JPRS L/10200

18 December 1981

Translation

SHIP BOUNDARY LAYER CONTROL

By

A.M. Basin, A.I. Korotkin and L.F. Kozlov

FBIS FOREIGN BROADCAST INFORMATION SERVICE

NOTE

JPRS publications contain information primarily from foreign newspapers, periodicals and books, but also from news agency transmissions and broadcasts. Materials from foreign-language sources are translated; those from English-language sources are transcribed or reprinted, with the original phrasing and other characteristics retained.

Headlines, editorial reports, and material enclosed in brackets [] are supplied by JPRS. Processing indicators such as [Text] or [Excerpt] in the first line of each item, or following the last line of a brief, indicate how the original information was processed. Where no processing indicator is given, the information was summarized or extracted.

Unfamiliar names rendered phonetically or transliterated are enclosed in parentheses. Words or names preceded by a question mark and enclosed in parentheses were not clear in the original but have been supplied as appropriate in context. Other unattributed parenthetical notes within the body of an item originate with the source. Times within items are as given by source.

The contents of this publication in no way represent the policies, views or attitudes of the U.S. Government.

FOR OFFICIAL USE ONLY

SHIP BOUNDARY LAYER CONTROL

Leningrad UPRAVLENIYE POGRANICHNYM SLOYEM SUDNA in Russian 1968
pp 2-491

[Book by Abram Moiseyevich Basin, Aleksandr Izrailevich Korotkin,
Leonid Filippovich Kozlov, Sudostroyeniye, submitted 3 June 1968,
2,800 copies, UDC 629.12:532.526]

Contents

FOR OFFICIAL USE ONLY

- c -

UDC 629.12:532.526

BOUNDARY LAYER CONTROL

Leningrad UPRAVLENIYE POGRANICHNYM SLOYEM SUDNA in Russian 1968 pp 2-491

[Book by Abram Moiseyevich Basin, Aleksandr Izrailevich Korotkin, Leonid Fillippovich Kozlov, Sudostroyeniye, submitted 3 June 1968, 2800 copies]

[Text] Abstract: The results of the most significant theoretical and experimental studies of a new area of modern ship hydrodynamics, which is of practical importance and is related to modern methods of the theory and calculation of a controlled boundary layer, are discussed in this monograph. Along with theoretical problems, physical models of the investigated phenomena are considered, experimental data and structural diagrams of various methods of boundary layer control are analyzed. Results are presented from studying fluid flow stability in a laminar boundary layer, various methods of laminarization (suction, flexible surfaces and coverings that alter the properties of the fluid), and turbulent boundary layer control by injecting materials with various properties into the region next to the wall. Practical recommendations are made which will permit the possibilities of one control method or another to be evaluated, and conclusions are drawn regarding the expediency of using boundary layer control for viscous drag reduction on ships.

The book is designed for engineering, scientific workers, postgraduates and students in the higher courses of the shipbuilding schools and departments.

There are 492 pages, 205 figures, 10 tables and 391 references.

1

PREFACE BY THE AUTHORS

At this time applied hydrodynamics has developed to the point that it is possible not only to determine the forces acting on a body in motion, but also to alter the direction of these forces in the direction required in practice. However, whereas there are a number of monographs on wave drag on a moving body in which methods of determination and reduction of wave drag are presented, the problems of determining viscous drag are discussed in only individual journal articles, which for the most part are unavailable and unknown to shipbuilders at large.

This situation is explained by the novelty of the problem and absence of a clear idea about the practical possibilities of one method or another of reducing viscous drag.

The monograph presented here is intended to fill this gap to some degree. It discusses boundary layer control methods and calculation procedures permitting estimation of the possibilities of one control method or another. Conclusions are drawn regarding expediency of boundary layer control to achieve viscous drag reduction.

Boundary layer control can theoretically be implemented by two methods. The first consists in injecting   materials the properties of which differ from the properties of water at the wall region. The second is based on the idea of laminarization of the boundary layer ; with large Reynolds numbers the friction in the boundary layer under laminar conditions is less than in a turbulent boundary layer.

Both of the indicated methods are investigated in the book. When discussing the first of them, problems are investigated which are connected with studying a boundary layer both with continuous distribution of the fluid properties across the boundary layer and in the presence of an interface between fluids (an air or gas interlayer between the surface over which flow takes place and the main water flow).

The problems of stability of the fluid flow in a laminar boundary layer and various methods of laminarization of the boundary layer (suction, flexible coverings, alteration of the fluid properties in the wall region) were investigated in the discussion of the second method.

Structural diagrams are presented for various methods of boundary layer control.

[Portions of the text are missing]

FOR OFFICIAL USE ONLY
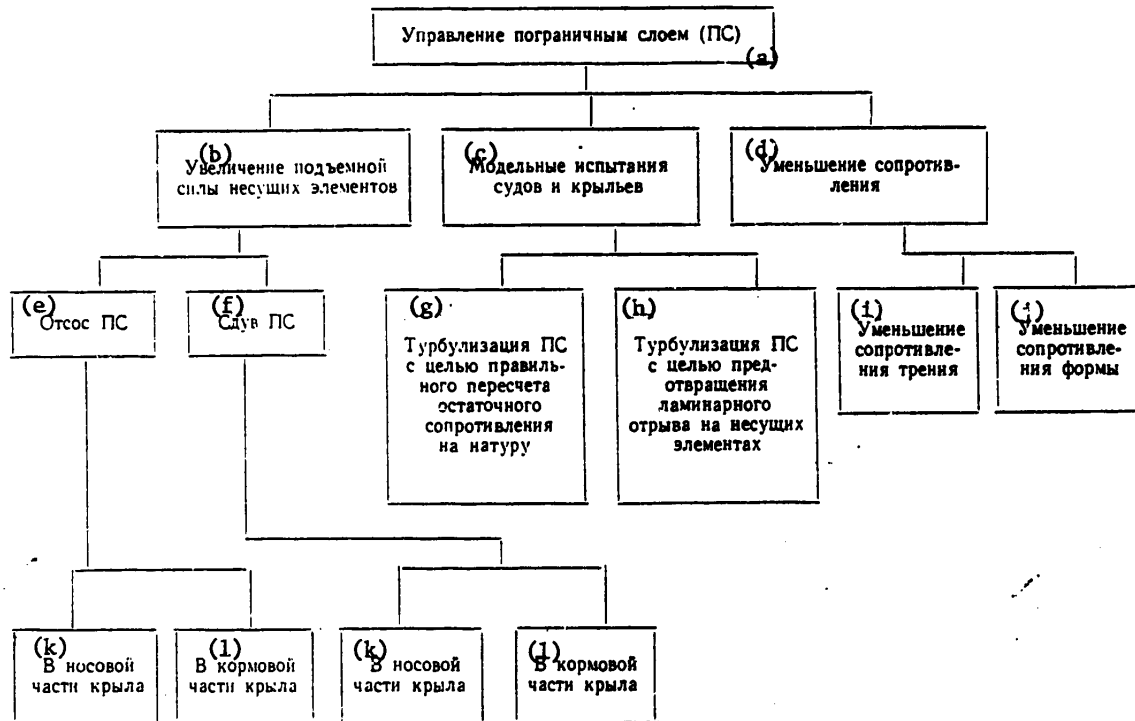
Diagram 1

Key: a. boundary layer (BL) control
b. increase in lift of the lifting surfaces
c. model basin testing of ships and foils
d. decrease in drag
e. boundary layer suction
f. boundary layer ventilation
g. turbulization of the boundary layer for proper recalculation of the residual drag to full scale
h. turbulization of the boundary layer to prevent laminar separation on the lifting surfaces
i. decrease in frictional drag
j. decrease in form drag
k. in the forward section of the foil
l. in the aft section of the foil

3

FOR OFFICIAL USE ONLY

... Reynolds number. Therefore the boundary layer characteristics of a model and full scale unit can differ significantly, which, in turn, can lead to noticeable variation of the force interaction of a body with a fluid and complicates the process of recalculating the results of model experiments to full scale. Under full scale conditions the Reynolds numbers are appreciably higher than during model experiments. The boundary layer of full-scale units in practice is completely turbulent. On the basis of relative smallness of the Reynolds numbers, in the case of models the boundary layer can remain laminar at significant distances from the forward end, and, consequently, the possibility of laminar separation arises. In addition, under laminar flow conditions the frictional drag is appreciably less than under turbulent conditions. Accordingly, the people conducting experiments are faced with the problem of turbulization of the boundary layer which is solved by various types of turbulence stimulators.

The turbulization problem also arises the simulating lifting surfaces if the experiment is performed with small Reynolds numbers.

For illustration of the effect of the nature of the flow in the boundary layer on the hydrodynamic properties of lifting surfaces let us consider the results of one of the experiments performed by G. G. Filippchenko and G. V. Anderson. A foil having NACA-2309 section, with 0.5 meter chord and 1 meter span was moved at a speed of 9.5 m/sec in a stationary air environment. The lift was measured, and the flow separation on the suction face of the foil was recorded by means of silk threads glued to it. A photograph of the upper surface of a foil set at an angle of attack of 18° is presented in Figure 0.1. The behavior of the silk threads indicates separation of the boundary layer over the greater part of the surface. The lift (C_y) was 0.8 in this case. Figure 0.2 shows the behavior of the silk threads in the presence of a trip wire 1 mm in diameter positioned with respect to the foil in accordance with the diagram illustrated in Figure 0.3. Judging by the silk threads, boundary layer separation is in practice absent over the entire foil although the towing speed and position of the foil with respect to the flow did not change. In the investigated case the lift was 1.15. Boundary layer separation is eliminated by turbulization exactly as in Prandtl's well-known experiment with flow over a sphere.

3. The next important area of application of boundary layer control is the class of problems connected with decreasing drag. Out of the three components of water resistance to the movement of vessels -- wave drag, form drag and frictional drag -- first form drag began to be decreased by giving streamlined, smooth lines to bodies moving in a fluid. It is also possible to reduce frictional drag by decreasing the wetted surface. In this case the bodies become relatively short and the form drag increases sharply as a result of flow separations occurring in the aft end. Suction or ventilation of the boundary layer in the vicinity of the aft end is proposed to eliminate the indicated separations.

4. The problems of influencing frictional drag have been the least studied. In practice, shipbuilding has no fully developed methods of reducing frictional drag. They are all in various stages of testing and determination of the expediency of their application.

It is the goal of the authors to outline to some degree the class of basic methods of lowering frictional drag which appear to be theoretically possible. These methods have been visually represented in diagram 2. The degree to which individual methods

4
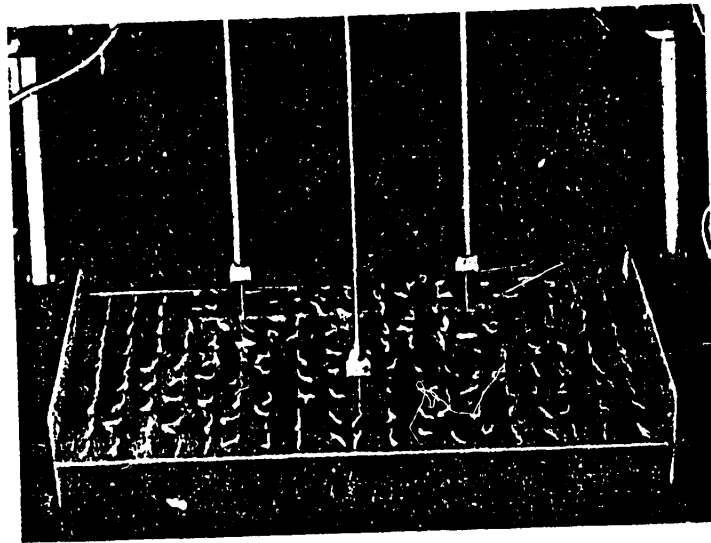
Figure 0.1. Behavior of silk threads on separation of the boundary layer over the greater part of a foil surface.
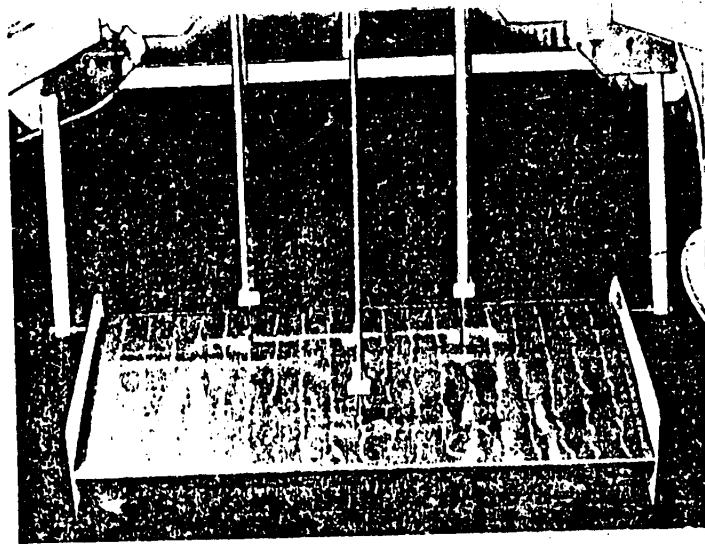
Figure 0.2. Behavior of silk threads in the presence of a longitudinal trip wire.

of lowering frictional drag have been developed differs. The most prospective and efficient means is ventilation of the wall region with gases. This follows from a comparison of the frictional stresses on the wall in fluids with different physical constants. Therefore the method of reducing frictional drag by creating thin air films, which has been checked out under full-scale conditions, is the closest to practical application. Although suction of the boundary layer to achieve laminarization has shown its best side in aviation, it is premature to recommend this

5
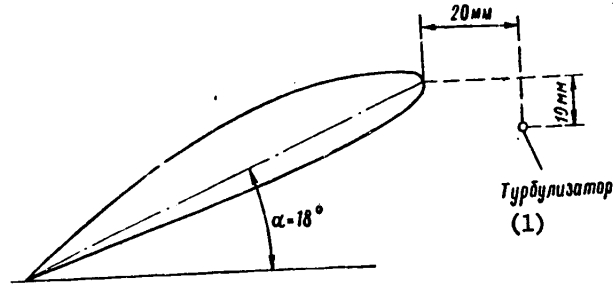
Figure 0.3. Diagram of trip wire positioned ahead
of a wing.

Key: 1. trip wire

method for practical use in shipbuilding, for there are no corresponding data from full-scale experiments.

The method of reducing drag by using flexible surfaces is the farthest from practical application. This method has been confirmed by a single experiment and theoretical developments.

Along with the indicated methods the classification presented in diagram 2 encompasses methods which have as their "assets" only theoretical developments (laminarization of the boundary layer by creating a positive kinematic viscosity gradient in the wall region). Finally, methods of lowering the frictional drag are mentioned there, the idea behind which has still be insufficiently completely confirmed by theoretical developments and experiments (for example, the effect of an elastic wall on a turbulent boundary layer).

When studying diagram 2 it is necessary to consider the known degree of arbitrariness in dividing laminarization methods into methods that increase the curvature of the velocity profile and methods directly influencing pulsating motion in the boundary layer. The presented classification was constructed by the principle of considering the primary mechanism of controlling disturbing motion. Thus, with suction, for example, not only is the steepness of the velocity profile increased, but the centers of pulsating motion are eliminated together with the fluid; in the case of decreasing the kinematic viscosity near the wall, the profile fills out significantly, but the pulsating motion damps more slowly.

Not all methods of reducing drag presented in diagram 2 are analyzed in the book. Only the most prospective in the sense of use for shipbuilding are touched on. Primary attention has been given to discussing new results and investigating the theoretical aspects of applying one method or another.

The apparatus of stability theory is used for theoretical evaluation of the possibility of boundary layer laminarization. This approach sometimes encounters objections in connection with the fact that there is a transition region between the point of loss of stability defined by this theory and the developed turbulent boundary layer zone. This transition region can also change in its extent. Therefore the following remarks are appropriate.

6
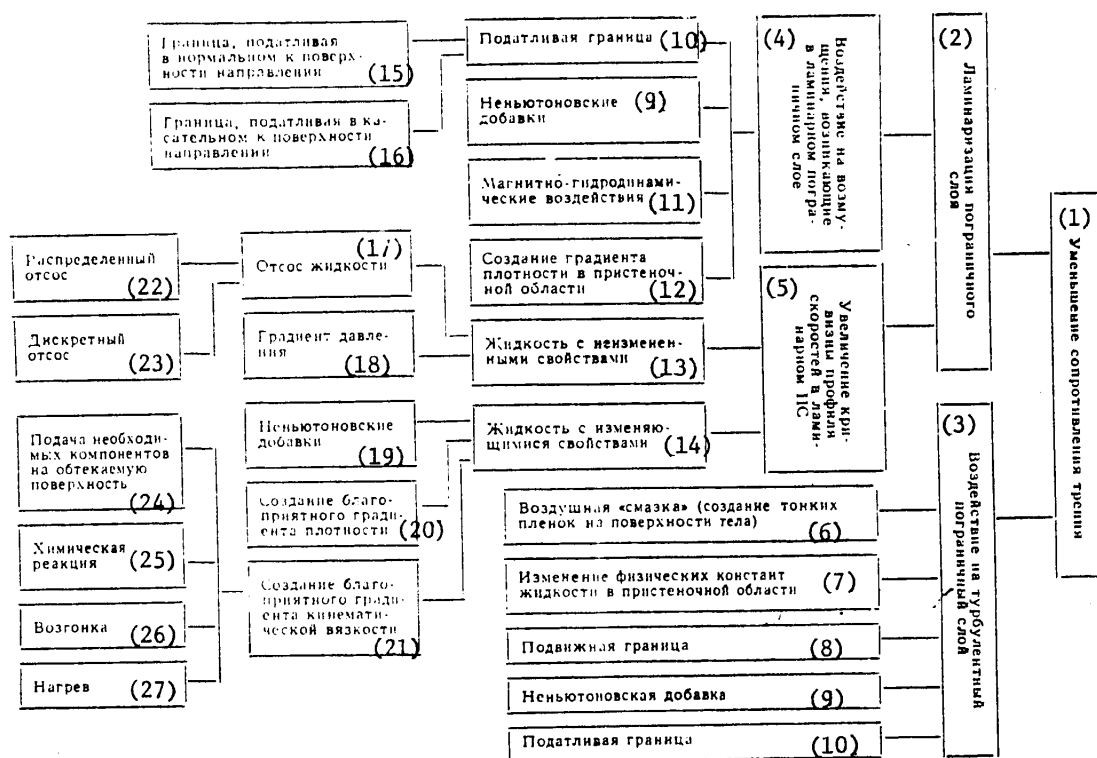
Diagram 2

Key: 1. decreasing frictional drag
2. laminarization of boundary layer
3. controlling a turbulent boundary layer
4. controlling disturbances occurring in a laminar boundary layer
5. increasing the curvature of the velocity profile in a laminar boundary layer
6. air "lubrication" (creation of thin films on the surface of a body)
7. alteration of the physical constants of the fluid in the wall region
8. moving boundary
9. nonnewtonian additive
10. compliant boundary
11. magnetohydrodynamic effects
12. creation of a density gradient in the wall region
13. fluid with unaltered properties
14. fluid with altered properties
15. boundary compliant in the direction normal to the surface
16. boundary compliant in the direction tangent to the surface
17. suction of fluid
18. pressure gradient
19. nonnewtonian additives
20. creation of a favorable density gradient
21. creation of a favorable kinematic viscosity gradient
22. distributed suction
23. discrete suction
24. injection of the required components at the surface over which flow is taking place
25. chemical reaction
26. volatilization
27. heating

7

Hydrodynamic stability theory has been confirmed by many experiments (see Chapter I) and correctly indicates the basic trend in the occurrence of turbulence. Based on the conclusions of stability theory, laminarized foil sections were built which under actual conditions demonstrated theoretically predicted better drag characteristics than ordinary sections (Figure 0.4).

This qualitative agreement between the stability theory conclusions and full-scale experimentation is also observed in boundary layer laminarization by suction of fluid from the surface over which flow is taking place.

Thus, the application of hydrodynamic stability theory for qualitative evaluation of the possibilities of one method of boundary layer laminarization or another appears to be justified, the more so in that calculations performed with respect to the loss of stability point always give a "margin" in determining the length of the laminar section (of course, if all of the significant factors of the phenomenon are taken into account).
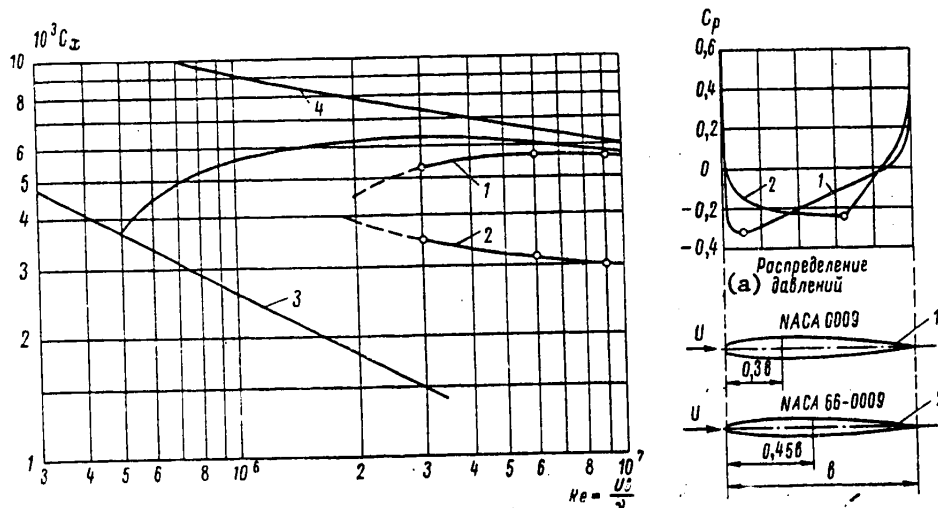
Figure 0.4. Frictional drag of a section, 1 — ordinary section; 2 — laminarized section; 3 — friction in the laminar boundary layer of a plate; 4 — friction in the turbulent boundary layer of a plate.

Key: a. pressure distribution

Laminarization of a boundary layer requires elimination of quite powerful disturbing factors: surface vibration and roughness, extraordinary external turbulence, local boundary layer separations. The effect of some of the indicated factors on transition of laminar flow to turbulent is discussed in Chapter V.

Hydrodynamic stability theory studies the behavior of small disturbances in a laminar boundary layer. It is obviously impossible exactly to define the boundary which separates small disturbances from finite ones at this time. It is necessary to define the admissible magnitude of the above-enumerated disturbances in each specific case on the basis of experimental data.

8

It has been pointed out that the most prospective means of reducing the frictional drag of flat-bottomed transport vessels is ventilation of the wall region of the flow with low-viscosity and low-density materials, that is, gases.

Accordingly, a theoretical study of a two-phase boundary layer is presented in the book.

Two boundary layer gas saturation modes are investigated: the film mode in which a clearly expressed, stable gas-liquid interface is observed, and the diffusion or bubble mode in which a gas-water mixture moves near the wall, the viscosity and density of which exceed the viscosity and density of the gas.

From the point of view of decreasing frictional drag the film gas saturation mode is of the greatest interest.

As a result of complexity of studying a two-phase boundary layer, the phase motion diagram is given, that is, the gas saturation mode (film or bubble) and the mode of motion of the liquid and gas (laminar or turbulent) are assumed in advance. This approach makes it possible to determine all of the hydrodynamic flow parameters. The problems of stability of the assumed form of the flow are not considered.

In view of significant difference in physical characteristics of a gas and a liquid two different methods of theoretical investigation of film gas saturation are presented in the book.

On the one hand, boundary layer theory is used to study film gas saturation considering the effect of the gas density and viscosity under the condition of neglecting the influence of the gas ventilation on the pressure distribution which is assumed to be given. The form of the interface is determined by the gas flow rate and method of injecting it into the flow.

On the other hand, for investigation of artificially created gas films the theory of developed cavitating flow is used in which real gas properties are not considered. Motion with an interface is considered as motion of an ideal fluid defined by the cavitation and Froude numbers with a free flow line subject to determination, the pressure on which is constant and equal to the gas pressure in the film.

Here a study is made of the problem of the limits of applicability of the indicated theories important in scientific and practical respects.

The efficient use of cavitating gas films to reduce drag is possible only if the basic physical laws defining the cavitating flow parameters are known.

In the proposed book a quite detailed discussion is presented of the results of theoretical and experimental studies determining the parameters of artificial gas films created on the bottom. The most important results of these studies was the conclusion of the existence of a limiting Froude number with respect to length of the gas film or, what amounts to the same thing, with given speed of the vessel -- limiting (maximum possible) length of the gas film. In addition, it is demonstrated that limiting gas films can be obtained for very small (theoretically zero) air flow rates, and the cavitation drag of the fittings used to form the gas films is very small.

9

The results presented in Chapter VIII can be used for practical solution of problems connected with the development of drag reduction devices for flat-bottomed transport vessels and planing vessels.

In the Soviet Union, papers by a number of researchers consider the problems connected with incompressible boundary layer control.

Hydrodynamic stability problems, which are closely intertwined with boundary layer laminarization, are being resolved by the Moscow Hydromechanics School under the direction of academician G. I. Petrov. Boundary layer laminarization by slot suction is the subject of papers by K. K. Fedyayevskiy, A. S. Ginevskiy, A. G. Prozorov, V. N. Nikolayeva, Yu. N. Alekseyev, L. F. Kozlov. Distributed suction from the boundary layer is represented by studies of Ya. S. Khodorkovskiy, S. S. Zolotov, Yu. N. Alekseyev, A. I. Korotkin, L. F. Kozlov. The influence of other discoveries on boundary layer laminarization was investigated in papers by A. I. Korotkin, V. B. Amfilokhiyev and N. A. Sergiyevskiy.

Turbulent boundary layer control is represented by papers by S. S. Kutateladze, A. I. Leont'yeva, L. Ye. Kalikhman, V. P. Mugalev, Yu. V. Lapin, Z. P. Shul'man, A. M. Basin, Yu. N. Karpeyev, I. P. Ginzburg.

In addition to the early works by L. G. Loytsyanskiy and K. K. Fedyayevskiy on two-phase boundary layers, it is necessary to note the studies of G. G. Chernyy, A. N. Ivanov, A. A. Butuzov, I. D. Zheltukhin, A. M. Basin and V. B. Starobinskiy. The influence of high-molecular additives on the characteristics of turbulent flows has been studied in experiments performed by a group of scientists under the direction of G. I. Barenblatt.

Hydrobionics problems have been investigated in papers by researchers directed by A. N. Patrashev.

A bibliography to which references are made in the text is presented at the end of each chapter. In some of these papers there are exhaustive lists and surveys of foreign research of the problems discussed in the book.

CHAPTER I. LAMINAR BOUNDARY LAYER STABILITY

§ I.1. Some General Problems of the Stability of the Laminar Form of Fluid Motion

During fluid flow two forms of motion can be observed in the boundary layer: laminar and turbulent. The laminar form of motion of the fluid (from the latin word *lamina* — plate) is characterized by the fact that its elements move in an orderly fashion, in layers, not mixing with adjacent layers. The turbulent form of fluid motion (from the latin word *turbulentus* — stormy, disordered) is characterized by disordered, nonsteady displacements of its elements along complex trajectories. Here the fluid particle velocities are of a random nature and vary with high frequency.

It must be emphasized that the presence of disorderliness in the motion of fluid particles only in time is insufficient for the motion to be considered turbulent [1]. Actually, one can conceive of defined quantity of fluid moving randomly as a solid body in space.

In exactly the same way, it is insufficient to have disorderliness of motion of the fluid particles only in space, for it is possible to imagine steady motion of a fluid with disorderly trajectories in any volume.

As an example, let us consider the flow behind a circular cylinder [2]. For small Reynolds numbers (Figure I.1a) the flow in the wake is of a laminar nature. With an increase in the flow velocity around the cylinder (Figure I.1b-d) a Karman vortex sheet forms behind the cylinder which, in spite of a quite complex nonsteady state law of development in time and space, cannot be classified as turbulent motion because of the absence of disorderliness of the displacements of the fluid elements. With a further growth of the flow velocity around the cylinder, the motion in the wake acquires a turbulent nature. An analogous picture of the laminar to turbulent flow transition is observed between coaxial cylinders [3].

It is possible to obtain a representation of the nature of velocity pulsations in the laminar, transition and turbulent regions of the boundary layer from investigation of some oscillograms (Figure I.2a-c) obtained by V. N. Nikolayeva and N. A. Sergiyevskiy during wind tunnel testing of a model of a wing using a thermoanemometric device.

The existence of two fluid flow conditions naturally imposes the problem of the conditions causing transition of one type of flow into the other. In practical applications usually we are dealing with transition of laminary flow into turbulent, in
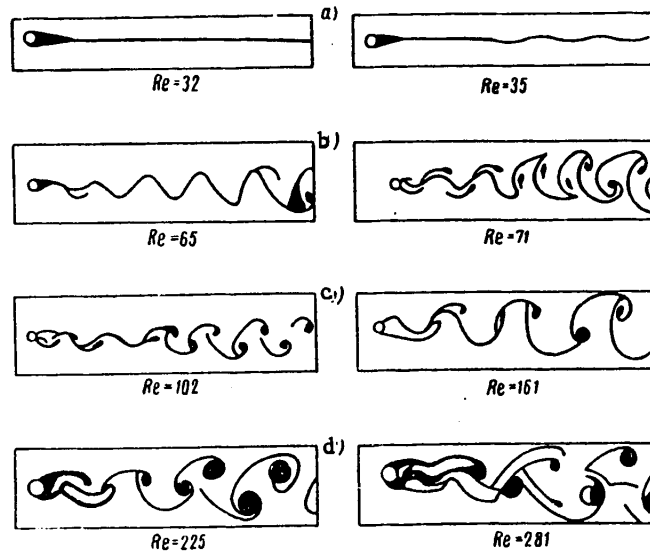
Figure I.1. Nature of motion in the wake behind a cylinder for various Reynolds numbers Re = ud/ν (d is the cylinder diameter).

conn.ection with which the primary attention of hydro and aeromechanics specialists is directed toward the discovery and study of the stability conditions of laminar fluid flow, the conditions of sustaining it [4]. However, recently problems have been discovered in which it was necessary for researchers to deal with transition of a turbulent flow to laminar [5]-[9]. A discussion is presented below of the problems connected only with the laminar-turbulent transition. The phenomenon of laminar to turbulent transition is highly complex. Thus, for example, for the case of fluid flow in a boundary layer the following regions are distinguished in the transition zone from the laminar boundary layer to a developed turbulent boundary layer [10]. The beginning of the first region (Figure I.3) is determined by the point of loss of stability of the laminar boundary layer with respect to small random disturbances incident in the boundary layer. As the experiments of Schubauer and Skramstad [11] demonstrated, relatively regular oscillations of the laminar flow can and do exist in this zone. These oscillations, developing downstream, increase with respect to amplitude and, acquiring an irregular nature, make the transition to the next region characterized by the presence of turbulent "spots" [4]. Increasing in size, the turbulent spots gradually fill the entire wall space, forming a turbulent boundary layer. Oscillograms of the recordings of velocity pulsations in the transition zone obtained by N. A. Sergiyevskiy using a thermoanemometer when testing plates in a model testing basin are presented in Figure I.4.

At the present time only the conditions of occurrence of the first region, that is, the conditions of stability of a laminar boundary layer with respect to small disturbances [12] have been sufficiently completely studied as applied to the boundary layer.

From what has been stated it follows that the state of the art in determining loss of stability in a boundary layer does not offer the possibility of indicating the beginning of developed turbulent flow in the layer, for the characteristics of the second

12
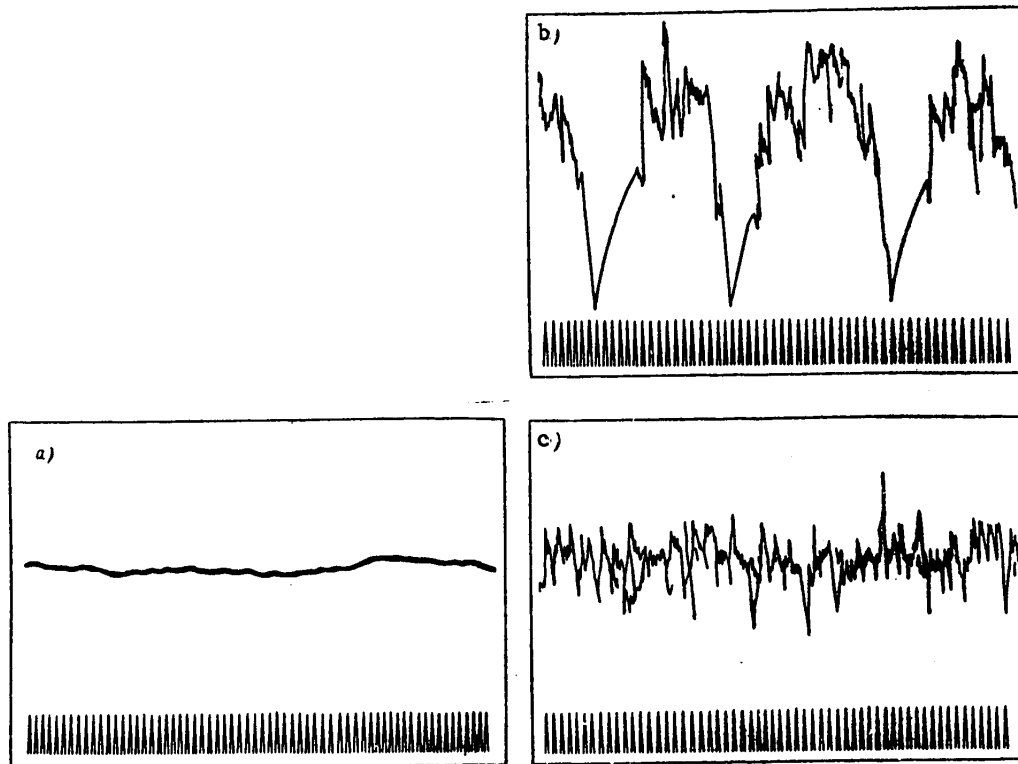
Figure I.2. Flow conditions in the boundary layer: a — laminar con-
ditions; b — transition conditions; c — turbulent conditions.
The distance between strokes corresponds to 0.002 second.
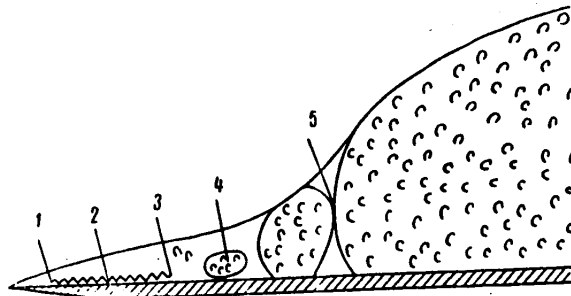
Figure I.3. Transition zone in a boundary layer. 1 — point of loss
of stability; 2 — developed disturbances in a laminar boundary
layer; 3 — beginning of the turbulent spot region; 4 — turbulent
spot region; 5 — beginning of the developed turbulent flow region.

transition region have still been insufficiently completely studied. However, the
calculation methods of stability theory as applied to a boundary layer permit sub-
stantiated comparison of laminar boundary layers developed under various conditions

13
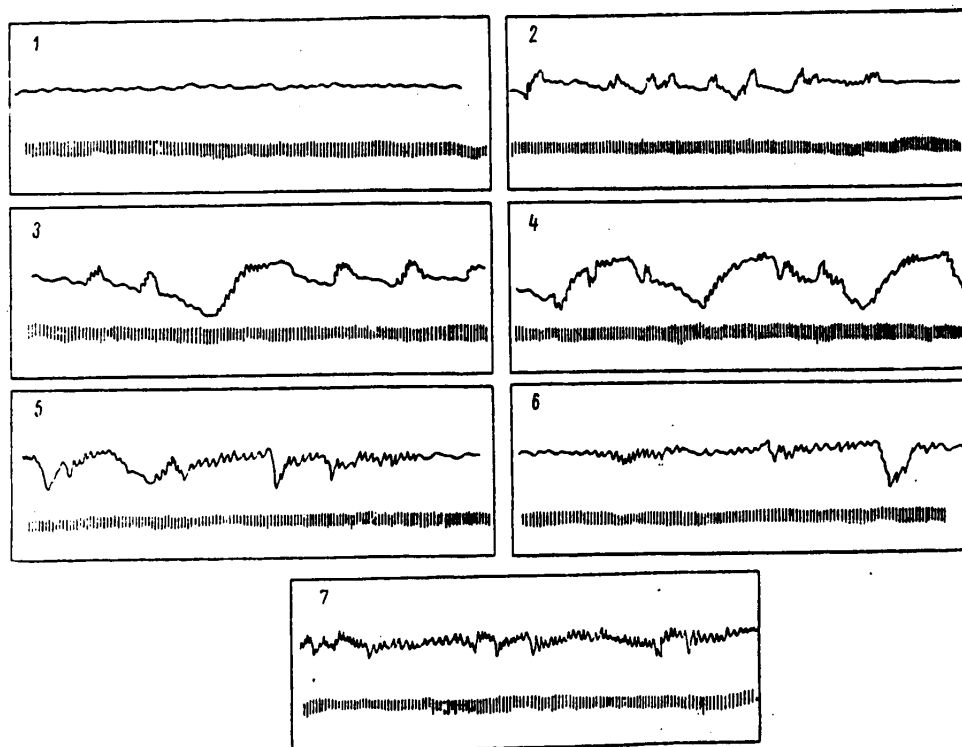
Figure I.4. Transition flow conditions in a boundary layer.
Spacing between strokes corresponds to 0.002 second. 1 — laminar
conditions; 2-6 — transition conditions; 7 — turbulent conditions.

from the point of view of their transition to the turbulent state. On the basis of
the conclusions of stability theory [13]-[15], laminarized foil sections have been
built which demonstrate better drag characteristics than ordinary sections [16].
Stability theory has also predicted [17], [18] significant possibilities of laminari-
zation of bodies by suction of fluid out of the boundary layer. As an example, in
Figure I.5 we see the results of determining the transition point by a thermoanemo-
metric device on a perforated foil with and without suction of air across its sur-
face (the experiment was performed by V. N. Nikolayeva). By the transition point in
the indicated experiment she meant the point of maximum intensity of the velocity
pulsations recorded by the instrument.

In connection with an investigation of the transition zone it must be noted that the
loss of stability of the initial laminar form of flow in a boundary layer need not
immediately cause turbulization. It can be found that the flow converts to another
laminar form more stable than the initial one [19], [20]. An analogous phenomenon
occurs in the wake behind a cylinder (see Figure I.1) when a rectilinear laminar
flow makes the transition to an oscillatory flow which, in turn, develops into a
Karman vortex sheet which is a more stable form of laminar motion than the initial
form. The transition of one laminar form of fluid motion into another can be
observed also in experiments with rotating coaxial cylinders [3], [21], when the
laminar flow in the gap between cylinders becomes proper vortex motion (so-called
"Taylor vortices").
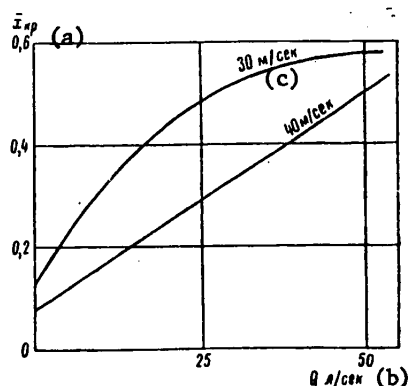
Figure I.5. Coordinates of the transition point on a perforated wing as a function of the degree of suction. Wing dimensions: chord ℓ = 1 m; span b = 1 m; perforated area S = 1 m^2; $\bar{x}_{cr}$ = x_{cr}/ℓ.

Key: a. $\bar{x}_{cr}$ b. Q, ℓ/sec   c. m/sec

Among researchers studying the problem of transition in a boundary layer there are two points of view with regard to its nature, Certain researchers (Taylor [22], Wieghardt [23]) consider that transition is a consequence of local separations of the laminar boundary layer occurring under the effect of finite disturbances incident in the boundary layer. Others (Tollmien [24], Schlichting [4], Lin [12]) explain transition as a consequence of loss of stability of the laminar boundary layer with respect to small random disturbances, Experiments performed under the corresponding conditions [11], [25], [26] and [27] confirm both theories. In reality, obviously the situation is such that in the presence of quite large disturbances transition takes place by a scheme close to the Taylor scheme, and for relatively small disturbances, phenomena develop as predicted by Tollmien-Schlichting theory.

At this time the Tollmien-Schlichting stability theory based on the classical method of small disturbances is considered generally accepted. This theory is very strictly substantiated and confirmed by many experiments. As will be obvious from what follows, it gives a picture of the development of small random disturbances in a laminar boundary layer which is quite close to reality.

When studying different methods of boundary layer laminarization, which will be discussed later, it is necessary to have a method of estimating the degree of stability of the laminar form of flow under various conditions. The method of small oscillations, a systematic discussion of which is presented in the following sections, was selected as this apparatus. Before proceeding with a description of this method, it is necessary to indicate its place among the existing methods of calculating stability: the Goertler method and the energy method. A brief description of the mentioned methods and their areas of application are considered below.

A discussion of various aspects of the problem of boundary layer control and flow stability problems in the wall region requires multiple references to the basic equations of motion of a fluid near boundaries, These equations with the corresponding boundary and initial conditions are presented in § I.2 in order to facilitate the subsequent discussion.

15

§ I.2. Laminar Boundary Layer Equations. Initial and Boundary Conditions

Equations of Motion of a Fluid in a Boundary Layer

The general equation of motion of a continuous medium [28]-[31] has the form:

$$\int_{\tau} (\vec{F} - \vec{w})\rho\, d\tau + \int_{S} \vec{p}_n\, dS = 0.$$

Here τ is an arbitrary volume isolated inside a fluid by the surface S;

ρ is the fluid particle density;

$\vec{w}$ is the fluid particle acceleration;

n is the direction of the external normal to the surface S;

$\vec{F}$ is the mass force vector reduced to a unit mass;

$\vec{p}_n$ is the surface force intensity vector.

Let us transform the surface integral entering into the equation of motion into a volumetric integral. Then we have

$$\int_{S} \vec{p}_n\, dS = \int_{S} [\vec{p}_x \cos(n,\ x) + \vec{p}_y \cos(n,\ y) +$$

$$+ \vec{p}_z \cos(n,\ z)]\, dS = \int_{\tau} \left(\frac{\partial \vec{p}_x}{\partial x} + \frac{\partial \vec{p}_y}{\partial y} + \frac{\partial \vec{p}_z}{\partial z} \right) d\tau.$$

The equation of motion assumes the form:

$$\int_{\tau} \left[(\vec{F} - \vec{w})\rho + \frac{\partial \vec{p}_x}{\partial x} + \frac{\partial \vec{p}_y}{\partial y} + \frac{\partial \vec{p}_z}{\partial z} \right] d\tau = 0.$$

Under the condition of continuity of the investigated functions and their derivatives the preceding equality exists only in the case where the function under the integral sign is zero at any time of motion, that is,

$$\vec{F} - \vec{w} + \frac{1}{\rho} \left(\frac{\partial \vec{p}_x}{\partial x} + \frac{\partial \vec{p}_y}{\partial y} + \frac{\partial \vec{p}_z}{\partial z} \right) = 0.$$

Denoting the projections of the mass force $\vec{F}$ on rectangular coordinate axes by F_x, F_y, F_z, the projections of the vectors $\vec{p}_x$, $\vec{p}_y$, $\vec{p}_z$ by p_{xx}, p_{xy}, p_{xz}, and so on and the projections of the acceleration $\vec{w}$ by du/t, dv/dt, dw/dt, we find the equations of motion in the following form:

$$\left. \begin{aligned} \frac{du}{dt} &= F_x + \frac{1}{\rho} \left(\frac{\partial p_{xx}}{\partial x} + \frac{\partial p_{yx}}{\partial y} + \frac{\partial p_{zx}}{\partial z} \right); \\ \frac{dv}{dt} &= F_y + \frac{1}{\rho} \left(\frac{\partial p_{xy}}{\partial x} + \frac{\partial p_{yy}}{\partial y} + \frac{\partial p_{zy}}{\partial z} \right); \\ \frac{dw}{dt} &= F_z + \frac{1}{\rho} \left(\frac{\partial p_{xz}}{\partial x} + \frac{\partial p_{yz}}{\partial y} + \frac{\partial p_{zz}}{\partial z} \right). \end{aligned} \right\}$$

(I.1)

The continuity equation must be added to these equations

$$\frac{\partial \rho}{\partial t} + \frac{\partial (\rho u)}{\partial x} + \frac{\partial (\rho v)}{\partial y} + \frac{\partial (\rho w)}{\partial z} = 0. \tag{I.2}$$

For an incompressible liquid the expressions for the intensities have the form [28]:

$$
\begin{aligned}
p_{xx} &= -p + 2\mu \frac{\partial u}{\partial x}; & p_{xy} = p_{yx} &= \mu \left(\frac{\partial u}{\partial y} + \frac{\partial v}{\partial x}\right); \\
p_{yy} &= -p + 2\mu \frac{\partial v}{\partial y}; & p_{xz} = p_{zx} &= \mu \left(\frac{\partial u}{\partial z} + \frac{\partial w}{\partial x}\right); \\
p_{zz} &= -p + 2\mu \frac{\partial w}{\partial z}; & p_{yz} = p_{zy} &= \mu \left(\frac{\partial v}{\partial z} + \frac{\partial w}{\partial y}\right).
\end{aligned}
\tag{I.3}
$$

Here μ is the internal friction coefficient or the coefficient of viscosity.

For a uniform viscous incompressible liquid the system (I.1)-(I.3) is simplified

$$
\begin{aligned}
\frac{du}{dt} &= F_x - \frac{1}{\rho}\frac{\partial p}{\partial x} + \nu \Delta u; \\
\frac{dv}{dt} &= F_y - \frac{1}{\rho}\frac{\partial p}{\partial y} + \nu \Delta v; \\
\frac{dw}{dt} &= F_z - \frac{1}{\rho}\frac{\partial p}{\partial z} + \nu \Delta w; \\
\frac{\partial u}{\partial x} + \frac{\partial v}{\partial y} + \frac{\partial w}{\partial z} &= 0.
\end{aligned}
\tag{I.4}
$$

Here $\nu = \mu/\rho$ is the kinematic coefficient of viscosity.

During motion of a fluid near curvilinear surfaces in some cases it is expedient to use curvilinear orthogonal coordinates q_1, q_2, q_3. The corresponding projections of the velocity vector will be denoted by v_1, v_2, v_3. In the indicated coordinates the equations (I.4) are written as follows [28]:

$$
\begin{aligned}
&\frac{\partial v_1}{\partial t} + \frac{v_1}{H_1}\frac{\partial v_1}{\partial q_1} + \frac{v_2}{H_2}\frac{\partial v_1}{\partial q_2} + \frac{v_3}{H_3}\frac{\partial v_1}{\partial q_3} + \frac{v_1 v_2}{H_1 H_2}\frac{\partial H_1}{\partial q_2} + \\
&+ \frac{v_1 v_3}{H_1 H_3}\frac{\partial H_1}{\partial q_3} - \frac{v_2^2}{H_1 H_2}\frac{\partial H_2}{\partial q_1} - \frac{v_3^2}{H_3 H_1}\frac{\partial H_3}{\partial q_1} = F_1 - \frac{1}{\rho}\frac{1}{H_1}\frac{\partial p}{\partial q_1} - \\
&- \frac{\nu}{H_2 H_3}\left\{\frac{\partial}{\partial q_2}\left[\frac{H_3}{H_1 H_2}\frac{\partial (v_2 H_2)}{\partial q_1} - \frac{H_3}{H_1 H_2}\frac{\partial (v_1 H_1)}{\partial q_2}\right] - \right. \\
&\left. - \frac{\partial}{\partial q_3}\left[\frac{H_2}{H_3 H_1}\frac{\partial (v_1 H_1)}{\partial q_3} - \frac{H_2}{H_3 H_1}\frac{\partial (v_3 H_3)}{\partial q_1}\right]\right\};
\end{aligned}
\tag{I.5}
$$

$$
\begin{aligned}
&\frac{\partial v_2}{\partial t} + \frac{v_2}{H_2}\frac{\partial v_2}{\partial q_2} + \frac{v_3}{H_3}\frac{\partial v_2}{\partial q_3} + \frac{v_1}{H_1}\frac{\partial v_2}{\partial q_1} + \frac{v_2 v_3}{H_2 H_3}\frac{\partial H_2}{\partial q_3} + \\
&+ \frac{v_2 v_1}{H_2 H_1}\frac{\partial H_2}{\partial q_1} - \frac{v_3^2}{H_2 H_3}\frac{\partial H_3}{\partial q_2} - \frac{v_1^2}{H_1 H_2}\frac{\partial H_1}{\partial q_2} = F_2 - \frac{1}{\rho}\frac{1}{H_2}\frac{\partial p}{\partial q_2} - \\
&- \frac{\nu}{H_3 H_1}\left\{\frac{\partial}{\partial q_3}\left[\frac{H_1}{H_2 H_3}\frac{\partial (v_3 H_3)}{\partial q_2} - \frac{H_1}{H_2 H_3}\frac{\partial (v_2 H_2)}{\partial q_3}\right] - \right. \\
&\left. - \frac{\partial}{\partial q_1}\left[\frac{H_3}{H_1 H_2}\frac{\partial (v_2 H_2)}{\partial q_1} - \frac{H_3}{H_1 H_2}\frac{\partial (v_1 H_1)}{\partial q_2}\right]\right\};
\end{aligned}
\tag{I.6}
$$

$$\frac{\partial v_3}{\partial t} + \frac{v_3}{H_3}\frac{\partial v_3}{\partial q_3} + \frac{v_1}{H_1}\frac{\partial v_3}{\partial q_1} + \frac{v_2}{H_2}\frac{\partial v_3}{\partial q_2} + \frac{v_3 v_1}{H_3 H_1}\frac{\partial H_3}{\partial q_1} +$$

$$+ \frac{v_3 v_2}{H_3 H_2}\frac{\partial H_3}{\partial q_2} - \frac{v_1^2}{H_3 H_1}\frac{\partial H_1}{\partial q_3} - \frac{v_2^2}{H_2 H_3}\frac{\partial H_2}{\partial q_3} = F_3 - \frac{1}{\rho}\frac{1}{H_3}\frac{\partial p}{\partial q_3} -$$

$$- \frac{\nu}{H_1 H_3}\left\{ \frac{\partial}{\partial q_1}\left[\frac{H_2}{H_3 H_1}\frac{\partial(v_1 H_1)}{\partial q_3} - \frac{H_2}{H_3 H_1}\frac{\partial(v_3 H_3)}{\partial q_1}\right] - \right.$$

$$\left. - \frac{\partial}{\partial q_2}\left[\frac{H_1}{H_2 H_3}\frac{\partial(v_3 H_3)}{\partial q_2} - \frac{H_1}{H_2 H_3}\frac{\partial(v_2 H_2)}{\partial q_3}\right]\right\}; \qquad (I.7)$$

$$\frac{\partial(v_1 H_2 H_3)}{\partial q_1} + \frac{\partial(v_2 H_3 H_1)}{\partial q_2} + \frac{\partial(v_3 H_1 H_2)}{\partial q_3} = 0. \qquad (I.8)$$

In equations (I.5)-(I.8) H_i (i = 1, 2, 3) are Lamé coefficients, the values of which can be obtained using the expression for an element of an arc in the adopted curvilinear coordinate system.

$$dS^2 = H_1^2(dq_1)^2 + H_2^2(dq_2)^2 + H_3^2(dq_3)^2. \qquad (I.9)$$
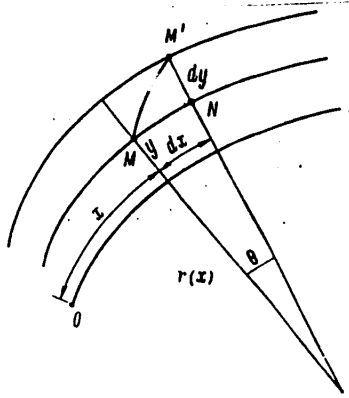
Figure I.6. Coordinate diagram on a curvilinear surface.

The above-described systems of equations of motion of a viscous fluid are basic when studying flow over bodies in cases where the forces of inertia in the flow greatly exceed the viscosity forces everywhere except the thin wall region where the indicated categories of forces are comparable with respect to magnitude. The Prandtl equations describing the motion of a fluid in this region called the boundary layer with good approximation, can be obtained by different methods [29], [32]-[35].
The derivation of the boundary layer equations for simplest plane-parallel flow based on the Mises scheme [33], [28], [39] is presented below.

Let us consider a cylindrical body of finite dimensions with generatrices perpendicular to the plane of the flow. A viscous liquid flows around the cylindrical body. Let s be the surface of this body. At each point of the surface let us draw

18

the external normal and take values of $q_1 = x$ and $q_2 = y$ as the coordinates of any point M, where x is reckoned along the surface from the selected initial point 0 and y is reckoned from the surface to the normal on through the point M (Figure I.6). We shall consider that in the flow region of interest to us ($0 \leq x \leq x_1$; $y \geq 0$) the values of v_1, v_2, p and their derivatives entering into equations (I.5)-(I.8) are finite values. In addition, let us assume for $0 \leq x \leq x_1$ the curvature of the surface of the body over which flow takes place also never goes to infinity anywhere.

Let us determine the length of the arc element MM' in the adopted coordinate system (Figure I.6)

$$dS^2 = (MM')^2 = (MN)^2 + dy^2;$$

$$MN = (r + y)\theta = (r + y)\frac{dx}{r} = \left(1 + \frac{y}{r}\right) dx,$$

where r(x) is the radius of curvature of the surface.

Thus,

$$dS^2 = \left(1 + \frac{y}{r}\right)^2 dx^2 + dy^2. \tag{I.10}$$

Comparing (I.9) and (I.10), we find the Lamé coefficients for the selected coordinate system

$$H_1 = 1 + \frac{y}{r}; \quad H_2 = 1. \tag{I.11}$$

If the wall is concave, then $H_1 = 1 - y/r$, $H_2 = 1$. Let us take u_0 -- the velocity of the oncoming flow far ahead of the body -- as the unit of measure of the velocities, let us take L -- the surface length of the body or any linear dimension depending on it -- as the unit of measure of distances. This can be done, because the body, by stipulation, has finite extent in the direction of the flow.

Using the indicated characteristic values, let us reduce the system of equations (I.5)-(I.8) to dimensionless form, considering the two-dimensional nature of the flow and the expression (I.11)

$$\frac{\partial u}{\partial t} + \frac{1}{1 + xy} u \frac{\partial u}{\partial x} + v \frac{\partial u}{\partial y} + \frac{x}{1 + xy} uv = -\frac{1}{1 + xy} \frac{\partial p}{\partial x} +$$

$$+ \frac{1}{Re} \left[\frac{1}{(1 + xy)^2} \frac{\partial^2 u}{\partial x^2} + \frac{\partial^2 u}{\partial y^2} - \frac{y}{(1 + xy)^3} \frac{\partial x}{\partial x} \frac{\partial u}{\partial x} + \right.$$

$$\left. + \frac{x}{1 + xy} \frac{\partial u}{\partial y} - \frac{x^2}{(1 + xy)^2} u + \frac{1}{(1 + xy)^3} \frac{\partial x}{\partial x} v + \frac{2x}{(1 + xy)^2} \frac{\partial v}{\partial x} \right]; \tag{I.12}$$

$$\frac{\partial v}{\partial t} + \frac{1}{1 + xy} u \frac{\partial v}{\partial x} + v \frac{\partial v}{\partial y} - \frac{x}{1 + xy} u^2 =$$

$$= -\frac{\partial p}{\partial y} + \frac{1}{Re} \left[\frac{1}{(1 + xy)^2} \frac{\partial^2 v}{\partial x^2} + \frac{\partial^2 v}{\partial y^2} - \frac{y}{(1 + xy)^3} \frac{\partial x}{\partial x} \times \right.$$

$$\times \frac{\partial v}{\partial x} + \frac{x}{1 + xy} \frac{\partial v}{\partial y} + \frac{x^2}{(1 + xy)^2} v - \frac{1}{(1 + xy)^3} \frac{\partial x}{\partial x} u -$$

$$\left. - \frac{2x}{(1 + xy)^3} \frac{\partial u}{\partial x} \right]; \tag{I.13}$$

19

$$\frac{\partial u}{\partial x} + (1 + \varkappa y)\frac{\partial v}{\partial y} + \varkappa v = 0. \tag{I.14}$$

In equations (I.12)-(I.14) the previous notation was retained for the dimensionless values u, v, p, x, y, $\varkappa(x) = \frac{L}{r(x)}$ is the dimensionless surface curvature, Re = $u_0 L/\nu$ is the Reynolds number. Striving to find solutions to the system (I.12-(I.14) for very large Re numbers, it would be possible to drop all terms of order (1/Re) if they do not contain higher-order derivatives of the desired functions u and v, for by lowering the order of the equations, at the same time we eliminate the possibility of satisfying all of the boundary conditions on the surface of the body, in particular, the physical condition of adherence of the fluid to the wall. The larger the Reynolds number, the thicker the wall layer where it is necessary to consider the viscous terms in the equations becomes, for the forces of inertia of the fluid exceed the viscosity forces more and more, and for Re → ∞ it approaches zero, but does not disappear.

In order to study the flow in a boundary layer it is expedient to introduce the scale for the transverse coordinate y such that the dimensions of the region where it is necessary to consider the influence of viscosity do not decrease to zero for R → ∞. It is natural that the scale selected in this way must be related to the Reynolds number. Considering the form of the dependence of the right-hand sides of equations (I.12), (I.13) on Re, let us set

$$y_1 = y \cdot Re^n. \tag{I.15}$$

On the basis of the continuity equation (I.14), which must be satisfied for any finite value of the curvature, including for $\chi = 0$, we conclude that the scale of the transverse velocity in the boundary layer must also be altered

$$v_1 = v \cdot Re^n, \tag{I.16}$$

for by the condition of the investigated problem $\partial u/\partial x$ is a finite value. The scales for u, x, t, p will remain as before, that is, we shall consider $u_1 = u$; $x_1 = x$; $t_1 = t$; $p_1 = p$.

Let us substitute new variables in the system (I.12)-(I.14) and, selecting the exponent in (I.15), (I.16) so that the terms of an inertial nature in equations (I.12), (I.13) for any finite surface curvature will have the same order as the higher order terms with respect to the Re number characterizing the influence of the viscosity, we find n = 1/2.

The discussed system of equations assumes the following form:

$$\frac{\partial u_1}{\partial t_1} + \frac{1}{1 + \varkappa y_1/Re^{1/2}} u_1 \frac{\partial u_1}{\partial x_1} + v_1 \frac{\partial u_1}{\partial y_1} +$$

$$+ \frac{\varkappa}{1 + \varkappa y_1/Re^{1/2}} u_1 \frac{v_1}{Re^{1/2}} = - \frac{1}{1 + \varkappa y_1/Re^{1/2}} \frac{\partial p_1}{\partial x_1} +$$

$$+ \frac{1}{Re} \frac{1}{(1 + \varkappa y_1/Re^{1/2})^2} \frac{\partial^2 u_1}{\partial x_1^2} + \frac{\partial^2 u_1}{\partial y_1^2} -$$

20

$$-\frac{y_1}{\mathrm{Re}^{3/2}(1+xy_1/\mathrm{Re}^{1/2})^3}\frac{\partial x}{\partial x_1}\frac{\partial u_1}{\partial x_1}+\frac{x}{\mathrm{Re}^{1/2}(1+xy_1/\mathrm{Re}^{1/2})}\frac{\partial u_1}{\partial y_1}-$$

$$-\frac{x^2 u_1}{\mathrm{Re}(1+xy_1/\mathrm{Re}^{1/2})^2}+\frac{v_1}{\mathrm{Re}^{3/2}(1+xy_1/\mathrm{Re}^{1/2})^3}\frac{\partial x}{\partial x_1}+$$

$$+\frac{2x}{\mathrm{Re}^{3/2}(1+xy_1/\mathrm{Re}^{1/2})^2}\frac{\partial v_1}{\partial x_1}\Big];$$

$$\frac{1}{\mathrm{Re}^{1/2}}\frac{\partial v_1}{\partial t_1}+\frac{u_1}{\mathrm{Re}^{1/2}(1+xy_1/\mathrm{Re}^{1/2})}\frac{\partial v_1}{\partial x_1}+\frac{1}{\mathrm{Re}^{1/2}}v_1\frac{\partial v_1}{\partial y_1}-$$

$$-\frac{x}{1+xy_1/\mathrm{Re}^{1/2}}u^2=-\mathrm{Re}^{1/2}\frac{\partial p_1}{\partial y_1}+\frac{1}{\mathrm{Re}^{3/2}(1+xy_1/\mathrm{Re}^{1/2})^2}\frac{\partial^2 v_1}{\partial x_1^2}+$$

$$+\frac{1}{\mathrm{Re}^{1/2}}\frac{\partial^2 v_1}{\partial y_1^2}-\frac{y_1}{\mathrm{Re}^2(1+xy_1/\mathrm{Re}^{1/2})^3}\cdot\frac{\partial x}{\partial x_1}\frac{\partial v_1}{\partial x_1}+$$

$$+\frac{x}{\mathrm{Re}(1+xy_1/\mathrm{Re}^{1/2})}\frac{\partial v_1}{\partial y_1}-\frac{x^2 v_1}{\mathrm{Re}^{3/2}(1+xy_1/\mathrm{Re}^{1/2})^2}-$$

$$-\frac{1}{\mathrm{Re}(1+xy_1/\mathrm{Re}^{1/2})^3}\frac{\partial x}{\partial x_1}u_1-\frac{2x}{\mathrm{Re}(1+xy_1/\mathrm{Re}^{1/2})^2}\frac{\partial u_1}{\partial x_1}\Big];$$

$$\frac{\partial u_1}{\partial x_1}+(1+xy_1/\mathrm{Re}^{1/2})\frac{\partial v_1}{\partial y_1}+\frac{x}{\mathrm{Re}^{1/2}}v_1=0.$$

In the obtained equations let us go to the limit for Re → ∞, dividing both sides of the second of the equations by $\mathrm{Re}^{1/2}$ in advance,

$$\frac{\partial u_1}{\partial t_1}+u_1\frac{\partial u_1}{\partial x_1}+v_1\frac{\partial u_1}{\partial y_1}=-\frac{\partial p_1}{\partial x_1}+\frac{\partial^2 u_1}{\partial y_1^2};$$

$$0=\frac{\partial p_1}{\partial y_1};$$

$$\frac{\partial u_1}{\partial x_1}+\frac{\partial v_1}{\partial y_1}=0.$$

(I.17)

The errors in equations (I.17) are on the order of

$$x\,\mathrm{R}^{-1/2},\ \mathrm{Re}^{-1},\ \mathrm{Re}^{-3/2}\frac{\partial x}{\partial x_1}.$$

If we go to the old variables x, y, t, u, v, p in (I.17), the Prandtl system of equations is obtained:

$$\frac{\partial u}{\partial t}+u\frac{\partial u}{\partial x}+v\frac{\partial u}{\partial y}=-\frac{\partial p}{\partial x}+\frac{1}{\mathrm{Re}}\frac{\partial^2 u}{\partial y^2};$$

$$\frac{\partial p}{\partial y}=0;$$

$$\frac{\partial u}{\partial x}+\frac{\partial v}{\partial y}=0,$$

(I.18)

describing the fluid motion in the laminar boundary layer on a curvilinear surface with moderate curvature with the indicated accuracy.

System (I.18) contains three unknowns u, v and p, where on the basis of the second equation the latter depends only on x. In order to solve the problem of fluid motion in a boundary layer with the help of two equations (first and third), it is necessary to give the function p(x) defined in the first approximation from the

21

corresponding problem of potential flow of an ideal fluid over the investigated surface.

Boundary and Initial Conditions. Excluding the transverse velocity component in the boundary layer by using the continuity equation,

$$v = v(x, 0, t) - \int_0^y \frac{\partial u}{\partial x} \, dy,$$

(I.19)

it is possible to reduce the problem of integration of the system (I.18) to finding the function u(x, y, t). Naturally the boundary and the initial conditions in this case will be set only for the function u(x, y, t) and its derivatives. As follows from (I.19), the function v(x, 0, t) which also must be given, constitutes an exception.

The main boundary conditions for the system (I.18) which fully determine the flow picture are the following expressions

$$u(x, 0, t) = f_1(x, t); \quad v(x, 0, t) = f_2(x, t);$$
$$u(x, y, t)/_{y \to \infty} \to U(x, t).$$

(I.20)

The last of the conditions (I.20) is defined insufficiently clearly, for the boundary layer region smoothly becomes the external potential flow region. In addition, it is necessary to remember that the Prandtl equations are valid only near the surface over which flow takes place. However, the use of this condition does not lead to any difficulties, for the equations themselves are such that even for finite and quite small values of y the velocity in the boundary layer in practice becomes equal to the velocity of the potential flow.

In the case of nonsteady motion in the investigated region it is necessary to give the function

$$u(x, y, 0) = f_3(x, y).$$

(I.21)

For practical solution of the problems of a nonsteady boundary layer, instead of the condition (I.21), the velocity of the body at the time t = 0 and law of subsequent variation of this velocity are given. If the initial velocity of the body $u_0 \neq 0$, then it is necessary to indicate how the body reaches this velocity; otherwise the problem will be incompletely formulated, for the function f_3 in equality (I.21) will not be defined.

Approximate methods of integrating the system (I.18), for example, the methods based on using the Karman integral relation, replace the problem of finding one function u(x, y, t) by the problem of defining several, but simpler functions with respect to structure. It is natural that to find these functions more boundary and initial conditions are required. These additional boundary conditions for the case of steady-state flow include the Karman-Pohlhausen condition consisting in the assumption of validity of the first equation of motion at the wall and also the expressions obtained by differentation of it with respect to the transverse coordinate. At the outer boundary of the boundary layer the conditions of smoothness of conjugacy of the velocity profile in the layer with the external flow velocity are used, equating the derivatives of the function u(x, y) with respect to the coordinate y to zero.

22

By methods analogous to those discussed above it is possible to obtain the equations and state the problem of a three-dimensional laminar boundary layer [35]-[38].

Axisymmetric Boundary Layer. In conclusion, let us consider the relation between a two-dimensional boundary layer and a boundary layer occurring during flow over a body of revolution. The equations of a steady axisymmetric boundary layer in dimensional form are obtained [16], [35] from the general system of equations (I.5)-(I.8) for a cylindrical coordinate system under ordinary assumptions of boundary layer theory and under the condition that the radius of transverse curvature of the surface $r_0(x)$ is significantly greater than the thickness of the boundary layer at the given point

$$u \frac{\partial u}{\partial x} + v \frac{\partial u}{\partial y} = -\frac{\partial p}{\rho \partial x} + \nu \frac{\partial^2 u}{\partial y^2} ;$$

$$\frac{\partial (r_0 u)}{\partial x} + \frac{(r_0 v)}{\partial y} = 0.$$

If we introduce the Stepanov-Mangler transformation [117], [118]

$$\bar{x} = \int_0^x r_0^2(\xi) d\xi ; \quad \bar{y} = r_0(x) y ; \quad \bar{u} = u ; \quad \bar{v} = \frac{v}{r_0} + \frac{r_0' y u}{r_0^2} ; \quad \bar{p} = p,$$

the preceding system of equations, considering the relation

$$\frac{\partial}{\partial x} = r_0^2 \frac{\partial}{\partial \bar{x}} + r_0' y \frac{\partial}{\partial \bar{y}} ; \quad \frac{\partial}{\partial y} = r_0 \frac{\partial}{\partial \bar{y}}$$

assumes the form

$$\bar{u} \frac{\partial \bar{u}}{\partial \bar{x}} + \bar{v} \frac{\partial \bar{u}}{\partial \bar{y}} = -\frac{\partial \bar{p}}{\rho \partial \bar{x}} + \nu \frac{\partial^2 \bar{u}}{\partial \bar{y}^2} ; \quad \frac{\partial \bar{u}}{\partial \bar{x}} + \frac{\partial \bar{v}}{\partial \bar{y}} = 0,$$

that is, it will exactly coincide with the system of equations of a plane boundary layer. Thus, the problem of the boundary layer in an incompressible fluid on a body of rotation can always be reduced to the problem of the boundary layer of a flat outline with corresponding velocity distribution in the potential external flow.

§ I.3. Methods of Calculating the Stability of a Laminar Boundary Layer

Equation of Disturbing Motion. When studying the stability of the laminary form of flow of a real fluid it is necessary to consider the process which is described by the nonlinear system of partial differential equations (I.5)-(I.8). If we do not consider the mass forces, then for flow over a cylindrical body with constant radius of curvature of the surface and generatrices perpendicular to the flow direction, the indicated system, analogously to the case investigated in § I.2, is written as follows:

For a convex surface:

$$\frac{\partial u}{\partial t} + \frac{r}{r+y} u \frac{\partial u}{\partial x} + v \frac{\partial u}{\partial y} + w \frac{\partial u}{\partial z} + \frac{1}{r+y} uv =$$

$$= -\frac{1}{\rho} \frac{r}{r+y} \frac{\partial p}{\partial x} + \nu \left[\left(\frac{r}{r+y} \right)^2 \frac{\partial^2 u}{\partial x^2} + \frac{\partial^2 u}{\partial y^2} + \frac{\partial^2 u}{\partial z^2} + \right.$$

$$+ \frac{2r}{(r+y)^2} \frac{\partial v}{\partial x} + \frac{1}{r+y} \frac{\partial u}{\partial y} - \frac{u}{(r+y)^2}\Big];$$

$$\frac{\partial v}{\partial t} + \frac{r}{r+y} u \frac{\partial v}{\partial x} + v \frac{\partial v}{\partial y} + w \frac{\partial v}{\partial z} - \frac{u^2}{r+y} = -\frac{1}{\rho} \frac{\partial p}{\partial y} +$$

$$+ \nu \Big[\Big(\frac{r}{r+y}\Big)^2 \frac{\partial^2 v}{\partial x^2} + \frac{\partial^2 v}{\partial y^2} + \frac{\partial^2 v}{\partial z^2} - \frac{2r}{(r+y)^2} \frac{\partial u}{\partial x} +$$

$$+ \frac{1}{r+y} \cdot \frac{\partial v}{\partial y} - \frac{v}{(r+y)^2}\Big];$$

$$\frac{\partial w}{\partial t} + \frac{r}{r+y} \cdot u \frac{\partial w}{\partial x} + v \cdot \frac{\partial w}{\partial y} + w \frac{\partial w}{\partial z} = -\frac{1}{\rho} \frac{\partial p}{\partial z} +$$

$$+ \nu \Big[\Big(\frac{r}{r+y}\Big)^2 \frac{\partial^2 w}{\partial x^2} + \frac{\partial^2 w}{\partial y^2} + \frac{\partial^2 w}{\partial z^2} + \frac{1}{r+y} \cdot \frac{\partial w}{\partial y}\Big];$$

$$\frac{\partial u}{\partial x} + \Big(1 + \frac{y}{r}\Big)\Big(\frac{\partial v}{\partial y} + \frac{\partial w}{\partial z}\Big) + \frac{v}{r} = 0;$$

For a concave surface

$$\frac{\partial u}{\partial t} + \frac{r}{r-y} u \cdot \frac{\partial u}{\partial x} + v \frac{\partial u}{\partial y} + w \frac{\partial u}{\partial z} - \frac{1}{r-y} \cdot u \cdot v = -\frac{1}{\rho} \times$$

$$\times \frac{r}{r-y} \cdot \frac{\partial p}{\partial x} + \nu \Big[\Big(\frac{r}{r-y}\Big)^2 \frac{\partial^2 u}{\partial x^2} + \frac{\partial^2 u}{\partial y^2} + \frac{\partial^2 u}{\partial z^2} - \frac{2r}{(r-y)^2} \times$$

$$\times \frac{\partial v}{\partial x} - \frac{1}{r-y} \cdot \frac{\partial u}{\partial y} - \frac{u}{(r-y)^2}\Big];$$

$$\frac{\partial v}{\partial t} + \frac{r}{r-y} \cdot u \cdot \frac{\partial v}{\partial x} + v \frac{\partial v}{\partial y} + w \frac{\partial v}{\partial z} + \frac{u^2}{r-y} = -\frac{1}{\rho} \times$$

$$\times \frac{\partial p}{\partial y} + \nu \Big[\Big(\frac{r}{r-y}\Big)^2 \frac{\partial^2 v}{\partial x^2} + \frac{\partial^2 v}{\partial y^2} + \frac{\partial^2 v}{\partial z^2} + \frac{2r}{(r-y)^2} \cdot \frac{\partial u}{\partial x} -$$

$$- \frac{1}{r-y} \cdot \frac{\partial v}{\partial y} - \frac{v}{(r-y)^2}\Big];$$

$$\frac{\partial w}{\partial t} + \frac{r}{r-y} \cdot u \frac{\partial w}{\partial x} + v \frac{\partial w}{\partial y} + w \cdot \frac{\partial w}{\partial z} = -\frac{1}{\rho} \cdot \frac{\partial p}{\partial z} +$$

$$+ \nu \Big[\Big(\frac{r}{r-y}\Big)^2 \frac{\partial^2 w}{\partial x^2} + \frac{\partial^2 w}{\partial y^2} + \frac{\partial^2 w}{\partial z^2} - \frac{1}{r-y} \cdot \frac{\partial w}{\partial y} \Big);$$

$$\frac{r}{r-y} \cdot \frac{\partial u}{\partial x} + \frac{\partial v}{\partial y} + \frac{\partial w}{\partial z} - \frac{v}{r-y} = 0.$$

(I.22)

Hereafter we shall consider the system (I.22), for the case of a concave surface is of special interest from the point of view of studying hydrodynamic stability of the boundary layer. The proposition of constancy of the radius of curvature of the surface permitting significant simplification of the problem appears to be justified for a qualitative study of the phenomenon of loss of stability by the boundary layer.

24

Stability of a flow described by equations (I.22) and the corresponding boundary conditions will be determined, as usually accepted, by the behavior of small random disturbances which can be imposed for any reasons on the investigated flow. If these random disturbances are damping with time, the given flow conditions will be stable; if they build with time, then the flow conditions will be unstable. The equations characterizing the development of the disturbances can be obtained if we consider u, v, w, p in (I.22) to consist of values defining the undisturbed motion $\bar{u}$, $\bar{v}$, $\bar{w}$, $\bar{p}$, and the corresponding disturbances v_x, v_y, v_z, p* so that

$$u = \bar{u} + v_x; \quad v = \bar{v} + v_y; \quad w = \bar{w} + v_z; \quad p = \bar{p} + p^*.$$

(I.23)

Substituting (I.23) in (I.22), using the assumption of smallness of the disturbances which permits us to obtain a linear system of equations with respect to v_x, v_y, v_z, p* and dropping the bar over the pressure and the velocities of the undisturbed motion, we arrive at the following system of partial differential equations

$$
\begin{aligned}
&\frac{\partial v_x}{\partial t} + \frac{r}{r-y} u \frac{\partial v_x}{\partial x} + \frac{r}{r-y} v_x \frac{\partial u}{\partial x} + v_y \frac{\partial u}{\partial y} + v \frac{\partial v_x}{\partial y} + \\
&+ v_z \frac{\partial u}{\partial z} + w \frac{\partial v_x}{\partial z} - \frac{1}{r-y} v_x v - \frac{1}{r-y} u v_y = \\
&= -\frac{1}{\rho} \frac{r}{r-y} \frac{\partial p^*}{\partial x} + \nu\left[\left(\frac{r}{r-y}\right)^2 \frac{\partial^2 v_x}{\partial x^2} + \frac{\partial^2 v_x}{\partial y^2} + \right. \\
&\left. + \frac{\partial^2 v_x}{\partial z^2} - \frac{2r}{(r-y)^2} \frac{\partial v_y}{\partial x} - \frac{1}{r-y} \frac{\partial v_x}{\partial y} - \frac{v_x}{(r-y)^2}\right]; \\
&\frac{\partial v_y}{\partial t} + \frac{r}{r-y} v_x \frac{\partial v}{\partial x} + \frac{r}{r-y} u \frac{\partial v_y}{\partial x} + v \frac{\partial v_y}{\partial y} + \\
&+ v_y \frac{\partial v}{\partial y} + v_z \frac{\partial v}{\partial z} + w \frac{\partial v_y}{\partial z} + \frac{2u v_x}{r-y} = -\frac{1}{\rho} \frac{\partial p^*}{\partial y} + \\
&+ \nu\left[\left(\frac{r}{r-y}\right)^2 \frac{\partial^2 v_y}{\partial x^2} + \frac{\partial^2 v_y}{\partial y^2} + \frac{\partial^2 v_y}{\partial z^2} + \right. \\
&\left. + \frac{2r}{(r-y)^2} \frac{\partial v_x}{\partial x} - \frac{1}{r-y} \frac{\partial v_y}{\partial y} - \frac{v_y}{(r-y)^2}\right]; \\
&\frac{\partial v_z}{\partial t} + \frac{r}{r-y} v_x \frac{\partial w}{\partial x} + \frac{r}{r-y} u \frac{\partial v_z}{\partial x} + v \frac{\partial v_z}{\partial y} + \\
&+ v_y \frac{\partial w}{\partial y} + w \frac{\partial v_z}{\partial z} + v_z \frac{\partial w}{\partial z} = -\frac{1}{\rho} \frac{\partial p^*}{\partial z} + \\
&+ \nu\left[\left(\frac{r}{r-y}\right)^2 \frac{\partial^2 v_z}{\partial x^2} + \frac{\partial^2 v_z}{\partial y^2} + \frac{\partial^2 v_z}{\partial z^2} - \frac{1}{r-y} \frac{\partial v_z}{\partial y}\right]; \\
&\frac{r}{r-y} \frac{\partial v_x}{\partial x} + \frac{\partial v_y}{\partial y} + \frac{\partial v_z}{\partial z} - \frac{v_y}{r-y} = 0.
\end{aligned}
$$

(I.24)

In system (I.24), u, v, w are considered to be given coordinate functions. For the case of a boundary layer when the velocities vary significantly more sharply with respect to the y coordinate than with respect to the x coordinate, it is possible to set u = u(y); v = w = 0. The variation of the velocity profile along the surface is taken into account by successive calculation of the stability characteristics for the velocity profiles in the boundary layer cross sections located at different distances from the transverse edge of the body. Some arguments indicating admissibility of the given simplification appear in § I.4.

25

The system (I.24) in the given case is written as follows:

$$
\left.
\begin{aligned}
&\frac{\partial v_x}{\partial t} + \frac{r}{r-y} u \frac{\partial v_x}{\partial x} + v_y \frac{\partial u}{\partial y} - \frac{1}{r-y} u v_y = \\
&= -\frac{1}{\rho} \frac{r}{r-y} \frac{\partial p^*}{\partial x} + \nu \left[\left(\frac{r}{r-y}\right)^2 \frac{\partial^2 v_x}{\partial x^2} + \frac{\partial^2 v_x}{\partial y^2} + \right. \\
&\left. + \frac{\partial^2 v_x}{\partial z^2} - \frac{2r}{(r-y)^2} \frac{\partial v_y}{\partial x} - \frac{1}{r-y} \frac{\partial v_x}{\partial y} - \frac{v_x}{(r-y)^2} \right] \\
&\frac{\partial v_y}{\partial t} + \frac{r}{r-y} u \frac{\partial v_y}{\partial x} + \frac{2}{r-y} u v_x = -\frac{1}{\rho} \frac{\partial p^*}{\partial y} + \\
&+ \nu \left[\left(\frac{r}{r-y}\right)^2 \frac{\partial^2 v_y}{\partial x^2} + \frac{\partial^2 v_y}{\partial y^2} + \frac{\partial^2 v_y}{\partial z^2} + \right. \\
&\left. + \frac{2r}{(r-y)^2} \frac{\partial v_x}{\partial x} - \frac{1}{r-y} \frac{\partial v_y}{\partial y} - \frac{v_y}{(r-y)^2} \right]; \\
&\frac{\partial v_z}{\partial t} + \frac{r}{r-y} u \frac{\partial v_z}{\partial x} = -\frac{1}{\rho} \frac{\partial p^*}{\partial z} + \\
&+ \nu \left[\left(\frac{r}{r-y}\right)^2 \frac{\partial^2 v_z}{\partial x^2} + \frac{\partial^2 v_z}{\partial y^2} + \frac{\partial^2 v_z}{\partial z^2} - \frac{1}{r-y} \frac{\partial v_z}{\partial y} \right]; \\
&\frac{r}{r-y} \frac{\partial v_x}{\partial x} + \frac{\partial v_y}{\partial y} + \frac{\partial v_z}{\partial z} - \frac{v_y}{r-y} = 0.
\end{aligned}
\right\}
\tag{I.25}
$$

The system (I.25) will be used to study the behavior of disturbances inside the boundary layer, that is, for $y/\delta \leq 1$. For bodies shaped like a ship, wings and aircraft in practice the following expression is always valid

$$
\frac{\delta}{r} \ll 1.
\tag{I.26}
$$

Considering (I.26) and the preceding inequality, let us neglect the value of y in the difference r − y. Then we obtain the following system of equations:

$$
\left.
\begin{aligned}
&\frac{\partial v_x}{\partial t} + u \frac{\partial v_x}{\partial x} + v_y \frac{\partial u}{\partial y} - \frac{1}{r} u v_y = -\frac{1}{\rho} \frac{\partial p^*}{\partial x} + \\
&+ \nu \left[\frac{\partial^2 v_x}{\partial x^2} + \frac{\partial^2 v_x}{\partial y^2} + \frac{\partial^2 v_x}{\partial z^2} - \frac{2}{r} \frac{\partial v_y}{\partial x} - \frac{1}{r} \frac{\partial v_x}{\partial y} - \frac{v_x}{r^2} \right]; \\
&\frac{\partial v_y}{\partial t} + u \frac{\partial v_y}{\partial x} + \frac{2}{r} u v_x = -\frac{1}{\rho} \frac{\partial p^*}{\partial y} + \\
&+ \nu \left[\frac{\partial^2 v_y}{\partial x^2} + \frac{\partial^2 v_y}{\partial y^2} + \frac{\partial^2 v_y}{\partial z^2} + \frac{2}{r} \frac{\partial v_x}{\partial x} - \frac{1}{r} \frac{\partial v_y}{\partial y} - \frac{v_y}{r^2} \right]; \\
&\frac{\partial v_z}{\partial t} + u \frac{\partial v_z}{\partial x} = -\frac{1}{\rho} \frac{\partial p^*}{\partial z} + \nu \left[\frac{\partial^2 v_z}{\partial x^2} + \frac{\partial^2 v_z}{\partial y^2} + \right. \\
&\left. + \frac{\partial^2 v_z}{\partial z^2} - \frac{1}{r} \frac{\partial v_z}{\partial y} \right]; \\
&\frac{\partial v_x}{\partial x} + \frac{\partial v_y}{\partial y} + \frac{\partial v_z}{\partial z} - \frac{v_y}{r} = 0.
\end{aligned}
\right\}
\tag{I.27}
$$

If $r \to \infty$ in (I.27), then the ordinary [12] system of equations of disturbing motion of a viscous fluid is obtained.

$$\frac{\partial v_x}{\partial t} + u\frac{\partial v_x}{\partial x} + v_y\frac{\partial u}{\partial y} = -\frac{1}{\rho}\frac{\partial p^*}{\partial x} + \nu\Delta v_x;$$

$$\frac{\partial v_y}{\partial t} + u\frac{\partial v_y}{\partial x} = -\frac{1}{\rho}\frac{\partial p^*}{\partial y} + \nu\Delta v_y;$$

$$\frac{\partial v_z}{\partial t} + u\frac{\partial v_z}{\partial x} = -\frac{1}{\rho}\frac{\partial p^*}{\partial z} + \nu\Delta v_z;$$

$$\frac{\partial v_x}{\partial x} + \frac{\partial v_y}{\partial y} + \frac{\partial v_z}{\partial z} = 0.$$

(I.28)

Goertler Instability in a Boundary Layer. The general solutions of systems (I.27)
and (I.28) under boundary conditions corresponding to the case of a boundary layer
are unknown at the present time. Researchers have been forced to consider the de-
fined forms of disturbing motion, selecting their form considering the equations of
motion. Here, being given the form of the velocities of the disturbing motion as a
function of three variables (usually x, z, t) the system of partial differential
equations was reduced to a system of ordinary differential equations, the solution
of which has been investigated. The special position of the variable y is connected
with essential dependence of the main flow characteristics on the transverse coordi-
nate. It is possible to indicate two basic forms of disturbing motion. The first
corresponds to giving small harmonic oscillations of the type of traveling waves in
the boundary layer

$$v_x = \hat{v}_x(y)\exp(iax + ibz - iact);$$

$$v_y = \hat{v}_y(y)\exp(iax + ibz - iact);$$

$$v_z = \hat{v}_z(y)\exp(iax + ibz - iact);$$

$$p^* = \hat{p}^*(y)\exp(iax + ibz - iact).$$

(I.29)

The sign of the imaginary part of the complex variable c in (I.29) permits us to
judge the increase or decrease in disturbances with time. When studying the behavior
of the second type of disturbances, the latter are given in the form of vortices with
axes along the flow

$$v_x = \hat{v}_x(y)\cos(az)e^{\beta t};$$

$$v_y = \hat{v}_y(y)\cos(az)e^{\beta t};$$

$$v_z = \hat{v}_z(y)\sin(az)e^{\beta t};$$

$$p^* = \hat{p}^*(y)\cos(az)e^{\beta t}.$$

(I.30)

The sign of the real exponent β in (I.30) defines the variation of the disturbances
in time. Relations (I.29) and (I.30) in which the variables x and t change places
can serve as a variation of the disturbing motion. In this case the development of
disturbances is investigated not in time, but downstream. If on the basis of the
equations of motion and boundary conditions the disturbances increase with an in-
crease in the x-coordinate, the motion is considered unstable; otherwise it is con-
sidered stable.

For the existence of disturbances of the type of (I.30) in the boundary layer, the
presence of a dynamic situation in which additional centrifugal forces of inertia
and the corresponding transverse pressure gradients arise (the second equation of
the system (I.27)) is necessary. These conditions occur, in particular, for flow
over a concave surface. If the wall is flat or convex, which in the majority of
cases is of the greatest interest, the vortex instability does not arise (see below).

Then disturbances of the type of (I.29) are considered which theoretically can exist both on convex and concave surfaces. Therefore they play a very important role in the theory of hydrodynamic stability of the boundary layer, a consequence of which is their detailed investigation in the following sections.

However, recently Goertler, et al. investigated some important aspects of the application of vortex theory which makes a brief discussion of its basic results necessary. When investigating the Goertler method we shall begin with the system of equations (I.27). Let us exclude pressure from the equations of motion and substitute the expressions for the velocities of the disturbing motion (I.30). Here we consider that the pressure of the disturbing motion does not depend on the x coordinate. In addition, in equations (I.27) we neglect values on the order of $1/r$. Since the thickness of the boundary layer δ is usually selected as the characteristic dimension, the corresponding errors will be on the order of $\delta/r \ll 1$. The term $(2/r)u \cdot v_x$ in the second equation of (I.27), constitutes an exception. It cannot be dropped, because the inertial forces are determined only by it for neutral disturbances ($\beta = 0$). For the case of neutral disturbances we find the following system of ordinary differential equations with respect to $\hat{v}_x(u)$, $\hat{v}_y(y)$, $\hat{v}_z(y)$:

$$\hat{v}_x'' - a^2\hat{v}_x = \frac{1}{\nu}u'\hat{v}_y;$$

$$\hat{v}_y^{IV} - 2a^2\hat{v}_y'' + a^4\hat{v}_y = -\frac{2}{r}u\hat{v}_x a^2\frac{1}{\nu};$$

$$\hat{v}_z = -\frac{1}{a}\hat{v}_y'.$$

(I.31)

Let us take the thickness of the boundary layer δ as the characteristic linear dimension and the velocity at the boundary of the boundary layer U_0 as the characteristic velocity. Then it is possible to write (I.31) in dimensionless form, using the notation

$$\alpha = a\delta; \quad Re_\delta = \frac{U_0\delta}{\nu},$$

and for convenience, omitting the circumflexes

$$v_x'' - \alpha^2 v_x = Re_\delta u' v_y;$$

$$v_y^{IV} - 2\alpha^2 v_y'' + \alpha^4 v_y = -2\frac{\delta}{r}uv_x\alpha^2 Re_\delta;$$

$$v_z = -\frac{1}{\alpha}v_y'.$$

(I.32)

The boundary conditions for the system (I.32) are determined from the assumption of equality of the disturbing motion velocity components on the wall to zero

$$v_x(0) = v_y(0) = v_y'(0) = 0.$$

(I.33)

In addition, the requirement of disappearance of the disturbing motion for $y \to \infty$ is imposed.

The system (I.32) with boundary conditions (I.33) was first obtained and investigated by Goertler[40], [41]. Later the following authors studied the solution of the investigated problem: Meksyn [42], Haemmerlin [43], [46], Prima [44], and Smith [45]. The last two researchers used the Galerkin method for approximate integration of the

system (I.32). A detailed discussion of the method and corresponding bibliography can be found in the monograph by Mikhlin [47]. Various problems of the application of the Galerkin method to the problems of hydrodynamic stability are contained in references [48]-[53], [81].

For explanation of the further course of the investigation of boundary layer stability in the presence of vortex disturbances, let us consider the solution of the problem (I.32)-(I.33) by the Galerkin method. The studies by Goertler [40], [41] demonstrated that the stability characteristics of a laminar bounary layer with respect to the investigated disturbances depend very slightly on the form of the velocity profile. Therefore, according to Prima, we consider

$$u = y; \ (0 \leqslant y \leqslant 1);$$
$$u = 1; \ (y \geqslant 1).$$

Proceeding according to the general scheme of the Galerkin method [47], let us select the following system of coordinate functions

$$f_k(y) = e^{-\nu} y^k \ (k = 1, 2 \ldots),$$

satisfying the boundary conditions of the problem. Limiting ourselves to the first terms of the series, we find the solution of the system (I.32) in the following form:

$$\begin{cases} v_{x_1} = e^{-\nu}(Ay + \ldots); \\ v_{y_1} = e^{-\nu}(By^2 + \ldots). \end{cases} \tag{I.34}$$

Let us transfer all the terms of the first two equations (I.32) to the left-hand side and denote them by $L_1(v_x, v_y)$, $L_2(v_x, v_y)$. The constant coefficients A, B in (I.34) will be selected from the conditions:

$$\begin{cases} \int_0^1 L_1(v_{x_1}, v_{y_1}) f_1(y) dy = 0; \\ \int_0^1 L_2(v_{x_1}, v_{y_1}) f_1(y) dy = 0. \end{cases} \tag{I.35}$$

Let us expand the relations (I.35):

$$\int_0^1 [A(y-2) - \alpha^2 Ay - \mathrm{Re}_\delta By^2] y e^{-2\nu} dy = 0$$

$$\int_0^1 \left[B(12 - 8y + y^2) - 2\alpha^2 B(2 - 4y + y^2) + \right.$$
$$\left. + \alpha^4 By^2 + 2\frac{\delta}{r} \alpha^2 \mathrm{Re}_\delta Ay^2 \right] y e^{-2\nu} dy = 0$$

$$\left.\begin{array}{l} \left| (1-\alpha^2)\left\{ \int_0^1 y^2 e^{-2y}\,dy - 2 \int_0^1 y e^{-2y}\,dy \right\} - B \operatorname{Re}_\delta \int_0^1 y^2 e^{-2y}\,dy = 0 \right. \\ A 2\dfrac{\delta}{r}\alpha^2 \operatorname{Re}_\delta \int_0^1 y^2 e^{-2y}\,dy + B\left[(1-2\alpha^2-\alpha^4)\int_0^1 y^2 e^{-2y}\,dy + \right. \\ \left. + 8(\alpha^2-1)\int_0^1 y^2 e^{-2y}\,dy + (12-4\alpha^2)\int_0^1 y e^{-2y}\,dy \right] = 0. \end{array}\right\}$$

Let us calculate the integrals sucessively:

$$\int_0^1 y e^{-2y}\,dy = -\frac{1}{2}y e^{-2y}\Big|_0^1 + \frac{1}{2}\int_0^1 e^{-2y}\,dy = 0.148499;$$

$$\int_0^1 y^2 e^{-2y}\,dy = -\frac{1}{2}y^2 e^{-2y}\Big|_0^1 + \int_0^1 y e^{-2y}\,dy = 0.080836$$

$$\int_0^1 y^3 e^{-2y}\,dy = -\frac{1}{2}y^3 e^{-2y}\Big|_0^1 + \frac{3}{2}\int_0^1 y^2 e^{-2y}\,dy$$

The preceding system of equations assumes the form:

$$\left.\begin{array}{l} (0{,}215 + 0{,}081\alpha^2)A + \operatorname{Re}_\delta 0{,}054B = 0; \\ \dfrac{\delta}{r}\alpha^2 \operatorname{Re}_\delta 0{,}107A + (1{,}181 - 0{,}051\alpha^2 + 0{,}536\alpha^4)B = 0. \end{array}\right\} \qquad (I.36)$$

In order that the system of equations (I.36) have nonzero solutions with respect to the constants A, B, satisfaction of the following equality is necessary and sufficient

$$\begin{vmatrix} 0{,}215 + 0{,}081\alpha^2 & 0{,}054\operatorname{Re}_\delta \\ \dfrac{\delta}{r}\alpha^2 \operatorname{Re}_\delta 0{,}107 & 1{,}181 - 0{,}051\alpha^2 + 0{,}536\alpha^4 \end{vmatrix} = 0. \qquad (I.37)$$

Thus, for neutral Goertler disturbances, the Reynolds number and parameter α characterizing the periodicity of the disturbances in the direction of the z-axis are related by the expression (I.37) which can be rewritten as follows:

$$\frac{\delta}{r}\operatorname{Re}_\delta^2 = \frac{(0{,}215 + 0{,}081\alpha^2)(1{,}181 - 0{,}051\alpha^2 + 0{,}536\alpha^4)}{0{,}0058\alpha^2}. \qquad (I.38)$$

The right-hand side of (I.38) is positive for all real values of α. Consequently, for a flat wall where the left-hand side of (I.38) is equal to zero or for a convex wall where it is less than zero, equality (I.38), which means also (I.37), will not be satisfied, that is, in the investigated approximation the vortex disturbances do not exist. For a concave wall it is possible to use (I.38) to construct a neutral curve in the plane $[(\delta/r)\cdot\operatorname{Re}_\delta^2, \alpha]$ separating the region of stability from the region of instability. By the region of stability here we mean the set of [one word illegible] parameters α and $(\delta/r)\cdot\operatorname{Re}_\delta^2$ for which the vortex disturbances damp. Usually

it is accepted to construct the curve of neutral disturbances on the axes [α**, Re** √δ**/r]. The values of α** [passage illegible] in the series (I.34) of two terms, Smith performed the calculations by the Galerkin method on the basis of six-term polynomials. Thus, by comparing curves I, II and III in Figure I.7 it is possible to establish convergence of the Galerkin method in the sense of determining the neutral stability curve to the exact Haemmerlin solution (curve IV). Strict proof of the convergence of this method as applied to problem (I.32)-(I.33) obviously is unavailable at the present time.
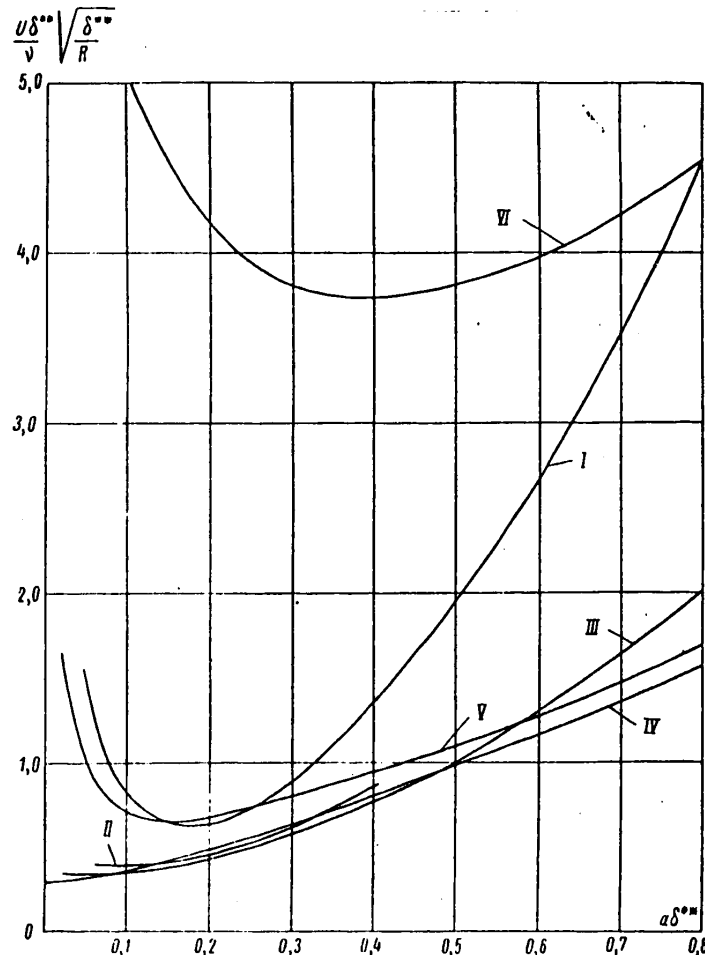
Figure I.7. Neutral stability curves for vortex disturbances. I — calculation by formula (I.38); II — Prima calculation; III — Smith calculation; IV — Haemmerlin calculation; V — Goertler calculation; VI — Maksyn calculation.

The regions of stability in Figure I.7 are below the corresponding neutral curves, and the regions of instability, above.

31
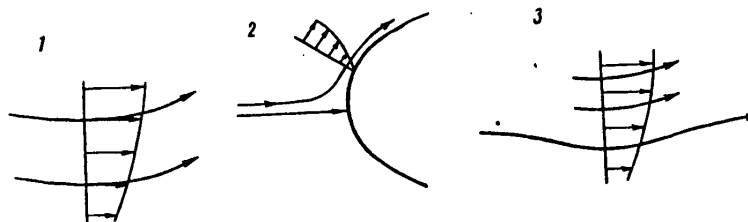
Figure I.8. Possible cases of the occurrence of Goertler vortexes.
1 — flow near a concave wall; 2 — flow in the vicinity of the
critical point; 3 — flow with wave current lines,

The instability of laminar flows with respect to vortex disturbances can be observed
not necessarily only near concave surfaces (Figure I.8). The studies by Goertler
[54] and Haemmerlin [55] detected an analogous picture of loss of stability for a
flow in the vicinity of the critical point. Significantly before the indicated
theoretical solutions, the fact of loss of stability of a flow near the frontal
point of a cylinder over which flow was taking place was established experimentally
by Piercy and Richardson [56], [57]. The noted fact of loss of stability of the
laminar form of flow in the vicinity of the critical point can have practical sig-
nificance, for the arbitray vortices formed in the flow can play the role of exter-
nal disturbances (turbulence of the external flow) the intensity of which essentially
determines the critical Reynolds number (see Chapter V). Accordingly, it is neces-
sary to recommend that the forward end of bodies with controlled boundary layer
(control for purposes of laminarization) be made with as little fullness as possible
so that the region of undesirable distortion of the current lines will be least.
The vortices with longitudinal axes can also arise in the boundary layer developed
on a plane or convex surface as a result of the appearance of the appearance of
wave disturbances of the type of (I.29). The studies of Goertler and Witting [58]
demonstrated that if the oscillation amplitude of the fluid particles in the bound-
ary layer reaches a value on the order of $1 \cdot 10^{-4} \delta*$, conditions are created for the
occurrence of a "secondary instability" connected with vortices of the type of
(I.30). The importance of the indicated result in connection with the creation of
the general theory of transition is obvious [59], [60]. In addition, it is possible
to expect that for unavoidable vibration of the skin of real bodies moving in the
water, the Goertler instability will have defined significance.

A list of basic papers studying vortex instability can be found in the surveys by
Goertler [61], [62], [63].

Energy Method of Investigating Instability. In addition to the above-discussed method
of small disturbances based on studying the behavior of a defined form of velocity
fluctuations in the boundary layer with the help of linearized equations cf motion,
there is the so-called energy method of investigating the stability of the laminar
form of flow [64], [66]. Its essence consists in the fact that the behavior of the
kinetic energy of the disturbing motion in time is investigated. If the kinetic
energy at any selected point in time is increasing, the motion is considered un-
stable; if it is decreasing, the laminar flow conditions are defined as stable.
The sign of the derivative of the kinetic energy of the disturbance with respect to
time is investigated using the relation obtained from the equations of disturbed

motion [32], [29]. It is natural that it is impossible to define all the values of v_x, v_y, p entering into one equation (the two-dimensional case) by using only one equation and the corresponding boundary under initial conditions. Therefore it is necessary to give the form of the disturbances. For the case of elliptic vortices proposed by Lorentz [64], detailed calculations appear in the monograph [29].

Let us discuss some of the assumptions used as the basis for deriving the energy balance equation of disturbing motion

$$\frac{d_1}{dt} \iint\limits_{(S)} \frac{1}{2} \rho \left(v_x^2 + v_y^2\right) dx\, dy = \varrho \iint\limits_{(S)} \left(- v_x v_y\right) \times$$
$$\times \frac{\partial u}{\partial y} dx\, dy - 4\mu \iint\limits_{(S)} \left(\frac{\partial v_y}{\partial x} - \frac{\partial v_x}{\partial y}\right)^2 dx\, dy. \qquad (I.39)$$

In equality (I.39) the basic motion is characterized by the presence of only velocity along the x-axis u = u(y); the velocity along the y-axis is absent (v = 0).

The derivative of the kinetic energy of a fluid with respect to time entering into (I.39) is calculated as follows:

$$\frac{d_1 T}{dt} = \frac{\partial T}{\partial t} + u \frac{\partial T}{\partial x}, \qquad (I.40)$$

that is, it is assumed that the fluid particles are transported only with the velocity of the main flow. This proposition appears to be sufficiently strong, for near the wall the velocity of the main flow in the boundary layer can be commensurate with the velocities of the disturbances. Writing the derivative in the form of (I.40) is actually equivalent to the condition of smallness of the disturbances.

Let us obtain the energy balance equation analogous to (I.39) using arguments free of the indicated assumption. Let us begin with the equation of motion of a viscous fluid written in vector form in the absence of mass forces

$$\frac{d\vec{V}}{dt} = - \frac{1}{\rho}\ \text{grad}\ p + \nu \Delta \vec{V}.$$
$$\text{div}\ \vec{V} = 0 \qquad (I.41)$$

Scalar-multiplying the first equation of system (I.41) by $\vec{V}$, we obtain the expression characterizing the variation of the kinetic energy of a fluid particle of unit mass

$$\vec{V} \frac{d\vec{V}}{dt} = - \frac{1}{\rho} \vec{V}\ \text{grad}\ p + \nu \vec{V} \Delta \vec{V}. \qquad (I.42)$$

If

$$\vec{V} = \vec{V}_0 + \vec{v},\ p = p_0 + p_1,$$

where $\vec{V}_0$, p_0 are the velocity and pressure of the basic flow;

$\vec{v}$, p_1 are the velocity and pressure of the disturbing motion of the fluid,

then the following equality obtained from (I.42) is valid:

33

$$(\vec{V}_0 + \vec{v})\frac{d(\vec{V}_0 + \vec{v})}{dt} = -\frac{1}{\rho}(\vec{V}_0 + \vec{v})\,\text{grad}\,(p_0 + p_1) +$$

$$+ \nu(\vec{V}_0 + \vec{v})\Delta(\vec{V}_0 + \vec{v}). \tag{I.43}$$

Equation (I.43) defines the variation of the kinetic energy of a fluid particle in disturbed motion. Since the basic motion ($\vec{V}_0$, p_0) satisfies (I.42), using (I.43) we find the expression demonstrating how the kinetic energy of a particle varies as a result of the presence of disturbing motion

$$\vec{V}_0\frac{d\vec{v}}{dt} + \vec{v}\frac{d\vec{V}_0}{dt} + \vec{v}\frac{d\vec{v}}{dt} = -\frac{1}{\rho}\vec{V}_0\,\text{grad}\,p_1 -$$

$$-\frac{1}{\rho}\vec{v}\,\text{grad}\,(p_0 + p_1) + \nu(\vec{V}_0\Delta\vec{v} + \vec{v}\Delta\vec{V}_0 + \vec{v}\Delta\vec{v}). \tag{I.44}$$

We shall consider that in the boundary layer grad $p_0 = 0$. Then for the two-dimensional case of motion from (I.44) we find

$$u\left[\frac{\partial v_x}{\partial t} + (u + v_x)\frac{\partial v_x}{\partial x} + (v + v_y)\frac{\partial v_x}{\partial y}\right] +$$

$$+ v\left[\frac{\partial v_y}{\partial t} + (u + v_x)\frac{\partial v_y}{\partial x} + (v + v_y)\frac{\partial v_y}{\partial y}\right] + v_x\left[(u + v_x)\frac{\partial u}{\partial x} + \right.$$

$$\left. + (v + v_y)\frac{\partial u}{\partial y}\right] + v_y\left[(u + v_x)\frac{\partial v}{\partial x} + (v + v_y)\frac{\partial v}{\partial y}\right] +$$

$$+ \frac{d\left(\frac{v_x^2 + v_y^2}{2}\right)}{dt} = -\frac{1}{\rho}\left(u\frac{\partial p_1}{\partial x} + v\frac{\partial p_1}{\partial y} + v_x\frac{\partial p_1}{\partial x} + v_y\frac{\partial p_1}{\partial y}\right) +$$

$$+ \nu(u\Delta v_x + v\Delta v_y + v_x\Delta u + v_y\Delta v + v_x\Delta v_x + v_y\Delta v_y). \tag{I.45}$$

The total derivative with respect to time in (I.45) is calculated according to the formula

$$\frac{d}{dt} = \frac{\partial}{\partial t} + (u + v_x)\frac{\partial}{\partial x} + (v + v_y)\frac{\partial}{\partial y}.$$

In the case of neutral disturbances, which is of the greatest interest, the process of variation of the velocity field is of a periodic nature. Therefore after averaging for the period, the terms of equation (I.45) which are linear with respect to velocities and pressures of the disturbing motion decrease, which allows consideration of the following simplified expression

$$\frac{d\left(\frac{v_x^2 + v_y^2}{2}\right)}{dt} = -\left[uv_x\frac{\partial v_x}{\partial x} + uv_y\frac{\partial v_x}{\partial y} + vv_x\frac{\partial v_y}{\partial x} + \right.$$

$$\left. + vv_y\frac{\partial v_y}{\partial y} + v_x^2\frac{\partial u}{\partial x} + v_xv_y\frac{\partial u}{\partial y} + v_xv_y\frac{\partial v}{\partial x} + v_y^2\frac{\partial v}{\partial y}\right] -$$

$$- \frac{1}{\rho}\left(v_x\frac{\partial p_1}{\partial x} + v_y\frac{\partial p_1}{\partial y}\right) + \nu(v_x\Delta v_x + v_y\Delta v_y). \tag{I.46}$$

34

Let us transform the series of terms entering into the right-hand side of (I.46) considering the continuity equation:

$$u \left(v_x \frac{\partial v_x}{\partial x} + v_y \frac{\partial v_x}{\partial y} \right) = u \left[\frac{\partial (v_x v_x)}{\partial x} + \frac{\partial (v_x v_y)}{\partial y} \right]; \tag{I.47}$$

$$v \left(v_x \frac{\partial v_y}{\partial x} + v_y \frac{\partial v_y}{\partial y} \right) = v \left[\frac{\partial (v_x v_y)}{\partial x} + \frac{\partial (v_y v_y)}{\partial y} \right]; \tag{I.48}$$

$$v_x \frac{\partial p_1}{\partial x} + v_y \frac{\partial p_1}{\partial y} = \frac{\partial (v_x p_1)}{\partial x} + \frac{\partial (v_y p_1)}{\partial y}; \tag{I.49}$$

$$v_x \Delta v_x + v_y \Delta v_y = 2 \left(v_y \frac{\partial \xi}{\partial x} - v_x \frac{\partial \xi}{\partial y} \right) = 2 \left(\frac{\partial v_y \xi}{\partial x} - \frac{\partial v_x \xi}{\partial y} - \xi \frac{\partial v_y}{\partial x} + \xi \frac{\partial v_x}{\partial y} \right) = 2 \left(\frac{\partial v_y \xi}{\partial x} - \frac{\partial v_x \xi}{\partial y} \right) - 4 \xi^2, \tag{I.50}$$

where

$$\xi = \frac{1}{2} \left(\frac{\partial v_y}{\partial x} - \frac{\partial v_x}{\partial y} \right).$$

Let us integrate both sides of equality (I.46) with respect to the so-called "basic rectangular S." Its boundaries are selected from the following arguments. The boundaries are selected by the variable y so that for $y = y_1$, $y = y_2$, the velocities of the disturbing motion will be absent. The boundaries are selected by the variable x in such a way that the velocity field of the disturbing motion for $x = x_1$ and $x = x_2$ will be entirely identical. With this type of integration, the terms (I.47)- (I.49) give zero, and from the term (I.50) only the integral of the square of the vortex remains. Actually,

$$\int_{x_1}^{x_2} \int_{y_1}^{y_2} \left[\frac{\partial (v_x v_x)}{\partial x} + \frac{\partial (v_x v_y)}{\partial y} \right] dx \, dy =$$

$$= \int_{y_1}^{y_2} (v_x v_x) \Big|_{x_1}^{x_2} dy + \int_{x_1}^{x_2} (v_x v_y) \Big|_{y_1}^{y_2} dx = 0.$$

Integration of the remaining terms is carried out analogously. As a result, we obtain the following equality:

$$\frac{d}{dt} \iint_{(S)} \frac{v_x^2 + v_y^2}{2} dx \, dy = - \iint_{(S)} \left[v_x^2 \frac{\partial u}{\partial x} + v_x v_y \times \right.$$

$$\left. \times \left(\frac{\partial u}{\partial y} + \frac{\partial v}{\partial x} \right) + v_y^2 \frac{\partial v}{\partial y} \right] dx \, dy - 4 v \iint_{(S)} \xi^2 dx \, dy. \tag{I.51}$$

Removal of the differentiation sign with respect to time outside the integral is possible, for the integration limits are constants, and the function under the integral sign depends continuously on time together with its derivatives [65].

Denoting $\Delta t = t_1 - t_0$

$$\iint_{(S)} \frac{v_x^2 + v_y^2}{2} dx \, dy = T,$$

let us perform the time averaging of both parts of equality (I.51) for the interval $\Delta t = t_1 - t_0$

35

$$\frac{T_{t_1} - T_{t_0}}{\Delta t} = - \iint_{(S)} \left[\overline{v_x^2} \frac{\partial u}{\partial x} + \overline{v_x v_y} \left(\frac{\partial u}{\partial y} + \frac{\partial v}{\partial x} \right) + \right.$$

$$\left. + \overline{v_y^2} \frac{\partial v}{\partial y} \right] dx\, dy - 4\nu \iint_{(S)} \overline{\xi^2}\, dx\, dy. \tag{I.52}$$

Averaging under the integral sign in the investigated case is possible [65] for the above-indicated reasons. If we consider that $\overline{v_x^2} \approx \overline{v_y^2}$, then

$$\overline{v_x^2} \frac{\partial u}{\partial x} + \overline{v_y^2} \frac{\partial v}{\partial y} \approx \overline{v_x^2} \left(\frac{\partial u}{\partial x} + \frac{\partial v}{\partial y} \right) = 0,$$

a corollary of which is the following equation obtained from (I.52):

$$\frac{T_{t_1} - T_{t_0}}{\Delta t} = - \iint_{(S)} \overline{v_x v_y} \left(\frac{\partial u}{\partial y} + \frac{\partial v}{\partial x} \right) dx\, dy - 4\nu \iint_{(S)} \overline{\xi^2}\, dx\, dy. \tag{I.53}$$

Equality (I.53) can also be obtained, assuming that u = u(y), and v = v(x). Absence of dependence of the transverse velocity component in the boundary layer on y occurs, for example, in the case of an asymptotic laminar boundary layer with suction.
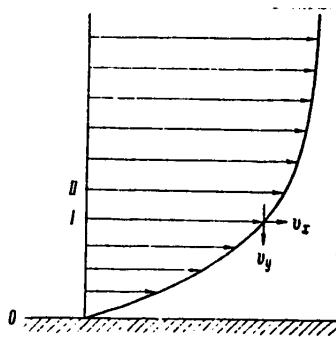
Figure I.9. Diagram of the occurrence of Reynolds stresses.

Investigation of expression (I.53) is useful for understanding the physical nature of the processes occurring in a laminar boundary layer on appearance of random disturbances in it. Actually, let us first consider the second term in the right-hand side. It is always positive and enters with the sign of the minimum, i.e., it promotes a decrease in the kinetic energy of the disturbing motion by converting it to heat. This process is naturally determined by the fluid viscosity. The first term of the right-hand side of the indicated equality characterizes the work of the so-called "Reynolds stress" $-\overline{\rho v_x v_y}$, which can transfer the energy from the basic motion to disturbances. In order that the kinetic energy of the disturbance increase, it is necessary in the simplest case where $\partial v / \partial x = 0$ that the signs of the Reynolds stress $(-\overline{\rho v_x v_y})$ and the velocity gradient of the basic flow $\partial u / \partial y$ compare. Let us explain this fact by the following schematic argument (Figure I.9). Let us assume that at the initial point in time there is no disturbance in the velocity profile of the laminar boundary layer. Then, at the next point in time for some reason the nature

of which is not significant in the given argument, a longitudinal velocity disturbance v_x appears in the fluid layer I. Let the coordinate of the point of appearance of the disturbance reckoned along the wall be x_0. Since for $x < x_0$ there is no disturbance, it is always possible to select the point x_0 so that $\left(\frac{\partial v_x}{\partial x}\right)_{x=x_0} > 0$.

This possibility is determined by continuous dependence of the velocity field in the fluid on the spatial coordinates. However, as soon as the derivative $\partial v_x/\partial x > 0$ appears at a point of the layer I with the coordinate x_0, in accordance with the continuity equation the derivative $\partial v_y/\partial y < 0$ appears at the same point, that is, fluid flow arises with velocity $(-v_y)$ from layer II to layer I. For positive velocity gradient of the basic flow $\partial u/\partial y > 0$, the fluid particles moving from layer II will have velocity in the direction of the main current greater than the fluid particle in the layer I, that is, they will promote an increase in the occurring disturbance v_x at the point of the layer I with the coordinate x_0. Here an increase in the disturbance will take place as a result of the kinetic energy of the main flow. It is obvious that the sign of the Reynolds stress $(-\rho v_x v_y)$ will be positive in the investigated case.

In Figure I.9, the velocities of the disturbing flow are illustrated for clarity in the right-hand side of the basic flow velocity diagram. In conclusion of the presented argument it is necessary again to consider the important role which is played by the property of continuity of the medium in the process of development of the disturbances expressed by the continuity equation.

If the equation (I.53) is written in dimensionless form, taking, for example, the thickness of the boundary layer δ as the characteristic thickness and the velocity at the boundary of the boundary layer u_0 as the characteristic velocity, then equating the right-hand side of (I.53) to zero, it is possible to determine the critical Reynolds number defining the existence of neutral disturbances, the kinetic energy of which does not vary in the time interval Δt

$$Re_\delta = \frac{\iint\limits_{(S)} \xi^2\, dx\, dy}{-\iint\limits_{(S)} \overline{v_x v_y} \left(\frac{\partial u}{\partial y} + \frac{\partial v}{\partial x}\right) dx\, dy}. \tag{I.54}$$

An actual calculation of the critical Reynolds number by formula (I.54) can be made for the known velocities of the disturbing motion. Functions defining the values of v_x, v_y must satisfy the equations of motion and continuity equation. For each form of disturbance, generally speaking, there will be a critical Reynolds number. The least critical Reynolds number out of the corresponding set for all-possible disturbances will define the boundary below which laminar motion will always exist, that is, all of the random disturbances entering the boundary layer will be damped.

Thus, one equation (I.54) is inadequate for determining the minimum critical Reynolds number for the boundary layer. It is also necessary to integrate the equations of motion for disturbances. If we consider any disturbances, not relating them to the equations of motion of a fluid, low Reynolds numbers are naturally obtained, for the region of possible disturbances increases sharply [12], [29].

Usually when investigating the work of the Reynolds stresses in the boundary layer, absence of a basic flow velocity normal to the surface v = 0 is assumed. For a boundary layer developed on an impermeable surface, this assumption is sufficiently substantiated. In the case of fluid suction across the surface, it is necessary to have a cautious attitude toward the indicated assumption. For example, for slot suction there are sections on the surface of the body where sharp variation of the basic flow velocity takes place in the direction of the y-axis. In these areas located in direct proximity to the slots, it is impossible obviously to neglect the derivative $\partial v/\partial x$ in the formula for the Reynolds stress

$$ -\rho \overline{v_x v_y} \left(\frac{\partial u}{\partial y} + \frac{\partial v}{\partial x} \right), $$

(I.55)

for, in spite of the small value of v, its variation near the wall takes place very rapidly. Formula (I.55) shows that the initial section of the slot has a favorable influence on the laminar boundary layer stability, for the turbulent Reynolds stress transferring the energy to the disturbance at the leading edge of the slot decreases as a result of the presence of $\partial v/\partial x < 0$. The trailing edge of the slot, conversely, has a negative influence on stability, for the presence of $\partial v/\partial x > 0$ increases the total Reynolds stress. The nature of the stress $-\rho v_x v_y \cdot \partial v/\partial x$ is exactly the same as $-\rho v_x v_y \cdot \partial u/\partial y$. The practical conclusion which can be drawn when investigating formula (I.55) is that from the point of view of increasing stability, the slot must be designed so that the normal suction velocity gradient in the direction of the x-axis on the trailing edge will be the least possible, and on the forward edge, the highest.

Of course, when selecting the form of the slot it is necessary also to consider the important requirement of least drag of the slot for the given fluid flow rate. In view of the necessity for solving the equations of disturbed motion to obtain a reliable value of the critical Reynolds number, in contrast to the small oscillation method, the energy method has not found significant practical development. Its basic value consists in the explanation of the physical aspects of the development and damping of disturbances in a boundary layer.

Surveys of research in laminar boundary layer stability can be found in references [4], [12], [67]-[73], [111], [112].

§ I.4. Small Oscillations Method. Orr-Sommerfeld Equation

In the linear statement of the problem, the velocity components of the disturbing motion must satisfy system (I.28). The basis for investigating small disturbances is the fact that it is always possible to assume conditions of development of the laminar form of flow such that the external random disturbances will not exceed a given value. The practical possibility of insuring such conditions is confirmed by experimental research (§ I.10) demonstrating very complete coincidence of the observed processes of development of disturbances in a laminar boundary layer with linear theory.

The problems of the behavior of finite disturbances in laminar flows are discussed in references [100]-[110]. However, the difficulties of studying a nonlinear system of partial differential equations describing the behavior of finite disturbances do not permit creation of a final theory of their development which, of course,

38

prevents understanding of the processes occurring between the loss of stability point and region of developed turbulent motion.

When deriving equations (I.28) it was assumed that the basic current satisfies the relations

$$u = u(y); \quad v = w = 0. \tag{I.56}$$

Condition (I.56) is strictly satisfied only for the Poiseuille flow which follows from the Navier-Stokes equations [29]. It is not valid for flow in the boundary layer. When studying laminar boundary layer stability, Pretsch [14] made an effort to consider the variation of u along the wall and also the presence of the velocity component v in the boundary layer. On the basis of the approximate nature of the methods of solving the problem of laminar flow stability in a boundary layer (see the following items) it turned out that the refinements of Pretsch are meaningless, for the corrections that he introduced are beyond the limits of the approximation in which the problem is solved.

The next simplifying assumption is two-dimensionality of the investigated disturbances. Here we base our arguments on the proof of Squire [74], [12], who demonstrated that two-dimensional disturbances of the traveling wave type are more dangerous in the sense of the occurrence of instability than three-dimensional ones. This problem was the subject of a paper by I. Tszya-Chun' [75]. It is possible to find interesting experimental confirmation of the discussed proposition in the paper by Schultz-Grunow [76]. Two-dimensional transverse oscillations corresponding to the points 1, 2, 3 in the vicinity of the neutral stability curve (Figure I.10) were also imposed on a two-dimensional laminar flow using an oscillating wing. The curve in Figure I.10 was constructed by the data of Tollmien [77]. Point 1 corresponds to the damping disturbances, and point 2 corresponds to mutual disturbances; point 3 corresponds to building disturbances. In addition to transverse disturbances longitudinal disturbances were created in the flow using individual roughness elements. Here it turned out that the presence of additional longitudinal disturbances was not felt at all at the beginning of loss of stability of the basic laminar flow (Figures I.11-I.13). In Figure I.11 it is obvious that longitudinal disturbances at point 1 damp, at point 2 (Figure I.12) they are of a steady nature, and at point 3 (Figure I.13) they build, that is, transverse planar disturbances for which the neutral curve is constructed (the method of construction is discussed in § I.7) are actually the most dangerous.

For two-dimensional disturbances system (I.28) is rewritten as

$$
\begin{aligned}
\frac{\partial v_x}{\partial t} + u\frac{\partial v_x}{\partial x} + v_y\frac{\partial u}{\partial y} &= -\frac{1}{\rho}\cdot\frac{\partial p^*}{\partial x} + \nu\Delta v_x; \\
\frac{\partial v_y}{\partial t} + u\frac{\partial v_y}{\partial x} &= -\frac{1}{\rho}\cdot\frac{\partial p^*}{\partial y} + \nu\Delta v_y; \\
\frac{\partial v_x}{\partial x} + \frac{\partial v_y}{\partial y} &= 0.
\end{aligned}
\tag{I.57}
$$
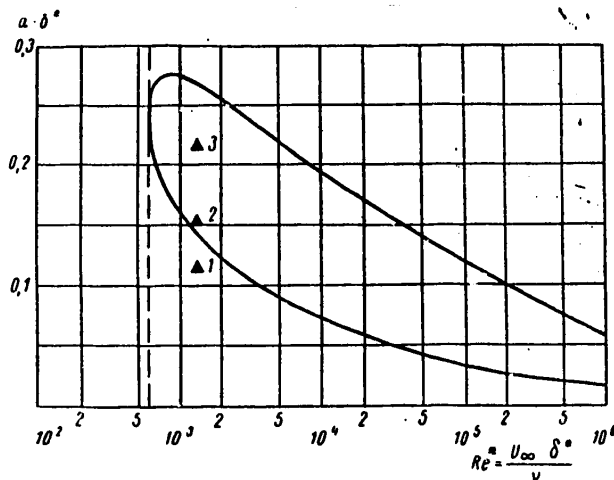
Figure I.10. Results of the Schultz-Grunow experiments.
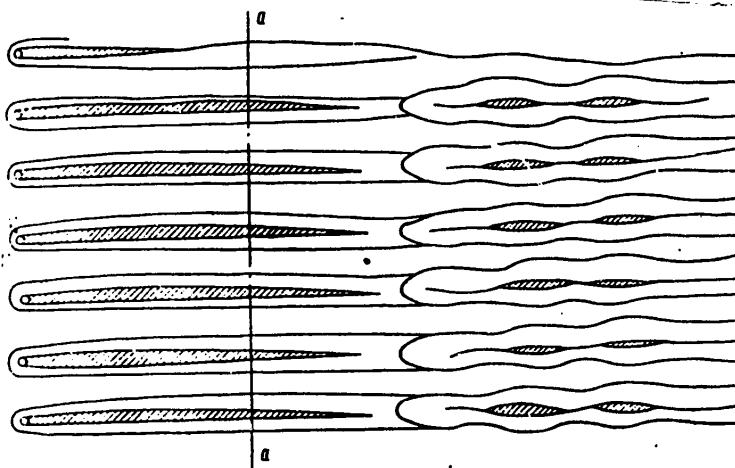
Figure I.11. Damping disturbance pattern. The axis of the oscillating wing was located along line a-a.

Using the coefficients of the linear system (I.57) as a function of only the y-coordinate, its solution is found in the form

$$v_x = \tilde{v}_x(y)\exp[i(ax-bt)];$$
$$v_y = \tilde{v}_y(y)\exp[i(ax-bt)].$$

(I.58)

The transition to a complex plane is convenient in the respect that being given complex values of the parameters a and b it is possible to obtain both oscillating and exponential solutions to system (I.57) with respect to the variables x and t. As the boundary conditions for equations (I.57) with respect to the variable x, the

40
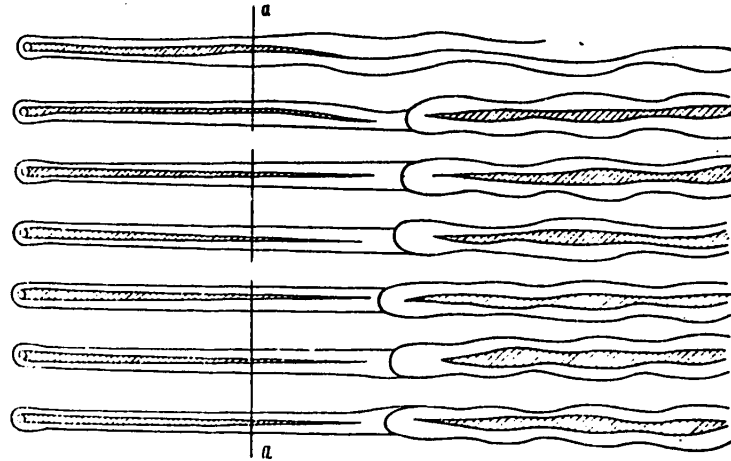
Figure I.12. Neutral disturbance pattern.

proposition of limited nature of the solution when x approaches both $+\infty$ and $-\infty$ is introduced [12], [78]. This leads to the conclusion that in expression (I.58) the parameter a must be a real value defining the wave length of the investigated disturbance $\lambda = 2\pi/a$. The parameter b can be complex. Its real part defines the propagation rate of the disturbance wave in the direction of reckoning the x-coordinate, and the imaginary part permits determination of the growth or damping of the disturbances with time. It is natural that only the real part of formulas (I.58) have physical meaning.
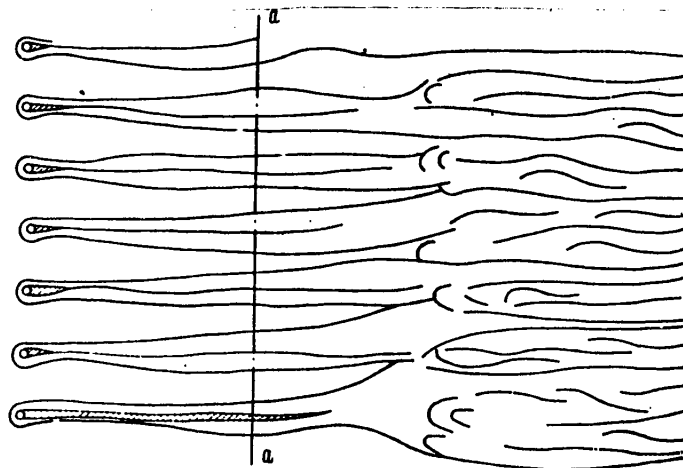
Figure I.13. Building disturbance pattern.

In the indicated formulation the problem has no initial conditions with respect to the variable t or boundary conditions with respect to the x-coordinate. It is

41

possible to find a formulation of the problem of hydrodynamic stability as a problem with initial data in references [78], [80], [116].

Excluding pressure from the first two equations of (I.57) and, on the basis of the continuity equation, introducing the current function

$$\varphi = \tilde{\varphi}(y)\exp[i(ax - bt)],$$

It is possible to obtain an ordinary fourth-order differential equation with respect to the amplitude of the current function $\tilde{\varphi}(y)$

$$\left(u - \frac{b}{a}\right)\left(\tilde{\varphi}'' - a^2\tilde{\varphi}\right) - u''\tilde{\varphi} = -\frac{i\nu}{a}\left(\tilde{\varphi}^{IV} - 2a^2\tilde{\varphi}'' + a^4\tilde{\varphi}\right),$$

which hereafter will be used in dimensionless form

$$(u - c)(\varphi'' - \alpha^2\varphi) - u''\varphi = -\frac{i}{\alpha Re}(\varphi^{IV} - 2\alpha^2\varphi'' + \alpha^4\varphi). \tag{I.59}$$

The velocity at the boundary of the boundary layer is taken as the characteristic velocity, and the thickness of the boundary layer, as the characteristic length.

The differential expression (I.59) is called [4], [12] the Orr-Sommerfeld equation [78]. It is the basis for studying the stability of laminar flows of the boundary layer type.

§ I.5. Boundary Conditions for the Orr-Sommerfeld Equation

When investigating stability of the laminar form of flow near a rigid surface it is natural to consider that adhesion conditions are observed on the wall, that is, for y = 0 both normal and tangential disturbance velocities are absent. Hence, two conditions on a rigid surface are found for the amplitude of the disturbing-motion current function

$$\varphi(0) = 0; \tag{I.60}$$
$$\varphi'(0) = 0. \tag{I.61}$$

Studying the stability of a laminar boundary layer, usually the concept of a boundary layer of finite thickness is used, considering that the effect of the fluid viscosity is felt only in the wall region bounded by dimensionless coordinate y = 1. Outside this region the influence of this viscosity both on the basic flow and on the development of the disturbances is neglected. In an ideal fluid, equation (I.59) is transformed to the simple form

$$\varphi'' - \alpha^2\varphi = 0, \tag{I.62}$$

for outside the boundary layer u"(y) = 0. It is easy to write the general solution of equation (I.62)

$$\varphi(y) = C_1 e^{\alpha y} + C_2 e^{-\alpha y}.$$

The parameter α characterizing the wavelength of a disturbing motion greater than zero, $\phi(y)$ must be limited for $y \to \infty$ on the basis of absence of disturbances far from the wall; therefore $c_1 = 0$. Imposing the requirement of continuity of transition to the solution for an ideal fluid at the boundary of the boundary layer with accuracy to the first derivative on the desired solution of equation (I.59), we arrive at the equalities

$$\varphi(1) = c_2 e^{-\alpha}; \quad \varphi'(1) = -c_2 \alpha e^{-\alpha},$$

on the basis of which [4], [12], the third uniform boundary condition is written for equation (I.59)

$$\alpha \varphi(1) + \varphi'(1) = 0. \tag{I.63}$$

A corollary of the limited nature of the solution for $y \to \infty$ is the fourth boundary condition

$$\varphi(y)|_{y \to \infty} < M < \infty. \tag{I.64}$$

§ I.6. Construction of Solutions of the Orr-Sommerfeld Equation

In the general case of giving the function $u(y)$ it is impossible to indicate exact solution of equation (I.59) under the boundary conditions (I.60), (I.61), (I.63), (I.64). Therefore various approximate methods of constructing partial solutions of the investigated equation are used. In (I.59) the coefficients are regular functions of the variable y in the interval $0 \le y \le 1$, that is, in the vicinity of any point y_0 from the indicated interval they can be expanded in converging series of the type

$$\sum_{k=0}^{\infty} a_k (y - y_0)^k, \text{ if } |y - y_0| < \rho_m,$$

where the values of $\rho_m > 0$ (the symbol m determines to which coefficient the given convergence radius pertains). Consequently [82], in this interval it is possible to find the solution of equation (I.59) in the form of a series with respect to powers of an independent variable. If series for four independent solutions of equation (I.59) can be constructed such that they will converge uniformly in the region of definition of y, the existence of the fundamental system of solutions of equation (I.59) will be proved at the same time. In view of the fact that the coefficients in (I.59) are also regular functions of certain parameters (α, c, 1/αRe), using smallness of some of them (c, 1/αRe) it is possible to construct solutions in the form of series with respect to powers of these parameters. Heisenberg [83] and Lin [67], who investigated the given method in detail proceeded in this fashion in their research.

Considering that the boundary layer stability is lost for large Re numbers, it is possible to find the solution of equation (I.59) in the form of the series

$$\varphi(y) = \varphi_0(y) + \frac{1}{\alpha Re} \cdot \varphi_1(y) + \left(\frac{1}{\alpha Re}\right)^2 \cdot \varphi_2(y) + \cdots \qquad (I.65)$$

The parameter $1/\alpha Re$ is assumed to be a   very   small value. Substituting (I.65) in (I.59) and equating the coefficients for identical powers of $1/\alpha Re$ in the expres-sion obtained, we arrive at the following system of differential equations:

$$(u - c)(\varphi_0'' - \alpha^2 \varphi_0) - u'' \cdot \varphi_0 = 0;$$
$$(u - c)(\varphi_\kappa'' - \alpha^2 \varphi_\kappa) - u'' \varphi_\kappa = -i(\varphi_{\kappa-1}^{IV} - 2\alpha^2 \varphi_{\kappa-1}'' + \alpha^4 \varphi_{\kappa-1}).$$
$$k = 1,2\ldots \qquad (I.66)$$

Determining the solutions of the first equation of system (I.66), it is then possible by the method of variation of arbitrary constants successively to determine all the functions ϕ_k. However, usually we are limited in the series (I.65) to only the first term, permitting an error in determining $\phi(y)$ on the order of $(\alpha Re)^{-1}$, and the problem thus reduces to integration of the equation

$$(u - c)(\varphi'' - \alpha^2 \varphi) - u'' \varphi = 0. \qquad (I.67)$$

Equation (I.67) determines the development of disturbances in an ideal fluid. It must be remembered, of course, that the effect of the viscosity is felt in the for-mation of the function $u(y)$, which, in turn, determines the variation across the boundary layer of the velocity pulsation amplitude. Neglecting the viscosity lowered the order of equation (I.59), in connection with which it is necessary to use another approximate method of integration (I.59) discussed below to find the missing solu-tions. The differential equation (I.67) has a singularity at the point $y = y_k$, where $u(y_k) = c$. This case corresponds to comparison of the propagation rate of a neutral disturbance in the boundary layer with the basic flow velocity. It is possible to explain the processes occurring in the layer $y = y_k$, which is called the "critical layer," by the following argument [84]. Let us introduce the disturbing motion vortex into the investigation

$$r = \frac{\partial v_y}{\partial x} - \frac{\partial v_x}{\partial y} = (\alpha^2 \varphi - \varphi'') e^{i\alpha(x - ct)}$$

and the basic motion vortex $R = -\partial u/\partial y$. Then equation (I.67) can be represented as follows:

$$(u - c)\frac{\partial r}{\partial x} + \frac{\partial R}{\partial y} \cdot v_y = 0. \qquad (I.68)$$

Equality (I.68) expresses the condition of preservation of the vortices in an ideal fluid. If for $y = y_k$, $\partial R/\partial y \neq 0$, then $(\partial R/\partial y)v_y \neq 0$, for in the general case $v_y(y_k) \neq 0$. Therefore for observation of the equality (I.68), its first term $(u - c)\partial r/\partial x$ must also be nonzero. For $u - c \to 0$ this can occur only in the case of $\partial r/\partial x \to \infty$, that is, in a critical layer in the absence of viscosity the vortex of the disturb-ing motion increases without limit. In order to bring the calculation scheme in accordance with reality in the critical layer it is necessary to consider the effect of viscosity which will also be done when finding the solutions of equation (I.59) as a function of viscosity.

The presence of a pole of the first order at the point $y = y_k$ in the function $u''/(u - c)$ determines [85] the form of the solution of equation (I.67)

$$\varphi(y) = (y - y_\kappa) P(y - y_\kappa). \tag{I.69}$$

where $P(y - y_k)$ is a series with respect to powers of $y - y_k$ with coefficients that depend on the parameter α. Since $u(y)$ is represented in the vicinity of $y = y_k$ by a series with respect to powers of $y - y_k$, it is possible to rewrite (I.69) as follows:

$$\varphi(y) = (u - c) P(y, \alpha).$$

Then the possibility of expansion of the function $P(y, \alpha)$ in a converging series with respect to powers of the parameter α^2 is proposed. Then, substituting

$$\varphi(y) = (u - c) \left| g_0(y) + \alpha^2 g_1(y) + \cdots + \alpha^{2n} g_n(y) + \cdots \right|$$

in equation (I.67) and equating the coefficients for identical powers of α^2, we obtain the system of differential equations

$$\left. \begin{aligned} g_0''(u - c) + 2u'g_0' &= 0 \\ g_n''(u - c) + 2u'g_n' &= g_{n-1} \cdot (u - c) \\ n &= 1, 2, \ldots \end{aligned} \right\} \tag{I.70}$$

Solving the first equation of system (I.70), we determine with accuracy to a constant factor

$$g_{0(1)} = 1; \quad g_{0(2)} = \int_0^y (u - c)^{-2} \, dy.$$

Knowing the function $g_n(y)$, it is possible to define g_{n+1}, using the equation

$$q_{n+1}'' + 2 \frac{u'}{u - c} g_{n+1}' = g_n$$

$$g_{n+1}(y) = \int_0^y (u - c)^{-2} \, dy \int_0^y (u - c)^2 g_n(y) \, dy. \tag{I.71}$$

The integral in (I.71) is calculated by the formula

$$\int_0^y (u \cdot c)^{-2} \left[\int_0^y (u - c)^2 g_n(y) \, dy \right] dy.$$

Thus, two solutions are found for equation (I.67)

$$\varphi_1(y) = (u - c) \sum_{n=0}^{\infty} g_n(y) \alpha^{2n}, \tag{I.72}$$

where

$$g_0(y) = 1; \quad g_{n+1}(y) = \int_0^y (u - c)^{-2} \, dy \int_0^y (u - c)^2 g_n(y) \, dy;$$

$$\varphi_2(y) = (u - c) \sum_{n=0}^{\infty} g_n(y) \cdot \alpha^{2n}; \tag{I.73}$$

45

where

$$g_0(y) = \int_0^y (u-c)^{-2}\, dy; \quad g_{n+1}(y) = \int_0^y (u-c)^{-2}\, dy \int_0^y (u-c)^2 g_n(y)\, dy.$$

The series (I.72), (I.73) converge for any fixed α, for with a sufficiently large n their terms are majorized [67] by the terms of the series

$$\frac{A\,(\alpha M)^{2n}}{(2n)!}.$$

It is possible to be convinced of this by substituting the expansion of u - c with respect to powers of $y - y_k$ in the coefficients of the investigated series.

Equation (I.67) is second order, in contrast to the fourth-order equation (I.59). Therefore only two independent solutions of equation (I.59) are obtained by the investigated method. Two more linearly independent solutions of equation (I.59) can be found [12] in exponential form

$$\varphi(y) = \exp\left[\int_0^y p(y)\, dy\right]. \tag{I.74}$$

Substituting (I.74) in (I.59), we obtain the equation for determining the function $p(y)$

$$(u-c)(p'+p^2-\alpha^2) - u'' = -\frac{i}{\alpha Re}\left[p^4 + 6p^2 p' + 3p'^2 + 4pp'' + \right.$$
$$\left. + p''' - 2\alpha^2(p'+p^2) + \alpha^4\right]. \tag{I.75}$$

The solution of equation (I.75) is represented by a series with respect to powers of $(\alpha Re)^{-1/2}$

$$p(y) = \sqrt{\alpha Re}\cdot p_0(y) + p_1(y) + \frac{1}{\sqrt{\alpha Re}}\cdot p_2(y) + \cdots \tag{I.76}$$

The exponent 1/2 is selected from the condition of equality of the higher-order terms in both sides of equation (I.75), which corresponds to the assumption of identical role of viscosity and forces of inertia. The function $p(y, \alpha Re)$ in the form of (I.76) has a singularity at Re $\to \infty$. This is necessary for the required solution of (I.74) to vanish when $\nu \to 0$. Substituting (I.76) in (I.75) and equating the coefficients before identical powers of $(\alpha Re)^{1/2}$, we find the system of equations:

$$(u-c)p_0^2 = -ip_0^4;$$
$$(u-c)(p_0' + 2p_0 p_1) = -i(4p_0^3 p_1 + 6p_0^2 p_0');$$
$$\cdots \cdots \cdots \cdots \cdots \cdots$$

from which it is possible to determine the following successively:

$$p_0(y) = \pm\sqrt{i(u-c)};$$
$$p_1(y) = -\frac{5}{2}\cdot\frac{p_0'}{p_0}\cdots \tag{I.77}$$

46

Two signs before the square root sign in formula (I.77) correspond to two linearly independent solutions of equation (I.59). Limiting ourselves to the first two terms in the expansion (I.76), by using (I.74) it is possible to determine:

$$\varphi_3(y) = (u-c)^{-\frac{5}{4}} \exp\left[-\int_0^y \sqrt{i\alpha\,\mathrm{Re}(u-c)}\,dy \right];$$ (I.78)

$$\varphi_4(y) = (u-c)^{-\frac{5}{4}} \exp\left[\int_0^y \sqrt{i\alpha\,\mathrm{Re}(u-c)}\,dy \right].$$ (I.79)

Approximate methods used to construct the solutions of $\phi_1(y)$ (I.72), $\phi_2(y)$ (I.73), $\phi_3(y)$ (I.78), $\phi_4(y)$ (I.79) lead to the appearance of a singularity for $y = y_k$ where $u(y_k) = c$. Here the problem of the sign of the argument of the value of $u - c$ for $u < c$ remains unexplained. If arg$(u - c) = \pi$, then on integration along the real axis the point $y = y_k$ must be rounded from above; if arg $(u - c) = -\pi$, it must be rounded from below. To study the behavior of the solution of equation (I.59) in the vicinity of the point $y = y_k$, a new independent variable is introduced [67], [83]

$$\eta = \frac{y - y_k}{\varepsilon},$$

where ε is a small parameter, the magnitude of which is determined from the following arguments.

Denoting $\phi(y) = \chi(\eta)$, on the basis of equation (I.59) we find

$$(u-c)(\chi'' - \alpha^2\varepsilon^2\chi) - \varepsilon^2\chi u'' = \frac{i}{\alpha\,\mathrm{Re}\cdot\varepsilon^2}(\chi^{IV} - 2\alpha^2\varepsilon^2\chi'' + \alpha^4\varepsilon^4\chi).$$ (I.80)

The functions u and u'' in the vicinity of the point $y = y_k$ can be represented by the series:

$$\left.\begin{aligned}
u - c &= u_k'\cdot\varepsilon\eta + \frac{1}{2}u_k''(\varepsilon\eta)^2 + \cdots \\
u'' &= u_k'' + u_k'''\cdot\varepsilon\eta + \frac{1}{2}u_k^{IV}(\varepsilon\eta)^2 + \cdots
\end{aligned}\right\}$$ (I.81)

The value of ε is assumed to be so small that the series (I.81) converge. The solution of equation (I.80) is found in the following form:

$$\varphi(y) = \chi(\eta) = \chi_0(\eta) + \varepsilon\chi_1(\eta) + \varepsilon^2\chi_2(\eta) + \cdots$$ (I.82)

Subsituting (I.81) and (I.82) in (I.80) and equating the coefficients for identical powers of ε, we obtain the system of differential equations for determining the functions $\chi_n(\eta)$:

$$\left.\begin{aligned}
i\chi_0^{IV} + u_k'\cdot\eta\chi_0'' &= 0, \\
i\chi_n^{IV} + u_k'\cdot\eta\chi_n'' &= L_{n-1}(\chi), \quad (n \geqslant 1);
\end{aligned}\right\}$$ (I.83)

where $L_{n-1}(\chi)$ are linear combinations of the functions χ_0, χ_1, ... χ_{n-1} and their derivatives. It is possible to determine the value ε from the assumption that the

47

highest terms in the left and right sides of equation (I.80) have the same order of smallness with respect to ε

$$(u-c)\chi'' \approx -\frac{i}{\alpha\,\mathrm{Re}\,\varepsilon^3}\chi^{IV}.$$

(I.84)

Considering the expansion of (I.81), on the basis of (I.84) we find the value of the parameter

$$\varepsilon = (\alpha\,\mathrm{Re})^{-1/3}.$$

(I.85)

Usually when determining the function $\chi(\eta)$ we are limited to the zero approximation, that is, it is considered that $\chi(\eta) \simeq \chi_0(\eta)$. Here an error on the order of $(\alpha\mathrm{Re})^{-1/3}$ is permitted, which is obvious from (I.82) and (I.85).

Let us consider the solution of the first equation of system (I.83). Let us use the known substitutions [86], reducing it to a Bessel equation. Let us denote $\chi_0'' = \psi$, $-iu_k' = a$, then the investigated equation becomes a second-order equation

$$\psi'' + a\eta\psi = 0,$$

(I.86)

which gives two linearly independent solutions to the equation

$$\chi_0^{IV} - iu_\kappa'\cdot\eta\chi_0'' = 0.$$

(I.87)

As the two remaining solutions it is possible to take the functions $\chi_{01} = 1$; $\chi_{02} = \eta$ which obviously satisfy equation (I.87). Let us introduce the new desired function $z = \psi/\sqrt{\eta}$. Here

$$\psi' = \frac{1}{2}\cdot\frac{1}{\sqrt{\eta}}\cdot z + z'\cdot\sqrt{\eta},$$

$$\psi'' = -\frac{1}{4}(\eta)^{-3/2}\cdot z + (\eta)^{-1/2}\cdot z' + \eta^{1/2}z'',$$

and equation (I.86) is written as follows

$$\frac{d}{d\eta}\left(\eta\frac{dz}{d\eta}\right) + \left(a\eta^2 - \frac{1}{4}\cdot\frac{1}{\eta}\right)z = 0.$$

(I.88)

Let us vary the independent variable, denoting

$$\eta = a^{-1/3}\cdot\left(\frac{3}{2}\xi\right)^{2/3}; \quad \frac{d\eta}{d\xi} = a^{-1/3}\cdot\left(\frac{3}{2}\xi\right)^{-1/3}.$$

From (I.88) in the new variables we obtain

$$\frac{d}{d\xi}\left(\xi\frac{dz}{d\xi}\right) + \left(\xi - \frac{1}{9\xi}\right)z = 0.$$

(I.89)

The solution of equation (I.89) is expressed in terms of the Bessel function of 1/3 order [87]

$$z = c_1 \cdot J_{1/3}(\xi) + c_2 J_{-1/3}(\xi),$$

or, considering the relation of the Bessel functions to the Hankel functions

$$J_{1/3}(\xi) = \frac{1}{2}\left[H_{1/3}^{(1)}(\xi) + H_{1/3}^{(2)}(\xi) \right],$$

$$J_{-1/3}(\xi) = \frac{1}{2}\left[e^{\pi i/3} \cdot H_{1/3}^{(1)}(\xi) + e^{\pi i/3} \cdot H_{1/3}^{(2)}(\xi) \right],$$

$$z = D_1 \cdot H_{1/3}^{(1)}(\xi) + D_2 \cdot H_{1/3}^{(2)}(\xi).$$

Thus, considering the substitutions made, we obtain the following two linearly independent solutions (I.86):

$$\chi_{03} \quad \sqrt{\eta} \cdot H_{1/3}^{(1)}\left[\frac{2}{3}(i\beta\eta)^{3/2} \right],$$

$$\chi_{04} \quad \sqrt{\eta} \cdot H_{1/3}^{(2)}\left[\frac{2}{3}(i\beta\eta)^{3/2} \right],$$

where it is assumed that $\beta \quad \sqrt[3]{u_c}$; $\arg(-i) \quad \frac{3}{2}\pi$.

Since

$$H_{1/3}^{(1)} \to 0 \quad \text{for } \eta \to \infty,$$

$$H_{1/3}^{(2)} \to 0 \quad \text{for } \eta \to -\infty,$$

then it is possible to take the following expressions as linearly independent solutions of the first equation of system (I.83):

$$\chi_{01} = 1; \quad \chi_{02} = \eta;$$

$$\chi_{03} = \int_{\infty}^{\eta} d\eta \int_{\infty}^{\eta} \sqrt{\eta} \cdot H_{1/3}^{(1)}\left[\frac{2}{3}(i\beta\eta)^{3/2} \right] d\eta; \qquad (I.90)$$

$$\chi_{04} = \int_{\infty}^{\eta} d\eta \int_{\infty}^{\eta} \sqrt{\eta} \cdot H_{1/3}^{(2)}\left[\frac{2}{3}(i\beta\eta)^{3/2} \right] d\eta. \qquad (I.91)$$

The solutions of (I.90) and (I.91) have no singularities in the critical layer for $\eta = 0$.

Replacing the Hankel functions in (I.90), (I.91) by their asymptotic representations, it is possible to reduce these expressions to the form (I.78) and (I.79). The region in which the investigated representations are valid thus determines the path of bypassing the singularity $y = y_k$.

Let us write [87] the asymptotic expansions of the Hankel functions of 1/3 order for small values of the argument

$$H_{1/3}^{(1)}(\xi) \approx \left(\frac{2}{\pi\xi} \right)^{1/2} \exp\left[i\left(\xi - \frac{5\pi}{12} \right) \right] \{1 + \cdots \}; \qquad (I.92)$$

$$(-\pi < \arg\xi < 2\pi)$$

$$H_{1/3}^{(2)}(\xi) \approx \left(\frac{2}{\pi\xi}\right)^{1/2} \exp\left[-i\left(\xi - \frac{5\pi}{12}\right)\right]\{1 + \cdots\}, \tag{I.93}$$

$$(-2\pi < \arg\xi < \pi),$$

where the dots indicate values on the order of $1/\xi$ and higher. Substituting (I.92) and (I.93) in formulas (I.90), (I.91), it is possible to obtain [67] the expressions for the functions χ_{03} and χ_{04} analogous to formulas (I.78) and (I.79). From the expansions of (I.92) and (I.93) it follows that the argument of the variable η must satisfy the conditions:

$$-\pi < \frac{3}{2}\arg\eta + \frac{3\pi}{4} < 2\pi;$$

$$-2\pi < \frac{3}{2}\arg\eta + \frac{3\pi}{4} < \pi,$$

or

$$-\frac{7}{6}\pi < \arg\eta < \frac{5}{6}\pi$$
$$-\frac{11}{6}\pi < \arg\eta < \frac{\pi}{6}. \tag{I.94}$$

From inequalities (I.94) the following estimate is obtained:

$$-\frac{7}{6}\pi < \arg\eta < \frac{\pi}{6}. \tag{I.95}$$

The inequality (I.95) shows that when going around the critical point $y = y_k$ it is necessary to select the path in the lower halfplane. This physically means that the motion approaches the neutral disturbances from the damping disturbance side. Then it appears possible to use both the solutions $\phi_1(y)$ (I.72), $\phi_2(y)$ (I.73) $\phi_3(y)$ (I.78), $\phi_4(y)$ (I.79), and the solutions χ_{01}, χ_{02}, χ_{03}, χ_{04}. The solutions ϕ_1, ϕ_2, ϕ_3, ϕ_4 were used by Heisenberg in his paper [83]. Tietjens [88] performed his calculations on the basis of χ_{01}, χ_{02}, χ_{03}, χ_{04}. Tollmien [24] and all subsequent authors used the solutions ϕ_1, ϕ_2, χ_{03}, χ_{04} as the basis for their research for ϕ_1 and ϕ_2 reflect the influence of the form of the velocity profile on the stability better than χ_{01}, χ_{02}, and the functions χ_{03}, χ_{04} consider the influence of viscosity on the stability of a laminar flow more precisely than ϕ_3, ϕ_4. Hereafter, by linearly independent partial solutions of equation (I.59) we shall mean the expressions $\phi_1(y)$ (I.72), $\phi_2(y)$ (I.73), $\phi_3(y) \equiv \chi_{03}(y)$ (I.90), $\phi_4(y) \equiv \chi_{04}(y)$ (I.91). The general solution of the Orr-Sommerfeld equation is then written as follows:

$$\varphi(y) = c_1\varphi_1(y) + c_2\varphi_2(y) + c_3\varphi_3(y) + c_4\varphi_4(y), \tag{I.96}$$

where c_1, c_2, c_3, c_4 are arbitrary constants determined from the boundary conditions.

§ I.7. Construction of the Neutral Stability Curve for Given Velocity Profile in the Boundary Layer

Beginning with the general form of the solution (I.96) and considering the boundary conditions (I.60), (I.61) and (I.63), it is possible to obtain a uniform system of linear algebraic equations with respect to the constants c_1, c_2, c_3:

$$
\begin{aligned}
& c_1\varphi_1(0) + c_2\varphi_2(0) + c_3\varphi_3(0) = 0; \\
& c_1\varphi_1'(0) + c_2\varphi_2'(0) + c_3\varphi_3'(0) = 0; \\
& c_1\left[\varphi_1'(1) + \alpha\varphi_1(1)\right] + c_2\left[\varphi_2'(1) + \alpha\varphi_2(1)\right] + \\
& \qquad + c_3\left[\varphi_3'(1) + \alpha\varphi_3(1)\right] = 0.
\end{aligned}
\qquad (I.97)
$$

From the condition of limited nature of the solution at infinity it follows that $c_4 = 0$. In order that the uniform system (I.97) have nonzero solutions with respect to c_1, c_2, c_3, it is necessary and sufficient that its determinant be equal to zero

$$
\begin{vmatrix}
\varphi_1(0) & \varphi_2(0) & \varphi_3(0) \\
\varphi_1'(0) & \varphi_2'(0) & \varphi_3'(0) \\
\varphi_1'(1) + \alpha\varphi_1(1) & \varphi_2'(1) + \alpha\varphi_2(1) & 0
\end{vmatrix} = 0.
\qquad (I.98)
$$

In equation (I.98) relating the values of α, Re, c, let us neglect the terms which include the sum $\phi_3'(1) + \alpha\phi_3(1)$, for the function $\phi_3'(y) + \alpha\phi_3(y)$ very quickly decreases with an increase in y, which is obvious from (I.78), and it is in practice equal to zero at the boundary of the boundary layer. It is possible also to see this, considering the results of the Holstein [89] and Schlichting [90] calculations.

Let us transform equation (I.98)

$$
\frac{\varphi_3(0)}{\varphi_3'(0)} = \frac{\varphi_1(0)\left[\varphi_2'(1) + \alpha\varphi_2(1)\right] - \varphi_2(0)\left[\varphi_1'(1) + \alpha\varphi_1(1)\right]}{\varphi_1'(0)\left[\varphi_2'(1) + \alpha\varphi_2(1)\right] - \varphi_2'(0)\left[\varphi_2'(1) + \alpha\varphi_1(1)\right]}.
$$

Using formulas (I.72) and (I.73), we find

$$
\varphi_1(0) = -c; \quad \varphi_1'(0) = u'(0) = u_0';
$$

$$
\varphi_2(0) = 0; \quad \varphi_2'(0) = -\frac{1}{c}.
$$

As a result, we obtain the complex equation

$$
-\frac{1}{y_\kappa} \cdot \frac{\varphi_3(0)}{\varphi_3'(0)} = \frac{c}{y_\kappa \cdot u_0'} \cdot \frac{z}{1+z},
\qquad (I.99)
$$

where

$$
z = \frac{u_0' \cdot c\left[\varphi_2'(1) + \alpha\varphi_2(1)\right]}{\varphi_1'(1) + a_L\varphi_1(1)}.
$$

Using (I.99), for real values of $c(c_i = 0)$ it is possible to obtain the function Re = R2(α) defining the neutral curve in the plane [α, Re] separating the region of stability from the region of instability. The left-hand side of equation (I.99) is represented as follows considering (I.90):

$$-\frac{1}{y_\kappa}\cdot\frac{\varphi_3(0)}{\varphi_3'(0)} = \frac{\int\limits_\infty^{-\infty}d\zeta\int\limits_\infty^{\zeta}\zeta^{1/2}H_{1/3}^{(1)}\left[\frac{2}{3}(i\zeta)^{3/2}\right]d\zeta}{-w\int\limits_\infty^{-\infty}\zeta^{1/2}H_{1/3}^{(1)}\left[\frac{2}{3}(i\zeta)^{3/2}\right]d\zeta} = F_r(w) + iF_i(w).$$

The following notation was introduced: $\zeta = \beta\cdot\eta$; $w = \frac{\beta y_\kappa}{e} = y_\kappa\,(u_\kappa'\alpha Re)^{1/3}$. The values of
the functions $F_r(w)$, $F_i(w)$ were first calculated by Tietjens [88]. They were later
calculated by various authors by expansion of the Hankel functions in series. A
comparative table of values of $F_r(w)$ and $F_i(w)$ calculated by Tietjens, Schlichting,
Pretsch, Maksyn, Holstein and Lin is presented in the paper by Holstein [89].
Table I.1 was compiled by the results of the Miles calculations [91].

The right-hand side of equation (I.99) can also be represented in the form

$$\frac{c}{y_\kappa\cdot u_0'}\cdot\frac{z}{1+z} = E_r + iE_i.$$

The values of $E_r(\alpha, c)$, $E_i(\alpha, c)$ depend on the velocity profile in the boundary layer.
The method of their calculation based on replacement of the true velocity profile by
parabolic or linear velocity distribution was used in the papers by Tollmien [24]
and Schlichting [92]. Pretsch [14] developed a method of calculating E_r and E_i when
using the velocity distribution profile corresponding to the third and fourth degree
polynomials and also sinusoidal velocity distribution. The Lin method [12] that
does not impose any restrictions on the form of the velocity profile in the boundary
layer, is used when determining E_r and E_i.

Let us transform the left-hand side of the preceding equality

$$\frac{c}{y_\kappa\cdot u_0'}\cdot\frac{z}{1+z} = \frac{c}{y_\kappa\cdot u_0'}\cdot\frac{z_r+iz_i}{1+z_r+iz_i} = \frac{z_r^2+z_r+z_i^2}{(1+z_r)^2+z_i^2}\cdot\frac{c}{y_\kappa\cdot u_0'} +$$
$$+ i\frac{z_i}{(1+z_r)^2+z_i^2}\cdot\frac{c}{y_\kappa\cdot u_0'}.$$

Using the expansions (I.72), (I.73) and considering only the terms with the first
powers of the parameter α which it is assumed is small, we find

$$z = u_0'c\frac{\varphi_2'(1)+\alpha\varphi_2(1)}{\varphi_1'(1)+\alpha\varphi_1(1)} = u_0'\cdot c\left[K_1 + \frac{1}{\alpha(1-c)^2} + 0(1)\right], \qquad (I.100)$$

where $K_1 = \int\limits_0^1(u-c)^{-2}\,dy$, the term $0(1)$ combines the terms of order one. On the
neutral curve where $c_i = 0$, the integral $K_1(c)$ has a singularity at $y = y_k$.

In the vicinity of the critical point we have the expansions:
$$u - c = u_\kappa'(y-y_\kappa) + \frac{1}{2}u_\kappa''(y-y_\kappa)^2 + \cdots$$
$$(u-c)^2 = u_\kappa'^2(y-y_\kappa)^2 + u_\kappa'\cdot u_\kappa''(y-y_\kappa)^3 + \cdots$$
$$(u-c)^{-2} = \frac{1}{u_\kappa'^2(y-y_\kappa)^2}\left[1 - \frac{u_\kappa''}{u_\kappa'}(y-y_\kappa) + \cdots\right].$$

52

FOR OFFICIAL USE ONLY

Table I.1

Example: $-0,1183\ 00 = -0,1183$: $0,1343\ 01 = 1,343$: $-0,7778 - 0,1 = -0,07778$

ω	$\mathfrak{S}_r$		$\mathfrak{S}_i$		$\mathfrak{S}'_r$		$\mathfrak{S}'_i$		F_r		F_i	
0,1	−0,1183	00	−0,7778	−01	−0,1249	01	−0,9281	00	0,6901	01	−0,3880	01
0,2	−0,2489	00	−0,1895	00	−0,1355	01	−0,1328	01	0,3544	01	−0,1936	01
0,3	−0,3867	00	−0,3485	00	−0,1380	01	−0,1879	01	0,2427	01	−0,1286	01
0,4	−0,5188	00	−0,5712	00	−0,1221	01	−0,2605	01	0,1871	01	−0,9593	00
0,5	−0,6194	00	−0,8741	00	−0,7156	00	−0,3467	01	0,1540	01	−0,7616	00
0,6	−0,6438	00	−0,1263	01	0,3311	00	−0,4283	01	0,1320	01	−0,6284	00
0,7	−0,5321	00	−0,1716	01	0,1995	01	−0,4641	01	0,1165	01	−0,5317	00
0,8	−0,2345	00	−0,2159	01	0,3949	01	−0,4029	01	0,1050	01	−0,4578	00
0,9	0,2409	00	−0,2484	01	0,5403	01	−0,2315	01	0,9613	00	−0,3989	00
1,0	0,8061	00	−0,2605	01	0,5689	01	−0,1210	00	0,8916	00	−0,3503	00
1,1	0,1342	01	−0,2522	01	0,4895	01	0,1672	01	0,8356	00	−0,3090	00
1,2	0,1770	01	−0,2298	01	0,3640	01	0,2662	01	0,7897	00	−0,2731	00
1,3	0,2042	01	−0,2012	01	0,2445	01	0,2973	01	0,7516	00	−0,2412	00
1,4	0,2268	01	−0,1717	01	0,1521	01	0,2897	01	0,7197	00	−0,2122	00
1,5	0,2386	01	−0,1438	01	0,8724	00	0,2659	01	0,6926	00	−0,1853	00
1,6	0,2450	01	−0,1186	01	0,4354	00	0,2385	01	0,6693	00	−0,1601	00
1,7	0,2478	01	−0,9606	00	0,1412	00	0,2129	01	0,6491	00	−0,1360	00
1,8	0,2461	01	−0,7590	00	−0,6314	−01	0,1910	01	0,6314	00	−0,1128	00
1,9	0,2467	01	−0,5774	00	−0,2138	00	0,1727	01	0,6157	00	−0,8996	−01
2,0	0,2439	01	−0,4126	00	−0,3339	00	0,1574	01	0,6014	00	−0,6742	−01
2,1	0,2401	01	−0,2619	00	−0,4378	00	0,1443	01	0,5863	00	−0,4491	−01
2,2	0,2352	01	−0,1235	00	−0,5334	00	0,1325	01	0,5760	00	−0,2227	−01
2,3	0,2294	01	0,3379	−02	−0,6242	00	0,1213	01	0,5641	00	0,6422	−03
2,4	0,2227	01	0,1191	00	−0,7107	00	0,1101	01	0,5523	00	0,2394	−01
2,5	0,2152	01	0,2234	00	−0,7912	00	0,9834	00	0,5403	00	0,4772	−01
2,6	0,2069	01	0,3155	00	−0,8625	00	0,8584	00	0,5277	00	0,7202	−01
2,7	0,1980	01	0,3948	00	−0,9208	00	0,7254	00	0,5143	00	0,9685	−00
2,8	0,1886	01	0,4604	00	−0,9625	00	0,5855	00	0,4995	00	0,1222	00
2,9	0,1788	01	0,5118	00	−0,9845	00	0,4418	00	0,4831	00	0,1479	00
3,0	0,1689	01	0,5487	00	−0,9851	00	0,2981	00	0,4646	00	0,1739	00
3,1	0,1592	01	0,5715	00	−0,9640	00	0,1593	00	0,4435	00	0,1998	00
3,2	0,1497	01	0,5809	00	−0,9225	00	0,2965	−01	0,4195	00	0,2252	00
3,3	0,1408	01	0,5779	00	−0,8632	00	−0,8679	−01	0,3922	00	0,2495	00
3,4	0,1325	01	0,5641	00	−0,7895	00	−0,1871	00	0,3611	00	0,2719	00
3,5	0,1250	01	0,5411	00	−0,7055	00	−0,2695	00	0,3264	00	0,2915	00
3,6	0,1184	01	0,5108	00	−0,6151	00	−0,3333	00	0,2881	00	0,3071	00
3,7	0,1127	01	0,4751	00	−0,5223	00	−0,3787	00	0,2468	00	0,3174	00
3,8	0,1080	01	0,4356	00	−0,4304	00	−0,4068	00	0,2036	00	0,3213	00
3,9	0,1041	01	0,3942	00	−0,3424	00	−0,4194	00	0,1600	00	0,3180	00

FOR OFFICIAL USE ONLY

Table I.1 (continued)

w	$\mathfrak{F}_r$		$\mathfrak{F}_i$		$\mathfrak{F}'_r$		$\mathfrak{F}'_i$		F_r		F_i	
4,0	0,1011	01	0,3522	00	—0,2603	00	—0,4183	00	0,1180	00	0,3072	00
4,1	0,9889	00	0,3109	00	—0,1859	00	—0,4058	00	0,7976	—01	0,2893	00
4,2	0,9737	00	0,2714	00	—0,1203	00	—0,3842	00	0,4699	—01	0,2656	00
4,3	0,9646	00	0,2343	00	—0,6392	—01	—0,3556	00	0,2103	—01	0,2378	00
4,4	0,9606	00	0,2004	00	—0,1708	—01	—0,3222	00	0,2384	—02	0,2081	00
4,5	0,9608	00	0,1700	00	0,2044	—01	—0,2859	00	—0,9187	—02	0,1785	00
4,6	0,9644	00	0,1433	00	0,4911	—01	—0,2483	00	—0,1455	—01	0,1507	00
4,7	0,9704	00	0,1203	00	0,6962	—01	—0,2109	00	—0,1493	—01	0,1258	00
4,8	0,9781	00	0,1010	00	0,8284	—01	—0,1749	00	—0,1164	—01	0,1045	00
4,9	0,9867	00	0,8524	—01	0,8974	—01	—0,1413	00	—0,5938	—02	0,8690	—01
5,0	0,9958	00	0,7267	—01	0,9134	—01	—0,1108	00	0,1128	—02	0,7289	—01
5,1	0,1005	01	0,6297	—01	0,8867	—01	—0,8371	—01	0,8728	—02	0,6212	—01
5,2	0,1013	01	0,5580	—01	0,8272	—01	—0,6041	—01	0,1625	—01	0,5416	—01
5,3	0,1021	01	0,5076	—01	0,7444	—01	—0,4092	—01	0,2329	—01	0,4855	—01
5,4	0,1028	01	0,4749	—01	0,6466	—01	—0,2514	—01	0,2958	—01	0,4482	—01
5,5	0,1034	01	0,4562	—01	0,5411	—01	—0,1285	—01	0,3498	—01	0,4257	—01
5,6	0,1039	01	0,4482	—01	0,4341	—01	—0,3737	—02	0,3942	—01	0,4143	—01
5,7	0,1043	01	0,4478	—01	0,3305	—01	0,2574	—02	0,4292	—01	0,4109	—01
5,8	0,1046	01	0,4525	—01	0,2339	—01	0,6497	—02	0,4553	—01	0,4130	—01
5,9	0,1048	01	0,4601	—01	0,1471	—01	0,8452	—02	0,4731	—01	0,4184	—01
6,0	0,1049	01	0,4689	—01	0,7167	—02	0,8851	—02	0,4836	—01	0,4255	—01
6,1	0,1049	01	0,4774	—01	0,8349	—03	0,8080	—02	0,4878	—01	0,4329	—01
6,2	0,1049	01	0,4848	—01	—0,4280	—02	0,6487	—02	0,4868	—01	0,4397	—01
6,3	0,1048	01	0,4902	—01	—0,8229	—02	0,4376	—02	0,4815	—01	0,4451	—01
6,4	0,1047	01	0,4935	—01	—0,1111	—01	0,2002	—02	0,4729	—01	0,4489	—01
6,5	0,1046	01	0,4942	—01	—0,1303	—01	—0,4284	—02	0,4620	—01	0,4506	—01
6,6	0,1045	01	0,4926	—01	—0,1415	—01	—0,2759	—02	0,4495	—01	0,4503	—01
6,7	0,1043	01	0,4888	—01	—0,1459	—01	—0,4876	—02	0,4360	—01	0,4481	—01
6,8	0,1042	01	0,4830	—01	—0,1451	—01	—0,6706	—02	0,4222	—01	0,4440	—01
6,9	0,1040	01	0,4755	—01	—0,1403	—01	—0,8210	—02	0,4084	—01	0,4384	—01
7,0	0,1039	01	0,4667	—01	—0,1328	—01	—0,9376	—02	0,3951	—01	0,4314	—01
7,1	0,1038	01	0,4568	—01	—0,1236	—01	—0,1021	—01	0,3825	—01	0,4234	—01
7,2	0,1037	01	0,4463	—01	—0,1136	—01	—0,1075	—01	0,3706	—01	0,4146	—01
7,3	0,1035	01	0,4354	—01	—0,1034	—01	—0,1101	—01	0,3597	—01	0,4054	—01
7,4	0,1035	01	0,4244	—01	—0,9351	—02	—0,1105	—01	0,3497	—01	0,3959	—01
7,5	0,1034	01	0,4134	—01	—0,8436	—02	—0,1091	—01	0,3406	—01	0,3863	—01
7,6	0,1033	01	0,4026	—01	—0,7615	—02	—0,1063	—01	0,3324	—01	0,3769	—01
7,7	0,1032	01	0,3922	—01	—0,6901	—02	—0,1024	—01	0,3248	—01	0,3676	—01
7,8	0,1031	01	0,3822	—01	—0,6294	—02	—0,9798	—02	0,3180	—01	0,3587	—01
7,9	0,1031	01	0,3726	—01	—0,5793	—02	—0,9317	—02	0,3117	—01	0,3502	—01

54

Table I.1 (continued)

w	$\mathfrak{F}_r$		$\mathfrak{F}_i$		$\mathfrak{F}'_r$		$\mathfrak{F}'_i$		F_r		F_i	
8,0	0,1030	01	0,3635	—01	—0,5388	—02	—0,8826	—02	0,3058	—01	0,3421	—01
8,1	0,1030	01	0,3549	—01	—0,5067	—02	—0,8344	—02	0,3004	—01	0,3343	—01
8,2	0,1029	01	0,3468	—01	—0,4818	—02	—0,7884	—02	0,2952	—01	0,3270	—01
8,3	0,1029	01	0,3392	—01	—0,4627	—02	—0,7455	—02	0,2903	—01	0,3201	—01
8,4	0,1028	01	0,3319	—01	—0,4481	—02	—0,7062	—02	0,2855	—01	0,3135	—01
8,5	0,1028	01	0,3250	—01	—0,4368	—02	—0,6708	—02	0,2810	—01	0,3073	—01
8,6	0,1027	01	0,3185	—01	—0,4279	—02	—0,6391	—02	0,2765	—01	0,3014	—01
8,7	0,1027	01	0,3122	—01	—0,4206	—02	—0,6109	—02	0,2721	—01	0,2957	—01
8,8	0,1027	01	0,3062	—01	—0,4140	—02	—0,5859	—02	0,2678	—01	0,2903	—01
8,9	0,1026	01	0,3005	—01	—0,4079	—02	—0,5638	—02	0,2636	—01	0,2851	—01
9,0	0,1026	01	0,2950	—01	—0,4017	—01	—0,5440	—02	0,2595	—01	0,2801	—01
9,1	0,1025	01	0,2896	—01	—0,3953	—02	—0,5262	—02	0,2554	—01	0,2752	—01
9,2	0,1025	01	0,2844	—01	—0,3886	—02	—0,5100	—02	0,2514	—01	0,2705	—01
9,3	0,1025	01	0,2794	—01	—0,3815	—02	—0,4951	—02	0,2475	—01	0,2659	—01
9,4	0,1024	01	0,2745	—01	—0,3741	—02	—0,4812	—02	0,2436	—01	0,2615	—01
9,5	0,1024	01	0,2698	—01	—0,3664	—02	—0,4681	—02	0,2399	—01	0,2572	—01
9,6	0,1024	01	0,2652	—01	—0,3584	—02	—0,4556	—02	0,2362	—01	0,2530	—01
9,7	0,1023	01	0,2607	—01	—0,3503	—02	—0,4436	—02	0,2326	—01	0,2488	—01
9,8	0,1023	01	0,2563	—01	—0,3422	—02	—0,4319	—02	0,2291	—01	0,2448	—01
9,9	0,1022	01	0,2520	—01	—0,3341	—02	—0,4206	—02	0,2251	—01	0,2409	—01
10,0	0,1022	01	0,2479	—01	—0,3261	—02	—0,4096	—02	0,2223	—01	0,2371	01
—0,1	0,1047	00	0,5379	—01	—0,9804	00	—0,4434	00	—0,6555	01	0,3880	01
—0,2	0,1964	00	0,9065	—01	—0,8557	00	—0,3020	00	—0,3197	01	0,1937	01
—0,3	0,2763	00	0,1156	00	—0,7451	00	—0,2019	00	—0,2080	01	0,1288	01
—0,4	0,3459	00	0,1320	00	—0,6492	00	—0,1308	00	—0,1523	01	0,9627	00
—0,5	0,4066	00	0,1424	00	—0,5667	00	—0,8004	—01	—0,1191	01	0,7671	00
—0,6	0,4597	00	0,1485	00	—0,4963	00	—0,4377	—01	—0,9699	00	0,6363	00
—0,7	0,5062	00	0,1515	00	—0,4360	00	—0,1782	—01	—0,8130	00	0,5425	00
—0,8	0,5472	00	0,1523	00	—0,3848	00	0,7189	—03	—0,6961	00	0,4721	00
—0,9	0,5834	00	0,1515	00	—0,3404	00	0,1389	—01	—0,6058	00	0,4171	00
—1,0	0,6155	00	0,1496	00	—0,3025	00	0,2314	—01	—0,5341	00	0,3730	00
—1,1	0,6441	00	0,1470	00	—0,2698	00	0,2954	—01	—0,4758	00	0,3368	00
—1,2	0,6696	00	0,1438	00	—0,2414	00	0,3383	—01	—0,4276	00	0,3066	00
—1,3	0,6925	00	0,1403	00	—0,2168	00	0,3658	—01	—0,3872	00	0,2810	00
—1,4	0,7131	00	0,1365	00	—0,1954	00	0,3819	—01	—0,3528	00	0,2590	00
—1,5	0,7316	00	0,1327	00	—0,1766	00	0,3896	—01	—0,3233	00	0,2399	00
—1,6	0,7484	00	0,1288	00	—0,1601	00	0,3911	—01	—0,2977	00	0,2232	00
—1,7	0,7637	00	0,1249	00	—0,1455	00	0,3882	—01	—0,2753	00	0,2085	00
—1,8	0,7776	00	0,1210	00	—0,1327	00	0,3821	—01	—0,2556	00	0,1954	00
—1,9	0,7903	00	0,1172	00	—0,1212	00	0,3737	—01	—0,2381	00	0,1836	00

55

Table I.1 (continued)

u'	$\mathfrak{F}_r$		$\mathfrak{F}_i$		$\mathfrak{F}'_r$		$\mathfrak{F}'_i$		F_r		F_i	
—2,0	0,8019	00	0,1135	00	—0,1111	00	0,3637	—01	—0,2225	00	0,1731	00
—2,1	0,8125	00	0,1099	00	—0,1020	00	0,3527	—01	—0,2086	00	0,1635	00
—2,2	0,8223	00	0,1065	00	—0 9390	—01	0,3411	—01	—0,1960	00	0,1549	00
—2,3	0,8314	00	0,1031	00	—0,8662	—01	0,3291	—01	—0,1846	00	0,1470	00
—2,4	0,8397	00	0,9990	—01	—0,8007	—01	0,3170	—01	—0,1743	00	0,1397	00
—2,5	0,8474	00	0,9679	—01	—0,7415	—01	0,3049	—01	—0,1649	00	0,1313	00
—2,6	0,8545	00	0,9380	—01	—0,6881	—01	0,2931	—01	—0,1563	00	0,1269	00
—2,7	0,8612	00	0,9093	—01	—0,6396	—01	0,2814	—01	—0,1484	00	0,1213	00
—2,8	0,8673	00	0,8817	—01	—0,5956	—01	0,2702	—01	—0,1412	00	0,1160	00
—2,9	0,8731	00	0,8552	—01	—0,5555	—01	0,2592	—01	—0,1345	00	0,1111	00
—3,0	0,8785	00	0,8298	—01	—0,5190	—01	0,2487	—01	—0,1283	00	0,1066	00
—3,1	0,8835	00	0,8055	—01	—0,4856	—01	0,2385	—01	—0,1226	00	0,1023	00
—3,2	0,8882	00	0,7821	—01	—0,4550	—01	0,2288	—01	—0,1172	00	0,9838	—01
—3,3	0,8926	00	0,7597	—01	—0,4269	—01	0,2195	—01	—0,1123	00	0,9467	—01
—3,4	0,8967	00	0,7382	—01	—0,4011	—01	0,2106	—01	—0,1077	00	0,9118	—01
—3,5	0,9006	00	0,7176	—01	—0,3774	—01	0,2021	—01	—0,1033	00	0,8791	—01
—3,6	0,9043	00	0,6978	—01	—0,3555	—01	0,1939	—01	—0,9931	—01	0,8483	—01
—3,7	0,9077	00	0,6788	—01	—0,3353	—01	0,1862	—01	—0,9552	—01	0,8192	—01
—3,8	0,9110	00	0,6605	—01	—0,3166	—01	0,1788	—01	—0,9197	—01	0,7917	—01
—3,9	0,9141	00	0,6430	—01	—0,2993	—01	0,1717	—01	—0,8862	—01	0,7658	—01
—4,0	0,9170	00	0,6262	—01	—0,2832	—01	0,1650	—01	—0,8547	—01	0,7412	—01

Let us calculate $K_1(c)$

$$K_1(c) = \int\limits_0^1 (u-c)^{-2} dy = -\frac{1}{u_\kappa'^2 \cdot y_\kappa (1-y_\kappa)} + \frac{\tilde{u}_\kappa}{u_\kappa'^3} \ln \frac{-y_\kappa}{1-y_\kappa}.$$

Selecting the integration path in the lower halfplane, which, as has already been noted, corresponds to the physical picture of the development of disturbances from damping ($c_i < 0$) to neutral ($c_i = 0$), we find

$$K_1(c) = -\frac{1}{y_\kappa \cdot u_\kappa'^2 (1-y_\kappa)} + \frac{\tilde{u}_\kappa}{u_\kappa'^3}\left(\ln \frac{y_\kappa}{1-y_\kappa} - \pi i\right). \qquad (I.101)$$

It is possible to simplify formula (I.101), assuming that $c \approx y_k u_k'$,

$$K_1(c) \simeq -\frac{1}{c(u_\kappa'-c)} + \frac{\tilde{u}_\kappa}{u_\kappa'^3}\left(\ln \frac{c}{u_\kappa'-c} - \pi i\right). \qquad (I.102)$$

Then considering that $c \ll 1$, we set $u_k' - c \approx u_k'$

$$\ln c - \ln(u_\kappa'-c) \approx \ln c - \ln u_\kappa' \approx \ln c,$$

for $u_k^1 \approx 1$. Then (I.102) is simplified further

$$K_1(c) = -\frac{1}{c \cdot u_\kappa'} + \frac{u_\kappa''}{u_\kappa'^3}(\ln c - \pi i).$$
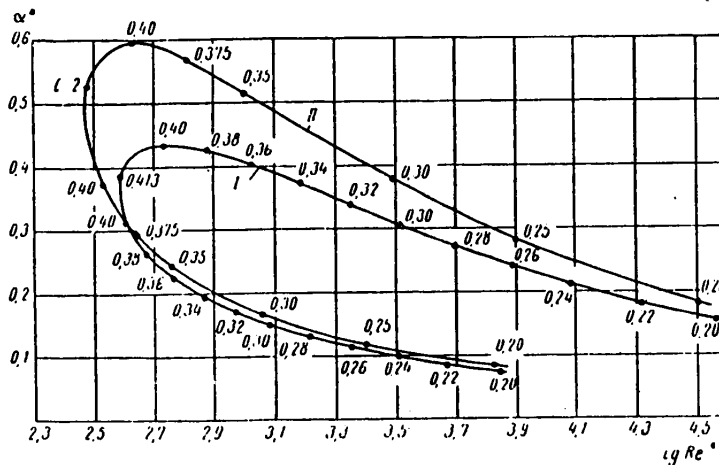
(I.103)

Figure I.14. Neutral curves for the Blasius profile.
I — calculation using formula (I.101); II — calculation using formula (I.103).

The results of the calculations performed for the Blasius profile using formulas (I.101) and (I.103) are represented in Figure I.14. Curve I calculated on the basis of formula (I.101) by V. V. Droblenkov is located very close to the Lin neutral stability curve. Curve II was constructed on the basis of expression (I.103).

All further arguments are made for $K_1(c)$ defined by (I.103), although it is possible to use formula (I.101) entirely analogously.

Substituting (I.103) in (I.100), we find the real and imaginary parts of the value of z

$$z_r = -\frac{u_0'}{u_\kappa'} + \frac{u_0' c u_\kappa''}{u_\kappa'^3}\ln c + \frac{u_0' c}{a(1-c)^2};$$

(I.104)

$$z_i = -\pi \cdot u_0' c \cdot \frac{u_\kappa''}{u_\kappa'^3}.$$

(I.105)

Thus, it is possible to propose the following scheme for calculating the neutral stability curve, which is an altered scheme for the known graphoanalytical method of the German school (Tietjens, Tollmien, Schlichting). The change in the direction of simplification took place when calculating the functions $E_r(\alpha, c)$, $E_i(\alpha, c)$.

57
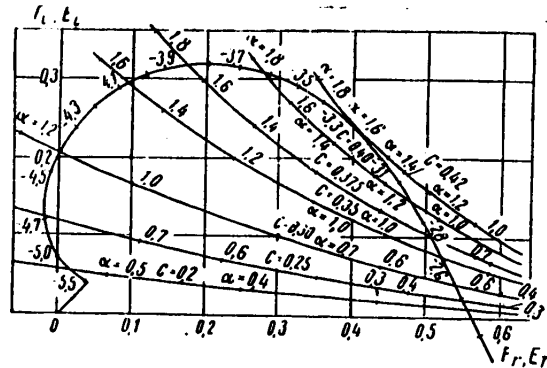
Figure I.15. Graphical solution of the characteristic
equation of the problem.

The curve $F_i = F_i(F_r)$ (Figure I.15) is constructed by Table I.1 on the coordinate axes $[F_r, F_i]$. The curves $E_i = E_i(E_r)$ are plotted on the same graph for fixed values of c and different α. The corresponding values of the variables w and α are noted on the curves. Preliminary calculations are performed by the formulas

$$E_r(\alpha, c) = \frac{c}{y_\kappa \cdot u_0'} \cdot \frac{z_r + z_r^2 + z_i^2}{(1 + z_r) + z_i^2};$$

$$E_i(\alpha, c) = \frac{c}{y_\kappa \cdot u_0'} \cdot \frac{z_i}{(1 + z_r)^2 + z_i^2},$$

(I.106)

where z_r and z_i are determined from (I.104), (I.105).

Joint values of α, c,w are found at the points of intersection of the curves $E_i(E_r)$ and $(F_i(F_r)$. Since the velocity profile investigated for stability is given, the values of y_k and u_k' are defined for the obtained value of c. Then the Re number corresponding to the obtained α is calculated

$$Re = \left(\frac{w}{y_\kappa}\right)^3 \cdot \frac{1}{\alpha u_\kappa'}.$$

Thus, a neutral curve in the plane [Re, α] will be constructed. Usually the neutral stability curve is constructed in the coordinates [Re*, α*] which are obtained from values of Re and α by multiplication by the ratio $\delta*/\delta$. The neutral stability curve for the Blasius profile, the data for which taken from reference [13] are presented in Table I.2, was calculated by the proposed scheme as an example. The graphical solution of the basic equation of the problem is illustrated in Figure I.15. Figure I.16 gives the neutral stability curves for the Blasius profile obtained by Tollmien [24], Schlichting [92], Pretsch [14], Lin [67], Zaat [95], and the curve constructed by the above-discussed scheme are plotted in Figure I.16.

The Tollmien-Schlichting method does not require any additional assumptions when solving equation (I.99). However, it is very labor-consuming, for the required range of variation of the parameter c in the general case of investigation of an arbitrary velocity distribution profile is unknown. Accordingly, let us discuss the analytical method of calculating a neutral curve by the basic ideas of Lin [67].

58
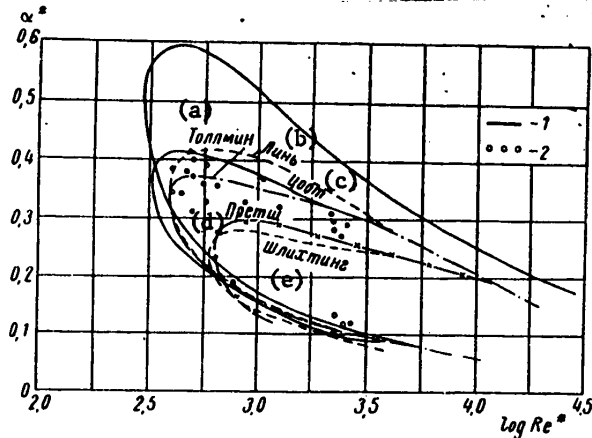
Figure I.16. Neutral stability curves for the Blasius profile (critical numbers Re^*_{cr}: Pretsch, 680; Schlichting, 575; Zaat, 321; Lin, 420; Tollmien, 420; proposed scheme, 295). 1 — calculation by the proposed scheme; 2 — Schubauer and Skramstad experiment.

Key: a. Tollmien   c. Zaat   e. Schlichting
      b. Lin   d. Pretsch

Figure I.17. Graph of the function $\mathfrak{F}_r = \mathfrak{F}_r(w)$.

The complex equation (I.99) is written as follows

$$F(w)(1 + \Delta) = \frac{z}{1 + z},$$ (I.107)

where the value of Δ is defined by the equality

59

Table I.2. Howarth Profiles

$$\eta = \frac{y}{\delta}, \qquad u = \frac{u}{U_m}, \qquad \bar{u}' = \frac{\delta}{U_m}\cdot\frac{du}{dy}, \qquad \bar{u}'' = \frac{\delta^2}{U_m}\cdot\frac{d^2u}{dy^2}$$

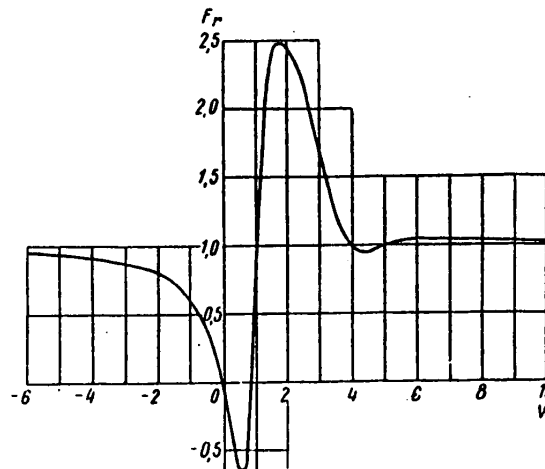| $r = 0$				$r = -0.025$				$r = -0.050$				$r = -0.075$			
η	$\bar{u}$	$\bar{u}'$	$\bar{u}''$	η	$\bar{u}$	$\bar{u}'$	$\bar{u}''$	η	$\bar{u}$	$\bar{u}'$	$\bar{u}''$	η	$\bar{u}$	$\bar{u}'$	$\bar{u}''$
0	0	1.680	0	0	0	1.776	-0.566	0	0	1.853	-1.014	0	0	1.916	-1.38
0.0395	0.066	1.678	-0.028	0.084	0.148	1.725	-0.662	0.089	0.161	1.760	-1.093	0.094	0.173	1.786	-1.42
0.079	0.133	1.676	-0.112	0.168	0.290	1.659	-0.942	0.178	0.312	1.654	-1.32	0.187	0.333	1.635	-1.62
0.1185	0.199	1.666	-0.252	0.252	0.425	1.563	-1.374	0.267	0.454	1.522	-1.67	0.281	0.479	1.747	-1.90
0.158	0.265	1.655	-0.445	0.337	0.551	1.426	-1.881	0.356	0.582	1.355	-2.07	0.374	0.609	1.287	-2.19
0.198	0.330	1.635	-0.685	0.421	0.664	1.248	-2.35	0.445	0.694	1.156	-2.40	0.468	0.719	1.077	-2.41
0.237	0.394	1.601	-0.964	0.505	0.760	1.048	-2.65	0.534	0.787	0.934	-2.56	0.561	0.809	0.845	-2.44
0.276	0.456	1.560	-1.270	0.589	0.858	0.810	-2.69	0.623	0.859	0.709	-2.47	0.655	0.877	0.624	-2.27
0.316	0.517	1.500	-1.595	0.673	0.897	0.592	-2.46	0.712	0.913	0.502	-2.17	0.748	0.926	0.428	-1.91
0.356	0.575	1.431	-1.920	0.757	0.938	0.401	-2.03	0.801	0.950	0.333	-1.71	0.842	0.959	0.280	-1.44
0.395	0.630	1.350	-2.220	0.841	0.965	0.254	-1.51	0.889	0.973	0.206	-1.21	0.935	0.978	0.159	-0.98
0.474	0.729	1.154	-2.690	0.926	0.982	0.149	-1.02	0.978	0.986	0.119	-0.48	1.029	0.990	0.085	-0.61
0.553	0.812	0.919	-2.900	1.004	0.991	0.080	-0.62	1.067	0.994	0.056	-0.45	1.122	0.995	0.042	-0.33
0.632	0.876	0.704	-2.790	1.093	0.996	0.038	-0.35	1.157	0.997	0.033	-0.24	1.218	0.998	0.019	-0.17
0.711	0.923	0.496	-2.420	1.178	0.998	0.019	-0.18	1.246	0.999	0.017	-0.11	1.312	0.999	0.008	-0.08
0.790	0.956	0.324	-1.900	1.262	0.999	0.008	-0.08	1.335	1.000	0.009	-0.05	1.403	1.000	0.003	-0.03
0.870	0.976	0.197	-1.345												
0.949	0.988	0.111	-0.864												
1.028	0.994	0.057	-0.505												
1.107	0.997	0.028	-0.269												
1.181	0.999	0.012	-0.131												

$r = -0.1$				$r = 0.025$				$r = 0.050$				$r = 0.075$				$r = 0.1$			
η	$\bar{u}$	$\bar{u}'$	$\bar{u}''$	η	$\bar{u}$	$\bar{u}'$	$\bar{u}''$	η	$\bar{u}$	$\bar{u}'$	$\bar{u}''$	η	$\bar{u}$	$\bar{u}'$	$\bar{u}''$	η	$\bar{u}$	$\bar{u}'$	$\bar{u}''$
0	0	1.972	-1.68	0	0	1.559	0.735	0	0	1.408	1.73	0	0	1.190	3.14	0	0	0.829	5.34
0.098	0.184	1.807	-1.73	0.074	0.116	1.610	0.607	0.068	0.100	1.523	1.58	0.062	0.079	1.362	2.97	0.055	0.053	1.117	5.17
0.195	0.352	1.632	-1.87	0.148	0.237	1.643	0.215	0.136	0.205	1.618	1.14	0.124	0.168	1.534	2.48	0.110	0.122	1.387	4.63
0.293	0.502	1.440	-2.07	0.176	0.282	1.645	0	0.205	0.317	1.675	0.423	0.186	0.267	1.658	1.67	0.164	0.205	1.620	3.74
0.391	0.633	1.226	-2.28	0.222	0.358	1.645	-0.404	0.235	0.367	1.682	0	0.248	0.373	1.731	0.572	0.219	0.299	1.787	2.48
0.489	0.741	0.999	-2.39	0.295	0.478	1.580	-1.17	0.273	0.430	1.674	-0.555	0.275	0.420	1.740	0	0.274	0.399	1.882	0.916
0.586	0.828	0.767	-2.33	0.369	0.591	1.464	-1.98	0.341	0.542	1.600	-1.53	0.310	0.480	1.730	-0.708	0.305	0.458	1.883	0
0.684	0.892	0.536	-2.07	0.443	0.692	1.290	-2.68	0.409	0.645	1.463	-2.49	0.372	0.585	1.625	-1.99	0.329	0.503	1.882	-0.803
0.782	0.936	0.367	-1.69	0.517	0.779	1.075	-3.09	0.477	0.739	1.266	-3.21	0.434	0.682	1.486	-3.13	0.384	0.605	1.795	-2.51
0.879	0.965	0.236	-1.23	0.591	0.850	0.843	-3.16	0.545	0.815	1.043	-3.56	0.496	0.767	1.270	-3.87	0.438	0.698	1.640	-3.94
0.977	0.982	0.120	-0.80	0.665	0.904	0.618	-2.97	0.614	0.876	0.789	-3.48	0.558	0.839	1.016	-4.15	0.493	0.781	1.391	-4.89
1.075	0.991	0.072	-0.48	0.739	0.942	0.421	-2.46	0.682	0.924	0.565	-3.06	0.620	0.894	0.759	-3.95	0.548	0.848	1.112	-5.16
1.172	0.996	0.037	-0.24	0.813	0.968	0.268	-1.90	0.750	0.953	0.391	-2.43	0.682	0.932	0.530	-3.48	0.603	0.901	0.834	-4.87
1.271	0.998	0.016	-0.12	0.886	0.984	0.159	-1.25	0.819	0.975	0.250	-1.75	0.744	0.960	0.354	-2.64	0.658	0.939	0.575	-4.16
1.370	0.999	0.007	-0.06	0.960	0.991	0.085	-0.75	0.886	0.987	0.150	-1.15	0.806	0.977	0.209	-1.86	0.712	0.965	0.378	-3.18
1.468	1.000	0.003	-0.02	1.035	0.996	0.045	-0.42	0.955	0.993	0.083	-0.70	0.868	0.990	0.119	-1.20	0.767	0.981	0.234	-2.23
				1.108	0.998	0.020	-0.22	1.023	0.997	0.043	-0.38	0.930	0.995	0.063	-0.71	0.822	0.990	0.131	-1.41
				1.180	0.999	0.009	-0.10	1.091	0.999	0.017	-0.19	0.992	0.998	0.024	-0.38	0.877	0.995	0.070	-0.82
				1.255	1.000	0.004	-0.04	1.160	1.000	0.008	-0.09	1.053	0.999	0.012	-0.19	0.932	0.998	0.036	-0.43
				1.329	1.000	0.001	-0.01	1.228	1.000	0.003	-0.04	1.116	1.000	0.003	-0.08	0.986	0.999	0.021	-0.20

$$\Delta = \frac{y_\kappa u_0'}{c} - 1.$$

In the first approximation it is possible to consider $\Delta = 0$, which, as the calculations demonstrate, gives good accuracy when calculating the critical Reynolds numbers. It is theoretically possible to make the following approximation, defining the numerical value of Δ by the first approximation. Hereafter, the approximate equality $\Delta \simeq 0$ will be used everywhere. It makes it possible to transform equation (I.107) to the form

$$-1 + F(w) = -1 + \frac{z}{1+z}, \quad \Re(w) = \frac{1}{1-F(w)} = 1 + z.$$

(I.108)

The complex equation (I.108) is equivalent to two real ones

$$\Re_r(w) = 1 + z_r;$$

(I.109)

$$\mathfrak{F}_i(w) = z_i.$$

(I.110)

The right-hand sides of (I.109) and (I.110) are defined by formulas (I.104), (I.105). The functions $\Re_r = \Re_r(w)$, $\Re_i = \Re_i(w)$ were first calculated by Lin [67]. In Table I.1, the results were studied from calculating $\mathfrak{F}_r$, $\mathfrak{F}_i$, made by Miles [91]. Figures I.17 and I.18 illustrate the graphs for the variation of $\Re_r(w)$ and $\Re_i(w)$. Then the calculation procedure consists in the following. Let us be given a defined value of w_1. By the graphs of $\Re_r(w)$, $\Re_i(w)$ let us determine $\Re_r(w_1)$, $\Re_i(w_1)$. From equation (I.110)

$$-\pi u_0' \cdot c \frac{u_\kappa''}{u_\kappa''^3} = \Re_i(w_1),$$

which is solved for a given velocity distribution profile graphically, we find c, which means also y_k, u_k^t, u_k'' corresponding to it. Using (I.104) and (I.109), let us determine the magnitude of the parameter α

$$\alpha = \frac{u_0' c}{(1-c)^2} \frac{1}{\mathfrak{F}_r(w_1) - 1 + \frac{u_0'}{u_\kappa'} - u_0' \cdot c \frac{u_\kappa''}{u_\kappa''^3} \ln c}.$$

(I.111)

Then let us calculate the value of

$$Re = \frac{1}{u_\kappa' \cdot \alpha} \left(\frac{w_1}{y_\kappa} \right)^3.$$

(I.112)

The neutral stability curves constructed graphoanalytically and by the method described which is based on the ideas of Lin, is illustrated in Figure I.19.

§ 1.8. Formulas for Finding the Critical Reynolds Number

The form of the graph $Re = Re(\alpha)$ having the shape of a loop is defined by the two-valued nature of the function $w = w(F_1)$. This fact is a reflection of the dual role of the viscosity in controlling the disturbances occurring in a laminar boundary layer. On the other hand, the viscosity is the cause of the occurrence of a phase shift in the vicinity of the wall between the velocity components of the

61
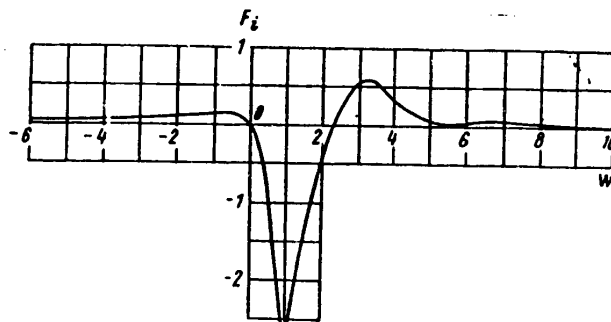
Figure I.18. Graph of the function $\mathfrak{F}_i = \mathfrak{F}_i (w)$.
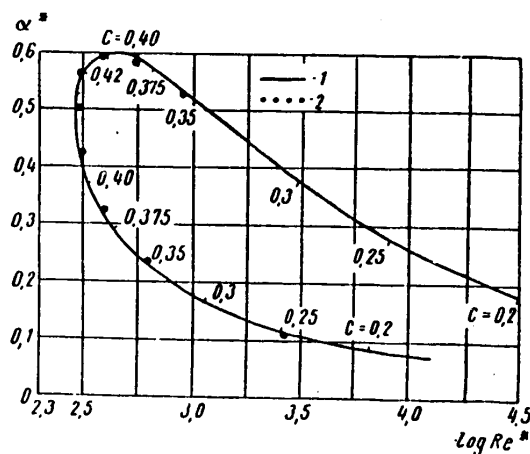
Figure I.19. Comparison of analytical and graphoanalytical methods of constructing a neutral curve. 1 -- graphoanalytical method; 2 -- analytical method.

disturbing motion, such that the Reynolds stress $\hat{t} = -\rho v_x v_y$ begins to transfer energy from the basic motion to the disturbances [12]. On the other hand, the viscosity has a damping effect on the disturbances occurring in the fluid.

Therefore the velocity profile without inflection points for Re $\rightarrow \infty$ ($v \rightarrow 0$) is stable with respect to sinusoidal oscillations of any wavelength, for the vorticity distribution across the boundary layer has a stabilizing influence on the disturbances that arise [12]. With an increase in viscosity, the Reynolds stresses arise, which insure an inflow of energy into the disturbances in the wall region at the expense of main flow energy. Thus, in some range of values of α and Re, the disturbances build with time. The instability region arises inside the neutral curve on the plane [α, Re]. Further increase in viscosity leads to an increase in energy dissipation, as a result of which all of the disturbances occurring in the laminar boundary layer are extinguished. The minimum Reynolds number for which neutral oscillations are still possible is called the critical Reynolds number for given velocity

62

profile. The curve $\tilde{N}_i = \tilde{N}_i(w)$ shown in Figure I.18 has a peak for w = 3.21 equal to 0.58. Therefore, if $z_i(c) < 0.58$, there are two values of w and, consequently, two values of Re corresponding to one value of c. If c is such that $z_i(c) = 0.58$, then there is only one value of w, and, consequently, one value of the Re number. The parameter α defining the disturbance wavelength will also be uniquely defined by formula (I.111).

In order to find the critical Reynolds number (Re_{cr}), it is possible to indicate the following procedure based on previous arguments. For a given velocity profile in the boundary layer for maximum value of $\tilde{N}_{i\,max} = 0.58$ a value of c is found from the equation

$$0.58 = -\pi \cdot u_0' \cdot c \frac{u_\kappa''}{u_\kappa'^3},$$ (I.113)

which is solved graphically. After determining c, we find the values of y_k, u_k', u_k''. Since the value of $\tilde{N}_i = 0.58$ corresponds to w = 3.21 and $\tilde{N}_r = 1.499 \simeq 1.5$, using formula (I.111), we find the critical Reynolds number

$$(a)\ Re_{\kappa p} = \frac{33(1-c)^2\left(0.5 + \frac{u_0'}{u_\kappa'} - \frac{u_0' \cdot c u_\kappa''}{u_\kappa'^3}\ln c\right)}{u_0' \cdot u_\kappa' y_\kappa'^3 \cdot c}.$$ (I.114)

Key: a. cr

Considering the assumption made earlier that $c \simeq y_k \cdot u_k'$, let us rewrite (I.114) as follows:

$$Re_{\kappa p} = \frac{33(1-c)^2\left(0.5 + \frac{u_0'}{u_\kappa'} - \frac{u_0' \cdot c u_\kappa''}{u_\kappa'^3}\ln c\right)}{u_0' \cdot c^2 y_\kappa^2},$$

or considering (I.113)

$$Re_{\kappa p} = \frac{33(1-c)\left(0.5 + \frac{u_0'}{u_\kappa'} + 0.185\ln c\right)}{u_0' \cdot c^2 y_\kappa^2}.$$ (I.115)

For small c when $u_0' \simeq u_k'$ and $c \simeq y_k u_0'$, formula (I.115) is still simplified

$$Re_{\kappa p} = \frac{33 u_0'(1-c)^2(1.5 + 0.185\ln c)}{c^4}.$$

For example, let us determine the critical Reynolds number for the Blasius profile (see Table I.2). Solving equation (I.113) graphically, we find c = 0.415, y_k = 0.25, u_k' = 1.59, u_k'' = -1.06, ln c = -0.883, u_0' = 1.68. By formula (I.115) let us calculate Re_{cr} = 942, Re^*_{cr} = 322.

Considering the curve for the function $\tilde{N}_i = \tilde{N}_i(w)$ (Figure I.18), it can be noted that in addition to the peak in the interval 2 < w < 5, there are peaks of the same type in the intervals -3 < w < 0; 5 < w < 8, where the behavior of the neutral curve can

63

formally be of the same nature as in the first interval. Detailed calculations by the scheme discussed in § I.7 demonstrated that in the region of negative w the critical Reynolds numbers are also found to be negative which has no physical meaning. In the range of 5 < w < 8, the neutral curve is actually deformed somewhat, but on the basis of insignificant variation of the curve $\tilde{N}_i = \tilde{N}_i(w)$, this deformation is found to be negligibly small and in no way is felt in the magnitude of the critical Reynolds number. Calculations with respect to investigating the behavior of the neutral curve in the indicated three intervals were performed for velocity profiles with $\lambda = -2, 0, 2$ (λ is the Pohlhausen parameter when using a sixth-degree polynomial for approximation of the velocity distribution in the boundary layer).

It must be noted that the formula for the critical Reynolds number (I.115) differs from the corresponding Lin formula [12], [67]. This difference is explained by the approximate nature of the methods of solving the problem of hydrodynamic stability of the laminar form of flow, on the basis of which various authors can use a different degree of approximation in their constructions. In particular, Lin [67] used the approximate equality $\alpha = u_0' c$ for determination of the parameter α at the same time as the value of α was determined from the expression (I.111) when deriving the formula (I.115).

§ I.9. Construction of Asymptotic Branches of a Neutral Stability Curve

The behavior of the neutral stability curve for the boundary layer for different Reynolds numbers was investigated in the papers by Tollmien [24], [96], Schlichting [13], Schlichting and Ulrich [15], and Lin [67]. In this section a study is made of the behavior of a neutral curve for large values of the Re number based on the expressions obtained above.

Let us consider the intersection of the polar diagram (Figure I.15) with the positive part of the x-axis. At this point $F_i = 0$, and consequently, in its vicinity the value of

$$z_i = -\pi \cdot c \cdot u_0' \cdot \frac{u_\kappa''}{u_\kappa'^3}$$

differs insignificantly from zero. Considering the case of a velocity profile without inflection points ($\lambda \geq 0$), we arrive at the conclusion that in the vicinity of the point where $F_r = 0.56$, w = 2.3, the value of $c \to 0$. Then in the expression

$$z_r = -\frac{u_0'}{u_\kappa'} + \frac{c u_0' \cdot u_\kappa''}{u_\kappa'^3} \ln c + \frac{u_0' \cdot c}{(1-c)^2 \alpha}$$

it is possible to neglect the second term, for $c \ln c \to 0$ for $c \to 0$, and it is possible to consider $u_0' \simeq u_k'$. Thus,

$$z_r = -1 + \frac{u_0' c}{\alpha}.$$

Considering the first equality of (I.106) and the approximate expression $c \simeq u_0' \cdot y_k$, we find

$$F_r = 0.56 = E_r = \frac{-\alpha + c u_0'}{c u_0}.$$

It is impossible to neglect the third term in the formula for z_r, for α can be quite small. For the Blasius profile $u_0' = 1.68$, and the preceding equality gives the expression

$$\alpha \cdot 0.738c. \tag{I.116}$$

From the expressions $w = y_\kappa (\alpha \operatorname{Re} u_\kappa)^{1/3}$, $y_\kappa = \dfrac{c}{u_\kappa}$ considering (I.116), we find

$$\operatorname{Re} = 13.8 \cdot \alpha^{-4} \quad \text{or} \quad \operatorname{Re} = 46.2c^{-4}. \tag{I.117}$$

For Tollmien [24], the corresponding branch of the neutral stability curve is described by the formula $\operatorname{Re} = 46 \cdot c^{-4}$. On transition to Re*, we obtain Re* = $15.75c^{-4}$ for the Blasius profile. Thus, the equation is obtained for the lower branch of the neutral curve.

The equation of the upper branch of the neutral stability curve is obtained from investigation of equation (I.99) in the vicinity of the origin of the coordinates of a plane [E_r, E_i]. Using (I.78), let us calculate the expression

$$-\frac{1}{y_\kappa} \cdot \frac{\varphi_3(0)}{\varphi_3'(0)} = -\frac{1}{u_\kappa} \cdot \frac{c}{\frac{5}{4} u_0' - c(1-i) \mid \frac{1}{2} \alpha c \operatorname{Re}}.$$

For large values of Re, we find

$$F_r + iF_i = \frac{1}{y_\kappa} \cdot \frac{1 + i}{\sqrt{2\alpha c \operatorname{Re}}}.$$

For the Blasius profile $u_\kappa'' = -18.4y_\kappa^2 = -6.55c^2$. Hence, considering smallness of c, it is possible to calculate $E_i = 2.6 \cdot c \cdot \alpha^2$. For large Reynolds numbers it is possible to set $F_r \simeq 0$, which, using the equality $E_r = F_r$, permits establishment of the relation of the parameters α and c.

$$E_r = \frac{-\alpha + u_0' \cdot c}{c \cdot u_0'} = 0, \quad \alpha = u_0' c.$$

In the case of the Blasius profile $\alpha = 1.68$. Considering the expression $F_i = E_i$, let us establish the relation $\operatorname{Re} = \operatorname{Re}(\alpha)$:

$$\left.\begin{array}{l} \dfrac{1.68}{c\sqrt{2\alpha c \operatorname{Re}}} = 2.6 \cdot c \cdot \alpha^2; \\[2mm] \operatorname{Re} = 2.8\alpha^{-10}; \quad \operatorname{Re} = 0.0156c^{-10}. \end{array}\right\} \tag{I.118}$$

According to Tollmien's calculations, the upper branch of the neutral stability curve is described by the equation $\operatorname{Re} = 0.0181c^{-10}$. The neutral stability curve for the Blasius profile, the asymptotic branches of which are constructed by formulas (I.117) and (I.118), is shown in Figure I.20. It is more convenient to use the following relations for the calculations:

for the lower branch of the curve

$$\lg \mathrm{Re}^* = \lg 13,8 - 5 \lg \frac{\delta}{\delta^*} - 4 \lg \alpha^*;$$

for the upper branch of the curve

$$\lg \mathrm{Re}^* = \lg 2,8 - 11 \lg \frac{\delta}{\delta^*} - 10 \lg \alpha^*.$$
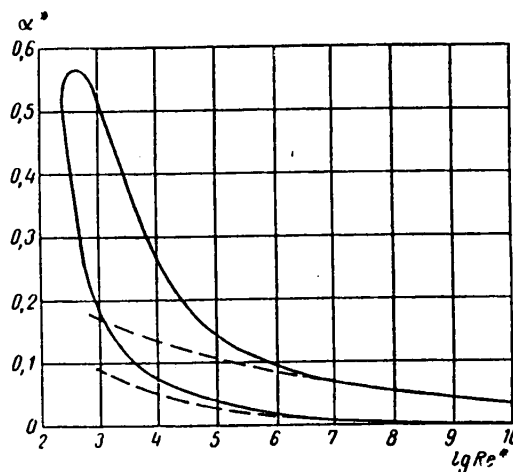
Figure I.20. Asymptotic branches of the neutral
stability curve.

Let us construct the formulas for the asymptotic branches of a neutral curve of
arbitrary velocity profile in a laminar boundary layer analogously. For the lower
branch of the neutral curve let us consider the vicinity of the intersection point
of the polar diagram with the real axis where $\tilde{n}_i = 0, \tilde{n}_r = 2,294, w = 2,3$. On the
basis of formula (I.111) we have:

$$\alpha = \frac{u_0' \cdot c}{(1 - c)^2} \cdot \frac{1}{1,3 + \frac{u_0'}{u_\kappa'} - \frac{c \cdot u_0' \cdot u_\kappa''}{u_\kappa'^3} \ln c}. \qquad (I.119)$$

Using the smallness of c, we shall consider $u_\kappa' \approx u_0', y_\kappa = \frac{c}{u_0'}.$ Then

$$\alpha = \frac{u_0' c}{2,3 - \frac{c \cdot u_\kappa''}{u_0'^2} \ln c};$$

$$\mathrm{Re} = \left(\frac{2,3}{y_\kappa}\right)^3 \cdot \frac{1}{\alpha \cdot u_\kappa'} \simeq \frac{28 \cdot u_0'}{c^4}.$$

As a result, the following formulas are obtained for calculating the lower branch
of the neutral stability curve for small c:

$$\alpha = \frac{c \cdot u'_0}{2,3}, \quad \text{Re} = \frac{28 \cdot u'_0}{c^4}.$$

The upper branch of the neutral curve corresponds to the vicinity of the null point of the polar diagram. At this point $F(w) = 0$; therefore $\tilde{v}_r(w) = 1$. The parameter α will be defined by a formula analogous to (I.119),

$$\alpha = \frac{u'_0 c}{(1-c)^2} \cdot \frac{1}{\dfrac{u'_0}{u'_\kappa} - \dfrac{u'_0 \cdot c \cdot u''_\kappa}{u'^3_\kappa} \ln c} \simeq u'_0 c. \qquad (I.120)$$

For establishment of the relation Re = Re(c) in the vicinity of the origin of the coordinates we shall use the equality $E_1 = F_1$

$$\frac{c}{u_\kappa \cdot u_0} \cdot \frac{-\pi \cdot u'_0 c \cdot \dfrac{u''_\kappa}{u'^3_\kappa}}{(1+z_r)^2 + \pi^2 u'^2_0 \cdot c^2 \dfrac{u''^2_\kappa}{u'^6_\kappa}} = \frac{u'_0}{c\sqrt{2\pi c \, \text{Re}}}. \qquad (I.121)$$

Considering that $c \ll 1$, $y_k \cdot u'_0 \simeq c$, $u^k_k \simeq u^k_0$ and using (I.120), we find

$$\text{Re} = \frac{u'^5_0}{2\pi^2} \cdot \frac{1}{c^6 \cdot u''^2_\kappa}. \qquad (I.122)$$

It is possible to obtain formula (I.118) directly from (I.122). Considering expression (I.121), it is possible to arrive at the conclusion that in the presence of an inflection point in the velocity profile ($u''_\text{II} = 0$) the left side can approach zero not only for $c \to 0$, but also for $c \to c_\text{II}$, which corresponds to y_II such that $u''(y_\text{II}) = 0$. Therefore for observation of the equality (I.121) when Re $\to \infty$, the upper branch of the neutral curve can approach $\alpha \neq 0$. This fact indicates the presence of non-viscous instability of the velocity profile with an inflection point [4].

Knowing the position of this point for the velocity profile with an inflection point ($\lambda < 0$), that is, the value of y_II, it is possible to find c_II and, using (I.120), to calculate the value of α_II, which is approached by the upper branch of the neutral stability curve for Re $\to \infty$

$$\alpha_\text{II} = \frac{u'_0 \cdot c_\text{II}}{(1-c_\text{II})^2}.$$

Proceeding to α^*, we obtain

$$\alpha^*_\text{II} = \frac{u'_0 \cdot c_\text{II}}{(1-c_\text{II})} \cdot \frac{\delta^*}{\delta}.$$

67

§ I.10. Experimental Confirmation of the Basic Conclusions of Stability Theory

The study of the stability of a laminar boundary layer has developed historically so that the first results were obtained in the theoretical studies by Tollmien and Schlichting. It was only after 13 years that Schubauer and Skramsted, creating a flow with a low degree of turbulence (0.02%), confirmed all the basic conclusions of the theoretical research of [4], [11], [16] and [12] well.

Schubauer and Skramsted performed experiments on a plate. Oscillations of different frequency were created in a boundary layer using a metal plate and electromagnets. Observing the development of these oscillations, it was possible to determine under what conditions the oscillations do not damp and do not build. The corresponding dimensionless frequency of neutral oscillations defined the point in the plane [$Re*$, $\beta_r \nu/U^2$], where $\beta_r = \alpha \cdot c \cdot U_0/\delta$. It is also possible to reconstruct the theoretical curve $Re* = Re*$, $(\alpha*)$ in the plane [$Re*$, $\beta_r \nu/U^2$], for each point $(\alpha*, Re*)$ of the indicated curve corresponds to a defined value of c (Figure I.19).

A comparison of the theoretical calculations with the experimental data of Schubauer and Skramsted is shown in Figure I.21. Schubauer and Skramsted made their measurements in the boundary layer using a thermoanemometric device.

Recently Burns, Childs, Nicol and Ross [97] performed analogous studies in the boundary layer. However, for measurements of the velocity pulsations they used a light plate which underwent oscillatory movements under the effect of the transverse component of the pulsation velocity in the boundary layer. The plate oscillations were recorded using a reflected beam. Experimental points are shown on Figure I.21.

Stability theory also found qualitative confirmation in the experimental paper by Berg [98]. Using smoke plumes, Berg observed oscillations of a wing in the boundary layer (NACA-0012). A display was obtained on a stroboscope. The oscillation source was a loud speaker generating sound of different frequency. The oscillations were observed near the wing surface in the region of positive pressure gradients.

In the three mentioned experimental papers studies were performed in air flows. Analogous experiments were set up in water by Wortmann [26], who used the telluric method for visual representation of the flow and Hama [99]. In both cases the oscillations in the boundary layer were created using a vibrating strip by the scheme first used by Schubauer and Skramstad.

The results of Wortmann and Hama, which agreed well with the theoretical results and the data of other authors are presented in Figure I.21.

Investigation of the expression for the amplitude of the disturbing motion current function (§ I.6 and § I.7) indicates that as a result of the presence of a singularity at the point $y = y_k$, for $y > y_k$ the disturbing motion is described by a formula of the type

$$[F_1(y) + F_2(y) \ln(y - y_\kappa)] e^{i\alpha(x - ct)},$$

and for $y < y_k$ the corresponding expression must have the following structure:
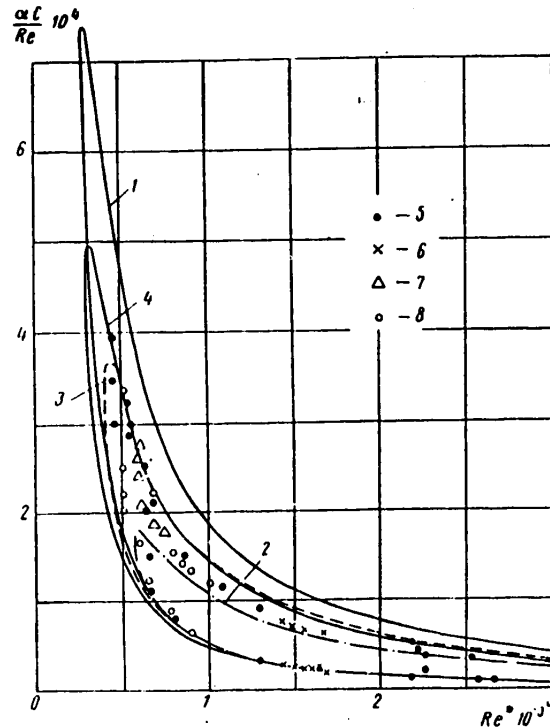
Figure I.21. Comparison of the calculated neutral stability curves
for the Blasius profile with experimental data. 1 — calculation
by the proposed formulas; 2 — Schlichting calculation; 3 — Lin
calculation; 4 — Zaat calculation; 5 — Schubauer and Skramstad
experiment; 6 - Burns, Childs, Nicol and Ross experiment; 7 —
Hama experiment; 8 — Wortmann experiment.

$$[F_1(y) + F_2(y) \ln |y_\kappa - y_\kappa| - i\pi \cdot P_2(y)] e^{i\alpha \, (x-ct)}.$$

Thus, for transition through a critical layer, a phase discontinuity arises in the
oscillations determining the disturbing motion. This conclusion was obtained
theoretically by Tollmien. The experiments of Schubauer and Skramstad confirmed
it brilliantly. They were also able to obtain surprising comparison of the amplitude
distribution of the oscillations across the boundary layer with the Schlichting
calculations [90].

It is also necessary to point out the recently published results of the experimental
studies of Schilz [27] which agreed satisfactorily with thetheoretical calculations
of the neutral stability curve. Using thermoanemometers, Schilz studied the be-
havior of small disturbances introduced into the boundary layer of a plate, a
surface over which flow was taking place vibrating by a known law.

In conclusion of this section, let us present a statement by one of the founders
of hydrodynamic stability theory, H. Schlichting [4]: "Experimental studies have

69

so brilliantly confirmed stability theory that it must be considered a fully checked-out component part of hydroaeromechanics."

§ I.11. Application of Stability Theory Results in Calculations of the Length of a Laminar Segment of a Boundary Layer

By the length of the laminar segment we mean the distance between the initial (frontal) point of the body over which the flow is taking place and the loss of stability point of the laminar boundary layer. We exclude the transition zone (see § I.1) from the investigation, for its extent depends on several factors [4], the most important of which are the degree of turbulence of the external flow, the external pressure gradient, and surface roughness.

Failure to consider the transition zone in the boundary layer leads to underestimation of the length of the laminar segment, which goes "into reserve" for the calculations connected with laminarization of the boundary layer. For practical calculations of the loss of stability point of a laminar boundary layer on bodies with a pressure gradient along the surface, it is necessary to have the function $Re^*_{cr} = Re^*_{cr}(\lambda)$. Instead of the Pohlhausen form parameter it is possible to use any other parameter reflecting the relation between the pressure forces and frictional forces in the boundary layer. Here it is necessary to consider that the families of profiles constructed by different methods using the same parameter $\lambda = U' \cdot \delta^2 / \gamma$ can differ from each other on the basis of the limited nature of the single-parametric method of approximating velocity profiles in the boundary layer. As an example it is possible to present a comparison of the family of profiles constructed by the Pohlhausen method with the application of a fourth-degree polynomial [13] and the analogous family in the case of using a sixth-degree polynomial [15].

For the possibility of determining how the form of the approximation of the velocity profiles in the laminar boundary layer influences the critical Reynolds number, calculations were made by the scheme in § I.8 of the functions $Re^*_{cr} = Re^*_{cr}(\lambda)$ based on the family of Pohlhausen profiles (sixth degree polynomial), the family of Howart profiles and the family of Basin profiles.

In the first case the velocity distribution across the boundary layer is expressed by the formula

$$u = F_6(y) + \lambda G_6(y),$$

$$0 \leqslant y \leqslant 1,$$

where the functions
$$F_6(y) = 2y - 5y^4 + 6y^5 - 2y^6,$$

$$G_6(y) = \frac{2}{10}y - \frac{1}{2}y^2 + y^4 - y^5 + \frac{3}{10}y^6.$$

together with their first and second derivatives are presented in Table I.3 taken from reference [15]. The family of Howart profiles is determined by the following dependence of the velocity at the boundary of the boundary layer on the longitudinal coordinate $U9x) = U_0(1 - r)$, where $U_0 = U(0)$; $r = -(\bar{x}/U_0)(dU/d\bar{x})$ ($\bar{x}$ is a dimensional variable). If $r < 0$, then the velocity increases with an increase in $\bar{x}$; if $r > 0$, the velocity decreases with an increase in $\bar{x}$. The velocity distribution in the boundary layer depends on the magnitude of the parameter r. The values of the functions $u(y)$, $u'(y)$, $u''(y)$ taken from reference [13] are presented in Table I.2.

Table I.3. Functions F_6 and G_6

y/δ_6	F_6	G_6	F_6'	G_6'	F_6''	G_6''
0	0	0	2	0,200	0	—1
0,05	0,1000	0,00876	1,997	0,150	—0,165	—0,966
0,10	0,1996	0,01509	1,983	0,104	—0,486	—0,900
0,15	0,2980	0,01918	1,946	0,061	—0,975	—0,793
0,20	0,3938	0,02130	1,884	0,025	—1,536	—0,662
0,25	0,4858	0,02175	1,793	—0,006	—2,109	—0,528
0,30	0,5726	0,02089	1,674	—0,028	—2,646	—0,388
0,35	0,6528	0,01905	1,528	—0,044	—3,105	—0,253
0,40	0,7252	0,01643	1,366	—0,054	—3,456	—0,126
0,45	0,7891	0,01380	1,185	—0,057	—3,675	—0,015
0,50	0,8438	0,01094	0,999	—0,056	—3,750	—0,067
0,60	0,9253	0,00584	0,634	—0,044	—3,456	0,170
0,70	0,9685	0,00232	0,326	—0,026	—2,646	0,181
0,80	0,9938	0,00056	0,116	—0,010	—1,536	0,126
0,90	0,9995	0,00005	0,017	—0,002	—0,486	0,044
1,00	1,0000	0	0	0	0	0

The stability calculations for the Howart profiles were performed as a function of the parameter r. Recalculation for the Pohlhausen parameter (λ_6) was made using the functional relation $r = r(\lambda_4)$ [13] and the approximate relation $\lambda_6 = 1.152\lambda_4$ [15]. The values of r and the values of λ_6 corresponding to them for which the stability was calculated appear in Table I.4.

The family of Basin profiles is defined by the following velocity distribution across the boundary layer [93]:

$$u = \left[1 + \lambda_B \cdot \frac{2}{\pi^2}\left(1 - \sin\frac{\pi y}{2}\right)\right]\sin\frac{\pi y}{2}. \tag{I.123}$$

The derivatives u' and u" are found by differentiation of (I.123) with respect to the y-coordinate. Using (I.123), it is possible to obtain [93] the expressions for the displacement thickness and pulse loss thickness

$$\frac{\delta^*}{\delta} = 0,363 - 0,028\lambda_B;$$

$$\frac{\delta^{**}}{\delta} = -0,00108\lambda_B^2 - 0,00296\lambda_B + 0,1366.$$

The stability calculations for the family of Basin profiles were performed for different values of the parameter λ_B. The relation between the parameters λ_6 and λ_B will be found from the condition of equality of the pulse loss thicknesses for the corresponding values of λ_6 and λ_B. Schlichting and Ulrich used the analogous condition when establishing the relation $\lambda_6 = \lambda_6(\lambda_4)$ [15]

$$\delta_6^2 \left(0{,}1366 - 0{,}00296\lambda_6 - 0{,}00108\lambda_6^2\right)^2 =$$

$$= \delta_6^2 \left(\frac{985}{9009} - \frac{19\lambda_6}{18018} - \frac{1}{6435}\lambda_6^2\right)^2. \tag{I.124}$$

Multiplying both sides of the equality (I.124) by $(dU/d\bar{x})(1/\nu)$, we find the relation:

$$\left.\begin{aligned} \lambda_6 &= \lambda_6(\lambda_6); \\ \lambda_6 \left(0{,}1366 - 0{,}00296\lambda_6 - 0{,}00108\lambda_6^2\right)^2 &= \\ = \lambda_6 \left(0{,}109 - 0{,}00105\lambda_6 - 0{,}000155\lambda_6^2\right)^2. \end{aligned}\right\} \tag{I.125}$$

The range of variation of λ_B, λ_6 in practice was bounded by the limits $10 > \lambda_6$, $\lambda_B > -10$. Therefore in equality (I.125) let us retain only the first-degree terms with respect to λ_6, λ_B, which leads to an approximate function $\lambda_B = 0{.}64\lambda_6$ or $\lambda_6 = 1{.}56\lambda_B$.

Table I.4. Relation of the form
parameters r and λ_6

r	λ_6
—0,100	3,88
—0,075	2,26
—0,050	1,64
—0,025	0,875
0	0
0,025	—1,04
0,050	—2,30
0,075	—3,86
0,100	—6,05

In order to simplify the calculations for each family of profiles graphs of the variable were constructed

$$M(c) = -\pi \cdot c \cdot u_0 \cdot \frac{u_\kappa''}{u_\kappa'^3}$$

for different values of λ_6, r, λ_B (Figure I.22, I.23, I.24). This type of graph greatly facilitates the graphical solution of equations of the type
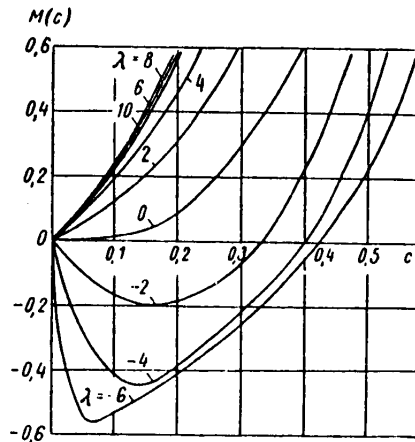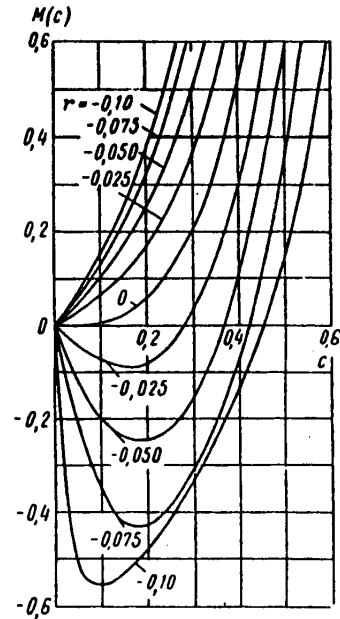
$$\mathfrak{F}_l = -\pi c u_0 \cdot \frac{u_\kappa''}{u_\kappa'^3}.$$

The critical Reynolds numbers were calculated by the scheme § I.8 using formulas (I.113) and (I.115). On transition from Re_{cr} to Re_{cr}^*, the following expressions were used:

for the family of Pohlhausen profiles [15]

$$\frac{\delta^*}{\delta} = \frac{2}{7} - \frac{\lambda_6}{105},$$

Figure I.22. Graph of the function M(c)
for the family of Pohlhausen profiles.

Figure I.23. Graph of the function
M(c) for the family of Howarth profiles.
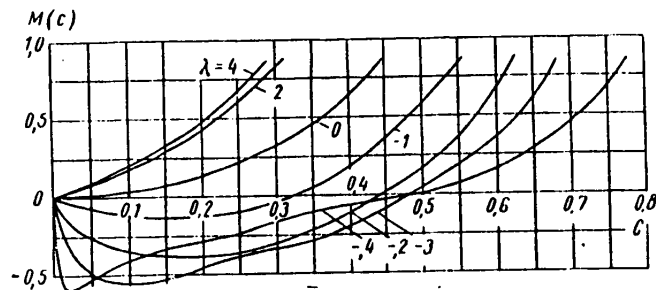
Figure I.24. Graph of the function M(c) for the
family of Basin profiles.

for the family of Howarth profiles [13]

$$\frac{\delta^*}{\delta} = 0,341,$$

for the family of Basin profiles [93]

$$\frac{\delta^*}{\delta} = 0,363 - 0,028\lambda_\text{5}.$$

The functions $\text{Re}^*_\text{cr} = \text{Re}^*_\text{cr}(\lambda)$ constructed on the basis of the investigated three-
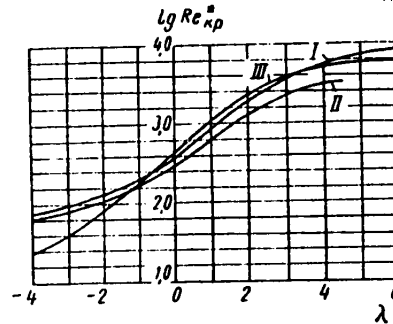families of velocity profiles in a laminar boundary layer are presented in Figure

73

Figure I.25. Curves for $Re^*_{cr}(\lambda_6)$ considering recalculation for the Pohlhausen parameter. I — family of Pohlhausen profiles; II — family of Howarth profiles; III — family of Basin profiles.

I.25. Here the parameters r and λ_B were recalculated by the above-presented formulas for the parameter λ_6. Agreement of the curves must be recognized as satisfactory.

If this recalculation is not made, the curves can differ significantly from each other, which can be seen from a comparison of the curve for the Pohlhausen family with the corresponding curve from the Basin family (Figure I.26). This fact indicates the necessity for a careful approach to the problem of which method is used to obtain the distribution of the parameter $\lambda = U'\delta^2/\nu$ with respect to length of the body when performing the stability calculations.
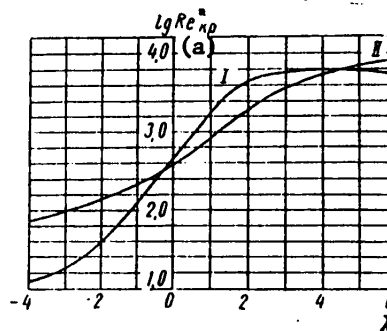
Figure I.26. Curves of $Re^*_{cr}(\lambda)$ without recalculation for the Pohlhausen parameter. I — family of Basin profile; II — family of Pohlhausen profile.

Key: a. cr

Figure I.27 shows the curves for the critical Reynolds numbers as a function of the parameter λ_6 calculated by various authors: Schlichting and Ulrich [15], Pretsch [14], Finston [94], Zaat [95], Soprunenko [114] and Tetervin [113]. For comparison, the same graph shows the curve obtained by calculations by formulas from § I.8 for the family of Pohlhausen profiles.   The basis for the Schlichting and Ulrich calculation, just as the Finston calculation using approximate Lin

74

formulas, was the family of profiles defined by the sixth-degree Pohlhausen poly-
nomials. In the calculations Soprunenko used the Howarth profiles. The basis for
the Pretsch and Tetervin calculations was the family of Hartree profiles with
power dependence of the velocity at the outer boundary of of the boundary layer on
the longitudinal coordinate. Zaat also selected a single-parametric family of
velocity profiles in the boundary layer for his calculations, but the parameter that
he used [95] differs from the Pohlhausen parameter. Comparison of the curves $Re^*_{cr} =$
Re^* (λ) indicates that the formulas obtained in § I.8 for calculations of the
critical Reynolds number give results that agree quite well with the data of other
authors.

Having the function $Re^*_{cr} = Re^*_{cr}(\lambda)$ available, by the known scheme of [4], [15], it
is possible to determine the position of the loss of stability point. Example cal-
culations appear in the following sections.

(a) $Lg\,R\dot{e}_{\kappa p}$

Key: a. $lg\,Re_{cr}$
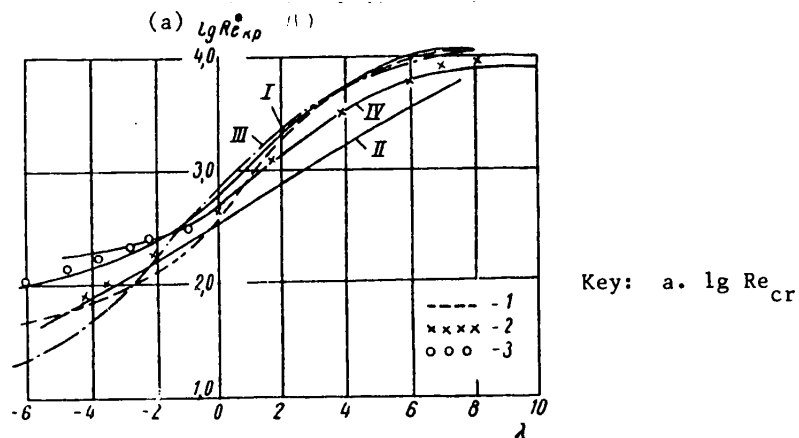
Figure I.27. Comparison of the curves Re^*_{cr} (λ) obtained by different
authors. I -- Schlichting curve; II -- Zaat curve; III -- Pretsch curve;
IV -- Finston curve; 1 -- proposed approximate formula; 2 -- Teterovih
calculation; 3 -- Soprunenko calculations [114].

§ I.12. Calculations of Stability of a Laminar Boundary Layer with Suction[1]

With relatively small removal of fluid from the wall, the stability of the laminar
boundary layer developed on it increases significantly [4], [17], [18]. During a
theoretical study of this phenomenon all of the researchers known to the authors of
this paper only considered the increase in fullness of the velocity profile in the
boundary layer with suction. The stability characteristics were calculated under
the assumption that the transverse velocities are absent in the boundary layer.
This statement of the problem makes it possible to use formulas § I.7. I.8 to calcu-
late the critical Reynolds number and neutral curve of any velocity profile obtained
during suction.

---

[1]The study discussed in this section was performed by Yu. N. Alekseyev and A. I.
Korotkin [115]

A study of the stability of the laminar boundary layer in the presence of constant transverse velocity in the wall region is presented below. The equation for the current function of the disturbing motion of an incompressible fluid is written [28] as follows:

$$\frac{\partial \Delta \hat{\varphi}}{\partial t} + \frac{\partial \theta}{\partial y} \cdot \frac{\partial \Delta \hat{\varphi}}{\partial x} + \frac{\partial \Delta \theta}{\partial x} \cdot \frac{\partial \hat{\varphi}}{\partial y} - \frac{\partial \theta}{\partial x} \cdot \frac{\partial \Delta \hat{\varphi}}{\partial y} - \frac{\partial \hat{\varphi}}{\partial x} \cdot \frac{\partial \Delta \theta}{\partial y} \quad v \Delta \Delta \hat{\varphi},$$ (I.126)

where θ is the current function of the undisturbed motion;

$\hat{\varphi}$ is the current function of the disturbing motion.

We shall consider that

$$\theta = \theta_1 (y) - \bar{v} \cdot x.$$ (I.127)

The value of $\bar{v}$ = const is the transverse velocity component of the main flow in the boundary layer. An example of a boundary layer with constant transverse velocity is the asymptotic boundary layer with fluid suction at the lower boundary.

Substituting (I.127) in (I.126) and considering the usual (§ I.4) expression for the current function of the disturbing motion

$$\hat{\varphi} = \hat{\varphi}(y) e^{i(\alpha x - bt)},$$

we obtain the following equation with respect to the amplitude of the current function

$$\left(u - \frac{b}{\alpha} \right) (\tilde{\varphi}'' - \alpha^2 \tilde{\varphi}) - u'' \tilde{\varphi} + \frac{\bar{v}}{i\alpha} (\tilde{\varphi}'' - \alpha^2 \tilde{\varphi}') =$$

$$- \frac{iv}{\alpha} (\tilde{\varphi}^{IV} - 2\alpha^2 \tilde{\varphi}'' + \alpha^4 \tilde{\varphi}),$$

where u(y) is the mean velocity distribution in the boundary layer.

Let us take the velocity at the boundary of the boundary layer as the characteristic velocity U and the thickness of the boundary layer as the characteristic dimension δ, and let us rewrite the preceding equation in dimensionless form, retaining the previous notation for the dimensionless variable U

$$(u - c)(\varphi'' - \alpha^2 \varphi) - u'' \varphi =$$

$$- \frac{i}{\alpha \operatorname{Re}} (\varphi^{IV} - 2\alpha^2 \varphi'' + \alpha^4 \varphi) - \frac{v}{i\alpha} (\varphi'' - \alpha^2 \varphi').$$ (I.128)

The boundary conditions for equation (I.128) will be found from the following prerequisites. On the wall for y = 0 the tangential component of the velocity of the disturbing motion is absent on the basis of the adhesion condition. This leads to expression (I.61). The presence of a constant transverse velocity of the main flow for y = 0 theoretically permits the existence of a normal velocity component of the disturbing motion at the wall $v_y(0) \neq 0$. However, the presence of transverse oscillations under the main flow conditions with a longitudinal velocity gradient for y $\geq$ 0

would have to unavoidably cause oscillations of the longitudinal component of the velocity, that is, would contradict the condition $v_x(0) = 0$. Therefore it is necessary to consider the identity $v_y(0) = 0$, valid, which gives condition (I.60). At the boundary of the boundary layer for $y = 1$ let us take the condition of smoothness cf the transition of the desired solution of equation (I.128) to the solution for an ideal fluid. This condition is written as follows with accuracy to the first derivative:

$$\varphi(1) = \varphi_0(1); \quad \varphi'(1) = \varphi_0'(1),$$

where $\phi_0(y)$ is the solution to equation (I.128) written for the region $y \geq 1$, where $u'' = 0$, $u = 1$, $(\alpha Re)^{-1} = 0$, for the viscosity is not considered

$$i\alpha(1-c)\left(\varphi_0'' - \alpha^2\varphi_0\right) + v\left(\varphi_0'' - \alpha^2\varphi_0'\right) = 0.$$

Denoting $\phi_0'' - \alpha^2\phi_0 = \Phi(y)$, we arrive at the equation

$$\Phi' + \frac{i\alpha(1-c)}{v}\Phi = 0,$$

which has the solution

$$\Phi(y) = A_1 e^{\frac{i(c-1)\alpha}{v}y},$$

where A_1 is an arbitrary constant. Thus, it is possible to define the function $\phi_0(y)$ using the following differential equation

$$\varphi_0'' - \alpha^2\varphi_0 = A_1 e^{\frac{i(c-1)\alpha}{v}y},$$

the general solution of which has the form

$$\varphi_0(y) = -\frac{A_1 v^2}{\alpha^2 v^2 + \alpha^2(c-1)^2} e^{\frac{i(c-1)\alpha}{v}y} + A_2 e^{\alpha y} + A_3 e^{-\alpha y}.$$

Since the parameters c, v and $\alpha > 0$ are real values, and at a sufficiently large distance from the surface there should be no disturbances ($\phi_0(y)/_{y\to\infty} \to 0$), $A_1 = A_2 = 0$, for the first term of the general solution has an oscillatory, nondamping nature with respect to the variable y, and the second term increases without limit with an increase in y. Thus, the smooth transition conditions have the form

$$\varphi(1) = A_3 e^{-\alpha}, \quad \varphi'(1) = -\alpha A_3 e^{-\alpha}.$$

On the basis of arbitrariness of the constant A_3 the two indicated equalities impose only one condition (I.63) on the values of $\phi(1)$ and $\phi'(1)$, which is obtained by finding A_3 from the first equality and substituting the value found in the second.

As a result, the boundary conditions of equation (I.128), which are a generalization of the Orr-Sommerfeld equation to the investigated case, are written in the form of the

expressions (I.60), (I.61), (I.63) and (I.64). In the latter, it is necessary to consider the value of $|M| = \varepsilon$ as small as one might like. Usually this restriction is not required when investigating stability problems by the small oscillation method.

Let us note that the relative magnitude of the transverse velocity v in the case of boundary layer control using laminarization is on the order of $(Re)^{-1}$, where $Re = U\delta/\nu$. Accordingly, as the first two solutions of equation (I.28) we take the analogous solutions of the Orr-Sommerfeld equation (I.72), (I.73), which are found under the assumption of smallness of the right-hand side of the equation as a function of viscosity.

In order to determine the remaining two solutions of equation (I.128) let us make the substitution (I.74), which converts (I.128) to the following expression:

$$(u - c)(p' + p^2 - \alpha^2) - u'' + \frac{v\,\mathrm{Re}}{i\alpha\,\mathrm{Re}}(p'' + 3pp' + p^3 - \alpha^2 p) =$$

$$= -\frac{i}{\alpha\,\mathrm{Re}}\,[p^4 + 6p^2 p' + 3p'^2 + 4pp'' + p''' -$$

$$- 2\alpha^2 (p' + p^2) + \alpha^4]. \qquad (I.129)$$

In turn, finding the solution of equation (I.129) in the form of the series (I.76) and limiting ourselves to the first two terms, which gives an error on the order of $(\alpha\mathrm{Re})^{-1/2}$, we find (see § I.6):

$$p_0(y) = \pm \sqrt{i(u - c)};$$

$$p_1(y) = -\frac{5}{2} \cdot \frac{p_0'}{p_0} + \frac{v\,\mathrm{Re}}{2};$$

$$\varphi_3(y) = (u - c)^{-\frac{5}{4}} \exp\left\{-\int_0^y \sqrt{i\alpha\,\mathrm{Re}(u - c)}\,dy + \frac{v\,\mathrm{Re}}{2}\,y\right\}; \qquad (I.130)$$

$$\varphi_4(y) = (u - c)^{-\frac{5}{4}} \exp\left\{\int_0^y \sqrt{i\alpha\,\mathrm{Re}(u - c)}\,dy + \frac{v\,\mathrm{Re}}{2}\,y\right\}. \qquad (I.131)$$

When removing fluid the value of v < 0. Let us consider the real part of the expression in the braces in the right-hand side of equality (I.131) for y → ∞

$$\left\{\int_0^y \sqrt{i\alpha\,\mathrm{Re}(u - c)}\,dy + \frac{v\,\mathrm{Re}}{2}\,y\right\}\bigg|_{y\to\infty} = \left\{\int_0^1 \sqrt{i\alpha\,\mathrm{Re}(u - c)}\,dy + \right.$$

$$\left. + i\sqrt{\frac{\alpha\,\mathrm{Re}(1 - c)}{2}}(y - 1) + \sqrt{\frac{\alpha\,\mathrm{Re}(1 - c)}{2}}(y - 1) + \frac{v\,\mathrm{Re}}{2}\,y\right\}_{y\to\infty},$$

for u(y) = 1 for y ≥ 1.

The value of v is on the order of 1/Re; therefore the product vRe/2 is on the order of 1 (for the asymptotic velocity profile vRe/2 = 2.3). The entire solution is constructed under the assumption αRe >> 1. The relative propagation rate of the disturbances c is always appreciably less than one. Thus, the real part of the

exponent in the solution of (I.131) for $y \to \infty$ is positive and, consequently, ϕ_4 does not satisfy the boundary condition (I.64). Therefore in the general solution of equation (I.128)

$$\varphi(y) = \sum_{\kappa=1}^{4} c_\kappa \varphi_\kappa(y)$$

the constant $c_4 = 0$.

The formula (I.130) shows that

$$\varphi_3(y) = \varphi_{30}(y) e^{\frac{v\,Re}{2} v},$$

(I.132)

where $\phi_{30}(y)$ is the corresponding solution for the Orr-Sommerfeld equation.

In order to determine the arbitrary constants c_1, c_2, c_3 from the uniform boundary conditions (I.60), (I.61), (I.64), the characteristic equation arises which for neutral disturbances relates the parameters of the disturbing motion α, c to the Reynolds number and the average motion characteristics. In the discussed case it has the form (§ I.7)

$$\left[1 + \frac{1}{y_\kappa} \frac{\varphi_3(0)}{\varphi_3'(0)} \right]^{-1} = 1 + z,$$

(I.133)

where the real and imaginary parts of the complex variable z are calculated by the formulas (I.104), (I.105). Considering (I.132), let us transform the left-hand side of (I.133), denoting it by $G(w)$,

$$G(w) = \left[1 - \frac{1}{y_\kappa} \cdot \frac{\varphi_{30}(0)}{\varphi_{30}'(0) + \varphi_{30}(0) \frac{v\,Re}{2}} \right]^{-1} =$$

$$= \left[1 - F(w) \frac{1}{1 - F(w) \frac{v\,Re\,y_\kappa}{2}} \right]^{-1} = \frac{1 - F(w)\,mw^3}{1 - F(w)(1 + mw^3)} =$$

$$= \frac{\left(1 - F_r w^3 m\right)\left(1 - F_r - mw^3 F_r\right) + mw^3 F_i^2\left(1 + mw^3\right)}{\left(1 - F_r - mw^3 F_r\right)^2 + F_i^2\left(1 + mw^3\right)^2} +$$

$$+ i \frac{F_i}{\left(1 - F_r - mw^3 F_r\right)^2 + F_i^2\left(1 + mw^3\right)^2},$$

where $F(w) = 1_r(w) + iF_i(w)$ is the Tietjens function (see § I.7),

$$w = y_\kappa \left(Re\,\alpha u_\kappa'\right)^{1/3}, \quad m = \frac{v}{2y_\kappa^2 \alpha u_\kappa'}.$$

Thus, it is possible to propose the following procedure for calculating the neutral stability curve.

1. The universal (independent of the velocity profile) functions $G_r(w, m)$, $G_i(w, m)$ are constructed for a series of values.

2. Being given the value of G_i, let us determine the values of w_1, w_2 for defined m by the graph $G_i(w, m)$, and also, using equality $G_i = z_i(c)$, let us determine the value of c. The nature of the function $g_i(w)$ is such that in the general case one value of the function corresponds to two values of the argument.

3. By the value of c found, let us determine y_k, u'_k, u''_k, for the velocity profile is known.

4. For the found values of w_1, w_2 and selected m let us calculate or define G_{r1}, G_{r2} by the graph.

5. Using equality $G_r = 1 + z_r$, we find α_1, α_2.

6. By the formula $Re = \left(\dfrac{w}{y_\kappa}\right)^3 \dfrac{1}{u\, u'_\kappa}$ we calculate Re_1, Re_2.

7. Let us determine the values of the relative ventilation $v = 2y_k^2\alpha u'_k m$, which correspond to the obtained points on the neutral curve.

It is possible to use the indicated scheme without alteration to find the critical Reynolds number directly if all the calculations are performed for a point on the curves $G_i = G_i(w, m)$, where $G_i = G_{i_{max}}$.

The numerical calculations were performed for the family of Wust profiles

$$u(y, l) \quad u_*(y) + l\,[u^*(y) - u_*(y)],$$

where $u_*(y)$ is the velocity distribution in the Blasius profile;

$u^*(y)$ is the velocity distribution in the asymptotic velocity profile;

ℓ is the parameter of the family which varied from 0 to 1.

The critical Reynolds number Re_{cr} as a function of the parameters m and ℓ is presented in Figure I.28. The dependence of Re_{cr} on the parameter ℓ and the relative transverse velocity in the boundary layer is shown in Figures I.29, I.30. From an investigation of this function it is possible to draw the conclusion of the existence of a relative velocity v_0 for each velocity profile such that for a suction velocity greater than v_0 the laminar boundary layer retains stability for all Reynolds numbers. The graphs of the function $v_0 = v_0(\ell)$ and the corresponding function $Re_0 = Re_0(\ell)$ are presented in Figures I.31, I.32. For suction velocities less than v_0, there are two critical Reynolds numbers — the upper Re_+ and lower Re_-. The flow in the boundary layer is stable if its Reynolds number is less than Re_- or greater than Re_+. If $Re_+ > Re > Re_-$, the flow is unstable.

For more complete explanation of the indicated fact, neutral stability curves were constructed for the velocity profile with the parameter $\ell = 0.2$. Each curve in Figure I.33 corresponds to a defined value of the parameter m. If we calculate the value of relative suction velocity v at each point of the neutral curves and join the points with $v = const$, then closed regions are obtained which are shown in Figure I.33 by the dotted line. Inside these regions the flow is unstable, and
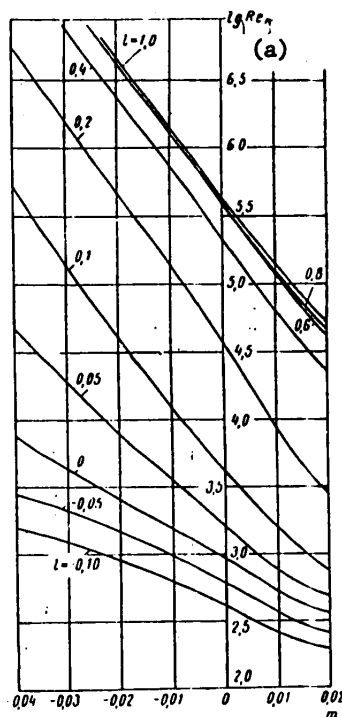
Figure I.28. Critical Reynolds number as a function
of the parameters m and ℓ. Key: a. cr

outside them it is stable. For a defined suction velocity (v_0), the instability
region degenerates to a point. Thus, for distributed suction, for purposes of
laminarization it is meaningful to increase the relative suction velocity only to a
defined amount corresponding to disappearance of the instability region. The pre-
sented calculation data allow estimation of the indicated velocity for velocity
profiles from the Blasius profile to the asymptotic profile.

§ I.13. Stability of the Asymptotic Velocity Profile

The study of the stability of an asymptotic velocity profile based on an infinite
plate with uniform and constant section with respect to the plate length plays a
special role in studies of the stability of a laminar boundary layer with suction.
The asymptotic profile has the greatest fullness of the velocity diagram, and there-
fore it has the greatest stability by comparison with all velocity profiles formed
on the plate with constant and uniform suction. The critical Reynolds number was
calculated for asymptotic velocity profile in references [17], [18]. For the
critical Reynolds number Pretsch obtained a value of $Re^*_{cr} = 5.52 \cdot 10^4$; Bussman and
Münz found $Re^*_{cr} = 7 \cdot 10^4$.

Since in the calculations of the stability of laminar boundary layers with suction
these figures (more frequently a value of $Re^*_{cr} = 7 \cdot 10^4$) are used to estimate the
required suction intensity and the calculations by the mentioned authors were

81

Figure I.29. Critical Reynolds number as afunction of the parameter ℓ and relative transverse velocity in the boundary layer $(-0.1 \leq \ell \leq 0.1)$.

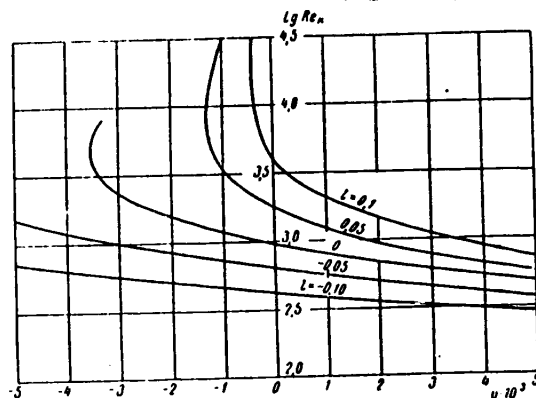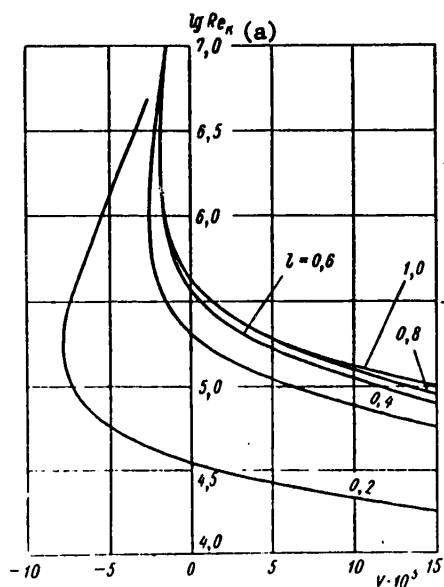Figure I.30. Critical Reynolds number as a function of the parameter ℓ and relative transverse velocity in the boundary layer $(1 \leq \ell \leq 0.2)$.

Key: a, cr

based on the Tollmien-Schlichting graphoanalytical scheme (see § I.7), it appears expedient to perform analogous calculations beginning with the scheme based on the ideas of Lin (see § I.7), which does not require approximation of the velocity

82
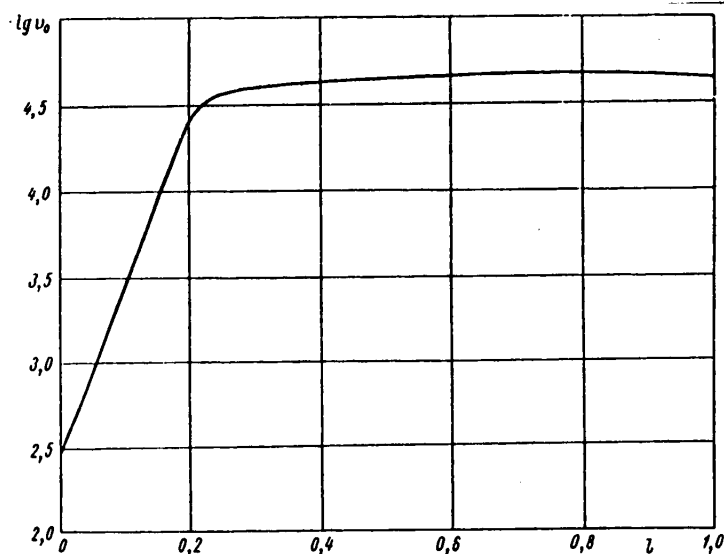
Figure I.31. Extremal suction velocity as a function
of the parameter ℓ,
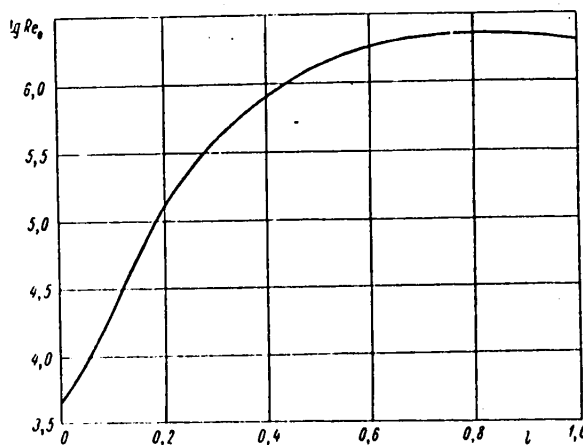
Figure I.32. Extremal Reynolds number as a function
of the parameter ℓ.

profile by polynomials   or   the application of the graphical method of solving
the characteristic equation.

Using the formula obtained in § I.8

$$\mathrm{Re}_{\kappa p} = \frac{33u_0'(1-c)^2(1,5+0,185\ln c)}{c^4},$$

(I.134)
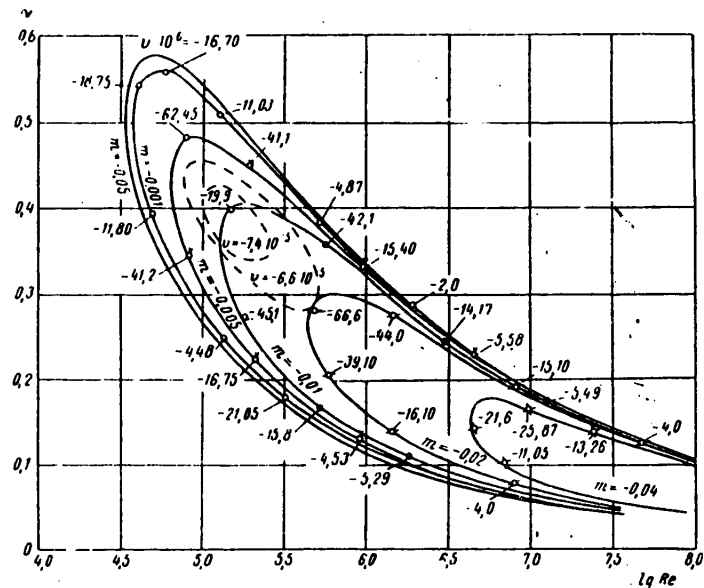
Figure I.33. Neutral stability curves considering
the transverse velocity of the main flow.

let us determine the critical Reynolds number for the asymptotic profile.

The velocity profile of an asymptotic boundary layer is defined [16] by the expression

$$u(y) = 1 - e^{\frac{v\bar{y}}{v}} = 1 - e^{\frac{v\delta}{v}\,v},$$
(I.135)

where $\bar{y} = \delta \cdot y$, $v < 0$.

On the basis of (I.135) let us calculate u_0', u_k', u_k'' entering into the equation (I.113), from which the parameter c is found

$$u_k' = -\frac{v\delta}{v} \epsilon^{\frac{v\delta}{v}\,v_k},$$

$$u_k'' = -\left(\frac{v\delta}{v}\right)^2 e^{\frac{v\delta}{v}\,v_k},$$

$$u_0' = u'(0) = -\frac{v\delta}{v}.$$

In the given case the equation (I.113) is written as follows:

$$0.58 = \pi\left(1 - e^{\frac{v\delta}{v}\,v_k}\right)e^{-2\frac{v\delta}{v}\,v_k}.$$

Let us solve it with respect to y_k. Let us introduce the notation $\xi = e^{\frac{v\delta}{v}\,v_k}$. Then, we find

84

$$0,58\xi^2 \quad \pi(1-\xi), \ \xi^3 + 5,41\xi - 5,41 = 0,$$
$$\xi_{1,2} = -2,705 \pm 3,57, \ \xi = 0,865.$$

The negative value of ξ is meaningless. Thus,

$$e^{\frac{v\delta}{v}\nu_\kappa} = 0,865,$$

$$y_\kappa = \frac{v}{v\delta}\ln 0,865,$$

$$c = 1 - 0,865 = 0,135.$$

Defining c, let us calculate the value of the critical Reynolds number, considering (I.134) and also the expression

$$\frac{\delta^*}{\delta} = -\frac{v}{v\delta} = \frac{1}{u_0^{'}},$$

valid for the asymptotic velocity profile [16],

$$Re^{\cdot}_{\kappa\rho} = \frac{\delta^*}{\delta}Re_{\kappa\rho} = \frac{33(1-c)^2(1,5+0,185\ln c)}{c^4} = 8,45 \cdot 10^4.$$

The above-presented results were obtained without considering the influence of the transverse velocity component of the main flow on the stability of the asymptotic velocity profile. In the preceding § I.12, this calculation was performed, but the magnitude of the relative pumping velocity was in no way connected with the velocity profile characteristics in the boundary layer. This statement of the problem is valid for the accelerating segment of the boundary layer ($\ell < 1$). In the case of an asymptotic velocity profile when the profile characteristics are rigidly connected with the suction belocity, consideration of the influence of the transverse component of the velocity on the stability of the laminar form of flow requires more precise definition. Let us perform this study, using the results of § I.12.

Let us transform the left-hand side of the characteristic equation (I.99), considering that for the asymptotic velocity profile

$$-v - \frac{1}{Re^*}, \ v\,Re = -\frac{\delta}{\delta^{'}} = -4,6.$$

The ratio δ/δ^* was found from the condition

$$1 - u(1) = e^{-\frac{\delta}{\delta^*}} = 0,01.$$

Considering equality (I.132), we have

$$-\frac{1}{y_\kappa}\frac{\varphi_3(0)}{\varphi_3^{'}(0)} = -\frac{1}{y_\kappa} \cdot \frac{\cdots_{30}(0)}{\cdots \ \cdots \ 1 - \varphi_{30}(0) \cdot \frac{v\,Re}{2}} = -\frac{1}{y_\kappa} \cdot \frac{1}{\frac{\varphi_{30}(0)}{\varphi_{30}^{'}(0)} - 2,3}.$$

In the right-hand side of (I.99) we set $c \simeq y_k u_0^t$, which is valid for the asymptotic velocity profile for the value of c in this case does not exceed 0.14. Then expression (I.99) assumes the form:

$$- \frac{1}{y_\kappa} \frac{\varphi_{30}(0)}{\varphi_{30}(0)} \quad \frac{z}{1 + (1 - 2.3y_\kappa)z}$$

or

$$F_r(w) + iF_i(w) = E_r(\alpha, c) + iE_i(\alpha, c),$$
(I.136)
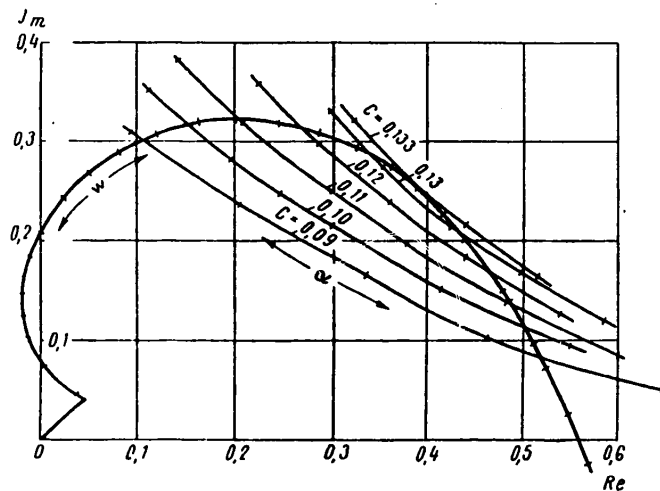
Figure I.34. Solution of the characteristic
equation considering the transverse flow velocity.

where $F(w) = F_r(w) + iF_i(w)$ is the Tietjens function (see § I.7),

$$E_r(\alpha, c) = \frac{(z_r^2 + z_i^2)(1 - 2.3y_\kappa) + z_r}{|1 + z_r(1 - 2.3y_\kappa)|^2 + (1 - 2.3y_\kappa)^2 z_i^2},$$

$$E_i(\alpha, c) = \frac{z_i}{|1 + z_r(1 - 2.3y_\kappa)|^2 + (1 - 2.3y_\kappa)^2 z_i^2}.$$

$w = y_k(\alpha Re\ u_k^t)^{1/3}$, the values of z_r and z_i are determined by formulas (I.104), (I.105).

The complex equation (I.136) is solved by the Tollmien-Schlichting graphoanalytical method (§ I.7). The graphical solution is presented in Figure I.34. For comparison of Figure I.35 shows the analogous solution for the asymptotic velocity profile in the case where the transverse component of the main flow velocity is not considered.

86
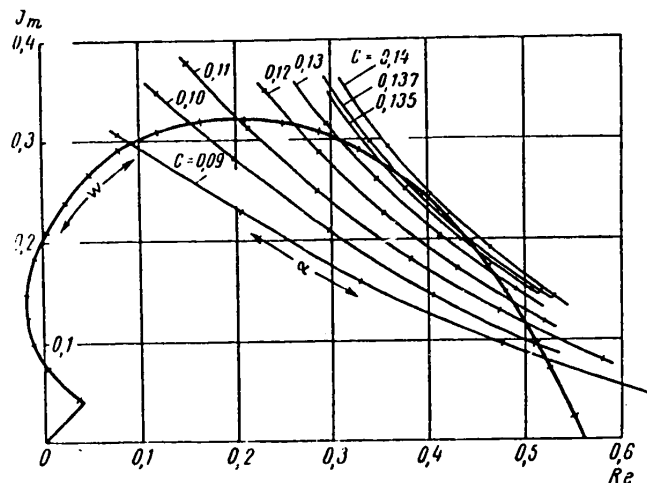
Figure I.35. Solution of the characteristic equation withou considering the transverse flow velocity.

The calculations are performed by the same formulas except the difference $1-2,3y_k$ is replaced by one, which is obvious from derivation of the final expressions. For the two indicated cases of calculating th stability of an asymptotic velocity profile neutral curves are constructed in Figure I.36. From an investigation of them it follows that consideration of the transverse component of the main flow velocity leads to an increase in the critical Reynolds number of the asymptotic boundary layer (curve I is constructed considering the transverse velocity, $Re^*_{cr} = 9.7 \cdot 10^4$, curve II is constructed without considering the transverse velocity, $^{cr}Re^*_{cr} = 7.9 \cdot 10^4$). Comparison of the values of the critical Reynolds number is $8.45 \cdot 10^4$ and $7.9 \cdot 10^4$ permits estimation of the difference in the analytical and graphical methods of solving the stability problem in the case of an asymptotic velocity profile.
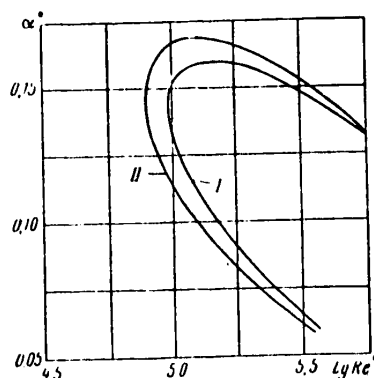
Figure I.36. Neutral stability curves for the asymptotic velocity profile. I — considering the transverse flow velocity; II — without considering the transverse flow velocity.

87

The cause of the difference is that $\mathfrak{F}_{i\,\text{max}} \sim 0.58$ does not exactly correspond to the minimum Reynolds number on the neutral stability curve (see § I.7).

BIBLIOGRAPHY

1. I. O.Khintse, TURBULENTNOST' (Turbulence), GIFML, Moscow, 1963.

2. F. Homann, "Einfluss grosser Zähigkeit bei Strömung um Zylinder und Kugel, FORSCHG. ING,- WES., Vol 7, No 1, 1936.

3. D. Coles, "Transition in Circular Couette Flow," J. FLUID MECH, Vol 21, No 3, 1965.

4. H. Schlichting, VOZNIKNOVENIYE TURBULENTNOSTI (Occurrence of Turbulence), Moscow, IL, 1962.

5. M. Ye. Deych, L. Ya. Lazarev, "Study of the Transition of a Turbulent Boundary Layer to Laminar," INZH.-FIZ. ZHURNAL (Engineering Physics Journal), Vol 7, No 4, 1964.

6. A. A. Sergiyenko, V. K. Gretsov, "Transition of a Turbulent Boundary Layer to Laminar," DAN SSSR (Reports of the USSR Academy of Sciences), Vol 125, No 4, 1959.

7. M. Sibulkin, "Transition from Turbulent to Laminar Pipe Flow," THE PHYSICS OF FLUIDS, Vol 5, No 3, 1962.

8. B. E. Launder, "Laminarization of the Turbulent Boundary Layer in a Severe Acceleration," TRANS. ASME, ser E, Vol 31, No 4, 1964.

9. A. Favre, R. Dumas, E. Verollet, "Conche limite sur paroi plane poreuse avec aspiration," PUBLICATIONS SCIENTIFIQUES ET TECHNIQUES DU MINISTERE DE L'AIRE, No 377, 1961.

10. K. Sewell, "A New Analytical Model for Boundary Layer Transition," PROCEEDINGS OF THE HEAT TRANSFER AND FLUID MECHANICS INSTITUTE, Stanford University Press, 1960.

11. G. B. Schubauer, H. K. Skramstad, "Laminar Boundary Layer Oscillations and Stability of Laminar Flow," J. AERON. SCI., Vol 14, 1947, p 69.

12. C. C. Lin, TEORIYA GIDRODINAMICHESKOY USTOYCHIVOSTI (Hydrodynamic Stability Theory), Moscow, IL, 1958.

13. H. Schlichting, "Über die theoretische Berechnung der kritischen Reynoldschen Zahl einer Reibungsschicht in beschleunigter und verzögerter Stromung," JB. D. D. LUFTFAHRFORSCHUNG, page I97, 1940.

14. J. Pretsch, "Die Stabilität einer ebenen Laminarströmung oei Druckgefälle und Druckanstieg," JB. D. D. LUFTFAHRTFORSCHUNG, Page 1 58, 1941.

15. H. Schlichting, A. Ulrich, "Berechnung des Umschlags Laminar — Turbulent," JB. D. D. LUFTFAHRTFORSCHUNG, page 1 8, 1942.

16. H. Shlichting, TEORIYA POGRANICHNOGO SLOYA (Boundary Layer Theory), Moscow, IL, 1956.

17. K. Bussman, H. Münz, "Die Stabilität der laminarer Reibungsschicht mit Absaugung," JB. D. D. LUFTFAHRTFORSCHUNG, page 1 36, 1942.

18. J. Pretsch, "Umschlagsbeginn und Absaugung," JB. D. D. LUFTFAHRTFORSCHUNG, page 1 1, 1942.

19. D. D. Landau, "Turbulence Problem," DAN SSSR, Vol 44, No 8, 1944.

20. L. D. Landau, Ye. M. Lifshits, MEKHANIKA SPLOSHNYKH SRED (Mechanics of Continuous Media), Moscow, GITTL, 1953.

21. F. Schultz-Grunow, H. Hein, "Beitrag zur Couette Strömung," Z. F. FLUGWISS, Vol 4, Ser A, 1936, p 307.

22. G. I. Taylor, "Statistical Theory of Turbulence," PROC. ROY. SOC., Ser. A, Vol 156, 1936, p 307.

23. K. Wieghardt, "Über die Wirkung der Turbulenz auf den Umschlagpunkt," ZAMM, Vol 20, No 1, 1940.

24. W. Tollmien, "W. Über die Entstehung der Turbulenz, Nachr. Ges. Wiss. Göttingen," MATH-PHYS., No 1, 1929.

25. H. L. Dryden, G. B. Schubauer, W. C. Mock, H. K. Skramstad, "Measurements of Intensity and Scale of Wind-tunnel Turbulence and their Relation to the Critical Reynolds Number of Spheres," NACA REPT., No 581, 1937.

26. F. K. Wortmann, "Study of Unstable Boundary Layer Oscillations in a Stream of Water by the Telluric Method," PROBLEMA POGRANICHNOGO SLOYA I VOPROSY TEPLOPE-REDACHI (Boundary Layer Problems and Heat Transfer Problems), Moscow-Leningrad, GEI, 1960.

27. W. Schilz, "Untersuchungen über den Einfluss biegeformiger Wand-schwingungen auf die Entwicklung der Strömungsgrenzschicht, ACUSTICA, Vol 15, No 1, 1965.

28. N. Ye. Kochin, I. A. Kibel', N. V. Rose, TEORETICHESKAYA GIDROMEKHANIKA (Theoretical Hydromechanics), Parts I, II, Moscow, GITTL, 1955.

29. N. A. Slezkin, DINAMIKA VYAZKOY NESZHIMAYEMOY ZHIDKOSTI (Dynamics of a Viscous Incompressible Fluid," Moscow, GITTL, 1955.

30. A. M. Mili-Tomson, TEORETICHESKAYA GIDRODINAMIKA (Theoretical Hydrodynamics), izd. Mir, 1964.

31. S. Goldstein, SOVREMENNOYE SOSTOYANIYE GIDRODINAMIKI VYAZKOY ZHIDKOSTI (Modern State of the Art in the Hydrodynamics of a Viscous Fluid), Moscow, IL, 1948.

32. L. Prandtl, "Mechanics of Viscous Fluids," AERODINAMIKA (Aerodynamics), Part III, Moscow-Leningrad, GIOP, 1939.

33. R. Mises, "Bemerkungen zur Hydrodynamik," ZAMM, Vol 7, 1927, p 425.

34. L. G. Loytsyanskiy, AERODINAMIKA POGRANICHNOGO SLOYA (Boundary Layer Aerodynamics), Gostekhizdat, 1941.

35. L. G. Loytsyanskiy, LAMINARNYY POGRANICHNYY SLOY (Laminar Boundary Layer), Moscow, GIFML, 1962.

36. R. I. Timman, Yu. A. Zaat, "Method of Calculating a Three-dimensional Laminar Boundary Layer," PROBLEMA POGRANICHNOGO SLOYA I VOPROSY TEPLOPEREDACHI (Boundary Layer Problem and Heat Transfer Problems), Moscow-Leningrad, Gosenergoizdat, 1960.

37. F. Muhr, "Three-dimensional Boundary Layer Theory," PROBLEMY MEKHANIKI (Problems of Mechanics), No II, Moscow, IL, 1959.

38. H. Schlichting, "Spatial Boundary Layer," MEKHANIKA, SBORN. PEREVODOV (Mechanics, Collection of Translations), No 3, 1964,

39. V. Golubev, "Boundary Layer Theory," TRUDY PO AERODINAMIKE (Works on Aerodynamics), Moscow-Leningrad, GITTL, 1957.

40. H. Görtler, "Über eine dreidimensionale Instabilität laminarer Grenzschichten an konkaven Wänden," NACHR. GES. WISS. GÖTTINGEN. MATH-PHYS. KLASSE, NEUE FOLGE, FACHGRUPPE I, Vol 2, No 1, 1940.

41. H. Görtler, "Instabilitat laminarer Grenzschichten an kankaven Wänden gegenüber gewissen dreidimensionalen Störungen," ZAMM, Vol 21, No 4, 1941.

42. D. Meksyn, "Stability of Viscous Flow Over Concave Cylindrical Surfaces," PROC. ROY. SOC., Ser. A, Vol 203, No 1073.

43. G. Hämmerlin, "Über das Eigenwertproblem dreidimensionalen Instabilität laminarer Grenzschichten langs konkaven Wänden," J. RATL. MECH. ANALYSIS, Vol 4, 1955.

44. R. C. Prima, "Application of the Galerkin Method to Problems in Hydrodynamic Stability," QUARTERLY OF APPLIED MECHANICS, Vol 13, No 1, 1955, Russian Translation: MEKHANIKA (Mechanics), collection of translations and surveys, No 3, 1956.

45. A. M. O. Smith, "On the Growth of Taylor-Görtler Vortices along highly Concave Walls," QUARTERLY OF APPLIED MATHEMATICS, Vol 13, No 3, 1955.

46. G. Hammerrlin, "Über die dreidimensionale Instabilität laminarer Grenzschichten," ZAMM, Vol 35, No 9/10, 1955.

47. S. G. Mikhlin, VARIATSIONNYYE METODY MATEMATICHESKOY FIZIKE (Variation Methods in Mathematical Physics), Moscow, GITTL, 1957.

48. G. I. Petrov, "Propagation of Oscillations of a Viscous Fluid and the Occurrence of Turbulence," TR. TSAGI (Works of the Central Aerohydrodynamics Institute), No 345, 1938.

49. G. I. Petrov, "Application of the Galerkin Method to the Problem of the Flow Stability of a Viscous Fluid," PMM (Applied Mathematics and Mechanics), Vol 4, No 3, 1940.

50. M. V. Keldysh, "B. G. Galerkin Method for Solving Boundary Problems," IZV. AN SSR, SER. MATEM. (News of the USSR Academy of Sciences, Mathematic Series), Vol 6, No 6, 1942.

51. N. I. Pol'skiy, "B. G. Galerkin Method," DOPOVIDI AKAD. NAUK. URSR, VILLIL. FIZ.-MAT. TA KHIM. NAU, (Reports of the Ukrainan SSR Academy of Sciences, Physical-Mathematical and Chemical Sciences Series), No 6, 1949.

52. V. A. Borodin, A. F. Dityakin, "Stability of Plane Flows of a Viscous Fluid between Two Walls," PMM, Vol 17, No 5, 1953.

53. V. A. Medvedev, "Application of the Bubnov-Galerkin Method in Hydrodynamic Stability Theory," PMM, Vol 28, No 4, 1964.

54. H. Görtler, "Three-dimensional Instability of a Plane Flow with Critical Point in the Presence of Vortex Disturbances," PROBLEMA POGRANICHNOGO SLOYA I VOPROSY TEPLOPEREDACHI, Moscow-Leningrad, GEI, 1960.

55. G. K. Hämmerlin, "Instability Theory of a Plane Flow in the Presence of a Critical Flow," PROBLEMA POGRANICHNOGO SLOYA I VOPROSY TEPLOPEREDACHI, Moscow-Leningrad, GEI, 1960.

56. N. A. Piercy, E. G. Richardson, "The Variation of Velocity Amplitude Close to the Surface of a Cylinder Moving Through a Viscous Fluid," PHIL. MAG., Vol 6, No 39, 1928.

57. N. A. V. Piercy, E. G. Richardson, "The Turbulence in Front of a Body Moving Through a Viscous Fluid," PHIL. MAG., Vol 9, No 60, 1930.

58. H. Görtler, "Theorie der sekundaren Instabilität der laminaren Grenzschichten," GREZSCHICHTFORSCHUNG SYMPOSIUM FREIBURG, Springer-Verlag, 1957, 1958.

59. P. S. Klebanoff, K. D. Tidstrom, L. M. Sargent, "The Three-dimensional Nature of Boundary-Layer Instability," JOURNAL OF FLUID MECHANICS, Vol 12, No 1, 1962.

60. J. Tani, H. Komoda, "Boundary Layer Transition in the Presence of Streamwise Vortices," JOURNAL OF THE AEROSPACE SCIENCES, Vol 29, No 4, 1962.

61. H. Görtler, "Dreidimensionales zur Stabilitäts theorie laminarer Grenzschichten," ZAMM, Vol 35, No 9/10, 1955.

62. H. Görtler, "Boundary Layer Effects in Aerodynamics," Z. F. FLUGWISS, Vol 3, No 6, 1955.

63. H. Görtler, "Einige neuere Ergebnisse zur hydrodynamischen Stabilitätstheorie," Z. F. FLUGWISS, Vol 8, No 1, 1960.

64. H. A. Lorentz, "Über die Entstehung turbulenter Flüssigkeitsbewegungen und über den Einfluss dieser Bewegungen bei der Strömung durch Röhren," ABHANDLUNGEN ÜBER THEORETISCHE PHYSIK, Leipzig, Vol 1, 1907, p 43.

65. V. I. Smirnov, KURS VYSSHEY MATEMATIKI (Course in Higher Mathematics), Vol II, Moscow, GITTL, 1954.

66. T. Karman, "Laminar Flow Stability and Turbulent Motion Theory," PROBLEMY TURBU-LENTNOSTI (Turbulence Problems), ONTI, 1936.

67. C. C. Lin, "On the Stability of Two-dimensional Parallel Flows, Parts I, II, III," QUART. APPL. MATH., Vol 3, 1945.

68. A. C. Monin, A. M. Yaglam, "Hydrodynamic Instability and the Occurrence of Tur-bulence (a Survey)," PMTF (Applied Mechanics and Technical Physics), No 5, 1962.

69. H. L. Dryden, "Transition of Laminar Flow to Turbulent," TURBULENTNYYE TECHENIYA (Turbulent Flows and Heat Transfer), Moscow, IL, 1963.

70. H. Schlichting, "Entwicklung der Grezschichttheorie in den letzten drei Jahrzehn-ten," Z. FÜR FLUGWIS., No 4, 1960.

71. H. Schlichting, "Über die Theorie der Turbulenzentsstenhung," FORSCHUNG AUF DEM GEBIETE DES INGENIEURWESENS, Vol 16, No 3, 1949/1950.

72. H. L. Dryden, "Modern Development of Boundary Layer Mechanics," PROBLEMY MEKHANIKI, IL, Moscow, 1955.

73. W. Tollmien, "Aspekte der Strömungsphysik 1962," Z. FÜR FLUGWISS, No 11, 1962.

74. H. B. Squire, "On the Stability for three-dimensional Disturbances of Viscous Fluid Flow between Parallel Walls," PROCEEDINGS OF THE ROYAL SOCIETY, Ser A, Vol 142, No 847, 1933.

75. I. Tszya-Chun', "Stability of Plane Parallel Flows in the Presence of Three-Dimensional Disturbances," MEKANIKA (Mechanics), Collection of translations and surveys, IL, No 1, 1956.

76. F. Schultz-Grunow, "Zur Entstehung von Längswirbeln in Grenzschichten," ZAMM, Vol 38, No 3/4, 1958.

77. W. Tollmien, "Über die Entschung der Turbulenz," NACHR. GES. WISS. GOTTINGEN. MATH-PHYS. KLASSE, No 1, 1929.

78. A. Sommerfeld, "Ein Beitrag zur hydrodynamischen Erklaerung der turbulenten Flüssigkeitshewegungen," ATTI DEL IV CONGRESSO INTERNAZIONALE DEL MATEMATICI, Rome, Vol 3, 1908.

79. K. M. Case, "Hydrodynamic Stability as a Problem with Initial Data," GIDRODINA-MICHESKAYA NEUSTOYCHIVOST' (Hydrodynamic Instability), Moscow, izd. Mir, 1964.

80. K. M. Case, "Stability of Inviscid Plane Couette Flow," PHYSICS OF FLUIDS, Vol 3, 1960, p 143.

81. A. M. Komarov, "Application of the Galerkin Method to Investigate the Develop-ment of Viscous Fluid Flow Disturbances in a Two-dimensional Channel," VEST. MGU. SER. MAT.-MEKH. (Moscow State University Vestnik, Mathematical and Mechanics Series), No 2, 1959.

82. N. M. Matveyev, METODY INTEGRIGOVANIYA OBYKNOVENNYKH DIFFERENTSIAL'NYKH URAVLENIY (Methods of Integrating Ordinary Differential Equations), Izd. LGU, 1955.

83. W. Heisenberg, "Über Stabilität und Turbulenz von Flüssigkeitsströmen," ANN. PHYS. LPZ, Vol 74, No 15, 1924.

84. R. Betchov, "Simplified Analysis of Boundary-Layer Oscillations," JOURNAL OF SHIP RESEARCH, Vol 4, No 2, 1960.

85. V. I. Smirnov, KURS VYSSHEY MATEMATIKI (Course in Higher Mathematics), Vol III, Part 2, GITTL, Moscow, 1953.

86. F. Trikomi, LEKTSII PO URAVNENIYAM V CHASTNYKH PROIZVODNYKH (Lectures on Partial Differential Equations), Moscow, IL, 1957.

87. J. N. Watson, TEORIYA BESSELEVYKH FUNKTSIY (Theory of Bessel Functions), Part I, Moscow, IL, 1949.

88. O. Tietjens, "Beiträge zur Entstehung der Turbulenz," ZAMM, Vol 5, No 3, 1925.

89. H. Holstein, "Über die aussere und innere Reibungsschicht bei Störungen laminarer Stromungen," ZAMM, Vol 30, No 1/2, 1950.

90. H. Schlichting, "Amplitudenverteilung und Energiebilanz der kleinen Störungen bei der Plattenströmung," NACHR. GES. WISS. GÖTTINGEN. MATH-PHYS. KLASSE, Fachgruppe, 1, Vol 1, No 4, 1935.

91. I. W. Miles, "The Hydrodynamic Stability of a Thin Layer of Liquid in Uniform Shearing Motion," JOURNAL OF FLUID MECHANICS, Vol 8, No 4, 1960.

92. H. Schlichting, "Zur Entstehung der Turbulenz bei der Plattenströmung," NACH. GES. WISS. GÖTTINGEN, MATH.-PHYS. KLASS, Fachgruppe II, No 38, 1933.

93. A. M. Basin, "A New Approximate Method of Calculating the Boundary Layer," DAN SSR, Vol 40, No 1, 1943.

94. E. Hahneman, I. C. Freeman, M. Finston, "Stability of Boundary Layers and of Flow in Entrance Section of a Channel," JOURNAL OF THE AERONAUTICAL SCIENCES, Vol 15, No 8, 1948.

95. I. A. Zaat, "Numerische Beiträge zur Stabilitätstheorie der Grenzschichten," GENZSCHICHTFORSCHUNG. SYMPOSIUM, Freiburg, 1957.

96. W. Tollmien, "Ein allgemeines Kriterium der Instabilität laminarer Gerschwindig-keitsverteilungen," NACHR. GES. WISS. GÖTTINGEN. MATH-PHYS. KLASSE, Frachgruppe I, Vol 1, No 5, 1935.

97. I. G. Burns, W. H. Childs, A. A. Nicol, M. A. Ross, "Development and Use of a Vane Device for Boundary-Layer Measurements," JOURNAL OF FLUID MECHANICS, Vol 6, No 1, 1959.

98. N. A. Bergh, "A Method for Visualizing Periodic Boundary-Layer Phenomena," GRENZSCHICHTFORSCHUNG SYMPOSIUM, Freiburg, 1957, Springer-Verlag, 1958.

93

99. F. R. Hama, "Boundary-Layer Transition Induced by a Vibrating Ribbon on a Flat Plate," PROCEEDINGS OF THE 1960 HEAT TRANSFER AND FLUID MECHANICS INSTITUTE, Stanford University Press, 1960.

100. C. C. Lin, "On the Instability of Laminar Flow and Its Transition to Turbulence," GRENZSCHICHTFORSCHUNG SYMPOSIUM, Freiburg, 1957, Springer-Verlag, 1958.

101. D. J. Benney, C. C. Lin, "On the Secondary Motion Induced by Oscillations in a Shear Flow, THE PHYSICS OF FLUIDS, Vol 3, No 4, 1960.

102. D. J. Benney, "Finite Amplitude Effects in an Unstable Laminar Boundary Layer," THE PHYSICS OF FLUIDS, Vol 7, No 3, 1964.

103. D. J. Benney, "A Nonlinear Theory for Oscillations in a Parallel Flow," JOURNAL OF FLUID MECHANICS, Vol 10, No 2, 1961.

104. C. C. Lin, D. J. Benney, "Flow Stability with Velocity Gradient," GIDRODINAMICH-ESKAYA NEUSTOYCHIVOST' (Hydrodynamic Instability), Moscow, izd. Mir, 1964.

105. S. T. Stuart, "Nonlinear Mechanics in Hydrodynamic Stability Theory," MEKHANIKA (Mechanics), collection of translations and surveys, No 3, 1959.

106. J. Watson, "On Spatially Growing Finite Disturbances in Plane Poiseuille Flow," JOURNAL OF FLUID MECHANICS," Vol 14, No 2, 1962.

107. A. Michalke, "Zur Instabilität und nichtlinearen Entwicklung einer gestörten Scherschicht," INGENIEUR-ARCHIV, Vol 33, No 4, 1964.

108. G. V. Schubauer, "Mechanism of Transition at Subsonic Speeds," GRENZSCHICHTFOR-SCHUNG. SYMPOSIUM, Freiburg, 1957, Springer-Verlag, 1958.

109. V. V. Struminskiy, "Nonlinear Theory of Aerodynamic Stability," DAN SSSR, Vol 151, No 5, 1963.

110. E. M. Khazen, "Nonlinear Theory of the Occurrence of Turbulence," DAN SSSR, Vol 153, No 6, 1963.

111. S. T. Stuart, "Hydrodynamic Stability," LAMINAR BOUNDARY LAYERS, edited by I. Rosenhead, Oxford, 1963.

112. D. W. Dunn, "Stability of Laminar Flows," CANADIAN AERONAUTICAL JOURNAL, April. 1961.

113. D. Tetervin, "A Study of the Stability of the Incompressible Boundary Layer on Infinite Wedges," TECH. NOTES NAT. ADV. COMM. AERO. WASH., No 2976, 1953.

114. I. P. Soprunenko, "Calculation of Flow Stability of a Boundary Layer with Positive Pressure Gradient," IZV. AN SSSR, MEKH. I MASH. (News of the USSR Academy of Sciences, Mechanics and Machinery), No 5, 1964.

115. Yu. N. Alekseyev, A. I. Korotkin, "Effect of Transverse Flow Velocity in an Incompressible Boundary Layer on the Stability of the Laminar Form of Flow," IZV. AN SSSR, MZHG (News of the USSR Academy of Sciences, MZhG), No 1, 1966.

116. L. A. Dikiy, "Stability of Plane-Parallel Flows of an Ideal Fluid," DAN SSSR, Vol 135, No 5, 1960.

117. Ye. I. Stepanov, "Integration of the Equations of a Laminar Boundary Layer for Motion with Axial Symmetry," PMM, Vol 11, No 1, 1947.

118. W. Mangler, "Zusammenhang zwischen ebenen und rotationssym-metrischen Grenzschichten in kompressiblen Flüssigkeiten," ZAMM, Vol 28, 1947, p 97.

CHAPTER II. INFLUENCE OF SURFACE FLEXIBILITY OF A BODY OVER WHICH FLOW IS TAKING PLACE ON LAMINAR BOUNDARY LAYER STABILITY

§ II.1. Brief Survey of Studies of the Influence of Surface Flexibility on the Drag of Bodies Moving in a Fluid

The idea of using a flexible surface for boundary layer control obviously was a consequence of observations of the motion of fish and marine animals. The opinion exists that marine animals, in particular, dolphins, have accomodations still unknown to man which permit them to move in the water at speeds greatly exceeding the maximum speeds calculated on the basis of estimating their power. Thus, it has been confirmed that the drag of a dolphin's body is less than that of the corresponding solid model.

It is possible to determine the hydrodynamic drag of moving fish and marine animals only indirectly, determining their power developed to sustain given speed. Accordingly, the question arises of a reliable method of determining the power and speed of animate moving objects. An analysis of the known data on hydrodynamic research performed with dolphins appears in the paper by Focke [23] written with the participation of H. Schlichting. The corresponding bibliography is presented in that paper.

Focke notes that the speed of dolphins has been determined by many observers both on shore and from a moving vessel. However, in none of the described cases are data presented on the equipment by which the observations were made so that the accuracy of the measurements is unknown. This fact appears to be significant, for in order to develop speeds of 9 and 11 m/sec, powers differing by approximately a factor of 2 are required. On observation from a moving vessel it is necessary to consider that dolphins can use the energy of the system of waves occurring near a ship in their movement (a method of riding the waves known in Australia and Polynesia), and they can also use the favorable pressure gradient in the vicinity of the bow. Focke performed calculations for a vessel 30 meters long and 6 meters wide moving at a speed of 10 m/sec. It turned out that in the vicinity of the stem a dolphin 2.75 meters long experiences a propelling force approximately equal to 140 kg at the same time as the drag of his body is about 15 kg at this speed. Analyzing the most reliable sources, Focke arrives at the conclusion that a dolphin can develop a speed of up to 10 m/sec.

The power of dolphins can theoretically be determined by several methods. The majority of researchers, including Focke, consider it possible to take a specific power of dolphins (power per kg of musculature) approximately the same as for man

and other mammals, that is, about 5 kg-m/sec. Some researchers have performed special experiments to determine the power of dolphins. The American scientist Hero observed a dolphin weighing 180 kg jumping. In 0.6-0.7 seconds this dolphin developed a speed permitting him to jump 2.1 meters out of the water (his speed ⁻ leaving the water was about 125 knots). Calculations show that his specific power was in this case 3.5 kg-m/sec. In the opinion of biologists, the most exact method of finding power is connected with measuring the consumed oxygen, but as applied to such relatively large subjects as dolphins, this procedure runs into technical difficulties.

Investigation of the available data at the present time does not permit definite conclusions to be drawn that the drag of the dolphin's body is appreciably less than the drag of the corresponding rigid models. However, it is necessary to mention the experimental studies of Kramer [1]-[3], which were an impetus to the development of the discussed method of boundary layer control.

In his first paper [1], M. O. Kramer describes experiments with a rotating cylinder (inside diameter 50.8 cm, height 25.4 cm), the inside walls of which, in contact with the water poured into the cylinder, were covered with a damping layer. The cylinder was rotated at a speed of up to 720 rpm. The given angular velocity was sustained for 10 minutes until the fluid in the cylinder began to turn as a solid body. Then the cylinder stopped, and the rotational velocity of the fluid in the cylinder was measured. The flow conditions in the cylinder were determined by the variation of the rotational velocity of the fluid with time.

The critical Reynolds number (the diameter of the inside circle of the cylinder was taken as the characteristic length, and the rotational velocity of the inside circle of the cylinder before stopping was taken as the characteristic velocity), using the best version of flexible covering, was 2.4 times greater than the corresponding critical Reynolds number in the case of a rigid surface.

Obtaining hopeful results in the experiments with a cylinder, Kramer performed the following series of tests under conditions closer to the actual nature of flow over bodies [2]. A solid of revolution (L = 2.44 m, D = 6.35 cm) in the form of a cylinder with adapter 47 cm long was towed behind a boat developing a speed up to 35 knots on a thin (d = 2.34 mm) steel line 5.18 meters long. The forward half of the model, covered with various coverings, was attached to a spring, the deformation of which was recorded by strain gages, made it possible to determine the drag acting on the tested surface. A comparison was made with a standard rigid surface.

The maximum gain in the drag was 59% for $Re_L = 1.5 \cdot 10^7$.

In reference [3] Kramer describes experiments which are a development of the preceding studies. Improvements pertained to the towboat (the boat speed could vary up to 40 knots) and the design of the covering which had ribs as the elements supporting the outer diaphragm instead of columns as in the preceding version.

Positive results were obtained from the experiments although the decrease in the drag was somewhat less than in the case of the "column" covering.

Soon after publication of the experimental results of M. O. Kramer, the paper by Benjamin [4] appeared in which the first effort was made to give a theoretical

97

analysis of the stability conditions of the laminar boundary layer on a flexible surface. Benjamin solved the problem for the following wall boundary conditions:

$$\varphi'(0) + u_0' \cdot a = 0, \tag{II.1}$$

$$\varphi(0) = c \cdot a, \tag{II.2}$$

where a is the complex amplitude of the harmonic oscillations of the wall surface.

The boundary condition (II.2) corresponds to the assumption that the normal component of the disturbance velocity at the wall is equal to the velocity of the movement of the wall in the direction of the y-axis. The boundary condition (II.1) relates the tangential velocity component of the disturbing motion to the deformation of the wall and velocity distribution in the main flow.

For determination of the surface deformati   .n the normal direction Benjamin uses a formula obtained from the Navier-Stokes equations without considering the terms that depend on the viscosity.

The indicated boundary conditions and adopted simplification when determining the pressure on the wall permitted Benjamin to obtain a relatively simple form of the basic characteristic equation of the problem · However, even in the case of surface deformation' by a trip wire vibrating in the resistant medium he was unable to come up with a method of calculating the critical Reynolds numbers for different characteristics of a flexible surface.

The article by Landahl [5] is a development of Benjamin's work. In this article the author, using Benjamin's ssumption, takes the first steps to discover general laws controlling the successful operation of flexible surface in the sense of laminarization.

The study by Becker [6], [7], where he investigates various conditions of supplying energy to a fluctuating wall from the incompressible laminar layer side, is very similar to the ideas of Benjamin's work.

R. Betchov demonstrated an original approach to the solution of the problem of laminar boundary layer stability [8]. He divided the disturbances in a laminar boundary layer into three parts: disturbances, the behavior of which is described by the inviscid Orr-Sommerfeld equation, disturbances connected with the presence of a "viscid" zone near the wall and disturbances determined by the effect of viscosity in the critical layer where the velocity in the boundary layer coincides with the disturbance propagation rate.

An equation equivalent to the characteristic equation was obtained from the expression $v_x(0) = 0$. It is proposed that this equation be solved graphically. The characteristic equation is generalized to the case of a surface that is compliant in the normal direction.

The strictest statement of the problem of laminar boundary layer stability on a flexible surface appears in the paper by Boggs and Tokita [9]. Writing out the relations for this surface deformation as a function of normal and tangential stresses on the wall, they then use the incomplete characteristic equation and present their

98

arguments without considering the conditions at the upper boundary of the boundary layer. However, even this simplification and neglecting the influence of the tangential deformation on stability did not offer them the possibility of indicating a specific way to calculate the critical Reynolds number for various characteristics of a flexible covering.

A qualitative investigation of the behavior of a flexible surface under the effect of a fluid flow over it appears in the papers by Nonweiler [10] and Benjamin [11], [15].

A description of experiments in determining the influence of foam polyurethane coverings on the position of the laminar-to-turbulent boundary layer transition point on models of wings is given in the paper by Gregory and Love [12].

The study of the stability conditions of a Poseuille flow in the presence of flexible boundaries made by Hains and Price [13], [16] is closely adjacent to the mentioned papers. They represented a flexible surface in the form of a compliant film stretched with known tension, the magnitude of which varied in the calculations. During oscillations the film experienced drag proportional to the first power of the velocity. The inertial forces connected with the mass of the film and the forces proportional to the shift of the film in the normal direction (flexibility of the base) were not taken into account. Calculations of neutral curves for different film tensions and drag coefficients were made on computers. The calculation results gave closed instability regions in some cases.

In connection with the discussed problem it is necessary to note the cycle of papers by Miles studying wind wave generation. The basic results of these papers with the corresponding references can be found in the survey article [14].

§ II.2. Boundary Conditions for the Orr-Sommerfeld Equation in the Case of a Flexible Surface

The problem of stability of the laminar form of flow near a flexible surface differs from the analogous problem for a rigid wall by the boundary condition for $y = 0$.

Whereas in the case of a rigid surface the velocity components of the disturbing motion at the wall are equal to zero, in the case of a flexible surface it is natural to assume that on the basis of satisfaction of the adhesion condition, they are equal to the corresponding velocity components of the wall surface points. Deformation of a flexible surface, in turn, is connected with tangential and normal stresses on the surface of the body caused by velocity pulsations of the disturbing motion in the flow. We shall consider only small deformations of the wall such that their influence on the basic velocity profile can be neglected.

Let us be given the following equations relating the surface stresses and strains [17], [18]

$$y = \bar{k} \cdot \tilde{p} e^{i\theta_1},$$

(II.3)

$$x = \bar{m} \cdot \tilde{\tau} \cdot e^{i\theta_2},$$

(II.4)

where $\bar{k}$, $\bar{m}$ are constants that depend on the properties of the covering;

99

$\tilde{p}$ is the variable component of the pressure on the surface of the body;

$\tilde{\tau}$ is the variable component of the tangential stress on the surface of the body;

θ_1, θ_2 are phase shifts between the oscillations of the stresses on the body surface and the corresponding deformations.

A normal stress acting in a viscous fluid on an area perpendicular to the y-axis is expressed (see § I.2) by the formula

$$\tilde{p} = p_{yy} = -p + 2\mu \frac{\partial \tilde{v}_y}{\partial y}.$$

If the wall does not deform in the tangential plane, then

$$\left. \frac{\partial \tilde{v}_x}{\partial x} \right|_{\bar{y}=0} = 0,$$

and, consequently, on the basis of the continuity equation which is assumed to be valid to the fluid boundary,

$$\left. \frac{\partial \tilde{v}_y}{\partial y} \right|_{\bar{y}=0} = 0.$$

Therefore, by $\tilde{p}$ we mean the static pressure p, including the minus sign in the phase shift.

Pressure pulsations on the wall can be determined from the linearized Navier–Stokes equations written for disturbing motion (I.28).

Just as in the case of a rigid surface, let us select the following form of the current function of disturbing motion

$$\tilde{\varphi} = \bar{\varphi}(\bar{y}) \exp\left[i\left(a\bar{x} - b\bar{t}\right)\right],$$

on the basis of which we shall define the values entering into the first equation (I.28):

$$
\begin{aligned}
\tilde{v}_x &= \frac{\partial \tilde{\varphi}}{\partial y} = \bar{\varphi}'(\bar{y}) \exp\left[i\left(a\bar{x} - b\bar{t}\right)\right]; \\
\tilde{v}_y &= -\frac{\partial \tilde{\varphi}}{\partial x} = -ia\bar{\varphi}(\bar{y}) \exp\left[i\left(a\bar{x} - b\bar{t}\right)\right]; \\
\frac{\partial \tilde{v}_x}{\partial t} &= -ib\bar{\varphi}'(\bar{y}) \exp\left[i\left(a\bar{x} - b\bar{t}\right)\right]; \\
\frac{\partial \tilde{v}_x}{\partial x} &= ia\bar{\varphi}'(\bar{y}) \exp\left[i\left(a\bar{x} - b\bar{t}\right)\right]; \\
\frac{\partial^2 \tilde{v}_x}{\partial x^2} &= -a^2\bar{\varphi}'(\bar{y}) \exp\left[i\left(a\bar{x} - b\bar{t}\right)\right]; \\
\frac{\partial^2 \tilde{v}_x}{\partial y^2} &= \bar{\varphi}''(\bar{y}) \exp\left[i\left(a\bar{x} - b\bar{t}\right)\right]; \\
\frac{\partial^3 \tilde{v}_x}{\partial y^3} &= \bar{\varphi}'''(\bar{y}) \exp\left[i\left(a\bar{x} - b\bar{t}\right)\right].
\end{aligned}
\qquad \text{(II.5)}
$$

100

Substituting (II.5) in the first equation of (I.28)

$$\frac{\partial \tilde{p}}{\partial x} = \rho \exp\left[i(a\bar{x}-b\bar{t})\right]\left\{ib\bar{\varphi}'(\bar{y})-u\cdot i\cdot a\bar{\varphi}'(\bar{y})+\right.$$
$$\left. + u'\cdot ia\bar{\varphi}(\bar{y}) + v\left[\bar{\varphi}'''(\bar{y})-a^2\bar{\varphi}'(\bar{y})\right]\right\}.$$

(II.6)

Let us integrate (II.6) with respect to $\bar{x}$

$$\tilde{p} = \frac{\rho}{ia}\exp\left[i(a\bar{x}-b\bar{t})\right]\left[v\bar{\varphi}'''(\bar{y})+ia\left(\frac{b}{a}-u-\frac{va}{i}\right)\times\right.$$
$$\left.\times \bar{\varphi}'(\bar{y}) + i\cdot au'\bar{\varphi}(\bar{y})\right] + Q(\bar{y}).$$

(II.7)

The value of $Q(\bar{y})$ can only be constant, for when determining the function $Q(\bar{y})$, the following relation is obtained

$$\frac{\partial \tilde{p}}{\partial \bar{y}} = f_1'(\bar{y})\exp\left[i(a\bar{x}-b\bar{t})\right] + Q'(\bar{y}) =$$
$$= f_2(\bar{y})\exp\left[i(a\bar{x}-b\bar{t})\right],$$

where $f_1'(\bar{y})$ is defined from (II.7), and $f_2(\bar{y})$ is found from the second equation of (I.28). Since $\partial\tilde{p}/\partial\bar{y} \equiv \partial\tilde{p}/\partial\bar{y}$ for all values of $\bar{x}$, $\bar{y}$, $\bar{t}$,

$$f_1'(\bar{y}) = f_2(\bar{y}) \text{ and } Q'(\bar{y}) \equiv 0.$$

It is necessary to consider the approximate nature of the equalities of (I.28).

Considering the equality (II.7) for $\bar{y} \to \infty$, we see that $Q(\bar{y}) \equiv 0$.

Let us differentiate (II.3) with respect to time, substituting the value of $\tilde{p}$ from (II.7) and the value of $\tilde{v}_y$ from (II.5),

$$ia\varphi(\bar{y}) = k\frac{b}{a}\cdot\rho\left[v\bar{\varphi}'''(\bar{y}) + ia\left(\frac{b}{a}-u-\frac{va}{i}\right)\times\right.$$
$$\left.\times \bar{\varphi}'(\bar{y}) + iau'\cdot\bar{\varphi}(\bar{y})\right]e^{i\theta_1}.$$

At the wall when $\bar{y} = 0$, the preceding equality gives the following boundary condition written in dimensionless form

$$\kappa c e^{i\theta_1}\left[\frac{\varphi'''(0)}{ia\,\mathrm{Re}} + \left(c + \frac{ai}{\mathrm{Re}}\right)\varphi'(0) + u'(0)\varphi(0)\right] - \varphi(0) = 0,$$

(II.8)

where the parameter

$$\kappa = \bar{\kappa}\frac{\rho U^2}{\delta}.$$

(II.9)

If the wall is unable to be deformed in the tangential plane, that is, $\tilde{v}_x(0) = 0$, then $\varphi'(0) = 0$, and condition (II.8) is simplified somewhat

101

$$\kappa c \, \frac{\varphi''(0)}{ia \, \mathrm{Re}} = \varphi(0) |e^{-i\theta_1} - \kappa c u'(0)|. \tag{II.10}$$

For a rigid surface the ordinary boundary condition is obtained from (II.8) and (II.10) for k = 0.

A tangential stress acting in a viscous fluid on an area normal to the y-axis is expressed by the formula

$$\tilde{\tau} = p_{xy} = \mu \left(\frac{\partial \tilde{v}_x}{\partial y} + \frac{\partial \tilde{v}_y}{\partial x} \right).$$

If the wall is not deformed in the normal direction, then

$$\frac{\partial \tilde{v}_y}{\partial x} \bigg|_{y=0} \equiv 0.$$

consequently,

$$\tilde{\tau} = \mu \frac{\partial \tilde{v}_x}{\partial y}. \tag{II.11}$$

In order to obtain the second boundary condition on the wall for the function ϕ let us substitute the value of $\tilde{\tau}$ from (II.11) and the expression $\partial \tilde{v}_x/\partial y$ from (II.5) in (II.4):

$$\bar{x} = \bar{m} \cdot \mu \bar{\varphi}''(\bar{y}) \exp [i(a\bar{x} - b\bar{t}) + \theta_2]. \tag{II.12}$$

Differentiating (II.12) with respect to time and considering that

$$\frac{\partial \tilde{x}}{\partial t} \bigg|_{y=0} = \tilde{v}_x(0) = \bar{\varphi}'(0) \exp [i(a\bar{x} - b\bar{t})],$$

we find

$$\bar{\varphi}'(0) = -i b \bar{m} \mu \cdot \bar{\varphi}''(0) e^{i\theta_2}. \tag{II.13}$$

Let us reduce the values entering into formula (II.13) to dimensionless form

$$\varphi'(0) = -im \frac{cu}{\mathrm{Re}} \varphi''(0) e^{i\theta_2}, \tag{II.14}$$

where

$$m = \bar{m} \frac{\rho U^2}{\delta}. \tag{II.15}$$

The boundary conditions on the outer boundary of the boundary layer will be taken in the same form as in the case of a rigid surface, that is, we shall use the expressions

$$af(1) + f'(1) = 0, \quad f(y)|_{y \to \infty} < M < \infty.$$

In subsequent sections of this chapter two problems will be considered: the first, on the stability of a laminar boundary layer on a surface that is compliant in the normal direction; the second, on the stability of a laminar boundary layer on a

102

surface that is compliant in the tangential plane.

Let us write the boundary conditions for these two cases, considering (II.10) and (II.14).

The boundary conditions of the first problem:

$$-\frac{kc}{iu\,\text{Re}}\,\varphi''(0) + \varphi(0)[e^{-i\theta_1} - \kappa c u'(0)] = 0;$$
$$\varphi'(0) = 0;$$
$$\alpha\varphi(1) + \varphi'(1) = 0;$$
$$|\varphi(y)|_{y \to \infty} < M < \infty.$$

$$(II.16)$$

The boundary conditions of the second problem

$$\varphi(0) = 0;$$
$$\varphi'(0) + i\,\frac{muc}{\text{Re}}\,\varphi''(0)e^{i\theta_1} = 0;$$
$$\alpha\varphi(1) + \varphi'(1) = 0;$$
$$|\varphi(y)|_{y \to \infty} < M < \infty.$$

$$(II.17)$$

The boundary conditions obtained on the wall are a consequence of the adopted relation between the surface deformation and the corresponding stresses (II.3), (II.4) which, in spite of its simplicity is very general. Thus, for example, relation (II.3) encompasses all coverings, the deformation of which is described by an equation of the type

$$L\left(y_c, \frac{\partial y_c}{\partial t},\ \frac{\partial y_c}{\partial x},\ \frac{\partial^2 y_c}{\partial t^2},\ \frac{\partial^2 y_c}{\partial x^2},\ \ldots,\ \frac{\partial^n y_c}{\partial x^n}\right) = p(x,\ t),$$

in which L is a linear combination of its arguments with constant coefficients, p is the pressure of the disturbing motion on the wall surface, y_c is the surface coordinate of the flexible covering. The same thing pertains also to equality (II.4). As usual in the method of small oscillations it is proposed that all the values connected with disturbing motion vary according to a harmonic law

$$A(x,\ y,\ t) = [A_r(y) + iA_i(y)]\exp[i\alpha(x - ct)].$$

For example, if the surface motion is described by the equation

$$a_1\frac{\partial^2 y_c}{\partial t^2} + a_2\frac{\partial y_c}{\partial t} + a_3 y_c + a_4\frac{\partial^2 y_c}{\partial x^2} = p(x,\ t),$$

where $p(x,\ t) = p_0 e^{i\alpha(x-ct)}$, then finding the forced oscillation of the wall in the form of $y_c = y_0 e^{i\alpha(x-ct)}$, we arrive at the expression

$$(-\alpha^2 c^2 a_1 - i\alpha c a_2 + a_3 - \alpha^2 a_4)y_0 e^{i\alpha(x-ct)} = p_0 e^{i\alpha(x-ct)},$$

or $y_c = K p e^{i\theta_1}$, where $\kappa e^{i\theta_1} = (a_3 - \alpha^2 c^2 a_1 - i\alpha c a_2 - \alpha^2 a_4)^{-1}$.

The values of a_i (i = 1, 2, 3, 4) define the specific mass, drag, elasticity and surface tension of the given covering.

The dimensionless parameters k (II.9) and m (II.15) play the role of similarity criteria characterizing the properties of the covering. For the same mechanical characteristics of the covering, its operating efficiency depends on the density of the fluid flowing over the body, the square of the flow velocity at the boundary of the boundary layer and the thickness of the boundary layer. It is necessary to consider the significant increase in relative compliance of the covering with an increase in velocity. Since the thickness of the laminar boundary layer is inversely proportional to $U^{1/2}$, with an increase in velocity the compliance of the covering varies proportionally to $U^{5/2}$. This fact makes it possible to hope for success in using damping coverings for laminarization at high flow velocities over a flexible surface.

§ II.3. Method of Calculating the Stability Characteristics of a Laminar Boundary Layer Developed at a Surface that is Compliant in the Normal Direction

Using boundary conditions (II.16), which are uniform with respect to the function ϕ and its derivatives, it is possible by the same method as in the case of a rigid surface (§ I.7) to find the following characteristic equation of the problem:

$$\begin{vmatrix} -\frac{\kappa c}{i\alpha Re}\varphi_1'''(0)+(e^{-i\theta_1}-\kappa c u_0')\varphi_1(0) - \frac{\kappa c}{i\alpha Re}\varphi_2''(0)+(e^{-i\theta_1}-\kappa c u_0')\varphi_2(0) - \frac{\kappa c}{i\alpha Re}\varphi_3''(0)+(e^{-i\theta_1}-\kappa c u_0')\varphi_3(0) \\ \varphi_1'(0) & \varphi_2'(0) & \varphi_3'(0) \\ \varphi_1'(1)+\alpha\varphi_1(1) & \varphi_2'(1)+\alpha\varphi_2(1) & 0 \end{vmatrix} = 0.$$

Let us expand the determinant obtained with respect to elements of the third column

$$\left(e^{-i\theta_1} - \kappa c u_0'\right)\frac{\varphi_3(0)}{\varphi_3'(0)} - \frac{\kappa c}{i\alpha Re}\cdot\frac{\varphi_3''(0)}{\varphi_3'(0)} =$$

$$= \frac{\left[\left(e^{-i\theta_1}-\kappa c u_0'\right)\varphi_1(0)-\frac{\kappa c}{i\alpha Re}\varphi_1''(0)\right]\left[\varphi_2'(1)+\alpha\varphi_2(1)\right] - \left[\left(e^{-i\theta_1}-\kappa c u_0'\right)\varphi_2(0)-\frac{\kappa c}{i\alpha Re}\varphi_2''(0)\right]\left[\varphi_1'(1)+\alpha\varphi_1(1)\right]}{\varphi_1'(0)\left[\varphi_2'(1)+\alpha\varphi_2(1)\right]-\varphi_2'(0)\left[\varphi_1'(1)+\alpha\varphi_1(1)\right]}.$$

Substituting the values of the functions

$$\left.\begin{aligned}
&\varphi_1(0) = -c; \quad \varphi_1'(0) = u'(0) = u_0'; \quad \varphi_1''(0) = u'' - \alpha^2 c; \\
&\varphi_1'''(0) = u_0''' + \alpha^2 u_0'; \quad \varphi_2(0) = 0; \quad \varphi_2'(0) = -\frac{1}{c}; \\
&\varphi_2''(0) = 0; \quad \varphi_2'''(0) = \frac{u_0''}{c^2} - \frac{\alpha^2}{c}; \\
&\frac{\varphi_3''(0)}{\varphi_3'(0)} = -i\sqrt{i\alpha Re \cdot c}; \quad \frac{\varphi_3'''(0)}{\varphi_3'(0)} = -ic\alpha Re,
\end{aligned}\right\} \qquad (II.18)$$

calculated on the basis of the known expansions of (§ I.6), considering smallness of the ratio $1/\alpha Re$ and also the condition $u''*(0) = 0$ valid for a laminar boundary layer at a wall, we arrive at the complex equality

$$-\frac{\varphi_3(0)}{y_\kappa\varphi_3'(0)} = -\frac{kc^2}{y_\kappa\left(e^{-i\theta_1}-\kappa c u_0'\right)} + \frac{c}{y_\kappa\cdot u_0'}\cdot\frac{z}{1+z}, \qquad (II.19)$$

where

$$z = z_r + iz_i;$$

$$z_r = -\frac{u_0'}{u_\kappa'} + \frac{u_0' c u_\kappa''}{u_\kappa'^3}\ln c + \frac{u_0' c}{\alpha(1-c)^3};$$

$$z_i = -\pi u_0' c \frac{u_\kappa''}{u_\kappa'^3}.$$

It is possible to solve equation (II.19) graphically as discussed in § I.7, except the values of E_r, E_i must be determined from the following expressions instead of formulas (I.106):

$$E_r(\alpha, c, \kappa, \theta_1) = \frac{c}{y_\kappa u_0} \frac{z_r + z_i^2 + z_r^2}{(1+z_r)^2 + z_i^2} +$$

$$+ \frac{\kappa c^2}{y_\kappa} \cdot \frac{\cos\theta_1 - \kappa c u_0'}{1 - 2\cos\theta_1 \cdot \kappa c u_0' + \kappa^2 c^2 u_0'^2};$$

$$E_i(\alpha, c, \kappa, \theta_1) = \frac{c}{y_\kappa u_0} \cdot \frac{z_i}{(1+z_r)^2 + z_i^2} +$$

$$+ \frac{\kappa c^2}{y_\kappa} \cdot \frac{\sin\theta_1}{1 - 2\cos\theta_1 \cdot \kappa c u_0' + \kappa^2 c^2 u_0'^2}.$$

(II.20)

The values of z_r and z_i entering into (II.20) are calculated by the above-presented formulas.

The difficulties in graphical solution of equation (II.19) noted in § I.7, increase significantly in the presence of additional parameters k, θ_1 reflecting the influence of a flexible surface on the laminar boundary layer stability.

Accordingly, it appears very useful to point out a calculation method of determining the critical Reynolds number for a laminar boundary layer developed on a flexible surface with known properties which, as before, is of interest to researchers studying laminarization.

Let us discuss the method beginning with the basic Lin concepts [19] which he developed when studying laminar boundary layer stability on a rigid surface.

Hereafter we shall use the approximate equality

$$c \simeq y_\kappa \cdot u_0'.$$ (II.21)

Let us rewrite (II.19) considering (II.21)

$$F(w) = \frac{z}{1+z} + A + iB,$$ (II.22)

where the following notation has been introduced

$$A = \frac{\kappa c u_0}{1 - 2\cos\theta_1 \cdot \kappa c u_0' + \kappa^2 c^2 u_0'^2}(\cos\theta_1 - \kappa c u_0');$$ (II.23)

$$B = \frac{\kappa c u_0}{1 - 2\cos\theta_1 \cdot \kappa c u_0' + \kappa^2 c^2 u_0'^2}\sin\theta_1.$$ (II.24)

Then setting $1 + z = \Phi$, we arrive at two real equations on the basis of the complex equation (II.19):

105

$$\left.\begin{array}{l}\Phi_r = G_{ri};\\ \Phi_i = G_i.\end{array}\right\} \tag{II.25}$$

The values entering into system (II.25), are defined by formulas

$$\Phi_r = 1 - \frac{u_0'}{u_\kappa'} + \frac{u_0' c u_\kappa''}{u_\kappa'^3}\ln c + \frac{u_0' c}{a(1-c)^2}. \tag{II.26}$$

$$\Phi_i = -\pi c u_0' \frac{u_\kappa''}{u_\kappa'^3}. \tag{II.27}$$

$$G_r = \frac{1 - F_r(w) + A}{(1 - F_r + A)^2 + (B - F_i)^2}. \tag{II.28}$$

$$G_i = \frac{F_i(w) - B}{(1 - F_r + A)^2 + (B - F_i)^2}, \tag{II.29}$$

where $F(w) = F_r(w) + iF_i(w)$ is the Tietjens function (§ I.7).

The scheme for calculating the critical Reynolds number as a function of the parameter k for a given velocity profile in the boundary layer and for a given value of the parameter θ_1 reduces to the following.

1. Being given the numerical value of the derivative kc and knowing the values of θ_1 and u_0' (the velocity profile is given), let us calculate A and B by formulas (II.23) and (II.24). Let us note that it is mpossible to give the value of k without relating it to the value of c, for in this case the right-hand sides of equalities (II.25) will be functions not only of w, but also the parameter c which excludes the possibility of using the basic Lin concept (§ I.7).

2. For the values of A and B found, using Table I.1 and formula (II.29), let us construct the graph $G_i = G_i(w)$.

3. Let us determine $G_{i_{max}}$ and the corresponding value of w_m by the graph of $G_i = G_i(w)$.

4. Solving the following equation graphically with respect to c

$$G_{i_{max}} = -\pi c \cdot u_0' \frac{u_\kappa''}{u_\kappa'^3},$$

which was obtained from the second equation of system (II.25) and formulas (II.27), let us determine the value of c_m and, consequently, the following parameters u_{km}', u_{km}'', y_{km}.

5. Let us determine G_{rm} by formula (II.28) for a value of $w = w_m'$.

6. Considering formula (II.26) and the first equation of system (II.25), we find α_m corresponding to the previously defined value of c_m

106

$$\alpha_m = \frac{u_0'c}{(1-c)^2} \cdot \frac{1}{G_{r_m} - 1 + \frac{u_0'}{u_\kappa'} - \frac{u_0'cu_\kappa''}{u_\kappa'^3} \ln c}.$$

7. Let us define the critical Reynolds number by the formula

$$\mathrm{Re}_{\kappa p} = \left(\frac{w_m}{y_{\kappa m}}\right)^3 \cdot \frac{1}{\alpha_m \cdot u_{\kappa m}'}.$$

8. Let us calculate the value of the parameter k which corresponds to the value found for the Reynolds number $k_m = kc/c_m$.

Performing the indicated calculations for different values of the parameter kc for a reinforced value of θ_1, it is possible to obtain the curve of $\mathrm{Re}_{cr} = \mathrm{Re}_{cr}(k)$ for a given velocity profile in a laminar boundary layer.

§ II.4. Calculations of the Critical Reynolds Number of a Laminar Boundary Layer as a Function of the Characteristics of a Compliant Surface in the Normal Direction and the Pohlhausen Form Parameter[1]

The methods discussed in this section permit calculation of the loss of stability point of a laminar boundary layer developed on an elastic surface with known characteristics k and θ_1. However, such calculations are very tedious. For significant simplification of the process of finding the loss of stability point on elastic surfaces the universal relations $\mathrm{Re}^*_{cr} = \mathrm{Re}^*_{cr}(k, \theta_1)$ were constructed for different values of the parameter λ.

As before, the nature of the following functions was studied:

$$\mathrm{Re}_{\kappa p}^{\cdot} = \mathrm{Re}_{\kappa p}^{\cdot}(\kappa, \; \theta_1 = \mathrm{const}),$$
$$\mathrm{Re}_{\kappa p}^{\cdot} = \mathrm{Re}_{\kappa p}^{\cdot}(\theta_1, \; \kappa = \mathrm{const}).$$
(a)

Key: a. cr

The calculations were performed on the basis of the grapho-analytical method (§ II.3) for the following values of the parameters

$$\kappa = 0,1; \; 360° > \theta_1 \geqslant 0°,$$
$$\theta_1 = 0°; \; -0,2 \leqslant \kappa \leqslant 0,4.$$

The results of determining the critical Reynolds numbers for the Blasius profile (see Table I.2) as a function of k and θ_1 are presented in Figures II.1 and II.2.

_____

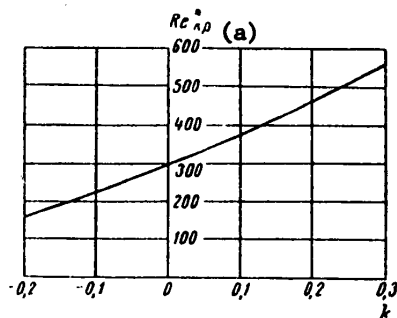[1]All the caLculations in this chapter were performed by Z. N. Smirnova and N. M. Savina.

107

Figure II.1. Critical Reynolds number as a function of the parameter k; $\theta_1=0$.
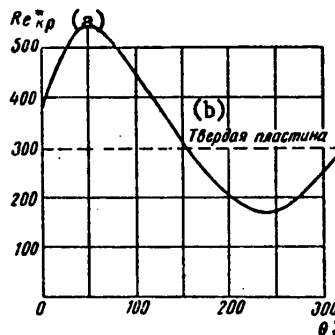
Key: a. cr

Figure II.2. Critical Reynolds number as a function of the parameter θ_1; k=0.1.

Key: a. cr   b. solid plate

The performed calculations indicate that the value of the critical Reynolds number varies monotonically with variation of the parameter k and has an obvious peak on variation of θ_1 within the interval $0° \leq \theta_1 < 360°$. Moreover, in some range of variation of θ_1 the critical Reynolds number on an elastic surface becomes less than the value for a rigid wall.

This fact has exceptionally important significance, for it indicates the necessity for careful selection of the coverings designed to damp   pulsations in a laminar boundary layer. It cannot be expected that the softer the coating, the greater the effect from using it. It can turn out to be the opposite if the damping properties are improperly selected.

In connection with what has been discussed, all of the following calculations were performed for a fixed value of $\theta_1 = 60°$. The basis for the calculations was the family of Pohlhausen profiles defined by a sixth-degree polynomial.

Figures II.3 and II.4 show the results of calculating a family of curves $Re^*_{cr} = Re^*_{cr}$ (λ, k) for $\theta_1 = 60°$. The rapid growth of the critical Reynolds number with variation of the parameter k in the interval $0 \leq k \leq 1$ attracts attention.

In addition to finding the critical Reynolds number which was determined by the scheme in § II.3 directly without constructing a neutral curve, it is of defined interest to consider the nature of variation of the wavelength of the disturbance which, as before, causes instability, and its propagation rate as a function of the characteristics of the elastic covering.

The corresponding graphs were constructed for three velocity profiles defined by values of the parameter $\lambda = 2, 0; -2$ (Figures II.5, II.6).

From Figure II.5 it is obvious that with an increase in k the wavelength of a dangerous disturbance increases sharply ($\bar{\lambda} = 2\pi\delta/\alpha$), and its propagation rate along the x-axis drops sharply (Figure II.6).
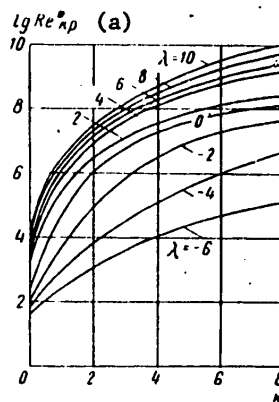
108

Figure II.3. Critical Reynolds number as a function of the parameter k for different values of the parameter λ; $\theta_1 = 60°$.
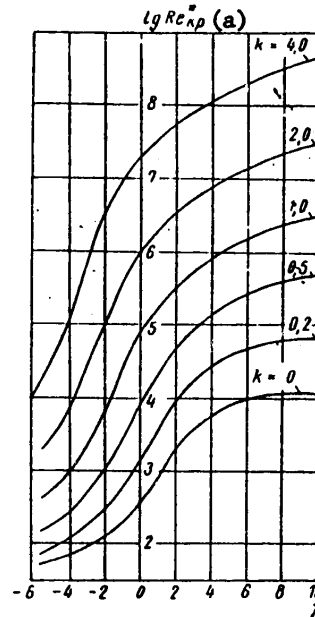
Key: a. cr

Figure II.4 Critical Reynolds number as a function of the parameters k and λ; $\theta_1 = 60°$.

Key: a. cr

§ II.5. Method of Calculating the Stability Characteristics of a Laminar Boundary Layer Developed on a Surface Compliant on the Tangential Direction

On the basis of the boundary conditions (II.17) which are uniform with respect to the function ϕ and its derivatives, we obtain the characteristic equation

$$\begin{vmatrix} \varphi_1'(0) + i\,\dfrac{mac}{Re}\,\varphi_1''(0)\,e^{i\theta_1} & \varphi_2'(0) + i\,\dfrac{mac}{Re}\,\varphi_2''(0)\,e^{i\theta_1} & \varphi_3'(0) + i\,\dfrac{mac}{Re}\,\varphi_3''(0)\,e^{i\theta_1} \\ \varphi_1(0) & \varphi_2(0) & \varphi_3(0) \\ \varphi_1'(1) + a\varphi_1(1) & \varphi_2'(1) + a\varphi_2(1) & 0 \end{vmatrix} = 0 \qquad (II.30)$$
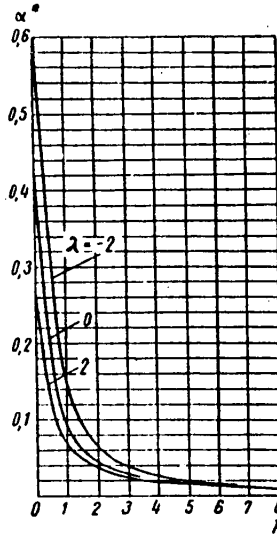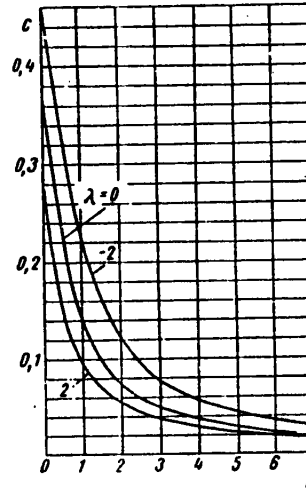
which relates the parameters of the boundary layer, the disturbances and the elastic surface.

Let us transform equation (II.30)

$$\left[\varphi_3'(0) + i\,\frac{mac}{Re}\,\varphi_3''(0)\,e^{i\theta_1}\right] \times$$

109

Figure II.5. Parameter α* as a function of compliance of the surface; $\theta_1 = 60°$.

Figure II.6. Propagation rate of a disturbance as a function of the parameter k; $\theta_1 = 60°$.

$$\times \begin{vmatrix} \varphi_1(0) & \varphi_2(0) \\ \varphi_1'(1) + \alpha\varphi_1(1) & \varphi_2'(1) + \alpha\varphi_2(1) \end{vmatrix} -$$

$$- \varphi_3(0) \begin{vmatrix} \varphi_1'(0) + i\frac{mac}{Re}\varphi_1''(0)e^{i\theta_1} & \varphi_2'(0) + i\frac{mac}{Re}\varphi_2''(0)e^{i\theta_1} \\ \varphi_1'(1) + \alpha\varphi_1(1) & \varphi_2'(1) + \alpha\varphi_2(1) \end{vmatrix} = 0.$$

$$\frac{\varphi_3(0)}{\varphi_3'(0)} = \left[1 + i\frac{mac}{Re}e^{i\theta_1}\frac{\varphi_3''(0)}{\varphi_3'(0)} \right] \times$$

$$\times \frac{\varphi_1(0)\dfrac{\varphi_2'(1) + \alpha\varphi_2(1)}{\varphi_1'(1) + \alpha\varphi_1(1)} - \varphi_2(0)}{\left[\varphi_1'(0) + i\dfrac{mac}{Re}\varphi_1''(0)e^{i\theta_1} \right]\dfrac{\varphi_2'(1) + \alpha\varphi_2(1)}{\varphi_1'(1) + \alpha\varphi_1(1)} - \left[\varphi_2'(0) + i\dfrac{mac}{Re}\varphi_2''(0)e^{i\theta_1} \right]}.$$ (II.31)

Substituting values of the functions ϕ_1, ϕ_2 and their derivatives at the wall (II.18) in the right-hand side of (II.31), we arrive at the equation

$$\frac{\varphi_3(0)}{\varphi_3'(0)} = \left[1 + \frac{ma^{3/2}c^{3/2}}{Re^{1/2}}e^{i\left(\theta_1 + \frac{\pi}{4}\right)} \right] \times$$

110

$$\lambda \ \frac{-c \ \dfrac{\varphi_2'(1) + \alpha\varphi_2(1)}{\varphi_1'(1) + \alpha\varphi_1(1)}}{\left[u_0' + \dfrac{imac}{Re}(u_0'' - c\alpha^2)e^{i\theta_1} \right] \dfrac{\varphi_2'(1) + \alpha\varphi_2(1)}{\varphi_1'(1) + \alpha\varphi_1(1)} + \dfrac{1}{c}} .$$

(II.32)

Since $m \approx 1$, $c < 1$, $\alpha \leq 1$, and the number $Re \gg 1$, in the sum $u_0' + imac/Re(U'' - c\alpha^2)e^{i\theta}2$, the second term can be neglected by comparison with u_0' in view of the fact that the value of u_0' varies within the limits of $0.8 \leq u_0' \leq 3.6$ within the most interesting range of variation of the parameter $\lambda = (U'\delta^2/\nu) \ (-6 \leq \lambda \leq 8)$.

Considering this fact, let us rewrite equality (II.32)

$$-\frac{1}{y_\kappa} \cdot \frac{\varphi_3(0)}{\varphi_3'(0)} = -\frac{c}{y_\kappa u_0'} \cdot \frac{z}{1+z} \left[1 + mac \left| \sqrt{\frac{c\alpha}{Re}} \cdot e^{i\left(\theta_1 + \frac{\pi}{4}\right)} \right| \right],$$

(II.33)

where

$$z = \frac{u_0' c \left[\varphi_2'(1) + \alpha\varphi_2(1) \right]}{\varphi_1'(1) + \alpha\varphi_1(1)} .$$

Then let us assume that the following inequality is valid:

$$\frac{m a^{1/2} c^{3/2}}{Re^{1/2}} < 1,$$

which defines the admissible values of the parameter

$$m < \frac{Re^{1/2}}{a^{3/2} c^{3/2}} .$$

In this case, on the basis of (II.33) we arrive at the expression

$$-\frac{1}{y_\kappa} \cdot \frac{\varphi_3(0)}{\varphi_3'(0)} \left[1 - \frac{m a^{1/2} c^{1/2}}{Re^{1/2}} e^{i\left(\theta_1 + \frac{\pi}{4}\right)} \right] = \frac{c}{y_\kappa u_0'} \cdot \frac{z}{1+z} .$$

(II.34)

Let us introduce the known notation (§ I.7)

$$-\frac{1}{y_\kappa} \cdot \frac{\varphi_3(0)}{\varphi_3'(0)} = F(w) = F_r(w) + iF_i(w); \quad w = y_\kappa (u_\kappa' \cdot \alpha \ Re)^{1/2}.$$

Then considering the assumption $c \approx y_k \cdot u_0'$ equality (II.34) is written as follows:

$$F(w) \left[1 - \frac{m a^2 c^2 y_\kappa}{w^{1/2}} e^{i\left(\theta_1 + \frac{\pi}{4}\right)} \right] = \frac{z}{1+z} .$$

Let us denote the product of the real parameters m, α^2, c^2, y_k by

$$M = m\alpha^2 c^2 y_\kappa .$$

(II.35)

111

Considering (II.35) the preceding equality assumes the form

$$F(w)\left[1 - \frac{M}{w^{3/2}} e^{i\left(\theta_2 + \frac{\pi}{4}\right)}\right] = \frac{z}{1+z}. \tag{II.36}$$

Let us transform equation (II.36) assuming for brevity the notation

$$P(\alpha, c) = P_r(\alpha, c) + iP_i(\alpha, c) = 1 + z = 1 + z_r + iz_i;$$

where

$$1 - F(w)\left[1 - \frac{M}{w^{3/2}} e^{i\left(\theta_2 + \frac{\pi}{4}\right)}\right] = D(w, M, \theta_2) = D_r + iD_i,$$

$$P_r(\alpha, c) = 1 - \frac{u_0'}{u_\kappa'} + \frac{u_0' c u_\kappa''}{u_\kappa'^3} \ln c + \frac{u_0' c}{\alpha(1-c)^2}; \tag{II.37}$$

$$P_i(\alpha, c) = -\pi u_0' c \frac{u_\kappa''}{u_\kappa'^3}; \tag{II.38}$$

$$D_r(w, M, \theta_2) = 1 - F_r(w) + F_r(w) \frac{M}{w^{3/2}} \cos\left(\frac{\pi}{4} + \theta_2\right) -$$

$$- F_i(w) \frac{M}{w^{3/2}} \sin\left(\theta_2 + \frac{\pi}{4}\right). \tag{II.39}$$

$$D_i(w, M, \theta_2) = -F_i(w) + F_i(w) \frac{M}{w^{3/2}} \cos\left(\theta_2 + \frac{\pi}{4}\right) +$$

$$+ F_r(w) \frac{M}{w^{3/2}} \sin\left(\theta_2 + \frac{\pi}{4}\right). \tag{II.40}$$

We obtain the complex equality P = 1/D which is equivalent to two real equalities

$$P_r(\alpha, c) = \frac{D_r(w, M, \theta_2)}{D_r^2 + D_i^2}; \tag{II.41}$$

$$P_i(\alpha, c) = -\frac{D_i(w, M, \theta_2)}{D_r^2 + D_i^2}. \tag{II.42}$$

Using formulas (II.37)-(II.42), it is possible to construct a neutral curve for any velocity profile in the boundary layer for given parameters M and θ_2 and also to find the critical Reynolds number without constructing the neutral stability curve.

Let us consider the procedure for finding the critical Reynolds number.

1. Being given values of M and θ_2, using Table I.1 and formulas (II.39), (II.40), let us construct the function

$$\Phi_i(w) = -\frac{D_i(w, M, \theta_2)}{D_r^2 + D_i^2}. \tag{II.43}$$

2. Let us define the maximum value of $\Phi_{i\ max}$ and the corresponding value of $w = w_m$ by this graph.

112

3. Solving the following equation graphically

$$-\pi u_0 c \frac{\ddot{u}_k}{\ddot{u}_k} = \Phi_{l\,\text{max}},$$

we determine the value of the parameter c and, consequently, the corresponding values of y_k, u_k^i, u_k^{ii}, for the velocity profile in the boundary layer is given.

4. For the value of w_m found, using formulas (II.39), (II.40), we calculate

$$\Phi_r(w_m, M, \theta_2) = \frac{D_r(w_m, M, \theta_2)}{D_r^2 + D_i^2}.$$

5. Using equalities (II.37) and (II.41), let us determine the value of the parameter α considering the values found for c, u_k^i, u_k^{ii},

$$\alpha_m = \frac{u_0 c}{(1-c)^2} \cdot \frac{1}{\Phi_r(w_m) - 1 + \frac{u_0}{u_k^i} - \frac{u_0 c u_k^{ii}}{u_k^{i3}} \ln c}.$$

6. Let us define the critical Reynolds number by the formula

$$\text{Re}_{\kappa p} = \left(\frac{w_m}{y_{km}}\right)^3 \frac{1}{\alpha_m u_{km}^i}$$

or, replacing the thickness of the boundary layer by the displacement thickness,

$$\text{Re}_{\kappa p}^{\bullet} = \text{Re}_{\kappa p}\left(\frac{2}{7} - \frac{\lambda}{105}\right)$$

7. Using formula (II.35) let us calculate the value of the covering parameter m which corresponds to the value found for the critical Reynolds number

$$m = \frac{M}{\alpha_m^2 c_m^2 y_{km}}.$$

Performing the indicated calculations for different values of the parameter M for reinforced θ_2, it is possible to obtain the function

$$\text{Re}_{\kappa p}^{\bullet} = \text{Re}_{\kappa p}^{\bullet}(m).$$
(a)

Key: a, cr

§ II.6. Calculations of the Critical Reynolds Number of a Boundary Layer as a Function of the Characteristics of a Surface Compliant in the Tangential Plane and the Pohlhausen Form Parameter

The corresponding calculations were performed for a plate in order to discover the nature of the critical Reynolds number as a function of the parameters m and θ_2. The velocity profile in the boundary layer was determined in this case by a sixth-degree polynomial with the parameter $\lambda = 0$.

113

Using formulas (II.39), (II.40), (II.43), the functions $\Phi_i = \Phi_i(w)$ were constructed for M = 0.1, 0.25 and 0.5 for different values of the parameter θ_2 which varied within the range from 0° to 360°.

On the basis of the indicated relations, for each combination of M and θ_2, values of $\Phi_{i_{max}}$ and the corresponding values of w_m were found. The functions $\Phi_{i_{max}} = \Phi_{i_{max}}(\theta_2)$, $w_m = w_m(\theta_2)$ are presented in Figure II.7 for M = 0.25. The functions $Re^*_{cr} = Re^*_{cr}(\theta_2)$, $m = m(\theta_2)$ for M = 0.1, 0.25 and 0.5 were constructed by the scheme described in the preceding section. The corresponding curves for M = 0.25 are illustrated in Figure II.8.

Beginning with these relations, graphs of the functions $Re^*_{cr} = Re^*_{cr}(\theta_2)$ were con-structed for consatnt values of the parameter m (Figure II.9).
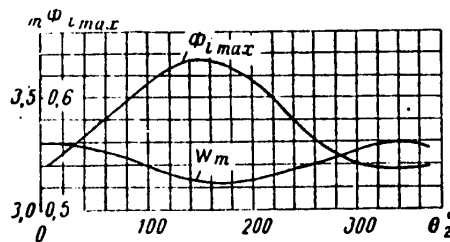
Figure II.7. Value of $\Phi_{i\ max}$ and w_m as a function of the parameter θ_2; M = 0.25; λ = 0.
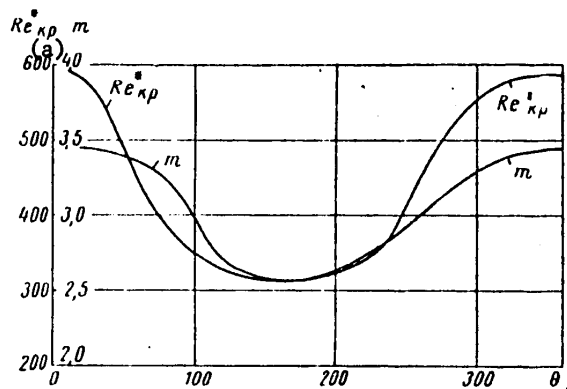
Figure II.8. Critical Reynolds number and m as a function of the parameter θ_2; M = 0.25; λ = 0.

Key: a, cr

Studying the behavior of the curves $Re^*_{cr} = Re^*_{cr}(\theta_2)$ for m = const, we arrive at the conclusion that from the point of view of increasing laminar boundary layer stabil-ity, a favorable phase shift between the tangential stress and deformations of the surface characterized by the parameter θ_2 will be found in the range of $0 \le \theta_2 \le 20°$.

114
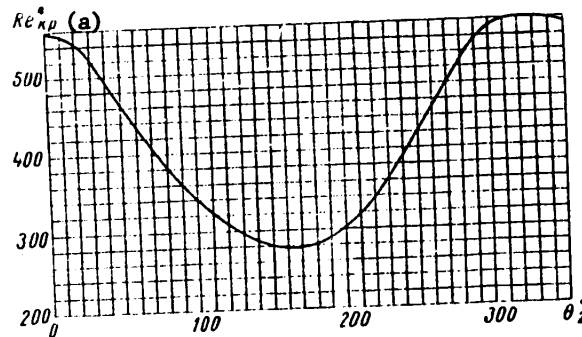
Figure II.9. Critical Reynolds number as a function
of the parameter θ_2; $m = 3$; $\lambda = 0$.

Key: a. cr
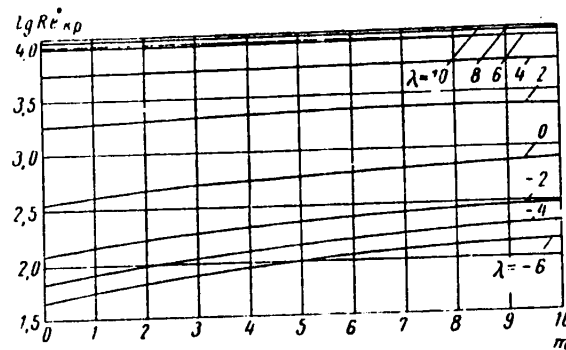
Figure II.10. Critical Reynolds number as a function
of the parameters λ and m; $\theta_2 = 0$.

Accordingly, the curves $Re^* = Re^*_{cr}(\lambda, m)$ were calculated for a constant value of the

angle $\theta_2 = 0$.

Figure IL.10 shows the functions $Re^*_{cr} = Re^*_{cr}(m)$ for different values of the parame-
ter λ and $\theta_2 = 0$.

The curves $Re^*_{cr} = Re^*_{cr}(\lambda)$ were constructed for different values of m on the basis of
these graphs (see Figure II.11). By using the family of curves $Re^*_{cr} = Re^*_{cr}(\lambda, m, \theta_2 =$
0), it is easily possible to find the loss of stability point of a laminar boundary
layer developed on any body with separated flow over it, the surface of which is
compliant in the tangential plane (of course, it is considered that the surface
characteristics are chosen optimal with respect to the parameter θ_2 which must be
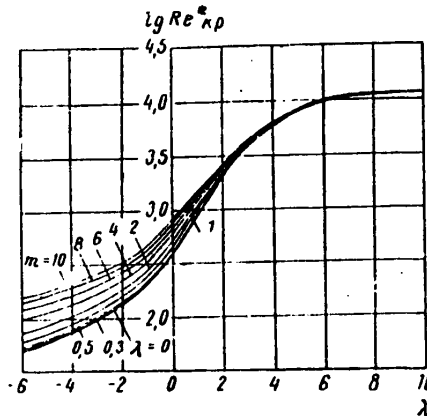close to zero).

115

Figure II.11. Critical Reynolds number as a function of the parameters m and λ; $\theta_2 = 0$.

Considering the family of curves $Re^*_{cr} = Re^*_{cr}(\lambda, m)$ (Figure II.11), it is possible to draw the conclusion that the compliance of the surface in the tangential plane over which flow takes place has insignificant influence on the laminar boundary layer stability. This infleunce, which is perceptible for small critical Reynolds numbers (the range of negative values of the parameter λ), decreases with an increase in λ, and for $\lambda > 4$, it becomes in practice negligibly small. This is explained by the fact that the influence of the surface compliance in the tangential plane on the boundary layer stability is inversely proportional to the Reynolds number as follows from the second boundary condition (II.17).

§ II.7. Energy Exchange of Oscillatory Motions of a Fluid and a Wall

Let us consider the direction of energy flow on interaction of a stream with a flexible wall. Knowing this direction makes it possible to determine the nature of the operation of the covering. If the energy flow is from the fluid to the wall, work is done by the pressure forces in the flow; consequently, the covering can be classified as passive, oscillating under the effect of the pressure forces. If the energy flow is directed from the wall to the fluid, work is done by certain external forces applied to the covering and not connected with pressures in the flow over the surface. Such a covering can be called "active."

Stability of the laminar form of flow in a boundary layer developed on an oscillatory surface does not depend directly on the direction of the energy flow at the investigated interface. For example, it cannot be said that if work is formed by the pressure forces from the fluid, the disturbances causing these pressures will damp, and vice versa, the direction of energy flow into the fluid does not necessarily lead to an increase in pulsation energy and, consequently, to buildup of the pulsations.

The indicated fact is connected with the presence of another source of energy transfer to a disturbing motion, which is basic. This source is the Reynolds stresses which define the process of energy transfer from the main flow to the disturbances. If it turns out to be possible to control the magnitude of the Reynold stresses, it

116

is possible to regulate the development of the disturbing motion. Therefore it can turn out that in the presence of an energy flow from the wall to the fluid the Reynolds stresses decrease, and the disturbances in the flow diminish. The opposite picture is also possible when the energy flow is directed to the wall, but the energy of the disturbing motion increases as a result of the energy of the main flow, for the magnitude of the Reynolds stresses increases.

The results of the calculations presented in § II.4 encompass all coverings, active and passive, for all possible phase shifts between the pressure in the flow and the wall displacements were considered there. Optimal phase shifts have been established for which the stability of a laminar boundary layer increases to the highest degree. Accordingly, it is of interest to determine what coverings (passive or active) have these phase angles that are the best from the point of view of laminarization.

Energy flow per unit surface displaced with a velocity v_{yw} under the effect of pressure p_w is calculated by the ordinary formula

$$N = -p_w \cdot v_{yw}.$$

(II.44)

The minus sign in (II.44) is taken because under the effect of a positive pressure in the flow the surface moves in the negative direction of the y-axis. If when calculating by formula (II.44), N > 0, then the work is done by the pressure forces and the covering is "passive." If N < 0, then the energy flow is directed to the fluid, and the covering operates as an "active" covering. The values of p_w and v_{yw} are complex variables which vary harmonically with respect to the x-coordinate and time. Therefore, considering an area with the coordinate $x = x_0$, we can write

$$p_w = |p_w| \cos(\alpha x_0 - \omega t),$$
$$v_{yw} = |v_{yw}| \cos(\alpha x_0 - \omega t + \theta_0),$$
$$N = -|p_w| |v_{yw}| \left[\cos^2(\alpha x_0 - \omega t) \cos\theta_0 - \frac{1}{2} \sin 2(\alpha x_0 - \omega t) \sin\theta_0 \right].$$

Performing the averaging for the period $T = 2\pi/\omega$, we obtain

$$N = -\frac{1}{2} |p_w| |v_{yw}| \cos\theta_0.$$

(II.45)

Formula (II.45) does not depend on the choice of the point x_0; therefore it is valid for the entire surface.

The stabili y calculations performed in § II.4 for the case of a surface that is compliant in the normal direction corresponded to the following relation of the surface deformation and pressure:

$$y_w = kpe^{i\theta_1}.$$

Here

$$y_w = y_{w0} e^{i\alpha(x-ct)}$$

Thus,

117

$$p = \frac{1}{k} y_{w0} e^{i\alpha(x-ct)-i\theta_1}.$$ (II.46)

In formula (II.46), k and y_{w0} are assumed to be real positive values. The surface deformation rate in the normal direction can be determined from the expression

$$v_{yw} = \frac{\partial y_w}{\partial t} = -i\alpha c y_{w0} e^{i\alpha(x-ct)}.$$ (II.47)

Values of α, c are also real and greater than zero. Let us write (II.47) as follows:

$$v_{yw} = \alpha c y_{w0} e^{i\alpha(x-ct)+\frac{3}{2}\pi i}.$$ (II.48)

From a comparison of (II.48) and (II.46) we see that the phase shift between the pressure on the wall and the velocity is defined by the sum

$$\theta_0 = \frac{3}{2}\pi + \theta_1.$$ (II.49)

Substituting (II.49) in (II.45), we arrive at the following expression for the energy flow at the interface of the fluid and elastic surface

$$N = -\frac{1}{2}|p_w|\cdot|v_{yw}|\sin\theta_1.$$ (II.50)

On the basis of (II.50), we obtain the following conclusions:

a) if $180° > \theta_1 > 0°$, then N < 0 and the covering must be considered "active":

b) if $360° > \theta_1 > 180°$, then N > 0, and the covering must be considered "passive";

c) if $\theta_1 = 0°$, $\theta_1 = 180°$, the energy flow is absent, and the covering can in this sense be considered "neutral."

Considering the results of calculating the critical Reynolds number of a laminar boundary layer on an elastic surface (§ II.4), we arrive at the conclusion that the greatest effect can be achieved by controlling the boundary layer using an active covering (case "a"). For the majority of shift angles characteristic of a "passive" covering, the critical Reynolds number decreases. There is a defined range of shift angles provided by a passive covering where the critical Reynolds number increases.

§ II.8. Examples of Calculating the Lengths of Laminar Segments of Boundary Layers on Bodies with Deforming Coverings

The loss of stability points in the case of a surface that deforms in the normal direction were calculation for an ellipsoid of revolution with L/B = 8.

The following formula [20] which defines the variation of the form parameter with respect to length of the body, was used to calculate the laminar boundary layer

$$f(x) = \frac{aU'(x)}{U^b(x)\,r^2(x)} \int_0^x U^{b-1}(\xi)\, r^2(\xi)\, d\xi. \tag{II.51}$$

The values entering into formula (II.51) were defined as follows.

The parameters a and b have constant values [20]: a = 0.45, b = 5.35.

The flow velocity at the boundary of the boundary layer was defined as a function of the $\bar{x}$ coordinate for an ellipsoid of revolution by a calculation [20] just as for the function U'(x). The corresponding curves are illustrated in Figure II.12. The distribution of the radii $r(\bar{x})$ with respect to length of the investigated bodies is shown in Figure II.12. Since the Pohlhausen parameter $\lambda_6(\bar{x}) = U'\delta^2/\nu$ calculated using a sixth-degree polynomial for approximation of the velocity profile in the boundary layer is assumed to be used for the stability calculation, beginning with the functions $f = f(\lambda_4)$ [21] and $\lambda_4 = \lambda_4(\lambda_6)$ [22] (Figure II.13), the function $f = f(\lambda_6)$ was constructed (Figure II.14), with the use of which the values of $\lambda_6(x)$ were determined for the indicated ellipsoid (Figure II.15).

Considering the function $f = f(\bar{x})$, beginning with determination of the form parameter f it is possible to obtain the variation with respect to body length of the value of

$$\frac{\delta^{**}}{L}\sqrt{\mathrm{Re}_L} = \sqrt{\frac{fU}{U'L}}.$$

Using the relation $f = f(\delta*/\delta**)$ [21] (Figure II.16), the graph of

$$\frac{\delta^*}{L}\sqrt{\mathrm{Re}_L} = F(\bar{x})$$

sas constructed for an ellipsoid of revolution (Figure II.17).

On the basis of the curves $\mathrm{Re}^*_{cr} = \mathrm{Re}^*_{cr}(\lambda,\ k,\ \theta_1 = 60°)$ (Figure II.4), using the relation $\lambda = \lambda(\bar{x})$, the curves for the critical Reynolds numbers Re^*_{cr} as a function of the dimensionless coordinate $\bar{x}/L$ (Figure II.18) were constructed. Further determination of the loss of stability point consists in the following. The curves $\mathrm{Re}^* = \mathrm{Re}^*(\bar{x})$ for different values of the Reynolds number $\mathrm{Re}_L = UL/\nu$ are constructed on the graph (Figure II.18) where the curves for the variation of the critical Reynolds numbers with respect to body length were constructed. These curves are obtained by multiplying $(\delta*/L)\sqrt{\mathrm{Re}_L}$ by $\sqrt{\mathrm{Re}_L}$. The x-axes of the points of intersection of the family of curves $\mathrm{Re}^*_{cr}(\bar{x}, k)$ with the curves $\mathrm{Re}^* = \mathrm{Re}^*(\bar{x})$ for different Re_L give the positions of the loss of stability points. The coordinates of the loss of stability point $\bar{x}_n$ as a function of the Reynolds number Re_L and the parameter k are presented on the graph (Figure II.19).

Analogous calculations can be performed on the basis of the function $\mathrm{Re}^*_{cr} = \mathrm{Re}^*_{cr}(m, \lambda, \theta_2 = 0)$ (see Figure II.11) for a body in the case where its surface has a covering that is compliant in the tangential plane.

119
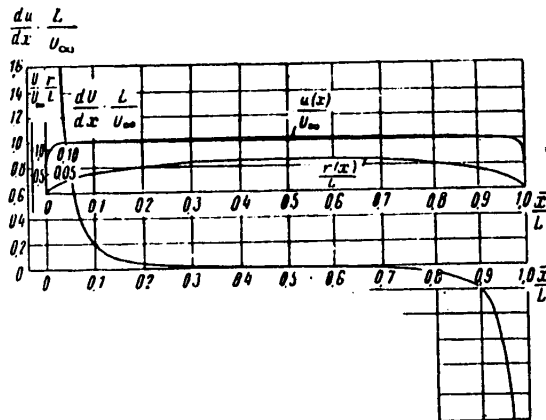
Figure II.12. Distribution of the values of $r(x)/L$; $U(x)/U_\infty$; $U'(x)L/U_\infty$ with respect to an ellipsoid of revolution with aspect ratio $L/2r_{max}=8$.
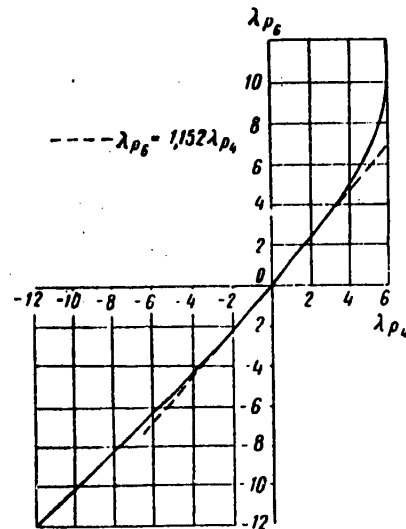
Figure II.13. The function $\lambda_{p_6} = \lambda_{p_6}(\lambda_{p_4})$.
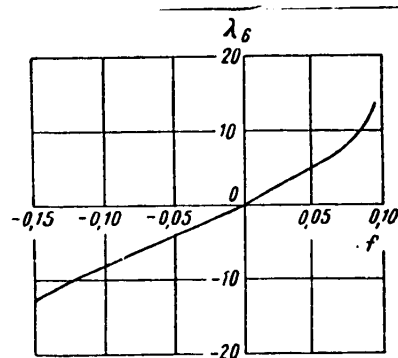
Figure II.14. Relation between form parameers f and λ_6.
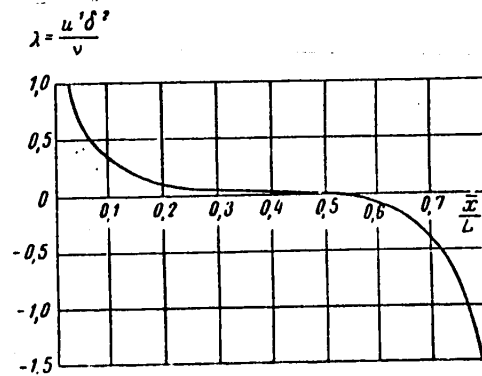
Figure II.15. Distribution of the parameter λ, with respect to length of an ellipsoid of revolution with $L/2r_{max} = 8$.

On the basis of the performed calculations it is possible to draw the conclusion that it is theoretically possible to laminarize the greater part of bodies over which streamlined flow takes place well (bodies without positive pressure gradients in the forward section) when using the appropriately selected coverings capable of deforming in the direction normal to the surface. For $Re_L = 10^9$ and $k \simeq 1$, the length of the laminar segment can reach 50% of the body length.

120
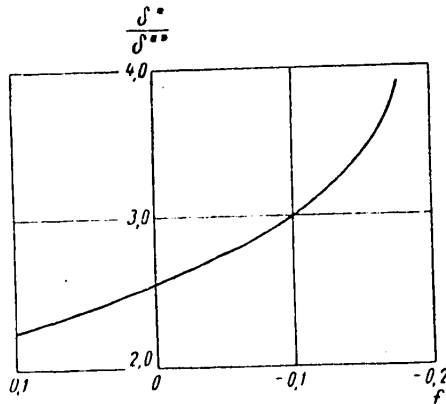
Figure II.16. Relation of the form parameter f to the ratio $\delta*/\delta**$.
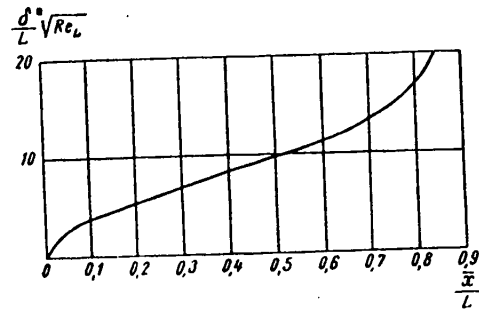
Figure II.17. Distribution of the displacement thickness with respect to an ellipsoid of revolution.
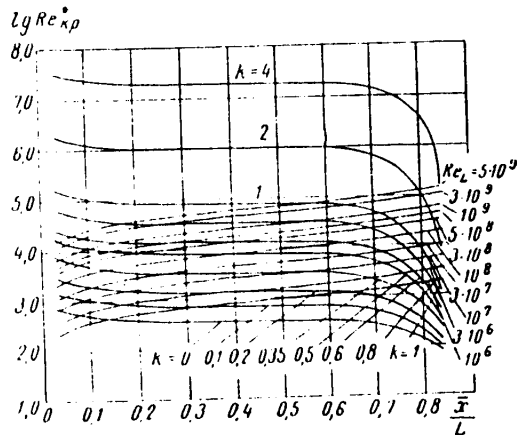
Figure II.18. Determination of the loss of stability point for an ellipsoid of revolution with aspect ratio $L/2r_{max} = 8$.
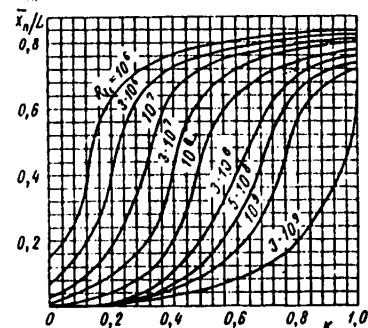
Figure II.19. Loss of stability point as a function of the Reynolds number Re_L and the parameter k for an ellipsoid of revolution with aspect ratio $L/2r_{max} = 8$, $\theta_1 = 60°$.

As the calculations performed by the Prandtl-Schlichting [21] formula demonstrate (Figure II.20), maintenance of the laminar form of flow in the boundary layer over %0% of the body length (calculations were performed on a plate) leads to a reduction in frictional drag by approximately 45% in the range of variation of the Reynolds numbers of $10^6 \leq Re_L \leq 5 \cdot 10^9$.

121
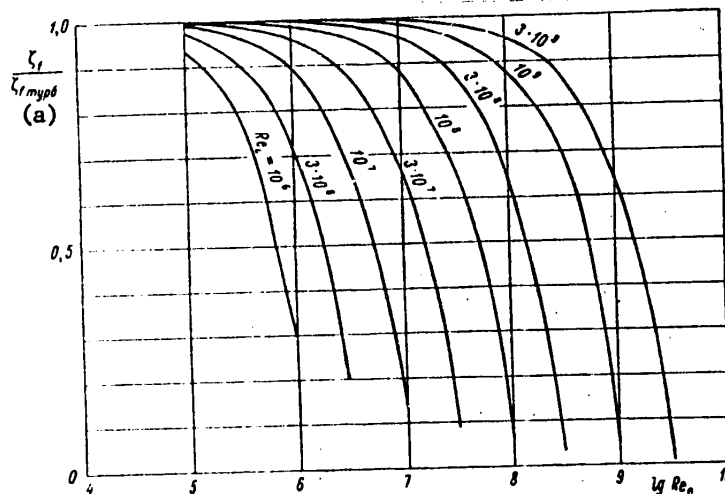
Figure II.20. Relative decrease in friction of a
plate as a function of the length of the laminar
section.

Key: a. turbulent

§ II.9. Some Structural Diagrams of Flexible Coverings Designed to Extinguish Pulsa-
tions in a Boundary Layer

Kramer obtained his first results with respect to reducing   the drag of bodies mov-
ing in water using the so-called "columnar covering," the structural design of which
appears in Figure II.21. Silicone fluid with different kinematic viscosity was used
as the filler. Figure II.22 shows the results of testing a model described in § II.1
with different versions of the columnar covering. Curve T corresponds to the fric-
tional drag of the model for a completely turbulent flow condition in the boundary
layer. Curve L corresponds to completely laminar flow in the boundary layer.
Curve 1 was obtained for a covering made of rubber with rigidity of 15.8 kg/cm^3 and
filled with a fluid having a viscosity of 400 centistokes. Curve 2 corresponds to
a covering with rigidity of 44.3 kg/cm filled with a viscosity of 1200 centistokes.
Curve 3 corresponds to a covering with rigidity 22.2 kg/cm^3 filled with a fluid
with viscosity of 300 centistokes. Curve E gives a representation of the drag of
an absolutely rigid standard under similar test conditions.

A structural design that is easier to put together for damping coverings tested by
Kramer appears in Figure II.23. The test results are presented in Figure II.22 in
the form of curve 4. As Kramer notes [3], this design allowed for maintaining
damping properties of the covering over a prolonged period of time at the same time
as the properties of "columnar coverings" changed in a negative direction during
prolonged storage for unknown reasons.

Kramer proposed several structural designs of damping coverings (Figure II.24, II.25).
The complexity of manufacturing them differs. However, common features include the

122

following: a) the presence of a flexible outer diaphragm which is supported on flexible bearing elements and b) the presence of cavities under this diaphragm filled with fluid with relatively high viscosity.
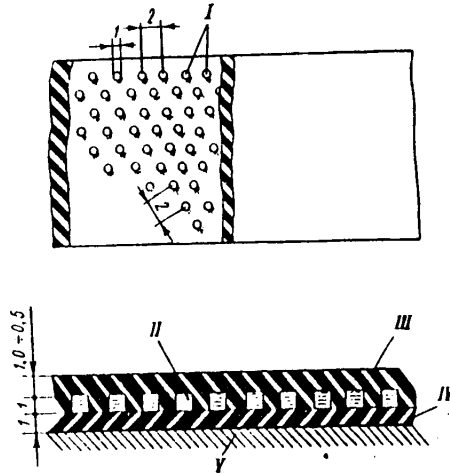
Figure II.21. Structural design of a columnar covering (dimensions in mm). I — projections; II — fluid filler; III — upper diaphragm; IV — lower diaphragm; V — solid base.
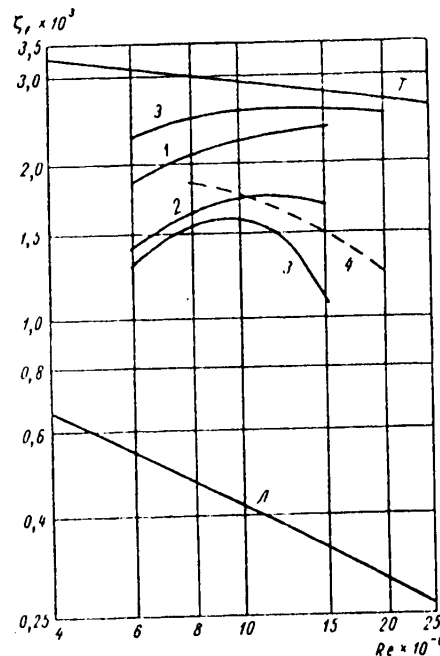
Figure II.22. Results of the Kramer experiments.

Figure II.23. Structural design of a ribbed Kramer covering (dimensions in mm). I -- flexible ribs; II -- flexible diaphragm; III -- rigid structure; IV -- fluid filler.
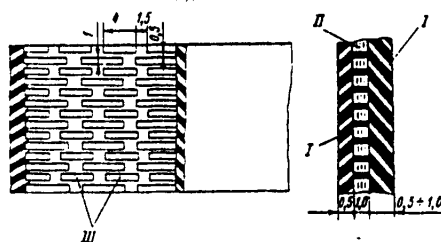
Figure II.24. Structural version of a damping covering (dimensions in mm). I -- flexible diaphragm; II -- liquid filler; III -- longitudinal cavities or projections.
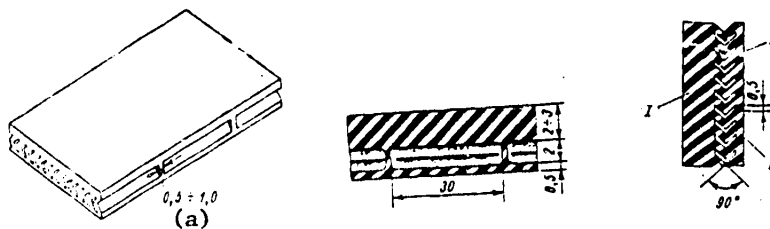
Figure II.25. Structural version of a damping covering (dimensions in mm). I -- flexible diaphragm; II -- cavity for fluid filler.

Key: a. 0.5 to 1.0
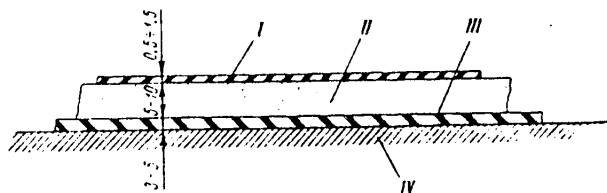
Figure II.26. Structural version of a damping covering (dimensions in mm). I -- flexible diaphragm; II -- porous layer; III -- flexible base; IV -- rigid base.

124

Apparently the simplest structural design is a three-layer covering (Figure II.26) consisting of a base, porous filler (sponge rubber, foam polyurethane) impregnated with a fluid with the corresponding viscosity and upper flexible diaphragm.

By varying the filler porosity, the fluid viscosity and pressure under which the fluid operates in the coating, it is possible to vary the damping characteristics of the investigated design.

BIBLIOGRAPHY

1. M. O. Kramer, "Boundary Layer Stabilization by Distributed Damping," JOURNAL OF THE AERONAUTICAL SCIENCES, Vol 24, No 6, 1957.

2. M. O. Kramer, "Boundary Layer Stabilization by Distributed Damping," JOURNAL OF THE AMERICAN SOCIETY OF NAVAL ENGINEERS, Vol 72, No 1, 1960.

3. M. O. Kramer, "Boundary Layer Stabilization by Distributed Damping," NAVAL ENGINEERS JOURNAL, Vol 74, No 2, 1962.

4. T. B. Benjamin, "Effects of a Flexible Boundary on Hydrodynamic Stability," JOURNAL OF FLUID MECHANICS, Vol 9, No 4, 1960.

5. M. T. Landahl, "On the Stability of a Laminar Incompressible Boundary Layer over a Flexible Surface," JOURNAL OF FLUID MECHANICS, Vol 13, No 4, 1962.

6. E. Becker, "Die laminare inkompressible Grenzschicht an einer durch laufende Wellen deformierten eben Wand," Z. I. FLUGWISS, Nos 10/11, 1960.

7. E. Becker, "Die laminare inkompressible Grenzschicht an einer durch laufende Wellen deformierten ebenen Wand," DEUTSCHE VERSUCHSANSTALT FUR LUFTFABRT, No 132, 1960.

8. R. Betchov, "Simplified Analysis of Boundary Layer Oscillations," JOURNAL OF SHIP RESEARCH, Vol 4, No 2, 1960.

9. E. W. Boggs, N. Tokita, "A Theory of the Stability of Laminar Flow along Compliant Plates," THIRD SYMPOSIUM ON NAVAL HYDRODYNAMICS, Wageningen, 1960.

10. T. Nonweiler, "Qualitative Solution of the Stability Equation for a Boundary Layer in Contact with Various Forms of Flexible Surface," ARC CURRENT PAPERS, London, No 622, 1963.

11. T. B. Benjamin, "The Threefold Classification of Unstable Disturbances in Flexible Surfaces Bounding Inviscid Flows," JOURNAL OF FLUID MECHANICS, Vol 16, October 1963.

12. N. Gregory, E. M. Love, "Progress Report on an Experiment on the Effect of Surface Flexibility on the Stability of Laminar Flow," ARC CURRENT PAPERS, London, No 602, 1962.

13. F. D. Hains, J. F. Price, "Effect of a Flexible Wall on the Stability of Poiseuille Flow," THE PHYSICS OF FLUID, Vol 5, No 3, 1962.

14. D. B. Miles, "Generation of Surface Waves by Flows with Velocity Gradient," GIDRODINAMICHESKAYA NEUSTOYCHIVOST' (Hydrodynamic Instability), Moscow, izd. Mir, 1964.

15. T. B. Benjamin, "Shearing Flow over a Wavy Boundary," JOURNAL OF FLUID MECHANICS, Vol 6, No 2, 1959.

16. F. D. Hains, J. F. Price, "Poiseuille Flow Stability in a Plane Channel with Flexible Walls," PRIKLADNAYA MEKHANIKA. TR. AMERIK. OBSHCH. INZH.-MEKH., (Applied Mechanics. Works of the American Society of Mechanical Engineers), Series E, Vol 29, No 2, 1962.

17. A. I. Korotkin, "Stability of a Plane Poiseuille Flow in the Presence of Flexible Boundaries," PMM (Applied Mathematics and Mechanics), No 6, 1965.

18. A. I. Korotkin, "Laminar Boundary Layer Stability in an Incompressible Fluid on Flexible Surface," IZV. AN SSSR, MZHG (News of the USSR Academy of Sciences, MZhG), No 3, 1966.

19. C. C. Lin, TEORIYA GIDRODINAMICHESKOY USTOYCHIVOSTN. (Hydrodynamics Stability Theory), Moscow, IL, 1958.

20. L. G. Loytsyanskiy, MEKHANIKA ZHIDKOSTI I GAZA (Fluid and Gas Mechanics), Moscow, GIFML, 1959.

21. G. Schlichting, TEORIYA POGRANICHNOGO SLOYA (Boundary Layer Theory), Moscow, IL, 1956.

22. H. Schlichting, A. Ulrich, "Zur Berechnung des Umschlages laminar-turbulent," JB. D. D. LUFTFAHRTFORSCHUNG, 1942, p I 8.

23. H. Focke, "Über die Ursachen der hohen. Schwimmgeschwindigkeitender Delphine," Z. F. FLUGWISS, Vol 13, No 2, 1965.

CHAPTER III. INFLUENCE OF VARIATION OF THE PHYSICAL CONSTANTS OF A FLUID (1
STABILITY OF AN INCOMPRESSIBLE LAMINAR BOUNDARY LAYER

§ III.1. Statement of the Problem. Equations of Motion of an Inhomogeneous Viscous
Fluid

The equations of motion and the continuity equation of an inhomogeneous incompres-
sible fluid are written in the form of   expressions (I.1)-(I.3).

In equations (I.1)-(I.3) the fluid density ρ and viscosity μ will be considered the
variables which depend on the space coordinates. Considering the study of fluid
flows in a boundary layer where variation of all of the variables with respect to
the y-coordinate is appreciably greater than with respect to the x-coordinate, let
us set

$$\rho = \rho(y), \quad \mu = \mu(y),$$
(III.1)

where $\nu = \mu/\rho = \nu(y)$. In order to discover the basic physical laws connected with
variability of the fluid properties in the boundary layer, it is expedient to con-
sider the relations $\rho(y)$ and $\nu(y)$ given. The methods of creating inhomogeneity in
the fluid boundary layer leading to specific definition of the indicated functions
are not considered in this section.

This approach greatly simplifies the problem, for it eliminates the necessity for
joint solution of the equations of hydrodynamics and equations characterizing the
material or heat transfer in the boundary layer. Possible inexactness connected
with noncorrespondence of the assumed functions $\nu(y)$, $\rho(y)$ to the real functions
obtained in each specific problem do not turn out to be significant, for the pur-
pose of this chapter is to discover qualitative laws and indicate the possible
order of magnitudes.

In the adopted statement, the fluid density is a function of the coordinates of a
point in space. Therefore let us introduce the gravitational force acting on a
unit volume of the fluid into the investigation

$$\rho \vec{F} = \rho \vec{g}.$$
(III.2)

The gravitational acceleration vector $\vec{g}$ has the projections g_x, g_y, g_z. Consider-
ing (III.1), (III.2), the equations of motion are written as follows:

127

$$\left. \begin{aligned} \rho\,\frac{\partial u}{\partial t} &= -\frac{\partial p}{\partial x} + \rho g_x + \mu\,\Delta u + \frac{\partial \mu}{\partial y}\left(\frac{\partial u}{\partial y} + \frac{\partial v}{\partial x}\right); \\ \rho\,\frac{\partial v}{\partial t} &= -\frac{\partial p}{\partial y} + \rho g_y + \mu\,\Delta v + 2\,\frac{\partial \mu}{\partial y}\cdot\frac{\partial v}{\partial y}; \\ \rho\,\frac{dw}{dt} &= -\frac{\partial p}{\partial z} + \rho g_z + \mu\,\Delta w + \frac{\partial \mu}{\partial y}\left(\frac{\partial v}{\partial z} + \frac{\partial w}{\partial y}\right). \end{aligned} \right\} \qquad (III.3)$$

The system of equations (III.3) together with the continuity equation (I.2) will be the basis for studying the characteristics of a laminar boundary layer in an inhomogeneous fluid.

Restriction of the problem to only laminar flow in a layer is connected with the fact that creation of inhomogeneity of the fluid in the wall region is used for laminarization of the flow in the boundary layer. The control of a turbulent boundary layer is the subject of the following sections of this paper.

In order to discover the conditions of maintaining the laminar form of flow in an inhomogeneous boundary layer, it is necessary to solve two problems successively. The first is determination of the characteristics of the laminar boundary layer in an inhomogeneous fluid for given laws of variation of $\rho(y)$, $\nu(y)$. The second is to study the stability of a laminar boundary layer with velocity profile in an inhomogeneous fluid obtained as a result of solving the first problem. For qualitative discovery of the basic laws of the influence of inhomogeneity of the fluid on the stability of a laminar fluid flow in a boundary layer and also simplify the problem, the case of variable density $\rho = \rho(y)$, $\nu = $ const and the case of variable kinematic viscosity $\nu = \nu(y)$, $\rho = $ const will be investigated separately below.

§ III.2. Laminar Boundary Layer in an Incompressible Liquid with Variable Kinematic Viscosity

Flows of the boundary layer type in an incompressible fluid with variable kinematic viscosity have been investigated both by Soviet authors [1]-[7] and foreign authors [8]-[14]. References [1]-[3], [8]-[10] study a laminar boundary layer in the presence of a kinematic viscosity gradient in the wall region. In references [4]-[7], [11]-[14] studies are made of flows in tubes and channels. The methods of solving the system of equations for a boundary layer in the indicated papers are divided into two groups. The first group includes approximate methods [1], [2], [8], [10]; the second can include the methods of numerical integration [7], [3], [9]. The authors of all the enumerated papers relate the kinematic viscosity distribution in the boundary layer to the fluid temperature variation across the flow which greatly complicates the problem. The studies [2], [8] were performed by the Pohlhausen method using a third-degree polynomial. The problem was stated as in references [15], [16].

In this section the Pohlhausen method is used, but approximation of the velocities in the boundary layer is made using the fourth-degree polynomial. In addition, calculated formulas were obtained for a flow with gradient velocity on the outer boundary of the boundary layer which, with respect to structure, correspond to the known Loytsyanskiy-Val'ts formulas, being a generalization of them to the case of variable kinematic viscosity.

The system of Prandtl equations obtained on the basis of (III.3) in the investigated case has the form

128

$$u \frac{\partial u}{\partial x} + v \frac{\partial u}{\partial y} = -\frac{1}{\rho} \cdot \frac{dp}{dx} + v \frac{\partial^2 u}{\partial y^2} + \frac{\partial v}{\partial y} \cdot \frac{\partial u}{\partial y};$$

$$\frac{\partial u}{\partial x} + \frac{\partial v}{\partial y} = 0;$$

$$\frac{\partial p}{\partial y} = 0.$$

(III.4)

The influence of gravity is not taken into account, for the corresponding term can be combined with a term characterizing the pressure gradient along the surface over which the flow takes place. For specific definition of the function $v = v(y)$ we assume that the viscosity distribution corresponds to the following law:

$$v = v_0 \left(1 + \frac{v_w - v_0}{v_0} e^{-B \frac{y}{\delta}} \right),$$

(III.5)

where v_0 is the viscosity of the oncoming flow;

v_w is the viscosity on the wall over which flow takes place.

The function

$$\frac{v - v_0}{v_w - v_0} = f \left(\frac{y}{\delta} \right)$$

is represented for different values of the parameter B in Figure III.1.

For solution of the problem let us use the Pohlhausen method [17], that is, we assume that the velocity distribution in the boundary layer can be represented in the form of the polynomial

$$\frac{u}{U} = a_1(x) \frac{y}{\delta} + a_2(x) \left(\frac{y}{\delta} \right)^2 + a_3(x) \left(\frac{y}{\delta} \right)^3 + a_4(x) \left(\frac{y}{\delta} \right)^4,$$

(III.6)

the coefficients of which are determined from the boundary conditions for $y = 0$:

$$u = 0; \quad v = v_1(x);$$

(III.7)

$$v_1(x) \frac{\partial u}{\partial y} \Big|_{y=0} = -\frac{1}{\rho} \cdot \frac{dp}{dx} + v \frac{\partial^2 u}{\partial y^2} \Big|_{y=0} + \frac{\partial v}{\partial y} \cdot \frac{\partial u}{\partial y} \Big|_{y=0};$$

(III.8)

for $y = \delta$:

$$u = U; \quad \frac{\partial u}{\partial y} = \frac{\partial^2 u}{\partial y^2} = 0.$$

(III.8)

Condition (III.8) corresponds to the assumption of validity of the first equation of system (III.4) in direct proximity to the wall. The second of the conditions in (III.7) will occur in the case where variability of the kinematic viscosity is reached by introducing a fluid with kinematic viscosity differing from the kinematic viscosity of the main flow through the wall.

129

Substituting (III.6) in conditions (III.7)-(III.9), we arrive at the system of equations

$$a_1 + a_2 + a_3 + a_4 = 1;$$
$$a_1 + 2a_2 + 3a_3 + 4a_4 = 0;$$
$$a_2 + 3a_3 + 6a_4 = 0;$$
$$\left(v_1 - \frac{\partial v}{\partial y}\Big|_{y=0}\right)\frac{a_1}{\delta} = -\frac{1}{\rho}\cdot\frac{1}{U}\cdot\frac{dp}{dx} + v_w\frac{2a_2}{\delta^2},$$

which has the solution

$$a_1(x) = 2 + \frac{K}{6}; \quad a_2(x) = -\frac{K}{2}; \quad a_3(x) = -2 + \frac{K}{2};$$

$$a_4(x) = 1 - \frac{K}{6},$$

where

$$K = \frac{\dfrac{\delta^2\frac{dU}{dx}}{v_0}\cdot\dfrac{v_0}{v_w} - 2\dfrac{\delta v_1}{v_w} + 2\dfrac{\delta}{v_w}\cdot\dfrac{\partial v}{\partial y}\Big|_{y=0}}{1 + \dfrac{1}{6}\cdot\dfrac{\delta v_1}{v_w} - \dfrac{1}{6}\cdot\dfrac{\delta}{v_w}\cdot\dfrac{\partial v}{\partial y}\Big|_{y=0}}.$$
(III.10)
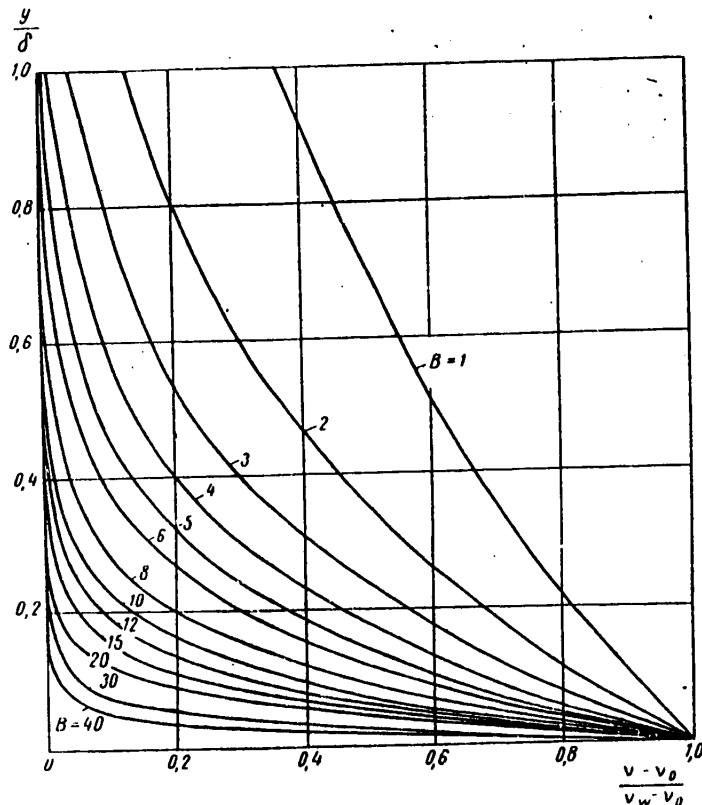
Figure III.1. Viscosity distribution in a boundary layer for various values of B.

130

If the law of variation of the kinematic viscosity corresponds to (III.5), then

$$K = \frac{\frac{\delta^2 U'}{\nu_0} \cdot \frac{\nu_0}{\nu_w} - 2\frac{\delta v_1}{\nu_w} - 2B\left(1 - \frac{\nu_0}{\nu_w}\right)}{1 + \frac{1}{6} \cdot \frac{\delta v_1}{\nu_w} + \frac{B}{6}\left(1 - \frac{\nu_0}{\nu_w}\right)} \cdots \tag{III.11}$$

Thus, a single-parametric family of velocity profiles in a boundary layer entirely analogous to the case of a homogeneous fluid was obtained except the parameter K (III.10), (III.11) is in the given case more general, characterizing not only the pressure gradient at the boundary of the boundary layer, but also the influence of the ventilation or suction velocity of the material at the wall and also the influence of the kinematic viscosity distribution law. The parameter K for a homogeneous fluid in the absence of ventilation (suction) of a material through the wall becomes the Pohlhausen parameter $\lambda = \delta^2 U'/\nu_0$. The velocity distribution in the boundary layer is represented [18] by the polynomial

$$\frac{u}{U} = F(\eta) + KG(\eta),$$

$$0 \leqslant \eta = \frac{y}{\delta} \leqslant 1,$$

where

$$F(\eta) = 1 - (1 - \eta)^3(1 + \eta); \quad G(\eta) = \frac{1}{6}\eta(1 - \eta)^3.$$

The displacement thickness and the pulse loss thickness are expressed by the following functions of the parameter K:

$$\frac{\delta^*}{\delta} = \frac{3}{10} - \frac{K}{120}; \quad \frac{\delta^{**}}{\delta} = \frac{37}{315} - \frac{K}{945} - \frac{K^2}{9072}. \tag{III.12}$$

The Karman integral relation obtained by integration of the first equation of (III.4) across the boundary layer under conditions (III.7), (III.9) is written as follows:

$$\frac{d\delta^{**}}{dx} + \frac{U'}{U}(2\delta^{**} + \delta^*) - \frac{v_1}{U} = \frac{\tau_w}{\rho U^2}, \tag{III.13}$$

where

$$\frac{\tau_w}{\rho U^2} = \frac{\nu_w}{U\delta}\left(2 + \frac{K}{6}\right). \tag{III.14}$$

From formula (III.11) it is possible to express δ^2 in terms of the parameter K

$$\delta^2 = \frac{\nu_w}{U'}(AK + D), \tag{III.15}$$

where

$$A = 1 + \frac{1}{6} \cdot \frac{\delta v_1}{\nu_w} + \frac{B}{6}\left(1 - \frac{\nu_0}{\nu_w}\right);$$

$$D = 2\left[\frac{\delta v_1}{\nu_w} + B\left(1 - \frac{\nu_0}{\nu_w}\right)\right].$$

131

In further arguments we shall consider the parameter $\delta v_1/v_w$ a constant. Then A and D also will be constant, depending on the ventilation characteristics and the viscosity distribution in the boundary layer. Substituting (III.12), (III.14) and (III.15) in (III.13) we arrive at a first-order ordinary nonlinear differential equation with respect to K

$$\frac{dK}{dx} = \frac{U''}{U'} f_1(K) + \frac{U'}{U} f_2(K),\tag{III.16}$$

where

$$f_1(K) = \frac{(AK+D)\left(\frac{37}{315} - \frac{K}{945} - \frac{K^2}{9072}\right)}{A\left(\frac{37}{315} - \frac{K}{945} - \frac{K^2}{9072}\right) - (AK+D)\left(\frac{2}{945} + \frac{K}{2268}\right)};$$

$$f_2(K) = 2\frac{2 + \frac{K}{6} + \frac{v_1\delta}{v_w} - (AK+D)\left(\frac{337}{630} - \frac{79K}{7560} - \frac{K^2}{4536}\right)}{A\left(\frac{37}{315} - \frac{K}{945} - \frac{K^2}{9072}\right) - (AK+D)\left(\frac{2}{945} + \frac{K}{2268}\right)}.$$

For solution of equation (III.16), according to reference [19], let us linearize the functions $f_1(I)$ and $f_2(K)$, considering that usually $|K| < 7$,

$$f_1(K) \approx \frac{\frac{37}{315}(AK+D)}{\frac{37}{315}A - \frac{2D}{945}} \simeq \frac{111A}{111A - 2D} K + \frac{111D}{111A - 2D} = p_{11} \cdot K + p_{12};$$

$$f_2(K) \simeq 2\frac{2 + \frac{v_1\delta}{v_w} + \frac{K}{6} - \frac{337}{630}(AK+D)}{A\frac{37}{315} - \frac{2D}{945}} =$$

$$= 1890\frac{\frac{1}{6} - \frac{337}{630}A}{111A - 2D} K + 1890\frac{2 + \frac{v_1\delta}{v_w} - \frac{337}{630}D}{111A - 2D} = p_{21}K + p_{22}.$$

The values of the coefficients p_{ik} (i, k = 1, 2) are clear from the above-presented formulas.

Let us write equation (III.16) in the assumed notation

$$\frac{dK}{dx} = \left(p_{11}\frac{U''}{U'} + p_{21}\frac{U'}{U}\right)K + p_{12}\frac{U''}{U'} + p_{22}\frac{U'}{U}.\tag{III.17}$$

During the process of deriving (III.17) it was assumed that $|K| < 7$, and p_{ik} (i, k = 1, 2) have finite values.

Under these conditions it is possible to use the discussed approximate method of calculation, the accuracy of which is higher for small K.

The general solution of a linear nonuniform equation (III.17) is written as follows [20]:

$$K \left[\int_{x_0}^{x} \left(p_{12} \frac{U''}{U'} + p_{22} \frac{U'}{U} \right) \exp \left\{ - \int \left(p_{11} \frac{U''}{U'} + p_{21} \frac{U'}{U} \right) dx \right\} dx + c \right] \times$$

$$\times \exp \left[\int \left(p_{11} \frac{U''}{U'} + p_{21} \frac{U'}{U} \right) dx \right].$$

Considering the expressions

$$\exp \left[\int \left(p_{11} \frac{U''}{U'} + p_{21} \frac{U'}{U} \right) dx \right] = (U')^{p_{11}} (U)^{p_{21}},$$

$$\exp \left[- \int \left(p_{11} \frac{U''}{U'} + p_{21} \frac{U'}{U} \right) dx \right] = (U')^{-p_{11}} (U)^{-p_{21}},$$

we obtain

$$K = (U')^{p_{11}} (U)^{p_{21}} \left[\frac{p_{12}}{p_{11}} U_0^{-p_{21}} (U_0')^{-p_{11}} - \frac{p_{12}}{p_{11}} U^{-p_{21}} (U')^{-p_{11}} + \right.$$

$$\left. + \left(p_{22} - \frac{p_{12} p_{21}}{p_{11}} \right) \int_{x_0}^{x} \frac{(U')^{1-p_{11}}}{U^{p_{21}+1}} dx + c \right],$$

where $U_0 = U(x_0)$, $U_0' = U'(x_0)$. Let us define the constant c from the condition $K(x_0) = K_0$

$$c = \frac{K_0}{(U_0')^{p_{11}} U_0^{p_{21}}}.$$

As a result, we arrive at the following solution of equation (III.17)):

$$K(x) = \left(K_0 + \frac{p_{12}}{p_{11}} \right) \left(\frac{U'}{U_0'} \right)^{p_{11}} \left(\frac{U}{U_0} \right)^{p_{21}} - \frac{p_{12}}{p_{11}} +$$

$$+ \left(p_{22} - \frac{p_{12} p_{21}}{p_{11}} \right) (U')^{p_{11}} (U)^{p_{21}} \int_{x_0}^{x} \frac{(U')^{1-p_{11}}}{U^{1+p_{21}}} dx. \tag{III.18}$$

Knowing the function K = K(x), let us determine $\delta = \delta(x)$ from expression (III.15); then using formulas (III.12) and (III.14), let us find $\delta^*(x)$, $\delta^{**}(x)$, $\tau_w(x)$. Using (III.6), it is possible to construct the velocity distribution in any cross section of the boundary layer.

If both sides of equality (III.18) are multiplied by the ratio

$$\left(\frac{\delta^{**}}{\delta} \right)^2 \simeq \left(\frac{37}{315} \right)^2,$$

we find the variation of the form parameter $f_1 = K \delta^{**2}/\delta^2$ along the surface of the body over which flow takes place. Then if we proceed to a homogeneous fluid, expression (II.18) is converted to the formula obtained by Loytsyanskiy [21] with constants a = 0.47, b = 6.25.

Using the Val'ts results, Schlichting [18] recommends that we set a = 0.47, b = 6.0. The values of the constants a and b obtained by Basin, Mel'nikov and certain other authors are presented in the monograph [21].

In the case of flow over a plate when $U' = 0$, $v_1 \delta / v_w = $ const, K = const, equation (III.13) is converted to the form

$$\frac{1}{2} \cdot \frac{U}{V_w} \left(\frac{37}{315} - \frac{K}{945} - \frac{K^2}{9072} \right) \frac{d\delta^2}{dx} = 2 + \frac{K}{6} + \frac{v_1 \delta}{v_w}. \tag{III.19}$$

Defining the integration constant from the condition $\delta(0) = 0$, on the basis of (III.19) we find

$$\delta = \sqrt{\frac{xv_w}{U}} \cdot \sqrt{\frac{4 + \frac{K}{3} + 2 \frac{v_1 \delta}{v_w}}{\frac{37}{315} - \frac{K}{945} - \frac{K^2}{9072}}}.$$

Knowing the function $\delta = \delta(x)$, it is possible to use (III.12) and (III.14) to construct the functions $\delta*(x)$, $\delta**(x)$, $\tau_w(x)$.

When investigating a boundary layer in a fluid with variable kinematic viscosity on the plate, the system of equations (III.4) can be reduced to the following equation by introducing the current function

$$\frac{\partial \psi}{\partial y} \cdot \frac{\partial^2 \psi}{\partial x \partial y} - \frac{\partial \psi}{\partial x} \cdot \frac{\partial^2 \psi}{\partial y^2} = \frac{\partial}{\partial y} \left(v \frac{\partial^2 \psi}{\partial y^2} \right). \tag{III.20}$$

Introduction of the Blasius variables

$$\zeta = \psi (Uxv_0)^{-\frac{1}{2}}, \quad \xi = y \left(\frac{U}{xv_0} \right)^{\frac{1}{2}}$$

converts (III.20) to an ordinary differential equation

$$\zeta''' + \frac{v_0}{v} \left(\frac{1}{2} \zeta + \frac{v'}{v_0} \right) \zeta'' = 0, \tag{III.21}$$

which must be integrated under the boundary conditions:

$$\zeta(0) = \zeta'(0) = 0, \quad \zeta'|_{\xi \to \infty} \to 1.$$

The equation (III.21) was integrated by Z. V. Borisova on the "Ural" computer with the following kinematic viscosity variation law:

$$\frac{v}{v_0} = 1 + \frac{v_w - v_0}{v_0} e^{-B_1 \xi}. \tag{III.22}$$

The integration results are presented in Table III.1. For putting formulas (III.5) and (III.22) in correspondence to each other, it is necessary to consider the difference in scales of the variables $\eta = y/\delta$ and ξ. For an identical viscosity distribution law, the following expression must be observed

$$B = B_1 \delta \sqrt{\frac{U}{xv_0}}. \tag{III.23}$$

The transition from the η coordinate to the ξ coordinate is made using the equality

$$\eta = \frac{\xi}{\delta} \sqrt{\frac{xv_0}{U}}.$$

Figures III.2-III.5 show the boundary layer thickness, the ratios $\delta*/\delta$, $\delta*/\delta**$ and the friction coefficient of a plate reduced to a wetted surface as a function of the parameter ν_w/ν_0. The exponent in the graphs of the indicated figures is taken as $B_1 = 1$.
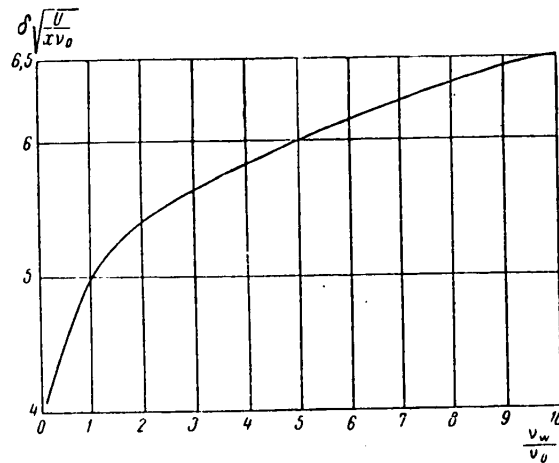

Figure III.2. Boundary layer thickness of a plate as a function of the ratio ν_w/ν_0; $B_1 = 1$.
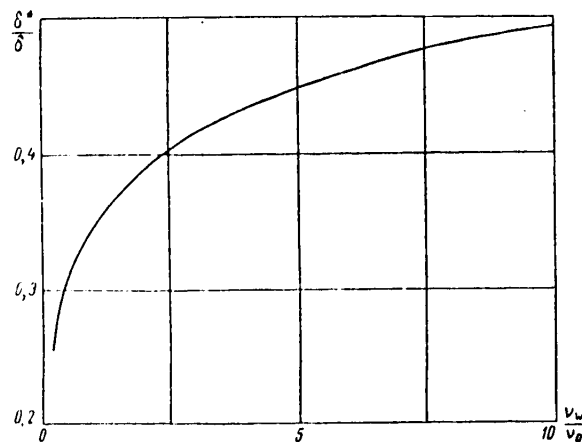
Figure III.3. Displacement thickness as a function of the ratio ν_w/ν_0; $B_1 = 1$.
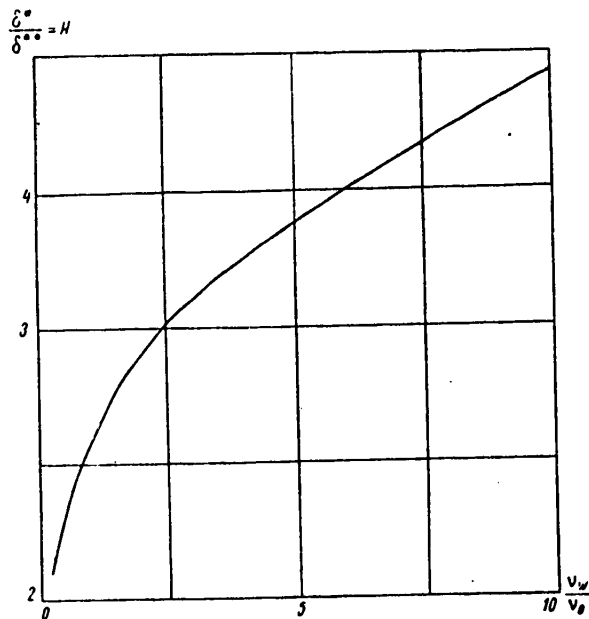
Figure III.4. The parameter H = */ ** as a function of the ratio v_w/v_0; B_1 = 0.
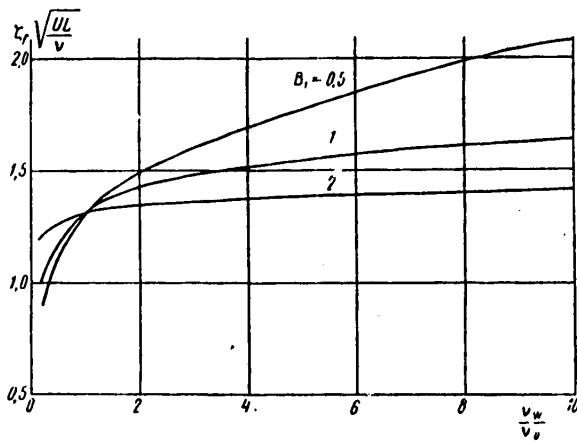
Figure III.5. Friction coefficient of a plate as a function of the ratio v_w/v_0.

136

Table III.1. Velocity profiles in a boundary layer with variable kinematic viscosity

$\dfrac{\nu_w}{\nu_0} = 1$ (Blasius profile)

$\eta \sqrt{\dfrac{U}{x\nu_0}}$				$\eta \sqrt{\dfrac{U}{x\nu_0}}$			
0	0	0	0.332060	4.2	2.498056	0.966962	0.050520
0.2	0.006641	0.066408	0.331986	4.4	2.692378	0.975875	0.038973
0.4	0.026560	0.132765	0.331472	4.6	2.888267	0.982688	0.029484
0.6	0.059735	0.198938	0.330081	4.8	3.085340	0.987794	0.021872
0.8	0.106109	0.264711	0.327391	5.0	3.283294	0.991546	0.015908
1.0	0.165573	0.329782	0.323009	5.2	3.481889	0.994250	0.011343
1.2	0.237950	0.383779	0.316591	5.4	3.680942	0.996160	0.007929
1.4	0.322984	0.456265	0.307867	5.6	3.880314	0.997482	0.005433
1.6	0.420324	0.516760	0.296665	5.8	4.079906	0.998380	0.003649
1.8	0.529522	0.574762	0.282933	6.0	4.279642	0.998977	0.002403
2.0	0.650029	0.629700	0.266753	6.2	4.479484	0.999367	0.001551
2.2	0.781199	0.681315	0.248352	6.4	4.679384	0.999616	0.000981
2.4	0.922297	0.728987	0.228093	6.6	4.879324	0.999773	0.000608
2.6	1.072514	0.772460	0.206455	6.8	5.072989	0.999869	0.000370
2.8	1.230986	0.811515	0.184007	7.0	5.279269	0.999927	0.000220
3.0	1.396818	0.846050	0.161360	7.2	5.479259	0.999961	0.000128
3.2	1.569106	0.876187	0.139128	7.4	5.679253	0.999980	0.000073
3.4	1.746962	0.901766	0.117876	7.6	5.879250	0.999992	0.000011
3.6	1.929538	0.923335	0.098086	7.8	6.079250	0.999998	0.000022
3.8	2.116044	0.941123	0.080126	8.0	6.279250	1.000001	0.000012
4.0	2.305762	0.955523	0.064234				

$B_1 = 0.5$; $\dfrac{\nu_w}{\nu_0} = 0.2$

$\eta \sqrt{\dfrac{U}{x\nu_0}}$				
0.0	0	0	1.1244	-2.2489
0.2	0.0200	0.1898	0.8122	-.0940
0.4	0.0729	0.3337	0.6411	-0.6762
0.6	0.1517	0.4499	0.5274	-0.4818
0.8	0.2516	0.5466	0.4426	-0.3759
1.0	0.3693	0.6280	0.3744	-0.3107
1.2	0.5020	0.6970	0.3169	-0.2658
1.4	0.6474	0.7554	0.2673	-0.2317
1.6	0.8035	0.8044	0.2239	-0.2033
1.8	0.9686	0.8453	0.1858	-0.1781
2.0	1.1411	0.8790	0.1525	-0.1551
2.2	1.3198	0.9066	0.1236	-0.1336
2.4	1.5034	0.9288	0.0989	-0.1137
2.6	1.6910	0.9464	0.0871	-0.0953
2.8	1.8817	0.9602	0.0607	-0.0786
3.0	2.0749	0.9709	0.0465	-0.0638
3.2	2.2699	0.9790	0.0351	-0.0508
3.4	2.4663	0.9851	0.0260	-0.0398
3.6	2.6638	0.9895	0.0190	-0.0306
3.8	2.8621	0.9928	0.0137	-0.0231
4.0	3.0609	0.9951	0.0097	-0.0172
4.2	3.2600	0.9967	0.0067	-0.0125
4.4	3.4596	0.9978	0.0046	-0.0089
4.6	3.6592	0.9986	0.0031	-0.0063
4.8	3.8589	0.9991	0.0020	-0.0043
5.0	4.0588	0.9994	0.0013	-0.0029
5.2	4.2588	0.9997	0.0008	-0.0019
5.4	4.4587	0.9998	0.0005	-0.0013
5.6	4.6587	0.9999	0.0003	-0.0008
5.8	4.8587	0.9999	0.0002	-0.0005
6.0	5.0586	0.9999	0.0001	-0.0003
6.2	5.2586	0.9999	0.0001	-0.0003
6.4	5.4586	0.9999	0.0000	-0.0002
6.6	5.6586	0.9999	0.0000	-0.0001
6.8	5.8586	1.0000	0.0000	0.0000

Table III.1 continued

$B_1 = 0.5; \quad \dfrac{v_w}{v_0} = 10$

$u\sqrt{U/xv_0}$	i	i'	i''	i'''
0,0	0	0	0,0521	0,0235
0,2	0,0011	0,0109	0,0571	0,0254
0,4	0,0044	0,0228	0,0623	0,0274
0,6	0,0103	0,0358	0,0680	0,0295
0,8	0,0188	0,0501	0,0741	0,0317
1,0	0,0304	0,0655	0,0807	0,0339
1,2	0,0452	0,0824	0,0877	0,0361
1,4	0,0634	0,1006	0,0951	0,0383
1,6	0,0855	0,1204	0,1030	0,0404
1,8	0,1117	0,1418	0,1113	0,0424
2,0	0,1424	0,1649	0,1199	0,0441
2,2	0,1778	0,1898	0,1289	0,0454
2,4	0,2184	0,2165	0,1381	0,0464
2,6	0,2645	0,2451	0,1474	0,0467
2,8	0,3166	0,2755	0,1567	0,0463
3,0	0,3749	0,3077	0,1658	0,0450
3,2	0,4398	0,3418	0,1746	0,0427
3,4	0,5117	0,3776	0,1828	0,0392
3,6	0,5909	0,4149	0,1902	0,0313
3,8	0,6777	0,4536	0,1965	0,0280
4,0	0,7724	0,4934	0,2013	0,0202
4,2	0,8751	0,5339	0,2044	0,0110
4,4	0,9860	0,5750	0,2056	0,0006
4,6	1,1051	0,6161	0,2046	—0,0109
4,8	1,2324	0,6567	0,2012	—0,0230
5,0	1,3678	0,6964	0,1954	—0,0353
5,2	1,5109	0,7347	0,1871	—0,0472
5,4	1,6615	0,7711	0,1766	—0,0581

$B_1 = 0.5; \quad \dfrac{v_w}{v_0} = 0.8$

$u\sqrt{U/xv_0}$	i	i'	i''	i'''
0,0	0	0	0,3937	—0,0192
0,2	0,0078	0,0778	0,3845	—0,0443
0,4	0,0310	0,1538	0,3757	—0,0427
0,6	0,0692	0,2281	0,3565	—0,0457
0,8	0,1221	0,3002	0,3584	—0,0527
1,0	0,1892	0,3707	0,3455	—0,0611
1,2	0,2702	0,4385	0,3323	—0,0709
1,4	0,3645	0,5035	0,3170	—0,0816
1,6	0,4714	0,5651	0,2996	—0,0923
1,8	0,5903	0,6232	0,2801	—0,1024
2,0	0,7204	0,6771	0,2588	—0,1109
2,2	0,8608	0,7266	0,2359	—0,1172
2,4	1,0107	0,7714	0,2121	—0,1208
2,6	1,1691	0,8114	0,1878	—0,1215
2,8	1,3350	0,8465	0,1637	—0,1192
3,0	1,5074	0,8769	0,1403	—0,1139
3,2	1,6854	0,9027	0,1182	—0,1063
3,4	1,8682	0,9243	0,0979	—0,0968
3,6	2,0549	0,9420	0,0796	—0,0860
3,8	2,2448	0,9563	0,0636	—0,0745
4,0	2,4372	0,9676	0,0498	—0,0631
4,2	2,6317	0,9764	0,0383	—0,0521
4,4	2,8277	0,9831	0,0289	—0,0421
4,6	3,0248	0,9881	0,0214	—0,0332
4,8	3,2228	0,9917	0,0155	—0,0256
5,0	3,4214	0,9944	0,0110	—0,0193
5,2	3,6205	0,9962	0,0077	—0,0142
5,4	3,8192	0,9976	0,0035	—0,0072
5,6	4,0192	0,9981	0,0023	—0,0050
5,8	4,2192	0,9989	0,0015	—0,0033
6,0	4,4191	0,9991	0,0009	—0,0022
6,2	4,6190	0,9996	0,0006	—0,0014
6,4	4,8189	0,9998	0,0004	—0,0009
6,6	5,0189	0,9998	0,0002	—0,0006
6,8	5,2188	0,9999	0,0001	—0,0003
7,0	5,4188	0,9999	0,0001	—0,0002
7,2	5,6188	1,0000	0,0000	—0,0001
7,4	5,8188	1,0000	0,0000	—0,0001
7,6	6,0188	1,0000	0,0000	0,0000
7,8	6,2188	1,0000	0,0000	0,0000

138

$$B_1 = 1; \quad \frac{v_w}{v_0} = 0,2$$

$u\sqrt{\dfrac{U}{xv_0}}$	I	I'	I''	I'''
0,0	0	0		
0,2	0,0213	0,1950	1,3174	−5,2690
0,4	0,0739	0,3246	0,7612	−1,4686
0,6	0,1492	0,4250	0,5661	−0,6923
0,8	0,2428	0,5083	0,4533	−0,4151
1,0	0,3518	0,5799	0,3844	−0,2886
1,2	0,4742	0,6426	0,3339	−0,2225
1,4	0,6083	0,6978	0,2936	−0,1849
1,6	0,7528	0,7465	0,2591	−0,1618
1,8	0,9065	0,7893	0,2283	−0,1465
2,0	1,0682	0,8267	0,2062	−0,1351
2,2	1,2369	0,8591	0,1742	−0,1255
2,4	1,4115	0,8868	0,1500	−0,1164
2,6	1,5913	0,9103	0,1276	−0,1071
2,8	1,7754	0,9298	0,1072	−0,0974
3,0	1,9630	0,9459	0,0887	−0,0872
3,2	2,1535	0,9589	0,0723	−0,0769
3,4	2,3464	0,9692	0,0579	−0,0664
3,6	2,5410	0,9773	0,0457	−0,0536
3,8	2,7371	0,9835	0,0354	−0,0468
4,0	2,9343	0,9881	0,0269	−0,0386
4,2	3,1323	0,9916	0,0201	−0,0303
4,4	3,3310	0,9911	0,0148	−0,0236
4,6	3,5299	0,9959	0,0106	−0,0180
4,8	3,7293	0,9972	0,0075	−0,0134
5,0	3,9288	0,9980	0,0052	−0,0098
5,2	4,1284	0,9986	0,0035	−0,0070
5,4	4,3282	0,9990	0,0024	−0,0049
5,6	4,5280	0,9993	0,0015	−0,0033
5,8	4,7279	0,9994	0,0009	−0,0022
6,0	4,9278	0,9995	0,0006	−0,0015
6,2	5,1277	0,9996	0,0004	−0,0009
6,4	5,3276	0,9996	0,0002	−0,0006
6,6	5,5275	0,9996	0,0001	−0,0004
6,8	5,7275	0,9996	0,0001	−0,0001
7,0	5,9274	1,0000	0,0000	0,0000

Table III.1 continued

$u\sqrt{\dfrac{U}{xv_0}}$	I	I'	I''	I'''
5,6	1,8192	0,8052	0,1640	−0,0674
5,8	1,9834	0,8366	0,1497	−0,0745
6,0	2,1536	0,8650	0,1343	−0,0791
6,2	2,3289	0,8963	0,1183	−0,0810
6,4	2,5095	0,9123	0,1021	−0,0800
6,6	2,6939	0,9312	0,0864	−0,0766
6,8	2,8818	0,9469	0,0716	−0,0711
7,0	3,0725	0,9599	0,0581	−0,0639
7,2	3,2656	0,9703	0,0461	−0,0559
7,4	3,4605	0,9784	0,0358	−0,0474
7,6	3,6568	0,9847	0,0271	−0,0390
7,8	3,8543	0,9894	0,0201	−0,0313
8,0	4,0525	0,9929	0,0146	−0,0243
8,2	4,2513	0,9953	0,0103	−0,0184
8,4	4,4506	0,9971	0,0071	−0,0136
8,6	4,6501	0,9982	0,0048	−0,0097
8,8	4,8499	0,9990	0,0032	−0,0068
9,0	5,0497	0,9996	0,0021	−0,0046
9,2	5,2197	0,9999	0,0013	−0,0031
9,4	5,4197	1,0000	0,0008	−0,0020
9,6	5,6198	1,0000	0,0005	−0,0013
9,8	5,8198	1,0000	0,0003	−0,0008
10,0	6,0198	1,0000	0,0002	−0,0005
10,2	6,2199	1,0000	0,0001	−0,0002
10,4	6,4199	1,0000	0,0000	−0,0001
10,6	6,6501	1,0000	0,0000	0,0000

Table III,1 continued

$\beta_1 = 1$; $\dfrac{v_\omega}{v_0} = 0{,}4$

$u = \sqrt{\dfrac{U}{\lambda v_0}}$	i	$i^\cdot$	$i^\cdot$	$i^\cdot$
0	0	0	0,7310	-1,0964
0,2	0,0134	0,1287	0,5741	-0,5619
0,4	0,0400	0,2340	0,4860	-0,3473
0,6	0,1061	0,3251	0,4280	-0,2440
0,8	0,1793	0,4062	0,3852	-0,1895
1,0	0,2680	0,4797	0,3506	-0,1596
1,2	0,3708	0,5468	0,3205	-0,1432
1,4	0,4864	0,6081	0,2928	-0,1344
1,6	0,6137	0,6640	0,2665	-0,1298
1,8	0,7516	0,7117	0,2408	-0,1270
2,0	0,8992	0,7603	0,2156	-0,1246
2,2	1,0554	0,8010	0,1910	-0,1216
2,4	1,2193	0,8368	0,1671	-0,1173
2,6	1,3898	0,8679	0,1442	-0,1116
2,8	1,5662	0,8946	0,1226	-0,1042
3,0	1,7474	0,9170	0,1026	-0,0955
3,2	1,9327	0,9357	0,0844	-0,0857
3,4	2,1215	0,9509	0,0683	-0,0753
3,6	2,3129	0,9632	0,0543	-0,0647
3,8	2,5066	0,9728	0,0423	-0,0544
4,0	2,7019	0,9803	0,0325	-0,0447
4,2	2,8985	0,9859	0,0244	-0,0360
4,4	3,0962	0,9901	0,0130	-0,0283
4,6	3,2945	0,9932	0,0131	-0,0217
4,8	3,4934	0,9954	0,0093	-0,0163
5,0	3,6927	0,9970	0,0065	-0,0120
5,2	3,8922	0,9981	0,0044	-0,0086
5,4	4,0919	0,9988	0,0029	-0,0061
5,6	4,2917	0,9993	0,0019	-0,0042
5,8	4,4916	0,9996	0,0012	-0,0028
6,0	4,6915	0,9998	0,0009	-0,0018
6,2	4,8915	0,9999	0,0005	-0,0012
6,4	5,0915	1,0000	0,0003	-0,0007
6,6	5,2915	1,0000	0,0002	-0,0005
6,8	5,4915	1,0000	0,0001	-0,0003
7,0	5,6915	1,0000	0,0001	-0,0002
7,2	5,8916	1,0000	0,0000	-0,0001
7,4	6,0916	1,0000	0,0000	-0,0000

$\beta_1 = 1$; $\dfrac{v_\omega}{v_0} = 0{,}6$

$u = \sqrt{\dfrac{U}{\lambda v_0}}$	i	$i^\cdot$	$i^\cdot$	$i^\cdot$
0	0	0	0,5165	-0,3443
0,2	0,0099	0,0973	0,4606	-0,2777
0,4	0,0383	0,1853	0,4219	-0,2277
0,6	0,0836	0,2667	0,3925	-0,1314
0,8	0,1446	0,3427	0,3682	-0,1131
1,0	0,2204	0,4141	0,3466	-0,1046
1,2	0,3100	0,4814	0,3260	-0,1021
1,4	0,4127	0,5445	0,3055	-0,1034
1,6	0,5276	0,6036	0,2845	-0,1066
1,8	0,6538	0,6583	0,2628	-0,1106
2,0	0,7906	0,7086	0,2403	-0,1142
2,2	0,9370	0,7544	0,2172	-0,1165
2,4	1,0920	0,7955	0,1938	-0,1171
2,6	1,2548	0,8319	0,1705	-0,1155
2,8	1,4245	0,8637	0,1478	-0,1116
3,0	1,6001	0,8911	0,1260	-0,1054
3,2	1,7807	0,9142	0,1057	-0,0974
3,4	1,9655	0,9335	0,0872	-0,0880
3,6	2,1538	0,9492	0,0706	-0,0776
3,8	2,3450	0,9619	0,0561	-0,0669
4,0	2,5384	0,9718	0,0438	-0,0563
4,2	2,7336	0,9795	0,0336	-0,0463
4,4	2,9301	0,9854	0,0252	-0,0372
4,6	3,1276	0,9897	0,0186	-0,0292
4,8	3,3259	0,9929	0,0134	-0,0225
5,0	3,5247	0,9952	0,0095	-0,0168
5,2	3,9234	0,9979	0,0045	-0,0089
5,4	4,1231	0,9986	0,0030	-0,0062
5,6	4,3229	0,9991	0,0020	-0,0043
5,8	4,5227	0,9995	0,0013	-0,0029
6,0	4,7226	0,9997	0,0008	-0,0019
6,2	4,9226	0,9998	0,0005	-0,0012
6,4	5,1226	0,9999	0,0003	-0,0008
6,6	5,3225	0,9999	0,0002	-0,0005
6,8	5,5225	0,9999	0,0001	-0,0003
7,0	5,7225	0,9999	0,0001	-0,0002
7,2	5,9225	1,0000	0,0000	-0,0001
7,4	6,1225	1,0000	0,0000	-0,0001
7,6	6,3225	1,0000	0,0000	-0,0001

Table III.1 continued

$B_1 = 1; \quad \dfrac{v_w}{v_0} = 0.8$

$u\sqrt{\dfrac{U}{xv_0}}$	f	f'	f''	f'''
0	0	0	0,4030	—0,1007
0,2	0,0079	0,0788	0,3854	—0,0773
0,4	0,0313	0,1544	0,3714	—0,0642
0,6	0,0695	0,2274	0,3592	—0,0583
0,8	0,1221	0,2981	0,3477	—0,0577
1,0	0,1886	0,3665	0,3359	—0,0609
1,2	0,2686	0,4325	0,3232	—0,0669
1,4	0,3614	0,4957	0,3090	—0,0748
1,6	0,4666	0,5560	0,2932	—0,0836
1,8	0,5836	0,6129	0,2756	—0,0926
2,0	0,7115	0,6661	0,2562	—0,1008
2,2	0,8498	0,7153	0,2351	—0,1076
2,4	0,9974	0,7601	0,2133	—0,1123
2,6	1,1535	0,8005	0,1906	—0,1145
2,8	1,3173	0,8364	0,1677	—0,1139
3,0	1,4878	0,8677	0,1452	—0,1106
3,2	1,6640	0,8945	0,1237	—0,1047
3,4	1,8453	0,9172	0,1035	—0,0968
3,6	2,0307	0,9360	0,0850	—0,0873
3,8	2,2175	0,9514	0,0686	—0,0768
4,0	2,4110	0,9636	0,0543	—0,0660
4,2	2,6048	0,9732	0,0422	—0,0553
4,4	2,8002	0,9807	0,0322	—0,0453
4,6	2,9969	0,9862	0,0241	—0,0364
4,8	3,1946	0,9904	0,0176	—0,0282
5,0	3,3930	0,9934	0,0127	—0,0216
5,2	3,5919	0,9956	0,0089	—0,0161
5,4	3,7912	0,9970	0,0062	—0,0117
5,6	3,9907	0,9981	0,0042	—0,0084
5,8	4,1904	0,9988	0,0028	—0,0058
6,0	4,3902	0,9992	0,0018	—0,0040
6,2	4,5900	0,9995	0,0011	—0,0026
6,4	4,7900	0,9997	0,0007	—0,0017
6,6	4,9899	0,9998	0,0004	—0,0011
6,8	5,1899	0,9999	0,0003	—0,0007
7,0	5,3899	0,9999	0,0002	—0,0004
7,2	5,5899	0,9999	0,0001	—0,0002
7,4	5,7898	0,9999	0,0001	—0,0001
7,6	5,9898	1,0000	0,0000	—0,0001
7,8	6,1898	1,0000	0,0000	0,0000

$B_1 = 1; \quad \dfrac{v_w}{v_0} = 2$

$u\sqrt{\dfrac{U}{xv_0}}$	f	f'	f''	f'''
0	0	0	0,1804	0,0902
0,2	0,0037	0,0379	0,1984	0,0891
0,4	0,0154	0,0793	0,2159	0,0856
0,6	0,0357	0,1242	0,2325	0,0797
0,8	0,0653	0,1722	0,2476	0,0712
1,0	0,1048	0,2231	0,2608	0,0601
1,2	0,1547	0,2763	0,2715	0,0467
1,4	0,2154	0,3315	0,2793	0,0311
1,6	0,2873	0,3879	0,2833	0,0137
1,8	0,3706	0,4448	0,2847	—0,0049
2,0	0,4652	0,5015	0,2818	—0,0241
2,2	0,5711	0,5572	0,2751	—0,0433
2,4	0,6880	0,6113	0,2646	—0,0614
2,6	0,8155	0,6628	0,2506	—0,0778
2,8	0,9530	0,7113	0,2336	—0,0915
3,0	1,0998	0,7561	0,2142	—0,1020
3,2	1,2551	0,7969	0,1931	—0,1088
3,4	1,4182	0,8333	0,1709	—0,1118
3,6	1,5882	0,8652	0,1486	—0,1109
3,8	1,7640	0,8928	0,1268	—0,1066

141

Table III.1 continued

$B_1 = 1$; $\dfrac{v_\infty}{v_0} = 10$

$y\sqrt{\dfrac{v}{xv_0}}$	i	i'	i''	i'''
0,0	0	0	0,0413	0,0372
0,2	0,8775	0,0090	0,0493	0,0434
0,4	0,0037	0,0198	0,0587	0,0504
0,6	0,0089	0,0326	0,0695	0,0578
0,8	0,0169	0,0477	0,0818	0,0655
1,0	0,0282	0,0655	0,0957	0,0732
1,2	0,0433	0,0861	0,1111	0,0805
1,4	0,0629	0,1160	0,1279	0,0869
1,6	0,0876	0,1373	0,1458	0,0918
1,8	0,1181	0,1684	0,1644	0,0944
2,0	0,1551	0,2031	0,1833	0,0943
2,2	0,1996	0,2417	0,2019	0,0972
2,4	0,2520	0,2838	0,2194	0,0834
2,6	0,3133	0,3293	0,2350	0,0721
2,8	0,3840	0,3776	0,2479	0,0569
3,0	0,4645	0,4282	0,2575	0,0384
3,2	0,5554	0,4804	0,2631	0,0172
3,4	0,6567	0,5332	0,2643	—0,0057
3,6	0,7686	0,5858	0,2608	—0,0290
3,8	0,8909	0,6372	0,2528	—0,0514
4,0	1,0234	0,6866	0,2404	—0,0716
4,2	1,1654	0,7331	0,2243	—0,0885
4,4	1,3164	0,7761	0,2053	—0,1012
4,6	1,4756	0,8151	0,1841	—0,1126

$y\sqrt{\dfrac{v}{xv_0}}$	i	i'	i''	i'''
4,0	1,9450	0,9160	0,1061	—0,0995
4,2	2,1302	0,9353	0,0872	—0,0902
4,4	2,3189	0,9510	0,0702	—0,0795
4,6	2,5104	0,9636	0,0554	—0,0683
4,8	2,7041	0,9733	0,0428	—0,0571
5,0	2,8996	0,9803	0,0325	—0,0466
5,2	3,0963	0,9865	0,0241	—0,0371
5,4	3,2941	0,9906	0,0176	—0,0288
5,6	3,4925	0,9936	0,0126	—0,0218
5,8	3,6915	0,9957	0,0088	—0,0161
6,0	3,8908	0,9972	0,0060	—0,0117
6,2	4,0903	0,9982	0,0040	—0,0082
6,4	4,2900	0,9989	0,0027	—0,0057
6,6	4,4898	0,9993	0,0017	—0,0038
6,8	4,6897	0,9996	0,0011	—0,0025
7,0	4,8897	0,9997	0,0007	—0,0016
7,2	5,0896	0,9998	0,0004	—0,0010
7,4	5,2896	0,9999	0,0002	—0,0006
7,6	5,4896	0,9999	0,0001	—0,0004
8,0	5,8896	1,0000	0,0000	—0,0001
8,2	6,0896	1,0000	0,0000	—0,0001
8,4	6,2896	1,0000	0,0000	0,0000

$B_1 = 2; \quad \dfrac{v_\omega}{v_0} = 0.2$

$\nu\sqrt{\dfrac{U}{xv_0}}$	t	r	r'	r''
0,0	0	0	1,5159	—12,1269
0,2	0,0205	0,1791	0,6444	—1,5046
0,4	0,0677	0,2866	0,4629	—0,5441
0,6	0,1337	0,3706	0,3852	—0,2785
0,8	0,2152	0,4429	0,3413	—0,1753
1,0	0,3103	0,5080	0,3114	—0,1293
1,2	0,4180	0,5678	0,2877	—0,1099
1,4	0,5372	0,6233	0,2666	—0,1025
1,6	0,6670	0,6745	0,2463	—0,1015
1,8	0,8067	0,7218	0,2258	—0,1032
2,0	0,9554	0,7648	0,2049	—0,1055
2,2	1,1124	0,8037	0,1837	—0,1068
2,4	1,2767	0,8383	0,1623	—0,1065
2,6	1,4474	0,8687	0,1413	—0,1039
2,8	1,6238	0,8949	0,1209	—0,0992
3,0	1,8051	0,9171	0,1017	—0,0924
3,2	1,9905	0,9356	0,0841	—0,0840
3,4	2,1792	0,9508	0,0682	—0,0745
3,6	2,3706	0,9631	0,0543	—0,0645
3,8	2,5642	0,9727	0,0425	—0,0554
4,0	2,7595	0,9802	0,0325	—0,0449
4,2	2,9562	0,9858	0,0244	—0,0361
4,4	3,1538	0,9900	0,0180	—0,0294
4,6	3,3521	0,9931	0,0130	—0,0218
4,8	3,5509	0,9953	0,0092	—0,0163
5,0	3,7502	0,9969	0,0064	—0,0119
5,2	3,9497	0,9979	0,0043	—0,0086
5,4	4,1493	0,9986	0,0029	—0,0060
5,6	4,3491	0,9991	0,0019	—0,0041
5,8	4,5489	0,9994	0,0012	—0,0028
6,0	4,7489	0,9996	0,0008	—0,0018
6,2	4,9488	0,9997	0,0005	—0,0012
6,4	5,1488	0,9998	0,0003	—0,0007
6,6	5,3487	0,9998	0,0002	—0,0004
6,8	5,5487	0,9999	0,0001	—0,0003
7,0	5,7487	0,9999	0,0001	—0,0002
7,2	5,9487	1,0000	0,0000	—0,0001
7,4	6,1486	1,0000	0,0000	0,0000

Table III.1 continued

$\nu\sqrt{\dfrac{U}{xv_0}}$	t	r	r'	r''
5,0	1,8152	0,8799	0,1394	—0,1113
5,2	1,9938	0,9055	0,1176	—0,1061
5,4	2,1771	0,9270	0,0972	—0,0979
5,6	2,3643	0,9445	0,0786	—0,0877
5,8	2,5547	0,9586	0,0623	—0,0758
6,0	2,7476	0,9696	0,0483	—0,0639
6,2	2,9474	0,9781	0,0367	—0,0524
6,4	3,1387	0,9844	0,0273	—0,0418
6,6	3,3361	0,9891	0,0199	—0,0325
6,8	3,5342	0,9925	0,0142	—0,0247
7,0	3,7330	0,9949	0,0099	—0,0183
7,2	3,9321	0,9966	0,0068	—0,0132
7,4	4,1316	0,9977	0,0046	—0,0093
7,6	4,3312	0,9984	0,0030	—0,0064
7,8	4,5310	0,9989	0,0019	—0,0043
8,0	4,7307	0,9992	0,0012	—0,0029
8,2	4,9306	0,9994	0,0008	—0,0018
8,4	5,1305	0,9995	0,0004	—0,0012
8,6	5,3304	0,9996	0,0003	—0,0007
8,8	5,5303	0,9996	0,0002	—0,0004
9,0	5,7303	0,9997	0,0001	—0,0002
9,2	5,9302	0,9997	0,0000	—0,0001
9,4	6,1302	1,0000	0,00000	—0,0001
9,6	6,330	1,0000	0,00000	0,0000

$B_1 = 2;\quad \dfrac{v_\infty}{v_0} = 10$

$\nu\sqrt{\dfrac{U}{xv_0}}$	i	i'	i''	i'''
0,0	0	0	0,0395	0,0648
0,2	0,0008	0,0086	0,0512	0,0878
0,4	0,0037	0,0208	0,0713	0,1143
0,6	0,0094	0,0375	0,0969	0,1415
0,8	0,0191	0,0599	0,1276	0,1642
1,0	0,0338	0,0888	0,1619	0,1766
1,2	0,0551	0,1248	0,1973	0,1744
1,4	0,0842	0,1676	0,2367	0,1569
1,6	0,1225	0,2167	0,2593	0,1275
1,8	0,1712	0,2709	0,2812	0,0917
2,0	0,2311	0,3287	0,2958	0,0544
2,2	0,3028	0,3887	0,3031	0,0190
2,4	0,3867	0,4495	0,3037	-0,0128
2,6	0,4826	0,5098	0,2983	-0,0404
2,8	0,5965	0,5685	0,2878	-0,0637
3,0	0,7099	0,6246	0,2731	-0,0829
3,2	0,8401	0,6775	0,2549	-0,0980
3,4	0,9806	0,7264	0,2342	-0,1090
3,6	1,1304	0,7711	0,2116	-0,1160
3,8	1,2887	0,8110	0,1880	-0,1189

Table III.1 continued $\qquad B_1 = 2;\quad \dfrac{v_\omega}{v_0} = 0,8$

$\nu\sqrt{\dfrac{U}{xv_0}}$	i	i'	i''	i'''
0,0	0	0	0,4099	-0,2050
0,2	0,0079	0,0786	0,3786	-0,1189
0,4	0,0311	0,11522	0,3595	-0,0771
0,6	0,0686	0,2228	0,3463	-0,0570
0,8	0,1200	0,2909	0,3359	-0,0439
1,0	0,1849	0,3572	0,3261	-0,0491
1,2	0,2628	0,4214	0,3159	-0,0539
1,4	0,3533	0,4834	0,3043	-0,0619
1,6	0,4560	0,5430	0,2910	-0,0717
1,8	0,5703	0,5997	0,2756	-0,0821
2,0	0,6956	0,6531	0,2582	-0,0920
2,2	0,8313	0,7028	0,2389	-0,1007
2,4	0,9765	0,7486	0,2180	-0,1074
2,6	1,1304	0,7900	0,1961	-0,1114
2,8	1,2922	0,8270	0,1737	-0,1126
3,0	1,4609	0,8595	0,1513	-0,1167
3,2	1,6357	0,8875	0,1296	-0,1061
3,4	1,8157	0,9114	0,1090	-0,0996
3,6	1,9999	0,9313	0,0907	-0,0901
3,8	2,1879	0,9475	0,0737	-0,0799
4,0	2,3788	0,9606	0,0581	-0,0692
4,2	2,5720	0,9709	0,0454	-0,0594
4,4	2,7670	0,9789	0,0348	-0,0481
4,6	2,9634	0,9850	0,0261	-0,0387
4,8	3,1609	0,9895	0,0192	-0,0304
5,0	3,3591	0,9928	0,0139	-0,0233
5,2	3,5579	0,9951	0,0098	-0,0175
5,4	3,7571	0,9968	0,0068	-0,0128
5,6	3,9566	0,9979	0,0046	-0,0092
5,8	4,1563	0,9987	0,0031	-0,0064
6,0	4,3561	0,9992	0,0020	-0,0044
6,2	4,5559	0,9995	0,0013	-0,0029
6,4	4,7559	0,9997	0,0008	-0,0019
6,6	4,9558	0,9998	0,0005	-0,0012
6,8	5,1558	0,9999	0,0003	-0,0005
7,0	5,3558	0,9999	0,0002	-0,0003
7,2	5,5558	0,9999	0,0001	-0,0003
7,4	5,7557	0,9999	0,0001	-0,0001
7,6	5,9557	1,0000	0,0000	0,0000

$$B_1 = 6; \quad \frac{v_w}{v_0} = 0{,}2$$

$y\sqrt{\dfrac{U}{xv_0}}$	I	I'	I''	I'''
0,0	0	0	2,8130	—67,5116
0,2	0,0142	0,0898	0,4360	—0,8345
0,4	0,0401	0,1668	0,3554	—0,1746
0,6	0,0804	0,2354	0,3349	—0,0587
0,8	0,1341	0,3014	0,3263	—0,0350
1,0	0,2009	0,3660	0,3194	—0,0360
1,2	0,2804	0,4291	0,3114	—0,0448
1,4	0,3724	0,4904	0,3013	—0,0564
1,6	0,4764	0,5495	0,2888	—0,0686
1,8	0,5920	0,6058	0,2737	—0,0811
2,0	0,7185	0,6588	0,2564	—0,0921
2,2	0,8553	0,7082	0,2370	—0,1014
2,4	1,0015	0,7535	0,2160	—0,1082
2,6	1,1564	0,7945	0,1939	—0,1121
2,8	1,3190	0,8311	0,1714	—0,1130
3,0	1,4885	0,8631	0,1489	—0,1108
3,2	1,6640	0,8907	0,1272	—0,1058
3,4	1,8445	0,9140	0,1068	—0,0984
3,6	2,0293	0,9335	0,0879	—0,0892
3,8	2,2177	0,9494	0,0711	—0,0789
4,0	2,4089	0,9621	0,0564	—0,0680
4,2	2,6023	0,9721	0,0439	—0,0572
4,4	2,7975	0,9798	0,0335	—0,0469
4,6	2,9941	0,9856	0,0251	—0,0376
4,8	3,1917	0,9899	0,0184	—0,0294
5,0	3,3900	0,9931	0,0133	—0,0225
5,2	3,5889	0,9954	0,0094	—0,0167
5,4	3,7881	0,9969	0,0065	—0,0122
5,6	3,9876	0,9980	0,0044	—0,0087
5,8	4,1873	0,9937	0,0029	—0,0061
6,0	4,3871	0,9992	0,0019	—0,0042
6,2	4,5870	0,9995	0,0012	—0,0028
6,4	4,7869	0,9997	0,0008	—0,0018
6,6	4,9868	0,9998	0,0005	—0,0011
6,8	5,1868	0,9999	0,0003	—0,0007
7,0	5,3868	0,9999	0,0002	—0,0004
7,2	5,5868	0,9999	0,0001	—0,0003
7,4	5,7868	1,0000	0,0001	—0,0002
7,6	5,9868	1,0000	0,0000	—0,0001
7,8	6,1863	1,0000	0,0000	0,0000

Table III.1 continued

$y\sqrt{\dfrac{U}{xv_0}}$	I	I'	I''	I'''
4,0	1,4545	0,8463	0,1643	—0,1181
4,2	1,6269	0,8768	0,1410	—0,1139
4,4	1,8049	0,9027	0,1189	—0,1068
4,6	1,9877	0,9244	0,0984	—0,0976
4,8	2,1744	0,9422	0,0799	—0,0868
5,0	2,3644	0,9566	0,0638	—0,0753
5,2	2,5569	0,9679	0,0499	—0,0637
5,4	2,7514	0,9767	0,0382	—0,0526
5,6	2,9474	0,9834	0,0288	—0,0424
5,8	3,1446	0,9883	0,0212	—0,0334
6,0	3,3427	0,9919	0,0153	—0,0256
6,2	3,5413	0,9946	0,0109	—0,0193
6,4	3,7400	0,9964	0,0076	—0,0141
6,6	3,9398	0,9976	0,0051	—0,0101
6,8	4,1395	0,9985	0,0034	—0,0071
7,0	4,3392	0,9990	0,0022	—0,0049
7,2	4,5391	0,9994	0,0014	—0,0033
7,4	4,7389	0,9996	0,0009	—0,0021
7,6	4,9389	0,9998	0,0006	—0,0014
7,8	5,1389	0,9999	0,0003	—0,0009
8,0	5,3388	0,9999	0,0002	—0,0005
8,2	5,5388	0,9999	0,0001	—0,0003
8,4	5,7388	0,9999	0,0001	0,0002
8,6	5,9388	1,0000	0,0000	—0,0001
8,8	6,1388	1,0000	0,0000	0,0000

Table III.1 continued

$B_1 = 6$; $\dfrac{v_w}{v_o} = 0.8$

$y\sqrt{\dfrac{U}{xv_o}}$				
0.0	0	0	0.4146	−0.6218
0.2	0.0077	0.0751	0.3526	−0.1371
0.4	0.0296	0.1437	0.3369	−0.0424
0.6	0.0651	0.2104	0.3310	−0.0217
0.8	0.1138	0.2762	0.3268	−0.0218
1.0	0.1755	0.3411	0.3218	−0.0292
1.2	0.2501	0.4048	0.3419	−0.0397
1.4	0.3373	0.4669	0.3058	−0.0517
1.6	0.4368	0.5270	0.2942	−0.0643
1.8	0.5479	0.5845	0.2801	−0.0767
2.0	0.6704	0.6389	0.2636	−0.0884
2.2	0.8033	0.6898	0.2449	−0.0984
2.4	0.9460	0.7367	0.2244	−0.106i
2.6	1.0977	9.7794	0.2026	−0.1112
2.8	1.2575	0.8177	0.1801	−0.1132
3.0	1.4245	0.8515	0.1576	−0.1122
3.2	1.5978	0.8808	0.1354	−0.1082
3.4	1.7765	0.9057	0.1144	−0.1016
3.6	1.9598	0.9266	0.0949	−0.0930
3.8	2.1469	0.9438	0.0773	−0.0830
4.0	2.3371	0.9577	0.0618	−0.0722
4.2	2.5298	0.9686	0.0484	−0.0613
4.4	2.7244	0.9772	0.0372	−0.0507
4.6	2.9206	0.9837	0.0281	−0.0410
4.8	3.1178	0.9886	0.0208	−0.0324
5.0	3.3159	0.9921	0.0150	−0.0249
5.2	3.5146	0.9947	0.0107	−0.0188
5.4	3.7137	0.9965	0.0071	−0.0138
5.6	3.9132	0.9977	0.0051	−0.0099
5.8	4.1128	0.9985	0.0031	−0.0070
6.0	4.3126	0.9991	0.0022	−0.0048
6.2	4.5124	0.9995	0.0014	−0.0032
6.4	4.7124	0.9997	0.0009	−0.0021
6.6	4.9123	0.9999	0.0006	−0.0014
6.8	5.1123	0.9999	0.0003	−0.0009
7.0	5.3123	1.0000	0.0002	−0.0005
7.2	5.5123	1.0000	0.0001	−0.0003
7.4	5.7123	1.0000	0.0000	−0.0002
7.6	5.9123	1.0000	0.0000	−0.0001
7.8	6.1123	1.0000	0.0000	0.0000

$B_1 = 6$; $\dfrac{v_w}{v_o} = 10$

$y\sqrt{\dfrac{U}{xv_o}}$				
0	0	0	0.0338	0.1823
0.2	0.0010	0.0117	0.0906	0.3973
0.4	0.0057	0.0388	0.1849	0.4985
0.6	0.0178	0.0819	0.2694	0.3170
0.8	0.0405	0.1436	0.3117	0.1230
1.0	0.0756	0.2077	0.3257	0.0306
1.2	0.1237	0.2731	0.3275	−0.0070
1.4	0.1849	0.3384	0.3241	−0.0259
1.6	0.2590	0.4026	0.3174	−0.0399
1.8	0.3458	0.4652	0.3081	−0.0529
2.0	0.4449	0.5256	0.2963	−0.0658
2.2	0.5559	0.5835	0.2818	−0.0783
2.4	0.6781	0.6382	0.2650	−0.0898
2.6	0.8109	0.6894	0.2460	−0.0998
2.8	0.9536	0.7365	0.2253	−0.1074
3.0	1.1052	0.7794	0.2032	−0.1123
3.2	1.2650	0.8178	0.1805	−0.1142
3.4	1.4320	0.8516	0.1578	−0.1130
3.6	1.6054	0.8809	0.1356	−0.1088
3.8	1.7841	0.9059	0.11+4	−0.1021
4.0	1.9674	0.9268	0.0948	−0.0933
4.2	2.1525	0.9435	0.0736	−0.0831
4.4	2.3448	0.9578	0.0616	−0.0723
4.6	2.5375	0.9688	0.0483	−0.0613
4.8	2.7321	0.9773	0.0371	−0.0507
5.0	2.9283	0.9837	0.0279	−0.0409
5.2	3.1256	0.9886	0.0206	−0.0323
5.4	3.3236	0.9921	0.0149	−0.0249
5.6	3.5223	0.9946	0.0106	−0.0187
5.8	3.7215	0.9964	0.0074	−0.0137
6.0	3.9209	0.9977	0.0050	−0.0099
6.2	4.1205	0.9985	0.0032	−0.0085
6.4	4.3203	0.9991	0.0022	−0.0047
6.6	4.5201	0.9994	0.0014	−0.0032
6.8	4.7200	0.9996	0.0009	−0.0021
7.0	4.9200	0.9998	0.0005	−0.0011
7.2	5.1199	0.9999	0.0003	−0.0009
7.4	5.3199	0.9999	0.0002	−0.0005
7.6	5.5199	0.9999	0.0001	−0.0003
7.8	5.7199	0.9999	0.0001	−0.0002
8.0	5.9199	1.0000	0.0000	−0.0001
8.2	6.1199	1.0000	0.0000	0.0000

§ III.3. Laminar Boundary Layer in a Fluid with Variable Density

Let us consider the two-dimensional, steady-state boundary layer under the assumption that $g_x = 0$, $g_y = -g$, where g is a gravitational acceleration. The system of equations of the boundary layer obtained on the basis of (III.3) is written as follows:

$$u \frac{\partial u}{\partial x} + v \frac{\partial u}{\partial y} = -\frac{1}{\rho} \cdot \frac{\partial p}{\partial x} + \nu \frac{\partial^2 u}{\partial y^2} + \nu \frac{1}{\rho} \cdot \frac{\partial \rho}{\partial y} \cdot \frac{\partial u}{\partial y};$$
$$\frac{\partial p}{\partial y} = -\rho g. \tag{III.24}$$

Let us consider the pressure p_1 related to p by the expression

$$p_1 = p + g \int_{y_0}^{y} \rho(y) \, dy.$$

Then system (III.24) together with the continuity equation assumes the form

$$u \frac{\partial u}{\partial x} + v \frac{\partial u}{\partial y} = -\frac{1}{\rho} \cdot \frac{\partial p_1}{\partial x} + \nu \frac{\partial^2 u}{\partial y^2} + \frac{\nu}{\rho} \cdot \frac{\partial \rho}{\partial y} \cdot \frac{\partial u}{\partial y};$$
$$\frac{\partial p_1}{\partial y} = 0; \quad \frac{\partial u}{\partial x} + \frac{\partial v}{\partial y} = 0. \tag{III.25}$$

It must be emphasized that the continuity equation (I.2) for an incompressible fluid has the above-indicated form in spite of the dependence of the density on the space point coordinates (see [28], Chapter I).

Defining the pressure gradient along the flow from the condition of validity of the first equation of (III.25) at the upper boundary of the boundary layer, we arrive at the expression

$$u \frac{\partial u}{\partial x} + v \frac{\partial u}{\partial y} = \frac{\rho_*}{\rho} U \frac{\partial U}{\partial x} + \nu \frac{\partial^2 u}{\partial y^2} + \frac{\nu}{\rho} \cdot \frac{\partial \rho}{\partial y} \cdot \frac{\partial u}{\partial y}, \tag{III.26}$$

where $\rho_* = \rho(\delta)$.

For solution of the problem, just as in § III.2, we use the Pohlhausen method. The velocity profile in the boundary layer will be approximated by the polynomial (III.6), the coefficients of which will be determined from the conditions (III.7), (III.9) and (III.27),

$$v_1 \frac{\partial u}{\partial y} \Big|_{y=0} = \frac{\rho_*}{\rho} U \frac{\partial U}{\partial x} + \nu \frac{\partial^2 u}{\partial y^2} \Big|_{y=0} + \nu \frac{1}{\rho} \cdot \frac{\partial \rho}{\partial y} \cdot \frac{\partial u}{\partial y} \Big|_{y=0}. \tag{III.27}$$

These coefficients are expressed by the formulas:

$$a_1 = 2 + \frac{K_1}{6}; \quad a_2 = -\frac{K_1}{2}; \quad a_3 = -2 + \frac{K_1}{2}; \quad a_4 = 1 - \frac{K_1}{6},$$

in which the value of

$$K_1 = \frac{\dfrac{\delta^2 U'}{\nu}\dfrac{\rho^*}{\rho_w} - 2\dfrac{\delta v_1}{\nu} + 2\dfrac{\delta}{\rho_w}\cdot\dfrac{\partial\rho}{\partial y}\Big|_{y=0}}{1 + \dfrac{1}{6}\cdot\dfrac{\delta v_1}{\nu} - \dfrac{1}{6}\cdot\dfrac{\delta}{\rho_w}\cdot\dfrac{\partial\rho}{\partial y}\Big|_{y=0}} \tag{III.28}$$

has the meaning of a Pohlhausen parameter in the case of a boundary layer with variable density. The velocity distribution across the boundary layer as a function of the parameter K_1 is entirely analogous to the case investigated in § III.2 except the role of the family parameter there was played by the value of K.

Let us give the law of density variation with respect to thickness of the boundary layer by the function

$$\rho(y) = \rho_w e^{-B\frac{y}{\delta}}, \tag{III.29}$$

then formula (III.28) is rewritten as follows:

$$K_1 = \frac{\dfrac{\delta^2 U'}{\nu}\cdot e^{-B} - 2\left(\dfrac{\delta v_1}{\nu} + B\right)}{1 + \dfrac{1}{6}\left(\dfrac{\delta v_1}{\nu} + B\right)}. \tag{III.30}$$

It is meaningful to use formulas (III.28), (III.30) just as, in general, the Pohlhausen method, under the condition where $-6 < K_1 < 7$. Let us add and subtract the value of $U\partial U/\partial x$ in the right-hand side of (III.26), and then let us integrate both sides of the equality with respect to the y-coordinate within the limits of the boundary layer. Considering the continuity equation, we obtain the following integral expression for an incompressible laminar boundary layer with variable density:

$$\frac{d\delta^{**}}{dx} + \frac{U'\delta^{**}}{U}\left(2 + \frac{\delta^*}{\delta^{**}}\right) - \frac{v_1}{U} + \frac{U'}{U}\int_0^\delta\left(\frac{\rho_*}{\rho} - 1\right)dy +$$

$$+ \frac{\nu}{U^2}\int_0^\delta\frac{1}{\rho}\cdot\frac{\partial\rho}{\partial y}\cdot\frac{\partial u}{\partial y}dy = \frac{\nu}{U^2}\frac{\partial u}{\partial y}\Big|_{y=0}, \tag{III.31}$$

where δ^*, δ^{**} are expressed in terms of the parameter K_1 using formulas entirely analogous to (III.12). Using (III.29), we determine the last two terms of the left-hand side of (III.31):

$$\frac{U'}{U}\int_0^\delta\left(\frac{\rho_*}{\rho} - 1\right)dy = \frac{U'}{U}\int_0^\delta\left(e^{B\left(\frac{y}{\delta}-1\right)} - 1\right)dy = \frac{U'\delta}{U}\left(\frac{1-e^{-B}}{B} - 1\right);$$

$$\frac{\nu}{U^2}\int_0^\delta\frac{1}{\rho}\frac{\partial\rho}{\partial y}\cdot\frac{\partial u}{\partial y}dy = \frac{\nu}{U^2}\int_0^\delta\left(-\frac{B}{\delta}\right)\frac{\partial u}{\partial y}dy = -\frac{B\nu}{\delta U}.$$

Let us substitute the obtained expressions in (III.31)

$$\frac{d\delta^{**}}{dx} + \frac{U'}{U}\left[2\delta^{**} + \delta^* + \delta\frac{1-B\cdot e^{-B}}{B}\right] -$$

$$- \frac{v_1}{U} - \frac{\nu}{U}\left(\frac{1}{U}\cdot\frac{\partial u}{\partial y}\Big|_{y=0} - \frac{B}{\delta}\right). \tag{III.32}$$

148

Using the expression for the velocity profile and formula (ΙΙΙ.30), we find

$$\frac{1}{U} \cdot \frac{\partial u}{\partial y}\Big|_{y=0} = \frac{1}{\delta}\left(2 + \frac{K_1}{6}\right);$$
(III.33)

$$\delta^2 = \frac{\nu}{U'} e^{B}(MK_1 + N),$$
(III.34)

where

$$M = 1 + \frac{1}{6}\left(\frac{\delta v_1}{\nu} + B\right); \qquad N = 2\left(\frac{\delta v_1}{\nu} + B\right).$$

Let us consider the value of $\delta v_1/\nu$ to be constant.

Considering (III.33) and (III.34), we reduce (III.32) to the form

$$\frac{dK_1}{dx} = \frac{U''}{U'}f_1(K_1) + \frac{U'}{U}f_2(K_1),$$
(III.35)

where

$$f_1(K_1) = \frac{(MK_1 + N)\cdot\left(\frac{37}{315} - \frac{K_1}{945} - \frac{K_1^2}{9072}\right)}{M\left(\frac{37}{315} - \frac{K_1}{945} - \frac{K_1^2}{9072}\right) - (MK_1 + N)\left(\frac{2}{945} + \frac{K_1}{2268}\right)};$$

$$f_2(K_1) = 2\frac{\left(\frac{v_1\delta}{\nu} + 2 + \frac{K_1}{6} + B\right)e^{-B} - (MK_1 + N)\left(\frac{337}{630} - \frac{79K_1}{7560} - \frac{K_1^2}{4536}\right)}{M\left(\frac{37}{315} - \frac{K_1}{945} - \frac{K_1^2}{9072}\right) - (MK_1 + N)\left(\frac{2}{945} + \frac{K_1}{2268}\right)}.$$

Linearizing the functions $f_1(K_1)$, $f_2(K_1)$, just as in § III.2, we obtain

$$f_1(K_1) \simeq \frac{\frac{37}{315}(MK_1 + N)}{\frac{37}{315}M - \frac{2N}{945}} = \frac{11M}{11M - 2N}K_1 +$$

$$+ \frac{11N}{11M - 2N} = q_{11}\cdot K_1 + q_{12};$$

$$f_2(K_1) \simeq 2\frac{\left(\frac{v_1\delta}{\nu} + 2 + \frac{K_1}{6} + B\right)e^{-B} - \frac{337}{630}(MK_1 + N)}{M\frac{37}{315} - \frac{2N}{945}} =$$

$$= 1890\frac{\frac{1}{6}e^{-B} - \frac{337}{630}M}{11M - 2N}K_1 + 1890 \times$$

$$\times \frac{\left(\frac{v_1\delta}{\nu} + 2 + B\right)e^{-B} \frac{337}{630}N}{11M - 2N} = q_{21}K_1 + q_{22}.$$

The simplifications made allow the solution to equation (III.35) to be found (see § III.2):

149

$$K_1(x) = \left(K_{10} + \frac{q_{12}}{q_{11}}\right)\left(\frac{U}{U_0'}\right)^{q_{11}} \left(\frac{U}{U_0}\right)^{q_{11}} - \frac{q_{12}}{q_{11}} +$$

$$+ \left(q_{22} - \frac{q_{12}q_{21}}{q_{11}}\right)(U')^{q_{11}} (U)^{q_{11}} \int_{x_0}^{x} \frac{(U')^{1-q_{11}}}{U^{1+q_{11}}} \, dx,$$

where

$$K_{10} = K_1(x_0); \quad U_0 = U(x_0); \quad U_0' = U'(x_0).$$

Knowing the function $K_1 = K_1(x)$, from expression (III.34) let us determine $\delta = \delta(x)$, after which we find $\delta^*(x)$, $\delta^{**}(x)$, and using (III.33), $\tau_w(x) = \rho_w v \frac{\partial u}{\partial y}\Big|_{y=0}$.

In the case of flow over an impermeable plate, where

$$U' = 0; \quad v_1 = 0; \quad K_1 = \frac{-12B}{6+B} = \text{const},$$

equation (III.32) is simplified significantly

$$\frac{1}{2} \cdot \frac{U}{v} \left(\frac{37}{315} - \frac{K_1}{945} - \frac{K_1^2}{9072}\right) \frac{d\delta^2}{dx} = 2 + \frac{K_1}{6} + B. \tag{II.36}$$

Integrating (III.36) under the condition $\delta(0) = 0$, we arrive at the expression for the boundary layer thickness

$$\delta(x) = \sqrt{\frac{xv}{U}} \cdot \sqrt{\frac{4 + \frac{K_1}{3} + 2B}{\frac{37}{315} - \frac{K_1}{945} - \frac{K_1^2}{9072}}}.$$

Using the formulas obtained for an impermeable plate, the boundary layer characteristics were calculated for various values of the ratio ρ_w/ρ_*. Here the value B was determined from expression (III.29): $B = \ln(\rho_w/\rho_*)$. The calculation results are presented in Figure III.6. The local friction coefficient was calculated by the formula

$$\zeta_f = \frac{\tau_w}{\rho_* U^2} = \frac{\rho_w}{\rho_*}\left(2 + \frac{K_1}{6}\right) \sqrt{\frac{\frac{37}{315} - \frac{K_1}{945} - \frac{K_1^2}{9072}}{4 + \frac{K_1}{3} + 2B}}.$$

If flow over an impermeable plate is considered, then in the case of density variable along the y-coordinate, the system of equations (III.25) can be reduced to the generalized Blasius equation

$$\zeta''' + \frac{1}{2} \zeta\zeta'' + \frac{\rho'}{\rho} \zeta'' = 0, \tag{III.37}$$

which, just as equation (III.21), must be integrated under the conditions

$$\zeta(0) = \zeta'(0) = 0; \quad \zeta'|_{\xi \to \infty} \to 1. \tag{III.38}$$

150

Selecting the law of variation of density across the boundary layer in the form

$$\rho(\xi) = \rho_w e^{-B_1 \xi},$$ (III.39)

where ξ is an independent Blasius variable, we obtain the following form of equation (III.37):

$$\zeta''' + \frac{1}{2} \zeta\zeta'' - B_1\zeta'' = 0.$$ (III.40)

For comparison of the values of B and B_1 in expressions (III.29) and (III.39) it is necessary to use equality (III.23) considering the difference in scales

$$\eta = \frac{y}{\delta} \quad \text{and} \quad \xi = y\left(\frac{U}{xv}\right)^{\frac{1}{2}}.$$

Making the substitution

$$\zeta = \zeta_* + 2B_1,$$

we convert equation (III.40) to the expression

$$\zeta_*''' + \frac{1}{2} \zeta_*\zeta_*'' = 0.$$ (III.41)

For equation (III.41), on the basis of (III.38), we obtain the following boundary conditions:

$$\zeta_*(0) = -2B_1; \quad \zeta_*'(0) = 0; \quad \zeta_*'|_{\xi \to \infty} \to 1.$$ (III.42)

The longitudinal and transverse velocity components in the boundary layer are defined [18] by the formulas:

$$u = \frac{\partial \psi}{\partial y} = U\zeta'(\xi); \quad v = -\frac{\partial \psi}{\partial x} = \frac{1}{2}\sqrt{\frac{vU}{x}}(\xi\zeta' - \zeta).$$

On the wall under the condition u = 0, the transverse velocity component is equal to

$$v(0) = -\frac{1}{2}\sqrt{\frac{vU}{x}} \cdot \zeta(0).$$

When the fluid is fed across the wall to the boundary layer $\zeta(0) < 0$,; when taking fluid from the boundary layer $\zeta(0) > 0$.

Thus, the problem of the velocity distribution in a boundary layer with density varying according to law (III.39), is equivalent to problem (III.41), (III.42) of a boundary layer with ventilation or removal of fluid across the wall over which flow takes place. Here the transverse velocity component on the wall must vary according to the law

$$v(0) = B_1\sqrt{\frac{vU}{x}}.$$ (III.43)

151
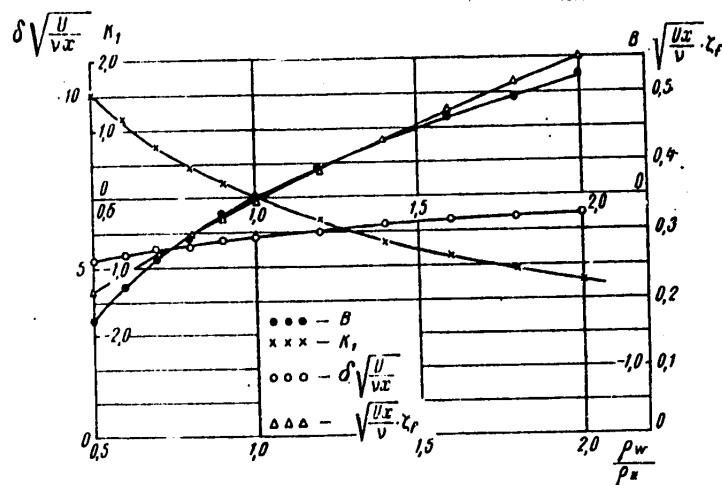
Figure III.6. Boundary Layer Characteristics as a
Function of the Ratio ρ_w / ρ_*

From formula (III.43) it is obvious that increasing the fluid density in the
direction of the wall ($B_1 > 0$) makes the velocity profile in the boundary layer
less full, and a decrease in density in the same direction ($B_1 < 0$) leads to fill-
ing out of the profile. Quantitative data can be found in reference [22], where
problem (III.41), (III.42) was solved numerically both for positive and for negative
values of $\zeta_*(0)$.

§ III.4. Laminar Boundary Layer Stability in an Incompressible Fluid with Variable
Kinematic Viscosity

The stability of plane-parallel flows of an incompressible fluid with variable kine-
matic viscosity in the presence of rigid·walls has been discussed in references [23]-
[27]. In reference [23] a study was made of Couette flow stability. The solution
method, which compares with the method of solving the problem indicated in the
title of [24], differs from the Tollmien-Schlichting method, for the expansion of
the solutions with respect to powers of αRe used presupposes smallness of this value.
The study [25] contains a general statement of the problem of stability of inhomo-
geneous fluids. In the paper b· Di Prima and Dunn [26], the Galerkin method was
used to investigate the stab?'.ity of a boundary layer with respect to vortex dis-
turbances in the case of variable kinematic viscosity. Since the development of
this type of disturbance depends weakly on the form of the velocity profile in the
boundary layer, noticeable variation of the viscosity had an insignificant influence
on the critical Reynolds number. The same problem is the subject of reference [27].
In the published literature we were unable to find references to studies of the
stability of a laminar boundary layer in an incompressible fluid with variable
kinematic viscosity with respect to disturbances of the Tollmien-Schlichting type
with the exception of the mention of an unpublished paper by Macintosh, who dis-
covered significant dependence of the critical Reynolds number on the viscosity
gradient.

152

In this section a study is made of the influence of the variability of the kinematic viscosity on boundary layer stability with respect to Tollmien-Schlichting waves.

Two approaches to studying the development of disturbances in an inhomogeneous fluid are possible. On the one hand, it is possible to assume that the displacement of the fluid particles causes no change in the distribution $\rho(y), \nu$ (y), that is, the velocity pulsations are not accompanied by pulsations of ρ and ν. This will occur if a fluid particle characterized by values of ρ_1, ν_1 incident in the layer with defined values of ν_2, ρ_2 instantaneously changes its properties so that ν becomes equal to ν_2 and, respectively, ρ acquires a value of ρ_2.

On the other hand, it is possible to consider that a fluid particle moving from layer 1 to layer 2 completely retains the properties which it had in layer 1. Here the velocity pulsations essentially cause pulsations of the values of ν and ρ.

In reality, obviously the phenomenon develops by some intermediate scheme, for on displacement in an inhomogeneous fluid the particle changes its properties. The degree of approximation of the process to the first or second scheme depends on the rate of these variations.

Studies of disturbances in a fluid that is inhomogeneous with respect to kinematic viscosity, discussed below, have the first scheme as their basis.

Using (III.3), let us write the system of equations of disturbing motion of a fluid with constant density for the two-dimensional case, not considering the influence of mass forces,

$$\frac{\partial v_x}{\partial t} + u\frac{\partial v_x}{\partial x} + v_y\frac{\partial u}{\partial y} = -\frac{1}{\rho}\cdot\frac{\partial p^*}{\partial x} + \nu\Delta v_x + \frac{\partial \nu}{\partial y}\left(\frac{\partial v_x}{\partial y} + \frac{\partial v_y}{\partial x}\right);$$

$$\frac{\partial v_y}{\partial t} + u\frac{\partial v_y}{\partial x} = -\frac{1}{\rho}\cdot\frac{\partial p^*}{\partial y} + \nu\Delta v_y + 2\frac{\partial \nu}{\partial y}\cdot\frac{\partial v_y}{\partial y}.$$

Excluding pressure and introducing the disturbing motion current function, just as in § I.4, we arrive at the equation

$$(u - c)(\varphi'' - \alpha^2\varphi) - u''\varphi = -\frac{i}{\alpha Re}\left[\nu_*(\varphi^{IV} - 2\alpha^2\varphi'' + \alpha^4\varphi) + \right.$$

$$\left. + 2\frac{\partial \nu_*}{\partial y}(\varphi''' - \alpha^2\varphi') + \frac{\partial^2 \nu_*}{\partial y^2}(\varphi'' + \alpha^2\varphi)\right], \qquad (III.44)$$

where $\nu_* = \frac{\nu(y)}{\nu_0}$, $Re = \frac{U\cdot\delta}{\nu_0}$, ν_0 is the viscosity of the main flow. All the values entering into (III.44) are dimensionless.

Defining the solutions of equation (III.44) by the methods discussed in § I.6, as the first two solutions we take the corresponding solutions of the nonviscous equation (I.72) and (I.73). In order to find partial solutions of ϕ_3, ϕ_4, let us consider equation (III.44) in the vicinity of the critical point $y = y_k$.

Let us introduce a new independent variable

153

$$\eta = \frac{y - y_\kappa}{\varepsilon}$$

and, proceeding analogously to the method discussed in § I.6, let us expand all the coefficients of equation (III.44) which depend on y with respect to powers of $y - y_k = \eta\varepsilon$. For specific definition of the law of variation of the kinematic viscosity, we set

$$\nu_* = 1 + \frac{\nu_w - \nu_0}{\nu_0} e^{-By},$$

so that

$$\nu_* = 1 + \frac{\nu_w - \nu_0}{\nu_0} e^{-B(\nu_\kappa + \varepsilon\eta)} = 1 + \frac{\nu_w - \nu_0}{\nu_0} e^{-B\nu_\kappa}(1 - B\eta\varepsilon + \cdots).$$

The value of $B\eta\varepsilon$ is on the order of $(\alpha Re)^{-1/3}$, which follows from (I.85) under the assumption of $B \sim 0\ (1)$. Therefore hereafter we shall consider in the vicinity of the point $y = y_k$

$$\nu_* = 1 + \frac{\nu_w - \nu_0}{\nu_0} e^{-B\nu_\kappa}.$$

Discussion of the expressions for the coefficients of the second and third terms of the right-hand side of (III.44) does not appear expedient, for in the approximation in which the problem is solved, they are not considered, for they have a higher order of smallness.

As a result of the solution, ϕ_3, ϕ_4 will be determined on the basis of an equation analogous to (I.87)

$$\chi_0^{IV} - i \frac{u_\kappa'}{1 + \frac{\nu_w - \nu_0}{\nu_0} e^{-B\nu_\kappa}} \cdot \eta \cdot \ddot{\chi_0} = 0.$$

The form of these solutions corresponds to formulas (I.90) and (I.91) except the parameter β has a somewhat different value

$$\beta = \left(\frac{u_\kappa'}{1 + \frac{\nu_w - \nu_0}{\nu_0} e^{-B\nu_\kappa}} \right)^{\frac{1}{3}}.$$

The neutral stability and critical Reynolds number curves for a boundary layer with variable kinematic viscosity are calculated by the scheme indicated in § I.7 for a homogeneous fluid. The velocity profile is assumed to be given. For the value of α found, which lies on a neutral curve, instead of formula (I.112), the Reynolds number is determined from the expression

$$Re = \left(1 + \frac{\nu_w - \nu_0}{\nu_0} e^{-B\nu_\kappa} \right) \frac{1}{\alpha u_k} \left(\frac{w_1}{y_\kappa} \right)^3. \tag{III.45}$$

Studying the influence of the viscosity gradient in a boundary layer on the form of the velocity profile (Figure III.7–III.9) and considering formula (III.45), it is

possible to draw the conclusion of the presence of two aspects in the problem of how the variability of the kinematic viscosity near the wall influences the stability of the laminar form of flow.

For example, let us assume that $\nu_w < \nu_0$. Then with a decrease in ν_w the fullness of the velocity diagram in the boundary layer increases significantly, which leads to an increase in stability under other equal conditions. However, a decrease in ν_w, on the other hand, weakens the stabilizing effect of the viscosity on the velocity pulsations, which is obvious from formula (III.45), and the critical Reynolds number for given, reinforced velocity profile decreases by comparison with a uniform fluid having kinematic viscosity ν_0.

The corresponding calculations were made in order to discover the total influence of both factors.
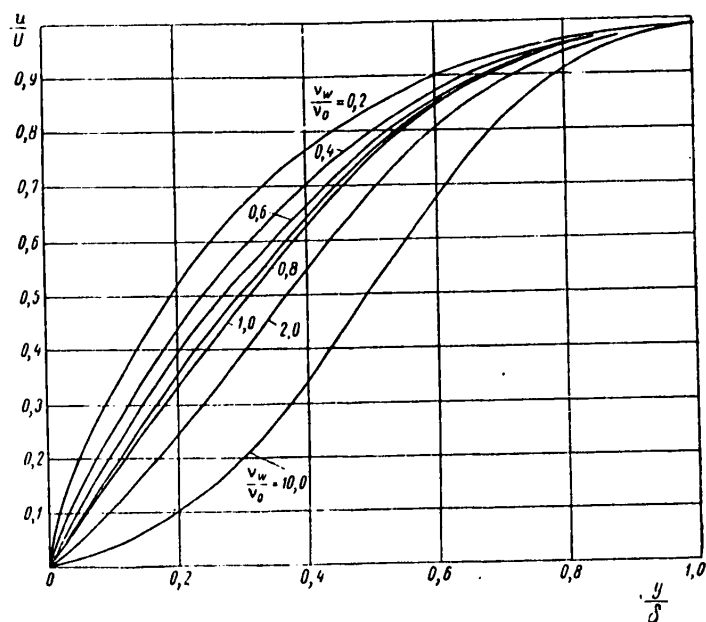
Figure III.7. The function $u/U = f_1(y/\delta, \nu_w/\nu_0)$.

Figure III.10 shows the neutral stability curves constructed on the basis of the profiles with characteristics presented in Figures III.7-III.9. These characteristics were obtained by the data in Table III.1 for $B_1 = 1$. The stability calculations were performed under the assumption that the fluid is homogeneous. The critical Reynolds numbers are shown in Figure III.11 and III.12 (curve 1) as a function of the parameter ν_w/ν_0. Then the stability was calculated by the scheme in this section for the same profiles using formula (III.45). The values of B_1 and B were compared using (III.23) and the graph in Figure III.2. The corresponding curves are also plotted in Figures III.11, III.12 (curve 2). In addition, Figure III.11

155

shows the calculated points obtained for velocity profiles calculated by the approximate method of § III.2. Investigation of the functions $Re^*_{cr} = Re^*_{cr}(\nu_w/\nu_0)$ permits the conclusion to be drawn that decreasing the kinematic viscosity of an incompressible fluid in the wall region by comparison with the kinematic viscosity of the main flow leads to a noticeable increase in fullness of the profile and growth of the critical Reynolds number. The destabilizing influence of decreasing the dispersion somewhat weakens the effect of increasing the stability.
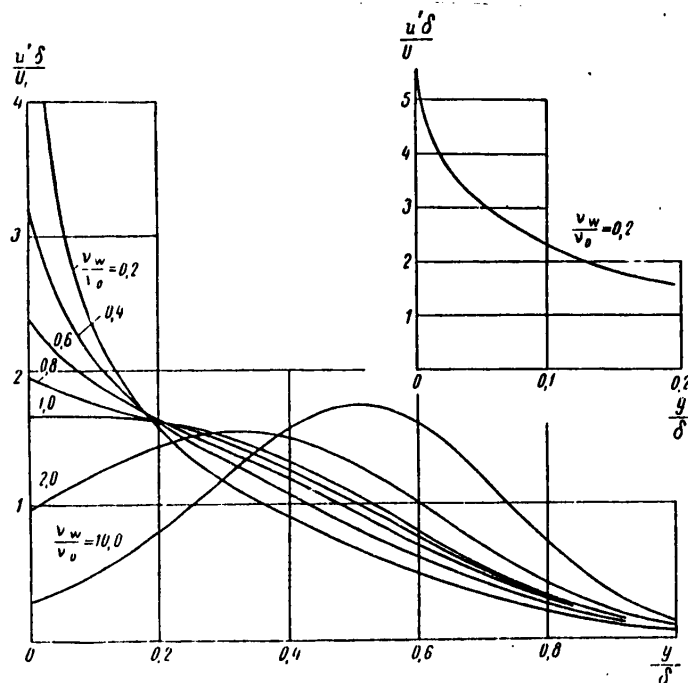
Figure III.8. The function $u'\delta/U = f_2\left(\frac{y}{\delta}, \frac{\nu_w}{\nu_0}\right)$.

It is possible to obtain an idea about the quantitative aspect of the problem by studying the graph in Figure III.11.

§ III.5. Stability of a Laminar Boundary Layer with Variable Density Across the Boundary Layer

References [28]-[36] investigated the stability of a laminar flow of an ideal fluid with variable density. Since the fluid viscosity was not considered, the mechanism of the occurrence of the instability differed significantly from that in a homogeneous viscous fluid, in particular, the transition to turbulent state in no way is related to the variation of the Reynolds number. For boundary layers where the viscosity has a significant influence on the flow formation, obviously this approach is inapplicable. Interesting arguments with respect to studying the behavior of oscillations in an inhomogeneous fluid appear in the monograph by Prandtl [37], but it was not possible to obtain quantitative determinations by this method.
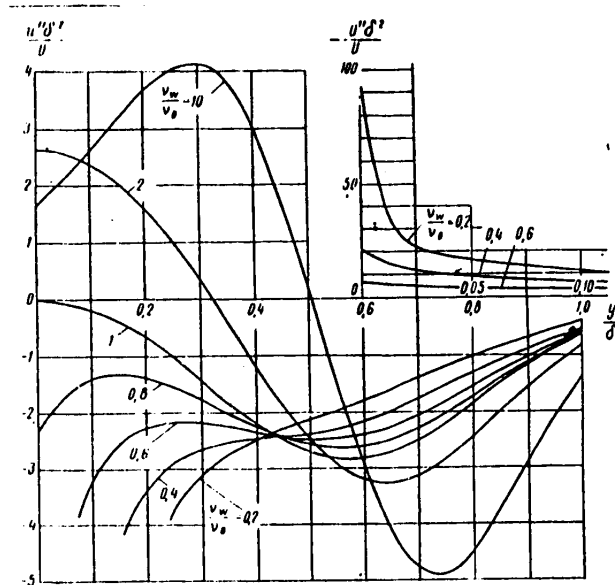
Figure III.9. The function $u''\delta^2/U = f_3\left(\dfrac{y}{\delta}, \dfrac{v_w}{v_0}\right)$.
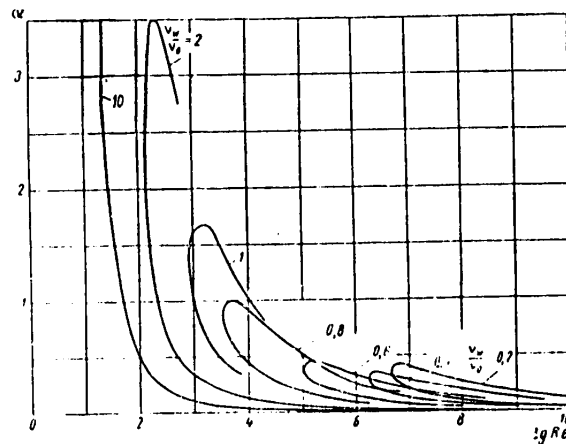
Figure II.10. Neutral stability curves of the boundary layer in a fluid with variable viscosity.

It is also necessary to mention the brief discussion of wave theory in a fluid that is inhomogeneous with respect to density contained in the book by Lamb [38].

The only study which takes up the problem of stability of a laminar boundary layer in an incompressible, viscous and inhomogeneous fluid with respect to density is the paper by Schlichting [39]. However, the method that he used can raise some objections [28], for in the process of deriving the basic equation with respect to

157
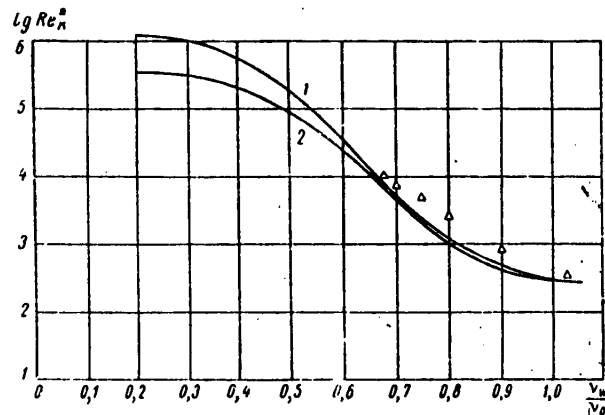
Figure III.11. Critical Reynolds number as a function of the parameter $v_w/v_0 \left(1 \geqslant \frac{v_w}{v_0} \geqslant 0\right)$.
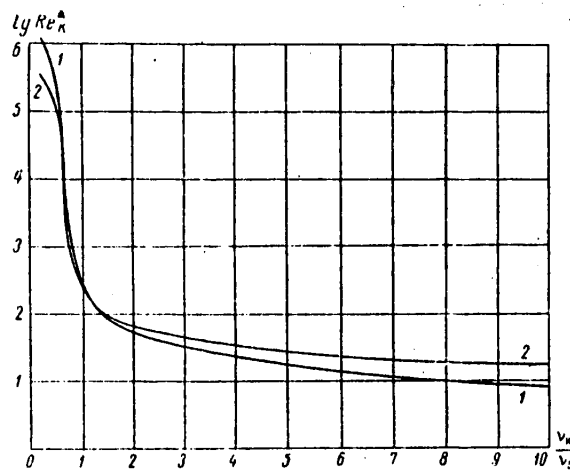
Figure III.12. Critical Reynolds number as a function of the parameter $v_w/v_0 \left(10 \geqslant \frac{v_w}{v_0} \geqslant 0\right)$.

the amplitude of the current function of the disturbing motion, Schlichting used the second scheme mentioned in § III.4 to determine the relation of the density pulsations to the velocity pulsations, which led to the appearance of a singularity in the total Orr-Sommerfeld equation.

Surveys of the principal papers on stability of fluid flows with variable density appear in the generalizing articles [40], [41]. A bibliography (primarily of English and American authors) on flow of inhomogeneous fluids can be found in the survey [42].

158

In the following study, the problem of the stability of a laminar boundary layer in a fluid with variable viscosity is solved under the assumption that the velocity pulsations do not cause density pulsations.

The system of equations of disturbing motion of an incompressible fluid that is inhomogeneous with respect to density based on relations (III.3) is written in the two-dimensional case as follows:

$$\rho \left(\frac{\partial v_x}{\partial t} + u \frac{\partial v_x}{\partial x} + v_y \frac{\partial u}{\partial y} \right) = - \frac{\partial p^*}{\partial x} + \mu \Delta v_x + $$
$$+ \frac{\partial \mu}{\partial y} \left(\frac{\partial v_x}{\partial y} + \frac{\partial v_y}{\partial x} \right);$$

$$\rho \left(\frac{\partial v_y}{\partial t} + u \frac{\partial v_y}{\partial x} \right) = - \frac{\partial p^*}{\partial y} + \mu \Delta v_y + 2 \frac{\partial \mu}{\partial y} \cdot \frac{\partial v_y}{\partial y};$$
$$\frac{\partial v_x}{\partial x} + \frac{\partial v_y}{\partial y} = 0.$$

(III.46)

In formulas (III.46) u(y) is the velocity distribution of the main flow; $\rho = \rho(y)$; $\mu = \mu(y)$, ν = const.

Substituting the following values in equations (II.46)

$$v_x = \bar{v}_x(y) e^{i(ax-bt)};$$
$$v_y = \bar{v}_y(y) e^{i(ax-bt)};$$
$$p^* = \bar{p}^*(y) e^{i(ax-bt)},$$

excluding the pressure and introducing the current function of the disturbing motion using the continuity equation, we arrive at the following differential expression:

$$\left(u - \frac{b}{a} \right) (\varphi'' - a^2 \varphi) - u'' \varphi + \frac{\rho'}{\rho} \left[\left(u - \frac{b}{a} \right) \varphi' - u' \varphi \right] =$$
$$= - \frac{\nu}{ia} \left\{ \varphi^{IV} - 2a^2 \varphi'' + a^4 \varphi + 2 \frac{\rho'}{\rho} (\varphi'' - a^2 \varphi') + \right.$$
$$\left. + \frac{\rho''}{\rho} (\varphi'' + a^2 \varphi) \right\}.$$

(III.47)

Let us reduce equation (III.47) to dimensionless form by the usual method (see § 14), continuing to use the previous notation for the dimensionless variables u, ϕ

$$(u - c)(\varphi'' - \alpha^2 \varphi) - u \varphi'' + \frac{\rho' \delta}{\rho} [(u - c) \varphi' - u' \varphi] =$$
$$= - \frac{1}{\alpha Re} \left[\varphi^{IV} - 2\alpha^2 \varphi'' + \alpha^4 \varphi + 2 \frac{\rho' \delta}{\rho} \times \right.$$
$$\left. \times (\varphi'' - \alpha^2 \varphi') + \frac{\delta^2 \rho''}{\rho} (\varphi'' + \alpha^2 \varphi) \right].$$

(II.48)

The solutions to equation (III.48) will be found by the method discussed in § I.6. Let us take the solutions of the equation

$$(u - c)(\varphi'' - \alpha^2\varphi) - u''\varphi + H\{(u - c)\varphi' - u'\varphi\} = 0,$$

(III.49)

as the first two solutions, where $H = \rho'\delta/\rho$ will be a constant if the density distribution is defined by formula (III.29) $H = -B$.

Expanding the solution of equation (III.49) in the form of a series

$$\varphi(y) = (u - c)\{g_0(y) + \alpha^2 g_1(y) + \cdots + \alpha^{2n}g_n(y) + \cdots\},$$

for the functions $g_i(y)$ (see § I.6) we obtain the following system:

$$g_0''(y) + \left(2\frac{u'}{u - c} + H\right)g_0'(y) = 0;$$

$$g_n''(y) + \left(2\frac{u'}{u - c} + H\right)g_n'(y) = g_{n-1}(y).$$

$$(n = 1, 2, \ldots)$$

Integrating the indicated equations successively, we find:

$$g_{0(1)}(y) = 1; \quad g_{0(2)}(y) = \int_0^y (u - c)^{-2}e^{-Hy}\,dy;$$

(III.50)

$$g_{n+1}(y) = \int_0^y (u - c)^{-2}e^{-Hy}\left[\int_0^y (u - c)^2 e^{Hy}g_n(y)\,dy\right]dy.$$

Thus,

$$\varphi_{(1)}(y) = (u - c)\sum_{n=0}^{\infty} g_n(y)\alpha^{2n}; \quad g_{01} = 1;$$

$$\varphi_{(2)}(y) = (u - c)\sum_{n=0}^{\infty} g_n(y)\alpha^{2n};$$

$$g_{02}(y) = \int_0^y (u - c)^{-2}e^{-Hy}\,dy,$$

the functions $g_n(y)$ are defined by relations (III.50).

For construction of the remaining two solutions of equation (III.48) let us use the expansions of these solutions in the vicinity of the point $y = y_k$, introducing the new variable (see § I.6)

$$\eta = \frac{y - y_\kappa}{\varepsilon},$$

where ε is a small parameter.

Denoting $\phi(y) = \chi(\eta)$, let us transform (III.48)

$$(u - c)(\chi'' - \alpha^2\varepsilon^2\chi) - \varepsilon^2 u''\chi + H\{(u - c)\varepsilon\chi' - u'\varepsilon^2\chi\} =$$

$$= -\frac{i}{\alpha R\varepsilon\varepsilon^2}\left[\chi^{IV} - 2\alpha^2\varepsilon^2\chi'' + \alpha^4\varepsilon^4\chi + \right.$$

$$\left. + 2H(\varepsilon\chi'' - \alpha^2\varepsilon^3\chi') + \frac{\delta^2\rho''}{\rho}(\varepsilon^2\chi + \alpha^2\varepsilon^4\chi)\right].$$

(III.51)

In equation (III.51)

$$u - c = u'_\kappa \varepsilon \eta + \frac{1}{2} u''_\kappa (\varepsilon \eta)^2 + \cdots,$$

$$u'' = u''_\kappa + u'''_\kappa \varepsilon \eta + \cdots,$$

$$u'' = u''_\kappa + u_\kappa^{IV} \varepsilon \eta + \cdots,$$

the values of $H = \delta\rho'/\rho$, $\delta^2\rho''/\rho$ for the selected law of density variation (III.29) are constant. The parameter ε is determined from the condition that the largest terms with respect to ε in the left and right-hand sides of equation (III.51) of the same order, that is, the forces of an inertial nature are commensurate with the forces of viscosity origin

$$u'_\kappa \varepsilon \eta \chi'' \approx \frac{1}{a\mathrm{Re}\varepsilon^2} \chi^{IV}.$$

Hence

$$\varepsilon = \frac{1}{(a\mathrm{Re})^{1/3}}.$$

By arguments analogous to the case of a homogeneous fluid, we arrive at the conclusion that the solutions $\phi_3(y)$, $\phi_4(y)$ are defined by formulas (I.90), (I.91). Thus, the density variability in the adopted statement of the problem and for an ordinary degree of approximation of the solution influences only the "inviscid part" of the general solution of equation (III.48). Using the generally accepted boundary conditions (see § I.5) and the approximate equality $c = u'_0 y_k$, we arrive at the characteristic equation

$$\delta(w) = 1 + z,$$ (III.52)

where

$$z = c u'_0 \left[\int_0^1 e^{Hy} (u - c)^{-2} dy + \frac{e^B}{a(1 - c)^2} \right].$$

The integral $J = \int_0^1 e^{Hy}(u - c)^{-2} dy$ will be calculated in the same approximation as in § I.7, considering the expansions

$$(u - c)^{-2} = \frac{1}{u_\kappa'^2 (y - y_\kappa)^2} - \frac{u''_\kappa}{u_\kappa'^3 (y - y_\kappa)} + O(1);$$

$$e^{Hy} = e^{Hy_\kappa} + B e^{Hy_\kappa} (y - y_\kappa) + \cdots;$$ (IIIL53)

$$J = -\frac{e^{Hy_\kappa}}{c u'_\kappa} + e^{Hy_\kappa} \left(\frac{u''_\kappa}{u_\kappa'^3} - \frac{B}{u_\kappa'^2} \right)(\ln c - \pi i).$$

The complex equation (III.52) is equivalent to two real equations which considering (III.53) are written as follows:

$$\delta_r(w) = 1 + \frac{u'_0}{u'_\kappa} e^{Hy_\kappa} + c u'_0 e^{Hy_\kappa} \left(\frac{u''_\kappa}{u_\kappa'^3} - \frac{B}{u_\kappa'^2} \right) \ln c + \frac{c u'_0 e^B}{a(1 - c)^2},$$ (III.54)

$$\tilde{\Re}_i(w) = -\pi c u_0' e^{By_\kappa}\left(\frac{u_\kappa''}{u_\kappa'^3} - \frac{B}{u_\kappa'^3}\right). \qquad\qquad \text{(III.55)}$$

On the basis of the system of equations (III.54), (III.55), it is possible to indicate the following scheme for calculating the neutral stability curve coinciding in its primary features with the calculation scheme for a homogeneous fluid (see § I.7). Being given a defined value of w_1, by the graphs of $\tilde{\Re}_r(w)$, $\tilde{\Re}_i(w)$ we determine $\tilde{\Re}_r(w_1)$, $\tilde{\Re}_i(w_1)$. Solving equation (III.55) graphically with known left-hand side $\tilde{\Re}_i(w_1)$. for the given velocity distribution and density distribution in the boundary layer we determine the value of the parameter c, which means the values of y_k, u_k' corresponding to it. Using (III.54), we find

$$\alpha = \frac{c u_0' e^B}{(1-c)^2}\left[\tilde{\Re}_r(w_1) - 1 + \frac{u_0'}{u_\kappa'}e^{By_\kappa} + \frac{\tilde{\Re}_i(w_1)}{\pi}\ln c\right]^{-1}. \qquad\qquad \text{(III.56)}$$

Then we calculate the neutral Reynolds number

$$\mathrm{Re} = \frac{1}{\alpha u_\kappa'}\left(\frac{w_1}{y_\lambda}\right)^3.$$

It is possible to obtain the critical Reynolds number if all the calculations are made for values of
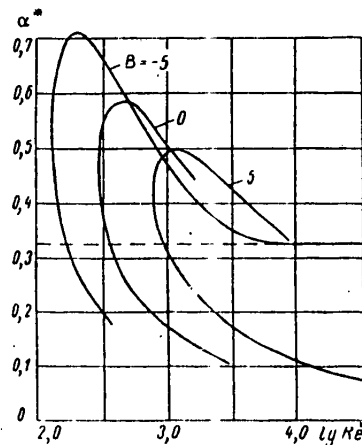
Figure III.13. Neutral stability curves of the boundary layer of a plate in a fluid with variable density.

In Figure III.13 we have the neutral stability curves for the Blasius profile for different values of the parameter B. Attention is drawn to the fact of an increase in the flow stability in the case of a negative density gradient (B > 0) in the wall region. Obviously this fact can be explained using the scheme for the occurrence of Reynolds stresses discussed in § I.3. With negative density gradient the magnitude of the Reynolds stresses will be less as a result of variability of ρ(y), and for a positive gradient (B < 0), larger by comparison with a homogeneous fluid. A

162

decrease in the value of the Reynolds stresses which transfer the energy of the main flow to the disturbances, naturally leads to an increase in the stability. In the case of an increase in density with respect to the y-coordinate, the form of the neutral curve resembles the corresponding curve for a velocity pro'ile with inflection point, that is, there is an "inviscid instability," and the region of instability does not disappear for $\nu \to 0$. For the upper branch of the neutral curve when $R \to \infty$, the parameter c is defined in this case by the condition $u_k'/u_k' - B = 0 (B < 0)$, and the value of the corresponding wave number α can be determined from (III.56) for $\tilde{r}_r = 1, \tilde{r}_i = 0$.

BIBLIOGRAPHY

1. S. M. Targ, OSNOVNYYE ZADACHI TEORII LAMINARNYKH TECHENIY (Basic Problems of Laminar Flow Theory), Moscow-Leningrad, GITTL, 1951.

2. I. I. Ibragimov, V. P. Kashkarov, "Laminar Boundary Layer of a Fluid with Variable Viscosity," TR. SEKTORA MATEM. I MEKHAN. AN KAZ. SSR (Works of the Mathematical and Mechanical Sector of the Kazakh SSR Academy of Sciences), Vol 2, 1963.

3. V. P. Kashkarov, A. T. Luk'yanov, "Calculation of Flow of a Drop Liquid with Variable Viscosity over a Plate," PMTF (Applied Mechanics and Technical Physics), No 5, 1964.

4. A. K. Pavlin, "A Case of Integration of the Equations of Motion of a Viscous Fluid with Variable Viscosity Factor," PMM (Applied Mathematics and Mechanics), Vol 19, No 5, 1955.

5. S. A. Regirer, "Some Thermohydrodynamic Problems of Steady State Uniform Flow of a Viscous Drop Liquid," PMM, Vol 21, No 3, 1957.

6. S. A. Regirer, "Thermal Effect on Viscous Drag in a Steady Uniform Flow of a Drop Liquid," PMM, Vol 22, No 3, 1958.

7. L. M. Simuni, "Numerical Solution of Some Problems of Motion of a Fluid with Variable Viscosity," TEPLO I MASSOPERENOS (Heat and Mass Transfer), Minsk, Belorussian SSR Academy of Sciences, Vol 5, 1963.

8. O. T. Hanna, I. E. Myers, "Laminar Boundary Layer Flow and Heat Transfer Past a Flat Plate for a Liquid of Variable Viscosity," AMER. I CH. E. JOURNAL, Vol 7, No 3, 1961.

9. I. E. Cross, C. F. Dewey, "Similar Solutions of the Laminar Boundary Layer Equations with Variable Fluid Properties," ARCHIWUM MECHANIKE STOSOWANEJ, Vol 16, No 3, 1964.

10. H. Schuh, "Über die Lösung der laminaren Grenzschichlgleichung an der ebenen Platte für Geschwindigkeite und Temperaturfeld bei veränderlichen Stoffwerten und für das Diffusions feld bei höheren Konzentrationen," ZAMM, Vol 25/27, No 2, 1947.

11. H. Hausenblas, "Die nichtisotherme laminare Strömung einer zähen Flüssigkeit durch enge Spalte und Kapillarröhren," ING.-ARCHIV., Vol 18, No 3, 1950.

12. E. W. Adams, "A Class of Similar Solutions for the Velocity and the Temperature Boundary Layer in Planar or Axially Symmetric Channel Flow," Z. F. FLUGWISS, No 3, 1963.

13. D. D. Joseph, "Variable Viscosity Effects on the Flow and Stability of Flow in Channels and Pipes," THE PHYSICS OF FLUIDS, Vol 7, No 11, 1964.

14. D. Daniel, "Variable Viscosity Effects on the Flow and Stability of Flow in Fluids," THE PHYSICS OF FLUIDS, Vol 7, No 11, 1964.

15. B. C. Sadiadis, "Boundary Layer Behavior on Continuous Solid Surfaces," I. AMER. I CH. E. JOURNAL, Vol 7, No 1, 1961.

16. B. C. Sadiadis, "Boundary Layer Behavior on Continuous Solid Surfaces," II. AMER. I. CH. E. JOURNAL, Vol 7, No 1, 1961.

17. K. Pohlhausen, "Zur näherungsweisen Integration der Differential gleichung der laminaren Grezschicht, ZAMM, Vol 1, No 4, 1921.

18. H. Schlichting, TEORIYA POGRANICHNOGO SLOYA (Boundary Layer Theory), Moscow, IL, 1956.

19. K. K. Fedyayevskiy, "Frictional Drag of Wings for Various Origins of the Point of Transition of a Laminar Boundary Layer to Turbulent," TEKHNIKA VOZDUSHNOGO FLOTA (Air Fleet Engineering), No 7-8, 1939.

20. N. M. Matveyev, METODY INTEGRIROVANIYA OBYKNOVENNYKH DIFFERENTIAL'NYKH URAVIYENIY (Methods of Integrating Ordinary Differential Equations), Izd., LGU, 1955.

21. L. G. Loytsyanskiy, MEKHANIKA ZHIDKOSTI I GAZA (Fluid and Gas Mechanics), Moscow, GIFML, 1959.

22. H. W. Emmons, D. C. Leigh, "Tabulation of Blasius Function with Blowing and Suction," AERONAUTIC. RES. COUN. CURRENT PAPER, No 157, 1954.

23. Ye. V. Semenov, "A Problem of Hydrodynamic Theory of Stability in the Case of Variable Viscosity," IZV. AN SSSR, MEKH. I MASH. (News of the USSR Academy of Sciences. Mechanics and Machinery), No 4, 1964.

24. Ye. V. Semenov, "Development of Waves on the Surface of Films with Variable Viscosity with Gas Flow over Them," IZV. AN SSSR, MEKH. I MASH., No 5, 1964.

25. P. C. Drazin, "On Stability of Parallel Flow of an Incompressible Fluid of Variable Density and Viscosity," PROCEEDINGS OF THE CAMBRIDGE PHILOSOPHICAL SOCIETY (MATH. AND PHYS. SC), Vol 58, No 4, 1962.

26. R. C. Di Prima, D. W. Dunn, "The Effect of Heating and Cooling on the Stability of the Boundary Layer Flow of a Liquid Over a Curved Surface," JOURNAL OF THE AERONAUTICAL SCIENCES, Vol 23, No 10, 1956, (Russian translation MEKHANIKA (Mechanics), collection of translations and surveys, No 4, 1956.

27. M. Morduchov, "Stability of Laminar Boundary Layer near a Stagnation Point over an Impermeable Wall and a Wall Cooled by Normal Fluid Injection," ADVIS. COMM. AERONAUT. TECH. NOTES, No 4037, 1957 (RZH MEKHANIKA (Mechanics Reference Journal) No 1543, 1959.

28. L. A. Dikiy, "Stability of Plane-Parallel Flows of a Inhomogeneous Fluid," PMM, Vol 24, No 2, 1960.

29. G. I. Taylor, "Effect of Variation in Density on the Stability of Superposed Streams of Fluid," PROC. ROY. SOC. LONDON, SER. A, Vol 132, 1931, p 499.

30. S. Goldstein, "On the Stability of Superposed Streams of Fluids of Different Densities," PROC. ROY. SOC. LONDON. SER. A., Vol 132, 1931, p 524.

31. P. G. Drazin, "The Stability of a Shear Layer in an Unbounded Heterogeneous Inviscid Fluid," JOURNAL OF FLUID MECHANICS, Vol 4, No 2, 1958.

32. J. W. Miles, "On the Stability of Heterogeneous Shear Flows," J. FLUID MECH., Vol 10, No 4, 1961.

33. L. N. Howard, "Note on a Paper of J. W. Miles," J. FLUID MECH., Vol 10, No 4, 1961.

34. J. W. Miles, "On the Stability of Heterogeneous Shear Flows, Part 2," J. FLUID MECH., Vol 16, No 2, 1963.

35. L. N. Howard, "Neutral Curves and Stability Boundaries in Stratified Flow," J. FLUID MECH., Vol 16, No 3, 1963.

36. J. W. Miles, L. N. Howard, "Note on a Heterogeneous Shear Flow," J. FLUID MECH., Vol 20, No 2, 1964.

37. L. Prandtl, GIDROAEROMEKHANIKA (Hydroaeromechanics), Moscow, IL, 1949.

38. G. Lamb, GIDRODINAMIKA (Hydrodynamics), Moscow-Leningrad, GITTL, 1947.

39. H. Schlichting, "Turbulenz bei Wärmeschichtung," ZAMM, Vol 15, No 6, 1935.

40. H. Schlichting, VOZNIKNOVENIYE TURBULENTNOSTI (Occurrence of Turbulence), Moscow, IL, 1962.

41. I. T. Stuart, "Hydrodynamic Stability," LAMINAR BOUNDARY LAYERS, edited by L. Rosenhead, Oxford, 1963.

42. D. R. F. Harleman, "Stratified Flow," HANDBOOK OF FLUID DYNAMICS," edited by V. L. Streeter, New York-London, 1961.

CHAPTER IV. EFFECT OF SUCTION OF A FLUID THROUGH A PERMEABLE SURFACE OF A BODY ON THE LAMINAR BOUNDARY LAYER CHARACTERISTICS

§IV.1. Similar Solutions of the Laminar Boundary Layer Equations in the Presence of Suction

Solutions of the laminar boundary layer equations which define the longitudinal velocity component profiles having similarity properties, that is, for each cross section of the boundary layer there is a characteristic linear dimension and characteristic velocity such that the dimensionless profile obtained with their help is identical for all cross sections of the layer, are called similar.

The system of equations of a two-dimensional steady-state boundary layer in dimensional form is described on the basis of (I.18) as follows:

$$u \frac{\partial u}{\partial x} + v \frac{\partial u}{\partial y} = - \frac{\partial p}{\rho \partial x} + v \frac{\partial^2 u}{\partial y^2};$$

$$\frac{\partial u}{\partial x} + \frac{\partial v}{\partial y} = 0; \frac{\partial p}{\partial y} = 0.$$

(IV.1)

It is possible to find the longitudinal pressure gradient by using the first equation of system (IV.1), considering the identity $\partial p/\partial y \equiv 0$. After defining the boundary of the boundary layer $y=\delta$ from the conditions $\frac{\partial u}{\partial y}\Big|_{y=\delta} = \varepsilon_1, \frac{\partial^2 u}{\partial y^2}\Big|_{y=\delta} = \varepsilon_2,$

where ε_1, ε_2 are negligibly small, we find

$$\frac{1}{\rho} \cdot \frac{\partial p}{\partial x}\Big|_{y=\delta} = \frac{1}{\rho} \frac{\partial p}{\partial x} = -U \frac{\partial U}{\partial x} = -UU'.$$

(IV.2)

The function $U=U(x)$ in the equality (IV.2) is the velocity distribution on the outer boundary of the boundary layer.

If we introduce the current function $\psi(x, y)$ on the basis of the continuity equation, the first equation of system (IV.1) is written as follows:

$$\frac{\partial \psi}{\partial y} \cdot \frac{\partial^2 \psi}{\partial x \partial y} - \frac{\partial \psi}{\partial x} \cdot \frac{\partial^2 \psi}{\partial y^2} = UU' + v \frac{\partial^3 \psi}{\partial y^3}.$$

(IV.3)

166

It is necessary to integrate equation (IV.3) in the case of a permeable surface under the following boundary conditions (see §I.2):

$$u(x, 0) = \frac{\partial \psi}{\partial y}\bigg|_{y=0} = f_1(x);$$
$$v(x, 0) = -\frac{\partial \psi}{\partial x}\bigg|_{y=0} = f_2(x); \qquad \text{(IV.4)}$$
$$u(x, y)_{y \to \infty} = \frac{\partial \psi}{\partial y}\bigg|_{y \to \infty} \to U(x).$$

The procedure for describing the last of the boundary conditions (IV.4) is of a somewhat formal nature, for equation (IV.3) itself correctly reflects the motion of the fluid only in the wall region and, generally speaking, it is impossible to consider its solution for y→∞. However, the calculations for the special cases of flow with boundary conditions (IV.4) give satisfactory correspondence to the experimental results, which is the basis for the application of the methods of an asymptotic boundary layer in practical applications of the methods in which the condition for y→∞ is used.

Finding similar solutions, according to the definition let us introduce [1] functions $\phi(x)$ and $\Phi(\eta)$ such that

$$y = \frac{\eta}{\phi(x)},$$
$$\psi = U(x)\frac{\Phi(\eta)}{\phi(x)},$$

as a result we obtain u/U(x)=Φ'(η), that is, the dimensionless velocity profile in the boundary layer does not depend on the longitudinal coordinate. In the new variables equation (IV.3) assumes the form

$$\frac{U'}{v\phi^2}\Phi'^2 - \frac{1}{v}\left(\frac{U'}{\phi^2} - \frac{U\phi'}{\phi^3}\right)\Phi\Phi'' = -\frac{U'}{v\phi^2} + \Phi''' . \qquad \text{(IV.5)}$$

$$U' = \frac{dU}{dx}; \quad \Phi^{(n)} = \frac{d^n\Phi}{d\eta^n}; \quad \phi' = \frac{d\phi}{dx}.$$

In order for the function Φ to depend only on the variable η, the following two conditions must be observed:

$$\frac{U'}{v\phi^2} = a = \text{const}, \qquad \text{(IV.6)}$$

$$\frac{1}{v}\left(\frac{U'}{\phi^2} - \frac{U\phi'}{\phi^3}\right) = b = \text{const}, \qquad \text{(IV.7)}$$

which are the equations for determining the functions U(x), $\phi(x)$. On satisfaction of the conditions (IV.6), (IV.7), equation (IV.5) is converted to the following form

$$a\Phi'^2 - b\Phi\Phi'' = a + \Phi'''. \qquad \text{(IV.8)}$$

167

We obtain the boundary conditions for the function $\Phi(\eta)$ based on the relations of (IV.4)

$$u(x,\,0) = \frac{\partial\psi}{\partial y}\Big|_{y=0} = \frac{\partial\psi}{\partial\eta}\,\varphi\Big|_{\eta=0} = U(x)\,\Phi'\Big|_{\eta=0} = f_1(x); \tag{IV.9}$$

$$v(x,\,0) = -\frac{\partial\psi}{\partial x}\Big|_{y=0} = -\left[\left(\frac{U'}{\varphi} - U\frac{\varphi'}{\varphi^2}\right)\Phi + U\frac{\Phi'\varphi'}{\varphi^2}\,\eta\right]_{\eta=0} =$$

$$= \left(U\frac{\varphi'}{\varphi^2} - \frac{U'}{\varphi}\right)\Phi\big|_{\eta=0} = f_2(x). \tag{IV.10}$$

$$\Phi'(\eta)\big|_{\eta\to\infty} \to 1.$$

Relations (IV.9), (IV.10) show that for existence of similar solutions the longitudinal and transverse velocity components on the wall in the boundary layer must vary by the laws

$$u(x,\,0) = f_1(x) = A \cdot U(x);$$
$$v(x,\,0) = f_2(x) = B\left(\frac{U\varphi'}{\varphi^2} - \frac{U'}{\varphi}\right) = Bbv\varphi(x). \tag{IV.11}$$

Here equation (IV.8) must be integrated under the boundary conditions:

$$\Phi(0) = B; \quad \Phi'(0) = A; \quad \Phi'(\eta)\big|_{\eta\to\infty} \to 1. \tag{IV.12}$$

Let us consider some special cases.

a) $U'=0$. The boundary layer on a plate. Parameter $a=0$. Let us find the function $\varphi(x)$, integrating equation (IV.7),

$$-\frac{\varphi'}{\varphi^3} = \frac{bv}{U}; \quad \varphi = \sqrt{\frac{1}{2}\cdot\frac{U}{bv(x+c_1)}},$$

where the integration constant c_1 is defined if the value of $\varphi(x)$ is known at any point x_1. Equation (IV.8) is converted to the form $\Phi''' + b\Phi\Phi''=0$. Making the substitution $\Phi=(1/b)\Phi_1$, $U=bU_1$, let us reduce the problem to integration of the equation

$$\Phi'' + \Phi\Phi'' = 0 \tag{IV.13}$$

under the boundary conditions

$$\Phi(0) = B_1 = Bb; \quad \Phi'(0) = A_1 = Ab; \quad \Phi'(\eta)\big|_{\eta\to\infty} \to 1.$$

Here the tangent and normal velocity components on the wall must vary by the laws

$$u(x,\,0) = A_1 U_1; \quad v(x,\,0) = B_1 v \sqrt{\frac{U_1}{v(x+c_1)}}.$$

The results of the numerical integration of equation (IV.13) for suction and blowing are contained in reference [2];

168

b) $U = A_2(x+B_2)$. In this case, from (IV.6) we have $\phi = (A_2/\nu a)^{1/2} = const$, which considering (IV.7) leads to the equality $a=b$. Thus, the problem reduces to integration of the equation

$$\Phi'' + b\left(1 + \Phi\Phi'' - \Phi'^2\right) = 0$$

under the boundary conditions (IV.12). If the fluid velocity components on the wall are nonzero, they must vary in accordance with (IV.11), where the normal velocity component must be constant;

c) It is possible to integrate the system of equations (IV.6) and (IV.7) in general form. For this purpose let us subtract expression (IV.7) from (IV.6)

$$\frac{U\psi'}{\phi^3} = \nu(a - b). \qquad (IV.14)$$

Writing (IV.7) in the form $(U/\phi)' = b\nu\phi$ and excluding U with the help of (IV.14), we arrive at the equation

$$(2a - 3b)\frac{\phi'}{\phi} = (a - b)\frac{\phi''}{\phi'}. \qquad (IV.15)$$

If $a=2b$, then (IV.15) has the solution $\phi(x) = c_2 e^{c_1 x}$ which corresponds to

$$U(x) = \nu b\frac{c_2^2}{c_1}e^{2c_1 x}; \quad \Phi'' + b\left(2 + \Phi\Phi'' - 2\Phi'^2\right) = 0.$$

The velocity distribution on the wall and the boundary conditions for the function $\Phi(\eta)$ are defined by the expressions (IV.11), (IV.12).

If $a \neq 2b$, then the solution of (IV.15) will be $\phi(x) = (c_3 x + c_4)^n$, where $n = (a-b)/(2b-a)$. The velocity at the outer boundary of the boundary layer can be found using (IV.14)

$$U(x) = \frac{\nu(a - b)}{c_3 n}(c_3 x + c_4)^{2n+1}.$$

Under the condition $U(0)=0$, the constant $c_4=0$, and the preceding expression gives

$$U(x) = \frac{\nu(a - b)}{n}c_3^{2n}x^{2n+1}. \qquad (IV.16)$$

In formula (IV.16) out of the three constant parameters a, b, c_3 one obviously can be selected arbitrarily. For example, let us set $b=1$. Let us introduce the following notation:

$$2n + 1 = \frac{a}{2b - a} = \frac{a}{2 - a} = m; \quad \frac{\nu(a - b)}{n}c_3^{2n} = c,$$

which makes it possible to write:

$$U(x) = cx^m;$$

$$\phi(x) = \left[\frac{c(m + 1)}{2\nu}\right]^{1/2}x^{\frac{m-1}{2}};$$

$$\Phi'' + \Phi\Phi'' = a\left(\Phi'^2 - 1\right),$$

where

$$a = \frac{2m}{m + 1}.$$

169

The boundary conditions and velocities on the wall are determined as before by (IV.11), (IV.12);

d) Let us consider the case b=0, a≠0. If a=b=0, equation (IV.8) has a solution in the form of a quadratic parabola, and the last of the conditions (IV.12) cannot be satisfied.

If b=0, equations (IV.6), (IV.7) give the following system for defining the functions U(x), ϕ(x):

$$\frac{U'}{\varphi^2} = av; \quad \frac{U'}{U} = \frac{\varphi'}{\varphi};$$

where it is proposed that ϕ(x)≠0. From the second equation we obtain U(x)=$c_5\phi$(x), which makes it possible to find the function ϕ(x) with the help of the first equation

$$\frac{\varphi'}{\varphi^2} = \frac{av}{c_5}; \quad \varphi(x) = \frac{1}{c_6 - \frac{av}{c_5}x},$$

and, consequently, the velocity distribution

$$U(x) = \frac{c_5}{c_6 - \frac{av}{c_5}x}.$$
(IV.17)

Analogously to the above-investigated case, one of the three constants in (IV.17) can be selected arbitrarily. For example, let us set c_5=a; then

$$U(x) = \frac{a}{c_6 - vx}.$$
(IV.18)

The velocity field on the outer boundary of the layer corresponding to (IV.18) can be characterized as the velocity field from the source (a>0) with its center at the point $x_0 = c_6/v$ or the source (a<0). Let us write the corresponding equation for the function Φ(n)

$$\Phi'' = a(\Phi'^2 - 1).$$
(IV.19)

Equation (IV.19) can be integrated in closed form [3].

The basic equation for the remaining enumerated cases usually is integrated by numerical methods to determine Φ(n). The solutions for U=const and U=cx^m for an impermeable surface are widely known and are put in the majority of monographs on boundary layers [3], [4], [5]. Integration of the boundary layer equations for a porous surface in the case of U=cx^m is presented in references [13], [52]. The problems of studying similar solutions of the boundary layer equations are investigated in the studies [6]-[8], [58]. A broad bibliography of papers on similar solutions of a laminar boundary layer with suction appears in the monograph [3]. N. I. Pol'skiy [53] studied similar solutions of boundary layer equations written in Mises form, and he detected that classes of similar solutions of Prandtl equations and the Mises equation coincide, that is, similar solutions of

the Mises equation exist only for the velocity distributions of the external flow for which similar solutions of Prandtl equations occur.

§IV.2. Use of Pulse and Energy Equations for Approximate Calculation of a Boundary Layer with Suction or Blowing.

In practical calculations of the boundary layer characteristics it is usually necessary to deal with highly varied velocity distribution laws at their outer boundary. The developed calculation schemes can be divided into three groups. The first group includes methods of numerical integration of the Prandtl control system. The application of numerical integration to the problems of boundary layer control using suction is discussed in §IV.9. The second group encompasses the methods connected with expansion of the velocity at the outer boundary of the layer in a series with respect to the variable which depends on the longitudinal coordinate [9], [10]. The desired function at which usually the current function is taken is also expanded in an analogous series, but with coefficients that depend on the transverse coordinate in the boundary layer. Using the system of equations (IV.1), the set of differential relations is obtained from which variable coefficients in a series which represents the desired solution are determined considering the boundary conditions. The complexity of the method consists in weak convergence of the series and the necessity of tabulating a large number of auxiliary functions. Recently, Goertler [11], [12] proposed modified series for solution of the problem which have better convergence, but, as before, require calculation of a significant number of auxiliary functions.

It is possible to consider approximate methods based on the application of integral relations of the boundary layer in the third group. Beginning with the known Karman-Pohlhausen method, the integral relations found broad application in practical calculations of the boundary layer, and they are used up to the present time.

Let us consider the case of axisymmetric flow over a body of rotation, the radius of which r_0 is appreciably larger than the thickness of the boundary layer. Using the ordinary assumptions adopted in boundary layer theory, the equations for an axisymmetric flow can be written in the following form [5]:

$$\rho \left(u \frac{\partial u}{\partial x} + v \frac{\partial u}{\partial y} \right) = - \frac{\partial p}{\partial x} + \frac{\partial \tau}{\partial y}; \tag{IV.20}$$

$$\frac{\partial (\rho u r_0)}{\partial x} + \frac{\partial (\rho v r_0)}{\partial y} = 0. \tag{IV.21}$$

On the upper boundary of the boundary layer we have

$$\frac{\partial p}{\partial x} = - \rho_1 U \frac{\partial U}{\partial x}.$$

The boundary conditions are assumed in the form

$$\left. \begin{array}{l} \text{for } y = 0 : u = u_0(x); \quad v = v_0(x); \quad \rho = \rho_0; \\ \text{for } y = \delta : u = U(x); \quad\quad\quad\quad \rho = \rho_1. \end{array} \right\} \tag{IV.22}$$

171

Here, u and v denote the average velocity components in the boundary layer ($0<y<\delta$) in the x and y direction, and U is the velocity at the boundary of the boundary layer. Here p is the pressure at the boundary of the boundary layer; τ is the tangential stress, ρ, ρ_0, ρ_1 are the density of the liquid at the boundary layer, at the surface of the body and at the boundary of the boundary layer, respectively.

For a planar flow, in equations (IV.20), (IV.21), just as in all subsequent formulas, it is necessary to set $r_0 \equiv 1$.

When $v_0 < 0$ we have the suction case, and when $v_0 > 0$, feeding a fluid to the boundary layer.

In order to obtain the generalized integral relation, let us perform the following transformations [14]. Let us multiply equation (IV.20) by u^k (k=0, 1, 2, ...), and (IV.21) by u^{k+1}/r_0(k+1) and let us add them. As a result, we obtain

$$-\frac{1}{r_0}\frac{\partial}{\partial x}\left(\rho u^{\kappa+2}r_0\right) + \frac{\partial}{\partial y}\left(\rho u^{\kappa+1}v\right) = (k+1)\,u^\kappa \times$$

$$\times \left(\rho_1 \frac{UdU}{dx} + \frac{\partial \tau}{\partial y}\right). \tag{IV.23}$$

The continuity equation (IV.21) is integrated from 0 to y, and under the adopted boundary conditions we obtain

$$\rho v = -\frac{1}{r_0}\cdot\frac{\partial}{\partial x}\int_0^y \rho u r_0\,dy + \rho_0 v_0. \tag{IV.24}$$

Substituting (IV.24) in (IV.23) and integrating the terms of the obtained equation from y=0 to y=δ, it is possible to obtain the generalized integral relation of a controlled boundary layer corresponding to the boundary conditions (IV.22)

$$\frac{1}{\rho_1 U^{\kappa+2}r_0}\cdot\frac{d}{dx}\left(\rho_1 U^{\kappa+2}\cdot r_0 f_1\right) + \frac{f_2}{U}\frac{dU}{dx} -$$

$$-\frac{\rho_0}{\rho_1}\frac{v_0}{U}\left[1 - \left(\frac{u_0}{U}\right)^{\kappa+1}\right] = f_3. \tag{IV.25}$$

where f_1, f_2, f_3 are the integral thicknesses of the boundary layer:

$$f_1 = \int_0^\delta \frac{\rho}{\rho_1}\frac{u}{U}\left[1 - \left(\frac{u}{U}\right)^{\kappa+1}\right]dy;$$

$$f_2 = -(k+1)\int_0^\delta \frac{u}{U}\left[\frac{\rho}{\rho_1} - \left(\frac{u}{U}\right)^{k-1}\right]dy;$$

$$f_3 = -(k+1)\int_0^\delta \left(\frac{u}{U}\right)^\kappa \frac{\partial}{\partial y}\left(\frac{\tau}{\rho_1 U^2}\right)dy.$$

172

Setting k=0, 1, 2, ..., it is possible to obtain a series of integral relations. For k=0 and k=1, from (IV.25) we have the pulse and energy equations of an axisymmetric controlled boundary layer, respectively.

The pulse equation (k=0)

$$\frac{1}{\rho_1 U^2 r_0} \cdot \frac{d}{dx}(\rho_1 U^2 r_0 \delta^{**}) + \frac{\delta^*}{U} \cdot \frac{dU}{dx} -$$

$$- \frac{\rho_0}{\rho_1} \frac{v_0}{U}\left(1 - \frac{u_0}{U}\right) = \frac{\tau_0}{\rho_1 U^2} \cdot \qquad\qquad (IV.26)$$

The energy equation (k=1)

$$\frac{1}{\rho_1 U^3 r_0} \cdot \frac{d}{dx}(\rho_1 U^3 r_0 \delta_3) + \frac{\delta_3^*}{U}\frac{dU}{dx} - \frac{\rho_0}{\rho_1}\frac{v_0}{U}\left(1 - \frac{u_0^2}{U^2}\right) =$$

$$= 2\int_0^\delta \frac{\partial}{\partial y}\left(\frac{u}{U}\right) \cdot \frac{\tau}{\rho U^2}\, dy + 2\frac{u_0}{U}\frac{\tau_0}{\rho_1 U^2} \cdot \qquad\qquad (IV.27)$$

Here

$$\delta^{**} = (f_1)_{k=0} = \int_0^\delta \frac{\rho}{\rho_1}\frac{u}{U}\left(1 - \frac{u}{U}\right) dy;$$

$$\delta^* = (f_2)_{k=0} = \int_0^\delta \frac{u}{U}\left[-\frac{\rho}{\rho_1} + \left(\frac{u}{U}\right)^{-1}\right] dy; \qquad\qquad (IV.28)$$

$$\delta_3 = (f_1)_{k=1} = \int_0^\delta \frac{\rho}{\rho_1}\frac{u}{U}\left[1 - \left(\frac{u}{U}\right)^2\right] dy.$$

$$\delta_3^* = (f_2)_{k=1} = -2\int_0^\delta \frac{u}{U}\left(\frac{\rho}{\rho_1} - 1\right) dy.$$

Equations (IV.25), (IV.26) and (IV.27) are valid for laminar and turbulent, incompressible and compressible, planar and axisymmetric flows, uncontrolled and controlled steady boundary layer.

Now let us propose that the fluid is incompressible ρ=const; in addition, let us assume that $\rho_1 = \rho_0 = \rho$, that is, the boundary layer is controlled by injecting or sucking fluid having the same density as the fluid at the external flow. In this case the pulse and energy equations (IV.26) and (IV.27) assume the following form:

$$\frac{1}{U^2 r_0} \cdot \frac{d}{dx}(U^2 r_0 \delta^{**}) + \frac{\delta^*}{U}\frac{dU}{dx} - \frac{v_0}{U}\left(1 - \frac{u_0}{U}\right) = \frac{\tau_0}{\rho U^2} \qquad\qquad (IV.29)$$

$$\frac{1}{U^3 r_0} \cdot \frac{d}{dx}(U^3 r_0 \delta_3) - \frac{v_0}{U}\left[1 - \left(\frac{u_0}{U}\right)^2\right] =$$

$$= 2\frac{u_0}{U} \cdot \frac{\tau_0}{\rho U^2} + 2\int_0^\delta \frac{\partial}{\partial y}\left(\frac{u}{U}\right) \cdot \frac{\tau}{\rho U^2}\, dy. \qquad\qquad (IV.30)$$

For the two-dimensional case the pulse equation (setting $r_0 = 1$) can be rewritten in the form

$$-\frac{1}{U^2} \cdot \frac{d}{dx}(U^2 \delta^{**}) + \frac{\delta^*}{U} \cdot \frac{dU}{dx} - \frac{v_0}{U}\left(1 - \frac{u_0}{U}\right) = \frac{\tau_0}{\rho U^2}$$ (IV.31)

or

$$-\frac{d\delta^{**}}{dx} + (2\delta^{**} + \delta^*)\frac{1}{U} \cdot \frac{dU}{dx} - \frac{\tau_0}{\rho U^2} + \frac{v_0}{U}\left(1 - \frac{u_0}{U}\right).$$ (IV.32)

The energy equation assumes the form

$$\frac{1}{U^3} \cdot \frac{d}{dx}(U^3 \delta_{,}) - \frac{v_0}{U}\left[1 - \left(\frac{u_0}{U}\right)^2\right] +$$

$$+ \frac{2u_0}{U} \cdot \frac{\tau_0}{\rho U^2} + 2\int_0^\delta \frac{\partial}{\partial y}\left(\frac{u}{U}\right)\frac{\tau}{\rho U^2} dy.$$ (IV.33)

Here δ^*, δ^{**}, δ_e are the provisional boundary layer thicknesses. The displacement flow thickness

$$\delta^* = \int_0^\delta \left(1 - \frac{u}{U}\right) dy.$$

The pulse loss thickness

$$\delta^{**} = \int_0^\delta \frac{u}{U}\left(1 - \frac{u}{U}\right) dy.$$

Energy loss thickness

$$\delta_{,} = \int_0^\delta \frac{u}{U}\left[1 - \left(\frac{u}{U}\right)^2\right] dy.$$ (IV.34)

Let us introduce the relations

$$H = \frac{\delta^*}{\delta^{**}},$$ (IV.35)

$$\overline{H} = \frac{\delta_{,}}{\delta^{**}}.$$ (IV.36)

into (IV.29) and (IV.30). Then we obtain the pulse and energy equations in the following form

$$\frac{1}{U^2 r_0} \cdot \frac{d}{dx}(U^2 r_0 \delta^{**}) + \frac{H\delta^{**}}{U} \cdot \frac{dU}{dx} = \frac{v_0}{U}\left(1 - \frac{u_0}{U}\right) + \frac{\tau_0}{\rho U^2};$$ (IV.37)

$$\frac{1}{U^3 r_0} \cdot \frac{d}{dx}(U^3 r_0 \overline{H} \delta^{**}) = \frac{v_0}{U}\left[1 - \left(\frac{u_0}{U}\right)^2\right] +$$

$$+ \frac{2u_0}{U} \cdot \frac{\tau_0}{\rho U^2} + 2\int_0^\delta \frac{\partial}{\partial y}\left(\frac{u}{U}\right)\frac{\tau}{\rho U^2} dy.$$ (IV.38)

174

For suction $v_0 = v(x, 0) < 0$. Equations (IV.37), (IV.38) can be obtained by applying the laws of conservation of momentum and energy to an element of the boundary layer on a permeable surface. For $k > 1$ the integral relations (IV.25) do not have an obvious physical interpretation.

For approximate calculation of a laminar boundary layer with an arbitrary velocity distribution law on its outer boundary, the integral relations of the pulses (IV.37) are used independently [16]-[19] or jointly with the energy equation (IV.38) [20]-[23].

The basic idea of these methods consists in using the approximate single-parametric family of profiles to approximate the velocity profiles in the boundary layer cross sections. Variation of the family parameter permits us to create a variety of shapes of profiles required for approximate description of the velocity distribution in the boundary layer. A survey of the single-parameteric methods is contained in the monograph [4]. It is possible to find a specific calculation system from the standard single-parametric Karman-Pohlhausen method in §III.1.

In conclusion, let us note that the set of Golubev integral relations cannot be considered from the point of view of their use in the sense of the method of successive approximations [4]. All of them, beginning with k=2, were obtained essentially by a formal procedure, and therefore they do not contain additional information about the fluid flow in a boundary layer. Consequently, using several integral relations in the boundary layer calculations, it is possible to obtain results that diverge with reality more than the data based on the application of only one pulse equation k=0.

§IV.3. Use of the K. K. Fedyayevskiy Method to Calculate a Laminar Boundary Layer with Oblique Blowing (Suction)[1]

Statement of the Problem. Basic Relations

We shall solve the problem based on the system of Prandtl equations for a plane steady laminar boundary layer (§IV.2):

$$\rho \left(u \frac{\partial u}{\partial x} + v \frac{\partial u}{\partial y} \right) = -\frac{\partial p}{\partial x} + \frac{\partial \tau}{\partial y} ; \qquad \left. \begin{array}{c} \\ \\ \end{array} \right\}$$
$$\frac{\partial u}{\partial x} + \frac{\partial v}{\partial y} = 0. \qquad \qquad \qquad$$

(IV.39)

According to K. K. Fedyayevskiy, let us assume that the tangential stress distribution in the boundary layer can be represented as follows:

$$\frac{\tau}{\tau_0} = a_0(x) + a_1(x)\frac{y}{\delta} + a_2\left(\frac{y}{\delta}\right)^2.$$

(IV.40)

$$0 \leqslant \frac{y}{\delta} \leqslant 1$$

_____

[1]The basic results of this section were obtained by I. P. Ginzburg and A. I. Korotkin.

Let us use the following boundary conditions for determination of a_0, a_1, a_2

$$\text{for } y = 0: \quad u = u_0; \quad v = v_0; \atop \text{for } y = \delta: \quad \tau = 0; \quad u = U.} \qquad \text{(IV.41)}$$

For y=0 let us consider the first equation of system (IV.39) valid. From these boundary conditions we find

$$u_0 = 1; \quad a_1 = \frac{\delta}{\tau_0}\left(\frac{dp}{dx} + \rho u_0 u_0'\right) + \frac{\delta v_0}{\nu}; \quad a_2 = -a_0 - a_1.$$

Expression (IV.40) for the stress distribution in the boundary layer can now be rewritten in the form

$$\frac{\tau}{\tau_0} = a_0 + a_1\left(\frac{y}{\delta}\right) + (-a_0 - a_1)\left(\frac{y}{\delta}\right)^2 =$$

$$= 1 - \left(\frac{y}{\delta}\right)^2 + \delta\left(\frac{1}{\tau_0}\frac{dp}{dx} + \frac{\rho}{\tau_0}u_0 u_0' + \frac{v_0}{\nu}\right)\left[\frac{y}{\delta} - \left(\frac{y}{\delta}\right)^2\right]. \qquad \text{(IV.42)}$$

Using relation (IV.42) and the first of the boundary conditions (IV.41), it is possible to determine the value of u

$$u = u_0 + \frac{1}{\mu}\int_0^y \tau\, dy = u_0 + f_1\left(\frac{y}{\delta}\right) + f_2\left(\frac{y}{\delta}\right)^2 + f_3\left(\frac{y}{\delta}\right)^3. \qquad \text{(IV.43)}$$

where

$$f_1 = \frac{\tau_0\delta}{\mu};$$

$$f_2 = \frac{1}{2}\frac{\tau_0\delta^2}{\mu}\left(\frac{1}{\tau_0}\frac{dp}{dx} + \frac{\rho}{\tau_0}u_0 u_0' + \frac{v_0}{\nu}\right);$$

$$f_3 = -\frac{\tau_0\delta}{3\mu} - \frac{1}{3}\frac{\tau_0}{\mu}\delta^2\left(\frac{1}{\tau_0}\frac{dp}{dx} + \frac{\rho}{\tau_0}u_0 u_0' + \frac{v_0}{\nu}\right).$$

From the second boundary condition (IV.41) (u=U for y=δ) we find the first equation relating δ and τ_0,

$$U = u_0 + \frac{\tau_0\delta}{\mu} - \frac{\tau_0\delta}{3\mu} + \frac{\delta^2}{\mu}\frac{1}{6}\left(\frac{dp}{dx} + \rho u_0 u_0'\right) + \frac{\tau_0\delta^2}{6\mu}\cdot\frac{v_0}{\nu},$$

or, otherwise,

$$\tau_0 = \frac{\mu\dfrac{U - u_0}{\delta} - \dfrac{\delta}{6}\left(\dfrac{dp}{dx} + \rho u_0 u_0'\right)}{\dfrac{2}{3} + \dfrac{1}{6}\dfrac{\delta v_0}{\nu}}. \qquad \text{(IV.44)}$$

We shall consider that the magnitude of the normal ventilation is such that $|v_0\delta/\nu| < 1$. This corresponds to the proposition

$$\frac{v_0}{U} < \frac{1}{\frac{U\delta}{v}} \cdot \frac{1}{Re_\delta} \cdot$$

Then expression (IV.44) can be approximately written as follows:

$$\tau_0 \simeq \frac{3}{2} \left[\mu \frac{U - u_0}{\delta} - \frac{\delta}{6} \left(\frac{dp}{dx} + \rho u_0 u_0' \right) \right] \left(1 - \frac{1}{4} \frac{\delta v_0}{v} \right). \tag{IV.45}$$

When deriving the basic Prandtl equations (IV.39) it was assumed that the boundary layer thickness δ is small, so that it is possible to neglect the squares and higher degrees of δ by comparison with the first degree. We shall make use of this assumption later.

Considering what has been stated, let us rewrite expression (IV.45) for τ_0 in the form

$$\tau_0 = \frac{a_1}{\delta} + a_2 + a_3 \delta. \tag{IV.46}$$

Here

$$a_1 = \frac{3}{2} \mu (U - u_0);$$

$$a_2 = \frac{3}{8} \rho (U - u_0) v_0;$$

$$a_3 = -\frac{1}{4} \left(\frac{dp}{dx} + \rho u_0 u_0' \right).$$

Beginning with expression (IV.43) for the velocity distribution u in the boundary layer, let us determine the provisional boundary layer thicknesses

$$\frac{\delta^*}{\delta} = \int_0^1 \left(1 - \frac{u}{U} \right) d \left(\frac{y}{\delta} \right) = \frac{\delta}{U} \left(U - u_0 - \frac{1}{2} f_1 - \right.$$
$$\left. - \frac{1}{3} f_2 - \frac{1}{4} f_3 \right); \tag{IV.47}$$

$$\frac{\delta^{**}}{\delta} = \int_0^1 \frac{u}{U} \left(1 - \frac{u}{U} \right) d \left(\frac{y}{\delta} \right) = \frac{\delta}{U^2} \left\{ u_0 (U - u_0) + \right.$$

$$+ \frac{1}{2} f_1 (U - 2u_0) + \frac{1}{3} |f_2 (U - 2u_0) - f_1^2| + \frac{1}{4} \times$$

$$\times |f_3 (U - 2u_0) - 2f_1 f_2| + \frac{1}{5} (-2f_1 f_3 - f_2^2) +$$

$$+ \frac{1}{6} \left(-2f_2 f_3 - \frac{1}{7} f_3^2 \right) \right\}. \tag{IV.48}$$

Considering the proposition of smallness of δ, which leads to approximate equalities

$$f_1 \simeq \frac{3}{2} (U - u_0); \quad f_2 \simeq 0; \quad f_3 \simeq \frac{1}{2} (U - u_0).$$

from (IV.47) and (IV.48) we obtain the following formulas for determing $\delta*$ and $\delta**$:

$$\frac{\delta^*}{\delta} = \frac{3}{8}\frac{U - u_0}{U};$$ (IV.49)

$$\frac{\delta^{**}}{\delta} = \left(1 - \frac{u_0}{U}\right)\left(\frac{39}{280} + \frac{43}{140}\frac{u_0}{U}\right).$$ (IV.50)

In the special case for $u_0{=}0$ expressions (IV.49) and (IV.50) exactly correspond to the third approximation in the Pohlhausen-Karman method of calculating a plane laminar boundary layer.

Basic Differential Equation of the Problem and its Solution. For the case of a homogeneous incompressible fluid and steady-state flow the integral relation of the laminar boundary layer to oblique ventilation (suction) has the form

$$\frac{d\delta^{**}}{dx} + \frac{U'\delta^{**}}{U}\left(2 + \frac{\delta^*}{\delta^{**}}\right) - \frac{v_0}{U}\left(1 - \frac{u_0}{U}\right) = \frac{\tau_0}{\rho U^2}.$$ (IV.51)

The integral relation (IV.51) gives a second equation that relates the values of δ and τ_0, for $\delta*$ and $\delta**$ are known functions of δ. Substituting $\delta*$ and $\delta**$ by formulas (IV.49) and (IV.50) in equation (IV.51) and τ_0 by formula (IV.46), we obtain the ordinary differential equation with respect to $\delta(x)$

$$\frac{d\delta}{dx} + \varphi_1(x)\delta + \frac{\varphi_2(x)}{\delta} = \varphi_3(x),$$ (IV.52)

where

$$\varphi_1(x) = \frac{1}{\left(1 - \frac{u_0}{U}\right)\left(\frac{39}{280} + \frac{43}{140}\frac{u_0}{U}\right)}\left\{\left[\left(1 - \frac{u_0}{U}\right)\times\right.\right.$$

$$\times \left.\left(\frac{39}{280} + \frac{43}{140}\frac{u_0}{U}\right)\right]'_x + \frac{U'}{U}\left(1 - \frac{u_0}{U}\right)\left(\frac{39}{280} + \frac{43}{140}\frac{u_0}{U}\right)\times$$

$$\times \left(2 + \frac{\frac{3}{8}}{\frac{39}{280} + \frac{43}{140}\cdot\frac{u_0}{U}}\right) + \left.\frac{1}{4\rho U^2}\left(\frac{dp}{dx} + \rho u_0 u_0'\right)\right\};$$

$$\varphi_2(x) = -\frac{3}{2}\cdot\frac{v}{U}\frac{1}{\frac{39}{280} + \frac{43}{140}\cdot\frac{u_0}{U}};$$

$$\varphi_3(x) = \frac{5}{8}\frac{v_0}{U}\frac{1}{\frac{39}{280} + \frac{43}{140}\cdot\frac{u_0}{U}}.$$

The obtained equation (IV.52) is a nonlinear differential equation, and in the general case it has no solution in quadratures. Therefore let us solve this equation by the method of successive approximations. As applied to the investigated equation, it is possible to point out two schemes for using the method of successive approximations.

The first scheme is based on smallness of $\phi_2(x)$, for

$$\varphi_2(x) = -\frac{3}{2} \cdot \frac{L}{Re_L} \cdot \frac{1}{\frac{39}{280} + \frac{43}{140} \cdot \frac{u_0}{U}},$$

where $Re_L = UL/\nu$ is a large value which follows from the basic proposition of boundary layer theory. Accordingly, as the first approximation for $\delta(x)$ we take the solution of the equation

$$\frac{d\delta}{dx} + \varphi_1(x)\delta = \varphi_3(x).$$

The solution of this equation for $\delta(0)=0$ gives

$$\delta_1(x) = e^{-\int_0^x \varphi_1(x)\,dx} \int_0^x e^{\int_0^x \varphi_1(x)\,dx} \varphi_3(x)\,dx. \qquad (IV.53)$$

Substituting the value obtained for $\delta_1(x)$ in the third term of the lefthand side of equation (IV.52), we find the equation for determining $\delta(x)$ in the second approximation

$$\frac{d\delta}{dx} + \varphi_1(x)\delta = \varphi_3(x) - \varphi_4(x),$$

where

$$\varphi_4(x) = \frac{\varphi_2(x)}{\delta_1(x)}.$$

Hence, under the condition $\delta(0)=0$ we find the thickness of the boundary layer in the second approximation

$$\delta_2(x) = e^{-\int_0^x \varphi_1(x)\,dx} \int_0^x e^{\int_0^x \varphi_1(x)\,dx} [\varphi_3(x) - \varphi_4(x)]\,dx. \qquad (IV.54)$$

For the calculations it is possible to limit ourselves to the second approximation and calculate $\delta(x)$ by formula (IV.54). Here the calculation error will be on the order of $(Re_L)^{-2}$.

The second scheme is based on the assumption of smallness of the value of $\phi_3(x)$, for the ratio v_0/U must be selected so that $\left|\frac{v_0}{U}\right| < \frac{1}{Re_\delta} \ll 1$.

As the first approximation let us take the solution to the equation

$$\frac{d\delta}{dx} + \varphi_1(x)\delta + \frac{\varphi_2(x)}{\delta} = 0.$$

The solution of this equation for $\delta(0)=0$ gives

$$\delta_1(x) = e^{-\int_0^x \varphi_1(x)\,dx} \sqrt{2} \left\{ \int_0^x e^{2\int_0^x \varphi_1(x)\,dx} [-\varphi_2(x)]\,dx \right\}^{1/2}. \qquad (IV.55)$$

Substituting the value obtained for $\delta_1(x)$ in the third term of the lefthand side of equation (IV.52), we find the relation for determining $\delta(x)$ in the second approximation

$$\frac{d\delta}{dx} + \varphi_1(x)\delta = \varphi_3(x) - \frac{\varphi_2(x)}{\delta_1(x)}.$$

Hence, under the condition $\delta(0)=0$, we find

$$\delta_2(x) = e^{-\int_0^x \varphi_1(x)\,dx} \int_0^x e^{\int_0^x \varphi_1(x)\,dx} \left[\varphi_3(x) - \frac{\varphi_2(x)}{\delta_1(x)}\right] dx. \qquad (IV.56)$$

The value of $\delta(x)$ in the second scheme must be calculated using formula (IV.56).

If $v_0=0$, then $\phi_3(x)=0$ and equation (IV.52) is integrated in quadratures. Under the condition $\delta(0)=0$, its integral is equal to

$$\delta(x) = \sqrt{2} e^{-\int_0^x \varphi_1(x)\,dx} \left\{\int_0^x e^{2\int_0^x \varphi_1(x)\,dx} [\varphi_2(x)]\,dx\right\}^{1/2}.$$

Separation Point of a Laminar Boundary Layer with Oblique Ventilation (Suction). Let us find the separation of the boundary layer from the condition $\tau_0=0$. Using expression (IV.46) for τ_0, we obtain the following equation for determining δ at the separation point ($\delta=\delta_s$):

$$\frac{a_1}{\delta_s} + a_2 + a_3\delta_s = 0; \quad (\delta_s \neq 0). \qquad (IV.57)$$

Solving (IV.57) with respect to δ_s, we obtain

$$\delta_s = -\frac{a_2}{2a_3} \pm \sqrt{\frac{a_2^2 - 4a_1a_3}{4a_3^2}}. \qquad (IV.58)$$

From expression (IV.58) we find the conditions under which separation occurs

$$a_2^2 - 4a_1a_3 > 0 \quad a_3^2 > 0. \qquad (IV.59)$$

Since for $U>u_0$ the product $a_1a_3<0$ and $\delta_s>0$, it is possible to draw the conclusion that the sign on the radical in formula (IV.58) must be selected positive.

Thus, the equation for determining the separation point coordinate x_s is written as follows:

$$\delta_s(x) = -\frac{a_2}{2a_3} + \sqrt{\frac{a_2^2 - 4a_1a_3}{4a_3^2}}. \qquad (IV.60)$$

The value of $\delta(x)$ defined by formulas (IV.54) or (IV.56) is substituted in (IV.60) in place of $\delta_s(x)$, after which the roots of the obtained equation are found. The least positive root gives the separation point coordinate x_s. In practice it is more convenient to solve equation (IV.60) graphically. Constructing the curves $\delta_s(x)$ and $\delta(x)$, let us determine the coordinates of the points of their intersection. The point with least positive coordinate defines the boundary layer separation.

Laminar Boundary Layer of a Plate with Oblique Ventilation [Suction]

As an example, on the basis of the relations obtained let us consider how oblique ventilation (suction) influences the boundary layer of a plate. We shall consider that along with U=const, the ventilation components u_0 and v_0 are constant.

Equation (IV.52) is rewritten in this case as follows:

$$\frac{d\delta}{dx} = \varphi_3 - \frac{\varphi_2}{\delta},$$
(IV.61)

where

$$\varphi_2 = -\frac{3}{2}\frac{v}{U}\frac{1}{\frac{39}{280} + \frac{43}{140}\cdot\frac{u_0}{U}};$$

$$\varphi_3 = \frac{5}{8}\frac{v_0}{U}\frac{1}{\frac{39}{280} + \frac{43}{140}\cdot\frac{u_0}{U}}.$$

ϕ_2 and ϕ_3 are constants. Integrating equation (IV.61) under the initial condition $\delta(0)=0$, we find

$$\delta + \frac{\varphi_2}{\varphi_3}\ln\left(1 - \frac{\varphi_3}{\varphi_2}\delta\right) = \varphi_3 x$$

or, otherwise,

$$\delta - \frac{12}{5}\frac{v}{v_0}\ln\left(1 + \frac{5}{12}\frac{v_0\delta}{v}\right) = \frac{5}{8}\cdot\frac{v_0 x}{U\left(\frac{39}{280} + \frac{43}{140}\frac{u_0}{U}\right)}.$$
(IV.62)

On the basis of (IV.62), it is possible to write the function $\delta=\delta(x)$ as follows:

$$\delta(x) = A(p)\sqrt{\frac{vx}{U + 2,2u_0}}, \quad A(p) = \left[\frac{140}{13}\cdot\frac{p^2}{p - \ln(1+p)}\right]^{1/2},$$
(IV.63)

where the coefficient A(p), $(p=5v_0\delta/12v)$ is presented in Figure IV.1.

It is necessary to define $\delta(x)$ using formula (IV.63) and the indicated graph A=A(p) by the method of successive approximations. In the first approximation, being given A(p=0), it is possible to find $\delta_1(x)$, then calculate the parameter $p_1=5v_0\delta_1/12v$, determine $A_1(p_1)$ by it and calculate δ_2. It is possible to make subsequent approximations analogously. In order to facilitate the calculations it is possible to use the graph depicted in Figure IV.2.
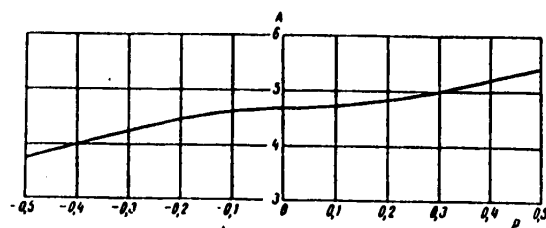
Figure IV.1.   Graph of the function A=A(p)
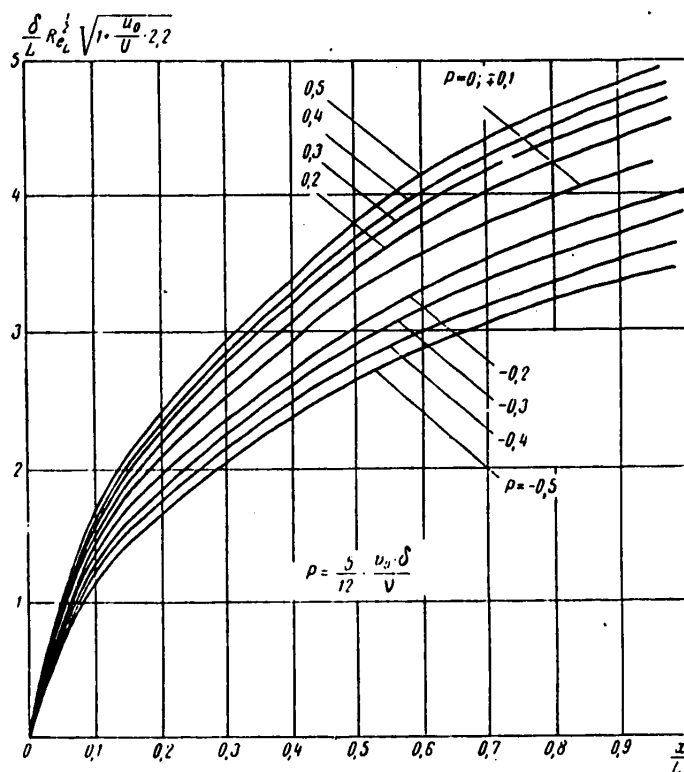
Figure IV.2.   Boundary layer thickness of a plate as a function of
the blowing   (suction) velocity at the wall
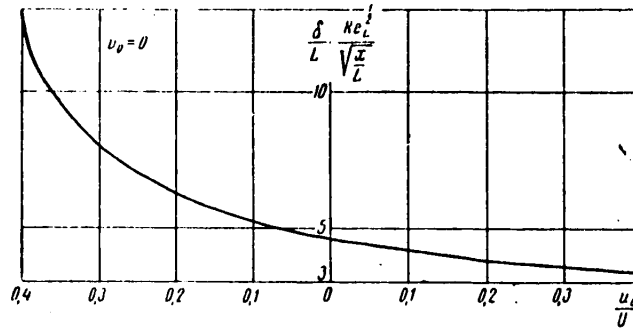
Figure IV.3. Boundary layer thickness of a plate as a function of the magnitude of the tangential component of the blowing velocity
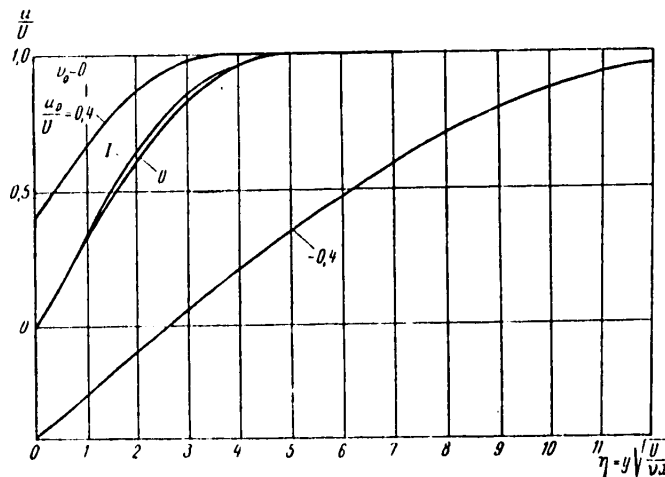
Figure IV.4. Velocity distribution in the boundary layer of a plate for various values of u_0/U; $v_0=0$.
1 -- Nikuradze experiment

183
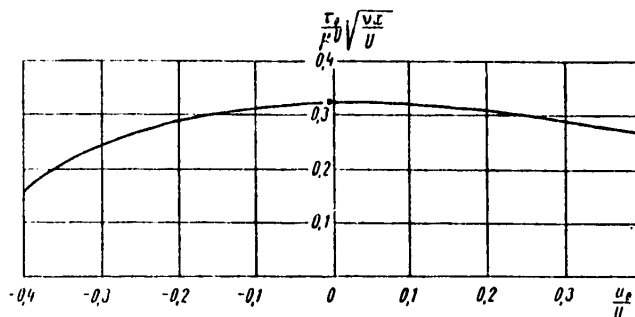
Figure IV.5. Local friction of a plate as a function of the value
of u_0/U; $u_0=0$;
(*) -- Blasius calculation
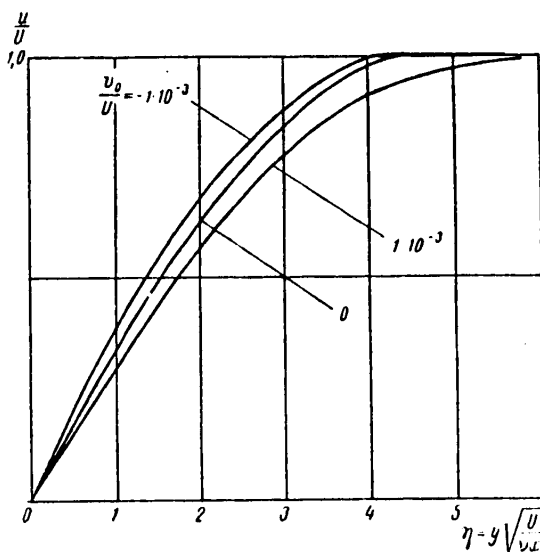
Figure IV.6. Velocity profile in the boundary layer of a plate
as a function of the magnitude of normal ventilation;
$u_0=0$, $Re_x=10^4$.

On the graphs shown in Figures IV.3-IV.7, the relations are presented for the
boundary layer thickness, the velocity distribution in the boundary layer and
local flow as a function of the ventilation components obtained by the above-
presented formulas.
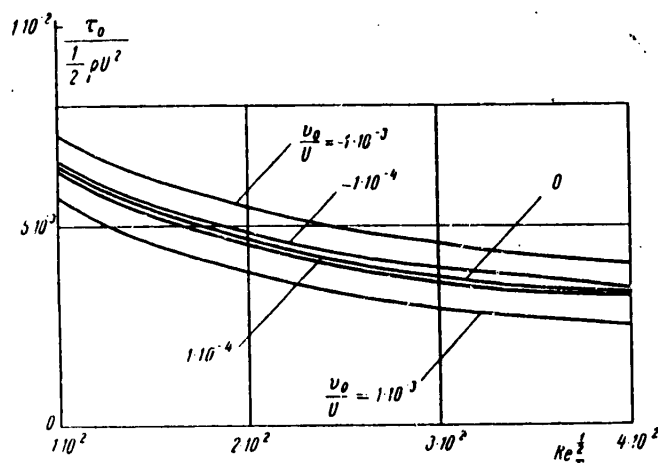
Figure IV.7. Local friction of a plate as a function of the magnitude of the normal ventilation; $u_0=0$

§IV.4. Use of a System of Three Equations of Moments for Approximate Calculation of a Laminar Boundary Layer

The existing methods of approximate integration of the equations of a laminar boundary layer on a porous surface are based on using the pulse equation or on joint application of the pulse and energy equations. The accuracy of these methods depends to a significant degree on successful approximation of the velocity profile across the boundary layer. For example, the velocity profile proposed in reference [16] very approximately reflects the effective variation of the velocities in the boundary layer on a porous surface, especially near the layer separation point. The use of a fourth degree polynomial also in this case leads to errors in calculating the boundary layer characteristics [17].

As was demonstrated in reference [24], by using the system of equations of "moments" of the basic differential equation of the boundary layer and applying simple families of velocity profiles, it is possible to develop an entirely satisfactory method of integrating the equations of a laminar boundary layer c an impermeable surface. In this section, a system of three equations of "moments" is used for approximate integration of equations (IV.1) of the laminar boundary layer on a porous surface in the presence of suction in an incompressible fluid [25].

For a body with porous surface the investigated system of differential equations must satisfy the following boundary conditions:

$$u = 0, \quad v = -v_0 \quad \text{for} \quad y = 0,$$
$$u \to U \quad \quad \quad \text{for} \quad y \to \infty. \quad\quad\quad\quad (IV.64)$$

Using the continuity equation, it is possible to give the first equation of
(IV.1) a more convenient form for future calculations

$$\frac{\partial}{\partial x}\left[u(U-u)\right]+\frac{\partial}{\partial y}\left[v(U-u)\right]+U'(U-u)-$$
$$-\nu\frac{\partial^2(U-u)}{\partial y^2}=0. \tag{IV.65}$$

Let us multiply both sides of equation (IV.65) by y^k, where k=0, 1, 2, 3, ...,
and let us integrate the expressions obtained with respect to y from zero to
infinity. As a result of the calculations we have

$$\frac{d}{dx}\int_0^\infty y^k u(U-u)\,dy+\int_0^\infty y_\kappa\frac{\partial}{\partial y}\left[v(U-u)\right]dy+$$
$$+U'\int_0^\infty y^k(U-u)\,dy-\nu\int_0^\infty y_\kappa\frac{\partial^2(U-u)}{\partial y^2}\,dy=0. \tag{IV.66}$$

Then it is assumed that the integrals in equations (IV.66) have finite values.

In the special case of k=0, equation (IV.66) becomes the integral relation of
pulses (IV.25), which on suction of the fluid from the wall $(v(x,)=-v_0)$ is
rewritten as

$$\frac{d\delta^{**}}{dx}+\frac{U'\delta^{**}}{U}(2+H)+\frac{v_0}{U}=\frac{\tau_0}{\rho U^2}, \tag{IV.67}$$

where $H=\delta^*/\delta^{**}$,

τ_0 is the local tangential stress on the surface.

Introducing the following dimensionless parameters into the investigation

$$f=\frac{\delta^{**2}}{\nu}\frac{dU}{dx};\quad \zeta=\frac{\tau_0\delta^{**}}{\mu U};\quad t^{**}=\frac{v_0\delta^{**}}{\nu}$$

and performing the algebraic transformations, equation (IV.67) is reduced to the
form

$$\frac{df}{dx}=\frac{U''}{U'^2}f+\frac{U'}{U}\left\{2\zeta-2\left[2+H\right]f-2t^{**}\right\}, \tag{IV.68}$$

where $U''=d^2U/dx^2$. Then equation (IV.68) will be called a zero moment equation.

For k=1, from equation (IV.66) we obtain the first moment equation. In this case
it is possible to write that

$$\frac{d}{dx}\int_0^\infty yu(U-u)\,dy+\int_0^\infty y\frac{\partial}{\partial y}\left[v(U-u)\,dy+U'\int_0^\infty y(U-u)\,dy=\right.$$
$$-\nu\int_0^\infty y\frac{\partial^2(U-u)}{\partial y^2}\,dy. \tag{IV.69}$$

156

Integrating the second and fourth integrals of equation (IV.69) by parts, under the assumption that:

$$y(U-u)\Big|_{y\to\infty}\to 0; \quad y\frac{\partial u}{\partial y}\Big|_{y\to\infty}\to 0;$$

$$\int_0^\infty y\frac{\partial}{\partial y}[v(U-u)]dy = -\int_0^\infty v(U-u)\,dy; \tag{IV.70}$$

$$\int_0^\infty y\frac{\partial^2(U-u)}{\partial y^2}\,dy = U. \tag{IV.71}$$

Considering formulas (IV.70) and (IV.71) equation (IV.69) is written in the form

$$\frac{d}{dx}\int_0^\infty yu(U-u)\,dy - \int_0^\infty v(U-u)\,dy + U'\int_0^\infty y(U-u)\,dy = vU. \tag{IV.72}$$

Let us introduce the notation for the first integral in the equality (IV.72)

$$\int_0^\infty yu(U-u)\,dy = H_1 U^2\delta^{**2}, \tag{IV.73}$$

where

$$H_1 = \int_0^\infty \eta\varphi(1-\varphi)\,d\eta, \quad \eta = \frac{y}{\delta^{**}}, \quad \frac{u}{U} = \varphi.$$

Noting that

$$\frac{d\eta}{dx} = -\frac{\eta}{\delta^{**}}\frac{d\delta^{**}}{dx}.$$

from the continuity equation and the boundary layer (IV.64), we have

$$v = -\int_0^y \frac{\partial u}{\partial x}\,dy - v_0 = -U'\delta^{**}\int_0^\eta \varphi\,d\eta - U\left(\int_0^\eta \varphi\,d\eta - \eta\varphi\right)\frac{d\delta^{**}}{dx} - v_0. \tag{IV.74}$$

Considering formula (IV.74), let us transform the second integral into the equations (IV.72)

$$-\int_0^\infty v(U-u)\,dy = H_2 U^2\delta^{**}\frac{d\delta^{**}}{dx} - H_3 UU'\delta^{**2} - v_0\int_0^\infty (U-u)\,dy =$$

$$= H_2 U^2\delta^{**}\frac{d\delta^{**}}{dx} - H_3 UU'\delta^{**2} - v_0 U\delta^*, \tag{IV.75}$$

where

$$H_2 = \int_0^\infty \left(\eta\varphi - \int_0^\eta \varphi\,d\eta\right)(1-\varphi)\,d\eta,$$

$$H_3 = \int_0^\infty \left(\int_0^\eta \varphi\,d\eta\right)(1-\varphi)\,d\eta.$$

Finally, the third integral in the equations is converted to the form

$$\int_0^\infty y(U-u)\,dy = H_4 U\delta^{**2}, \tag{IV.76}$$

where

$$H_4 = \int_0^\infty \eta(1 - \varphi)d\eta.$$

Substituting the calculated integrals (IV.73), (IV.75), and (IV.76) in equation (IV.72), we obtain

$$-\frac{d}{dx}\left(H_1 U^2 \delta^{**2}\right) - H_2 U^2 \delta^{**} \frac{d\delta^{**}}{dx} + H_3 UU' \delta^{**2} +$$

$$+ v_0 U \delta^* + H_4 UU' \delta^{**2} = \nu U.$$

(IV.77)

Substituting $\dfrac{\delta^{**2}}{\nu} \quad \dfrac{f}{U'}$, in equation (IV.77), we find under the assumption

that $H_i(i=1, \ldots, 4)$ do not depend on x,

$$\frac{df}{dx} \quad \frac{1}{\left(H_1 - \frac{1}{2} H_2\right)} \frac{U'}{U} \{1 - Hf^{**} - (2H_1 + H_3 + H_4)f\} + \frac{U''}{U'} f.$$

(IV.78)

For k=2, from expression (IV.66), we obtain the second moment equation

$$-\frac{d}{dx}\int_0^\infty y^2 u(U - u)\,dy - 2\int_0^\infty yv(U - u)\,dy + U'\int_0^\infty y^2(U - u)\,dy =$$

$$= 2\nu \int_0^\infty (U - u)\,dy.$$

(IV.79)

Let us denote

$$\int_0^\infty y^2 u(U - u)\,dy = H_5 U^2 \delta^{**3};$$

(IV.80)

$$\int_0^\infty yv(U - u)\,dy = H_6 U^2 \delta^{**2} \frac{d\delta^{**}}{dx} - H_7 UU' \delta^{**3} - H_4 v_0 \delta^{**2} U,$$

(IV.81)

$$\int_0^\infty (U - u)\,dy = U\delta^{**} H; \quad \int_0^\infty y^2(U - u)\,dy = U\delta^{**3} H_8,$$

(IV.82)

where

$$H_5 = \int_0^\infty \eta^2 \varphi(1 - \varphi)\,d\eta;$$

$$H_6 = \int_0^\infty \eta\left(\eta\varphi - \int_0^\eta \varphi\,d\eta\right)(1 - \varphi)\,d\eta;$$

$$H_7 = \int_0^\infty \eta\left(\int_0^\eta \varphi\,d\eta\right)(1 - \varphi)\,d\eta;$$

$$H_8 = \int_0^\infty \eta^2(1 - \varphi)\,d\eta.$$

188

Then considering equations (IV.80)-(IV.82), after certain transformations of formula (IV.79), we obtain the desired equation in final form

$$\frac{df}{dx} = \frac{U''}{U} \frac{4}{(3H_5 - 2H_6)} \left[H - H_4 t^{**} - \left(H_5 + H_7 + \frac{1}{2} H_8 \right) f \right] + \frac{U''}{U'} f.$$

(IV.83)

For calculation of the three unknowns H, ζ and f, a system of three equations (IV.68), (IV.78) and (IV.83) was put together. These equations are a generalization of the zero, first and second moment equations proposed in reference [24] to the case of a porous surface.

Introducing the constants

$$a = \frac{1}{H_1 - \frac{1}{2} H_2}; \quad b = \frac{2H_1 + H_3 + H_4}{H_1 - \frac{1}{2} H_2};$$

$$c = \frac{H_5 + H_7 + \frac{1}{2} H_8}{H_0}; \quad H_0 = \frac{3H_5 - 2H_6}{4\left(H_1 - \frac{1}{2} H_2\right)},$$

the first and second moment equations are written in the form

$$\frac{df}{dx} = a \frac{U'}{U}\left(1 - Ht^{**} - \frac{b}{a} f\right) + \frac{U''}{U'} f,$$

(IV.84)

$$\frac{df}{dx} = \frac{a}{H_0} \frac{U'}{U}(H - H_4 t^{**} - H_0 c f) + \frac{U''}{U'} f.$$

(IV.85)

The range of variation of the form parameter H is comparatively small. For example, for a plate with suction of the boundary layer H=2.0 to 2.59. Let us propose that in the first moment equation (IV.84) the form parameter H is approximately equal to 2, that is, its exact value for the asymptotic boundary layer on a porous plate [3]. Then in order to find the function H(f, t**) we subtract equation (IV.84) term by term from equation (IV.85), and after simple transformations considering condition U'≠0 we obtain

$$H = H_0 - (2H_0 - H_4) t^{**} - H_0\left(\frac{b}{a} - c\right) f.$$

(IV.86)

Setting t**=0 in this formula and considering that in this case formula (IV.86) must correspond to the known interpolation formula proposed in [24], let us determine the numerical values of the coefficients: H_0=2.59 and $H_0((b/a)-c)$=7.55.

Let us define the constant H_4 by the formula (IV.76), using the asymptotic velocity profile in the boundary layer on a porous plate. As a result of these calculations it was found that H_4=4.

Determining the numerical values of the constant coefficients, it is possible to write the interpolation formula in final form:

$$H = 2.59 - 1.18 t^{**} - 7.55 f.$$

(IV.87)

189

A comparison of this formula with the data from numerical integration of the laminar boundary equations for a porous plate [2] demonstrates satisfactory correspondence of them (Figure IV.8). A comparison of analogous data for a porous wedge [26] demonstrated that for t**=0.462 and f=0.01675, the exact value of H=2.03, and the approximate value of H=1.97.

Solving the zero and first moment equations jointly, we obtain

$$\zeta = \frac{a}{2} + (1-a)t^{**} + \left(2 + H - \frac{b}{2}\right)f. \qquad (IV.88)$$

Here let us set t**=0, and then from the condition of correspondence of equation (IV.88) to the known solution obtained in reference [24], let us determine the numerical values of the coefficients: a=0.4408 and b=5.48.
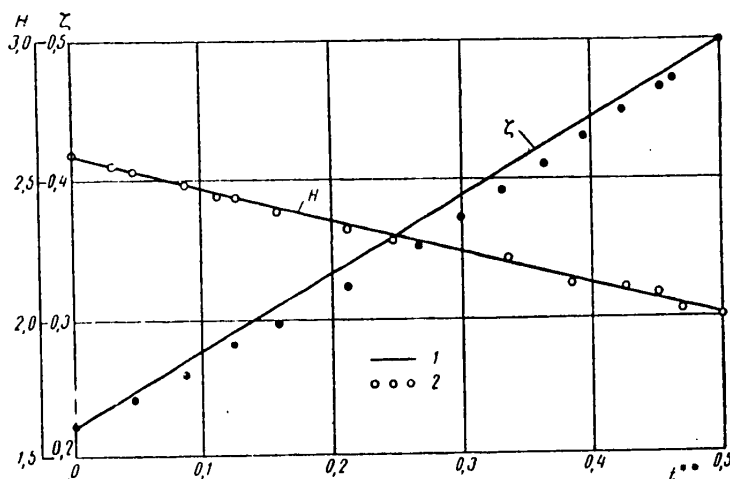
Figure IV.8. Comparison of the calculation results by the approximate formulas (IV.87), (IV.89) with the exact solutions. 1 -- by the formulas; 2 -- exact solution [2].

Using formula (IV.87) and the values of the coefficients a and b, from equation (IV.88) we obtain

$$\zeta = 0,22 + 0,56t^{**} - 1,18 f f^{**} + 1,85 f - 7,55 f^2. \qquad (IV.89)$$

A comparison of the data calculated by formula (IV.89) with the exact values of ζ for a porous plate [2] gives satisfactory correspondence of them in the range of values of the parameter t** from 0 to 0.5 (see Figure IV.8). Here the maximum error does not exceed 5%.

It is of interest to compare the exact numerical data calculated in reference [26] for a porous wedge with the results of the calculations by the obtained formulas. The comparison demonstrated that for t**=0.462 and f=0.01675, the exact value of ζ=0.488, and the approximate value calculated by the formula (IV.89), ζ=0.498.

190

Setting $\zeta=0$ in equation (IV.89), we obtain the formula for calculating the form parameter $f_s(t^{**})$ at the boundary layer separation point:

$$f_s = \frac{(1.85 - 1.18t^{**}) - \sqrt{(1.85 - 1.18t^{**})^2 + 4 \cdot 7.55 (0.22 + 0.56t^{**})}}{15.1}.$$

(IV.90)

For an impermeable surface, formula (IV.90) gives $f_s=-0.0875$.

For calculation of the form parameter f it is possible to use any of the three equations of moments inasmuch as, as the calculations demonstrated, the results obtained here are very close to each other. In later calculations for determinacy we shall use the zero moment equation in the following form:

$$\frac{df}{dx} = \frac{U''}{U'} f + \frac{U'}{U} (F - 2t^{**}).$$

(IV.91)

Here

$$F(f, t^{**}) = 2\zeta(f, t^{**}) - 2[2 + H(f, t^{**})]f.$$

(IV.92)

Substituting the values of H and ζ in formula (IV.92), it is possible to show that the function F is a linear function of the form parameter f, that is,

$$F(f, t^{**}) = A(t^{**}) - Bf,$$

(IV.93)

where

$$A(t^{**}) = 0.44 + 1.12t^{**}; \quad B = 5.48.$$

Inasmuch as F(f, t**) is a linear function of f, the integral of the equation (IV.91) can be written in the following form:

$$f(x) = \frac{U'(x)}{[U(x)]^B} \int_0^x [A(x) - 2t^{**}(x)] [U(x)]^{B-1} dx + c \frac{U'(x)}{U^B(x)}.$$

(IV.94)

Let us expand the system of coordinates so that for x=0, U=0. Then from the condition of finiteness of f for x=0 it follows that the integration constant c=0, and f(0)=A/B. The form parameter at the forward critical point as a function of the suction parameter is presented in Figure IV.9.

Calculating the values of the form parameter $f_{(x)}$ by formula (IV.94), it is possible to determine all the remaining characteristics of a laminar boundary layer:

$$\delta^{**} = \sqrt{\frac{\nu f(x)}{U'(x)}};$$

(IV.95)

$$\delta^+ = \delta^{**} H(f, t^{**});$$

(IV.96)

$$\frac{\tau_0}{\frac{1}{2} \rho U^2} = \frac{2\nu}{U\delta^{**}} \zeta(f, t^{**});$$

(IV.97)

$$v_0 = \frac{\nu t^{**}}{\delta^{**}}.$$

(IV.98)

191

For calculation of the boundary layer characteristics with given normal velocity component on the porous surface of a body v_0, it is necessary to use the method of successive approximations. Being given the expected variation of the parameter t^{**} in the first approximation by formulas (IV.94) and (IV.95), it is possible to calculate the function δ^{**} and inasuch as v_0 is given, by the values of this function it is possible to find the variation of the parameter t^{**} in the second approximation. Repeating the process of successive approximations, it is possible with sufficient accuracy to calculate all the boundary layer characteristics.
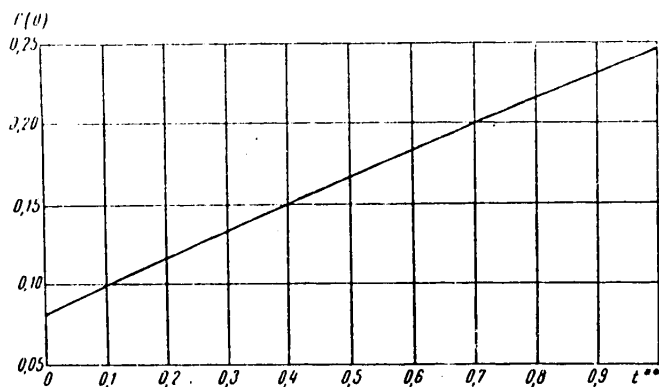
Figure IV.9. Value of the form parameter f at the critical point as a function of the suction parameter t^{**}

As the first approximation of the expected variation of the parameter t^{**} it is necessary to take the corresponding values for a porous plate with given distribution v_0. It is recommended that the required values of t^{**} for a porous plate be defined as follows. First the values of $f_1(0)$ are calculated by the formula

$$f_1(0) = \frac{v_0}{U} \cdot 2 \sqrt{\frac{Ux}{v}}$$

and the expected variation of the parameter t^{**} in the first approximation is determined by the graph (Figure IV.10). The mentioned graph is proposed in reference [27].

Calculating the values of the form parameters f and t^{**} with the required accuracy, we can determine all the remaining boundary layer characteristics by formulas (IV.95)-(IV.98).

The discussed procedure can be used also to calculate the laminar boundary characteristics and the function $v_0(x)$ by the given values of the functions δ^{**}, U and U'. If the recalculated values are given, it is possible to calculate the functions f and df/dx, and from equations (IV.91) and (IV.98), determine the desired functions t^{**} and v_0.

The case where the suction velocity is approximately proportional to the thickness of the boundary layer pulse loss, that is, $v_0 \sim \delta^{**}$, is of practical interest. In this case $t^{**}=t_0^{**}=$const, and equation (IV.94) is simplified, converting to the form

$$f_{(x)} = \frac{0.44 \left| 1 - 2 t_0^{**} \right|}{U^B{}_{(x)}} \frac{dU}{dx} \int_0^x U^{B-1} \, dx.$$

Let us also consider the special case of uniform suction of a laminar boundary on a plate. In this case $v_0=$const and the zero moment equation (IV.67) is written in the following form

$$\frac{d\delta^{**}}{dx} + \frac{v_0}{U} = \frac{\tau_0}{\rho U^2}.$$

(IV.99)

Using equation (IV.99), let us determine the laminar boundary layer characteristics in the presence of uniform suction over the entire surface of the plate. Let us introduce the new variables

$$\xi = \left(\frac{-v_0}{U} \right)^2 \cdot \frac{Ux}{\nu}$$

and

$$t^{**} = \frac{-v_0 \delta^{**}}{\nu}.$$
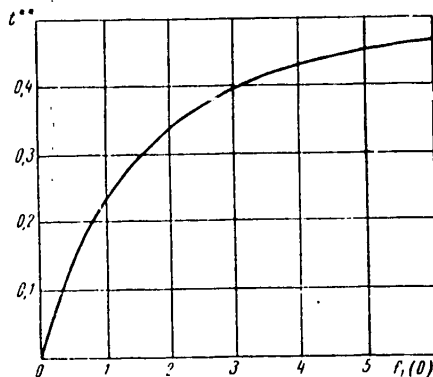
Figure IV.10. Graph of the function $f_{1(0)}$ as a function of the suction parameter t^{**}

In these variables equation (IV.99) is transformed to the following:

$$t^{**} \frac{dt^{**}}{d\xi} - t^{**} = \zeta.$$

(IV.100)

For arbitrary suction velocity distribution along a porous plate, the dimension-less local friction coefficient (see equality IV.88) is equal to

$$\zeta = \zeta_0 - p t^{**},$$

(IV.101)

193

where $\zeta_0=0.22$; $p=0.56$ and $t^{**}\leq0$. A comparison of the results of calculations by formula (IV.101) with the data from numerical integration of the differential equations of a laminar boundary layer on computers demonstrated that in the range of values of t^{**} from 0 to 0.5, the maximum error in formula (IV.101) does not exceed 3%.

Let us transform equation (IV.100) considering formula (IV.101). After separation of variables and determination of the integration limits we obtain the simple equation

$$\int_0^{t^{**}} \frac{t^{**}dt^{**}}{\zeta_0 + (1-p)\, t^{**}} = \int_0^{\xi} d\xi.$$

(IV.102)

Equation (IV.102) has the solution

$$\xi = \frac{t^{**}}{1-p} -$$

$$- \frac{\zeta_0}{(1-p)^2} \ln\left|1 + \frac{(1-p)}{\zeta_0}\, t^{**}\right|.$$

(IV.103)
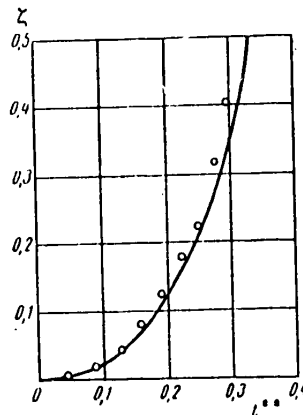
Figure IV.11. Comparison of the exact and approximate solutions for uniform suction of a laminar boundary layer on a plate.

The exact solution of the problem of determining the characteristics of an incompressible laminar boundary layer for uniform suction on a porous plate by numerical integration of the L. Prandtl differential equations is presented in reference [28]. The results of the exact solution (the circles) are compared with the approximate values calculated by formula (IV.103) (the solid line) in Figure IV.11.

§IV.5. Approximate Method of Calculating Optimal Suction of a Fluid from the Boundary Layer of Wing Sections with Porous Surface

By optimal suction of a fluid from a boundary layer through a porous surface we mean the distribution of the normal component of the velocity along the surface when the local Reynolds number in each cross section of the boundary layer is equal to its lower critical value.

The problem of optimal suction of a fluid from the boundary layer of a porous plate was solved for the first time by numerical integration of the L. Prandtl equation in reference [29]. The papers [30], [32] are also devoted to an approximate solution of the analogous problem for the boundary layer with arbitrary pressure gradient at the outer boundary. The last two papers are based on using the pulse and energy equation for the boundary layer. In this section a system of zero and second moment equations (see §IV.4) is used to calculate the optimal suction of a fluid from the boundary layer of wing sections with porous surface in an incompressible fluid [33].

Let us write the zero moment equation in the following form:

$$\frac{df}{dx} = \frac{U''}{U'} f + \frac{U'}{U} [a + (B - 2) t^{**} - bf].$$

(IV.104)

Here f is the boundary layer form parameter;

x is the profile surface coordinate;

U is the given longitudinal velocity at the outer boundary of the layer;

U', U'' are the first and second derivatives of the longitudinal velocity at the outer boundary of the layer with respect to x;

t** is the suction parameter of the fluid through a porous surface;

a=0.44, b=5.48 and B=1.12 are constants.

Inasmuch as

$$f = \frac{\delta^{**2}U'}{\nu} = \frac{\nu U'}{U^2} \text{Re}^{**2} \left(\text{Re}^{**} = \frac{U\delta^{**}}{\nu} \right),$$

(IV.105)

by differentiating equality (IV.105) we find that

$$\frac{df}{dx} = \frac{\nu U''}{U^2} \text{Re}^{**2} - \frac{2\nu U'^2}{U^3} \text{Re}^{**2} + \frac{\nu U'}{U^2} \frac{d\text{Re}^{**2}}{dx}.$$

(IV.106)

Substituting formulas (IV.105) and (IV.106) in equation (IV.104) and performing algebraic transformations, we obtain

$$\frac{\nu}{U} \frac{d\text{Re}^{**2}}{dx} + \frac{\nu U'}{U^2} (b - 2) \text{Re}^{**2} - (B - 2) \frac{v_0}{U} \text{Re}^{**} - a =$$
$$= 0 \left(t^{**} = \frac{v_0}{U} \text{Re}^{**} \right),$$

(IV.107)

where $v_0(x)$ is the local rate of suction of the fluid from the boundary layer.

We shall use the second-moment equation in the following form:

$$\frac{df}{dx} = \frac{U''}{U'} f + \frac{U'}{U} \frac{a}{H_0} (H - H_1 t^{**} - H_0 cf),$$

(IV.108)

where H is the boundary layer form parameter;

$c=9.54$, $H_0=2.59$ and $H_4=4$ are constants.

After substituting formulas (IV.105) and (IV.106) in equation (IV.108) we have

$$\frac{v}{U}\frac{dRe^{**2}}{dx} + \frac{vU'}{U^2}(ac-2)Re^{**2} + a\frac{H_4}{H_0}\frac{v_0}{U}Re^{**} - a\frac{H}{H_0} = 0. \qquad \text{(IV.109)}$$

Excluding the value of v_0/U from equations (IV.107) and (IV.109), we obtain the differential equation for calculating the local Reynolds number

$$\frac{dRe^{**2}}{dx} + \frac{U'}{U}\kappa_0 Re^{**2} - \frac{\frac{a}{H_0}\left(\frac{aH_4}{B-2}-H\right)}{\frac{v}{U}\left(1+\frac{a}{B-2}\frac{H_4}{H_0}\right)} = 0, \qquad \text{(IV.110)}$$

where

$$\kappa_0 = \frac{\left[(ac-2)+\frac{a(b-2)}{B-2}\frac{H_4}{H_0}\right]}{\left(1+\frac{a}{B-2}\frac{H_4}{H_0}\right)}.$$

Integrating equation (IV.110) for the boundary condition $Re^{**}=Re_0^{**}$ for $x=x_0$, where x_0 is the coordinate of the loss of stability point without fluid suction, we find

$$Re^{**2} = \exp\left[-\kappa_0 \ln\frac{U(x)}{U(x_0)}\right]\left\{\frac{a}{v[H_0(B-2)+aH_4]}\times\right.$$

$$\left.\times \int_{x_0}^{x}[aH_4+(B-2)H]U(x)\exp\left[\kappa_0 \ln\frac{U(x)}{U(x_0)}\right]dx + Re_0^{**}\right\}. \qquad \text{(IV.111)}$$

Calculations of optimal fluid suction from the boundary layer begin with the Reynolds number Re_0^{**} at the loss of stability point of the layer before which the flow in the layer is stable with respect to small disturbances without suction of the fluid. For known velocity distribution at the outer boundary of the wing section layer U(x) and given values of the form parameter H, we calculate Re^{**} by formula (IV.111). Obtaining a family of curves for Re^{**} (x, H) and local critical Reynolds numbers corresponding to each value of the form parameter H, let us determine the function $Re^{**}_{cr}(x)$ graphically. Here it is recommended that the values of $Re^{**}_{cr}(H)$ be calculated by the following formula [21]:

$$Re^{**}_{cr} = \exp(A_1 - B_1 H),$$
$$\text{(1)}$$

Key: 1. cr

where A_1 and B_1 are constants.

From the zero moment equation (IV.107) we obtain the formula for calculating the optimal fluid suction rate distribution

$$\frac{v_0}{U} = \frac{v}{U}\frac{1}{B-2}\cdot\frac{1}{Re^{**}_{cr}}\frac{dRe^{**2}_{cr}}{dx} + \frac{vU'}{U^2}\frac{(b-2)}{(B-2)}Re^{**}_{cr} - \frac{a}{B-2}\frac{1}{Re^{**}_{cr}}. \qquad \text{(IV.112)}$$
$$\text{(1)}$$

Key: 1. cr

The first term in the righthand side of formula (IV.112) is defined from the differential equation (IV.110). After corresponding transformations we have

$$\frac{v}{U} \frac{1}{B-2} \frac{1}{\mathrm{Re}_{\kappa p}^{\bullet\bullet}} \cdot \frac{d\,\mathrm{Re}_{\kappa p}^{\bullet\bullet\,2}}{dx} = -\frac{vU'}{U^2} \frac{\kappa_0}{B-2} \mathrm{Re}_{\kappa p}^{\bullet\bullet} +$$

$$+ \frac{a}{(B-2)} \frac{[aH_4 + H(B-2)]}{[H_0(B-2)+aH_4]} \frac{1}{\mathrm{Re}_{\kappa p}^{\bullet\bullet}}$$

Substituting this expression in equation (IV.112) and performing the required calculations, we find the formula in final form for determining the optimal distribution of the rate of fluid suction from the boundary layer through a porous surface along the chord of the wing section

$$\frac{v_0}{U} = \frac{vU'}{U^2} \frac{(b-2-\kappa_0)}{B-2} \mathrm{Re}_{\kappa p}^{\bullet\bullet} + \frac{a(H-H_0)}{[H_0(B-2)+aH_4]} \frac{1}{\mathrm{Re}_{\kappa p}^{\bullet\bullet}}. \qquad (IV.113)$$

Determining the optimal suction velocity distribution by formula (IV.113) using the approximate method proposed in reference [25], it is possible to calculate all the boundary layer characteristics and frictional drag of the wing section.

The discussed method of calculating the distribution of the optimal fluid suction velocity from the boundary layer was developed as applied to plane flows. Using the known Ye. I. Stepanov transformation [34], this procedure can be extended to the case of axisymmetric flows.

For the special case of a porous plate expressions (IV.111) and (IV.113) reduce to an integral exponential function. The zero moment equation (IV.104) will in this case be written in the form of an integral expression

$$\frac{d}{dx} \int_0^\infty u(U-u)dy + v_0 U = \frac{\tau_0}{\rho}. \qquad (IV.114)$$

Let us transform expression (IV.114) to the following

$$\mathrm{Re}^{\bullet\bullet} \frac{d\,\mathrm{Re}^{\bullet\bullet}}{d\,\mathrm{Re}_x} + f^{\bullet\bullet} = \zeta. \qquad (IV.115)$$

By optimal boundary layer suction, just as before, we mean the distribution of the normal velocity component at the surface of a plate where in each boundary layer cross section the local Reynolds number is equal to its lower critical value, that is,

$$\mathrm{Re}^{\bullet\bullet}(x) = \mathrm{Re}_{H}^{\bullet\bullet}. \qquad (IV.116)$$

When calculating the lower critical Reynolds numbers by the small oscillations method, usually the fluid flow stability in a laminar boundary layer is investigated. This method of investigation is very tedious. In addition it is, however, possible to use the fact that the influence of various suction velocity distribution laws along the plate on the flow stability loss in a laminar boundary layer can be established using the form parameter H. It is known that the value of the lower critical Reynolds number can be calculated by the following approximate formula:

$$\mathrm{Re}_H^{\cdot\cdot} = \exp\,(a - bH).$$

(IV.117)

The following two pairs of constants are recommended in references [21], [32]:
a=26.3, b=8 and a=29.1, b=9.

With the first pair of constants formula (IV.117) satisfactorily approximates the
results of calculations of the boundary layer stability of wedges and also the
asymptotic boundary layer on a porous plate (for H from 2 to 2.8). The data from
calculations by formula (IV.117) with the second pair of constants correspond better
to the lower critical Reynolds numbers for Schlichting sections with boundary
layer pumping and for a six-term Pohlhausen polynomial without suction of the
layer (for H from 2.2 to 2.7).

The results of further calculations depend to a significant degree on the assumed
values of the constants a and b. Accordingly, the data from calculations of the
hydrodynamic stability of a fluid flow in a laminar boundary layer of a porous
plate were analyzed again with entirely different suction velocity distribution
along the plate surface: namely, with uniform suction v_0=const [28] and with
suction by the law $v_0 \sim 1/\sqrt{x}$ [36]. This analysis made it possible to establish that
in the range of values of H from 2.15 to 2.80 the mentioned data are approximated
with high accuracy (to 2%) by formula (IV.117) for the next pair of constants:
a=31.3 and b=10. The calculations demonstrated that for optimal suction of the
laminar layer on a porous plate this range of values of H approximately corresponds
to the range of Reynolds numbers Re_x from $0.\cdot 10^6$ to $1000\cdot 10^6$.

In §IV.4 it is demonstrated that for arbitrary suction velocity distribution along
a porous plate for ζ and H the following approximate formulas are valid:

$$\zeta = \zeta_0 - p t^{**},$$

(IV.118)

$$H = H_0 + c t^{**}.$$

(IV.119)

Here ζ_0=0.22, p=0.56, H_0=2.59 and c=1.18 are constants, and $t^{**} \leq 0$.

A comparison of the results of the calculations by formulas (IV.118) and (IV.119)
with the data from numerical integration by computer of the differential equations
of a laminary boundary layer [2] demonstrated that in the range of values of
t^{**} from 0 to -0.5 the maximum error in formula (IV.118) does not exceed 3%, and
formula (IV.119), 1%.

Substituting formulas (IV.116)-(IV.119) in equation (IV.115) and separating
variables, we obtain an ordinary differential equation

$$(-bc)\,\frac{\exp\,[2\,(a - H_0 b - bc t^{**})]}{\zeta_0 - (p + 1)\,t^{**}}\,dt^{**} = d\,\mathrm{Re}_x.$$

(IV.120)

Integrating equation (IV.120) by substitution of the variable $z \cdot \dfrac{2bc\zeta_0}{p+1} - 2bc t^{**}$

under the boundary condition: for t^{**}=0,

$$\mathrm{Re}_x = \mathrm{Re}_{x_0},$$
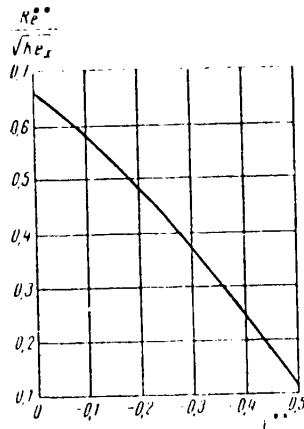
Figure IV.12. Ratio $Re^{**}/Re_x^{1/2}$ as a function of the suction parameter t^{**}
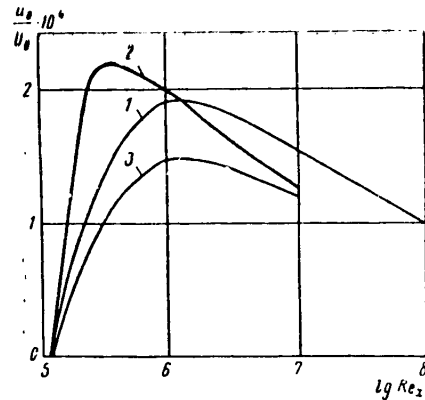
Figure IV.13. Comparison of different values with respect to optimal suction of a laminar boundary layer.
1 -- by formula (IV.113); 2 -- by the data of [21]; 3 -- by the data of [32]

we find that

$$\mathrm{Re}_x - \mathrm{Re}_{x_0} = \frac{bc}{p+1}\exp\left[2\left(a - H_0 b - \frac{bc\zeta_0}{p+1}\right)\right]\times$$

$$\times\left\{E_i\left(\frac{2bc\zeta_0}{p+1} - 2bct^{**}\right) - E_i\left(\frac{2bc\zeta_0}{p+1}\right)\right\},\qquad\text{(IV.121)}$$

where E_i is an integral exponential function.

Inasmuch as [3] $Re_H^{**}=225$, it is easy to find that $Re_{x_0}=0.115\cdot10^6$.

Calculating the function $Re_x(t^{**})$ by formula (IV.121) and using the graphical dependence of $Re^{**}/\sqrt{Re_x}$ on t^{**} (Figure IV.12) proposed in reference [37], it is possible to determine the local flow rate factor

$$\frac{v_0}{U} = \frac{t^{**}}{Re^{**}}.$$

Comparison of the functions obtained by different authors for optimal suction velocity on a porous plate v_0/U_0 for different Reynolds numbers $Re_x=U_0x/\nu$, where U_0 is the velocity of the oncoming flow, is presented in Figure IV.13. The results of calculations by the proposed formula (IV.113) (curve 1) and also by the data of references [21], [32] are plotted on this graph (curves 2 and 3, respectively). In these calculations it was proposed that the constants $A_1=26.3$ and $B_1=8$. Comparison shows satisfactory ·correspondence of the calculation results by the proposed formula with the corresponding data from reference [29]. The obtained results also make it possible to draw the conclusion that the distribution of the optimal rate of fluid suction from the boundary layer depends to a significant degree on the Reynolds number.

The laminar frictional drag with optimal boundary layer suction on a porous plate is calculated by the formula

$$
\zeta_f = \frac{2\int_0^x \tau_0 \, dx}{\rho U_0^2 x} = \frac{2}{R_x} \int_0^{Re_x} \frac{\zeta \frac{v_0}{U_0}}{t^{**}} \, dR_x.
$$

which, by expression (IV.118), is transformed to the following:

$$
\zeta_f = \frac{2u}{Re_x} \int_0^{Re_x} \frac{d\,Re_x}{Re^{**}} - \frac{2p}{Re_x} \int_0^{Re_x} \frac{v_0}{U_0} \, dRe_x.
$$

Considering that for $Re_x \leqslant Re_{x0}$: $v_0/U_0 = 0$ and $Re^{**} = 0.664\sqrt{Re_x}$, in final form we obtain

$$
\zeta_f = \frac{1.328\sqrt{Re_{x_0}}}{Re_x} + \frac{0.44}{Re_x} \int_{Re_{x_0}}^{Re_x} \frac{d\,Re_x}{Re^{**}} - \frac{1.12}{Re_x} \int_{Re_{x_0}}^{Re_x} \frac{v_0}{U_0} \, dRe_x. \qquad \text{(IV.122)}
$$

Both integrals in formula (IV.122) were determined by graphical integration using function (IV.121) and the data presented in Figures IV.12 and IV.13. Here it was considered that $v_0/U_0 \leqslant 0$.

The results of using formula (IV.122) to calculate the laminar frictional drag with optimal boundary layer suction are presented in column 2 of Table IV.1. For cases of uniform boundary layer suction ($v_0/U_0 = -1.18 \cdot 10^{-4}$ and $-2.0 \cdot 10^{-4}$), the laminar frictional drag is presented in columns 3-4 of the table using the data from reference [28], and a laminar and turbulent frictional drags for a plate calculated by the Blasius and Prandtl-Schlichting formulas are presented in columns 5-6. The decrease in hydrodynamic drag of the plate (in %) with respect to turbulent friction is presented in column 7 of the table for the case of optimal boundary layer suction. From the presented data it follows that as the Reynolds number increases, the reduction in drag increases, reaching about 84% for $Re_x = 100 \cdot 10^6$.

For practical calculations it is necessary to calculate the total flow rate factor defined by the formula

$$
c_q = \frac{Q}{U_0 x} = \frac{1}{Re_x} \int_{Re_{x_0}}^{Re_x} \frac{v_0}{U_0} \, dRe_x. \qquad \text{(IV.123)}
$$

The function $c_q(Re_x)$ calculated by formula (IV.123) is presented in column 8 of the table for optimal boundary layer suction on a porous plate.

Table IV.1. Friction Coefficient as a Function of Amount of Suction

$Re_x \cdot 10^{-6}$	$\zeta_{f_0} \cdot 10^3$ $\left(\frac{v_*}{U_*}\right)_{opt}$	$\zeta_{fc} \cdot 10^3$ $\left(\frac{v_*}{U_*}\right) = -1.18 \times 10^{-4}$	$\zeta_{fc} \cdot 10^3$ $\left(\frac{v_*}{U_*}\right) = -2.0 \times 10^{-4}$	$\zeta_{ff} \cdot 10^3$ по Блазиусу (a)	$\zeta_{ff} \cdot 10^3$ по Прандтлю—Шлихтингу (b)	$\frac{\Delta\zeta_f}{\zeta_f} \cdot \%$	$\zeta_q \cdot 10^4$
1	2	3	4	5	6	7	8
0.115	3.920	4.220	4.360	3.920	7.100	45	0
1.00	1.338	1.471	1.680	1.328	4.450	70	0.216
10.0	0.683	0.590	0.736	0.421	3.100	78	1.552
100	0.340	0.332	0.450	0.133	2.131	84	1.206

Key:
   a. Blasius
   b. Prandtl-Schlichting

§IV.6. Calculation of an Axisymmetric Laminar Boundary Layer in the Presence of Suction

Arguments analogous to the case of plane flow [4] make it possible to obtain the following system of equations for an axisymmetric layer on a body of revolution:

$$u\frac{\partial u}{\partial x} + v\frac{\partial u}{\partial y} = U\frac{\partial U}{\partial x} + v\frac{\partial^2 u}{\partial y^2};$$
$$\frac{\partial(ru)}{\partial x} + \frac{\partial(rv)}{\partial y} = 0, \tag{IV.124}$$

where r(x) is the dynamic radius of the body of revolution.
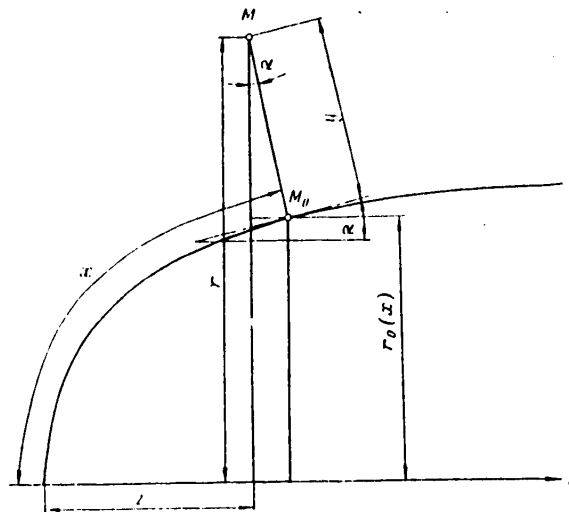
Figure IV.14. Coordinate system in an axisymmetric boundary layer

Inasmuch as (Figure IV.14) $r(x) = r_0(x) + y \cos \alpha$, it is possible to set $r(x) \cong r_0(x)$ in the second equation of (IV.124) everywhere in the boundary layer except the region close to the aft critical point where the boundary layer is comparatively thick, and the radius of transverse curvature of the surface of the body r_0, on the contrary, approaches zero.

Considering this remark, using the system of equations (IV.124) or applying the law of variation of momentum to an element of an axisymmetric boundary layer on a porous surface in the presence of suction, we obtain the integral relation of the pulses (see §IV.2)

$$\frac{d}{dx} \int_0^\delta \rho u^2 r_0 \, dy - U \frac{d}{dx} \int_0^\delta \rho u r_0 \, dy - \rho U \frac{dU}{dx} \delta r_0 - \rho v_0 r_0 U = -\tau_0 r_0. \qquad \text{(IV.125)}$$

When deriving expression (IV.125), the origin of the coordinates was located at the forward critical point; the x-axis was directed along the meridian of an axisymmetric body, and the y-axis, along the normal to the meridian. It must also be noted that expression (IV.125) and all subsequent calculations are valid only for small values of δ/r_0. Departure from the latter restriction greatly complicates the problem and does not allow its solution in finite form. Expression (IV.125) is transformed to the following

$$\frac{df}{dx} = \frac{dU}{dx} \frac{1}{U} (F - 2t^{**}) + \left(\frac{d^2 U}{dx^2} : \frac{dU}{dx} - 2 \frac{dr_0}{dx} : r_0 \right) f, \qquad \text{(IV.126)}$$

where

$$F = 2\zeta - (2 + H)f.$$

Equation (IV.126) is a variation of the integral expression (IV.125) based on the assumption of the possibility of replacing the true velocity profile in different cross sections of the boundary layer by an approximate single-parametric family. Equation (IV.126) differs from the analogous expression given in reference [38] only by the term $2t^{**}$, which takes into account the boundary layer suction through a porous surface.

Inasmuch as in the investigated axisymmetric case the function F has the same form as for a plane laminar boundary layer, according to formula (IV.93) we have

$$F = A - Bf, \qquad \text{(IV.127)}$$

where $A = 0.44 + 1.12t^{**}$; $B = 5.48$.

Integrating equation (IV.126), considering (IV.127), we obtain

$$f(x) = \frac{dU}{dx} \frac{1}{U^B r_0^2} \int_0^x \left[A(\xi) - 2t^{**}(\xi) \right] U^{B-1}(\xi) r_0^2(\xi) \, d\xi + c \frac{dU}{dx} \frac{1}{U^B}. \qquad \text{(IV.128)}$$

For a body with impermeable surface (t**=0) formula (IV.128) compares with the solution obtained in reference [38].

Since the origin of the coordinates was selected so that U=0 for x=0, from the condition of finiteness of the value of the form parameter f(0) it follows that c=0, and f(0)=A/B.

It is recommended that the characteristics of the axisymmetric boundary layer on a porous surface in the presence of suction be calculated using the method of successive approximations, analogously to the case of a plane boundary layer. As the first approximation of the expected variation of the parameter t** it is recommended that the corresponding values be taken for a porous plate according to the data of Figure IV.10. Repeating the process of successive approximations, it is possible to calculate f(x) with the required accuracy. The calculations demonstrated that for elongated axisymmetric bodies (L/B>6) it is sufficient to limit ourselves to the third approximation.
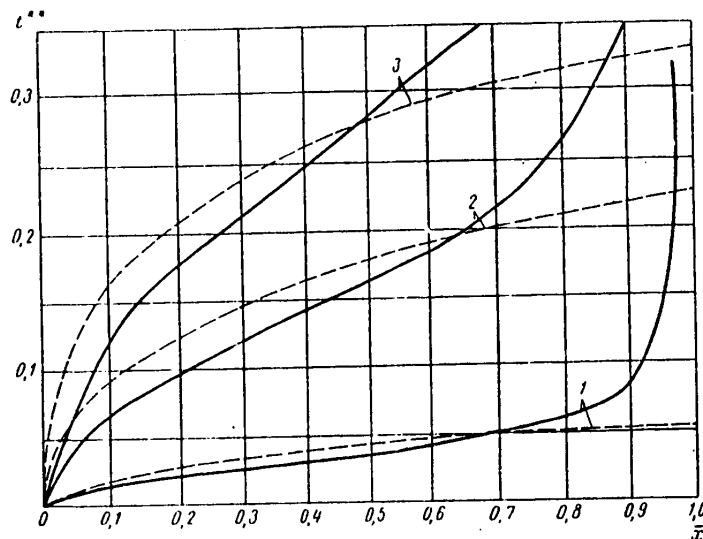
Figure IV.15. Results of calculating an axisymmetric laminar boundary layer on a body of revolution in the presence of suction

Calculating the values of the form parameters f and t** with the required accuracy, it is possible to determine all the remaining characteristics of an axisymmetric boundary layer:

$$\delta^{**} \cdot \left[\nu f(x) : \frac{dU}{dx} \right]^{1/2}; \quad \delta^* \cdots \delta^{**}H;$$

$$\frac{\tau_0}{\frac{1}{2}\rho U^2} \cdots \frac{2\nu}{U\delta^{**}}\zeta; \quad v_0 \cdots \frac{\nu t^{**}}{\delta} .$$

(IV.129)

The values of H and ζ are calculated by the interpolation formulas (IV.87) and (IV.89).

As an example, the results of calculating the laminar boundary layer characteristics for an ellipsoid of revolution L/B=8 with porous surface are presented in Figure IV.15 for constant values of $v_0/U=0.1\cdot10^{-4}$, $0.5\cdot10^{-4}$, $1.0\cdot10^{-4}$ (curves 1, 2, 3) and Reynolds number $U_0B/v=Re_B=6.25\cdot10^6$. The dotted lines on the graph give the first-approximation calculation results.

§IV.7. Approximate Method of Calculating a Laminar Boundary Layer in the Presence of Slot Suction

The existing methods of calculating a laminar boundary layer with fluid suction through transverse slots located on the surface of the body are based on the proposition that suction does not change the pressure distribution on the outer boundary of the boundary layer.

An approximate method of calculating a laminar boundary layer on a plate with slot suction was proposed for the first time by Wuest [39]. The procedure is based on the application of a single-parametric family of profiles

$$u = F(\eta, \kappa),$$

where k is the form parameter, $\eta = y/\delta$, and also on joint use of pulse and energy equations.

A very simple method of calculating the pulse loss thickness for a laminar boundary layer with suction through transverse slots was proposed by G. Lachmann [40]. For calculation of δ^{**} in the profile between the slots $x_{n-1} \leq x \leq x_n$, let us use the known expression of [4]

$$\left(\frac{\delta^{**}}{L}\right)^2 = \frac{1}{Re}\frac{u}{(U/U_0)^b}\left(\int_{\frac{x_{n-1}}{L}}^{\frac{x}{L}}\left(\frac{U}{U_0}\right)^{b-1}dx + \left[\frac{\left(\frac{\delta^{**}}{L}\right)^2 Re\left(\frac{U}{U_0}\right)^b}{a}\right]_{x=x_{n-1}}\right),$$

where a=0.45, b=6.

Let $(\delta^{**}/L)_n$ be the ratio of the pulse loss thickness to the length of a body on reaching the n-th slot. As a result of suction, this ratio decreases to a value of $(\delta^{**}/L)'_n$. During the development process, the pulse loss thickness behind the slot increases again and reaches a value of $(\delta^{**}/L)_{n+1}$ at the n+1 slot.

According to Lachmann, from the condition of transition of a laminary boundary layer to turbulent, we limit the value of the critical Reynolds number constructed by the pulse loss thickness to a value of $Re^{**}_{cr} = 1250$.

From the following expressions

$$\left(\frac{\delta^{**}}{L}\right)_n = \frac{Re_{\kappa p}^{**}}{Re\left(\frac{U}{U_0}\right)_n};$$

$$\left(\frac{\delta^{**}}{L}\right)_{n+1} = \frac{Re_{\kappa p}^{**}}{Re\left(\frac{U}{U_0}\right)_{n+1}}$$

we obtain the relation

$$\frac{(\delta^{**}/L)_n'}{(\delta^{**}/L)_n} = \frac{\sqrt{\left(\frac{U}{U_0}\right)_{n+1}^4 - c_n\Delta_{n+1}l}}{\left(\frac{U}{U_0}\right)_n^2},$$

where

$$n\Delta_{n+1}l = \int_{(x/L)_n}^{(x/L)_{n+1}} \left(\frac{U}{U_0}\right)^5 d\left(\frac{x}{L}\right), \quad c = \frac{0.45\,Re}{\left(Re\,\delta_{\kappa p}^{**}\right)^2}.$$

It remains to find the relation between the suction coefficient $c_Q = Q/U_0 L$ and the ratio of the pulse loss thicknesses $(\delta^{**}/L)_n/(\delta^{**}/L)_n'$. Let us propose that it is possible to find the profile after the slot, dropping the lower part of the profile before the slot through which the fluid is sucked at a distance y from the surface. The area of the dropped part of the slot corresponds to the amount of sucked fluid. If the slot width S is very small, we neglect the variation of the profile shape in the first approximation.

Inasmuch as the sucked fluid flow rate through the slot

$$Q = \int_0^y u\,dy = U\delta^{**} \int_0^{y/\delta^{**}} \frac{u}{U} d\left(\frac{y}{\delta^{**}}\right),$$

the flow rate coefficient

$$c_Q = \frac{\delta^{**}U}{U_0 L} \int_0^{y/\delta^{**}} \frac{u}{U} d\left(\frac{y}{\delta^{**}}\right). \qquad (IV.130)$$

For any slot expression (IV.130) is written

$$\frac{c_{Q_n}}{(\delta^{**}/L)_n} = \frac{U}{U_0} \int_0^{y/\delta_n^{**}} \frac{u}{U} d\left(\frac{y}{\delta_n^{**}}\right). \qquad (IV.131)$$

On the other hand,

$$\frac{(\delta^{**}/L)_n'}{(\delta^{**}/L)_n} = 1 - \int_0^{y/\delta^{**}} \frac{u}{U}\left(1 - \frac{u}{U}\right) d\left(\frac{y}{\delta^{**}}\right). \qquad (IV.132)$$

In parametric form equations (IV.131) and (IV.132) define the dependence of $\dfrac{c_{Q_n}}{(\delta^{**}/L)_n}$ on $\dfrac{(\delta^{**}/L)_n'}{(\delta^{**}/L)_n}$. This function was calculated by Lachmann

(Figure IV.16) under the assumption that it is possible to use the Blasium profile for the velocity distribution across the boundary layer [40].
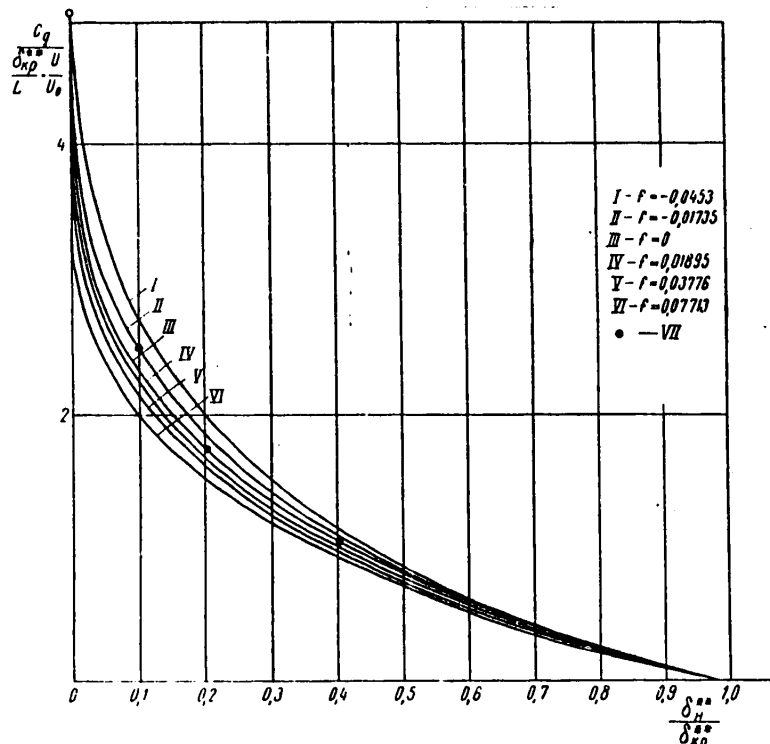
Figure IV.16. Value of $c_q \left(\dfrac{\delta_{кр}^{**}}{L} \cdot \dfrac{U}{U_0} \right)^{-1}$ as a function of the

form parameter f and degree of suction of a laminar boundary layer $\delta_H^{**}/\delta_{cr}^{**}$.

VII -- Lachmann data for f=0

Let us consider the flow in the boundary layer near the slot (Figure IV.17). At some distance y_s from the surface we have the current line AB. The point B is the critical point on the rear edge of the slot. Consequently, the liquid flowing between the current line AB and the surface is completely sucked through the slot, and the other part remains in the boundary layer. Let us consider cross sections 1 and 2 which are located directly on the front and rear edges of the slot, and let us calculate the flow dissipation energy and also the variation of the momentum in the vicinity of the slot.

206
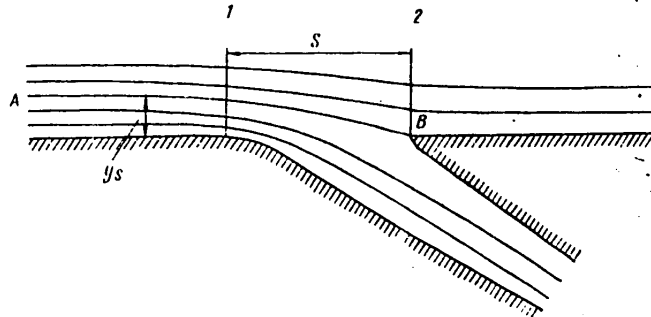
Figure IV.17. Flow diagram in the vicinity of a slot

Let us direct the x coordinate axis along and the y-axis normal to the surface. The momentum equation is written in the form

$$\frac{dM}{dx} + \rho U \frac{dU}{dx} \delta^* = \tau_0,$$

(IV.133)

where U is the velocity at the outer boundary of the boundary layer;

τ_0 is the tangential stress on the surface;

δ^* is the displacement flow thickness;

ρ is the fluid density;

$M = \rho \int_0^{\delta^*} u(U - u)dy$ is the variation of the momentum;

u is the longitudinal velocity component in the boundary layer.

Let us propose that the slot width is so small that in the interval $x_1 \leqslant x \leqslant x_2$ ($x_2-x_1=S$ is the slot width), the displacement flow thickness and velocity at the outer boundary vary according to a linear law:

$$\delta^* = a_0 + a_1 x;$$
$$U = b_0 - b_1 x,$$

Inasmuch as in the vicinity of the slot the flow is not in contact with the solid surface, it is possible to propose that $\tau_0 = 0$, and equation (IV.133) is written as follows, neglecting the term with x^2:

$$\frac{dM}{dx} = \rho b_1 \int_0^S [a_0 b_0 + (a_1 b_0 - a_0 b_1) x] dx =$$

$$= \rho a_0 b_0 b_1 S \left[1 + \frac{1}{2} \left(\frac{a_1}{a_0} - \frac{b_1}{b_0} \right) S \right].$$

(IV.134)

In the majority of practical cases, the value of

$$\frac{1}{2} \left(\frac{a_1}{a_0} - \frac{b_1}{b_0} \right) S \ll 1.$$

207

Then equation (IV.134) is rewritten in the form

$$M_2 - M_1 = \rho \delta_1^{\bullet} U_1 (U_1 - U_2),$$

where the indices 1 and 2 pertain to the corresponding cross sections, and varia-
tion of the momentum as a result of frictional drag in the vicinity of a very
narrow slot $U_2 \cong U_1$) is neglected.

Thus, in cross section 1 we have

$$M_1 = \rho \int_0^{\infty} u_1 (U_1 - u_1) \, dy = \rho \int_0^{\nu_s} u_1 (U_1 - u_1) \, dy +$$

$$+ \rho \int_{\nu_s}^{\infty} u_1 (U_1 - u_1) \, dy.$$

In cross section 2 the momentum

$$M_2 = \rho \int_{\nu_s}^{\infty} u_1 (U_1 - u) \, dy.$$

Then the variation of momentum

$$M_1 - M_2 = \rho \int_0^{\nu_s} u_1 (U_1 - u_1) \, dy.$$

Inasmuch as the corresponding displacement thicknesses are equal to

$$\delta_1^{\bullet\bullet} = \frac{M_1}{\rho U_1^2}, \qquad \delta_2^{\bullet\bullet} = \frac{M_2}{\rho U_2^2}, \quad \text{and} \quad U_2 \cong U_1.$$

then

$$\frac{\delta_2^{\bullet\bullet}}{\delta_1^{\bullet\bullet}} = 1 - \int_0^{\nu_s} \frac{u_1}{U_1} \left(1 - \frac{u_1}{U_1} \right) d \left(\frac{y}{\delta^{\bullet\bullet}} \right).$$

(IV.135)

Then the sucked amount of fluid per unit slot length

$$Q = \int_0^{\nu_s} u_1 \delta y_1,$$

or in dimensionless form

$$c_Q = \frac{Q}{U_0 L} = \frac{U_1}{U_0} \frac{\delta_1^{\bullet\bullet}}{L} \int_0^{\nu_s/\delta^{\bullet\bullet}} \frac{u_1}{U_1} d \left(\frac{y}{\delta^{\bullet\bullet}} \right),$$

(IV.136)

where U_0 is the oncoming flow velocity,

L is the length of the body.

Equations (IV.135) and IV.136) are parametric equations obtained from somewhat different Lachmann expressions. In order to obtain the dependence of c_Q on $\delta**/\delta**$ the Blasius profile was used in reference [40]. For consideration of the longitudinal velocity gradient on the outer boundary of the boundary layer when calculating the dependence of c_Q on $\delta**/\delta**$, by formulas (IV.135) and (IV.136) Coleman proposed that the Hartree profiles be used. However, it is simpler to perform these calculations using analytical velocity profiles. A comparison of the exact and approximate solutions demonstrated that the most acceptable function is the family of profiles proposed by A. M. Basin [57]

$$\frac{u}{U} = \left\{ 1 + \frac{2}{\pi^2}\, f\, \frac{1}{H^{**2}}\left[1 - \sin\frac{\pi}{2}\, H^{**}\left(\frac{y}{\delta^{**}}\right)\right] \times \right.$$

$$\left. \times \sin\frac{\pi}{2}\, H^{**}\left(\frac{y}{\delta^{**}}\right)\right\}. \tag{IV.137}$$

where $f = \frac{\delta^{**}}{\nu}\frac{dU}{dx}$ is the boundary layer form parameter;

$H** = \delta**/\delta$ is the ratio of the provisional thickness of the boundary layer.

Substituting formula (IV.137) in equation (IV.135), after simple transformations we obtain

$$\frac{\delta_{\kappa p}^{\cdot\cdot}}{\delta_{H}^{\cdot\cdot}} = 1 - \int_{0}^{y/\delta^{**}}\left\{1 + \frac{2}{\pi^2}f\frac{1}{H^{**2}}\left[1 - \sin\frac{\pi}{2}H^{**}\left(\frac{y}{\delta^{**}}\right)\right] \times \right.$$

$$\left. \times \sin\left[\frac{\pi}{2}H^{**}\left(\frac{y}{\delta^{**}}\right)\right]d\left(\frac{y}{\delta^{**}}\right)\right\} +$$

$$+ \int_{0}^{y/\delta^{**}}\left\{1 + \frac{2}{\pi^2}f\frac{1}{H^{**2}}\left[1 - \sin\frac{\pi}{2}H^{**}\left(\frac{y}{\delta^{**}}\right)\right]\right\} \times \tag{IV.138}$$

$$\times \sin^2\left[\frac{\pi}{2}H^{**}\left(\frac{y}{\delta^{**}}\right)\right]d\left(\frac{y}{\delta^{**}}\right).$$

The value of $H**$ in formula (IV.138) depends only on the form parameter f.

After calculating the integrals and reducing similar terms, formula (IV.138) acquires the form

$$\frac{\delta_{\kappa p}^{\cdot\cdot}}{\delta_{H}^{\cdot\cdot}} = 1 - a_1 + a_2\left(\frac{y}{\delta^{**}}\right) - a_3\sin\left[\pi H^{**}\left(\frac{y}{\delta^{**}}\right)\right] +$$

$$+ a_4\sin\left[2\pi H^{**}\left(\frac{y}{\delta^{**}}\right)\right] + a_5\cos\left[\frac{\pi}{2}H^{**}\left(\frac{y}{\delta^{**}}\right)\right] - \tag{IV.139}$$

$$- a_6\cos^3\left[\frac{\pi}{2}H^{**}\left(\frac{y}{\delta^{**}}\right)\right],$$

where

$$a_1 = \frac{2}{\pi H^{**}} + \frac{20}{3} f \frac{1}{H^{**3}} + \frac{32}{3\pi^6} f^2 \frac{1}{H^{**5}};$$

$$a_2 = \frac{1}{2} + f \frac{3}{\pi^2} \frac{1}{H^{**2}} + \frac{7}{2\pi^4} f^2 \frac{1}{H^{**6}};$$

$$a_3 = \frac{1}{2\pi H^{**}} + f \frac{3}{\pi^3} \frac{1}{H^{**2}} + \frac{7}{2\pi^4} f^2 \frac{1}{H^{**4}};$$

$$a_4 = f^2 \frac{1}{4\pi^5} \frac{1}{H^{**5}};$$

$$a_5 = \frac{2}{\pi H^{**}} + f \frac{12}{\pi^3} \frac{1}{H^{**3}} + f^2 \frac{16}{\pi^5} \frac{1}{H^{**5}};$$

$$a_6 = f \frac{8}{3\pi^3} \frac{1}{H^{**3}} + f^2 \frac{16}{3\pi^5} \frac{1}{H^{**3}},$$

Analogous calculations, as applied to formula (IV.136), lead to the expression

$$\frac{c_Q}{\delta_{\kappa p}^{**} \frac{U}{L} \frac{U}{U_0}} = a_7 - a_8 \left(\frac{y}{\delta^{**}}\right) +$$

$$+ a_9 \sin\left[\pi H^{**} \left(\frac{y}{\delta^{**}}\right)\right] - a_{10} \cos\left[\frac{\pi}{2} H^{**} \left(\frac{y}{\delta^{**}}\right)\right], \tag{IV.140}$$

where

$$a_7 = \frac{2}{\pi H^{**}} + f \frac{4}{\pi^3} \frac{1}{H^{**3}};$$

$$a_8 = f \frac{1}{\pi^2} \frac{1}{H^{**2}},$$

$$a_9 = f \frac{1}{\pi^3} \frac{1}{H^{**3}};$$

$$a_{10} = \frac{2}{\pi H^{**}} + f \frac{4}{\pi^3} \frac{1}{H^{**3}}.$$

Equations (IV.130) and (IV.140) in parametric form express the dependence of

$$\frac{c_Q}{\delta_{\kappa p}^{**} \frac{U}{L} \frac{U}{U_0}} \qquad \text{on} \qquad \frac{\delta_{\kappa p}^{**}}{\delta_{II}^{**}}.$$

The numerical values of the coefficients are presented in Table IV.2. The final calculation results are depicted in Figure IV.16 in the form of the dependence of

$$\frac{c_q}{\delta_{\kappa p}^{**} \frac{U}{L} \frac{U}{U_0}} \qquad \text{on} \qquad \frac{\delta_{II}^{**}}{\delta_{\kappa p}^{**}} \qquad \text{for different values of the form parameter. The data}$$

obtained for f=0 agree satisfactorily with the Lachmann results.

i	u''	a_1	a_2	a_3	a_4	a_5	a_6	a_7	a_8	a_9	a_{10}
0.0153	0.0958	31.0182	2.8756	9.9704	0.2077	39.8760	8,8631	13.2919	0,5001	1.6616	13,2919
0.03164	0.1266	10.7950	1.2396	3.1160	0.0251	12.6724	1.8772	7,0408	0,06367	0,5024	7,0408
0.01735	0.1326	7.2959	0.8348	2.0159	0.0060	8.0635	0,7676	5,7609	0.1000	0,2400	5,7609
0	0.1366	4.561	0.5000	1.162	0	4,561	0	4,551	0	0	4,561
−0.01893	0.1385	2.6968	0.2350	0.5516	0,0057	2,2065	−0,4903	3,6773	0,1000	−0,2298	3,6773
−0.03776	0.1383	1.2893	0.04000	0.1376	0,0230	0.5503	−0,7368	2,7618	−0,2000	−0,4603	2,7618
−0.5529	0.1359	0.3523	−0.0880	−0,0983	0,0539	−0,3930	−0,7452	1,8426	−0,3033	−0,7105	1,8426
−0.6826	0.1315	−0.0648	−0.1400	−0.1463	0,0968	−0,5809	−0,5167	0,9687	−0,3999	−0,9681	0,9687
−0.07413	0.1250	−0.0081	−0.1264	−0.0037	0.1589	−0.0170	−0,0047	−0,0003	−0,5001	−1,2733	−0,0003

§IV.8. Determination of the Elements of a Slot Suction System Insuring Boundary Layer Laminarization

The optimal removal of fluid from a boundary layer is distributed suction through a porous surface. With corresponding smoothness and porosity of the surface, this organization of fluid removal introduces the least disturbances into the boundary layer and, acting continuously on the flow along its entire surface, it creates the most favorable flow stabilization conditions. However, for a number of process reasons, the most important of which is danger of rapid clogging of the pores under actual operating conditions, in contrast to discrete, primarily slot suction, distributed suction still has not found practical application for boundary layer laminarization purposes.

For slot suction, the slot width must be selected quite small so that the surface roughness will not exceed a defined level, for the edges of the slot play the role of disturbance sources in the flow even when they do not protrude above the surface. Small slot width with defined flow rate through the entire surface implies relatively large local fluid flow velocities in the slot by comparison with distributed suction. Therefore, by using the apparatus of boundary layer theory based on the proposition of smallness of transverse velocities, it appears possible to determine the flow characteristics near the slot.

The indicated facts give rise to an empirical nature of all of the existing calculation methods of determining the parameters of slot suction systems. A discussion is presented below of an approximate method developed by Yu. N. Alekseyev. Calculation practice shows that for longitudinal flow over symmetric wings and axisymmetric elongated bodies with Reynolds numbers $U_0 L/\nu \geq 4 \cdot 10^7$ the influence of individual forms of the body on the amount of sucked fluid and location of the slots is small. The obtained number of slots and sucked fluid flow rates required for boundary layer laminarization differ little from the corresponding values for a plate with longitudinal flow over it. Consequently, for approximate estimation of the parameters of the suction system for wings and bodies of revolution, it is possible to use the relations obtained for a plate.

The basis for the calculations was the Blasius profile which is presented in Figure IV.18 in dimensionless coordinates U/U_0, y/δ^{**}. The studies of [43] demonstrated that the velocity profile in the indicated coordinates on the plate behind the slot very quickly assumes the initial form during suction, then developing as on an impermeable surface. Therefore, according to the solution of [47], let us propose that the velocity profile on the entire surface remains unchanged in dimensionless form, except the pulse loss thickness varies in the vicinity of the slot, which is defined as the difference $\delta_B^{**} - \delta_H^{**}$, where δ_B^{**} is the pulse loss thickness of the profile ABC (Figure IV.18) before the slot, δ_H^{**} is the pulse loss thickness of the profile A_1DBC after the slot. It is considered that the velocity profile filled out as a result of fluid suction from the boundary layer can be obtained, dropping the lower part of the initial profile characterized by the y-axis y_0. Thus,

$$\delta_H^{**}(x, y_0) = \int_{y_0}^{\infty} \frac{u}{U_0}\left(1 - \frac{u}{U_0}\right) dy; \tag{IV.141}$$

$$\delta_B^{**}(x) = \int_0^{\infty} \frac{u}{U_0}\left(1 - \frac{u}{U_0}\right) dy. \tag{IV.142}$$

The amount of fluid pumped through the slot per second is defined here by the expression

$$Q = \int_0^{y_0} u\,dy = Q(y_0), \tag{IV.143}$$

or in dimensionless form

$$\bar{Q} = \frac{Q(y_0)}{U_0 \delta_B^{**}} = f\left(\frac{y_0}{\delta_B^{**}}\right). \tag{IV.144}$$

The function (IV.144) borrowed from reference [47] is presented in Figure IV.19.
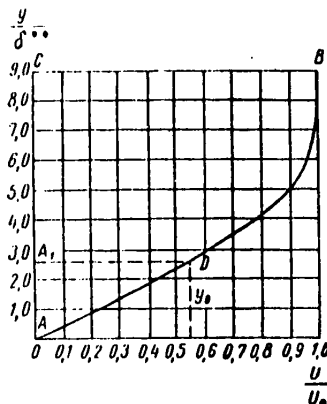
Figure IV.18. Dimensionless velocity profile on a plate

If boundary layer suction takes place in such a way that an increase in δ^{**} in the interval between slots is entirely compensated by suction, then, using formula

$$\delta^{**} = 0.664 \ \sqrt{\frac{vx}{U_0}},$$

(IV.145)

which is valid for the Blasius profile, it is possible to find

$$S = x_{n+1} - x_n = \left(\frac{\delta_B^{**}}{0.664}\right)^2 \frac{U_0}{v} - \left(\frac{\delta_H^{**}}{0.664}\right)^2 \frac{U_0}{v},$$

(IV.146)

or

$$\frac{U_0 S}{v} = \mathrm{Re}_S = \frac{\left(\mathrm{Re}_B^{**}\right)^2 - \left(\mathrm{Re}_H^{**}\right)^2}{0.441}.$$

(IV.147)

For description of the boundary layer suction, the dimensionless flow rate is used

$$c_Q = \frac{Q}{U_0 S} = \frac{v_0 h}{U_0 S} = \frac{v_0}{U_0} \frac{\mathrm{Re}_h}{\mathrm{Re}_S},$$

(IV.148)

where v_0 is the mean velocity of the fluid in the slot,

h is the slot width,

S is the distance between slots.
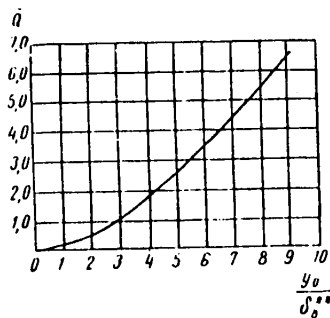
Figure IV.19. Amount of sucked fluid as a function of the degree of suction
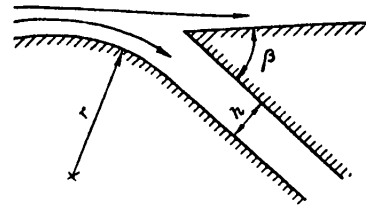
Figure IV.20. Slot form for boundary layer suction

213
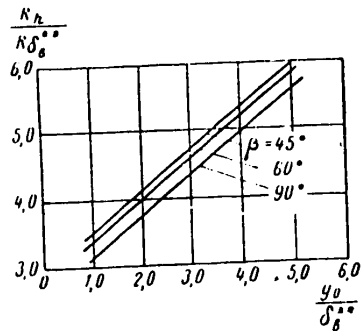
Figure IV.21. Slot width as a function of degree of suction and angle of inclination of the slot
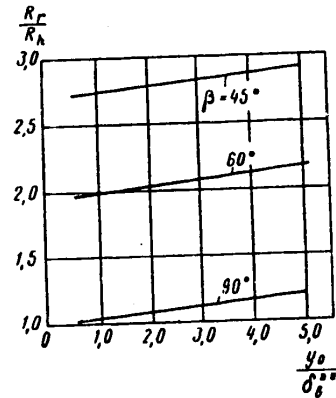
Figure IV.22. Radius of rounding of the inside edge as a function of the degree of suction and angle of inclination of the slot

By visual observation of the nature of the flow in a slot (Figure IV.20), in reference [48] the relations were obtained which insure attached flow of the fluid through a slot of maximum width h (Figure IV.21) and minimum radius of rounding of the entrance edge r (Figure IV.22) as a function of the angle of inclination of the slot and degree of suction of the fluid from the boundary layer. Attached fluid flow in the slot is necessary in connection with the fact that separation of the boundary layer at the entrance to the slot blocks the slot useful cross section, decreasing the flow rate, and it is an additional source of disturbances in the layer. The experimental relations $h = h\left(\frac{y_0}{\delta_B^{**}}, \beta\right)$, $r = \left(\frac{y_0}{\delta_B^{**}}, \beta\right)$ in the range

of $40° < \beta < 90°$ can be expressed by empirical formulas

$$\frac{h}{\delta_B^{**}} = \frac{Re_h}{Re_B^{**}} = 0,615 \frac{y_0}{\delta_B^{**}} - 0,45\beta + 3,25, \qquad (IV.149)$$

$$\frac{r}{h} = \frac{Re_r}{Re_h} = 0,038 \frac{y_0}{\delta_B^{**}} + 0,917\beta^2 - 4,18\beta + 5,3. \qquad (IV.150)$$

When calculating the suction system it is natural to select the critical Reynolds number as Re_B^{**}. The critical Reynolds number Re_{cr}^{**} depends on the roughness, surface waviness, turbulence of the oncoming flow, vibration, noise, and the external pressure gradient. It is possible to determine the value of Re_{cr}^{**}, using the materials of Chapter V.

When designing a slot suction system it is necessary to find the following parameters S, h, v_0, r, β or, for given U_0, the values of Re_S, Re_h, c_Q, Re_r, β. The value of Re_B^{**} is considered known. From structural arguments usually we select $\beta = 90°$. Considering formulas (IV.145)-(IV.150), it is easy to establish that all the indicated characteristics of the suction system are parametrically related to each other using the degree of suction y_0/δ_B^{**}. The value of δ_B^{**} is given, for $Re_B^{**} = Re_{cr}^{**}$ is selected for known velocity U_0. Excluding the parameter y_0/δ_B^{**}, it is possible to find the direct relations between the values of Re_S, Re_h, Re_r, c_Q. To facilitate the calculations of the slot suction system elements

for β=90°, a nomogram is presented in Figure IV.23, by means of which it is possible to solve the following problems:

1) Determine the system parameters providing for boundary laminarization with given value of c_Q;

2) Determine the maximum admissible slot width and minimum fluid flow rate for given distance between slots;

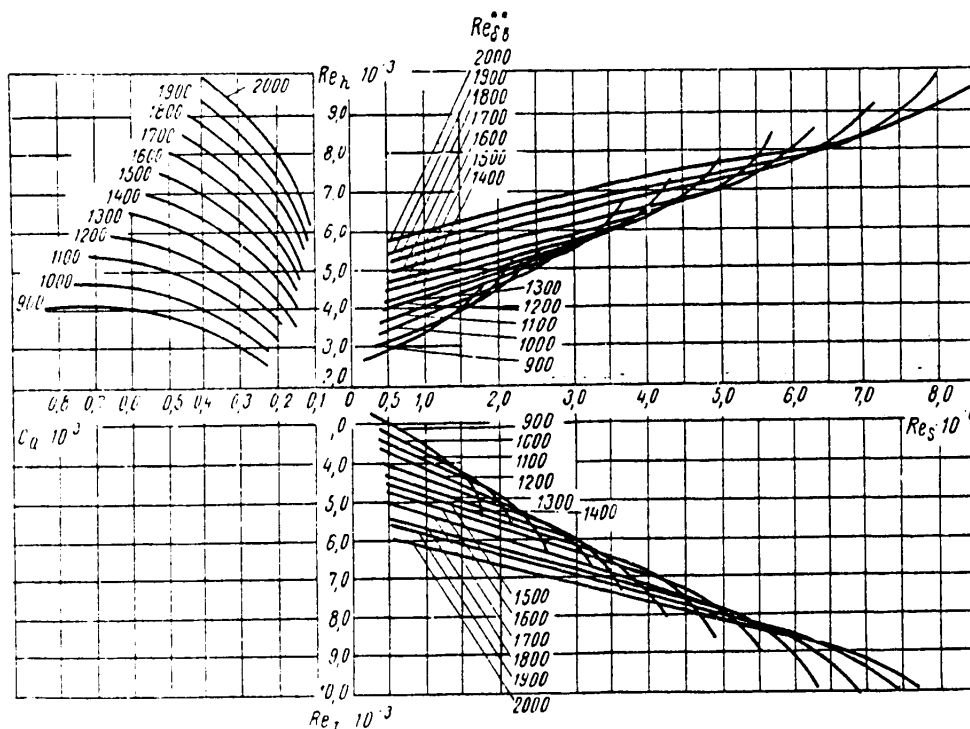3) Calculate the minimum flow rate and distance between slots for given slot width.

Figure IV.23. Nomogram for calculating the suction system parameters

When solving these problems the minimum radius of rounding r of the entrance edge of the slot is also determined. When calculating the boundary layer suction system elements for $\beta \neq 90°$ it is necessary to introduce corrections into the values of Re_h and Re_r according to the formulas (IV.149) and (IV.150).

Figure IV.24. Example of determining slot system elements

Key:
   1. Point ...

As an example of using a nomogram let us consider the procedure for calculating a slot system for a wing section moving in water at a velocity 13 m/sec with zero angle of attack. It is assumed that the chord of the wing is 6 meters, the wetted surface is 30 m^2, $\nu=1.3\cdot 10^{-6}$ m^2.sec, $Re^{**}_{cr}=10^3$. From process arguments let us set the distance between slots as 100 mm, which corresponds to $Re_S=1\cdot 10^6$. Let us plot this point on the nomogram (point 1 in Figure IV.24). Then, by the corresponding curves let us determine the slot width h=0.36 mm (point 2), the radius of rounding of the leading edge r=0.38 mm (point 3), the flow rate coefficient $c_Q=3.2\cdot 10^{-4}$ (point 4), which corresponds to Q=0.125 m^3/sec.

In the region where the curves $Re_h=Re_h(R_S)$ begin to deviate from linear sections sharply, the accuracy of the obtained method is reduced. The proposition that the pulse loss thickness after the slot develops approximately the same as on an ordinary impermeable surface used as the basis for the method is confirmed by the experiments of N. N. Kornilova and Ya. S. Khodorkovskiy [49]. More precise definitions of the method of calculating a slot system connected with considering the influence of the velocity gradient on the outer boundary of the boundary layer can be found in references [50], [51].

§IV.9. Numerical Integration of the Equations of Motion of a Fluid in a
Laminar Boundary Layer with Suction

The methods of calculating a laminar boundary layer investigated in §IV.2-IV.4
and based on the application of integral relations and a set of boundary conditions,
offer the possibility of comparatively quickly calculating the desired layer
characteristics for distributed suction on bodies of revolution and profiles. How-
ever, the accuracy of the calculation is in this case limited by a number of
specific assumptions and forced mathematical simplifications. Examples of such
assumptions, in particular, are to a known degree the subjective assumptions of
the possibility of representing the velocity profile or tangential stresses in the
form of a function of one or several parameters and the method of approximating it.
Using the methods of calculating a laminar boundary for discrete suction, it must
be noted that the assumptions on which they are based are still more approximate.
Therefore, for comparative estimation of the quality of different calculation
methods and degree of reliability of the results obtained by them, experimental
and theoretical checking are required. Inasmuch as the experimental data on a
sucked laminar boundary layer are meager and basically are of a qualitative nature,
a great deal of significance is attached to the possibility of theoretical analysis,
for which primarily the methods of numerical integration of the equations of motion
of a fluid in a laminar boundary layer can be used.

It is known that the equations of a laminar boundary layer are among the parabolic
type equations of mathematical physics. It is possible to obtain the solution to
these equations in quadratures only in individual special cases, for example, in
the case of an asymptotic boundary layer with uniform suction on a plate. As for
solutions obtained using series, according to the evidence of Schlichting [3],
this calculation of the boundary layer is in the majority of cases highly complex,
tedious, and it cannot be performed with admissible expenditure of time in practice.

The numerical method of integration which is called the "continuation method" in
some papers on boundary-layer theory makes it possible for us to obtain solutions
which are more accurate than the solutions using series, and this numerical inte-
gration method has been adapted well for computer use. The development of the
methods of numerical integration of the boundary layer equations have attracted
the attention of a number of researchers (Prandtl, Goldstein, Schroeder, Goertler,
Witting, Reinboldt in the German Democratic Republic and Federal Republic of Germany,
Hartree, Womersly, Manogar, Smith and Clutter in the United States and A. A.
Dorodnitsyyn in the USSR).

Among the German papers, the following are of practical interest: the paper by
Goertler [41] on the application of the finite-difference method of numerical
integration to the laminar boundary layer equations for an impermeable surface and
the paper by Witting [42] which introduces corrections into the Goertler method.
Generalization of reference [41] to the case of suction was accomplished by
Reinboldt [43]. The primary content of his research was determination of the
variation of the flow characteristics at the boundary condition discontinuity points
on the wall. The data on the effect of suction on a laminar boundary layer were
also obtained by numerical integration by Smith and Clutter [44].

Below, a discussion is presented of the method of integrating the boundary layer equations in the case of boundary conditions on a wall corresponding to distributed suction.

Let U, L be the characteristic velocity and length for the given problem. Then the dimensionless coordinates, the velocities and pressure are defined by the expressions

$$x = \frac{x^*}{L}; \quad u = \frac{u^*}{U}; \quad u_\infty = \frac{u^*_\infty}{U}, \quad u_\infty = \lim_{y^* \to \infty} u^*(x^*, y^*).$$

$$y = \frac{y^*}{L} \sqrt{Re}; \quad v = \frac{v^*}{U} \sqrt{Re};$$

$$v_0 = \frac{v^*_0}{U} \sqrt{Re}; \quad p = \frac{p^*}{\rho U^2}; \quad Re = \frac{UL}{\nu},$$

where the index * corresponds to the dimensional values.

The boundary layer equation and the corresponding boundary conditions in dimensionless notation have the form

$$u \frac{\partial u}{\partial x} + v \frac{\partial u}{\partial y} = u_\infty \frac{d u_\infty}{dx} + \frac{\partial^2 u}{\partial y^2}; \quad \frac{\partial u}{\partial x} + \frac{\partial v}{\partial y} = 0, \tag{IV.151}$$

on the wall: $y = 0$, $u = 0$, $v = v_0(x)$; on the outer boundary of the boundary layer: $\lim_{y \to \infty} u = u_\infty(x)$.

In addition, the velocity profile is given in the initial cross section x_1 of the boundary layer: $u|_{x=x_1} = \tilde{u}(y)$.

The transition of equations (IV.151) to a system of finite-difference equations is made as follows. Let us divide the interval of the variable x into i parts with stepsize h; let us divide the segment of variation of the variable y analogously into k parts with stepsize 1. The set of nodes formed on intersection of the straight lines x = ih (i = 0, 1, 2,...) and y = kl (k = 0, 1, 2, ...) is a rectangular grid. It is possible to write the following approximate relations in this grid:

$$\frac{\partial u}{\partial y}\Big|_{x_i, y_\kappa} = \frac{u_{i, \kappa+1} - u_{i, \kappa-1}}{2l} = \frac{\nabla_{i\kappa}}{2l};$$

$$\frac{\partial^2 u}{\partial y^2}\Big|_{x_i, y_\kappa} = \frac{\nabla_{i, \kappa+1} - \nabla_{i, \kappa-1}}{4l^2} = \frac{\nabla^{(2)}_{i\kappa}}{4l^2}; \tag{IV.152}$$

$$\frac{\partial u}{\partial x}\Big|_{x_i, y_\kappa} = \frac{u_{i+1, \kappa} - u_{i\kappa}}{h} = \frac{\Delta_{i\kappa}}{h},$$

which are then substituted in the equation obtained from system (IV.151) as a result of exclusion of the transverse velocity component v. This exclusion is done using the expression

$$v = - \int_0^y \frac{\partial u}{\partial x}\, dy + v_0(x),$$
(IV. 153)

which follows from the continuity equation and boundary conditions at the wall. Approximating (IV.153) by finite differences and calculating the integral by the trapezoid rule, we obtain

$$v|_{x_i,\, y_\kappa} = -\frac{l}{2h}\left(2 \sum_{\nu=1}^{\kappa-1} \Delta_{i,\, \nu} + \Delta_{i,\, \kappa}\right) + v_0|_{x_{i,\, 0}}.$$
(IV.154)

Substituting (IV. 154) and (IV.152) in the first of equations (IV.151), we have after setting for simplicity of notation,

$$u|_{x_i y_\kappa} = u_{i,\, \kappa},\ v|_{x_i y_\kappa} = v_{i,\, \kappa};$$

$$u_{i,\, \kappa}\frac{\Delta_{i,\, \kappa}}{h} + \left[v_{i0} - \frac{l}{2h}\cdot\left(2\sum_{\nu=1}^{\kappa-1}\Delta_{i,\, \nu} + \Delta_{i,\, \kappa}\right)\right] \times$$

$$\times \frac{v_{i\kappa}}{2l} = u_{\infty i}u'_{\infty i} + \frac{v_{i,\, \kappa}^{(2)}}{4l^2}.$$
(IV.155)

Equation (IV.155) can be resolved with respect to $\Delta_{i,\, k}$

$$\Delta_{i,\, \kappa} = \frac{hu_{\infty i}u'_{\infty i} + \frac{h}{4l^2}\, v_{i,\, \kappa}^{(2)} - v_{0i}\frac{h}{2l}\, v_{i,\, \kappa} + \frac{v_{i,\, \kappa}}{2}\sum_{\nu=1}^{\kappa-1}\Delta_i}{u_{i,\, \kappa} - \frac{v_{i,\, \kappa}}{4}}.$$
(IV.156)

The structure of formula (IV.156) is such that the values of $\Delta_{i,k}$ calculated by it are calculated successively, beginning with the layer k=1, for $(\Delta_{i0}=0)$, as a result of the presence in the numerator (IV.156) of a sum by the index ν assuming values from 1 to k-1. From the boundary conditions it follows that at the nodes k=0, i=0, 1, 2, ...

$$u_{i,0} = 0; \quad v_{i,0} = v_0|_{x_{i,0}}. \tag{IV.157}$$

In addition, inasmuch as the initial velocity profile is considered given at the nodes i=1; k=0,1,2,..., the values are known

$$u_{1,\kappa} = u_{i,\kappa}|_{x_1 v_\kappa}. \tag{IV.158}$$

Thus, the problem of integration of the boundary layer equations is reduced to a purely algebraic problem of solving a system of "explicit finite-difference" equations (IV.156) considering (IV.157) and (IV.158) with an error called the "approximation error."

The calculated values of $\Delta_{ik}=u_{i+1,k}-u_{i,k}$ are the velocity increments in layers with the index k on transition from cross section i to cross section i+1. Consequently, if the velocity profile is given in the initial cross section, it is possible to calculate the velocity profile in the subsequent cross section downstream, that is, it is possible to calculate the deformation of the velocity profile during the process of development of a laminar boundary layer and all of its characteristics: integral thicknesses, form parameter, frictional stress at the wall.

It must be noted that expression (IV.156) has a significant deficiency which does not permit its use to calculate the velocity increment for small k=1, 2. From analysis of this expression it is possible to conclude that the value of y exists (in practice within the limits of the first layer) for which indeterminacy of the type of 0/0 arises in equation (IV.156). This fact leads to significant calculation errors $\Delta_{i,k}$ for k=1,2 and forces us to resort to special methods of obtaining more exact calculation formulas for the layers closest to the wall. For k>2, expression (IV.156) is applicable without any stipulations.

The mentioned formulas for k=1, 2 were obtained in Witting's paper [42] in the case of impermeable surfaces; the method of successive approximations for calculating the velocity increment by these formulas is also discussed there.

Yu. N. Karpeyev generalized the Witting method to the case of arbitrary boundary conditions on the wall. This generalized method was used to investigate the development of a laminar boundary layer on a plate on transition from the impermeable section of surface to a permeable section through which distributed suction is uniformly performed. In order to get around the difficulties connected with the presence of a normal velocity discontinuity at the wall, a suction law shown in Figure IV.25 was adopted. The values of u*∞=7 m/sec, L*=0.5 m were taken as the characteristic velocity and length; here, Re=2.5·10⁵. The dimensionless suction

velocity was taken as $\quad v_0 = \dfrac{v_0}{U_\infty^*}\sqrt{\text{Re}} = -2.5\left(\dfrac{v_0}{U_\infty^*} = 0.005\right)$, and the cell dimensions

were taken as the following: $\ell=0.4$, which corresponds to giving the initial profile

(the Blasius profile for x=1) by 20 points, the step size h along the x-axis varied in accordance with the nature of variation of the investigated layer parameters. In Figure IV.26, the variation of $\left.\frac{\partial u}{\partial y}\right|_{y=0}$, proportional to the tangential stress on the wall is presented, and the step distribution h is indicated. The results of the Reinboldt [43], Smith and Clutter [144] calculations are presented there also. The nature of deformation of the velocity profile in the calculated example (v₀=02.5) is explained in Figure IV.27, where it is possible to trace a gradual transition from the Blasius profile to the asymptotic velocity profile. It is of interest that the suction effect is first manifested in the wall region, and then it is propagated to greater distances from the wall on going downstream.
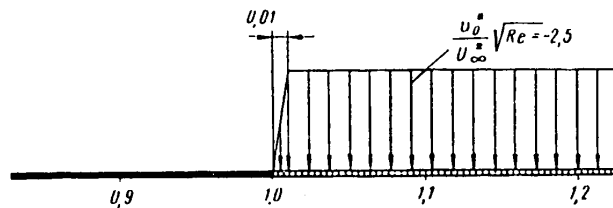
Figure IV.25. Distribution of suction velocity in the calculated example

It was noted above that the application of the methods of numerical integration permits investigation of the development of a laminar boundary layer for arbitrary suction laws and, in particular, discrete suction with precision not available to approximate methods based on using integral relations. One such problem is the problem of the boundary layer with uniform suction through a short permeable section simulating a slot. The results of the Reinboldt, Smith and Clutter calculations illustrating the process of layer development on transition through a permeable section 1.0<x≤1.15 in length (suction velocity v₀=-1.5) are depicted in Figure IV.28. By variation of the values proportional to the displacement thickness and tangential stress in the vicinity of the slot and after it, it is possible to judge the intensity of the development of slot suction. At some quite large distance downstream by comparison with the slot width, the velocity profile approaches the Blasius profile, but the boundary layer thicknesses and tangential stresses are not restored to values which would occur in the absence of discrete suction.

221

$\left(\dfrac{\partial u}{\partial y}\right)_{y=0}$
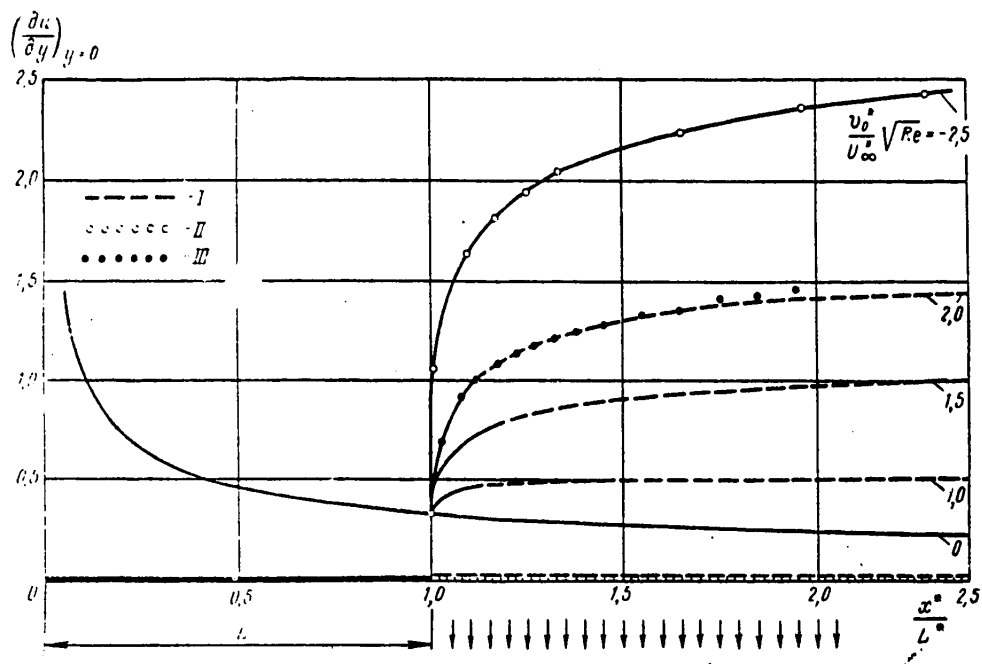
Figure IV.26. Tangential stress on a plate with uniform suction.
1 -- Reinboldt calculation [43]; I -- calculation by formulas presented in this paper; III -- Smith and Clutter calculation [44]
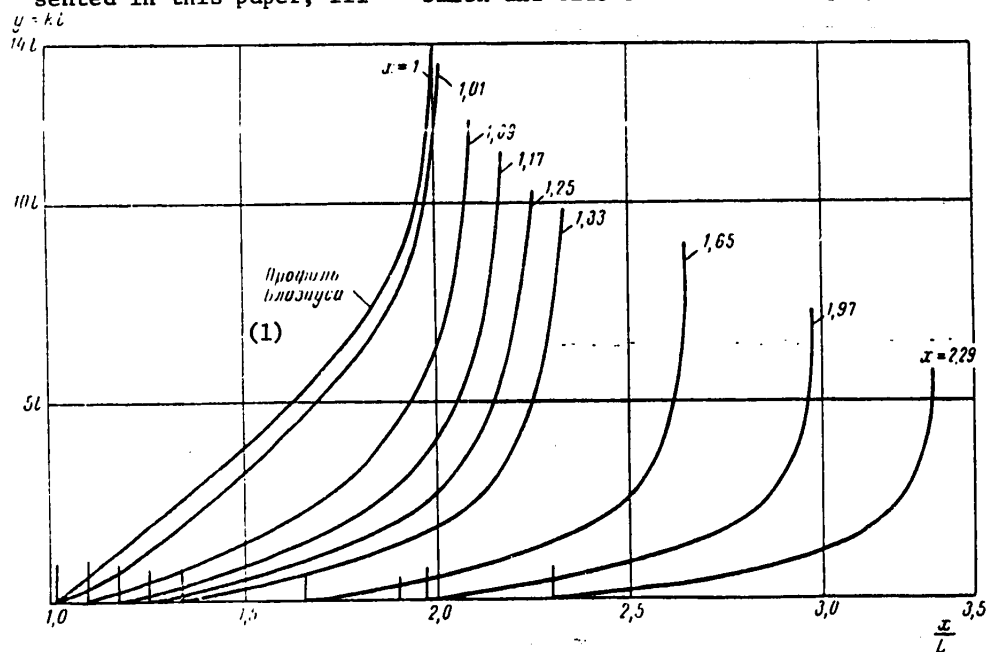
Figure IV.27. Velocity profile deformation on a permeable surface with uniform suction $v_0\sqrt{Re}=-2.5$.

Key: 1 -- Blasius profile

222
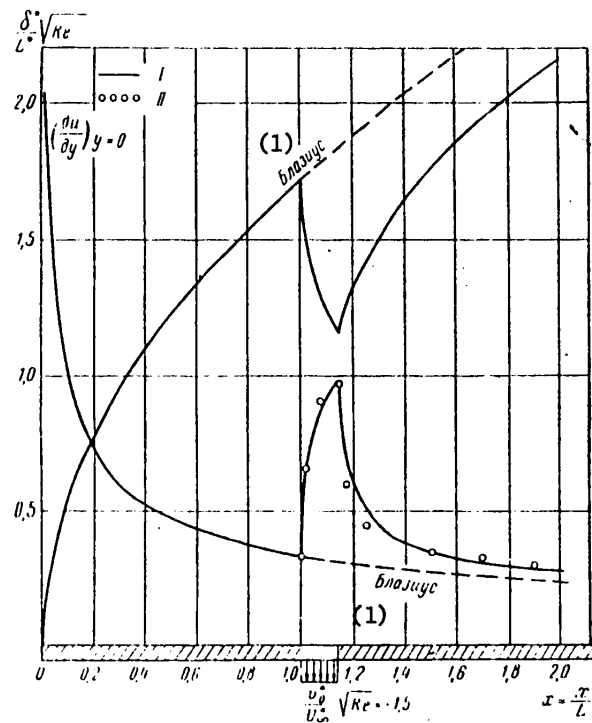
Figure IV.28. Effect of suction through a permeable section of a
plate on variation of the displacement thickness of the boundary
layer and the tangential stress on the wall.
I -- Reinboldt calculation; II -- Smith and Clutter calculation
Key:
   1. Blasius

Application of the A. A. Dorodnitsyn Method for Calculating a Controlled Laminar Boundary Layer

The original method of numerical solution of the laminar boundary layer equations
was proposed by A. A. Dorodnitsyn [59]. This method allows the solution to be
found to the specific problem of calculating the laminar boundary parameters with
any degree of accuracy using high-speed computers.

The A. A. Dorodnitsyn calculation method is discussed below for a more general case
of a laminar boundary layer when fluid is either injected or sucked out.

Let us first transform the initial system of laminar boundary layer equations
(IV.1) to dimensionless form, introducing the following expressions:

$$\bar{x} = \frac{x}{L}; \quad \bar{y} = y\frac{\sqrt{Re}}{L}; \quad \bar{u} = \frac{u}{U}; \quad \bar{v} = v\frac{\sqrt{Re}}{U};$$

$$\bar{U} = \frac{U}{U_0}; \quad Re = \frac{U_0 L}{\nu}; \quad \xi = \int_0^{\bar{x}} \bar{U}\,dx; \quad \eta = \int_0^{\bar{y}} \bar{U}\,d\bar{y}. \qquad (IV.159)$$

223

When using expressions (IV.159), the initial system of laminar boundary layer equations assumes the form indicated by A. A. Dorodnitsyn

$$\bar{u}\,\frac{\partial\bar{u}}{\partial\xi} + \left(\bar{v} + \frac{\dot{U}}{U}\,\eta\bar{u}\right)\frac{\partial\bar{u}}{\partial\eta} = \frac{\dot{U}}{U}(1 - \bar{u}^2) + \frac{\partial^2\bar{u}}{\partial\eta^2}, \qquad\text{(IV.160)}$$

$$\frac{\partial\bar{u}}{\partial\xi} + \frac{\partial\bar{u}}{\partial\eta}\left(\bar{v} + \frac{\dot{U}}{U}\,\eta\bar{u}\right) = 0. \qquad\text{(IV.161)}$$

Here

$$\dot{U} = \frac{\partial U}{\partial\xi} = \frac{U'}{U}.$$

Let us introduce the notation

$$w = \bar{v} + \frac{\dot{U}}{U}\,\eta\bar{u}$$

and let us write equations (IV.160) and (IV.161) in the following form:

$$\bar{u}\,\frac{\partial\bar{u}}{d\xi} + w\frac{\partial\bar{u}}{\partial\eta} = \frac{\dot{U}}{U}(1 - \bar{u}^2) + \frac{\partial^2\bar{u}}{\partial\eta^2}, \qquad\text{(IV.162)}$$

$$\frac{\partial\bar{u}}{\partial\xi} + \frac{\partial w}{\partial\eta} = 0. \qquad\text{(IV.163)}$$

The boundary conditions assume the form:

$$\left.\begin{array}{l} \bar{u} = 0;\ w = \bar{v}_0 \text{ for } \eta = 0 \\[4pt] \bar{u} = 1 \ \text{ for } \eta = \infty \end{array}\right\} \qquad\text{(IV.164)}$$

Here

$$\bar{v}_0 = v_0\,\frac{\sqrt{Re}}{U}.$$

The following notation is adopted in the presented formulas:

U_0, L are the characteristic velocity and length — constants selected in accordance with the solved problem;

x, y are coordinates along the wall and along the normal to it;

u, v are the corresponding velocity components;

U is the velocity at the outer boundary of the boundary layer.

Hereafter, for convenience of notation we shall drop the bars over the letters, remembering that they denote the above-indicated dimensionless values.

In accordance with A. A. Dorodnitsyn, we now obtain integral relations of a general type for the system (IV.162) and (IV.163), analogously to how this is done for the nontransformed system. For this purpose let us multiply equation (IV.163) by an arbitrary function f(u), equation (IV.162) by f'(u), and let us add them. Then we have

$$-\frac{\partial}{\partial \xi} uf(u) + \frac{\partial}{\partial \eta} wf(u) = \frac{U}{U} f'(u)(1 - u^2) + f''(u)\frac{\partial^2 u}{\partial \eta^2} \cdot \quad (IV.165)$$

The arbitrary function f(u) must satisfy only one condition, that it approach zero sufficiently rapidly for $\eta \to \infty$.

Let us integrate equation (IV.165) with respect to η

$$-\frac{d}{d\xi} \int_0^\infty uf(u)d\eta = \frac{U}{U} \int_0^\infty (1 - u^2)f'(u)d\eta$$

$$+ \bar{v}_0 f(0) - f'(0)\left(\frac{\partial u}{\partial \eta}\right)_{\eta=0} - \int_0^\infty \left(\frac{\partial u}{\partial \eta}\right)^2 f''(u)d\eta. \quad (IV.166)$$

Let us introduce the notation

$$\theta = \frac{1}{\frac{\partial u}{\partial \eta}}; \qquad \theta_0 = \frac{1}{\left(\frac{\partial u}{\partial \eta}\right)_0} .$$

Then the integral expression (IV.166) can be written in the form

$$\frac{d}{d\xi} \int_0^1 \theta uf(u)du = \frac{U}{U} \int_0^1 \theta(1 - u^2)f'(u)du + \bar{v}_0 f(0) -$$

$$- \frac{f'(0)}{\theta_0} - \int_0^1 \frac{f''(u)}{\theta} du. \quad (IV.167)$$

The special case of equation (IV.167) for f(u)=1-u is the analog of the Karman integral relation for the system (IV.162) and (IV.163)

$$\frac{d}{d\xi} \int_0^1 \theta u (1 - u) du = \frac{U}{U} \int_0^1 \theta(1 - u^2)du + \frac{1}{\theta_0} - \bar{v}_0 f(0).$$

As the functions f(u), hereafter we shall take the power system $f(u)=(1-u)^n$, (n=1, 2 ..., k). Let us represent the desired function θ by an interpolation series in the k-th approximation

$$\theta = \frac{1}{1 - u}(a_0 + a_1 u + \cdots + a_{k-1}u^{k-1}). \quad (IV.168)$$

The coefficients a_m will be selected so that for u=m/k (m=0, 1, ..., k-1) expression (IV.168) will compare exactly with the corresponding value of θ_m.

Analogously, we take

$$\int_0^1 (1 - u)(b_0 + b_1 u + \cdots + b_{k-1}u^{k-1}).$$

225

When compiling the interpolation series for θ and $1/\theta$, consideration is given to the singularity of the desired function θ, namely, $\theta \to \infty$ for $u=1$. Coefficients b_m are selected just as a_m.

Let us then compile the integral relations for k functions $f(u)$. Substitution of the interpolation expressions for θ and $1/\theta$ in (IV.167) gives a system of ordinary differential equations with respect to values of θ_0, θ_1, ..., θ_{k-1} $[\theta_m = \theta \ (\xi, u_m)]$. This system is called the k-th approximation system.

Let us present the final form of the approximating expressions and the systems of equations for the first three approximations. These systems are "universal," for values connected with specific assignment of the calculated case are the coefficients $\dot{U}/u$ and $\bar{v}_0$.

1. First approximation system.

Approximating the expressions:

$$\theta = \frac{\theta_u}{1-u}; \quad \frac{1}{\theta} = \frac{1}{\theta_0}(1-u).$$ (IV.169)

The differential equations (the dot-dash differentiation with respect to ξ):

$$\dot{\theta}_u + 3\frac{\dot{U}}{U}\theta_u = \frac{2}{\theta_0} + 2\bar{v}_0.$$ (IV.170)

3. The second approximation system:

Approximating expression:

$$\theta = \frac{1}{1-u}[\theta_u(1-2u) + \theta_1 u];$$

$$\frac{1}{\theta} = (1-u)\left[\frac{1}{\theta_u}(1-2u) + \frac{1}{\theta_1}4u\right].$$ (IV.171)

Differential equations:

$$\left.\begin{array}{l}\dot{\theta}_u + \frac{\dot{U}}{U}(9\theta_u + 7\theta_1) = \frac{31}{\theta_u} - \frac{32}{\theta_1} + 18\bar{v}_0; \\[2mm] \dot{\theta}_1 + \frac{\dot{U}}{U}(40\theta_u + 60\theta_1) = \frac{20}{\theta_u} - \frac{16}{\theta_1} + 12\bar{v}_0.\end{array}\right\}$$ (IV.172)

3. Third approximation system.

Approximating expressions:

226

$$0 = \frac{1}{1-u}\left[\theta_0\left(1 - \frac{9}{2}u + \frac{9}{2}u^2\right) + \theta_1(4u - 6u^2) + \right.$$
$$\left. + \theta_2\frac{1}{2}(-u + 3u^2)\right];$$
$$\frac{1}{\theta} = (1-u)\left[\frac{1}{\theta_0}\left(1 - \frac{9}{2}u + \frac{9}{2}u^2\right) + \right.$$
$$\left. + \frac{1}{\theta_1}\frac{9}{2}(2u - 3u^2) + \frac{1}{\theta_2}\cdot\frac{9}{2}(-u + 3u^2)\right].$$

(IV.173)

Differential equations:

$$\dot{\theta}_0 + \frac{\dot{U}}{U}\left(\frac{67}{2}\theta_0 + 40\theta_1 - \frac{7}{2}\theta_2\right) = \frac{225}{\theta_0} - \frac{234}{\theta_1} + \frac{9}{\theta_2} + 72\bar{v}_0;$$
$$\dot{\theta}_1 + \frac{\dot{U}}{U}\left(\frac{67}{12}\theta_0 + \frac{28}{3}\theta_1 + \frac{13}{12}\theta_2\right) = \frac{39}{\theta_0} - \frac{51}{2\theta_1} - \frac{12}{\theta_2} + 18\bar{v}_0;$$
$$\dot{\theta}_2 + \frac{\dot{U}}{U}\left(-\frac{83}{6}\theta_0 - \frac{52}{3}\theta_1 + \frac{31}{6}\theta_2\right) = -\frac{99}{\theta_0} + $$
$$+ \frac{120}{\theta_1} - \frac{15}{\theta_2} - 24\bar{v}_0.$$

(IV.174)

Let us consider the special case where $U = x^m$. Converting to the coordinates ξ and η, we have

$$\xi = \int_0^x U\,dx = \frac{x^{m+1}}{m+1}; \quad x = (m+1)^{\frac{1}{m+1}}\xi^{\frac{1}{m+1}};$$
$$\eta = \int_0^x U\,dy = x^m y; \quad y = \eta x^{-m} = (m+1)^{-\frac{m}{m+1}}\xi^{\frac{-m}{m+1}}.$$

As a result, we obtain

$$U = (m+1)^{\frac{m}{m+1}}\xi^{\frac{m}{m+1}};$$
$$\frac{\dot{U}}{U} = \frac{m}{(m+1)\xi} = \frac{\beta}{2\xi}; \quad \beta = \frac{2m}{m+1}.$$

Here by x, y, U, just as before, we mean the dimensionless values.

In the investigated case the approximating systems have an exact solution [59]

$$\theta_\kappa = A_\kappa \sqrt{\xi}.$$

(IV.175)

Here the values of A_k are found as solutions of the corresponding algebraic systems obtained by substitution of expression (IV.175) in the systems of differential equations (IV.170), (IV.172), (IV.174) for different approximations.

Thus, for the first approximation we shall have

$$A_0(1 + 3\beta) = \frac{4}{A_0} + 4\bar{v}_0\sqrt{\xi},$$

227

in the second approximation:

$$A_0 + \beta(9A_0 + 7A_1) = \frac{68}{A_0} - \frac{64}{A_1} + 36\bar{v}_0 \sqrt{\xi};$$

$$A_1 + \beta(4A_0 + 6A_1) = \frac{40}{A_0} - \frac{32}{A_1} + 24\bar{v}_0 \sqrt{\xi}$$

and analogously for systems of higher approximations.

In order to obtain the solutions of algebraic systems it is necessary to take the dimensionless ventilation law in the form

$$\bar{v}_0 \approx \frac{1}{\sqrt{\xi}}.$$

In dimensional form this law is rewritten as

$$\frac{v_0}{U_0} \approx \frac{U}{U_0} \frac{\sqrt{Re}}{\sqrt{\xi}} = (m+1)^{\frac{m}{m+1}} \xi^{\frac{m-1}{2(m+1)}}. \tag{IV.176}$$

The ventilation law (IV.176) gives physically real results only for m<1 and, correspondingly, for β<1.

For $v_0=0$, from the above-presented formulas, the results of A. A. Dorodnitsyn are obtained.

The investigated case of $U=x^n$ permits investigation of the problem of convergence of successive approximations and accuracy of the approximate systems. The calculations performed by A. A. Dorodnitsyn for an uncontolled laminar boundary layer demonstrated that the third approximation gives satisfactory results, especially far from separation. Therefore it is possible to state that when solving the problem of suction of a laminar boundary layer, the accuracy of the approximate systems increases significantly.

In accordance with the recommendations of A. A. Dorodnitsyn for an arbitrary velocity law $U(\xi)$ the solutions of the type of (IV.175) can be used as initial values for θ_k which permit us to depart from the singular point $\xi=0$ and then apply any methods of numerical integration of the systems of ordinary differential equations.

After determining the values of θ_k, it is easy to determine all of the boundary layer characteristics.

The frictional stress on the wall τ_0 is expressed in terms of dimensionless values as follows:

$$\frac{2\tau_0}{\rho U_0^2} = 2\rho \bar{U}^2 \left(\frac{\partial \bar{U}}{\partial \eta}\right)_{\eta=0} \frac{1}{\sqrt{Re}}.$$

The local friction coefficient will be defined by the formula

$$\zeta_f = \frac{2\tau_0}{\rho \bar{U}^2 U_0^2} = \frac{2}{\sqrt{Re}} \frac{1}{\theta_n}.$$

228

The expressions for the provisional thicknesses of the boundary layer δ* and δ** depend on the approximation number.

The general formulas for δ* and δ** have the form

$$\bar{\delta}^* = \frac{\delta^*}{L} = \frac{1}{\sqrt{Re}} \cdot \frac{1}{\bar{U}} \int_0^1 \theta\,(1-u)\,du;$$

$$\bar{\delta}^{**} = \frac{\delta^{**}}{L} = \frac{1}{\sqrt{Re}} \cdot \frac{1}{\bar{U}} \int_0^1 \theta u\,(1-u)\,du.$$

(IV.177)

Substituting the approximating expressions (IV.169), (IV.171) and (IV.173) in place of θ in (IV.177), we find

$$\delta^* \bar{U} \sqrt{Re} \approx \theta_0 \approx \frac{1}{2}\,\theta_1 \approx \frac{1}{4}\,(\theta_0 + \theta_2);$$

$$\delta^{**} \bar{U} \sqrt{Re} \approx \frac{1}{2}\,\theta_0 \approx \frac{1}{3}\,\theta_1 - \frac{1}{6}\,\theta_0 \approx \frac{1}{8}\,\theta_0 - \frac{1}{6}\,\theta_1 + \frac{5}{24}\,\theta_2$$

for the 1st, 2d, and 3d approximations, respectively.

It must be noted that the above-presented formulas become meaningless at the separation point, for here θ_0 goes to infinity. A. A. Dorodnitsyn recommends using the following approximating epxressions at the separation point, which must replace the interpolation series (IV.168)

$$\theta = \frac{1}{(1-u)\sqrt{u}}\,(c_0 + c_1 u + \cdots + c_{K-2} u^{K-2}).$$

(IV.178)

The coefficients c_m are selected from the condition of insuring identical coincidence of expression (IV.178) with values of θ_m at the points u=m/k (m≠0, k≠0).

BIBLIOGRAPHY

1. Fabrikant, N. Ya. AERODINAMIKA [Aerodynamics], Moscow, Izd. Nauka, 1964.

2. Emmons, H. W.; Leigh, D. C. "Tabulation of the Blasius Function with Blowing and Suction," AERONAUTIC. RES. COUN. CURRENT PAPER, No 157, 1954.

3. Schlichting, H. TEORIYA POGRANICHNOGO SLOYA [Boundary Layer Theory], Moscow, IL, 1956.

4. Loytsyanskiy, L. G. LAMINARNYY POGRANICHNYY SLOY [Laminar Boundary Layer], Moscow, GIFML, 1962.

5. Loytsyanskiy, L. G. AERODINAMIKA POGRANICHNOGO SLOYA [Boundary Layer Aerodynamics], Moscow-Leningrad, Gostekhizdat, 1941.

6. Goldstein, S. "A Note on the Boundary Layer Equations," PROC. CAMBR. PHIL. SOC., Vol 35, 1939, p 338.

7. Mangler, W. "Die 'ähnlichen" Lösungen der Prandtlischen Grenzschicht gleichungen," ZAMM, Vol 23, 1943, p 243.

8. Wuest, W. "Survey of Calculation Methods of Laminar Boundary Layers with Suction in Incompressible Flow," BOUNDARY LAYER AND FLOW CONTROL, Vol 2, ed. Lachmann, G. V., Pergamon Press, 1961.

9. Blasius, H. "Grenzschichten in Flüssigkeiten mit kleiner Reibung," Z. MATH U. PHYS., Vol 56, 1908, p 1.

10. Howarth, L. "On the Solution of the Laminar Boundary Layer Equations," PROC. ROY. SOC., London, Ser. A., Vol 164, No 919, 1938.

11. Görtler, H. "A New Series for the Calculation of Steady Laminar Boundary Layer Flows," J. MATH. MECH., Vol 6, 1957, p 1.

12. Görtler, H. "On the Calculation of Steady Laminar Boundary Layer Flows with Continuous Suction," J. MATH. MECH., Vol 6, 1957, p 323.

13. Kozlov, L. F.; Pikin, Yu. D. "Computer Integration of the Faulkner-Skan Equation for the Case of a Porous Surface," ISSLEDOVANIYA PO PRIKLADNOY GIDRODINAMIKE [Research in Applied Hydrodynamics], Kiev, izd. Naukova dumka, 1965.

14. Kochin, N. Ye.; Kibel', I. A.; Roze, N. V. TEORETICHESKAYA GIDROMEKHANIKA [Theoretical Hydromechanics], Part II, ONTI, 1937.

15. Leybenzon, L. S. "Energy Form of the Integral Condition in Boundary Layer Theory," TR. TSAGI [Works of the Central Institute of Aerohydrodynamics], No 240, 1935.

16. Schlichting, H. "Ein Näherungsverfahren zur Berechnung der laminaren Reibungsschict mit Absaugung," ING.-ARCHIV, Vol 16, 1948, p 201.

17. Torda, T. P. "Boundary-Layer Control by Continuous Surface Suction or Injection," J. MATH. PHYS., Vol 31, 1952, p 206.

18. Truckenbrodt, E. "Ein einfaches Näherungsverfahren zum Berechnen der laminaren Reibungsschict mit Wbsaugung," FORSCH. ING. WES., Vol 22, 1956, p 147.

19. Kozlov, L. F.; Tsyganyuk, A. I. "Use of Sixth-Degree Polynomials for Calculating a Boundary Layer in the Presence of Suction," Kiev, PRIKLADNAYA MEKHANIKA [Applied Mechanics], No 4, 1966.

20. Wieghardt, K. "Über einen Energiesatz zur Berechnung laminarer Grenzschichten," ING.-ARCHIV, Vol 16, 1948, p 231.

21. Wighardt, K. "Zur Berechnung ebener und drehsymmetrischer Grenzschicten mit kontinuierlicher Absaugung," ING.-ARCHIV, Vol 22, 1954, p 368.

22. Wuest, W. "Entwicklung einer laminaren Grenzschicht hinter einer Absaugestelle," ING.-ARCHIV, Vol 17, 1949, p 199.

23. Head, M. R. "Approximate Methods of Calculating the Two-Dimensional Laminar Boundary Layer with Suction," BOUNDARY LAYER AND FLOW CONTROL, Vol 2, ed. by G. V. Lachmann, Pergamon Press, 1961.

24. Loytsyanskiy, L. G. "Approximate Method of Integrating Laminar Boundary Layer Equations in an Incompressible Gas," PMM [Applied Mathematics and Mechanics], Vol 13, No 5, 1949.

25. Kozlov, L. F. "Approximate Integration of Laminar Boundary Layer Equations on a Porous Surface in an Incompressible Fluid," PMTF [Applied Mechanics and Technical Physics], No 5, 1962.

26. Schaefer, H. "Laminare Grenzschicht zur Potentialströmung U=u, x^m mit Absaugung und Ausblasen," DEUTSCHE LUFTFAHRTFORSCHUNG, UM, 1944, p 2043.

27. Kozlov, L. F. "Calculation of an Axisymmetric Laminar Boundary Layer on a Porous Body in an Incompressible Fluid," INZHENERNO-FIZICHESKIY ZHURNAL [Engineering Physics Journal], No 2, 1962.

28. Iglisch, R. "Exacte Berechnung der laminaren Grenzschicht an der längsangeströmten ebenen Platte mit homogener Absaugung," SCHRIFTEN D. D. AKAD. LUFTFAHRTFORSCHUNG, Vol 8, 1944, p 1.

29. Pretsch, I. "Die Leistungsersparins durch Crenzschichtbeeinflüssung, beim Schleppen ebenen Platte," DEUTSCHE LUFTFAHRTFORSCHUNG, UM, No 3048, 1943.

30. Zolotov, S. S.; Khodorkovsky, V. S. "Optimum Suction Distribution to Obtain a Laminar Boundary Layer," INT. J. HEAT MASS TRANSFER, Vol 6, 1963, p 897, Pergamon Press.

32. Wortmann, F. "Grenzschicht-Absaugung," GRENZSCHICHTFORSCHUNG, SYMPOSIUM, Freiburg, Springer-Verlag, 1958.

33. Kozlov, L. F. "Approximate Method of Calculating Optimal Suction of Fluid from a Boundary Layer of Wing Sections with Porous Surface," PMTF, No 3, 1964.

34. Stepanov, Ye. I. "Integration of Laminar Boundary Layer Equations for Motion with Axial Symmetry," PMM, Vol 11, No 1, 1947.

36. Schlichting, H.; Bussman, K. "Exakte Lösungen für die laminare Grenzschicht mit Absaugung und Ausblasen," DTSCH. AKAD. LUFTFAHRTFORSCHUNG, Vol 7, 1943, p 25.

37. Kozlov, L. F. "Optimal Boundary Layer Suction on a Porous Plate in an Incompressible Fluid," INZH.-FIZ. ZHURNAL [Engineering-Physics Journal], No 10, 1963.

38. Loytsyanskiy, L. G. "Laminar Boundary Layer on a Solid of Revolution," DAN SSSR [Reports of the USSR Academy of Sciences], Vol 36, No 6, 1942.

39. Wuest, W. "Naherungsweise Berechnung und Stabilitätsverhalten von laminaren Grenzschichten mit Absaugung durch Einzelschlitze," ING.-ARCHIV, Vol 21, 1953, p 90.

40. Lachmann, G. F. "Laminarization Through Boundary Layer Conrol, AERON. ING. REV., Vol 13, No 8, 1954.

41. Görtler, H. "Ein Differenzenverfahren zur Berechnung der laminaren Grenzschichten," ING.-ARCHIV, Vol 16, 1948.

42. Witting, H. "Verbesserung des Differenzverfahrens von H. Görtler zur Berechnung laminaren Grenzschichten," Z. ANGEW. MATH. UND PHYS., Vol 4, 1953.

43. Reinboldt, W. "Zur Berechnung stazionärer Grenzschichten beikantinuierlicher Absaugung mit unstetig veränderlicher Absaugegeschwindigkeit," J. RATIONAL. MECH. AND ANAL., Vol 5, No 3, 1956.

44. Smith, A. M. O.; Clutter, D. W. "Solution of the Incompressible Laminar Boundary Layer Equation," AIAA JOURNAL, Vol 1, No 9, 1963.

45. Witting, H. "Unstable Form of Prandtl Boundary Layer Equations," PROBLEMA POGRANICHNOGO SLOYA I VOPROSY TEPLOPERADACHI [Boundary Layer Problem and Heat Transfer Problems], Moscow-Leningrad, Gosenergoizdat, 1960.

46. Saul'yev, V. K. INTEGRIROVANIYE URAVNENIY PARABOLICHESKOGO TIPA METODOM SETOK [Integration of Parabolic Type Equations by the Finite-Difference Method], Moscow, Fizmatgiz, 1960.

47. Lachmann, G. V. "The Case for Laminarization," SELECTED PAPERS ON ENGINEER-ING MECHANICS, 1955.

48. Fage, A.; Sargent, R. "Design of Suction Slots. Aeronautical Research Council," REPORTS AND MEMORANDA, No 2177, 1944.

49. Kornilova, N. N.; Khodorkovskiy, Ya. S. "Experimental Study of a Laminar Boundary Layer on a Plate with Transverse Slot," TR. LKI [Works of Leningrad Shipbuilding Institute], No 48, 1965.

50. Aliyev, R. Z.; Demin, V. Ya. "Calculation of Laminar Boundary Layer with Continuous Suction," TR. LPI [Works of Leningrad Polytechnical Institute], No 230, 1964.

51. Khodorkovskiy, Ya. S. "Calculation of Discrete Fluid Suction from a Boundary Layer," TR. LKI, No 48, 1965.

52. Besedin, L. N.; Khodorkovskiy, Ya. S. "Numerical Integration of the Faulkner-Skan Equation for Nonzero Boundary Conditions," TR. LPI, No 52, 1966.

53. Pol'skiy, N. I. "Self-Similar Solutions of the Mises Equation," TECHENIYA ZHIDKOSTEY I GAZOV [Fluid and Gas Flows], Kiev, izd. Nauka dumka, 1965.

56. Struminskiy, V. V. SBORNIK TEORETICHESKIKH RABOT PO AERODINAMIKE [Collection of Theoretical Papers on Aerodynamics], TsAGI, Oborongiz, 1957.

57. Basin, A. M. "A New Approximate Method of Calculating a Laminar Layer," DAN SSSR, Vol 40, No 1, 1943.

58. Shul'man, Z. P.; Berkovskiy, B. M. "Self-Similar Problem of a Laminar Boundary Layer on a Permeable Curvilinear Surface," IFZH [Engineering Physics Journal], Vol 6, No 12, 1963.

59. Dorodnitsyn, A. A. "A Method of Solving Laminar Boundary Layer Equations," PMTF, No 3, 1960.

CHAPTER V. LAMINAR-TO-TURBULENT BOUNDARY LAYER TRANSITION

§V.1. Theory of Laminar Boundary Layer Transition to Turbulent Under the Effect of Initial Flow Turbulence

The existing methods of determining the transition point can be divided into two groups.

The first group includes empirical methods based on the results of statistical processing of the experimental data. In these methods the influence of the initial turbulence of an external flow on transition of the laminar boundary layer to turbulent is for the most part considered in implicit form. Surveys of this type of research appear in references [27], [28].

The second group combines semi-empirical methods, which include the known methods of A. A. Dorodnitsyn and L. G. Loytsyanskiy [1], A. P. Mel'nikov [2], Van-Drist and Bloomer [32]. These methods permit consideration of the effect of the initial turbulence in an external flow on the extent of the laminar section in the boundary layer.

The basis for semi-empirical methods is the proposition that the cause of occurrence of turbulence in a laminar boundary layer under the effect of external disturbances is eddies. These eddies are generated near the surface of the body as a result of instantaneous local separations of the laminar layer formed as a result of pressure disturbances in the external flow. The idea of such a mechanism of influence of finite-amplitude external disturbances on transition of a laminar boundary layer to turbulent was apparently first stated by Taylor [3]. Empirical studies [4] have demonstrated that this transition mechanism in a boundary layer occurs only for initial turbulence of the flow, the degree of which exceeds 0.1 to 0.2%. The indicated scheme for the occurrence of a laminar boundary layer transition to turbulent permits an equation to be written for determining the transition point.

In order to explain the basic principles of the semi-empirical transition theory let us discuss the method of A. A. Dorodnitsyn and L. G. Loytsyanskiy [30] for calculating the transition point. Let us consider the condition of occurrence of separation in a laminar boundary layer which is written in the form [22]

$$f_s = \frac{U'\delta^{*2}}{\nu} = -0.089,$$

where f_s is the value of the boundary layer form parameter at the separation point;

U'=dU/dx, U(x) are the velocity distribution at the outer boundary of the layer.

The separating laminar flow has significantly less stability by comparison with the laminar boundary layer [28]; therefore in direct proximity to the separation point turbulent motion of the fluid sets up. It is expedient to rewrite the separation condition in the form

$$\frac{\nu U'}{U^2} \cdot \text{Re}^{**2} = f_s = -0,089,$$

for the value of Re**=Uδ**/ν in practice does not vary under the effect of small disturbances of the external flow velocity. Small random nonsteady disturbances can noticeably influence the dimensionless parameter $\nu U'/U^2$, changing it on the average by defined amount γ having negative significance so that the boundary layer separation will be shifted upstream. The indicated fact is explained in that the spatial frequency of the disturbances can be so great that the derivative of the longitudinal velocity of the disturbing motion d$\tilde{U}$/dx can be of the same order as U'. Thus, the condition of occurrence of separation of a laminar boundary layer under the effect of random disturbances can be written as follows:

$$\left(\frac{\nu U'}{U^2} + \gamma \right) \text{Re}^{**2} = f_s = -0,089.$$

Let us substitute the following value in the obtained expression

$$\frac{\delta^{**2}}{\nu} = \frac{0,46}{U^6} \int_0^x U^5(\xi)\, d\xi,$$

$$\text{Re}^{**2} = \text{Re}\varphi(\bar{x}),$$

where Re=U$_b$/ν; b is the characteristic linear dimension

$$\varphi(\bar{x}) = \frac{0,46}{\bar{U}^6} \int_0^{\bar{x}} \bar{U}^5(\xi)\, d\xi,$$

$$\left(\frac{1}{\text{Re}} \cdot \frac{\bar{U}'}{\bar{U}^2} + \gamma \right) \cdot \text{Re}\,\varphi(\bar{x}) = -0,089. \qquad (V.1)$$

The value of f_s and also the constants in the formula for δ** can be somewhat different [22], depending on the method of calculating the laminar boundary layer. In particular, the method of A. M. Basin [20] gives a value of f_s=-0.077 for the form parameter at the separation point. The dimensionless values are denoted by a bar at the top.

If the velocity distribution at the external boundary of the layer is known, the values of γ and Re, then, constructing the graph of the lefthand side of formula (V.1), it is possible to find a dimensionless coordinate x for which equality (V.1) occurs. This will be the transition point of the laminar boundary layer to turbulent. It is necessary to determine the value of γ in the discussed method on the basis of analyzing the experimental data.

Using the Taylor hypothesis [3], it is possible to establish the relation of γ to the turbulence characteristics of the external flow. For this purpose let us rewrite the basic equation for determining the coordinate of the separation point in the following dimensionless form

$$\left(-\frac{\mu}{\rho^2 U^3}\cdot\frac{dp}{dx}+\gamma\right)\mathrm{Re}^{**2} = -0,089. \tag{V.2}$$

In accordance with reference [30], we shall consider that

$$\gamma \sim \frac{\mu}{\rho^2 U^3}\left[\frac{\widetilde{\partial p}}{\partial x}\right], \tag{V.3}$$

where $[\widetilde{\partial p}/\partial x]$ denotes the square root of the mean square value of the pressure pulsations on the outer boundary of the boundary layer. Making some additional assumptions [30], it is possible to find the relation of the pulsation pressure to the characteristics of the oncoming flow, obtaining the equality

$$\gamma = \frac{\gamma_0}{\sqrt{\mathrm{Re}}}\,\Omega\,(\overline{U}),$$

where $\gamma_0 < 0$ is an experimental constant;

$$\Omega\,(\overline{U}) = \frac{\overline{U}^{-4}}{(1+\overline{U}^{-4})^{5/4}}; \quad \mathrm{Re} = \frac{Ub}{\nu}.$$

The transition point is calculated by a formula obtained from (V.1),

$$\mathrm{Re}\,\gamma = -\frac{0,089}{\varphi\,(\overline{x})} - \frac{\overline{U}'}{\overline{U}^2},$$

and the expression $\mathrm{Re}\,\gamma = \gamma_0 \sqrt{\mathrm{Re}}\cdot\Omega\,(\overline{U})$.

Constructing the righthand sides of these equations as a function of $\overline{x}$ for given γ_0 and Re, we find the intersection of the corresponding curves, thus defining the transition point coordinate. The empirical nature of the method is manifested in the method of finding γ_0. The scheme for the occurrence of turbulent motion inside the boundary layer is qualitatively confirmed by the fact that external turbulence causing transition is significantly less with respect to intensity than the turbulent motion formed in the boundary layer.

For practical use of the method of A. A. Dorodnitsyn and L. G. Loytsyanskiy, difficulties arise in selecting the value of the parameter γ_0 characterized, in accordance with the authors' proposition, only by the magnitude of the velocity disturbances in the external flow. However, Ye. M. Minskiy [29] demonstrated experimentally that the parameter γ_0 depends also on the longitudinal pressure gradient at the outer boundary of the boundary layer.

Let us proceed with the discussion of a somewhat different method of determining the critical Reynolds number at the transition point [6]. As before, we shall consider that turbulence in the boundary layer occurs under the effect of finite-amplitude disturbances caused by eddies generated at the surface of the body and formed as a result of local separations of the boundary layer. In the investigated case, finite disturbances are introduced into the boundary layer by turbulence of the oncoming flow.

236

Considering (V.3) let us represent formula (V.2) as follows:

$$\frac{\delta_t^{**}}{\nu} \cdot \frac{1}{\rho U} \left\{ \left| \frac{dp}{dx} \right| + \left| \frac{\tilde{\partial p}}{dx} \right| \right\} = |f_s| = 0,089. \tag{V.4}$$

Oncoming flow turbulence will be considered isotropic. Let us assume that the surface of the body does not distort the isotropicity of the turbulence at the outer boundary of the boundary layer. Then for the relation between the longitudinal pressure gradient pulsations $[\partial p/\partial x]$ and the velocity pulsations at the outer boundary of the boundary layer, it is possible to use the relations of statistical turbulence theory [3]

$$\lambda_1 \sim L_\delta \sqrt{\frac{\nu}{u_1' L_\delta}}; \quad \left[\frac{\tilde{\partial p}}{\partial x} \right] \sim \frac{\rho u_1'^2}{\lambda_1}, \tag{V.5}$$

where u'_1 is the mean square value of the velocity pulsation at the outer boundary of the boundary layer;

λ_1 is the size of the "least vortex";

L_δ is the scale of the turbulence in the external flow.

Isolating the critical Reynolds number $Re_t^{**} = U\delta_t^{**}/\nu$ and the Taylor parameter $\left[\varepsilon \left(\frac{L}{L_0} \right)^{1/5} \right]$, at the transition point, the transition condition of (V.4) is transformed by the expressions of (V.5) to the form

$$Re_t^{**} = \frac{A_1 \left(|f_s| + f \right)^{1/2}}{\left[\varepsilon \left(\frac{L}{L_0} \right)^{1/5} \right]^{5/4} \left[\left(\frac{u_0'}{u_1'} \right) \left(\frac{U_0}{U} \right) \left(\frac{L_0}{L_\delta} \right)^{1/5} \right]^{5/4} \cdot \left(\frac{\nu}{uL} \right)^{1/4}}, \tag{V.6}$$

where $\varepsilon = u'_0/U_0$ is the degree of turbulence in the oncoming flow;

U_0 is the velocity of the oncoming flow;

u_0 is the mean square value of the velocity pulsation in the oncoming flow;

L is the body length;

L_0 is the scale of the oncoming flow turbulence.

With an increase in the degree of turbulence of the external flow the critical Reynolds number calculated by formula (V.6) diminishes and can reach a value less than the critical Reynolds number at the loss of stability point. However, experiments show [27] that the critical Reynolds number calculated by the loss of stability point is the limit below which turbulent motion cannot exist in the boundary layer. Therefore it is expedient to introduce the lower value of the critical Reynolds number Re_H^{**} into formula (V.6), writing it as follows:

$$Re_l^{\cdot\cdot} = Re_\mu^{\cdot\cdot} + \frac{A_1 \left(|f_s| + f\right)^{1/2}}{\left[f\left(\frac{L}{L_0}\right)^{1/5}\right]^{5/4}\left[\left(\frac{u_0'}{u_1'}\right)\left(\frac{U_0}{U}\right)\left(\frac{L_0}{L_\delta}\right)^{1/5}\right]^{5/4}\left(\frac{1}{Re}\right)^{1/4}}.$$

(V.7)

It is recommended that the values of the lower critical Reynolds numbers for different pressure gradients and distributed fluid suction laws be calculated by the approximate formula (IV.117)

$$Re_\mu^{\cdot\cdot} = \exp\left(A - BH\right),$$

where $H = \delta^*/\delta^{**}$ is the ratio of the provisional thicknesses of the boundary layer;

$A = 25.9$ and $B = 7.76$ are constants.

For more exact calculation of the lower values of the critical Reynolds numbers it is necessary to investigate the fluid flow stability in the boundary layer (see Chapter I).

The values of u_1' and L_δ entering into formula (V.4) are the mean square value of the velocity pulsation and turbulent scale on the outer boundary of the layer, respectively. Since usually the turbulence characteristics of the oncoming flow u_0' and L_0 are known in the calculations, it is necessary to express u_1' and L_δ in terms of the mentioned characteristics. In order to establish this function let us use the known relations of [1]

$$\frac{u_1'}{u_0'} \sim \frac{\left(\frac{U}{U_0}\right)^3}{1 + \left(\frac{U}{U_0}\right)^4},$$

(V.8)

$$\frac{L_\delta}{L_0} \sim \left(\frac{U}{U_0}\right).$$

(V.9)
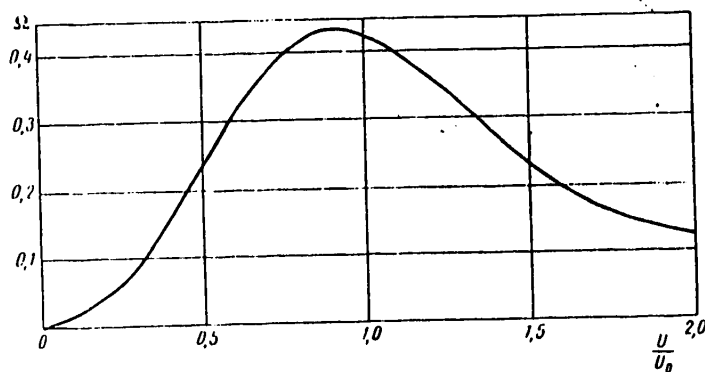
Figure V.1. Graph of the function $\Omega(U/U_0)$

Substituting expressions (V.8) and (V.9) in formula (V.7) and performing the necessary transformations, we obtain the final expression for the critical Reynolds number at the transition point

$$\mathrm{Re}_t^{**} = \mathrm{Re}_H^{**} + \frac{A_1 \left(|f_s| + f\right)^{1/2}}{\left[\nu \left(\frac{L}{L_0}\right)^{1/5}\right]^{5/4} \mathrm{Re}^{-1/4} \, \Omega \left(\frac{U}{U_0}\right)}, \qquad (V.10)$$

where the function $\Omega = \dfrac{\left(\frac{U}{U_0}\right)^2}{\left[1 + \left(\frac{U}{U_0}\right)^4\right]^{5/4}}$ is illustrated in Figure V.1.

In the case where the surface of the body is smooth, for given turbulence of the oncoming flow the difference $\mathrm{Re}_t^{**} - \mathrm{Re}_H^{**}$ is proportional to the value of $(|f_s|+f)^{1/2}$ [see equation (V.10)].

At the same time, by the data in reference [2] the mentioned difference is proportional to $(|f_s|+f)^{2/3}$. A comparison of these results with the experimental data indicates (Figure V.2) that formula (V.10) corresponds better to reality.
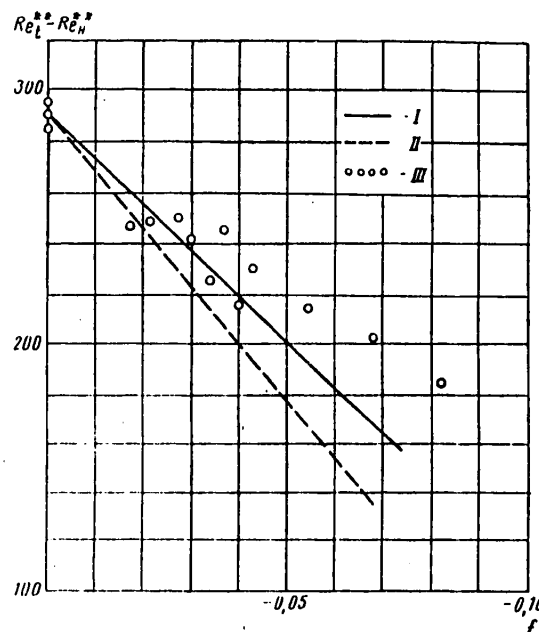
Figure V.2. Comparison of the function $\mathrm{Re}_t^{**}-\mathrm{Re}_H^{**}=\phi(f)$ with the experimental data.
I -- calculation by formula (V.10); II -- by the Mel'nikov data;
III -- experiments of [7].

239

Formula (V.10) includes the constant A_1, the values of which cannot be determined theoretically. Analysis of the experimental data of [4], [5] demonstrated that $A_1=0.22$.

In order to check the semi-empirical formula (V.10), the results of the calculations and experiments on an elliptic cylinder with L/B=3 were compared. The comparison (Figure V.3) demonstrated satisfactory correspondence of the calculated results to the experimental data.

In the practical calculations the scale of the turbulence is not always known, for its definition is related to fine, tedious measurements. This value enters into equation (V.10) to a power of 1/4 so that even with significant variation of it the critical Reynolds number varies little. The value of the function Ω also varies insignificantly in the calculations of the transition point.

Comparison of the calculated and experimental data demonstrated that it is approximately possible to assume

$$A_1\left(\frac{U_0 L}{\nu}\right)^{1/4}\Omega^{-1}\left(\frac{U}{U_0}\right)=2.$$

Then formula (V.10) is simplified significantly and reduces to the form

$$\mathrm{Re}_t^{\bullet\bullet} = \mathrm{Re}_u^{\bullet\bullet} + \frac{c\,(|f_s|+f)^{1/2}}{e^{5/4}}, \tag{V.11}$$

which is very convenient for practical use. The constant c in formula (V.11) is equal to 1.88.
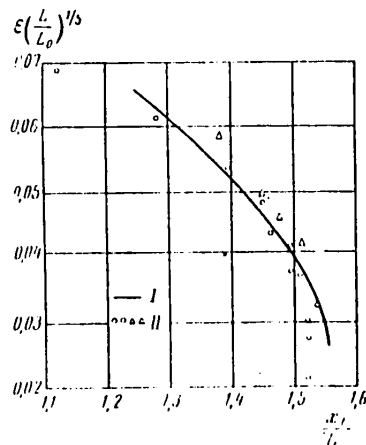
Figure V.3. Comparison of the results of calculating the transition point with experimental data.
I -- calculation; II -- experiment
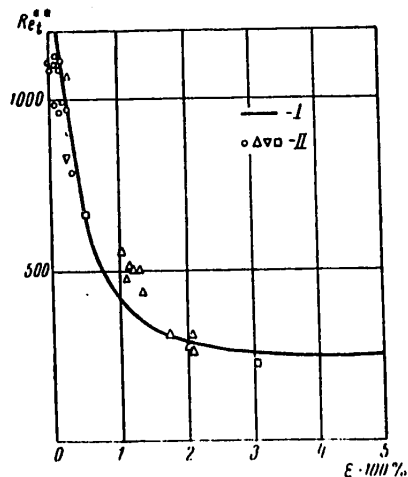
Figure V.4. Comparison of the experimental values of the critical Reynolds number with the calculated values
I -- calculation; II -- experiment

240

The dependence of the critical Reynolds number for a plate on the degree of turbulence can be calculated by the formula

$$\text{Re}''_{t_{nn}} = 225 + \frac{0.089^{1/2}c}{\varepsilon^{5/4}}.$$

(1)

(V.12)

Key: 1. plate

The calculated and experimental values of the local critical Reynolds numbers at the transition point as a function of the degree of turbulence of the oncoming flow were compared in Figure V.4 (see formula V.12). Considering the dispersion of the experimental points, it is possible to recognize the comparison as entirely satisfactory with the exception of the segment of the curve corresponding to an insignificant (no more than 0.1%) degree of turbulence of the oncoming flow. The reason for the divergences in this case is unsuitability of the transition scheme used in this section for very small velocity disturbances introduced into the boundary layer by turbulence of the oncoming flow.

It is of interest to note that comparison of the data obtained with the graphs for calculating the transition point proposed in references [8]-[10] indicates correspondence of the mentioned graphs to formula (V.11) for $\varepsilon=0.15$ to 0.35%. This fact is an additional confirmation of correctness of formula (V.11) inasmuch as the experimental data used for comparison of these graphs were obtained in the indicated range of the degree of turbulence of the oncoming flow.

In practice, calculation of the transition point for a body with given shape consists in calculating the Reynolds number Re** and also the parameter f for a laminar layer, depending on the coordinate x reckoned from the front critical point along the lines of the body. The characteristics of a laminar boundary layer are calculated by the usual method. For the calculated parameters by formula (V.11) values are determined for the critical Reynolds number Re^{**}_t, and the following equation is solved graphically

$$\text{Re}''(x) = \text{Re}''_t.$$

(V.13)

The value of the root of equation (V.13) is the transition point coordinate.

§V.2. Influence of Surface Roughness on the Laminar Boundary Layer Transition to Turbulent

One of the basic factors defining the position of the transition point of a laminar boundary layer to turbulent is surface roughness of the body. Accordingly, studies aimed at investigating the effect of roughness on turbulization of the boundary layer have significant theoretical and practical interest.

The study of the effect of roughness on the laminar boundary layer transition to turbulent is found in a large number of experimental papers. H. Dryden [11], classifying his experimental results, arrived at the conclusion that the ratio of the critical Reynolds number at the transition point for a rough plate to the corresponding value for a smooth plate is a "universal function" of the ratio of the height of a roughness element to the pulse loss thickness or the displacement

flow at the location of the roughness element. Universality of the mentioned
function consists in its independence of the initial turbulence of the oncoming
flow. A comparison [12] of the "universal function" with the experimental data of
Feindt [7] obtained on a setup with large initial flow turbulence did not confirm
Dryden's proposition. We also arrive at an analogous conclusion when analyzing
the experimental results of Japanese researchers [13], [14]. Accordingly, when
determining the influence of roughness on the laminar boundary layer transition to
turbulent, Dryden's "universal function" must be used with caution. Nevertheless,
this function is widely used in aerodynamic calculations, for example, in the
calculation technique proposed by G. Lachmann [15].

A nonuniform flow caused by the stagnating effect of the fluid viscosity near the
body surface hits a roughness element located in the boundary layer. By the
effect on the roughness element, it is possible approximately to replace the non-
uniform flow in a boundary layer by a uniform flow with an average velocity.
Analysis of the experimental data of [11], [7], [13], [14], [16], [17], [33]
demonstrated that the roughness element becomes the cause of premature turbuliza-
tion of the boundary layer.when the Reynolds number constructed by the average
velocity and height of the roughness element is greater than 30-40. After circular
cylinders and other poorly streamlined bodies in a uniform flow, when the mentioned
Reynolds numbers are reached, a Benard-Karman vortex sheet is formed. Accord-
ingly, it is possible to assume that flow over a roughness element is also
accompanied by periodic vortex formation. As a result of the shielding effect of
the body surface, after the roughness element a vortex chain must be formed, and
not the vortex sheet as in the case of unlimited flow over a circular cylinder.

Experiments in visual representation of the flow in the boundary layer by dyed
streams confirmed this proposition [17]. After passage by a two-dimensional rough-
ness element located on a plate, the dyed stream of fluid twists into rectilinear
vortex plaits. Then, from the individual vortex plaits formed periodically on flow
over a roughness element, a vortex chain is formed. At a significant distance from
the roughness element, the vortex plait assumes a sawtooth shape with clearly
expressed periodicity in the transverse direction.

Passage of a vortex chain must cause periodic velocity pulsations in the boundary
layer, which influence the velocity redistribution across the layer and also
obviously serve as a source of turbulent disturbances in the layer. The velocity
profile in a boundary layer in the absence of a roughness element (1) is depicted
shematically in Figure V.5. As a result of the disturbing effect of the vortex
plaits, the velocity profile acquires the shape denoted by 2 at some point in time,
and the state of the boundary layer becomes close to preseparation. Then the pre-
maturely separated laminar layer decomposes into individual vortices and becomes
turbulent. Schematizing the flow in this way, it is possible to see a direct
relation between premature separation of a laminar boundary layer and transition
of the laminar layer to turbulent caused by a roughness element.

This schematization of the flow permits generalization of Taylor's hypothesis
regarding the mechanism of transition of the laminar boundary layer to turbulent
to the investigated case of a rough surface. The mentioned hypothesis was formu-
lated by Taylor [3] when studying the effect of the initial turbulence of a flow
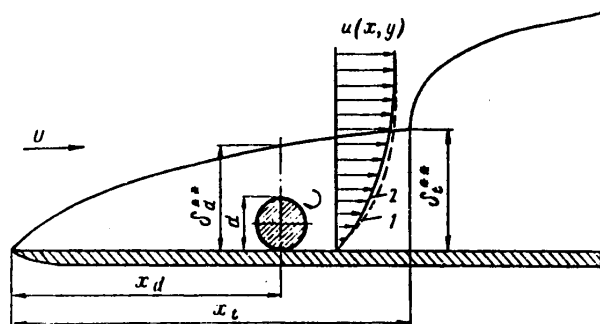on the transition of a laminar layer to turbulent.

Figure V.5. Diagram of the transition of a laminar boundary layer
to turbulent after a single roughness element

In the majority of cases the transition of a laminar layer to turbulent is simultaneously influenced by the initial turbulence and the surface roughness. In this section we shall limit ourselves to studying the effect of roughness on the laminar layer transition to turbulent. This approach has practical significance for low-turbulent flows (less than 0.1-0.2%).

For determination of the conditions of local separation we shall use formula (V.4).

A turbulent flow formed as a result of the formation of vortices on the roughness element will be considered isotropic. Then, using the results of statistical turbulence theory [3], let us apply the first formula of (V.5).

Inasmuch as the formation of vortices on flow around a roughness is taken as the only cause of premature transition of a laminar boundary layer to turbulent in this section, the size of the "least vortex" in formula (V.5) will be taken as a value proportional to the height of the roughness element, that is, λ_1~d, where d is the roughness element height.

Considering velocity pulsations resulting from the formation of vortices on flow over a roughness element, it is possible approximately to consider that near the body surface

$$u' \sim \frac{\Gamma}{d},$$

(V.14)

where Γ is the circulation of a vortex separating from the roughness element.

H. Schlichting [18] demonstrated that flow over a roughness element located in the boundary layer can be approximately considered as uniform flow over this element with a velocity equal to the corresponding value in the boundary layer at a roughness element height in place of the location of the roughness element. Taking this into account, in the investigated case it is possible to write that the circulation of a vortex formed on flow around a roughness element

$$\Gamma \sim d u_\delta$$

(V.15)

243

FOR OFFICIAL USE ONLY

where u_1 is the velocity in the boundary layer at the height of the roughness element from the surface.

Using the linear velocity distribution law in a laminary boundary layer, we obtain

$$u_1 \sim U\left(\frac{d}{\delta_1^{**}}\right),$$ (V.16)

where δ_1^{**} is the pulse loss thickness in the boundary layer at the location of the roughness element;

U is the velocity on the outer boundary of the layer.

Expression (V.16) is a version of one of the velocity profiles in a laminar boundary layer proposed by K. Pohlhausen [19].

Substituting expressions (V.15) and (V.16) in expression (V.14),we obtain

$$u' \sim U\left(\frac{d}{\delta_1^{**}}\right).$$ (V.17)

Then, isolating the critical Reynolds number at the transition point of the laminar boundary flow to turbulent $Re_t^{**}=U\delta_t^{**}/\nu$ by relations (V.5) and (V.17), we convert condition (V.4) to the following form:

$$Re_t^{**} = Re_n^{**} + \frac{A_1\left[(|f_s|+f)\dfrac{Ud}{\nu}\right]^{1/2}}{\left(\dfrac{d}{\delta_1^{**}}\right)^2},$$ V.18)

where A_1 is a constant.

The value of Re_H^{**} is introduced into equation (V.18) analogously to the case investigated in §V.1.

The values of the lower critical Reynolds numbers for different pressure gradients on the outer boundary of the boundary layer are determined using hydrodynamic stability theory. Formula (IV.117) is recommended for approximate estimation of this value.

It must be noted that the constant A_1 in formula (V.18) is the only value which cannot be determined theoretically. Comparison and analysis of the calculated and experimental data demonstrated that this value is universal and equal to $A_1=70$ to 80.

For check purposes, the calculated data using formula (V.18) were compared with the known experimental data of [11], [7], [13], [14]. The comparison results which are shown in Figure V.6 (the circles are the experimental data; the solid line is the calculations by the presented formulas) permit confirmation of good correspondence of formula (V.18) to the experimental data.

244

—

APPROVED FOR RELEASE: 2007/02/09: CIA-RDP82-00850R000400080056-8

FOR OFFICIAL USE ONLY

In the proposed theory it was considered that the only cause of premature transition is surface roughness. Therefore it is natural that comparison of the theoretical and experimental data (Figure V.6) turned out to be better, the smaller the initial turbulence of the flow.

Let us consider a special case of laminar boundary layer transition on a plate under the effect of roughness which is of importance for practical applications. The calculations by formula (V.18) for this case (f=0) allowed the graphical relation (Figure V.7) for the local critical Reynolds number of the transition Ux_t/ν to be obtained as a function of the Reynolds number Ux_1/ν constructed by the velocity of the oncoming flow and the distance of a single roughness element from the forward edge x_1.

The proposed diagram makes it possible to solve various practical problems. From the presented graph, in particular, it follows that the transition of a laminar boundary layer to turbulent will take place directly after a single roughness element $(x_t=x_1)$ if

$$\frac{Ud}{\nu} \geqq 800 \text{ to } 900.$$
(V.19)

Using the formula of A. M. Basin [20] for the velocity distribution across the boundary layer, let us transform expression (V.19) to the form

$$\frac{u_1 d}{\nu} = (800 \text{ to } 900) \sin \frac{\pi}{2} \frac{d}{\delta_1},$$
(V.20)

where δ_1 is the boundary layer thickness for $x=x_1$.

The relation obtained in this form is of interest in connection with the formula proposed by Fage [16]

$$\frac{u_1 d}{\nu} = 400.$$
(V.21)

This formula permits determination of the height of a single roughness element, for which at the given flow velocity the transition of the laminar boundary layer to turbulent takes place directly after the roughness element.

Figure V.8 shows the comparison of the calculation results by formulas (V.20) (the solid line) and (V.21) (the dotted line with the corresponding experimental data of Fage [16] and Japanese researchers [13], [14] (noted by the circles). These data confirm the correctness of the proposed formula (V.20), and they agree with the theoretical results obtained in reference [21].

Practical calculation of the transition point for a body of given shape and known surface roughness consists in calculation of the local Reynolds number Re** and also the parameters f and d/δ** for a laminar layer as a function of the coordinate x reckoned from the forward critical point along the lines of the body. It is possible to calculate the characteristics of the laminar boundary layer by ordinary methods [22]. Values of the critical Reynolds number Re_t** are determined for the calculated parameters by formula (V.18), and the equation of the type of (V.13) is solved graphically. The root of this equation is the transition point coordinate.

245

FOR OFFICIAL USE ONLY

APPROVED FOR RELEASE: 2007/02/09: CIA-RDP82-00850R000400080056-8
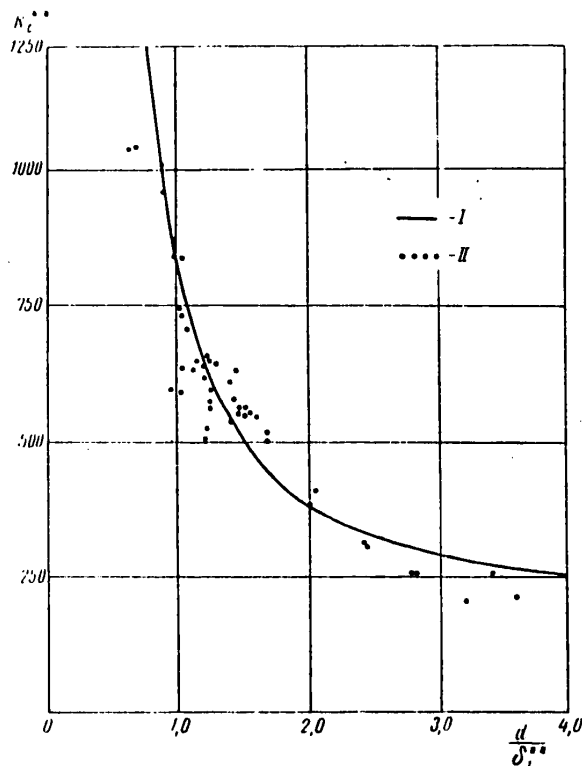
Figure V.6. Comparison of the calculation results with experimental data.
I -- calculation by formula (V.18); II -- experiment

The papers that study the influence of various types of surface roughness on the transition are finding broad application in model experiments in the model testing basins. Small Reynolds numbers by comparison with the full-scale units lead to the appearance of significant laminar sections of boundary layer on the ship models. The viscous drag of the models decreases compared to the turbulent flow conditions in the boundary layer, which is a cause for undesirable errors when recalculating to actual Reynolds numbers. Therefore special measures to turbulize the boundary layer of the models are taken in all of the model testing basins [40]-[42].

It is possible to accelerate the transition of the laminar boundary layer to the turbulent state by various methods:

a) By increasing the local surface roughness in the forward part of the model (pins of different shape, trip wires, strips with large grainy roughness);

b) By increasing the turbulence of the oncoming flow using gratings towed in front of the model;

c) By varying the physical properties of the fluid in order to increase the Reynolds number (for example, heating the water in the basin).

246
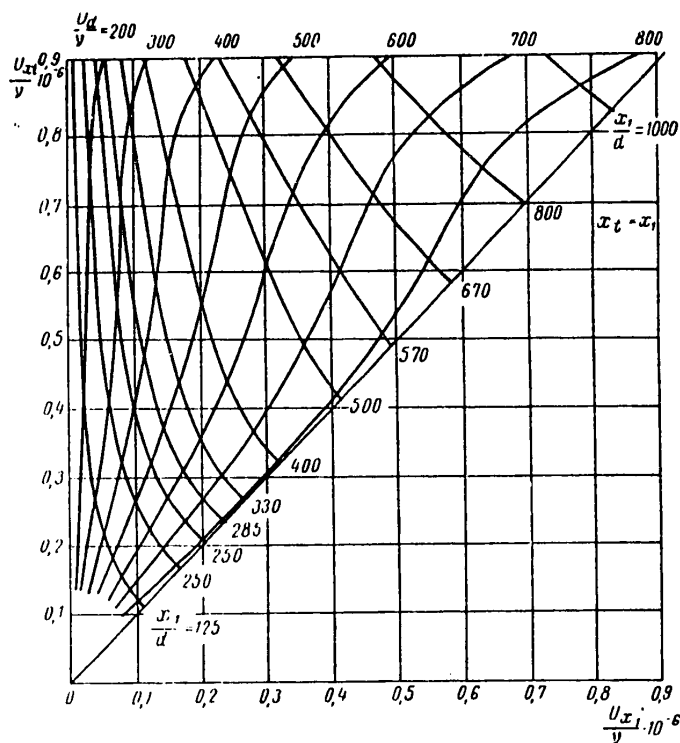
Figure V.7. Diagram for determining the local critical Reynolds
number at the transition point on a plate as a function of the
roughness element height and its location
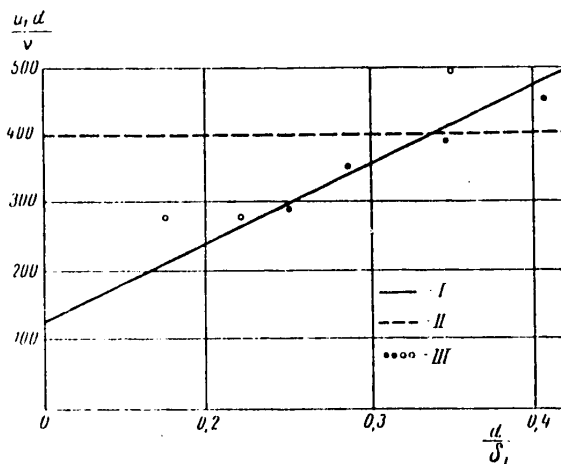
Figure V.8. Comparison of the results of calculating $u_1 d/\nu$ by
formulas (V.20) and (V.21) with the experimental data.
I -- formula (V.20); II -- formula (V.21); III --experimental data.

247

§V.3. Joint Influence of Initial Turbulence and Surface Roughness on Transition in the Boundary Layer

For determination of the transition point coordinate we shall use expression (V.4).

The value of the form parameter f_s in formula (V.4) depends on the intensity of sucking the fluid through the surface of the body characterized by the suction parameter $t^{**} = v_0 \delta^{**}/\nu$, where v_0 is the local fluid suction velocity through the surface. Figure V.9 shows the form parameter f_s as a function of t^{**}.
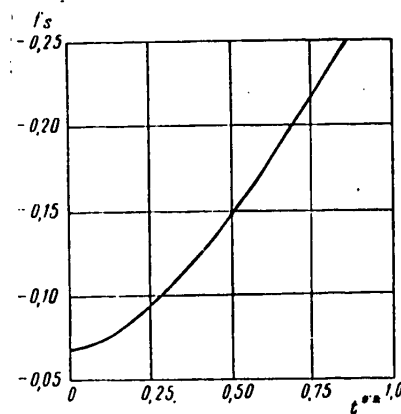
Figure V.9. Form parameter at the separation point f_s as a function of the suction parameter

Since the pressure pulsations caused by turbulent movements of a fluid are subject to a random phenomenon law, it is possible to assume that the mean square pressure pulsations at the outer boundary of the boundary layer are subject to the following addition rule:

$$\left[\frac{\tilde{\partial p}}{\partial x}\right] = \left[\frac{\tilde{\partial p}}{\partial x}\right]_1 + \left[\frac{\tilde{\partial p}}{\partial x}\right]_2,$$

(V.22)

where $\left[\frac{\partial p}{\partial x}\right]_1$ is the component caused by turbulence in the external flow;

$\left[\frac{\tilde{\partial p}}{\partial x}\right]_2$ is the component caused by vortices formed on flow around a roughness element on the surface of the body.

We shall consider the turbulence of the oncoming flow to be isotropic. Then according to the results discussed in §V.1, for the relation between the longitudinal pressure gradient pulsations and velocity pulsations at the outer boundary of the boundary layer it is possible to use the relations of statistical turbulence theory (V.5).

248

In order to calculate the pulsation flow caused by the vortices trailing off the roughness element located on the surface of the body, according to the data of (§V.2), it is possible to use formulas (V.14), (V.15) and (V.17).

Isolating the critical Reynolds number at the transition point $Re_t^{**}=U\delta_t^{**}/\nu$ and the Taylor parameter $\left[\varepsilon\left(\dfrac{L}{L_0}\right)^{1/5}\right]$, using relations (V.22), (V.5), (V.14) and (V.17),

the transition condition (V.4) is converted to a form analogous to formulas (V.6) and (V.18),

$$Re_t^{**} = Re_n^{**} : \frac{A_1(\lg D + D)^{1/2}}{\left[\varepsilon\left(\frac{L}{L_0}\right)^{1/5}\right]^{5/4}\left[\left(\frac{u_0}{u_1'}\right)\left(\frac{U_0}{U}\right)\left(\frac{L_0}{L_\delta}\right)^{1/5}\right]^{5/4}\cdot Re^{-1/4} + B\left(\frac{Ud}{\nu}\right)^{-1/2}\left(\frac{d}{\delta_1^{**}}\right)^2}$$

(V.23)

where $\varepsilon = u'_0/U_0$ is the degree of turbulence in the oncoming flow;

U_0 is the velocity of the oncoming flow;

u'_0 is the mean square magnitude of velocity pulsation in the oncoming flow;

L is the length of the body.

The values of u'_1 and L_δ entering into formula (V.23) are the mean square velocity pulsations and turbulent scale at the outer boundary of the layer, respectively. Since usually the turbulence characteristics of the oncoming flow u'_0 and L_0 are known in the calculations, it is necessary to express u'_1 and L_δ in terms of the mentioned characteristics. In order to establish this relation let us use expressions (V.8) and (V.9). Substituting these expressions in formula (V.23) and performing the necessary transformations, we obtain the final expression for the critical Reynolds number at the transition point

$$Re_t^{**} = Re_n^{**} : \frac{A_1(\lg D + D)^{1/2}}{\left[\varepsilon\left(\frac{L}{L_0}\right)^{1/5}\right]^{5/4}Re^{-1/4}\Omega\left(\frac{U}{U_0}\right) + B\left(\frac{Ud}{\nu}\right)^{-1/2}\left(\frac{d}{\delta_1^{**}}\right)^2}$$

(V.24)

The graph of the function $\Omega(U/U_0)$ is shown in Figure V.1.

Equation (V.24) includes two constants A_1 and B, the values of which cannot be determined theoretically. Analysis of the experimental data demonstrated that $A_1=0.22$ and $B=0.21$.

In the practical calculations, the turbulent scale is not always known, for its determination is connected with fine, tedious measurements. This value enters into equation (V.24) to a power of 1/4, so that even with significant variation of it the critical Reynolds number varies little. In addition, the value of the functions $\Omega(U/U_0)$ and $(Ud/\nu)^{1/2}$ varies insignificantly also in the transition point calculations.

249

Comparison of the calculated and experimental data demonstrated that it is possible to set

$$A_1 \left(\frac{U_0 l_0}{\nu}\right)^{1/4} \Omega^{-1} = 2; \quad \frac{A_1}{B} \left(\frac{U d}{\nu}\right)^{1/2} = 2250.$$

Then formula (V.24) is simplified significantly, and it reduces to the form

$$\mathrm{Re}_l^{**} = \mathrm{Re}_H^{**} + \frac{c\,(|f_s|+1)^{1/2}}{\varepsilon^{5/4} + D\left(\frac{d}{\delta_1^{**}}\right)^2}, \qquad (V.25)$$

which is very convenient for practical use. The constants c and D in formula (V.25) are equal to 1.88 and $0.25 \cdot 10^{-3}$, respectively.

The relation for the critical Reynolds number Re_t^{**} for a plate as a function of the degree of turbulence ε and the surface roughness parameter d/δ_1^{**}

$$\mathrm{Re}_{t_{nn}}^{**} = 225 + \frac{(0.089)^{1/2} c}{\varepsilon^{5/4} + D\left(\frac{d}{\delta_1^{**}}\right)^2}$$
$$(1)$$

Key: 1. plate

is illustrated in Figure V.10.

Figure V.11 gives the calculated and experimental values of the critical Reynolds numbers for a body with different surface roughness. The experiments were performed for small ($\varepsilon=0.15\%$) and comparatively large ($\varepsilon=0.5$ to 0.6%) degree of turbulence of the oncoming flow. Comparison shows satisfactory correspondence of the calculation results by formula (V.25) to the experimental data except for the case of small values of the turbulence and roughness ($\varepsilon \leqslant 0.15\%$ and $d/\delta_1^{**}=0$ to 0.5). A cause of divergence in this case is unsuitability of the transition scheme adopted in this section for very small velocity disturbances introduced into the boundary layer by turbulence of the oncoming flow or surface roughness of the body.
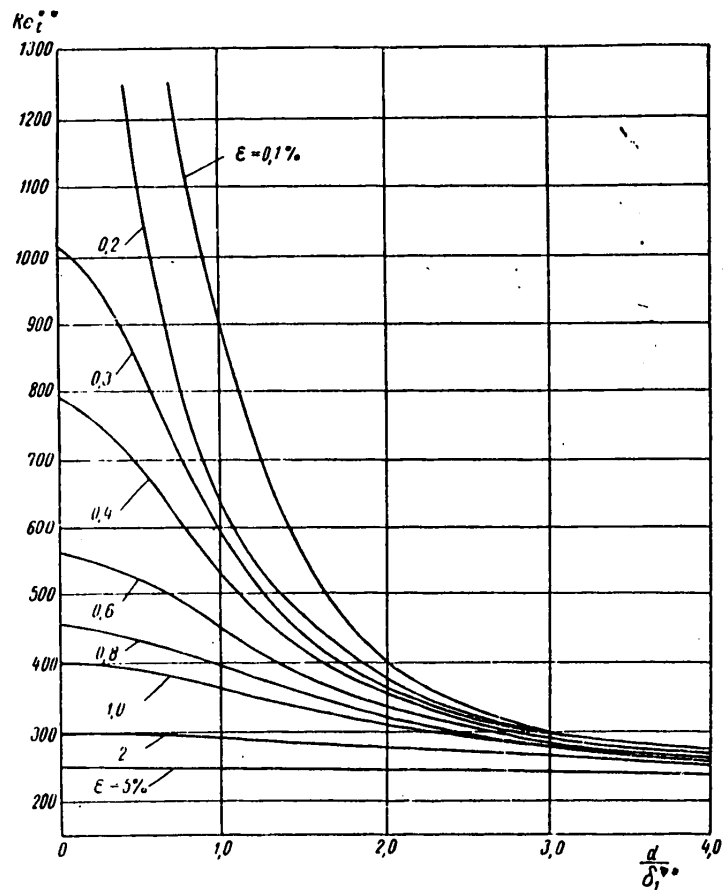
Figure V.10. Critical Reynolds number at the transition point for a plate as a function of the degree of initial turbulence and the roughness parameter
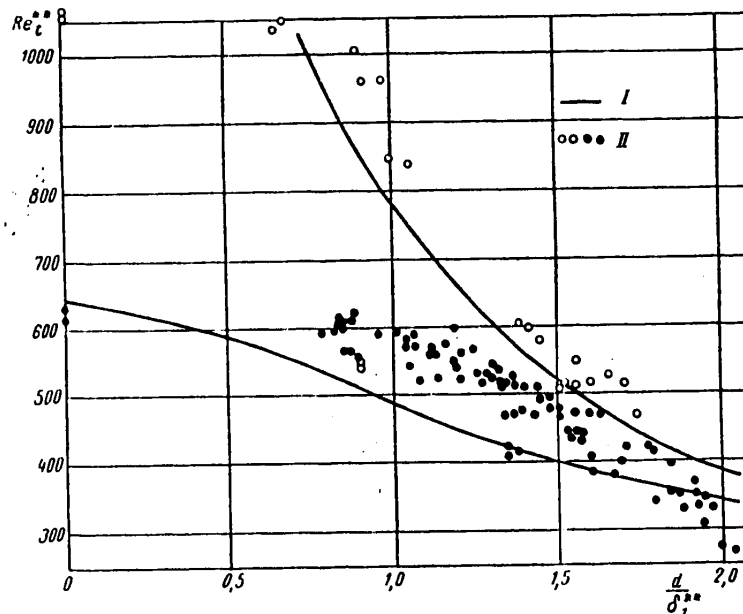
Figure V.11. Comparison of calculated and experimental values of local critical Reynolds number at the transition point
I -- calculation; II -- experimental data

§V.4. Flow Structure and Frictional Drag in the Transition Region of a Boundary Layer

A study is made below of some of the quantitative relations pertaining to the calculation of boundary layer characteristics in a transition region. In connection with the fact that such relations have been insufficiently studied, it is possible to establish such relations at the present time only for a plate [25].

The experimental observations show that in some stage the development of Tollmien-Schlichting waves leads to the formation of a concentrated vortex which then is formed into vortex loops in the boundary layer. Rupture of the vortex loops leads to the occurrence of turbulent spots which, moving along the flow, develop along and across the laminar boundary layer. The spots are generated randomly, and as they grow they overlap each other, leading to the, formation of a completely turbulent boundary layer.

The passage of the spots over different sections of the body surface leads to alternation of laminar and turbulent flows. This alternation is described quantitatively by the "intermittence factor":

$$\gamma = 1 - \exp\left[-0.412\left(\frac{x - x_t}{\lambda}\right)^2\right],$$ (V.26)

252

where x_t is the beginning of the transition region;

λ is the extent of the transition region defined by the expression
$\lambda = x_{\nu} = 0.75 - x_{\nu} = 0.25$.
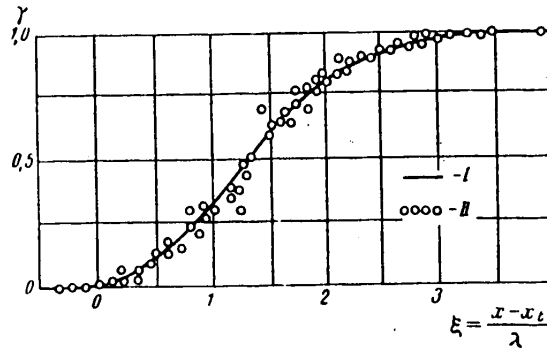
Figure V.12. Comparison of the universal dependence of
γ on ξ with experimental data
I -- calculation; II -- experimental data

A comparison of formula (V.26) with the experimental data is presented in
Figure V.12. The presented graph confirms universality of the relation obtained.
This means that the "intermittence factor" is defined only by the value of λ.
However, this says nothing about the location of the transition region on the
surface over which flow takes place. It is recommended that the value of the
critical Reynolds number at the transition point be calculated by the formulas
investigated in the preceding sections of this chapter. Analyzing the experi-
mental data (Figure V.13), Narasimha and Dhawan [25] established the following
relation between the transition Reynolds number $Re_{\lambda} = \lambda u/\nu$ and the critical Reynolds
number at the transition point Re_t:

$$Re_{\lambda} = 0.5 Re_t^{0.8}. \tag{V.27}$$

Analysis of the experimental data and obvious theoretical arguments demonstrated
that the instantaneous value of the velocity in the transition region of the
boundary layer is defined from the equation

$$u = (1 - \gamma)\, u_L + \gamma u_T, \tag{V.28}$$

where u_L is the velocity profile in a laminar boundary layer;

u_T is the corresponding value for a turbulent boundary layer.

Figure V.14 gives the calculated velocity profiles in the transition region of
the boundary layer for different values of the "intermittence factor" γ.

253
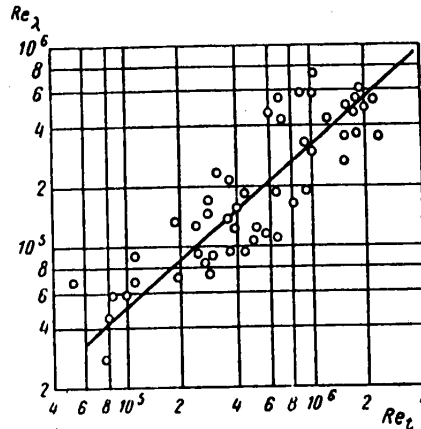
Figure V.13. Establishment of the experimental dependence of
Re_t on Re_λ

Let us proceed to an investigation of the basic characteristics of the boundary layer in the transition region: the displacement flow thicknesses δ^*_t, the pulse loss thicknesses δ^{**}_t and the form parameter H_t:

$$\delta'_t = \int_0^{\delta_t} \left(1 - \frac{u}{U}\right) dy, \qquad (V.29)$$

$$\delta''_t = \int_0^{\delta_t} \frac{u}{U}\left(1 - \frac{u}{U}\right) dy, \qquad (V.30)$$

where U is the velocity at the outer boundary of the boundary layer.

Substituting (V.28) in expressions (V.29) and (V.30), after some simplifications we obtain the following formulas:

$$\delta'_t = (1 - \gamma)\delta'_L + \gamma\delta'_T;$$

$$\delta''_t = (1 - \gamma)\left[(1 - \gamma)\delta''_L - \gamma\delta'_L\right] + \gamma\left[\gamma\delta''_T - (1 - \gamma)\delta'_T\right] + 2\gamma(1 - \gamma)F(\delta_t);$$

$$H_t = \frac{(1 - \gamma)H_L + \gamma H_T \dfrac{\delta''_T}{\delta''_L}}{(1 - \gamma)^2\left[1 - \dfrac{\gamma}{1 - \gamma}H_L\right] + \gamma^2\left[1 - \dfrac{1 - \gamma}{\gamma}H_T\right]\dfrac{\delta''_T}{\delta''_L} + 2\gamma\dfrac{F(\delta_t)}{\delta''_L}},$$

where δ^*_L, δ^*_T, δ^{**}_L, δ^{**}_T, H_L and H_T are the displacement thicknesses, the pulse losses and form parameter, respectively, for laminar and turbulent velocity profiles, and the function

$$F(\delta_t) = \int_0^{\delta_t} \left[1 - \left(\frac{u}{U}\right)_L\left(\frac{u}{U}\right)_T\right] dy.$$

254

Analysis of the experimental data demonstrated that the value of the critical
Reynolds number at the transition point Re_t has little influence on the magnitude
of the form parameter H_t. Accordingly, for calculation of this form parameter it
is possible to use a simpler formula

$$H_t = H_T + (H_L - H_T)\exp\left[-0.412\left(\frac{x-x_t}{\lambda}\right)^2\right].$$
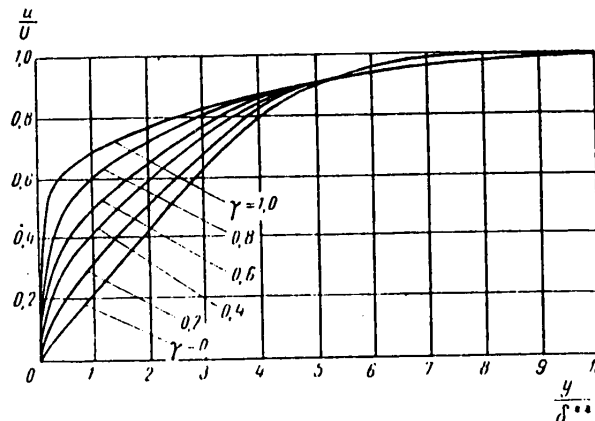
Figure V.14. Velocity profiles in the transition region of
the boundary layer as a function of the magnitude of γ

Let us proceed to calculation of the local frictional drag which is determined in
the transition region by the equality

$$\zeta_{ft} = (1-\gamma)\zeta_{fL} + \gamma\zeta_{fT},\qquad (V.31)$$

where ζ_{fL} and ζ_{fT} are the local frictional drags, respectively, for the laminar
and turbulent boundary layers.

Substituting γ in formula (V.31), we obtain

$$\zeta_{ft} = \zeta_{fL} + \left\{1 - \exp\left[-0.412\left(\frac{x-x_t}{\lambda}\right)^2\right]\right\}(\zeta_{fT} - \zeta_{fL}).\qquad (V.32)$$

The calculation results demonstrated that the difference $(\zeta_{fT}-\zeta_{fL}) \cong 3\cdot10^{-3}$
does not depend on the Reynolds number. This fact satisfactorily explains the
experimental fact noted by Narasimha and Dhawan [25] that the difference $\zeta_{fT}-\zeta_{fL}$
in the transition region does not depend on the Reynolds number, that is,

$$\zeta_{ft} - \zeta_{ft\mid\gamma=0} = \psi(\xi),\qquad (V.33)$$

where

$$\xi = \frac{x-x_t}{\lambda}.$$

255

Comparison of expressions (V.32) and (V.33) shows that

$$\psi(\xi) = 3 \cdot 10^{-3} \left\{ 1 - \exp\left[-0{,}412 \left(\frac{x - x_t}{\lambda} \right)^2 \right] \right\}.$$ (V.34)

Equation (V.33) in Figure V.15 is compared with the experimental data.

Let us use the variation of the local friction in the transition region (V.32) to calculate the total friction of a plate with transition region in its boundary layer. Integration of equations (V.31) for a plate of length ℓ with transition region beginning at the point $x_1 = x_t$ using formulas (V.27), (V.34) makes it possible to obtain the relations for the total frictional drag $\xi_F = \xi_F(Re)$ presented in Figure V.16 for a number of values of Re_t.

A comparison with the calculations of Emmons, the Prandtl-Schlichting formula and the known experimental data of Hebers is presented on the same graph. The presented data allow the conclusion to be drawn that there is a steeper rise of ζ_F in the transition region that Emmons obtained, and a smoother nature of the transition curve at the beginning of the transition region, and not such a sharp one as obtained when using the semi-empirical Prandtl-Schlichting function.

In Soviet literature the calculation of boundary layer characteristics in the transition region is the subject of references [34]-[36].
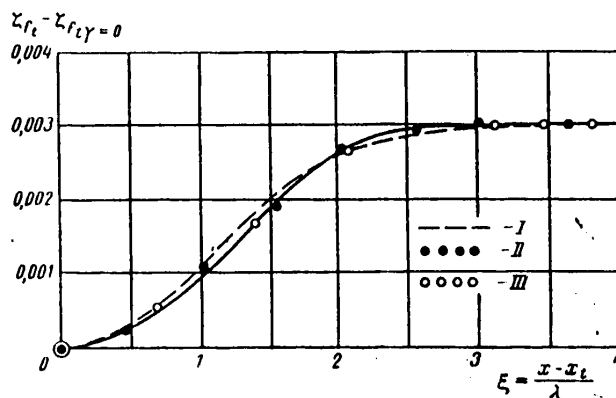
Figure V.15. Comparison of the function $\psi(\zeta)$ with experimental data.
I -- equation (V.33); II -- experiment for $Re_t = 4.3 \cdot 10^5$; III -- experiment for $Re_t = 2.31 \cdot 10^6$
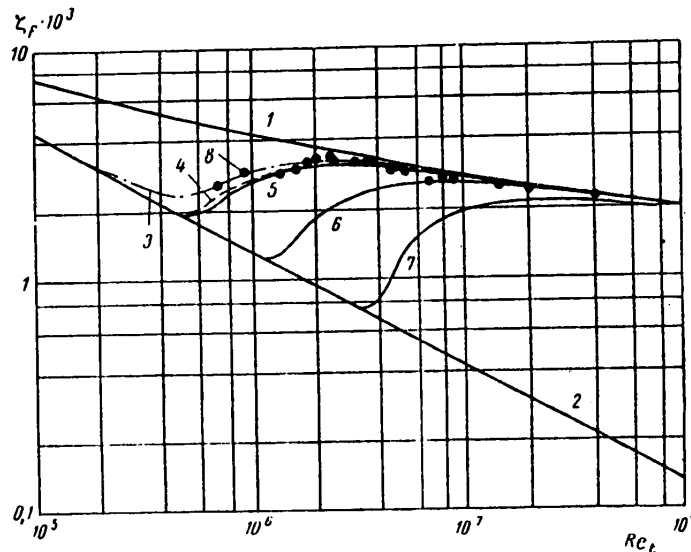
Figure V.16. Frictional coefficient of a smooth plate as a
function of the Reynolds number in the transition region.
1 -- turbulent conditions; 2 -- laminar conditions; 3 --
Prandtl calculation; 4 -- Emmons calculation; 5, 6, 7 --
calculation by formulas (V.27)-(V.34) for $Re_t = 4 \cdot 10^5$; 10^6; $3 \cdot 10^6$

BIBLIOGRAPHY

1. Dorodnitsyn, A. A.; Loytsyanskiy, L. G. "Theory of Laminar Layer Transition
   to Turbulent," PMM [Applied Mathematics and Mechanics], Vol 9, No 4, 1945.

2. Mel'nikov, A. P. "Turbulent Transition, Its Theory and Calculations,"
   TR. LKVVIA, No 12, 1947.

3. Taylor, G. I. "Statistical Theory of Turbulence, Effect of Turbulence on
   Boundary-Layer," PROC. ROY. SOC., Ser. A., Vol 156, 1936.

4. Schubauer, G. B. "Laminar Boundary Layer Oscillations and Stability of
   Laminar Flow," J. AERONAUT. SCI., Vol 14, 1947.

5. Schubauer, G. B.; Skramstad, H. K. "The Effect of Turbulence on Transition
   in the Boundary Layer of an Elliptic Cylinder." PROC. 5. INT.CONGR. APPL.
   MECH., Cambridge, Mass., 1938, p 321.

6. Kozlov, L. F. "Calculation of the Transition of a Laminar Boundary Layer to
   Turbulent Under the Effect of Turbulence of the Oncoming Flow," INZH.-FIZ.
   ZHURN. [Engineering Physics Journal], No 3, 1962.

257

7. Feindt, E. G. "Untersuchungen über die Abhändigkeit des Umschlages laminar-turbulent von der Oberflachenrauhigkeit und der Druckverteilung," D.F.L. INST. AERODYNAMIK, Braunschweig. Bericht. 56/10, 1956, JB. DER SCHIFFBAUTECHN. GES., Vol 50, 1956.

8. Preston, I. H. "Prediction of Transition on the Boundary Layer on an Aero-foil," J. ROY. AERON. SOC., No 12, 1958.

9. Grabtry, L. F. "Prediction of Transition in the Boundary Layer on an Aero-Foil," J. ROY. AERON. SOC., No 7, 1958.

10. Granville, P. S. "The Calculation of Viscous Drag of Bodies of Revolution," Navy Department, The David Taylor Model Basin, Rep. No 849, 1953.

11. Dryden, H. L. "Review of Published Data on the Effect of Roughness on Transition from Laminar to Turbulent Flow," J. AERONAUT. SCI., Vol 20, 1953, p 477.

12. Kozlov, L. F. "Modern Studies in the Resistance of Water to the Motion of Ships," SUDOSTROYENIYE [Shipbuilding], No 3, 1960.

13. Tani, I.; Hama, F. R.; Mituisi, S. "On the Effect of a Single Roughness Element on Boundary Layer Transition," REP. INST. SCI. AND TECHNOL. UNIV., Tokyo, Vol 8, 1954, p 125.

14. Tani, I.; Luchi, M.; Yamamoto, K. "Further Experiments on the Effect of a Single Roughness Element on Boundary-Layer Transition," REP. INST. SCI. AND TECHNOL. UNIV., Tokyo, Vol 8, 1954, p 171.

15. Lachmann, G. V. "Laminarization Through Boundary Layer Control," AERON. ENG. REV., Vol 13, No 8, 1954.

16. Fage, A. "Study of the Flow in a Boundary Layer Using a Hydrodynamic Microscope," PROBLEMA POGRANICHNOGO SLOYA I VOPROSY TEPLOPEREDACHI [Boundary Layer Problem and Heat Transfer Problems], Moscow-Leningrad, Gosenergoizdat, 1960.

17. Hama, F. R.; Long, I.; Hegarty, I. "On Transition from Laminar to Turbulent Flow," J. APPL. PHYS., Vol 28, No 4, 1957.

18. Schlichting, H. "Experimentelle Untersuchungen zum Rauhigkeitsproblem," ING.-ARCHIV., No 7, 1936.

19. Pohlhausen, K. "Zur näherungsweisen Integration der Differentialgleichung der laminare Reibungsschict," ZAMM, No 1, 1921, p 235.

20. Basin, A. M. "A New Approximate Method of Calculating a Laminar Layer," DAN SSSR [Reports of the USSR Academy of Sciences], Vol 40, No 1, 1943.

21. Kozlov, L. F. "Problem of the Relation Between Natural Drag and the Critical Parameter of a Single Cylindrical Roughness," GIDRODINAMIKA BOL'SHIKH SKOROSTEY [High-Velocity Hydrodynamics], Kiev, Naukova dumka, 1965.

22. Loytsyanskiy, L. G. LAMINARNYY POGRANICHNYY SLOY [Laminar Boundary Layer], Fizmatgiz, Moscow, 1962.

23. Kozlov, L. F. "Approximate Integration of the Equations of a Laminar Boundary Layer on a Porous Surface in an Incompressible Fluid," ZHURN. PRIKL. MEKH. I TEKHN. FIZ. [Journal of Applied Mechanics and Technical Physics], No 5, 1962.

24. Kozlov, L. F. "Approximate Method of Calculating Optimal Suction of a Fluid from the Boundary Layer of Wing Profiles with Porous Surface," PMTF [Applied Mechanics and Technical Physics], No 3, 1964.

25. Dhawan, S.; Narasimha, R. "Some Properties of Boundary Layer Flow During the Transition from Laminar to Turbulent Motion," J. FLUID, MECH., Vol 3, No 4, 1958.

26. Emmons, H. W. "The Laminar-Turbulent Transition in a Boundary Layer," PROC. FIRST US NAT. CONGR. APPL. MECH., 1952, p 859.

27. Shlichting, H. VOZNIKNOVENIYE TURBULENTNOSTI [Occurrence of Turbulence], Moscow, IL, 1962.

28. Dryden, H. L. "Transition of a Laminar Flow to Turbulent," TURBULENTNYYE TECHENIYA I TEPLOPEREDACHA, Moscow, IL, 1963.

29. Minskiy, Ye. M. "Transition Point of a Laminar Layer to the Turbulent State," TEKHN. OTCHETY TSAGI [Technical Notes of the Central Aerohydrodynamics Institute], No 74, 1947.

30. Dorodnitsyn, A. A.; Loytsyanskiy, L. G. "Transition of a Laminar Boundary Layer to Turbulent and Laminar Profiles," TR. TSAGI [Works of the Central Aerohydrodynamics Institute], No 563, 1945.

31. Prandtl, L.; Tietjens, O. GIDRO- I AEROMEKHANIKA [Hydro and Aeromechanics], Vol 2, ONTI, 1935.

32. Van Drist, E. R.; Bloomer, K. B. "Influence of Turbulence of the External Flow and Pressure Gradient on Transition in the Boundary Layer of a Laminar Form of Flow to Turbulent," RAKETNAYA TEKHNIKA I KOSMONAVTIKA [Rocket Engineering and Astronautics], Vol 1, No 6, 1963, Russian translation, IL, Moscow.

33. Gertsenshteyn, S. Ya. "Influence of a Single Roughness Element on the Occurrence of Turbulence," IZV. AN SSSR, MZHG [News of the USSR Academy of Sciences, MZhG], No 2, 1966.

34. Zysina-Molozhen, L. M. "Nature of Transition from Laminar to Turbulent Flow Conditions in a Boundary Layer," ZHURN. TEKHN. FIZIKI [Journal of Technical Physics], Vol 25, No 7, 1955.

259

35. Zysina-Molozhen, L. M. "Some Quantitative Characteristics of Transition from Laminar to Turbulent Flow in a Boundary Layer," ZHURN. TEKHN. FIZIKA, Vol 25, No 7, 1955.

36. Vulis, L. A. "Interpolation Formula for the Transition Flow Region," IZV. AN SSSR, MEKHAN. I MASHINOSTROYENIYE [News of the USSR Academy of Sciences, Mechanization and Machine Building], No 3, 1962.

37. Smith, A. M. O.; Clutter, D. W. "The Smallest Height of Roughness Capable of Affecting Boundary-Layer Transition," J. AERO/SPACE SCIENCES, Vol 26, No 4, 1959.

38. Dryden, H. L. "Combined Effects of Turbulence and Roughness on Transition," Z. ANGEW. MATH. PHYS., Vol 96, No 5/6, 1958.

39. Wells, K. S. "Influence of Turbulence of the Oncoming Flow on Transition in a Boundary Layer," RAKETNAYA TEKHNIKA I KOSMONAVTIKA [Rocket Engineering and Cosmonautics], Russian translation, Vol 5, No 1, 1967.

40. Prishchemikhin, Yu. N.; Pustoshnyy, A. F. "Study of Methods of Turbulizing the Boundary Layer of Ship Models During Testing in a Model Testing Basin," NTO SUD. PROM. MATERIALY PO OBMENU OPYTOM [Scientific and Technical Society of the Shipbuilding Industry, Exchange of Experience Materials], Leningrad, Izd. Sudostroyeniye, No 76, 1966.

41. Bazilevskiy, Yu. S.; Pustoshnyy, A. F. "Methods of Turbulizing the Boundary Layer During Tow Testing of Models in Small Model Testing Basins," NTO SUD. PROM. MATERIALY PO OBMENU OPYTOM, Leningrad, izd. Sudostroyeniye, No 76, 1966.

42. Pustoshnyy, A. F. "Study of Boundary Layer Characteristics and Local Frictional Forces on Ship Models Under Artificial Turbulization Conditions," NTO SUD. PROM. MATERIALY PO OBMENU OPYTOM, Leningrad, izd. Sudostroyeniye, No 46, 1963.

CHAPTER VI. CONTROLLED TURBULENT BOUNDARY LAYER

§VI.1. Some Results of Experimental Studies of a Turbulent Boundary Layer of a Plate on Injecting or Removing Fluid at the Wall

All of the calculation techniques for determining the characteristics of a turbulent boundary layer (TBL) both in the case of an impermeable surface and a permeable surface, are based on the application of a defined number of experimental relations relating certain parameters of the boundary layer.

In this section a study is made of some of the experimental results of investigating the TBL of a plate with distributed removal or injection of a fluid on the surface over which flow takes place. The fluid entering the boundary layer has physical properties that coincide completely with the fluid properties of the main flow. The experimental materials presented below are used hereafter to construct and check out semi-empirical methods of calculating a controlled TBL.

One of the first and most significant experimental studies in the indicated area is the paper by Mickley, Ross, Sguyers and Stewart [1].

The experimental setup used in these studies was a wind tunnel more than 6 meters long. The permeable surface made of 15 isolated sections with a total area of 3.048×0.3048 m and chambers required to incure uniformity of suction or injection was the upper wall of a rectangular channel of a closed operating section. The lower wall was made flexible; its displacements (using special adjustment attachments) made it possible approximately to insure constancy of the pressures along the channel. In order to isolate the boundary layer developed on the permeable surface from the boundary layer of other sections of the wind tunnel, suction was used before the beginning and on the side walls of the working section.

The capabilities of the setup permitted various suction or injection laws to be realized within defined limits and also studies to be made of both laminar and turbulent boundary layers inasmuch as artificial turbulization is not used. During the experiments, the velocity and temperature profiles and also the flow rates of the injected or sucked air were measured.

The data obtained permit determination with sufficient completeness of the effect of injecting or suction on the TBL characteristics. In Figure VI.1, in particular, velocity profiles in the TBL cross section located at a distance of 1190 mm from the beginning of the permeable surface are presented for injection and suction of

261

different intensity. Comparing these profiles, it is possible to note the increase in thickness of the boundary layer on injecting the fluid and the decrease in fullness of the velocity profiles with an increase in v_0/U.

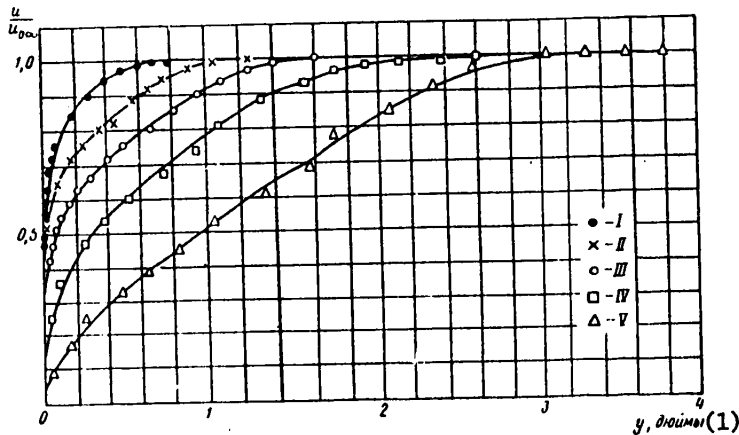

Figure VI.1. TBL velocity profile on a plate for injection or suction in a cross section x=1190 mm from the beginning of the permeable surface (according to the data of [1])

	$Re_x \cdot 10^{-6}$	v_0/U
I	5.98	−0.002
II	5.95	0
III	6.00	+0.002
IV	5.98	+0.005
V	6.07	+0.010

Key:
  1. y, inches

From the point of view of the possibility of lowering drag, the results of calculating the local friction coefficients (Figure VI.2) are of the greatest interest. It must be noted that in the Mickley experiments direct measurements of the turbulent tangential stresses were not taken. Their values were determined at the wall by using the pulse equation and approximate differentiation of the experimentally obtained relations for $\delta^{**}(x)$ considering the presence of injection or suction and possible deviations from the conditions of constancy of the pressures along the working section. In Figure VI.2, the results of calculating the relative local friction coefficient ζ_f/ζ_{f_0} as a function of the injection or suction parameter are presented in universalized form, that is, a form suitable for different Reynolds numbers Re_x. The universalizing factor here is a value which is the inverse of the local friction coefficient ζ_{f_0} in the case of $v_0=0$. The graph in Figure VI.2 offers the possibility of estimating the variation of ζ_f for given Re_x as a function of variation of v_0/U. More generalized data were obtained in reference [2] only for the case of injection. These results are presented in Figure VI.3. The value of $v_0/U \times 1/\sqrt{\zeta_{f_0}/2}$ is used as the injection parameter. The

tangential stress on the wall was also measured in the case of injection by
D. Hacker [3]. He obtained a universal relation (Figure VI.4) between the variables
analogous to the corresponding Mickley parameter [1] if we consider that in the
region of variation of Re_x, in the Hacker experiments $\zeta_{f0} \sim Re_x^{-1/5}$. Since the
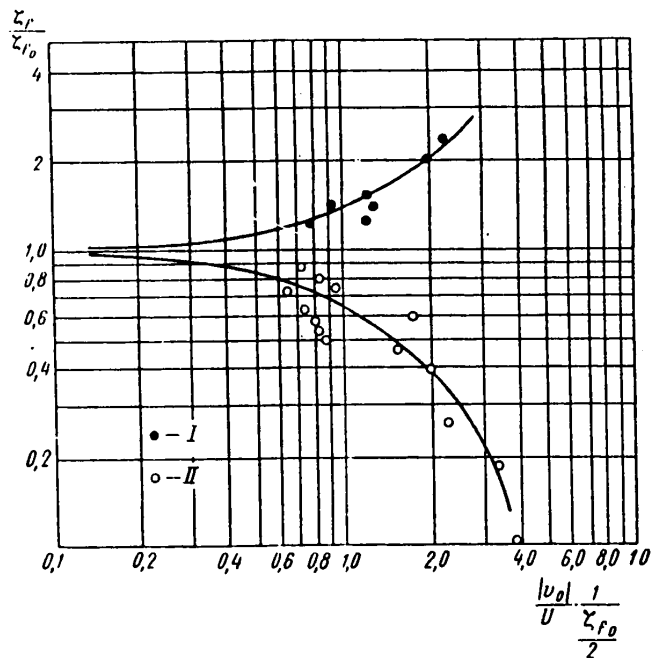
Figure VI.2. Local frictional stress coefficient ζ_f as a
function of the injection or suction intensity.
I -- suction; II -- injection

Stanton tube was used for the measurements, the accuracy of the measurements in
the small stress and high injection intensity range is doubtful in view of the
strong influence of the transverse velocity component in the boundary layer on the
tube readings. Therefore it is necessary to exercise caution with regard to
Hacker's data in the range of $(v_0/U)Re_x^{1/5}$=0.06 to 0.01, just as it is also
necessary to exercise caution with regard to the critical value of the injection
parameter indicated by him $(v_0/U)Re_x^{1/5}$=0.08, for which ζ_f=0.

From the Soviet experimental studies of injection of a material into the TBL, it
is necessary to mention the papers of V. P. Mugalev [4], P. N. Romanenko and
V. N. Kharchenko [5]. An interesting analogy was detected in reference [4]
between the effect of uniformly distributed injection and the effect of a positive
pressure gradient in the outer flow on the boundary layer characteristics of a
plate.

The study of the effect of uniformly distributed suction on the TBL characteristics
was performed by Kay [6], who, studying the laminarization problem, was interested
in the problem of what happens to the boundary layer parameters on a permeable
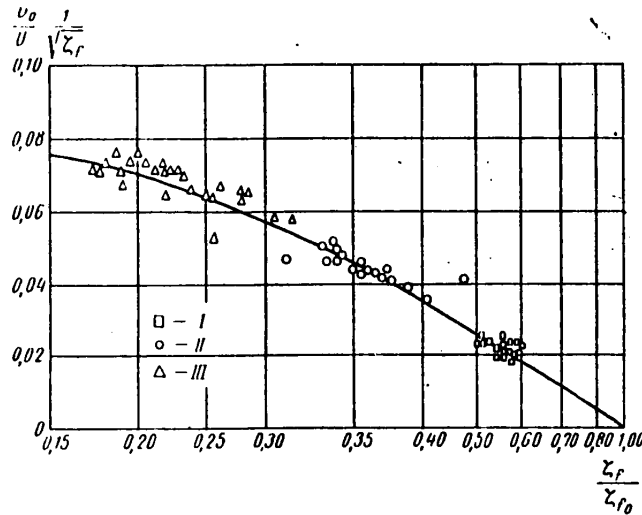
Figure VI.3. The function $\zeta_f/\zeta_{f0} = f\left(\frac{v_0}{U} \cdot \frac{1}{\sqrt{\zeta_{f0}/2}}\right)$ by the data of reference [2]:

	u_0/U
I	0,001
II	0,002
III	0,003

surface if for some reason the laminar flow conditions are violated. Kay's experimental setup resembles Mickley's in general outline. Kay measured velocity profiles in the boundary layer on a plate made of porous bronze (610×305 mm) and the sucked air flow rate. During the course of the tests, a noteworthy fact of achievement of an asymptotic state by the TBL with uniform suction was detected. Another significant result of Kay's work consisted in detecting a laminar sublayer of the TBL during suction. The velocity distribution in the sublayer turned out to correspond to the exponential law

$$u = U_\infty \left(1 - e^{-\frac{v_0 y}{\nu}}\right). \tag{VI.1}$$

The studies by Kay received further development in the paper by Dutton [7], where a study was made of the effect of suction on the characteristics of an artificially turbulized TBL on a plate 1676 mm long. Dutton tested two versions of a permeable surface. In the first version the surface was formed from two perforated sheets 0.5 mm thick separated by a layer of blotting paper. The outer sheet had fine, partial perforation (hole diameter 0.51 mm with spacing of 1.52 mm between holes). In the other version the surface was made of calendered nylon, which insured more uniform permeability and less roughness.
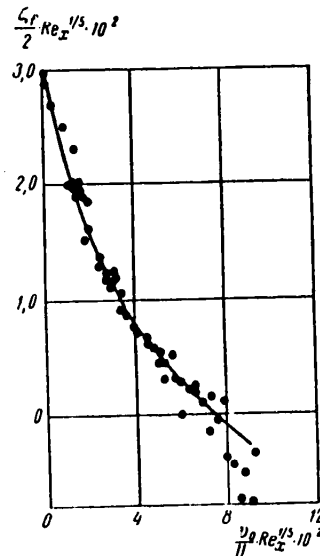
Figure VI.4. Local friction coefficient ζ_f as a function of
the injection parameter according to Hacker's data [3]

The noted difference in quality of the skin was also reflected in the results of
measuring the boundary layer characteristics presented in Figures VI.5 and VI.6.
As is obvious from the figures, for every two surface versions there is a suction
velocity for which the pulse loss thickness along the plate remains unchanged and
equal to this value at the beginning of the permeable section. For a nylon skin
this relative velocity $v_0/U=0.0044$, and for perforated skin 0.0073, which indi-
cates significant influence of the surface quality on the flow rate of the sucked
air required to maintain constancy of the thickness of the TBL.

Dutton's experiments again confirmed the possibility of obtaining an asymptotic
turbulent boundary layer with uniformly distributed suction; in addition, during
these experiments it was discovered that for a defined, sufficiently high suction
intensity, inverse transition from turbulent to laminar flow conditions in the
boundary layer is possible.

Favre, Dumas and Verolet [8] studied TBL under uniform suction conditions through
a porous surface using measuring devices analogous to those used in reference [1]-
[7] and with the help of a thermoanemometric device. A characteristic feature of
these experiments was significant thickness of the boundary layer at the
beginning of the porous section as a result of the presence of an impermeable
surface 1 meter long ahead of it with a total plate length of about 2 meters.
The permeable part of the plate model was made of material with porosity of 50%
and pore sizes from 1 to 10 microns. The following were found for different
boundary layer cross sections and different suction intensities (v_0/U varied from
0 to 0.02): velocity profiles, profiles of the mean square values of the pulsa-
tion velocity components, turbulent stress profiles $\rho \overline{u'v'}$, correlation
coefficients $\overline{u'v'}/\sqrt{\overline{u'^2}}\sqrt{\overline{v'^2}}$ and the longitudinal pulsation energy spectra. Velocity
profiles are presented in Figure VI.7 for the cross section x=300 mm from the

265

beginning of the porous section. The influence of suction is already noticeable for minimum intensity ($v_0/U=0.0007$); for large values of v_0/U, the velocity profiles reveal an inflection point.
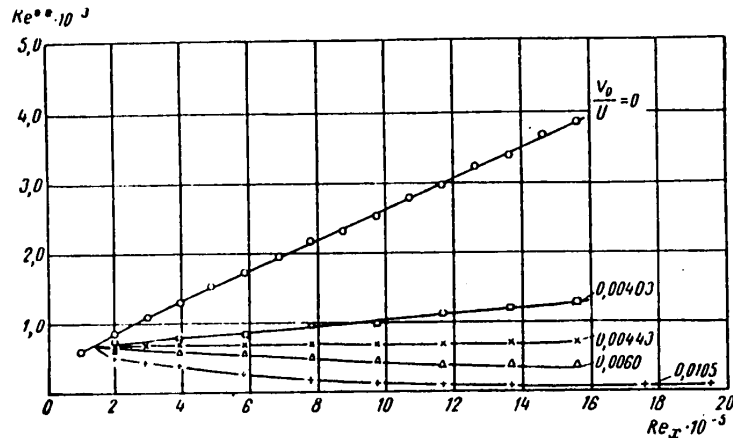

Figure VI.5. Re**(Re$_x$) for uniform suction [7]. Surface made of calendered nylon.

Favre notes that the wall part of the velocity profile is approximated satisfactorily by expression (VI.1), which is valid for the asymptotic state of a laminar boundary layer with uniform suction if the value of U_i at the velocity profile inflection point is taken as the velocity outside the boundary layer U. The nature of variation of the values of H(x), δ**(x) (Figure VI.8) calculated by the velocity profiles is in general close to the Kay and Dutton data. However, the asymptotic state of the TBL was not reached in Favre's experiments. Even with powerful suction the velocity profiles were still a weak function of distance, which can be explained by the previously noted characteristic of the experiments which consists in the fact that suction begins not with the leading edge, but significantly back along the length of the impermeable section in which sufficiently developed TBL is formed.

The profiles of the values of $\sqrt{\overline{u'^2}}$ and $\sqrt{\overline{v'^2}}$ presented in Figures VI.9 and VI.10 reveal the significant influence of suction on the longitudinal and transverse components of the pulsation component of the velocity.

The suction effect on the magnitudes and nature of distribution of the turbulent stresses (Figure VI.11) is manifested quite characteristically. In spite of the fact that the tangential stress on the wall increases with suction, the turbulent stresses decrease with an increase in suction intensity. The maximum distribution shifts from the wall into the inner region of the TBL. Near the wall in the sublayer zone the tangential stresses of a viscous nature $\tau=\mu\,\partial u/\partial y$ significantly exceed the maximum turbulent stresses $\rho\overline{u'v'}$ in the sucked boundary layer.
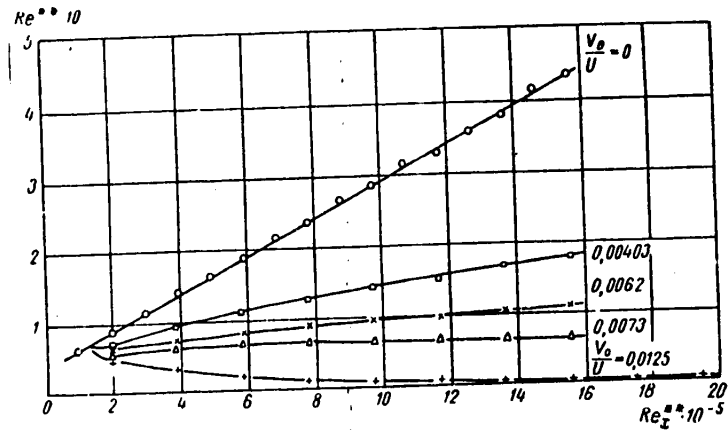
Figure VI.6. Function Re**(Re$_x$) for uniform suction [7]. Surface made of finely perforated sheet metal
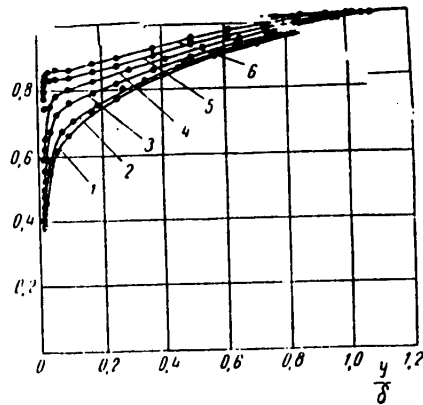

Figure VI.7. Velocity profiles of a sucked TBL in the cross section x=300 mm from the beginning of the porous section [8].

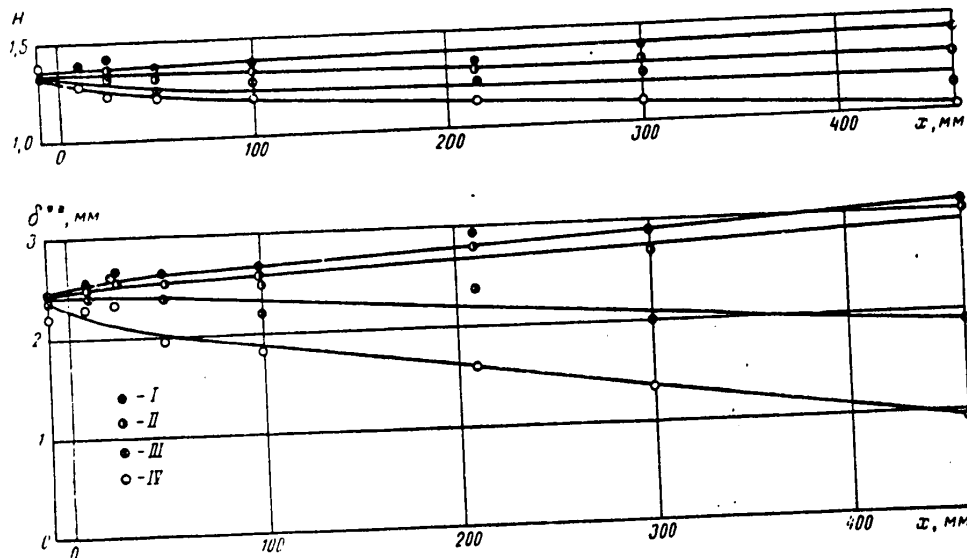|	Suction intensity v_0/U
1	0
2	0.0007
3	0.0025
4	0.0045
5	0.0097
6	0.0153

Figure VI.8. H and δ** as functions of the distance x from the beginning of the porous section for various suction intensities [8]

Suction intensity

$$v_0/U$$

I	0
II	0.001
III	0.005
IV	0.016

In contrast to the powerful effect of suction on the pulsation velocity components according to Favre's data suction has only insignificant influence on

the correlation coefficient $\dfrac{\overline{u'v'}}{\sqrt{\overline{u'^2}}\ \sqrt{\overline{v'^2}}}$ and the energy spectrum of the longitud-

inal velocity pulsations u'.

When comparing the above-presented experimental data with the results of the theoretical calculations it is necessary to consider that experiments with injection and suction of material were performed on porous surfaces having a defined degree of roughness. It is possible to judge the influence of the roughness by Dutton's results [7]. Therefore, representation of the experimental results in the form of the function $\zeta_f/\zeta_{f_0}=f((v_0/U)(2/\zeta_{f_0}))$ is the most expedient for comparison with the calculation data. In this case it is possible to expect that the roughness influence is approximately identically felt in the value of ζ_f both for $v_0=0$ and for $v_0\neq0$, as a result of which the ratio ζ_f/ζ_{f_0} will depend little on the roughness.
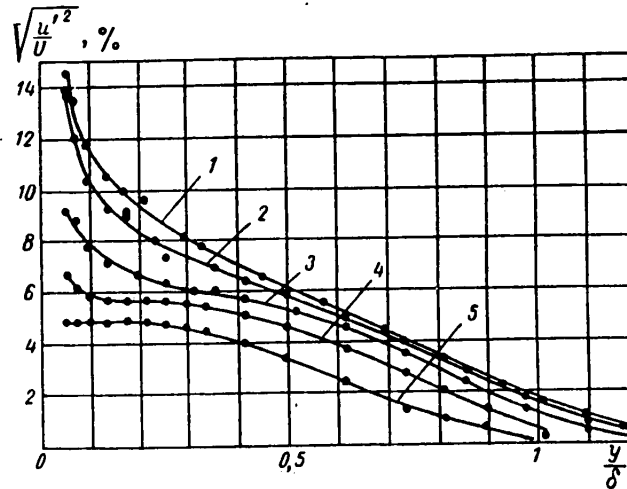
Figure VI.9. Profiles of mean square values of the transverse component of the pulsation velocity $\sqrt{v'^2}$ in the TBL cross section at a distance 300 mm from the beginning of the porous section with a flow velocity of 11 m/sec and different section intensities (layer thickness $\delta=24.9$ mm)
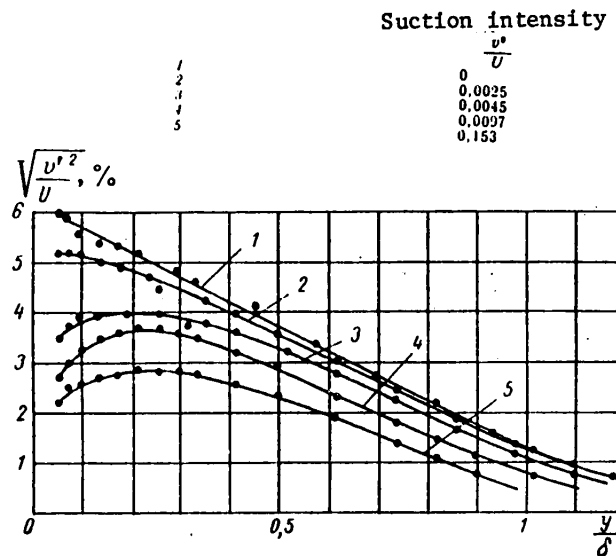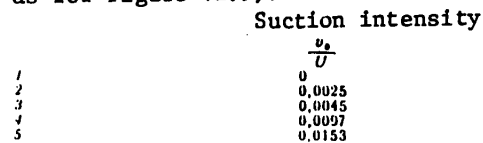
Suction intensity
$$\frac{v^0}{U}$$

1	0
2	0.0025
3	0.0045
4	0.0097
5	0.153

Figure VI.10. Profiles of the mean square values of the transverse component of the pulsation velocities $\sqrt{u'^2}$ (measurement conditions and notation the same as for Figure VI.9).

Suction intensity
$$\frac{v_0}{U}$$

1	0
2	0.0025
3	0.0045
4	0.0097
5	0.0153

269
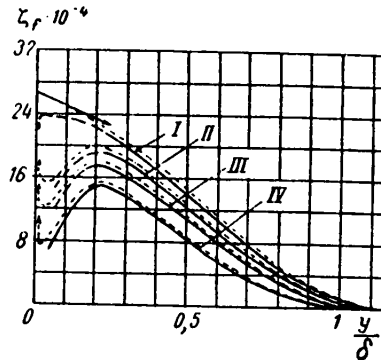
Figure VI.11. Profiles of dimensionless turbulent and viscous
stresses for different suction intensities in the TBL cross
section located 100 mm from the beginning of the porous section
(flow velocity U=11 m/sec, solid line -- $\rho u'v'/1/2\rho U^2$, dotted
line -- $\tau/1/2\rho U^2$)

	Suction intensity v_0/U
I	0
II	0.0026
III	0.0046
IV	0.0165

§VI.2. Methods of Calculating a Controlled Turbulent Boundary Layer, Which Are
a Development of the Truckenbrodt Method

Approximate methods of calculating the turbulent boundary layer characteristics
can be provisionally divided into two groups: the first group includes methods
based on using the pulse equation, and the second group, methods based on joint
use of the pulse equations (IV.29) and energy equations (IV.30). The Truckenbrodt
and Eppler methods, which belong to the second group, are considered in this sec-
tion as applied to TBL control by suction and injection of material. Surveys of
various methods of calculating TBL appear in monographs [44] (uncontrolled TBL)
and [45] (TBL on a permeable surface).

The system of equations (IV.29), (IV.30) contains five unknown functions:

$\delta^*(x)$, $\delta^{**}(x)$, $\delta_3(x)$, $\tau_0(x)$ and $c_D(x) = \int_0^\delta \frac{\tau}{\rho U^3} \frac{\partial u}{\partial y} dy$. For complete solution of the

problem it is necessary to have three more functions relating the indicated
desired functions. These additional relations must be taken from the experimental
data. Relations recommended in references [20]-[25] are used below:

$$\frac{2\tau_0}{\rho U^2} = \zeta_f(\text{Re}^{**}, H) = 0.058\left(\lg \frac{8.05}{H^{1.818}}\right)^{1.705} \cdot (\text{Re}^{**})^{-0.268}; \tag{VI.2}$$

$$10^5 > \text{Re}^{**} \geq 10^2, \ 1.2 \leqslant H \leqslant 2.5;$$

$$c_D = c_D(\text{Re}^{**}, H) = \frac{\beta(H)}{\text{Re}^{**n}};$$

270

$$n = -\frac{1}{6}; \quad \beta(H) \approx \text{const} = 5,21 \cdot 10^{-3}; \tag{VI.3}$$

$$H = 1 + 1,48(2 - \overline{H}) + 104(2 - \overline{H})^{6,7}. \tag{VI.4}$$

The parameters H and $\overline{H}$ are defined by formulas (IV.35) and (IV.36).

Let us assume that the functions (IV.2)-(VI.4) are universal, that is, they can be used for any boundary conditions on the wall permitted by boundary layer theory. The influence of injection or suction is only felt in variation of the parameters H, $\overline{H}$, Re**, ζ_f, c_D when maintaining the relation between them. Experiments with known accuracy confirm the proposition of universality of the function $\overline{H}=\overline{H}(H)$ (Figure VI.12). At the present time the required experimental data for confirmation of universality of the functions $c_D(Re^{**}, H)$, $\zeta_f(Re^{**}, H)$ in the case of a controlled TBL are unavailable.

Generalization of the Truckenbrodt Method.[1] In the case of injection or suction of a fluid along the normal to the surface over which flow takes place, considering (VI.3), the energy equation (VI.4.3) is written as follows:

$$\frac{1}{U^3 r_0} \cdot \frac{d}{dx}(U^3 \cdot r_0 \overline{H} \cdot \delta^{**}) - \frac{v_0}{U} = \frac{2\beta(H)}{Re^{**n}}. \tag{VI.5}$$

Let us introduce an auxiliary variable

$$\chi = U^{2n+3} \cdot \overline{H}^{n+1} \cdot r_0^{n+1} \cdot Re^{**n} \cdot \delta^{**} \tag{VI.6}$$

and let us denote

$$\psi = U^3 \cdot r_0 \cdot \overline{H} \cdot \delta^{**}. \tag{VI.7}$$

Then we obtain

$$\chi = \psi^{n+1} \left(\frac{1}{\nu}\right)^n; \quad \frac{d\chi}{dx} = (n+1)\psi^n \left(\frac{1}{\nu}\right)^n \frac{d\psi}{dx}. \tag{VI.8}$$

Substituting (VI.6)-(VI.8) in the energy equation, we have

$$\frac{d\chi}{dx} = (n+1) \cdot U^{2n+3} \cdot r_0^{n+1} \cdot \overline{H}^n \cdot Re^{**n} \left(\frac{2\beta(H)}{Re^{**n}} + \frac{v_0}{U}\right). \tag{VI.9}$$

Integration of (VI.9) gives

$$\chi = \chi_1 + \int_{x_1}^{x} (n+1) \cdot \overline{H}^n \cdot U^{2n+3} \cdot r_0^{n+1} \left[2\beta(H) + \frac{v_0}{U} Re^{**n}\right] dx, \tag{VI.10}$$

Here

$$\chi_1 = Re_1^{**n} \cdot \delta_1^{**} \cdot U_1^{2n+3} \cdot r_{10}^{n+1}.$$

[1]Yu. N. Karpeyev generalized the Truckenbrodt method to the case of a permeable surface.
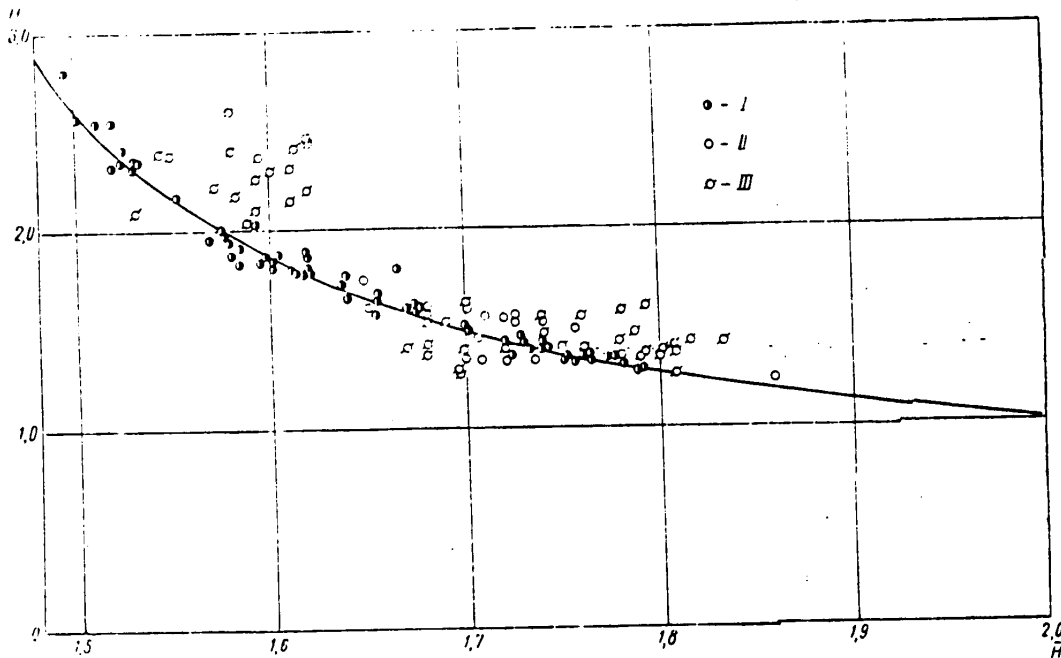
271

Figure VI.12. Form parameter H as a function of $\bar{H}$ in the case
of TBL control.
I -- uncontrolled TBL; II -- data from processing the measurements
of [1], [2] undertaken by Pechau [26]; III -- results of measure-
ments by Wust [27] on a plate with suction.

The subscript "1" corresponds to the values in the layer cross section $x=x_1$ where
the distributed injection or suction of a fluid from the TBL begins.

Let us introduce a new variable

$$0(x) = Re^{**n} \cdot \delta^{**}. \tag{VI.11}$$

Then from (VI.6), we obtain

$$0(x) = \frac{\chi}{\bar{H}^{n+1} \cdot U^{2n+3} \cdot r_0^{n+1}}. \tag{VI.12}$$

Considering (VI.10), from (VI.12) we have

$$0(x) = \frac{\chi_1 + \int_{x_1}^{x} (n+1) \cdot \bar{H}^n \cdot U^{2n+3} \cdot r_0^{n+1} \left[2\beta(') + \frac{v_0}{U} Re^{**n} \right] dx}{\bar{H}^{n+1} \cdot U^{2n+3} \cdot r_0^{n+1}}. \tag{VI.13}$$

Let us rewrite (VI.13) as follows:

$$0(x) = \frac{\chi_1 + \int_{x_1}^{x} E(H) \cdot U^{2n+3} \cdot r_0^{n+1} \left(1 + \frac{1}{2\beta} \frac{v_0}{U} Re^{**n} \right) dx}{\bar{H}^{n+1} \cdot U^{2n+3} \cdot r_0^{n+1}}, \tag{VI.14}$$

272

where $E(H)=2(n+1)\beta\overline{H}^n$ is a function which depends weakly on the Reynolds number and form parameter. It is possible approximately to take it constant and outside the integral sign. In accordance with Truckenbrodt, let us make another assumption: namely, let us take the value of $\overline{H}$ as constant (considering that in practice the range of variation of $\overline{H}$ in the calculations is $1.6<\overline{H}<1.8$). Denoting the quotient $E(H)/\overline{H}^{n+1}=A$, for calculation of $\theta(x)$ we obtain the following expression:

$$\theta(x) = \frac{\chi_1 + A\int_{x_1}^{x} U^{2n+3}\cdot r_0^{1+n}\left(1+\frac{1}{2\beta}\frac{v_0}{U}Re^{**n}\right)dx}{U^{2n+3}r_0^{n+1}}.$$ (VI.15)

The constant A can be determined from the condition of applicability of (VI.15) for the special case of a TBL on a plate ($U=U_\infty=const$; $v_0=0$; $r_0\equiv1$). If we set $\chi_1=0$, for $x_1=0$, then from (VI.15) in this case we have

$$\theta(x)_{plate} = A\cdot x.$$ (VI.16)

Key: 1. plate

Considering that for a plate of length L with flow over it on one side with a velocity U_∞, we have the expression

$$\frac{\delta_L^{**}}{L} = \frac{\zeta_F}{2},$$ (VI.17)

from comparison of (VI.16) and (VI.17) we obtain

$$A = \left(\frac{U_\infty L}{\nu}\right)^n\left(\frac{\zeta_F}{2}\right)^{n+1}.$$ (VI.18)

On the basis of analyzing the data on the drag of a plate for Reynolds numbers $U_\infty L/\nu>3\cdot10^6$ it is recommended in reference [21] that we take $A=0.765\cdot10^{-2}$.

The parameter θ and the value Re^{**} uniquely related to it are calculated by the method of successive approximations. As the first approximation it is possible to take either the function $\theta(x)$ calculated for the case $v_0=0$ or the function obtained under the assumption of constancy of the complex $(v_0/U)Re^{**}=\xi=const$. The choice of θ in the first approximation is defined by the conditions of the specific calculation, in particular, the suction or injection velocity distribution law.

For determination of the form parameter H, according to Truckenbrodt, we use the equation obtained on subtraction of the pulse equation (IV.29), the terms of which are multiplied by $\overline{H}$, from the energy equation (IV.30),

$$\delta^{***}\frac{dH}{dx} = (H-1)\overline{H}\frac{\delta^{**}}{U}\frac{dU}{dx}+2c_D-\overline{H}\frac{1}{2}\zeta_f+(1-\overline{H})\frac{v_0}{U}.$$ (VI.19)

After certain algebraic transformations and introduction of a substitution

$$l = \int \frac{d\overline{H}}{(H-1)\overline{H}} \tag{VI.20}$$

(VI.19) is converted to the form

$$\theta(x)\frac{dl}{dx} = \theta\frac{d\ln U}{dx} - K(\text{Re}^{**}, H) + \varphi(H)\frac{v_0}{U}\text{Re}^{**}, \tag{VI.21}$$

where

$$K(\text{Re}^{**}, H) = -\frac{\left(2c_D - \overline{H}\frac{1}{2}\zeta_1\right)}{(H-1)\overline{H}}\text{Re}^{**n}, \quad \varphi(H) = \frac{1-\overline{H}}{H(\overline{H}-1)}$$

can be approximated by linear relations (the form parameters $\overline{H}$, H and ℓ are uniquely related on the basis of (VI.4)):

$$K(\text{Re}^{**}, H) = a(l-b), \tag{VI.22}$$

$$\varphi(H) = -(cl+d). \tag{VI.23}$$

In (VI.22) and (VI.23) the coefficients have the following values:

$$a = 3.04\cdot10^{-2}, \quad b = 0.07\cdot\lg\text{Re}^{**} - 0.230, \quad c = 4.52, \quad d = 1.06.$$

After linearization of the function K and ψ, the equation (VI.21) becomes a linear first-order differential equation

$$\frac{dl}{dx} + \frac{(a+c\xi)}{\theta}l = \frac{d\ln U}{dx} + \frac{ab-d\xi}{\theta}, \tag{VI.24}$$

the common integral of which is the expression

$$l(x) = \exp\left\{-\int_{x_0}^{x} p(x)\,dx\right\}\left[l(x_1) + \int_{x_0}^{x} q(x)\exp\left\{\int_{x_0}^{x} p(x)\,dx\right\}dx\right],$$

where

$$p(x) = \frac{a+c\xi}{\theta}, \quad q = \frac{U'}{U} + \frac{ab-d\xi}{\theta}, \quad \xi = \frac{v_0}{U}\text{Re}^{**n}$$

are known functions of the variable x, for the function $\theta(x)$, and, consequently, also Re**(x) (see formula (VI.11)), has already been defined as a result of integration of equation (VI.5). It is possible to determine the initial value of $\ell(x_1)$ by the graph of $\ell=\ell(H)$ (Figure VI.13) constructed using expressions (VI.4) and (VI.20), for the magnitude of $H(x_1)$ at the beginning of the permeable section of the surface over which flow takes place is found as a result of calculating the TBL on an impermeable wall to the point $x=x_1$. The calculation basically ends

274

with determination of θ' $_{;)}$ and $\ell(x)$. All the remaining TBL characteristics such as Re**, H, $\bar{H}$, $\tau_0/\rho U^2$ are related to θ and ℓ and are calculated by formulas (VI.11), VI.4) and by the graph presented in Figure VI.13.

For the case of distributed suction or injection with constant velocity under plate conditions ($u=U_\infty$; $r_0\equiv1$), equation (VI.15) can be integrated in closed form. Here, considering the "initial" condition Re**=0; x=0, it assumes the form

$$\mathrm{Re}^{**^{n+1}} = A\,\mathrm{Re}_x + \frac{A}{2\beta}\frac{v_0}{U_\infty}\int_0^{\mathrm{Re}_x} \mathrm{Re}^{**^n}\,d\mathrm{Re}_x \qquad\text{(VI.25)}$$

(here $\mathrm{Re}_x = U_\infty x/\nu$).
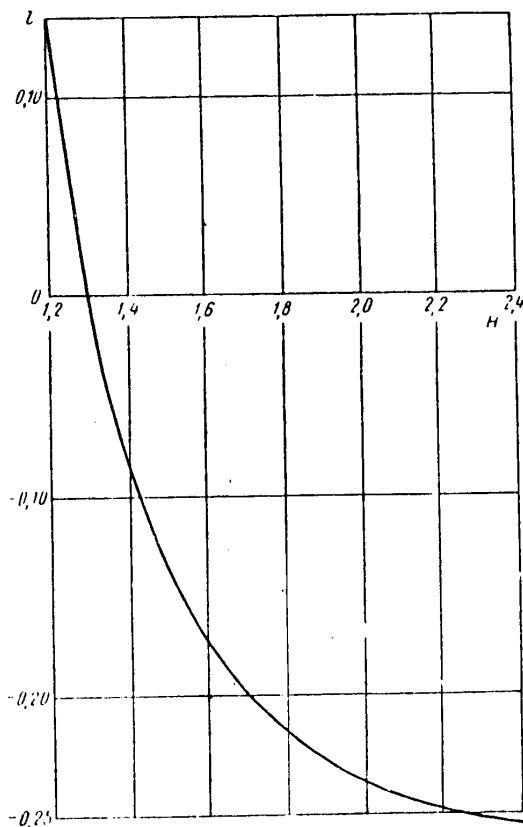
Figure VI.13. The function $\ell(H)$

Single differentiation of the components of (VI.25) with respect to Re_x leads to the equation

$$\mathrm{Re}^{**^n}\frac{d\,\mathrm{Re}^{**}}{d\,\mathrm{Re}_x} = \frac{A}{(n+1)}\left(1 + \frac{1}{2\beta}\frac{v_0}{U_\infty}\mathrm{Re}^{**^n}\right), \qquad\text{(VI.26)}$$

275

the integral of which (for n=1/6) obtained by the method of separation of variables can be written in the form

$$Re_x = \frac{Re^{**7/6}}{A} \frac{7}{(z-1)^7} \left(\frac{z^6}{6} - \frac{6}{5} z^5 + \frac{15}{4} z^4 - \frac{20}{3} z^3 + \right.$$

$$\left. + \frac{15}{2} z^2 - 6z + \ln z + \frac{49}{20} \right),$$ (VI.27)

where

$$z = 1 + \frac{1}{2\beta} \frac{v_0}{U_\infty} Re^{**1/6}; \quad A = 0,765 \cdot 10^{-2}; \quad \beta = 0,521 \cdot 10^{-2}.$$

For $v_0/U \to 0$ and, consequently, $z \to 1$ (VI.27) reduces to the expression that follows from the known Faulkner equality [26]

$$Re^{**} = 0,0153 \, Re_x^{6/7}.$$ (VI.28)

The local friction coefficient is determined from the pulse equation, which for the given case has the form

$$\frac{\zeta_f}{2} = \frac{d \, Re^{**}}{d \, Re_x} - \frac{v_0}{U_\infty}.$$ (VI.29)

Hence, considering (VI.27) we have

$$\frac{\zeta_f}{2} = \frac{v_0}{U_\infty} \left[\frac{A}{2(n+1)\beta} \frac{z}{z-1} - 1 \right].$$ (VI.30)

For $v_0 \to 0$, this expression becomes the expression given by Faulkner

$$\frac{\zeta_{f_0}}{2} = 0,00655 \cdot Re^{**-1/6} = 0,0132 \, Re_x^{-1/7}.$$ (VI.31)

The results of calculating the value of ζ_f by formulas (VI.27)-(VI.30) for the given v_0/U_∞ and also the corresponding results of the experimental studies of [1] are presented in Figure VI.14.

Equations (VI.5) and (VI.19) can also be used to investigate the other special case of control which permits creation of flow with characteristics close to separated flow in the entire controlled section of the TBL. This result can be reached using distributed injection by a defined law. Considering that the TBL form parameters in this section are constant and have values of $\overline{H} \approx H_{sep}$ and $\overline{H} \approx H_{sep}$, and the tangential frictional stress on the wall is close to zero, from (VI.19) we obtain the following expression for the injection velocity distribution law

$$\frac{v_0}{U} = \frac{H_{\text{orp}}^{(1)} (H_{\text{orp}}^{(1)} - 1)}{(H_{\text{orp}} - 1)} \frac{\delta^{**}}{U} \frac{dU}{dx} - \frac{2\beta}{Re^{**n} (1 - \overline{H}_{\text{orp}})}.$$ (VI.32)

Key: 1. sep

For the special case of a plate (dU/dx=0), from (VI.32) we have

$$\frac{v_0}{U} Re^{**n} = \frac{2\beta}{\overline{H}_{\text{orp}} - 1} = \xi = const.$$ (VI.33)

276

If we assume that the distributed injection velocity is defined in the first approximation by formula (VI.33), it is possible to find the function $\theta(x)$ in the same approximation

$$\theta(x) = \frac{\chi_1 + A\frac{\overline{H}_{\text{отр}}^{(1)}}{\overline{H}_{\text{отр}} - 1}\int_{x_1}^{x} U^{2n+3}r_0^{n+1}\,dx}{U^{2n+3}r_0^{n+1}},$$

Key: 1. sep

where $\theta(x)$, Re** and δ** are uniquely related to each other. Substitution of their values in (VI.32) makes it possible to calculate the distributed injection velocity in the first approximation.

The Eppler method [28] belongs to the group of methods following the basic principles of the paper by Truckenbrodt. The initial equations of the method are also the pulse and energy equations. Additional semi-empirical relations, as before, include the functions $\zeta_f(\text{Re**}, H)$; $c_D(\text{Re**}, H)$ and $H(\overline{H})$. However, the form of these relations is somewhat altered, beginning with the specific requirements which, in Eppler's opinion, they must satisfy in the case of suction. Eppler considered the necessity for expanding the region of application of the above-mentioned functions in the direction of values of H<1.2, in view of the fact that suction leads to a decrease in the magnitude of this form parameter. The mentioned requirements basically consist in the following:

a) Mandatory observation of the condition lim H=1 for $\overline{H}{\to}2$;

b) Restriction of the influence of fast growth of δ** for H→1 on ζ_f and c_D, which in the absence of such a restriction, approach zero.

Considering the enumerated requirements, Eppler recommends the following expressions for the additional functions:

$$H = \frac{11\overline{H} + 15}{48\overline{H} - 59};\qquad\qquad\qquad\text{(VI.34)}$$

$$2\zeta_f = \frac{\tau_0}{\rho U^2} = 0.045716\,[(H-1)\,\text{Re**}]^{-0.232};\qquad\text{(VI.35)}$$

$$C_D = 0.050\,[(H-1)\,\text{Re**}]^{1/6}.\qquad\qquad\text{(VI.36)}$$

In the region of variation of 1.2<H<2.6, these expressions agree well with the experimental data and expression (VI.2), (VI.3), (VI.4).

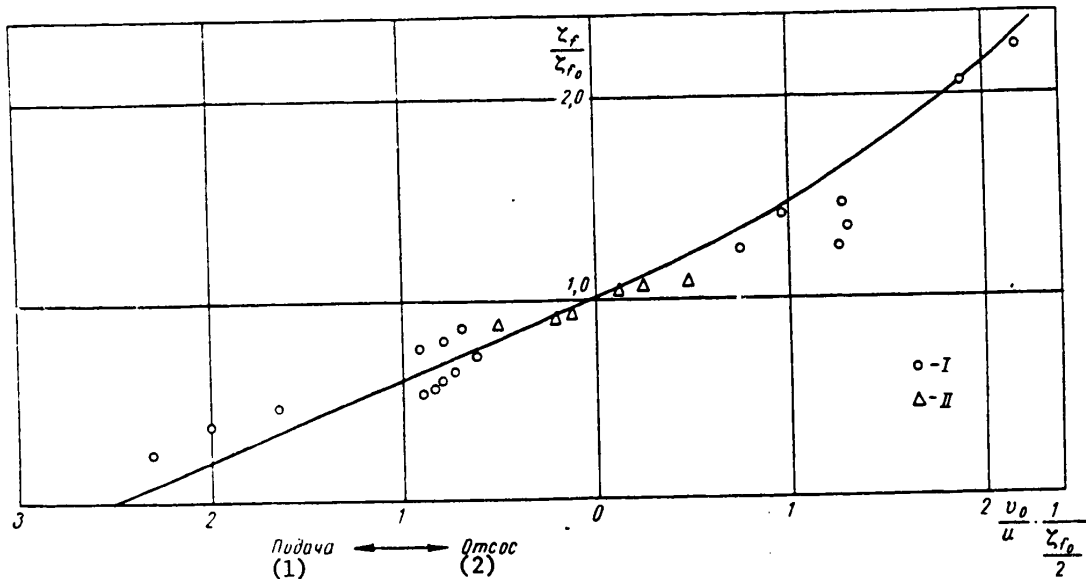Figure VI.14. Ratios ζ_f/ζ_{f0} as a function of the parameter $v_0/U_\infty^{1} \cdot/\zeta_{f0}/2$.
I -- experimental data [1]; II -- calculation by the
K. K. Fedyayevskiy method; solid line -- calculation by formula
(VI.30)

Key:
1. Injection
2. Suction

An important characteristic feature of Eppler's method is the application of numerical integration of the system of initial equations, which has the following form for the investigated problem[1]

$$\frac{d\,Re^{**}}{d\bar{x}} = -Re^{**}(H+1)\frac{d\ln\bar{U}}{d\bar{x}} + Re\bar{U}\left(\frac{\zeta_f}{2} + \bar{v}_0\right);$$
$$\frac{d\,Re_{\vartheta}}{d\bar{x}} = -2Re_{\vartheta}\frac{d\ln\bar{U}}{d\bar{x}} + Re\bar{U}(2c_D + \bar{v}_0),$$

(VI.37)

where

$$Re_{\vartheta} = \frac{U\delta_{\vartheta}}{\nu}; \quad Re = \frac{U_\infty L}{\nu}; \quad \bar{U} = \frac{U}{U_\infty}; \quad \bar{x} = \frac{x}{L}; \quad \bar{v}_0 = \frac{v_0}{U},$$

here U_∞ and L are the velocity and length characteristic of the given problem.

In order more clearly to emphasize the mathematical characteristics of the equations (VI.37), it is expedient to write them in the form

$$\frac{d\,Re^{**}}{d\bar{x}} = f_1(\bar{x}, Re^{**}, Re_{\vartheta}); \quad \frac{d\,Re_{\vartheta}}{d\bar{x}} = f_2(\bar{x}, Re^{**}, Re_{\vartheta}).$$

(VI.38)

---

[1]In reference [28] equations (VI.37) were used in the dimensional form of notation. The dimensionless form has the advantage that it permits calculations by a more compact scheme.

278

For numerical integration of this system Eppler recommends the Runge method.

If the initial values of Re**, Re_e, $\bar{U}$, v_0 at the point $\bar{x}_i$ and finite values of $\bar{U}$, v_0 at the point $x_i + \Delta x$ are given, then the increments of the variables Re** and Re_e in the segment from x_i to $x_i + \Delta x$ will be defined by the following expressions, respectively, in the first and second approximations

$$
\begin{aligned}
\Delta Re_i^{**(1)} &= f_1\left(\bar{x}_i,\ Re_i^{**},\ Re_{3_i}\right)\Delta\bar{x}; \\
\Delta Re_{3i}^{(1)} &= f_2\left(\bar{x}_i,\ Re_i^{**},\ Re_{3_i}\right)\Delta\bar{x}; \\
\Delta Re_i^{**(2)} &= f_1\left(\bar{x}_i + \frac{\Delta\bar{x}}{2};\ Re_i^{**} + \frac{\Delta Re_i^{**(1)}}{2};\ Re_{3_i} + \frac{\Delta Re_{3_i}^{(1)}}{2}\right)\Delta\bar{x}; \\
\Delta Re_{3i}^{(2)} &= f_2\left(\bar{x}_i + \frac{\Delta\bar{x}}{2};\ Re_i^{**} + \frac{\Delta Re_i^{**(1)}}{2};\ Re_{3_i} + \frac{\Delta Re_{3_i}^{(1)}}{2}\right)\Delta\bar{x}.
\end{aligned}
\qquad (VI.39)
$$

In spite of the apparent awkwardness of formulas (VI.39), the calculation scheme by them is simple. On breakdown of the steps usually used in the practice of calculating TBL, the tediousness of this calculation does not differ very much from the tediousness of calculations by other methods. The advantages of the numerical method of integration consist in absence of mathematical simplifications and additional assumptions, without which it is impossible to obtain a solution by other methods, and also convenience of implementation of this method on computers. The accuracy of calculating the TBL characteristics by Eppler's method can be very high. As Eppler notes, it is expedient to achieve an increase in accuracy as a result of a decrease in step size Δx and not by using more complex numerical integration procedures.

For fast variation of the functions $\bar{U}(\bar{x})$ or $\bar{v}_0(\bar{x})$ and also for large $\Delta\bar{x}$, instability of the solution expressed in disturbance of smoothness of variation of the calculated TBL characteristics and an increase in the error can arise during the calculation process. Conditions insuring stability consist in restrictions imposed on the step size Δx. According to Eppler, the instability arises when

$$|H_i - 2H_{i+1/2} + \bar{H}_{i+1}| \geqq \varepsilon_1 \ (\varepsilon_1 \approx 0.001 \text{ to } 0.01).$$

If during the calculation the lefthand side of this equality exceeds the admissible value, it is necessary to resort to a decrease in step size. Near the separation point it is necessary to consider the additional destabilization condition

$$|\bar{H}_{i+1} - H_i| \geqq \varepsilon_2 \ (\varepsilon_2 \approx 0.01 \text{ to } 0.03).$$

Developing his own method, Eppler had in mind its application for TBL calculation with suction, in particular for calculating the suction velocity v_0 providing for satisfaction of special requirements imposed on the variation law of some of the boundary layer characteristics. A number of practical purposes of the application of suction are satisfied by the condition of constancy of the TBL form parameter on the surface over which flow takes place. For example, maintenance of the pre-separation value of the form parameter promotes elimination of the danger of separation in the case of large positive pressure gradients.

Calculations of the characteristics of uncontrolled TBL for the experimental conditions described by Dryden [30] were made by the modified Eppler method [29]. Figure VI.15 shows the results of the calculations and the experimental data, a comparison of which demonstrates very satisfactory agreement of them outside the preseparation region (H$\lesssim$1.8). The curves presented on this graph for H(x) are the most indicative for such comparisons, for the peculiarities of one method of calculating the TBL or another are felt most sharply in the values of the form parameters.

In Figure VI.15 results are also presented from the calculation for the case of distributed suction with constant relative velocity v_0/U=0.0005, beginning with $\bar{x}$=0.5. These data show that suction even with low intensity effectively promotes the prevention of separation with significant positive pressure gradients.

Each of the methods investigated in this section has its advantages and disadvantages. For example, direct generalization of the Truckenbrodt method, permitting us to obtain a relatively precise solution, is distinguished by complexity. The Eppler method which is free of mathematical simplifications as a result of the application of numerical integration of the initial system of differential equations is more effective. This fact advantageously distinguishes the Eppler method among others from the point of view of performing the calculation on computers. When using ordinary computing means the calculation by the Eppler method with the same number of calculation points differs little with respect to labor intensiveness from other methods. at the same time giving more reliable results.
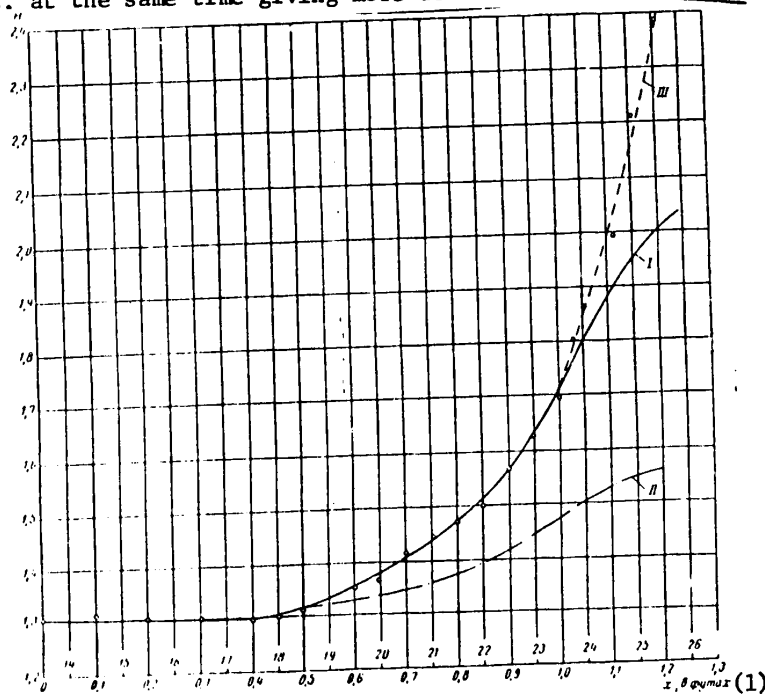

Figure VI.15. Results of the calculation by the modified Eppler method. I -- uncontrolled TBL; II -- TBL with suction with an intensity v_0/U=0.0005; III -- experimental data [30]

Key: 1. x, in feet

§VI.3. Application of the K. K. Fedyayevskiy Method to Calculation of a Turbulent Boundary Layer in the Presence of Injection and Suction

In this section a discussion is presented of the methods of calculating the turbulent boundary layer characteristics in the presence of injection and suction using the semi-empirical turbulence theory.

The method of calculating a turbulent boundary layer in the presence of a longitudinal pressure gradient proposed by K. K. Fedyayevskiy and A. S. Ginevskiy [32], [33], [34] was taken as the initial method.

As will be demonstrated below, the advantage of this method is that with a fixed value of the K. K. Fedyayevskiy form parameter the basic relations relating the values which enter into the integral relations of the investigated problem for a controlled layer with respect to form coincide with the corresponding uncontrolled layer functions.

It is recommended that the turbulent boundary layer be calculated in the presence of injection and suction by the method of successive approximations, beginning with the assumption of the possibility of extension of the empirical constants and a number of relations for the characteristics of the uncontrolled boundary layer to the case of a controlled layer. The parameters of the uncontrolled turbulent boundary layer were taken as the zero approximation.

In order to simplify the method of calculating the zero approximation and avoid tedious calculations it is possible to use A. V. Kolesnikov's recommendations [35], which permit improvement of the calculation part of the K. K. Fedyayevskiy method.

As A. V. Kolesnikov has demonstrated, calculation of the uncontrolled boundary layer on the basis of the semi-empirical turbulence theory by the K. K. Fedyayevskiy method can be made as simple as the semi-empirical calculation technique of L. G. Loytsyanskiy [36] based on the analogy between turbulent and laminar layers.

As a result of introducing a new form parameter analogous to the L. G. Loytsyanskiy form parameter, it was possible to convert the integral relation of the boundary layer pulses to a linear nonuniform first-order differential equation, the solution of which is expressed in quadratures. Thus, it was possible greatly to simplify the K. K. Fedyayevskiy and A. S. Ginevskiy method for calculation of an uncontrolled turbulent boundary layer. A comparison of the calculation results by this method with experiments demonstrated satisfactory correspondence. Hereafter the Fedyayevskiy-Ginevskiy-Kolesnikov method is used as zero approximation for calculating a controlled turbulent boundary layer.

Theoretical Principles of the Method of Calculating a Turbulent Boundary Layer with Fluid Injection and Suction. The equations of the nonstationary turbulent boundary layer have the form

$$\frac{\partial u}{\partial t} + u\frac{\partial u}{\partial x} + v\frac{\partial u}{\partial y} = \frac{\partial U}{\partial t} + U\frac{\partial U}{\partial x} + \frac{1}{\rho}\frac{\partial \tau}{\partial y}, \qquad (VI.40)$$

$$\frac{\partial u}{\partial x} + \frac{\partial v}{\partial y} = 0. \qquad (VI.41)$$

281

In accordance with K. K. Fedyayevskiy [32], let us represent the square root of the ratio of the frictional stress in the boundary layer τ to the frictional stress on the wall τ_0 in the form of a polynomial with respect to powers of $\eta = y/\delta$ (δ is the thickness of the boundary layer)

$$\sqrt{\frac{\tau}{\tau_0}} = \sum_{n=0}^{n} a_n \eta^n. \tag{VI.42}$$

The coefficients of the polynomial will be defined from the following boundary conditions for $\sqrt{\tau/\tau_0}$ and its derivatives on the wall ($y=0$) and on the outer boundary ($y=\delta$):

a) For a wall when $\eta = y/\delta = 0$:

$$\sqrt{\frac{\tau}{\tau_0}} = 1; \quad u = u_0(x); \quad v = v_0(x). \tag{VI.43}$$

Here u_0, v_0 are the given fluid injection law ($v_0 > 0$) or fluid suction law ($v_0 < 0$) for $\eta = 0$. In addition, for $\eta = 0$, as follows from (VI.40)

$$\left(\frac{\partial \tau}{\partial y}\right)_{y=0} = -\rho\left(\frac{\partial U}{\partial t} + U\frac{\partial U}{\partial x} - u_0\frac{\partial u_0}{\partial x}\right) + \rho v_0\left(\frac{\partial u}{\partial y}\right)_{y=0}, \tag{VI.44}$$

which gives

$$\left|\frac{\partial}{\partial \eta} \cdot \sqrt{\frac{\tau}{\tau_0}}\right|_{\eta=0} = \frac{1}{2}A, \tag{VI.45}$$

where A is the generalized form parameter of K. K. Fedyayevskiy.

$$A = \frac{\rho\delta}{\tau_0}\left(u_0\frac{\partial u_0}{\partial x} - U\frac{\partial U}{\partial x} - \frac{\partial U}{\partial t}\right) + \frac{v_0\delta}{v}. \tag{VI.46}$$

When writing (VI.46) it is also considered that within the limits of a laminar sublayer the tangential stress is defined by the Newton formula

$$\tau = \mu\frac{\partial u}{\partial y}. \tag{VI.47}$$

Hence, it follows that

$$\left(\frac{\partial u}{\partial y}\right)_{y=0} = \frac{\tau_0}{\mu}; \tag{VI.48}$$

b) On the outer boundary of the boundary layer for $\eta = y/\delta = 1$ we have

$$\sqrt{\frac{\tau}{\tau_0}} = 0. \tag{VI.49}$$

In expression (VI.42), just as in the case of an uncontrolled turbulent boundary layer we shall limit ourselves to only three terms and for determination of the coefficients a_n we shall use the above-indicated boundary conditions (VI.43), (VI.44), (VI.49). As a result, we obtain

$$a_0 = 1; \quad a_1 = \frac{A}{2}; \quad a_2 = -\left(1 + \frac{A}{2}\right).$$

Then from (VI.42) we find

$$\sqrt{\frac{\tau}{\tau_0}} = 1 + \frac{A}{2}\eta - \left(1 + \frac{A}{2}\right)\eta^2. \qquad \text{(VI.50)}$$

From investigation of the above-presented formulas it is obvious that the tangential stress distribution across the layer described by the polynomial (VI.50) is universal and applicable both for the uncontrolled layer and for the controlled turbulent boundary layer with fluid injection and suction. The effect of the conditions of motion and boundary conditions of the problem is felt only through the magnitude of the form parameter A.

Therefore, hereafter when deriving the corresponding formulas for the velocity profile and the resistance law we shall proceed in accordance with the papers by K. K. Fedyayevskiy and A. S. Ginevskiy [33], [34].

Just as for the uncontrolled nonstationary turbulent boundary layer we shall use the Prandtl formula for tangential stress in a turbulent layer

$$\tau = \rho l^2 \left(\frac{\partial u}{\partial y}\right)^2. \qquad \text{(VI.51)}$$

Here l is the mixing path length.

From (VI.51) we obtain the following differential equation:

$$\frac{d\left(\frac{u}{v^*}\right)}{d\eta} = \frac{\sqrt{\frac{\tau}{\tau_0}}}{\frac{l}{\delta}}, \qquad \text{(VI.52)}$$

where v* is the dynamic velocity

$$v^* = \sqrt{\frac{\tau_0}{\rho}}. \qquad \text{(VI.53)}$$

Integrating (VI.52) within the limits from 1 to η, we find

$$\frac{u}{v^*} = \frac{U}{v^*} + \int_1^\eta \frac{\sqrt{\frac{\tau}{\tau_0}}}{\frac{l}{\delta}} d\eta. \qquad \text{(VI.54)}$$

Let us express the dimensionless mixing path in the form

$$\bar{l} = \frac{l}{\delta} = \varkappa\eta, \qquad \text{(VI.55)}$$

where $\varkappa$ is a universal constant determined experimentally. The experiments show that for an uncontrolled boundary layer $\varkappa=0.4$.

283

Substituting (VI.50) and (VI.55) in (VI.54), after integration we obtain the
following expression for the velocity profile in a turbulent boundary layer:

$$\frac{u}{U} = 1 + \frac{1}{z}\left[\ln\eta - \frac{1}{2}(A-\eta) + \frac{1}{2}\left(1+\frac{A}{2}\right)\cdot\left(1-\eta^2\right)\right].$$ (VI.56)

Here

$$z = \frac{\varkappa U}{v^*}.$$ (VI.57)

Formula (VI.56) is valid only outside the limits of the laminar sublayer, for
directly at the wall, from (VI.56) we do not obtain u/U=0, but u/U→−∞.

In order to find the relation between the frictional stress at the wall and other
turbulent boundary layer characteristics, it is necessary to consider the laminar
sublayer.

In the laminar sublayer ($y/\delta \le \delta_\ell/\delta \le 1$, δ_ℓ is the sublayer thickness), the velocity
distribution u/U will be found beginning with the following formula for the tan-
gential stress distribution:

$$\tau = \tau_0\left(1+\frac{A}{2}\eta\right)^2.$$ (VI.58)

Comparing expression (VI.47) and (VI.58), we find

$$\frac{\partial u}{\partial y} = \frac{\tau_0}{\mu}\left(1+\frac{A}{2}\eta\right)^2.$$

Integrating this expression, we obtain

$$u = u_1(x) + \frac{\tau_0}{\mu}\left(y + \frac{A}{2\delta}y^2 + \frac{1}{12}\cdot\frac{A^2}{\delta^2}y^3\right) \simeq$$

$$\simeq u_1(x) + \frac{\tau_0}{\mu}\left(y + \frac{A}{2\delta}y^2\right).$$ (VI.59)

Let us define the function $u_1(x)$ from the condition $u_{y=0}=u_0$. Then we find

$$u = u_0 + \frac{\tau_0}{\mu}\left(y + \frac{A}{2\delta}y^2\right)$$ (VI.60)

or

$$\frac{u}{v^*} = \frac{u_0}{v^*} + \text{Re}_{v^*}\eta + \frac{A}{2}\text{Re}_{v^*}\eta^2.$$ (VI.61)

Here

$$\text{Re}_{v^*} = \frac{v^*\delta}{v}.$$ (VI.62)

On the outer boundary of the laminar sublayer $\eta=\eta_\ell=\delta_\ell=\delta$, the velocity u will be
determined from (VI.61), setting

$$\frac{u_\ell}{v^*} = \frac{u_0}{v^*} + \text{Re}_{v^*}\frac{\delta_\ell}{\delta} + \frac{A}{2}\text{Re}_{v^*}\left(\frac{\delta_\ell}{\delta}\right)^2.$$ (VI.63)

Let us define the thickness of the laminar sublayer by the Karman formula

284

$$\delta_n = \alpha \frac{\nu}{v^*}.$$

(VI.64)

Here α is the universal constant defined experimentally (for an uncontrolled boundary layer $\alpha = 11.5$). Substituting (VI.64) in (VI.63), we find

$$\frac{u_n}{v^*} = \frac{u_0}{v^*} + \alpha + \frac{A}{2} \cdot \frac{\alpha^2}{\mathrm{Re}_{v^*}}.$$

(VI.65)

Another expression for u_ℓ will be determined from (VI.56), substituting $\eta = \eta_\ell = \delta_\ell / \delta$.

Equating the values of u_ℓ from (VI.65) and (VI.56) for $\eta = \delta_\ell / \delta$, we obtain the following formula for the resistance law:

$$u_0 + \alpha v^* + A \frac{\alpha^2 v^*}{2\mathrm{Re}_{v^*}} = U + \frac{v^*}{\kappa} \left\{ \ln \frac{\delta_n}{\delta} - \frac{1}{2} \left(A - \frac{\delta_n}{\delta} \right) + \right.$$

$$\left. + \frac{1}{2} \left(1 + \frac{A}{2} \right) \cdot \left[1 - \left(\frac{\delta_n}{\delta} \right)^2 \right] \right\}.$$

(VI.66)

After substituting formula (VI.64) in (VI.66) and the corresponding transformations we obtain the following expression for the resistance law:

$$z = \frac{1}{1 - \frac{u_0}{U}} \left[\left(\kappa\alpha - \ln \alpha - \frac{1}{2} \right) + \frac{\alpha}{2} \cdot \frac{A}{\mathrm{Re}_{v^*}} (\kappa\alpha - 1) + \right.$$

(VI.67)

$$\left. + \ln \mathrm{Re}_{v^*} + \frac{A}{4} + \frac{A}{4} \cdot \frac{\alpha^2}{\mathrm{Re}_{v^*}^2} \right],$$

or

$$z = \frac{1}{1 - \frac{u_0}{u}} \left[\left(\kappa\alpha - \ln \alpha - \frac{1}{2} \right) + \frac{\alpha}{2} (\kappa\alpha - 1) \frac{AH^{**}z}{\kappa \mathrm{Re}^{**}} + \right.$$

$$\left. + \ln \frac{\kappa \mathrm{Re}^{**}}{zH^{**}} + \frac{A}{4} + \frac{A}{4} \cdot \frac{\alpha^2}{\kappa^2} \left(\frac{H^{**}}{\mathrm{Re}^{**}} \right)^2 z^2 \right].$$

(VI.68)

Here

$$H^{**} = \frac{\delta^{**}}{\delta}; \quad \mathrm{Re}^{**} = \frac{U\delta^{**}}{\nu}; \quad \mathrm{Re}_{v^*} = \frac{v^*\delta}{\nu} = \frac{\kappa}{z} \cdot \frac{\mathrm{Re}^{**}}{H^{**}}.$$

(VI.69)

Let us use formula (VI.65) for determination of the provisional boundary layer thicknesses. Here, on the basis of smallness of δ_ℓ / δ, integration with respect to y will be carried out not within the limits from δ_ℓ to δ, but from 0 to δ. Calculations show that the logarithmic singularity of the function $u/U = f(\eta)$ for $\eta = 0$ has little influence on the values of δ^*, δ^{**} and δ_e.

As a result, we obtain the following expressions for the provisional thicknesses of the boundary layer:

$$H^* = \frac{\delta^*}{\delta} = \frac{1}{\delta}\int_0^\delta \left(1 - \frac{u}{U}\right) dy = \frac{8 + A}{12Z};$$

$$H^{**} = \frac{\delta^{**}}{\delta} = \frac{1}{\delta}\int_0^\delta \frac{u}{U}\left(1 - \frac{u}{U}\right) dy = \frac{8 + A}{12Z} -$$

$$-\frac{1}{z^2}\left(\frac{56}{45} + \frac{83}{360}A + \frac{1}{80}A^2\right);$$

$$H_\vartheta \quad \frac{\delta_\vartheta}{\delta} = \frac{1}{\delta}\int_0^\delta \frac{u}{U}\left(1 - \frac{u^2}{U^2}\right) dy \quad \frac{8 + A}{6z} - \frac{3}{z^2}\left(\frac{56}{45} + \frac{83}{360}A +\right.$$

$$\left.+ \frac{1}{80}A^2\right) + \frac{1}{z^3}(3,6673 + 0,7936A + 0,0678A^2 + 0,0022A^3).$$

(VI.70)

Let us represent the form parameter A in the following form

$$A \quad \frac{\mu\delta}{\tau_0}\left(u_0 \frac{\partial u_0}{\partial x} - U\frac{\partial U}{\partial x} - \frac{\partial U}{\partial t}\right) + \frac{v_0\delta}{v} = \frac{z^2}{x^2}R_\delta Q + \mathrm{Re}_{v_0}.$$

(VI.71)

Here

$$Q = \frac{1}{\bar{U}\,\mathrm{Re}}\left(\bar{u}_0 \frac{\partial \bar{u}_0}{\partial \bar{x}} - \bar{U}\frac{\partial \bar{U}}{\partial \bar{x}} - \frac{\partial \bar{U}}{\partial \bar{t}}\right);$$

$$\bar{U} = \frac{U}{U_0}; \quad \bar{u}_0 = \frac{u_0}{U_0}; \quad \bar{x} = \frac{x}{L}; \quad \bar{t} = \frac{tU_0}{L};$$

$$\mathrm{Re} = \frac{U_0 L}{v}; \quad \mathrm{Re}_\delta = \frac{U\delta}{v}; \quad \mathrm{Re}_{v_0} = \frac{v_0\delta}{v}.$$

(VI.72)

In these formulas L is the characteristic linear dimension;

U_0 is the velocity at the initial point in time.

The presented formulas show that the parameters

$$H^*; \; H^{**}; \; H_\vartheta; \; H = \frac{\delta^*}{\delta^{**}} = \frac{H^*}{H^{**}}; \; \bar{H} = \frac{\delta_\vartheta}{\delta^{**}} = \frac{H_\vartheta}{H^{**}}$$

depend on the values of z, Q and Re_{v_0} which are independent arguments. Hereafter, we shall limit ourselves to the case where the fluid is injected only along the normal to the body surface, that is, we set $u_0 = 0$; $v_0 \neq 0$.

Inasmuch as expressions (VI.68), (VI.70) for the nonsteady controlled boundary layer in the case of $v_0 = 0$ coincide with the corresponding formulas of a nonsteady uncontrolled turbulent boundary layer for fixed values of the parameters A and Re**, when calculating a nonsteady controlled boundary layer the graphs of z=f(lg Re**,A) constructed by K. K. Fedyayevskiy and A. S. Ginevskiy [33] can be used.

In connection with the fact that the auxiliary graphs presented in reference [33] were constructed for a small number of fixed values of A and on a small scale, the graphs constructed by A. V. Kolesnikov will be presented below [35].

286

In accordance with A. V. Kolesnikov's recommendations, let us introduce a new form parameter into the investigation

$$f = -AH^{**}\left(\frac{z_0}{z}\right)^2. \tag{VI.73}$$

Here A is the generalized K. K. Fedyayevskiy form parameter defined by (VI.71); z_0 is the drag in the gradientless uncontrolled steady boundary layer corresponding to the Reynolds number Re**=U$_0\delta^{**}/\nu$.

From (VI.68) when A=0 and u_0=0, we find

$$z_0 = \varkappa\alpha - \ln\alpha - \frac{1}{2} + \ln\text{Re}^{**} - \ln\frac{\frac{2z_0}{3} - \frac{56}{45}}{\varkappa z_0}. \tag{VI.74}$$

When obtaining expression (VI.74), formula (VI.70) was used for H** when A=0.

After introduction of the value of the form parameter f in accordance with (VI.73) in place of A in (VI.68), the resistance law (VI.68) is reduced to the following form:

$$\frac{z}{z_0} = 1 + \ln\frac{z_0 H_0^{**}}{z H^{**}} - \frac{f}{z H^{**}}\left(\frac{z}{z_0}\right)^3 \times$$

$$\times \left[0.5 + \frac{z H^{**}}{\varkappa\,\text{Re}^{**}}\left(\varkappa\alpha^2 - \alpha + \frac{u^2 z H^{**}}{2\varkappa\,\text{Re}^{**}}\right)\right]. \tag{VI.75}$$

From expressions (VI.70) and (VI.73), we have

$$z H^{**} = \frac{2}{3} - \frac{1}{12}\frac{f}{H^{**}}\left(\frac{z}{z_0}\right)^2 - \frac{1}{z} \times$$

$$\times \left[\frac{56}{45} - \frac{83}{360}\frac{f}{H^{**}}\left(\frac{z}{z_0}\right)^2 + \frac{1}{80}\left(\frac{f}{H^{**}}\frac{z^2}{z_0^2}\right)^2\right]. \tag{VI.76}$$

Investigation of expressions (VI.73)-(VI.76) shows that for fixed values of A and Re** the magnitude of the form parameter f will be identical both for controlled and uncontrolled turbulent boundary layers. Therefore all of the above-presented formulas for a controlled turbulent layer written as a function of the form parameter f will compare with the corresponding formulas of a steady-state uncontrolled boundary layer for fixed values of A and Re**. Thus, when calculating a nonsteady or steady controlled turbulent layer, the graphs of A. V. Kolesnikov presented below can be used [35].

In Figure VI.16 we see the graphical dependence of ζ_f/ζ_{f0} on the form parameter f and the Reynolds number Re**

$$\frac{\zeta_f}{\zeta_{f_0}} = \left(\frac{z_0}{z}\right)^2 \varphi(f, \lg\text{Re}^{**}). \tag{VI.77}$$

Here ζ_f is the local drag factor;

ζ_{f_0} is the same for a plate with the same number Re**.

The curves in Figure VI.16 were obtained as a result of joint solution of the equations (VI.75) and (VI.76).

287

From expressions (VI.70) and (VI.73) the following formula is obtained for calculation of the displacement thickness:

$$zH^* = \frac{2}{3} - \frac{1}{\cdot H^{**}} \cdot \frac{f}{12}\left(\frac{z}{z_0}\right)^2.$$

(VI.78)

On the basis of (VI.76) and (VI.78), the parameter H was calculated as a function of the form parameter f for fixed values of Re**, which is also presented in Figure VI.16.

It is obvious that with an increase in the absolute magnitude of the form parameter f the ratio $\zeta_f/\zeta_{f_0} = (z_0/z)^2$ decreases, and the parameter H increases. For a value of $|f| = |f_s|$ corresponding to flow separation, we obtain $\zeta_f/\zeta_{f_0} = 0$. The value of $|f| = |f_s|$ depends on Re**: with an increase in Re** separation comes for large values of $|f_s|$. The value of H at the separation point fluctuates within the lmits of $1.75 < |f_s| < 1.80$.

The value of

$$z_0^{..} = \frac{2x^2}{-f_0}$$

(VI.79)

is expressed for a gradientless flow with the help of (VI.80).

The calculations demonstrated that the relation between $\lg \chi = \lg (Re^{**} \times z_0^2/\chi^2)$ and $\lg Re^{**}$ with a high degree of approximation can be replaced by two segments of a straight line as shown in Figure VI.17.
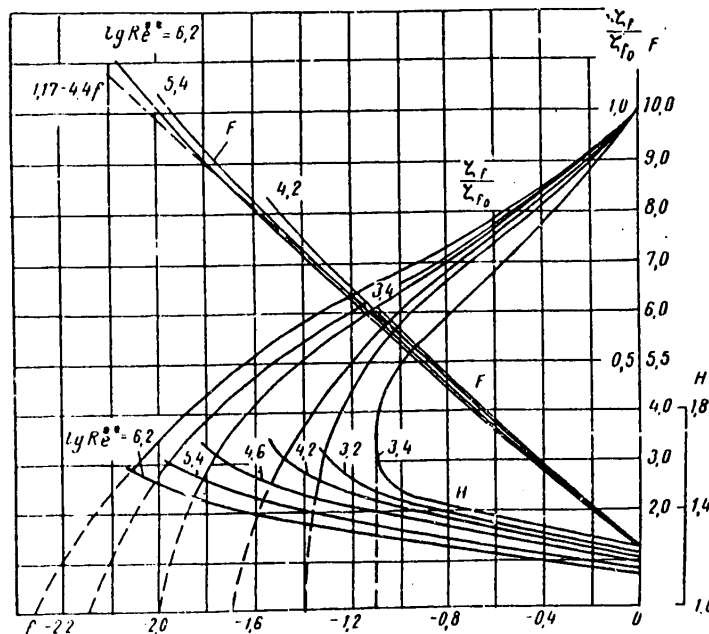
Figure VI.16. The dependence of the functions F, H, ζ_f/ζ_{f_0} on the parameter f.

288

Accordingly, the relation between $\chi = 2Re^{**}/\zeta_{f_0}$ and Re^{**} was presented by A. V. Kolesnikov in the form of the following relations:

for lg $Re^{**}=1$ to 3:

$$Re^{**} \quad 0.0348\chi^{0.776}; \quad \frac{\zeta_{f_0}}{2} \quad 0.01316(Re^{**})^{0.29};$$

(VI.80)

for lg $Re^{**}=3$ to 7:

$$Re^{**} = 0.0132\chi^{0.863}; \quad \frac{\zeta_{f_0}}{2} \quad = 0.00652(Re^{**})^{-0.16};$$

(VI.81)

Formula (VI.81) in practice coincides with the Faulkner formula obtained as a result of processing a large number of experimental data. Depending on the values of the form parameter f and the Reynolds number Re^{**}, the coefficients H^{**} and $\overline{H}=H_e/H^{**}$ are determined by Figures VI.18 and VI.19. In the case of a plate with steady-state uncontrolled boundary layer the values of H_0 and H_0^{**} are determined by Figure VI.17.
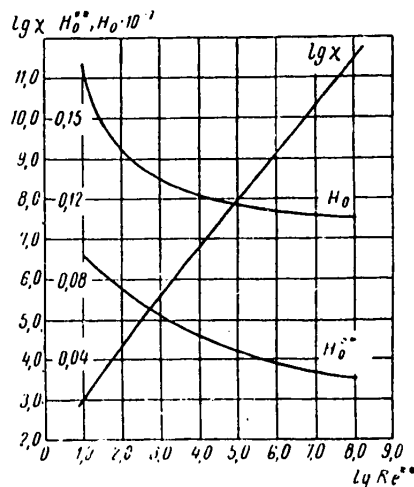
Figure VI.17. Dependence of the functions χ, H_0, H_0^{**} on the Reynolds number Re^{**}

Calculating the Characteristics of an Uncontrolled Turbulent Boundary Layer. Usually when calculating the controlled turbulent boundary layer characteristics, the method of successive approximations is used, and it is recommended that the results of calculating an uncontrolled layer be taken as the zero approximation.

From the existing methods of calculating an uncontrolled turbulent boundary layer, the most operative is the method proposed by K. K. Fedyayevskiy and A. S. Ginevskiy [33], which was later significantly simplified by A. V. Kolesnikov [35].

Below, this method of calculating the characteristics of the uncontrolled turbulent boundary layer is discussed in accordance with the paper by A. V. Kolesnikov [35].

289

By analogy with the form parameter of L. G. Loytsyanskiy, a new form parameter f is introduced in the paper by A. V. Kolesnikov using expression (VI.73)

$$f \quad \frac{2\delta^{*'}U'}{\zeta_{f_0}U} \approx \frac{\delta^{**}U'}{U} \frac{z_0^2}{\chi^3} = -AH^{**} \left(\frac{z_0}{z}\right)^2. \qquad (VI.82)$$

Here, and hereafter the subscript "H" on the values characterizing the uncontrolled boundary layer will be omitted, A is the K. K. Fedyayevskiy form parameter

$$A = \frac{-\rho\delta UU''}{\tau_0}, \qquad (VI.83)$$

$\zeta_{f_0}=2\chi^2/z_0^2$ is the local drag factor in a gradientless flow corresponding to the Reynolds number $Re^{**}=u_0\delta^{**}/\nu$ defined by formulas (VI.80) and (VI.81).
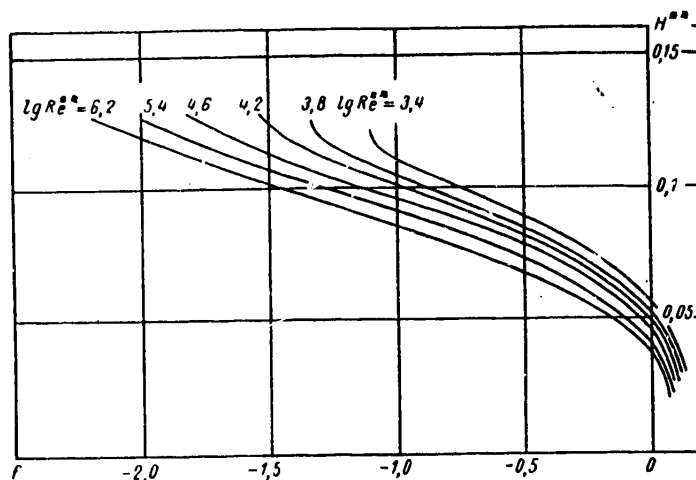
Figure VI.18. Dependence of the function H** on the parameter f
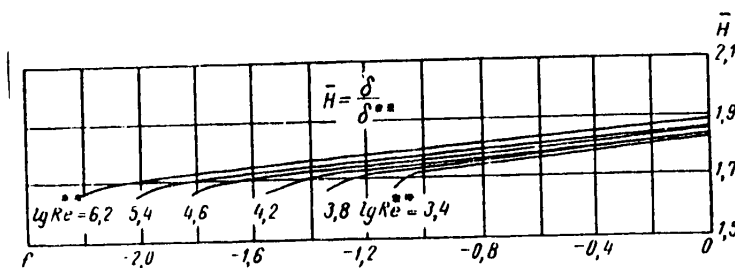
Figure VI.19. Dependence of the function $\overline{H}$ on the parameter f

290

It is easy to see that the form parameter f coincides with respect to form with the form parameter $f=(U'/U)\delta^{**}G(Re^{**})$, used to calculate a laminar boundary layer [36] if we take the value

$$G(Re^{**}) = \frac{z_0^2}{x^2} = \frac{2}{\zeta_{f_0}}.$$

as the function $G(Re2^*)$. Let us find the equation satisfied by the form parame r f. We have

$$\frac{d\delta^{**}}{dx} = \frac{d}{dx}\left[f\,\frac{U}{U'}\,\frac{x^2}{z_0^2}\right] = \frac{x^2}{z_0^2}\,\frac{d}{dx}\left(f\,\frac{U}{U'}\right) + f\,\frac{U}{U'}\,\frac{d}{dx}\left(\frac{x^2}{z_0^2}\right). \qquad (VI.84)$$

Since according to equation (VI.74), z_0 is a function only of Re^{**}, it is possible to obtain

$$f\,\frac{U}{U'}\,\frac{d}{dx}\left(\frac{x^2}{z_0^2}\right) = f\,\frac{U}{U'}\,\frac{d}{d\,Re^{**}}\left(\frac{x^2}{z_0^2}\right)\frac{dRe^{**}}{dx} =$$

$$= \frac{d}{d\,Re^{**}}\left(\frac{x^2}{z_0^2}\right)f\,\frac{U}{U'}\left(\frac{U}{v}\,\frac{d\delta^{**}}{dx} + \delta^{**}\,\frac{U'}{v}\right).$$

Substituting this expression in the preceding one, after transformations we obtain

$$\frac{z_0^2}{x^2}\,(1+m)\,\frac{d\delta^{**}}{dx} = \frac{d}{dx}\left(f\,\frac{U}{U'}\right) - fm, \qquad (VI.85)$$

where

$$m = -\frac{d\ln\left(\frac{x^2}{z_0^2}\right)}{d\ln Re^{**}}. \qquad (VI.86)$$

The integral relation of the pulses for an uncontrolled steady boundary layer has the form

$$\frac{d\delta^{**}}{dx} + \frac{U'}{U}\,(2+H)\,\delta^{**} = \frac{\tau_0}{\varrho U^2} = \frac{\zeta_f}{2}. \qquad (VI.87)$$

Let us rewrite (VI.87) in the form

$$\frac{z_0^2}{x^2}\,\frac{d\delta^{**}}{dx} = \frac{z_0^2}{z^2} - f\,(2+H). \qquad (VI.88)$$

Multiplying the left and right sides of equality (VI.88) by (m+1) and subtracting the relation obtained term by term from (VI.87), we find

$$\frac{d}{dx}\left(f\,\frac{U}{U'}\right) = (1+m)\,\frac{z_0^2}{z^2} - [1+(1+m)\,H]\,f$$

or

$$\frac{df}{dx} = \frac{U'}{U}\,F(f,\,Re^{**}) + \frac{U''}{U'}\,f. \qquad (VI.89)$$

where

$$F(f, \text{Re}^{**}) = (1 + m)\frac{z_0^2}{z^2} - [2 + (1 + m)(1 + H)]f,$$

(VI.90)

and the coefficient m is determined from (VI.86) and (VI.74)

$$m = \frac{2}{z_* + \frac{1.244}{(0.667z_* - 1.244)}}.$$

(VI.91)

Equation (VI.89) has similarity with the analogous laminar boundary layer equation. However, in the investigated case the values entering into the function F depend not only on the form parameter f, but also on Re**. The calculations performed by A. V. Kolesnikov demonstrated that the function F in practice does not depend on Re**, and the function F(f) is close to linear (see Figure VI.16)

$$F = a - bf,$$

(VI.92)

where a=1.17; b=4.4.

The coefficients a and b are close to the corresponding coefficients in the L. G. Loytsyanskiy method [36]. Substituting expression (VI.92) in equation (VI.89), we obtain

$$\frac{df}{dx} = \frac{U'}{U}(a - bf) + \frac{U^*}{U'}f.$$

(VI.93)

The solution of this equation gives

$$f = \frac{U'}{U}\left[\frac{U_t^b}{U_t'}f_t + a\int_{x_t}^{x} U^{b-1}\,dx\right],$$

(VI.94)

where f_t, U_t, U'_t are the values of the form parameter, the velocity and its derivative with respect to x at the point $x=x_t$.

If the turbulent boundary layer begins with the leading edge ($x_t=0$), from (VI.94) we obtain

$$f = \frac{aU'}{U}\int_{0}^{} U^{b-1}\,dx.$$

(VI.95)

The value of the form parameter at the critical point (U=0) is determined from the condition of finiteness of the derivative df/dx [36] f(0)=a/b=0.266.

Substituting expression (VI.82) in (VI.94) for the form parameter f, we obtain

$$\frac{2\bar{\delta}^{**}}{\zeta_{/0}} = \frac{1}{\bar{U}^{b-1}}\left[\frac{\bar{U}_t^{b-1}2\bar{\delta}_t^{**}}{\zeta_{/\,t}} + a\int_{\bar{x}_t}^{\bar{x}} \bar{U}^{b-1}\,d\bar{x}\right],$$

(IV.96)

where

$$\bar{\delta}^{**} = \frac{\delta^{**}}{L}; \quad \bar{x} = \frac{x}{L}; \quad \bar{U} = \frac{U}{U_0};$$

L and U_0 are the characteristic linear dimension of the body and the flow velocity.

It is also possible to represent the equality (IV.96) in the form

$$\frac{2\,\mathrm{Re}^{**}}{\zeta_{f_*}} = \frac{1}{\bar{U}^{b-2}} \left[\frac{2\bar{U}_t^{b-2}}{\zeta_{f_{0t}}} + a\,\mathrm{Re} \int_{x_t}^{\bar{x}} \bar{U}^{b-1}\,d\bar{x} \right],$$

(VI.97)

where $\mathrm{Re}=U_0 L/\nu$ is the Reynolds number.

The final calculation formula of A. V. Kolesnikov for calculating the characteristics of the uncontrolled turbulent boundary layer will be obtained if we substitute equation (VI.81) in equality (VI.97)

$$\mathrm{Re}^{**} = \frac{0.0132}{\bar{U}^{2.07}} \left[\bar{U}_t^{2.4} \cdot 153\,(\mathrm{Re}_t^{**})^{1.16} + 1.17\,\mathrm{Re} \int_{x_t}^{\bar{x}} \bar{U}^{3.4}\,d\bar{x} \right].$$

(VI.98)

Formula (VI.98) is applicable for $\mathrm{Re}^{**}=10^3$ to 10^7.

The value of ζ_f/ζ_{f_0} will be determined by Figure VI.16 as a function of the form parameter f and the Reynolds number Re^{**}.

For $\mathrm{Re}^{**}=10^3$ to 10^7 the value of the form parameter f can also be determined by the approximate function

$$f = -153.15 Q_0 (\mathrm{Re}^{**})^{1.16},$$

(VI.99)

where

$$Q_0 = -\frac{1}{\mathrm{Re}}\frac{\bar{U}'}{\bar{U}^2}; \quad \bar{U}' = \frac{\partial \bar{U}}{\partial x}.$$

(VI.100)

The coefficient H is defined by the curves in Figure VI.16, and the coefficients H^{**} and $\bar{H}=H_e/H^{**}$, by the curves in Figures VI.18 and VI.19, on which these values are presented as a function of f and Re^{**}. For a plate the coefficients H_0 and H_0^{**} are determined by the curves in Figure VI.17.

For an axisymmetric boundary layer on solids of revolution the value of Re^{**} is defined by the formula

$$\mathrm{Re}^{**} = \frac{0.0132}{r_0^{1.88}\cdot\bar{U}^{2.07}} \left[153\bar{U}_t^{-2.4}\bar{r}_{0t}^{-2.18}(\mathrm{Re}_t^{**})^{1.16} + \right.$$

$$\left. + 1.17\,\mathrm{Re} \int_{x_t}^{\bar{x}} \bar{U}^{3.4}\bar{r}_0^{2.18}\,d\bar{x} \right]^{0.863}.$$

(V.101)

Here $r_0(x)$ is the radius of transverse curvature of the body. When obtaining formula (VI.101) it is assumed that the thickness of the layer is small by comparison with $r_0(x)$ and $m=1.18$.

The assumed approximation for τ/τ_0 cannot serve as a basis for determining the position of the separation point from the condition $\tau=0$. Accordingly, the value of f_s corresponding to the position of the separation point must be defined by extrapolation of the functions ζ_f/ζ_{f_0} in Figure VI.16 to the point $\zeta_f=0$. Knowing f_s, it is possible to use formula (VI.99) to calculate the corresponding value of $Q=-(1/Re)(\overline{U'}/\overline{U^2})$ and construct the graph of Re^{**} at the separation point as a function of the parameter Q. The function $Re^{**}_s=f(Q)$ is presented in Figure VI.20. For determination of the separation point it is necessary to have the curve $Q=f(x)$. Using the curve in Figure VI.20, let us define $Re^{**}_s(x)$, and then let us plot this function on the $Re^{**}(x)$ curve calculated by formula (VI.98). The intersection point of these curves defines the desired coordinate x_s of the boundary layer separation point.
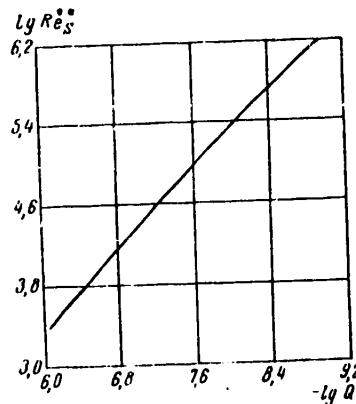
Figure VI.20. The function Re^{**}_s as a function of the value of Q

Calculations of a nonsteady turbulent boundary layer [34] demonstrated that for slow movements of the body ($\partial U/\partial t<0$), under other equal conditions, the separation point advances toward the leading edge of the body. Positive acceleration ($\partial U/\partial t>0$) leads to protraction of separation.

The methods of calculating a controlled turbulent boundary layer can be generalized to the case of a rough surface by the V. F. Droblenkov procedure [37].

When $U'(x)>0$ it is possible to use the Loytsyanskiy formulas [36] to calculate the uncontrolled TBL.

Methods of Solving the Integral Relation of Pulses for a Controlled Turbulent Boundary Layer. For complete solution of the problem of a turbulent boundary layer with injection and suction of a fluid it is necessary to define the values of Re^{**}, z and $H=\delta^*/\delta^{**}$. Previously formulas (VI.68) and (VI.70) were obtained which characterize the values of z and H as functions of the form parameter A, the Reynolds number Re^{**} and the known injection and suction parameters U_0/U and v_0/U.

The integral pulse relation which in the case of a uniform nonsteady controlled boundary layer assumes the following form can be used as the additional equation relating three unknowns Re**, z and H:

$$\frac{\partial \delta^{**}}{\partial x} + \frac{1}{U}\frac{\partial U}{\partial x}(2\delta^{**} + \delta^*) + \frac{1}{U^2}\frac{\partial}{\partial t}(U\delta^*) =$$

$$= \frac{\zeta_f}{2} + \frac{v_0}{U}\left(1 - \frac{u_0}{U}\right). \tag{VI.102}$$

Here

$$\zeta_f = \frac{2\tau_0}{\rho U^2} = \frac{2\kappa^2}{z^2} = \frac{2(v^*)^2}{U^2}. \tag{VI.103}$$

After transformations, it is possible to rewrite equation (VI.102)

$$\frac{\partial \operatorname{Re}^{**}}{\partial x} + \frac{\bar{U}'}{\bar{U}}(H + 1)\operatorname{Re}^{**} = \operatorname{Re}\bar{U} \times$$

$$\times \left[\frac{1}{2}\zeta_f + \frac{v_0}{U}\left(1 - \frac{u_0}{U}\right) - \frac{1}{U^2}\frac{\partial}{\partial t}(U\delta^*)\right]. \tag{VI.104}$$

Here

$$\bar{U}' = \frac{\partial \bar{U}}{\partial x};\ \bar{U} = \frac{U}{U_0}.$$

For solution of the pulse equation (VI.104), we use the method of successive approximations of K. K. Fedyayevskiy and A. S. Ginevskiy.

Assuming the values of ζ_f and δ^* to be known in the first approximation and taking t as the parameter, after integrating (VI.104), we obtain

$$\operatorname{Re}^{**} = \left\{\operatorname{Re}\int_{x_t}^{} \bar{U}\left[\frac{\zeta_f}{2} + \frac{\bar{v}_0}{U}\left(1 - \frac{\bar{u}_0}{U}\right) - \frac{1}{U^2}\frac{\partial}{\partial t}(\bar{U}_x^*,\ \delta^*)\right] \times \right.$$

$$\left. \times e^{\varphi(\bar{x})}\,d\bar{x} + \operatorname{Re}_t^{**}\right\}e^{-\varphi(\bar{x})}. \tag{VI.105}$$

Here

$$\varphi(\bar{x}) = \int_{x_t}^{\bar{x}} \frac{\bar{U}'}{\bar{U}}(H + 1)\,d\bar{x}. \tag{VI.106}$$

The subscript "t" denotes values at the initial point of calculating the controlled turbulent boundary layer.

In this case, if the fluid is injected in the entire turbulent boundary layer region, then the point of transition of the laminar boundary layer to turbulent is taken as the initial point of the calculation. For a completely turbulent boundary layer $\operatorname{Re}_t^{**}=0$; $x_t=0$.

When solving the problem of a nonsteady turbulent controlled boundary layer, the following functions are assumed given

$$u = u(x, t); \frac{\partial U}{\partial t} = \frac{\partial U(x, t)}{\partial t};$$

$$u_0 = u_0(x); \quad v_0 = v_0(x),$$

the number Re=$U_0 L/\nu$ and also the controlled boundary layer parameters at the initial point in time t=0 are assumed given also. Then using expressions (VI.105) and (VI.70), on the basis of successive approximations we find the boundary layer parameter distribution along the body at various points in time. The successive approximations calculation technique for a nonsteady controlled turbulent boundary layer does not differ theoretically from the analogous method for a nonsteady uncontrolled boundary layer [34].

The results obtained for a plane, nonsteady controlled boundary layer can also be generalized to the case of motion of a body of revolution with zero angle of attack if we consider that the boundary layer thickness δ is appreciably less than the radius of curvature of the transverse cross section of the body of revolution $r_0(x)$.

If

$$\bar{U} = \tilde{U}(x)\bar{U}_m(\bar{t}), \tag{VI.107}$$

then

$$\frac{\partial \bar{U}}{\partial x} = \bar{U}_m(\bar{t}) \tilde{U}'(\bar{x}), \quad \frac{\partial \bar{U}}{\partial \bar{t}} = \tilde{U}(\bar{x}) \frac{\partial \bar{U}_m}{\partial \bar{t}}. \tag{VI.108}$$

For a solid of revolution, formula (VI.105), considering (VI.107) and (VI.108) for a completely turbulent controlled boundary layer assumes the form

$$\mathrm{Re}^{**} = \left\{ \mathrm{Re}\bar{U}_m \int_0^{\bar{x}} r_0 \tilde{U}(\bar{x}) \left[\frac{x^2}{z^2} + \frac{\bar{v}_0 \left(1 - \frac{\bar{u}_0}{\bar{U}}\right)}{\tilde{U}(\bar{x}) \bar{U}_m(\bar{t})} \right. \right.$$

$$\left. \left. - \frac{\frac{\partial}{\partial \bar{t}}(\bar{U}_m \delta^*)}{\bar{U}_m^2 \tilde{U}(\bar{x})} \right] e^{\varphi(\bar{x})} d\bar{x} \right\} r_0^{-1} \cdot e^{-\psi(\bar{x})}, \tag{VI.109}$$

where

$$\varphi(\bar{x}) = \int_0^{\bar{x}} \frac{\tilde{U}'}{\tilde{U}} (H + 1) d\bar{x}, \tag{VI.110}$$

$r_0 = r_0(\bar{x})$ is the radius of transverse cross section of the body of revolution. The remaining formulas of a plane boundary layer retain their form also for a body of revolution.

For the special case of a steady turbulent controlled boundary layer, the integral relation in formula (VI.102) assumes the form

$$\frac{d\delta^{**}}{dx} + \frac{U'}{U}\left(2 + \frac{\delta^{*}}{\delta^{**}}\right)\delta^{**} = \left(\frac{v^{*}}{U}\right)^{2} + \frac{v_{0}}{U}\left(1 - \frac{u_{0}}{U}\right),$$

(VI.111)

or

$$\frac{d\,\mathrm{Re}^{**}}{dx} + \frac{\bar{U}'}{\bar{U}}(1 + H)\,\mathrm{Re}^{**} = \mathrm{Re}\,\bar{U}\left[\frac{\varkappa^{2}}{z^{2}} + \frac{\bar{v}_{0}}{\bar{U}}\left(1 - \frac{\bar{u}_{0}}{\bar{U}}\right)\right].$$

(VI.112)

Equation (VI.112) is solved by the method of successive approximations, assuming $\zeta_{f} = \tau_{0}/\rho/2U^{2} = 2\varkappa^{2}/z^{2}$ and H known in the first approximation.

As a result of integration of (VI.112) we obtain

$$\mathrm{Re}^{**} = \left\{\mathrm{Re}\int_{x_{l}}^{\bar{x}}\bar{U}\left[\frac{\varkappa^{2}}{z^{2}} + \frac{\bar{v}_{0}}{\bar{U}}\left(1 - \frac{\bar{u}_{0}}{\bar{U}}\right)\right]e^{\varphi\,(\bar{x})}\,d\bar{x} + \mathrm{Re}_{l}^{**}\right\}e^{-\omega\,(\bar{x})}.$$

(VI.113)

Formula (VI.113) is simplified when the parameter H differs little along the outline. In this case

$$e^{\varphi\,(x)} = e^{\int^{x}\frac{U'}{U}(H+1)\,d\bar{x}} = e^{(H+1)\int\frac{U'}{U}\,d\bar{x}} = U^{H+1}$$

and formula (VI.113) assumes the form

$$\mathrm{Re}^{**} = \frac{1}{U^{H+1}}\left\{\mathrm{Re}\int_{x_{l}}^{\bar{x}}U^{H+2}\left[\frac{\varkappa^{2}}{z^{2}} + \frac{\bar{v}_{0}}{\bar{U}}\left(1 - \frac{\bar{u}_{0}}{\bar{U}}\right)\right]\times\right.$$

$$\left.\times d\bar{x} + U_{l}^{H+1}\mathrm{Re}_{l}^{**}\right\}.$$

(VI.113a)

The controlled turbulent boundary layer characteristics are calculated by the method of successive approximations. The values of z_{H}, Re_{H}^{**}, H_{H} pertaining to the case of an uncontrolled turbulent boundary layer are taken as the zero approximation. The method of determining all of the uncontrolled layer characteristics was presented above. The first approximation for a controlled turbulent boundary layer is obtained as follows. Let us calculate Q by formula (VI.72), setting $\partial U/\partial t = 0$ in it. By the values of z_{H}, Re_{H}^{**}, H_{H}, z_{0} known from calculating the zero approximation, let us determine the form parameter A in the zero approximation by the formula (VI.71)

$$A_{0} = \frac{z_{H}^{2}}{\varkappa^{2}}\frac{\mathrm{Re}_{H}^{**}}{H_{H}^{**}}Q + \frac{v_{0}}{U}\frac{\mathrm{Re}_{H}^{**}}{H_{H}^{**}}.$$

By formula (VI.73) we find the value of the form parameter f in the zero approximation

$$f_{0} = -A_{0}H_{H}^{**}\left(\frac{z_{0}}{z_{H}}\right)^{2}.$$

By the known values of f_0 and Re_H^{**}, we obtain $\left(\frac{\zeta_l}{\zeta_{l_*}}\right)_1 = \left(\frac{z_0}{z}\right)_1^2$, H_1 and H_1^{**} in the

first approximation. Then by the known values of $z=z_1$, $H=H_1$, by formula (VI.113) or (VI.113a), we determine the new value of Re_1^{**} in the first approximation. The values of the form parameters A and f are determined in the first approximation by formulas (VI.71) and (VI.73):

$$A_1 = \frac{z_1^2}{\varkappa^2}\frac{\text{Re}_1^{**}}{H_1^{**}}Q + \frac{v_0}{U}\frac{\text{Re}_1^{**}}{H_1^{**}}; \quad f_1 = -A_1 H_1^{**}\left(\frac{z_0}{z_1}\right)^2.$$

The controlled turbulent boundary layer characteristics can be calculated in the second approximation analogously.

Calculation of a Turbulent Boundary Layer with Injection and Suction for a Plate.[1] As an example let us consider the special case of flow over a plate (U=const) for which the injection velocity (suction velocity) of the fluid in the turbulent boundary layer is constant, that is, v_0=const and u_0=const. For the boundary layer of a plate the basic equations (VI.111) and (VI.66) assume the form

$$\frac{d\delta^{**}}{dx} - \frac{v_0}{U}\left(1 - \frac{u_0}{U}\right) = \left(\frac{v^*}{U}\right)^2; \tag{VI.114}$$

$$\frac{v^*\delta}{\nu} = Be^{\varkappa\left(1 - \frac{u_0}{U}\right)\frac{U}{v^*}}e^{-\frac{v_0\delta}{4\nu}}. \tag{VI.115}$$

Equation (VI.115) will be obtained from (VI.66) if we neglect small values containing δ_ℓ/δ, $(\delta_\ell/\delta)^2$ and the term $A\alpha^2/2\varkappa v^*/\text{Re}_\delta$ in it and introduce the notation $\ln B = \ln \alpha + 1/2 - \alpha\varkappa$.

From formulas (VI.70) we have

$$\frac{\delta^{**}}{\delta} = \frac{8+A}{12z} - \frac{1}{z^3}(1.3 + 0.28A + 0.0125A^2). \tag{VI.116}$$

For the plate

$$A = \frac{v_0\delta}{\nu}; \quad z = \frac{\varkappa U}{v^*}. \tag{VI.117}$$

Let us transform expression (VI.114) based on smallness of the value of v_0/U.

We shall consider the fluid injections in the boundary layer for which $|v_0|\delta/\nu < 1$, which is equivalent to the proposition

$$\frac{|v_0|}{U} < \frac{1}{\text{Re}_\delta}. \tag{VI.118}$$

[1] The results of this section were obtained by I. P. Ginzburg and A. I. Korotkin.

Then from (VI.115) we obtain

$$\frac{v^* \delta}{v} \simeq Be^{\left(1 - \frac{u_\bullet}{U}\right) z}\left(1 - \frac{v_0 \delta}{4v}\right),$$

or

$$\frac{U\delta}{v}\left(\frac{\varkappa}{z} + \frac{1}{4}\frac{v_0}{U}Be^{\left(1 - \frac{u_\bullet}{U}\right) z}\right) = Be^{\left(1 - \frac{u_\bullet}{U}\right) z}. \qquad (VI.119)$$

Let us assume that

$$\frac{v_0}{U}\frac{z}{\varkappa}Be^{\left(1 - \frac{u_\bullet}{U}\right) z} < 1.$$

If we consider the values of $z/\chi = 10$; $\chi = 0.4$; $B = 0.25$, then from (VI.119) we obtain the following estimate for the normal fluid injection velocity in the boundary layer

$$\frac{|v_0|}{U} < \frac{1}{220}. \qquad (VI.120)$$

Considering this inequality, expression (VI.119) can be represented in the form

$$\delta = \frac{z}{\varkappa}\frac{v}{U}Be^{\left(1 - \frac{u_\bullet}{U}\right) z}\left[1 - \frac{1}{4}\frac{v_0}{U}Bze^{\left(1 - \frac{u_\bullet}{U}\right) z}\right]. \qquad (VI.121)$$

Expression (VI.116) for δ^{**} can be approximately written as follows considering that for the given assumptions $|A| < 1.0$:

$$\frac{\delta^{**}}{\delta} = \frac{2}{3z} - \frac{1.3}{z^3}. \qquad (VI.122)$$

Substituting (VI.121) in (VI.122), we find

$$Re^{**} = \left[Be^{z\left(1 - \frac{u_\bullet}{U}\right)} - B^2\frac{z}{\varkappa}\frac{1}{4}\frac{v_0}{U}e^{\left(1 - \frac{u_\bullet}{U}\right) z}\right] \times$$

$$\times \left(\frac{2}{3\varkappa} - \frac{1.3}{\varkappa z}\right). \qquad (VI.123)$$

From expression (VI.123) we obtain

$$\frac{d\,Re^{**}}{dz} = \frac{2}{3\varkappa}\left(1 - \frac{u_0}{U}\right)Be^{\left(1 - \frac{u_\bullet}{U}\right) z} + \frac{1.3}{z^2\varkappa}Be^{\left(1 - \frac{u_\bullet}{U}\right) z} -$$

$$- \frac{1.3}{z\varkappa}\left(1 - \frac{u_0}{U}\right)Be^{\left(1 - \frac{u_\bullet}{U}\right) z} - \frac{1}{3}\left(1 - \frac{u_0}{U}\right)\frac{v_0}{U}\frac{z}{\varkappa^3} \times$$

$$\times e^{2\left(1 - \frac{u_\bullet}{U}\right) z} - \frac{1}{6\varkappa^3}\frac{v_0}{U}B^2e^{2\left(1 - \frac{u_\bullet}{U}\right) z} +$$

$$+ \frac{1.3}{2\varkappa^2}\left(1 - \frac{u_0}{U}\right)\frac{v_0}{U}B^2e^{2\left(1 - \frac{u_\bullet}{U}\right) z}. \qquad (VI.124)$$

The integral relation (VI.114) can be rewritten as follows:

$$\frac{d\,\mathrm{Re}^{**}}{\frac{z^2}{z^2}\cdot\frac{v_0}{U}\left(1-\frac{u_0}{U}\right)} = d\,\mathrm{Re}_x.$$

(VI.125)

We shall consider $\frac{z^2}{x^2}\cdot\frac{v_0}{U}\left(1-\frac{u_0}{U}\right) < 1.$ Hence, we have another estimate for v_0/U:

$$\frac{v_0}{U} < \frac{x^2}{z^2\left(1-\frac{u_0}{U}\right)}.$$

(VI.126)

Then it is possible to represent equality (VI.125) in the form

$$\frac{z^2}{x^2}\left[1-\frac{z^2}{x^2}\frac{v_0}{U}\left(1-\frac{u_0}{U}\right)\right]d\,\mathrm{Re}^{**} \simeq d\,\mathrm{Re}_x.$$

(VI.127)

Substituting (VI.124) in (VI.127), integrating for the condition $z(0)=0$ and leaving the higher-order terms with respect to z and the lower ones with respect to v_0/U, we obtain the equation relating z and Re_x,

$$\frac{z^2}{x^2}e^{\left(1-\frac{u_0}{U}\right)z}\left[1-\frac{v_0}{U}\left(1-\frac{u_0}{U}\right)\frac{z^2}{x^2}\right] = \mathrm{Re}_x\,\frac{3x}{2B}.$$

(VI.128)

Let us logarithmize (VI.128) and express z in terms of the local friction coefficient

$$\ln\frac{z^2}{x^2}+\left(1-\frac{u_0}{U}\right)z+\ln\left[1-\frac{v_0}{U}\left(1-\frac{u_0}{U}\right)\frac{z^2}{x^2}\right]$$

$$= \ln\mathrm{Re}_x + \ln\frac{3x}{2B};$$

(VI.129)

$$z = x\sqrt{\frac{U^2\rho}{\tau_0}} = x\sqrt{\frac{2}{\zeta_l}}.$$

(VI.130)

Then from (VI.129) we find

$$\frac{1}{\sqrt{\zeta_l}} = \frac{1}{0.434x\sqrt{2}\left(1-\frac{u_0}{U}\right)}\left[\lg\left(\frac{3x}{B}\cdot\frac{\mathrm{Re}_x\zeta_l}{1-\frac{v_0}{U}\left(1-\frac{u_0}{U}\right)\frac{2}{\zeta_l}}\right)\right].$$

(VI.131)

In the absence of injection (suction) formula (VI.131) coincides with the formula for the local frictional drag of a plate, which has the form

$$\frac{1}{\sqrt{\zeta_l}} = M + N\lg(\mathrm{Re}_x\zeta_l),$$

(VI.132)

where the constants M and N are, according to the experiments of Kempf, equal to $M=1.7$, $N=4.15$.
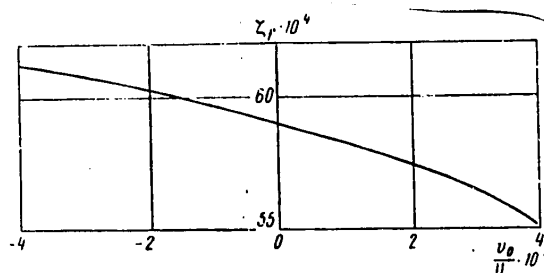
Figure VI.21. ζ_f as a function of v_0/U for $u_0=0$, $Re_x=10^5$

Using these values of M and N, it is possible to rewrite formula (VI.132) as follows:

$$\frac{1}{\sqrt{\zeta_f}} = \frac{M}{1-\frac{u_0}{U}} + \frac{N}{1-\frac{u_0}{U}} \lg \frac{Re_x \zeta_f}{1-\frac{v_0}{U}\left(1-\frac{u_0}{U}\right)\frac{2}{\zeta_f}}.$$

(VI.133)

Here, we consider the previously made estimates for the value of v_0/U. From the above-presented estimates, the estimate $|v_0|/U<1/Re_\delta$ is defining, for in a turbulent boundary layer $Re_\delta>2000$. The functions $\zeta_f(v_0/U)$, $\zeta_f(u_0/U)$ calculated by formula (VI.133) are presented in Figures VI.21-VI.24. For comparison with the Mickley experiments [1] the points corresponding to $v_0/U=\pm4\cdot10^{-4}$ for Reynolds numbers $Ux/\nu=10^5$, 10^6, 10^8 are shown in the graph in Figure VI.14 by the triangles.
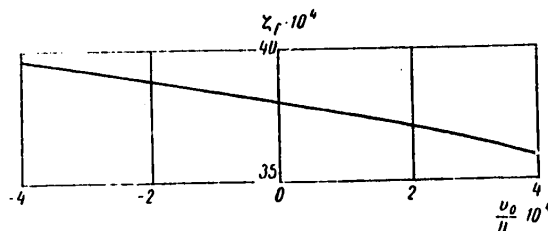
Figure VI.22. ζ_f as a function of v_0/U for $u_0=0$, $Re_x=10^6$
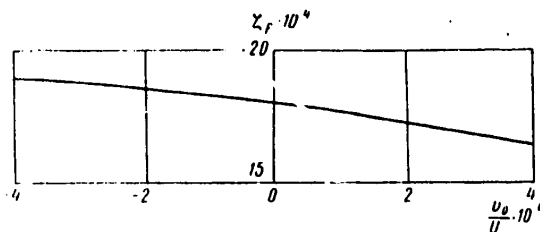
Figure VI.23. ζ_f as a function of the value of v_0/U for $u_0=0$, $Re_x=10^8$

301
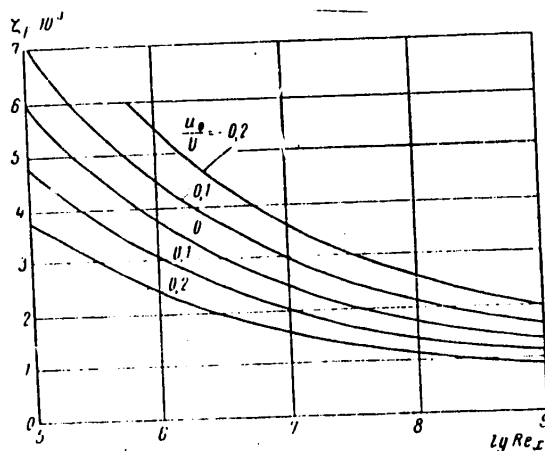
Figure VI.24. ζ_f as a function of the value of u_0/U for $v_0=0$

§VI.4. Effect of a High-Speed Jet Aimed Tangentially to a Surface Over Which Flow Takes Place on the TBL Characteristics for Positive Pressure Gradient

The boundary layer is separated as a result of the fact that the fluid particles in the wall layer do not have sufficient energy to overcome the positive pressure gradient in the diverging region of the flow. If the missing energy is fed from the outside, separation can be eliminated. One of the methods of communication of additional momentum to the stagnated particles in the flow direction is injection of a thin jet having significant energy and directed along the tangent to the surface over which flow takes place into the preseparation zone. This method has found practical application as a means of increasing the lift factor of   wing sections with large angles of attack. The possibility of applying the investigated control method in order to decrease the drag (in particular, the pressure drag) is unquestioned, but this problem has been studied little.

The first indications that "ventilation" of the boundary layer (as this method of control is sometimes called) can lead to elimination of separation and alteration of the aerodynamic characteristics of the profiles, were presented in 1921 by K. Baumann, and the first experimental results were obtained by F. Seewald in 1927. During World War II broad studies of "ventilation" were performed on wings by W. Schwier.   After World War II, numerous experiments studying the effect of high-speed jets propagated along surfaces over which flow took place on the boundary layer and the profile characteristics were performed in England (J. Williams, et al.), in France (P. Carriere, A. Poisson-Quinton, E. Eichelbrenner), in the United States (J. Attinello, J. Dode, M. B. Kelly), in the Soviet Union (Ya. G. Vilenskiy, V. M. Stepanov, S. T. Kashafundinov), and in the Federal Republic of Germany (F. Thomas).

A representation of the possibilities and some of the peculiarities of the investigated method of controlling a turbulent boundary layer can be put together, in particular, by the results of the paper by F. Thomas [39] in which a study was made of the effect of "ventilation" of the boundary layer of the flaps on the characteristics of the section. The object of investigation in this paper was

302

a wing section NACA-0010 with flap amounting to 25.7% of the wing chord with respect to length. The angle of setting the flap η_k was varied from 0 to 105° during tests in a wind tunnel. In the case of absence of "ventilation," separation of the boundary layer began at the point of "bending" of the section caused by setting the flap even for comparatively small angles. In order to protract the elimination of the separation, ejection of a thin, high-speed jet from a slot through the leading edge of the flap (Figure VI.25) was used.
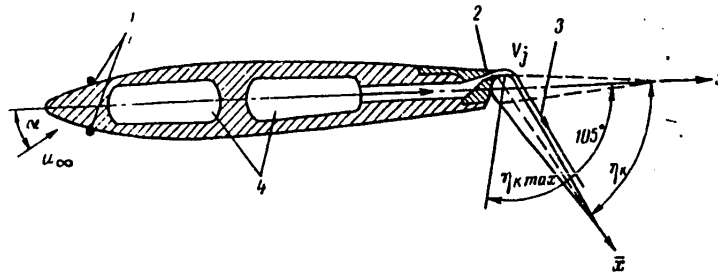
Figure VI.25. Diagram of the organization of "ventilation"
on a flap
1 -- turbulence stimulators; 2 -- slot; 3 -- jet; 4 -- channels
for injecting air

Fitting of the jet to the surface of the forward part of the flap was insured as a result of the Coande effect.[1] Further development of the flow in the boundary layer of a flap depended significantly on the magnitude of the jet momentum. An increase in the momentum was accompanied by a shift of the separation point in the direction of the trailing edge and an increase in lift of the section. The latter occurred as a result of partial or complete maintenance of the rarefaction peak at the "break" point under "ventilation" conditions. As Figure VI.26 shows, in the absence of escape of the jet, this peak becomes diffuse.

As a dimensionless characteristic of the jet momentum in reference [39] and also in other studies devoted to boundary layer control by "ventilation" the "jet momentum factor" -- c_μ -- is used:

$$c_\mu = \frac{\text{mass of ejected fluid} \times \text{ejection velocity}}{(1/2) \times \text{velocity head} \times \text{wing area}} .$$

---

[1] By the Coande effect we mean the capacity of jets (in particular, plane jets) propagated near solid surfaces to fit to these surfaces. The capacity to fit to a known limit is not influenced by the orientation of the jet or the location of its initial section with respect to the surface [40].
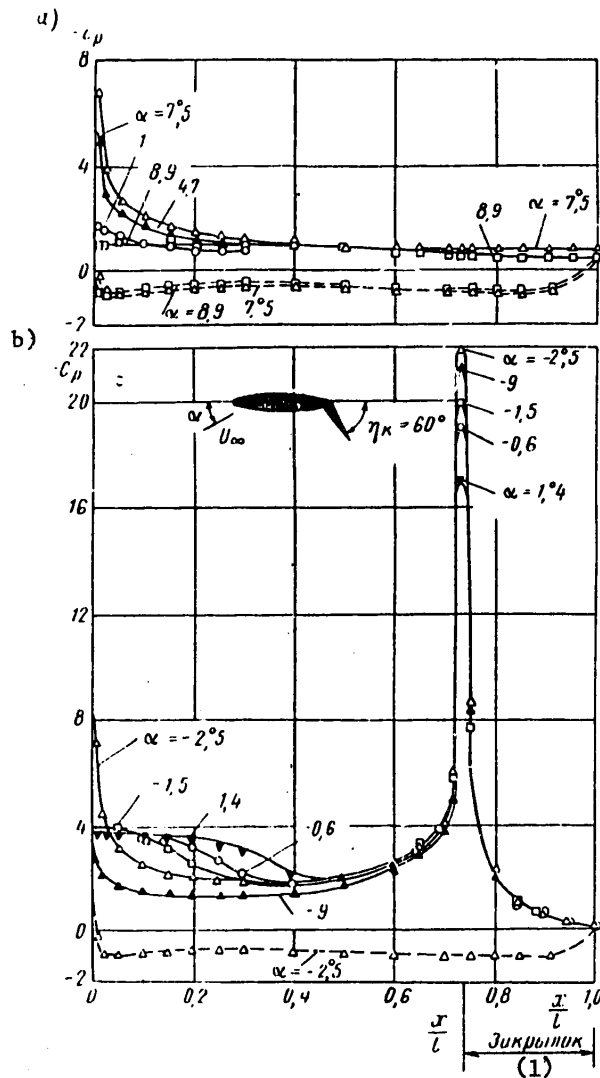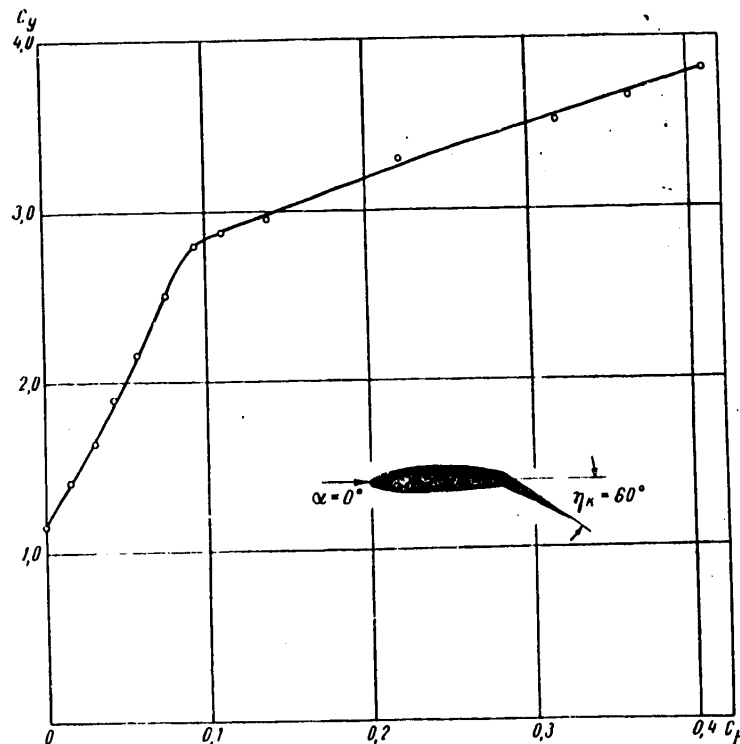
303

Figure VI.26. Pressure distribution on the surface of a section and flap:
a -- without "ventilation" $c_\mu=0$, $\eta_k=60°$, b -- with ventilation $c_\mu=0.35$, $\eta_k=60°$

Key:
   1. flap

304

Figure VI.27.   Function $c_y(c_\mu)$ ($\alpha=0$, $\eta_k=60°$)

Until the separation point reaches the trailing edge, the lift factor increases rapidly with an increase in c_μ and becomes close to the theoretical value calculated using the Chaplygin-Zhukovskiy hypothesis.

With an increase in momentum of the jet above that required for displacement of the separation point to the trailing edge (the corresponding value of the coefficient c_μ is denoted $c_{\mu A}$) the growth rate of the lift is sharply decelerated (Figure IV.27). Therefore knowing $c_{\mu A}$ is of interest for engineers designing a "ventilation" system, for this value of the momentum is optimal from the point of view of economy.

The dependence of $c_{\mu A}$ on the angle of setting the flap by different experimental data is presented in Figure VI.28. Inasmuch as to a defined degree η_k characterizes the magnitude of the positive pressure gradient, it is obvious that a larger value of $c_{\mu A}$ must correspond to a larger η_k. The experimental data presented in Fig VI.28 indicate that the effectiveness of "ventilation" is significantly influenced by variation of the ratio of the slot width to the wing chord with a flap s/ℓ. The smaller this ratio, the smaller the corresponding value of $c_{\mu A}$ and, together with this, the higher the TBL control efficiency. Decreasing the slot width is, in turn, connected with an increase in the ejection velocity; therefore the noted effect can be interpreted as evidence in favor of the application of relatively

thinner and higher-speed jets. As is obvious from Figure VI.28, especially favorable results were obtained in the ONERA studies, during which the ratio $s/\ell=2.5$ to $3.5 \cdot 10^{-4}$ was least by comparison with other studies.
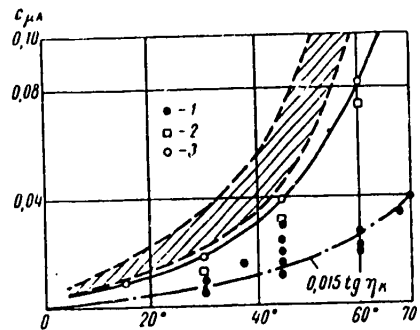

Figure VI.28. Values of the momentum factor $c_{\mu A}$ required to eliminate separation as a function of the angle of setting the flap η_k.

	Source of experimental data	$10^3 s/\ell$
1	OHERA	0.25 to 0.35
2	Williams	0.33
3	Thomas	1.67
cross hatched	Schwier	5-7

The approximate theoretical-experimental methods of determining $c_{\mu A}$ can be found in references [39]-[42]. The discussed method of insuring given displacement of the separation point downstream in the boundary layer can be used not only in studies aimed at increasing the lift of the sections, but also when studying the problem of decreasing drag of poorly streamlined bodies. It is known that any reduction in dimensions of the separation zone leads to a decrease in width of the wake and together with this, a reduction in pressure drag and also total drag. However, up to now the problem of boundary layer control by high-speed jets remains almost entirely uninvestigated for this purpose. In addition to lowering the drag it is also possible to use "ventilation" to increase the efficiency of turbomotors and marine devices having diverging exit cones in their makeup and, in addition, to decrease the vibration of various types of struts around which flow takes place if this vibration is caused by separation of the vortices.

§VI.5. Use of High-Molecular Additives to Decrease Surface Friction in a Turbulent Flow

The interest of hydrodynamic specialists studying the problems of the resistance of water to motion of bodies, to anomalous or nonnewtonian fluids is caused by recent experiments with flow in pipes of weak water solutions of high-molecular compounds. Usually the flow of such fluids is a subject of investigation in rheology. The experiments performed by a number of researchers both abroad [46]-[49] and in the Soviet Union [50]-[52] demonstrated that addition of a small

amount of a defined type of polymer to water leads to a significant reduction in the surface friction (in individual cases, to 60-70%).

It is impossible to explain the noted effect from the point of view of quantitative variation of the density and viscosity of the medium inasmuch as the density of a weak solution of the polymer in water almost does not differ from the density of the solvent, and its viscosity measured by ordinary methods, for example, by a capillary viscosimeter, as a rule, somewhat exceeds the viscosity of pure water. It is obvious that the introduction of polymer additives into water lends it new qualities, converting it to an anomalous fluid.

Theoretical explanation of the indicated phenomenon has still not been forthcoming at the present time; therefore a brief study is made below of some of the basic experimental results. The greater part of the experiments performed with weak aqueous solutions of polymers in pipes are devoted to establishing the relations between the pressure gradient in the measuring section of the pipe and the flow velocity of the fluid or its flow rate. The results of the experiments of Savins [48] with aqueous solutions of cellulose and vinyl derivatives are presented in the graphs in Figures VI.29 and VI.30; the results of Metzner and Graham [49] with a J-100 polymer solution are presented in Figure VI.31.

Investigation of the curves presented in Figures VI.29-VI.31 permits a number of peculiarities to be noted that are characteristic of flows of weak polymer solutions. First of all, the addition of not all polymers will lead to a decrease in pressure gradient with invariant flow rate. In Figure VI.29 the function $\Delta p = f(Q)$ was constructed from experiments with a 0.286% solution of cellulose derivatives; in Figure VI.30, the same relation reflects the behavior of a 0.143% solution of vinyl derivative. From the graphs it is obvious that the addition of vinyl derivative to water only causes an increase in drag, whereas in the case of cellulose it is clearly possible to note a reduction in drag. Attention is attracted by the difference in the transition from laminar flow to turbulent in the two solutions: whereas for the vinyl solution it is possible definitely to indicate the critical velocity for which the laminar motion shifts to turbulent, in the case of cellulose solution there is a less sharply expressed broad transition region which is protracted with respect to the velocities.

Another characteristic feature of flows of weak aqueous solutions of polymers and pipes is the existence of a velocity zone favorable in the sense of drag reduction. As is obvious from Figure VI.29, the curve for the pressure gradient as a function of the water flow rate with the addition of polymer first goes below the analogous curve for pure water (region of unfavorable velocities), and then for some value of the velocity intersects it (region of favorable velocities). Further increase in velocity leads to the fact that the points lie on a straight line corresponding to water flow in a large-diameter pipe, that is, with smaller hydraulic losses. This fact indicates that the drag reduction reached in the experiments, increasing with an increase in flow rate or flow velocity, is not unlimited, but approaches some value which depends on the type of polymer and flow conditions. Figure VI.32 shows the results of the Savins experiments in the form of the relation for the ratio of the pressure gradient with a solution flow to the pressure gradient with a water flow with the same volumetric flow rate. These curves are an illustration of the statement above.
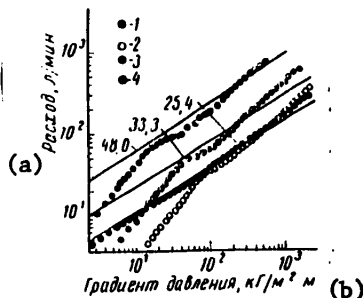
Figure VI.29. Flow rate of an aqueous solution of cellulose for flow in a circular pipe as a function of the pressure gradient [48]

	Polymer concentration, %	Pipe diameter, mm
1	0.0358	25.4
2	0.286	25.4
3	0.286	33.3
4	0.286	48.0

Solid line -- experiments with pure water

Key:
a. Flow rate, liters/min
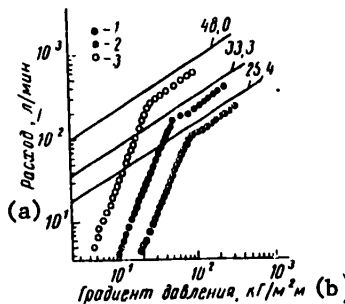b. Pressure gradient, kg/m2-m

Figure VI.30. Flow rate of a 0.143% aqueous solution of vinyl for flow in a circular pipe as a function of pressure gradient [48]

	Pipe diameter, mm
1	25.4
2	33.3
3	48

Solid line -- experiments with pure water

Key:
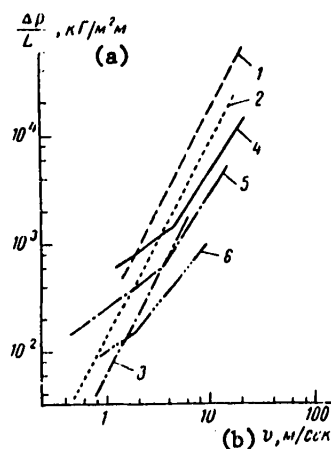a. Flow rate, liters/min
b. Pressure gradient, kg/m2-m

308

Figure VI.31. Pressure gradient as a function of the flow velocity of an aqueous solution of J100 polymer in a circular pipe [49]:

Pipe diameter, mm	Water	J100 solution
12.7	1	4
25.4	2	5
50.8	3	6

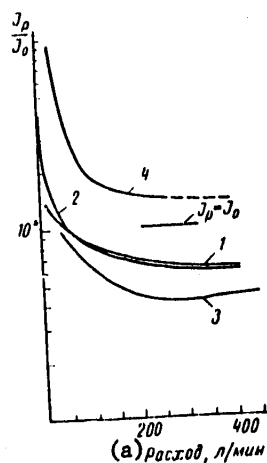Key:

a. kg/m^2-m

b. v, m/sec

Figure VI.32. Ratio J_p/J_0 as a function of the fluid flow rate in a cylindrical pipe [48], where J_p is the pressure gradient during flow of the solution, and J_0 is the pressure gradient for a water flow.
1 -- cellulose II; 2 -- cellulose I; 3 -- vinyl I; 4 -- vinyl II. Pipe diameter 25.4 mm, concentration 0.0716%

Key:

a. flow rate, liters/min

309

A third characteristic feature of the motion of dilute aqueous solutions of high-molecular compounds is the influence of the pipe diameter on the drag reduction. The greatest pressure gradient reduction with invariant flow velocity is reached, as is obvious from Figure VI.31, in a pipe of smaller diameter.

Finally, the inclination of some, as a rule, the most effective solutions, toward aging, toward loss of properties insuring drag reduction, is a characteristic feature of flows of dilute polymer solutions important in practical respects. Thus, Savins [48] points out that deterioration and depolymerization of the solution of vinyl I derivative was so intense and fast that during the experiment with invariant volumetric flow rate constant buildup of the measured pressure gradient was noted with time in the pipe.

As has already been pointed out, the greater part of the experiments in flow of dilute polymer solutions in water in pipes have been connected with determining characteristics of practical importance -- drag and flow rate. The form of the average velocity profile and turbulent motion characteristics have been studied much more weakly. The Bogu measurements in pipes with an aqueous solution of carboxylmethyl cellulose and also the Shaver and Merril experiments [47] demonstrated that in the solution the velocity profile is less full than in water. Some information about the nature of turbulent mixing was obtained by G. I. Barenblatt, et al. [50]. In his experiments a stream of colored liquid was introduced into a pure water flow in a transparent tube; on addition of some amount of carboxylmethyl cellulose solution to the water, the nature of diffusion of the colored stream was altered, the mixing of the stream became smoother, there were no high-frequency pulsations noted on dissipation of the colored stream in the water.

A natural continuation of the experiments with aqueous solutions of polymers in pipes was experiments measuring the drag of bodies towed in weak aqueous solutions of high-molecular compounds and also the study of the influence on the drag which comes from introducing polymer solutions into the boundary layer of bodies around which water is flowing.

Among the papers of the first of the above-indicated areas it is necessary to note the studies by Hoyt and Fabula [53], Emerson [54], Levy and Davis [55]. Hoyt and Fabula established that under certain conditions the turbulent friction coefficient in weak aqueous solutions of polymers with defined molecular chain length is 70% less than in water.

During tow testing of models in the basin at the University of Newcastle, Emerson [54] obtained data on turbulent friction in aqueous solutions of WSR-301 polyox. The rated concentrations by weight of the solutions were 0.000125, 0.00025, 0.0005, 0.002 and 0.005%. The effective polymer concentration during the tests turned out to be noticeably lower than the rated value as a result of precipitation of the polymer out of solution on the bottom of the basin and also as a result of depolymerization of its molecules with time.

Drag determination experiments were performed with KS-116, KS-119 models and also with a plate and pontoon. The KS-116 model 2.44 meters long corresponded to a single-screw vessel with prismatic coefficient of 0.65.

310

The y-axes of the KS-119 model 2.44 meters long were given by the expression

$$\frac{y}{b} = \left(1 - \frac{x^2}{l^2}\right)\left(1 - \frac{z^2}{d^2}\right),$$

where b is half of the breadth;

l is half the length;

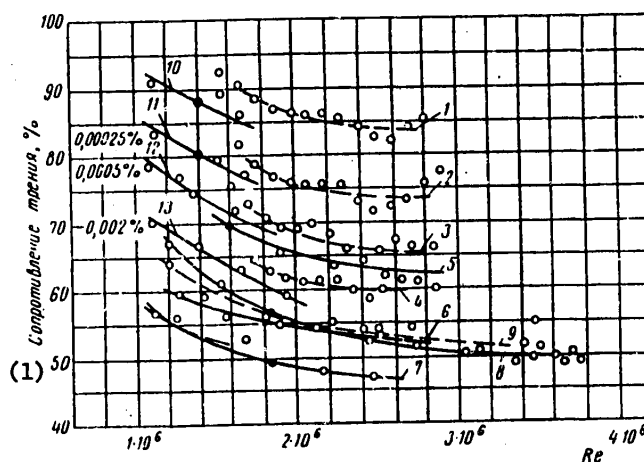d is the draft of the model. The ratios $l/b=10$, $l/d=8$.

Figure VI.33. Frictional drag (in percentages of the frictional drag in pure water) as a function of the Re number for towed testing of models in a polyox solution [54]

KS-116 model: 1 — concentration 0.000125%;
                          2 — concentration 0.00025%;
                          3 — concentration 0.0005%;
                          4 — concentration 0.002%;
Pontoon: 5 — concentration 0.002%;
                          6 — concentration 0.005%; polyox (1)
                          7 — concentration 0.005%; polyox (2)
                          8 — concentration 0.005%; polyox (3)
KS-119 model: 9 — concentration 0.005%;
Plate: 10; 11; 12; 13 — concentration 0.000125%; 0.00025%; 0.0005%; 0.002%, respectively.
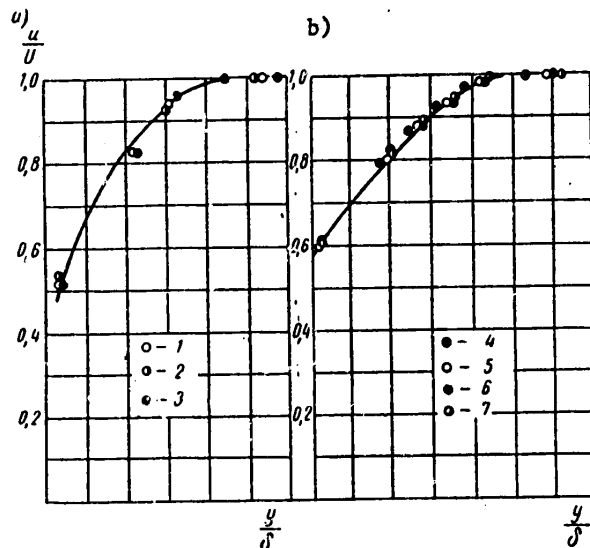Key:
    a. Frictional drag, %

Figure VI.34. Mean velocity profile in the boundary layer cross section of a plate [54:

a -- in 0.002% polyox solution
1 -- U=1.22 m/sec; δ=2.14 cm;
2 -- U=0.927 m/sec; δ=2.18 cm;
3 -- U=1.54 m/sec; δ=2.03 cm;

b -- in pure water
4 -- U=0.92 m/sec; δ=3.7 cm;
5 -- U=1.21.m/sec; δ=3.43 cm;
6 -- U=1.5 m/sec; δ=3.3 cm;
7 -- U=1.82 m/sec; δ=3.25 cm.

A plate made in the form of a slab with rounded edges, with ballast on the lower edge was 2.13 meters long, 3.8 cm thick and 0.61 meters high. Six Pitot tubes were installed at a distance of 1.72 m from the leading edge of the plate to measure the velocity profile in the boundary layer cross section.

The pontoon 2.44 m long, 0.61 m wide and with a draft of 0.95 cm was flat-bottomed and had slightly raised ends. Trip wires were installed on all the models in the forward end.

The results of the testing of the above-enumerated models are presented in Figure VI.33 in the form of the percentage drag reduction of the models when towing them in polymer solutions of different concentration by comparison with the towing drag of models in water as a function of the Reynolds number. As is obvious, with an increase in Reynolds number (constructed by the kinematic viscosity of water), an increase in drag reduction is noted. Figure VI.34 shows the average velocity profiles in the cross section of the boundary layer of a plate measured by Pitot tubes: the velocity profile in the polymer solution is less full, which agrees with the above-mentioned measurements in pipes. Levy and Davis towed a plate in a circular channel with an aqueous solution of WSR-301 polyox. For a polyox concentration by weight of $1.5 \cdot 10^{-6}$, the drag of the plate was reduced by 32%, and with a concentration of 15 to $20 \cdot 10^{-6}$, by 63% as compared to the tow testing in pure water. The Reynolds number range constructed by the length of the plate and speed of towing was $3 \cdot 10^6$ to $1 \cdot 10^7$ in the Levy and Davis experiments.

312

Emerson proposes that the property of polymer solutions having in practice the same density and viscosity as water to significantly (by 50-60%) decrease the turbulent friction coefficient be used to obtain full-scale values not only of the wave drag factor, but also the frictional drag coefficient when using polymer solutions of the corresponding concentration under model experimentation conditions. The basis for this procedure is identicalness of the shape of the curve for the total drag factor as a function of the Froude number for models in pure water and polymer solutions. Figure VI.35 shows the curves of the total drag factors as a function of the Froude number for the KS-119 model 2.44 m long in water and 0.005% aqueous solution of polymer and models of the same lines 6.1 meters long tested in water qualitatively confirming the proposition stated above. Quantitative comparison of the wave drag curves as a function of the Froude number for water and aqueous solutions of polymers can be achieved if the turbulent friction coefficient of an equivalent flat plate multiplied by some factor which depends on the shape of the model and takes into account the deviation of the frictional resistance of the model from the flat plate drag (see Figure VI.35) is subtracted from the total drag factor measured experimentally.

On the basis of Emerson's tests, he concludes that towing a model 5.5 meters long with $U/\sqrt{Lg}=0.8$ and $Re=8.4 \cdot 10^6$ in a polymer solution that decreases the viscous drag by 50% can give results equivalent to testing a full-scale unit 120 meters long ($Re=9 \cdot 10^8$).

Just as for certain experiments with flow of polymer solutions in a pipe, Emerson noted aging of the polyox polymer in his experiments. The high molecular weight ($4 \cdot 10^6$) of polyox obviously is the reason for disbehavior of its aqueous solutions which are dstroyed under the effect of an acid medium, light, ultrasonic oscillations and mechanical shear. Hoyt [56] presents noteworthy data in this sense in a discussion of Emerson's article. Polyox solutions in water were pumped through a pipe 40 cm long and 1.09 mm in diameter at a speed of about 14 m/sec in Hoyt's experiments (the Reynolds number constructed by the kinematic viscosity of water is 14,000). Whereas at first the drag reduction in the experiments was 32 and 64.5% by comparison with pure water for polymer concentrations of $3 \cdot 10^{-6}$ and $9 \cdot 10^{-5}$, respectively, when pumping the same solutions through a pipe the third time pressure gradients less than for pure water by 18.5 and 63.2%, respectively,were obtained. Nevertheless, Emerson and Hoyt point out the possibility of using the more stable Guar-Guma polymer as an additive leading to drag reduction. This polymer is inferior to polyox only in the sense that somewhat greater quantity of it is required to obtain the same effect. In Hoyt's experiments described above, aqueous solutions of Guar-Guma with concentrations of 10^{-4} and $5 \cdot 10^{-4}$ revealed stable drag reduction by 54 and 68% by comparison with pure water in three experiments.

The above-described experiments with respect to a flow of dilute aqueous solutions of polymers in pipes and also with respect to towing models in such solutions indicating the possibility of a sharp decrease in surface friction led to statement of a number of experiments with respect to the introduction of these solutions into the boundary layer of models around which water is flowing. Thus, in a discussion of the above-investigated paper by Emerson, A. Vosper [56] reported preliminary results of testing a model which had a polyox solution injected in its

boundary layer. These experiments performed at AEW (Admiralty Research Center in Huslar, England) demonstrated that the greatest drag reduction is detected for high speeds of the oncoming water flow. At low speeds the degree of dispersion of the solution in the boundary layer obviously is insufficient to obtain the required polymer concentration in the wall region. Above all, the experiments demonstrated that even at high velocity the introduction of a solution into the boundary layer in cross sections located farther than a quarter of the length of the model from the bow in practice does not change the drag.
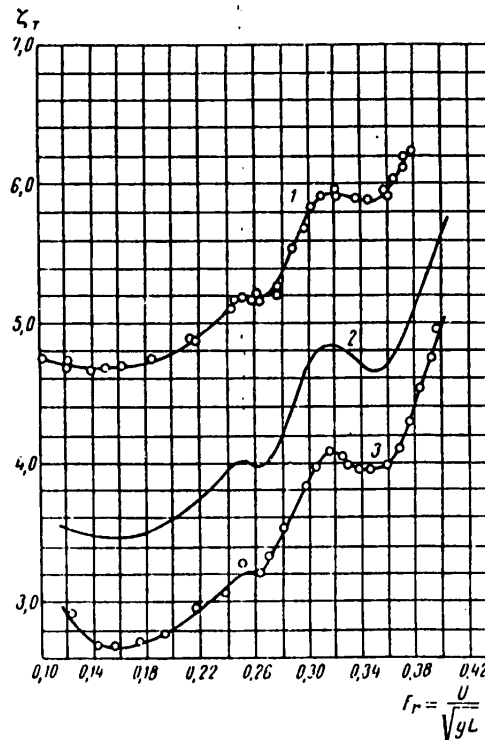

Figure VI.35. Total drag as a function of the Froude number [54] for the KS-119 model 2.44 meters long in water (curve 1) and in a 0.005% aqueous solution of polymer (curve 3). Curve 2 -- a model 6.1 meters long with the same lines as the KS-119.

The effect of injecting solutions of high-molecular compounds on hydrodynamic drag of a cylinder placed across an oncoming flow was examined in reference [50], the work for which was done at the Mechanics Institute of the USSR Academy of Sciences. A cylindrical pipe 40 mm in diameter and 400 mm long had openings 0.5 mm in diameter used to let the polymer solution into its forward and aft sections. The tests were run in an open channel at low speeds (on the order of 1.6 m/sec) so that the Reynolds number constructed by the cylinder diameter was $6.5 \cdot 10^4$. Therefore in order to obtain transcritical conditions of flow around the cylinder surface, it was covered with a screen 5×5 mm made of longitudinal and annular slots 0.5 mm deep.

314

An aqueous solution of carboxylmethyl cellulose, an aqueous solution of polyvinyl alcohol and an aluminum naphthenate solution in chemically pure kerosene were used as the high-molecular additives. The solution concentrations varied from 10 to 0.5%.

The experiments demonstrated that injection of water or glycerine solutions in water of different concentration at low velocities does not change the cylinder drag, whereas injecting polymer additives at low escape velocities from the openings leads to drag reduction, the magnitude of which depends both on the type of polymer and its concentration. A maximum decrease in drag was noted when using 5-10% solutions of polyvinyl alcohol, and it amounted to 31-34%; a 0.6% solution of carboxylmethyl cellulose decreased the hydrodynamic drag by 10%.

In conclusion, let us mention the experiments of Thurston and Jones [57] performed with models of bodies of revolution, on the forward surface of which weather-soluble polymer compounds were applied. Two models were tested: with a blunt forward section and a model, the forward section of which had smooth lines. Different coverings including WSR-301 polyox were used. The tests concluded with measuring the speed of the models under the effect of gravity in a vertical tank 6.1 m high filled with water. It was discovered that at such low velocities as were achieved in the experiments ($Re \approx 10^6$, $L \approx 0.5$ meter), drag reduction (by 16-18%) is observed only on a model with blunt forward section on which the boundary layer was turbulent and high solution rate of the coating was noted. On a model with well-streamlined forward section obviously under laminar flow conditions, no change in drag was recorded.

The above-investigated experimental data, therefore, demonstrate that introduction of polymer additives into a boundary layer leads to a decrease in hydrodynamic drag, but the effectiveness of these additives is determined not only by the properties of the polymer, but it also depends on the method by which the polymer additive is introduced into the flow. There are grounds for expecting that with appropriate organization of polymer injection in the wall region a significant reduction in surface friction will be achieved which was obtained in experiments with polymer solution flows in pipes and when towing models in such solutions.

BIBLIOGRAPHY

1. Mickley, H. S.; Ross. R. C.; Sguyers, A. L.; Stewart, W. E. "Heat, Mass and Momentum Transfer for Flow Over a Flat Plate with Blowing or Suction," NACA TH, No 3208, July 1954.

2. Mickley, H. S.; Devis, R. C. "Momentum Transfer for Flow Over a Flat Plate with Blowing," NACA TH, No 4017, November 1957.

3. Hacker, D. S. "Empirical Prediction of Turbulent Boundary Layer Instability a Flat Plate with Constant Mass Addition at the Wall," JET PROPULSION, Vol 26, No 9, 1959.

4. Mugalev, V. P. "Experimental Study of a Subsonic Turbulent Boundary Layer on a Plate with Ventilation," IZV. VYSSH. TEKH. UCH. ZAVED. MVO SSSR, SERIYA "AVNATSIONNAYA TEKHNIKA" [News of the Higher Institutions of Learning of the

315

USSR Ministry of Higher Education, Aviation Engineering Series], No 3, 1959.

5. Romanenko, P. N.; Kharchenko, V. N. "Influence of a Transverse Mass Flow on Drag and Heat Exchange During Turbulent Flow of a Compressible Gas," PMTF [Applied Mechanics and Technical Physics], No 1, 1962.

6. Kay, I. M. "Boundary-Layer Flow Along a Flat Plate with Uniform Suction," ARC REP. AND MEM., No 2628, 1948.

7. Dutton, R. A. "The Effects of Distributed Suction on the Development of Turbulent Boundary Layers," ARC. REP. AND MEM., No 3155, 1960.

8. Favre, A.; Dumas, R.; Verolet, E. "Couche limite sur paroi plane poreuse avec aspiration," PUBLICATIONS SCIENTIFIQUES ET TECHNIQUES DU MINISTERE DE L'AIR No 377, 1961.

9. Tennekes, H. "Similarity Laws for Turbulent Boundary Layers with Suction or Injection," J. FLUID. MECH., Vol 21, Part 4, 1965.

10. Dorrance, W. H.; Dore, F. I. "The Effect of Mass Transfer on the Compressible Turbulent Boundary-Layer Skin-Friction and Heat Transfer," JOURN. OF THE AERONAUTICAL SCIENCES, Vol 21, No 6, June, 1954, collection of translations and surveys MEKHANIKA [Mechanics], No 3(31), 1955.

11. Kalikhman, L. Ye. "Turbulent Boundary Layer of an Incompressible Fluid on a Porous Wall," ZHTF [Journal of Technical Physics], No 11, 1955.

12. Rubesin, M. W. "Analytical Estimation of the Effect of Transpiration Cooling on the Heat Transfer and Skin Friction Characteristics of a Compressible Turbulent Boundary Layer," NACA, TN 3341, December 1954.

13. Driest, Van. "On the Aerodynamic Heating of Blunt Bodies," ZAMP, Vol 9, special volume Nos 5-6, 1958.

14. Turcotte, D. L. "A Sublayer Theory for Fluid Injection into the Incompressible Turbulent Boundary Layer," JOURNAL OF THE AEROSPACE SCIENCES, Vol 27, No 9, September 1960.

15. Kutateladze, S. S.; Leont'yev, A. I. "Turbulent Boundary Layer of a Gas on a Permeable Wall," PMTF, No 1, 1962.

16. Ginzburg, I. P.; Krest'yaninova, N. S. "Turbulent Boundary Layer of a Plate in an Incompressible Fluid with Mass Injection," INZH.-FIZ. ZHURNAL [Engineering-Physics Journal], Vol 9, No 4, 1965.

17. Rannie, W. D. "Heat Transfer in Turbulent Shear Flow," J. AERONAUTICAL SCIENCES, Vol 25, No 5, 1956.

18. Leadon, B. M. "A Sublayer Theory for Fluid Injection," JOURNAL OF THE AERONAUTICAL SCIENCES, Vol 28, No 10, 1961.

19. Rotta, I. "Beitrag zur Berechnung turbulenter Grenzshichten, ING.-ARCHIV, Vol 19, 1951.

20. Rotta, I. "Schubspannungsverteilung und Energiedissipation bei turbulenten Grenzschichten," ING.-ARCHIV, Vol 20, 1952.

21. Truckenbrodt, E. "Ein Quadraturverfahren zur Berechnung der laminaren und turbulenten Reibungsschict bei ebener und rotationssymmetrischer Strömung," ING.-ARCHIV, Vol 20, 1952.

22. Fernholz, H. "Halbempirische Gesetzte zur Berechnung turbulenter Grenzschichten nach Methode der Integralbedingungen," ING.-ARCHIV, Vol 23, 1964.

23. Ludwieg, H.; Tillmann, W. "Untersuchungen über die Wandschubspannung in turbulenten Reibungsschichten," ING.-ARCHIV, Vol 17, 1949.

24. Uram, E. M. "A Method of Calculating Velocity Distribution for Turbulent Boundary Layers in Adverse Pressure Distributions," J. AERO/SPACE, Vol 27, No 9, 1960.

25. Markov, N. M. RASCHET AERODINAMICHESKIKH KHARAKTERISTIK LOPATOCHNOGO APPARATA TURBOMASHIN [Calculating the Aerodynamic Characteristics of the Blade System of Turbomotors], Moscow-Leningrad, Mashgiz, 1955.

26. Pechau, W. "Ein Näherungsverfahren zur Berechnung der ebenen und rotationssymmetrischen turbulenten Grenzschicht mit beliebiger Absaugung oder Ausblasung," 1958 FARBOUCH DER WUSL.

27. Wust, W. "Theory of Boundary-Layer Suction to Prevent Separation," BOUNDARY LAYER AND FLOW CONTROL, Vol 1, Pergamon Press, Oxford, 1961.

28. Eppler, R. "Praktische Berechnung laminarer und turbulenter Absauge-Grenzschichten," ING. ARCHIV, Vol 32, No 4, 1963.

29. Karpeyev, Yu. N. "Some Modern Methods of Calculating Turbulent Boundary Layer and Possible Ways of Improving Them," TR. VNIITOS [Works of the VNIITOS Institute], No 73, 1966.

30. PROBLEMY MEKHANIKI [Problems of Mechanics], IL, 1955.

31. Doenhoff, A. E.; Tetervin, N. "Determination of General Relations for the Behavior of Turbulent Boundary Layers," NACA, Rep. No 772, 1943.

32. Fedyayevskiy, K. K. "Turbulent Boundary Layer of a Wing," Part I, TR. TSAGI [Works of the Central Aerohydrodynamics Institute], No 282, 1936; Part II, TR. TSAGI, No 316, 1937.

33. Fedyayevskiy, K. K.; Ginevskiy, A. S. "Method of Calculating a Turbulent Boundary Layer in the Presence of a Longitudinal Pressure Gradient," ZHTF, Vol 27, No 2, 1957.

34. Fedyayevskiy, K. K.; Ginevskiy, A. S. "Nonsteady Turbulent Boundary Layer of a Wing Section," ZHTF, Vol 29, No 7, 1957.

35. Kolesnikov, A. V. "Calculating the Turbulent Boundary Layer by the K. K. Fedyayevskiy Method," TR. TSAGI, No 940, 1964.

36. Loytsyanskiy, L. G. MEKHANIKA ZHIDKOSTI I GAZA [Fluid and Gas Mechanics], Moscow, Gostekhizdat, 1967.

37. Droblenkov, V. F. "Turbulent Boundary Layer on a Rough Curvilinear Surface," IZV. AN SSSR. OTN [News of the USSR Academy of Sciences, Technical Sciences Department], NO 8, 1955.

38. Granvill, P. S. "The Effect of Fluid Injection on the Drag of Flat Plates at High Reynolds Numbers," INTERNATIONAL SHIPBUILDING PROGRESS, Vol 10, No 101, 1963.

39. Thomas, F. "Untersuchungen über die Erhöhung des Auftriebes von Tragflügein mittels Grenzschichtbeeinflüssung durch Ausblasen, Z. FÜR FLUGWISS, Vol 10, No 2, 1962.

40. "Newman, B. G. "The Deflection of Plane Jets by Adjacent Boundaries — Coande Effect," BOUNARY LAYER AND FLOW CONTROL, Pergamon Press, Oxford, 1961.

41. Carriere, P.; Eichelbrenner, E.; Poisson-Quinton, P. "Contribution theoretique et experimentale a l'etude du controle de la couche limite par soufflage," PROCEEDINGS OF THE FIRST CONGRESS IN THE AERONAUTICAL SCIENCES, Madrid, 1958.

42. Carriere, P.; Eichelbrenner, E. "Theory of Flow Reattachment by a Tangential Jet Discharging Against a Strong Adverse Pressure Gradient," BOUNDARY LAYER AND FLOW CONTROL, edited by G. V. Lachmann, Pergamon Press, Oxford, 1961.

43. Martensen, S. E. "Berechnung der Druckverteilung an dicken Gitterprofilen mit Hilfe von Fredholmischen Integralgleichungen zweiter Art.," ARCH. RAT. MECH. ANALYSIS, Vol 3, 1959, p 235.

44. Rotta, I. K. "TURBULENTNYY POGRANICHNYY SLOY V NESZHIMAYEMOY ZHIDKOSTI [Turbulent Boundary Layer in an Incompressible Fluid], Leningrad, izd. Sudostroyeniye, 1967.

45. Romanenko, P. N. TEPLOOBMEN I TRENIYE PRI GRADIYENTNOM TECHENII ZHIDKOSTEY [Heat Exchange and Friction During Gradient Flow of Fluids], Moscow-Leningrad, izd. Energiya, 1964.

46. Dodge, D. W.; Metzner, A. B. "Turbulent Flow of Nonnewtonian System," A. J. CH. JOURN., Vol 5, 1959, p 189.

47. Shaver, R. G.; Merril, E. W. "Turbulent Flow of Pseudoplastic Polymer Solutions in Straight Cylindrical Tubes," A. I. CH. JOUR., Vol 5, 1959, p 181.

48. Savins, I. G. "Drag Reduction Characteristics of Solutions of Macromolecules in Turbulent Pipe Flow," SOC. PETROL. ENGNG. J., Vol 4, No 3, 1964.

49. Metzner, A. B.; Graham, P. M. "Turbulent Flow Characteristics of Viscoelastic Fluids," J. FLUID MECH., Vol 20, No 2, 1964.

50. Barenblatt, G. I.; Bulina, I. G.; Myasnikov, V. P. "Influence of Solutions of Some High-Molecular Compounds on Drag Reduction with Turbulent Flow over Bodies," PMTF, No 3, 1965.

51. Barenblatt, G. I.; Bulina, I. G.; Myasnikov, V. P.; Sholomovich, G. I. "Influence of Small Additions of Soluble High-Molecular Compounds on Fluid Flow Conditions," PMTF, No 4, 1965.

52. Barenblatt, G. I.; Bulina, I. G.; Zel'dovich, Ya. B.; Kalashnikov, V. N.; Sholomovich, G. I. "Possible Mechanism of the Influence of Small Additions of High-Molecular Compounds on Turbulence," PMTF, No 5, 1965.

53. Hoyt, I. W.; Fabula, A. C. "The Effect of Additives on Fluid Friction," FIFTH SYMPOSIUM ON NAVAL HYDRODYNAMICS, September 1964.

54. Emerson, A. "Model Experiments Using Dilute Polymer Solutions Instead of Water," TRANS. N. E. COAST INST. ENGRS AND SHIPBUILDERS, Vol 81, No 4, 1965.

55. Levy, J.; Davis, S. "Drag Measurements on a Thin Plate in Dilute Polymer Solutions," INTERNAT. SHIPBUILDING PROGRESS, Vol 14, No 152, 1967.

56. "Discussion on Model Experiments Using Dilute Polymer Solutions Instead of Water," NORTH EAST COAST INSTITUTION OF ENGINEERS AND SHIPBUILDERS TRANSACTIONS, Vol 81, No 7, 1965.

57. Thurston, S.; Jones, R. D. "Experimental Model Studies of Nonnewtonian Soluble Coatings for Drag Reduction," J. AIRCRAFT, Vol 2, No 2, 1965.

CHAPTER VII. TWO-PHASE BOUNDARY LAYER

§VII.1. Introduction. General Statement of the Problem of a Gas Film on a Body

An effective means of decreasing surface friction is injection of materials with low viscosity and density into the wall region. This follows from a comparison of the frictional stress on the wall in fluids with different physical constants -- $\mu_1\rho_1$ and $\mu_2\rho_2$.

In the case of laminar motion, for example, in the first fluid

$$\tau_1 \sim \mu_1 \frac{U}{\delta_1}, \quad \text{where} \quad \delta_1 \sim \frac{L}{\sqrt{\frac{UL\rho_1}{\mu_1}}},$$

and in the second,

$$\tau_2 \sim \mu_2 \frac{U}{\delta_2}, \quad \text{where} \quad \delta_2 \sim \frac{L}{\sqrt{\frac{UL\rho_2}{\mu_2}}},$$

so that the relative magnitude of the surface friction

$$\frac{\tau_1}{\tau_2} \sim \sqrt{\frac{\mu_1\rho_1}{\mu_2\rho_2}}.$$

Hence, it follows that significant friction reduction on a wall over which water is flowing should be expected on gas ventilation of the wall region inasmuch as the value of $\mu_1\rho_1$ is a very small proportion of $\mu_2\rho_2$ for them (for air and water, for example, $\mu_1\rho_1/\mu_2\rho_2 \sim 10^{-5}$ under normal conditions).

With respect to nature of gas distribution in a water flow it is possible to distinguish two gas saturation conditions: film in which the clearly expressed, stable gas-fluid interface is observed, and diffusion or bubble, in which a gas-water mixture -- a fluid saturated with gas bubbles -- moves near the wall. The viscosity and density of such a mixture exceed the viscosity and density of gas, as a result of which the study of film gas saturation conditions is of the greatest interest from the point of view of drag reduction.

A characteristic feature of two-phase flow caused by participation of two immiscible components -- fluid and gas -- in the motion consists in the fact that for gas velocities given on the body surface (that is, essentially for the given gas flow rate and method of injecting it in the water flow) and known conditions at infinity, the form of the joint motion of the phases and, in particular, gas distribution in the flow are unknown. Accordingly, the phase motion diagram usually is given in advance, that is, it is designated in advance how (in the form of a solid film or individual bubbles) the gas is distributed and also how the motion in the fluid and gas occurs -- laminar or turbulent. With this approach determination of the hydrodynamic parameters of a flow which is frequently a very complicated problem, is only part of the problem as a whole. A study of the stability of the a priori proposed form of motion is no less important.

Some examples of the indicated method of constructing solutions of the equations of hydrodynamics are presented in the following sections.

Significant difference in the physical concepts of fluid and gas has given rise to a dual approach to the investigation of film gas saturation conditions. On the one hand, in order to study artificially created gas interlayers, the theory of a developed cavitation flow is used. Actual gas properties are not used in the calculation, and motion with an interface is interpreted as motion of an ideal fluid with free current lines subject to determination, the pressure at which is constant and equal to the gas pressure in a film. The characteristics of developed cavitating flow depend slightly on the method of injection of the gas into the flow (that is, the method of creating the required pressure in the cavity), and they are determined by the cavitation and Froude numbers (see Chapter VIII).

Another approach to the investigation of film gas saturation conditions is boundary layer theory. The finite magnitude of the density and viscosity of the gas is taken into account in it, but the influence of its injection on the pressure distribution which, in accordance with the basic assumption of the theory is considered known, is neglected. The form of the interface in this case is determined essentially by the gas flow rate and the method of injecting it into the flow, for example, in the case of a porous surface, the distribution of the ventilation velocity with respect to length.

Discovery of the region of applicability of the indicated theories and determination of the boundary layer stability conditions in a developed cavitating flow and in the boundary layer is an important problem in practical respects.

In connection with the first of tne indicated problems it is natural to consider the statement of the problem of a gas film on a body in general form.

For determinacy let us consider flow over a plane contour, selecting (Figure VII.1) the system of curvilinear coordinates x, y made up of normals to the contour (curves x=const) and curves orthogonal to the normals (curves y=const) in such a way that the elements of length along the coordinate lines will be $(1+ky)dx$ and dy respectively (see Chapter I), and the Lamé coefficients $h_1 \equiv h = 1+ky$, $h_2 = 1$. Here $k=1/R$ is the curvature of the contour, which is a function of x.

Let us assume that as a result of gas ventilation through the permeable surface of the contour a boundary layer arises in the wall region, the equation for which in the selected coordinate system is y=f(x).
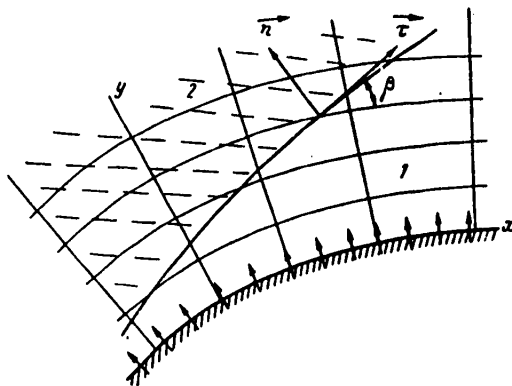

Figure VII.1. Flow diagram with gas-liquid interface

The boundary problem corresponding to this case reduces to joint investigation of the Navier-Stokes equations:

$$
\left\{ \frac{1}{h} u \frac{\partial u}{\partial x} + v \frac{\partial u}{\partial y} + \frac{\kappa}{h} uv \right\}_i = \left\{ -g_x - \frac{1}{\rho h} \frac{\partial p}{\partial x} + \right.
$$

$$
+ \nu \left[\frac{1}{h^2} \frac{\partial^2 u}{\partial x^2} + \frac{\partial^2 u}{\partial y^2} - \frac{1}{h^3} y \frac{\partial \kappa}{\partial x} \frac{\partial u}{\partial x} + \frac{\kappa}{h} \frac{\partial u}{\partial y} - \right.
$$

$$
\left. \left. - \frac{\kappa^2}{h^2} u + \frac{1}{h^3} \frac{\partial \kappa}{\partial x} v + 2 \frac{\kappa}{h} \frac{\partial v}{\partial x} \right] \right\}_i ;
$$

$$
\left\{ \frac{1}{h} u \frac{\partial v}{\partial x} + v \frac{\partial v}{\partial y} - \frac{\kappa}{h} u^2 \right\}_i = \left\{ -g_y - \frac{1}{\rho} \frac{\partial p}{\partial y} + \right.
$$

$$
+ \nu \left[\frac{1}{h^2} \frac{\partial^2 v}{\partial x^2} - \frac{\partial^2 v}{\partial y^2} + \frac{y}{h^3} \frac{\partial \kappa}{\partial x} \frac{\partial v}{\partial x} + \frac{\kappa}{h} \frac{\partial v}{\partial y} - \right.
$$

$$
\left. \left. - \frac{\kappa^2}{h^2} v - \frac{1}{h^3} \frac{\partial \kappa}{\partial x} u - 2 \frac{\kappa}{h} \frac{\partial u}{\partial x} \right] \right\}_i ;
$$

$$
\left[\frac{\partial u}{\partial x} + \frac{\partial}{\partial y} (hv) \right]_i = 0,
$$

(VII.1)

written for each of the components of motion: gas (i=1) and liquid (i=2). As the initial data, along with the ordinary conditions at infinity, we have the gas flow rate across the permeable surface and the method of injecting the gas into the flow (slots, holes, porous surface). In other words, on the body surface (for y=0) the gas velocities are given (zero in the impermeable sections and nonzero in the gas ventilation sections).

At the phase interface -- the discontinuity line of the physical properties of the medium -- the form of which is not given and is subject to determination, the following relations are satisfied. These relations follow [4] from the mass and momentum conservation laws:

322

for y=f(x)

$$\rho_1(D - v_{n1}) = \rho_2 \overline{(D - v_{n2})};$$ (VII.2)

$$\rho_1 \vec{v}_1 (D - v_{n1}) + \vec{p}_{n1} = \rho_2 \vec{v}_2 (D - v_{n2}) + \vec{p}_{n2},$$ (VII.3)

where ρ_1, ρ_2 are the densities of the phases separated by the discontinuity line;

D is the normal velocity of points on the boundary;

$\vec{v}_1$, $\vec{v}_2$ are the velocities of the media;

$\vec{p}_{n1}$, $\vec{p}_{n2}$ are the stresses operating in the liquid and gas in an area with normal to the boundary.

In the coordinate system connected with the discontinuity line, D=0, and the normal velocity components of the media v_{n1} and v_{n2} are determined by the phase conversion rate for y=f(x). In the case of joint motion of water and air of interest to us, this velocity is so small that it can be considered that

$$v_{n1} = 0; \quad v_{n2} = 0,$$ (VII.4)

as a result of which, as follows from expression (VII.3),

$$\vec{p}_{n1} = \vec{p}_{n2},$$ (VII.5)

that is, the conditions of equality of tangential and normal stress components operating in an area with normal $\vec{n}$ at the given point for y=f(x) are satisfied on the phase interface,

$$p_{n\tau 1} = p_{n\tau 2};$$ (VII.6)

$$p_{nn1} = p_{nn2}.$$ (VII.7)

The system of boundary conditions on the boundary becomes complete if we add the kinematic condition of equality of the tangential velocity components of the phases to the expressions obtained above

$$v_{\tau 1} = v_{\tau 2},$$ (VII.8)

which expresses the well-known experimental fact [12] of absence of shearing of the liquid with respect to the gas.

Let us assume that the gas interlayer is thin in the sense that the y-axes of the boundary are much smaller than the radius of curvature of the contour [f(x)<<R]; otherwise, we shall consider that the radii of curvature of the boundary and the contour are approximately identical, and with respect to order of magnitude they correspond to the body length L. Let us denote by β the angle between the direction of the boundary at some point of it and the tangent to the contour at the point with the same coordinate x; then the velocity and stress components on the normal and tangent to the interface are defined by formulas [11]:

$$v_n = -u \sin \beta + v \cos \beta; \tag{VII.9}$$

$$v_\tau = u \cos \beta + v \sin \beta; \tag{VII.10}$$

$$p_{nn} = -p_{xy} \sin \beta + p_{yy} \cos \beta; \tag{VII.11}$$

$$p_{n\tau} = -p_{xx} \sin \beta + p_{yx} \cos \beta, \tag{VII.12}$$

where

$$
\left.
\begin{aligned}
p_{xx} &= -p + 2\mu \left(h \frac{\partial u}{\partial x} + h\kappa v \right); \\
p_{xy} &= p_{yx} = \mu \left(\frac{\partial u}{\partial y} + h \frac{\partial v}{\partial x} - h\kappa u \right); \\
p_{yy} &= -p + 2\mu \frac{\partial v}{\partial y},
\end{aligned}
\right\}
\tag{VII.13}
$$

and u and v denote the velocity components with respect to the coordinate axes. The angle β is related to the elements of the curve y=f(x) by the obvious expression

$$\lg \beta = \frac{\frac{\partial y}{dx}}{h}. \tag{VII.14}$$

Neglecting the effect of viscous forces, the problem of a gas film formulated above reduces to investigation of the Euler equations written for a liquid and gas and obtained from the initial equations (VII.1) for $\nu_1 = 0$. In view of extraordinary smallness of the gas density by comparison with the liquid density ($\rho_1/\rho_2 \sim 10^{-3}$), in the majority of cases it is possible to neglect the force of inertia in the gas so that the equations of motion for it

$$\frac{\partial p}{\partial x} \simeq 0; \quad \frac{\partial p}{\partial y} \simeq 0,$$

will have the integral $p = \text{const} = p_k$ everywhere in the gas film region. For the region corresponding to motion of a fluid [y≥f(x)], as follows from equalities (VII.4), (VII.7), (VII.11)-(VII.13), the problem reduces to determining the form of the interface (the so-called free current line) as a function of pressure in the film (more precisely, the cavitation number $(p_\infty - p_k)/\rho_2 U^2/2)$) and the Froude number (for given conditions at infinity). This is the problem of developed cavitating flows.

Its defining conditions contain only a unique parameter characterizing the state of the gas — pressure in the cavity p_k. Accordingly, the method by which the indicated value of p_k is reached, in other words, the gas ventilation method, is insignificant if we a priori assume that the flow conditions are film.

The distinguishing feature of developed cavitating flow is the presence of a positive pressure gradient directed into the liquid. The pressure at the boundary of a cavitating film is minimal and increases with an increase in the y-coordinate. This fact gives rise to stable nature of the gas-liquid interface confirmed by experimental observations. In order to discover the influence of the viscosity

forces, let us proceed to the dimensionless form of the equations (VII.1), expressing all of the values in certain scales characteristic of them. Here it is necessary to consider not only the difference in the wall region of the scales of the longitudinal and transverse coordinates and velocities, as is done in boundary layer theory in a homogeneous liquid, but it is necessary to consider that these scales, generally speaking, are different in regions corresponding to motion of a liquid and a gas. Correspondence between them must be established using conditions of jointness of movement of phases at the interface. Selecting the scale L for x and R, for y, u and v we select still undefined scales: Y_1, U_1, V_1 for gas and Y_2, U_2, V_2 for liquid. From the continuity equation it follows that the scales for the transverse velocity are defined by the expressions

$$V_1 = Y_1 \frac{U_1}{L}; \quad V_2 = Y_2 \frac{U_2}{L}. \tag{VII.15}$$

The condition of equality of the tangential velocity components of media on both sides of the discontinuity (VII.8) considering (VII.10) is represented in the form

$$U_1 \left(u_1' + \frac{V_1}{U_1} v_1' \operatorname{tg} \beta \right) = U_2 \left(u_2' + \frac{V_2}{U_2} v_2' \operatorname{tg} \beta \right), \tag{VII.16}$$

where the apostrophe pertains to dimensionless variables. Hence, it follows that the scales of the longitudinal velocities both in the liquid and in the gas can be selected identical $U_1 = U_2 = U$.

The condition of equality of normal stresses at the interface (VII.7) considering expressions (VII.11), (VII.13) in dimensionless form reduces to the following relation:

$$-p_2' + \frac{2}{Re} \frac{\partial v_2'}{\partial y'} - \frac{1}{Re} \frac{L}{Y_2} \frac{\partial u_2'}{\partial y'} \operatorname{tg} \beta' - \frac{1}{Re} \frac{V_2}{U} \frac{1}{h'} \frac{\partial v_2'}{\partial x'} \operatorname{tg} \beta' +$$

$$+ \frac{1}{Re} \frac{u_2' \kappa'}{h'} \operatorname{tg} \beta' = -p_1' + \frac{2}{Re} \frac{\mu_1}{\mu_2} \frac{\partial v_1'}{\partial y'} - \frac{\mu_1}{\mu_2} \frac{1}{Re} \frac{L}{Y_1} \frac{\partial u_1'}{\partial y'} \operatorname{tg} \beta' -$$

$$- \frac{\mu_1}{\mu_2} \frac{1}{Re} \frac{1}{h'} \frac{V_1}{U} \frac{1}{h'} \frac{\partial v_1'}{\partial x'} \operatorname{tg} \beta' + \frac{\mu_1}{\mu_2} \frac{1}{Re} \frac{u_1' \kappa'}{h'} \operatorname{tg} \beta', \tag{VII.17}$$

where

$$\operatorname{tg} \beta' = \frac{\frac{Y}{L} \frac{dy'}{dx'}}{h'}, \quad h' = 1 + \frac{Y}{L} \kappa' y'.$$

When deriving (VII.17), a value identical for both the liquid and the gas equal to $\rho_2 U^2$ was used as the scales for the pressures. From equality (VII.17) it follows that for large Reynolds numbers $Re = UL/\nu_2$, it is possible to neglect the effect of the contribution of the part of the normal stress which depends on viscous forces, as a result of which, just as in an ideal liquid, at the interface we must have

$$p_1' = p_2'. \tag{VII.18}$$

Finally, from the condition of equality of the tangential stresses (VII.6) considering expressions (VII.12), (VII.13) we have the equation

$$
\mu_2 \frac{U}{Y_2} \left[\frac{\partial u_2'}{\partial y'} + \frac{Y_2^2}{L^2} \frac{U}{L} \frac{1}{h'} \frac{\partial v_2'}{\partial x'} - \frac{Y_2}{L} \frac{u_2' \kappa'}{h'} - 2 \frac{Y_2}{L} \frac{1}{h'} \frac{\partial u_2'}{\partial x'} \lg \beta' - \right.
$$

$$
\left. - 2 \frac{Y_2}{L} \frac{V_2}{U} \frac{v_2' \kappa'}{h'} \lg \beta' \right] = \mu_1 \frac{U}{Y_1} \left[\frac{\partial u_1'}{\partial y'} + \frac{Y_1^2}{L^2} \frac{U}{L} \frac{1}{h'} \frac{\partial v_1'}{\partial x'} - \right.
$$

$$
\left. - \frac{Y_1}{L} \frac{u_1' \kappa'}{h'} - 2 \frac{Y_1}{L} \frac{1}{h'} \frac{\partial u_1'}{\partial x'} \lg \beta' - 2 \frac{Y_1}{L} \frac{V_1}{U} \frac{v_1' \kappa'}{h'} \lg \beta' \right],
$$

(VII.19)

from which it follows that the ratio of the scales of the transverse coordinates is equal to the ratio of the viscosities of the media participating in the motion

$$
\frac{Y_1}{Y_2} = \frac{\mu_1}{\mu_2}. \tag{VII.20}
$$

This means that if when estimating the order of magnitude of the terms in the Navier-Stokes equation for gas a scale of Y_1 is selected, the scale Y_2 cannot be given arbitrarily, but must be taken in accordance with equality (VII.20). Physically this corresponds to a discontinuity of the derivative $\partial u / \partial y$ at the interface (identical tangential stress is obtained in the fluid for smaller velocity gradients, and in the gas, for larger velocity gradients).

Let us reduce the initial equations (VII.1) to dimensionless form for a fluid $y \geq f(x)$:

$$
\frac{1}{h'} u' \frac{\partial u'}{\partial x'} + v' \frac{\partial u'}{\partial y'} + \frac{Y_2}{L} \frac{\kappa' u' v'}{h'} = - \frac{gL}{U^2} g_x' - \frac{1}{h'} \frac{\partial p'}{\partial x'} +
$$

$$
+ \frac{1}{h'^2 \mathrm{Re}} \frac{\partial^2 u'}{\partial x'^2} + \frac{1}{\mathrm{Re}} \left(\frac{L}{Y_2} \right)^2 \frac{\partial^2 u'}{\partial y'^2} - \frac{1}{\mathrm{Re}} \frac{Y_2}{L} \frac{1}{h'^3} y' \frac{\partial \kappa'}{\partial x'} \frac{\partial u'}{\partial x'} +
$$

$$
+ \frac{1}{\mathrm{Re}} \frac{L}{Y_2} \cdot \frac{1}{h'} \frac{\partial u'}{\partial y'} - \frac{1}{\mathrm{Re}} \frac{1}{h'^3} \kappa'^2 u' + \frac{1}{\mathrm{Re}} \frac{Y_2}{L} \frac{1}{h'^3} \frac{\partial \kappa'}{\partial x'} v' +
$$

$$
+ \frac{1}{\mathrm{Re}} \frac{Y_2}{L} \frac{2\kappa'}{h'} \frac{\partial v'}{\partial x'} ;
$$

(VII.21)

$$
\left(\frac{Y_2}{L} \right)^3 \frac{1}{h'} u' \frac{\partial v'}{\partial x'} + \left(\frac{Y_2}{L} \right)^2 v' \frac{\partial u'}{\partial y'} - \frac{1}{h'} \frac{Y_2}{L} \kappa' u'^2 =
$$

$$
= - \frac{gL}{U^2} \frac{Y_2}{L} g_y' - \frac{\partial p'}{\partial y'} + \frac{1}{\mathrm{Re}} \left(\frac{Y_2}{L} \right)^2 \frac{1}{h'^2} \frac{\partial^2 v'}{\partial x'^2} +
$$

$$
+ \frac{1}{\mathrm{Re}} \frac{\partial^2 v'}{\partial y'^2} - \frac{1}{\mathrm{Re}} \left(\frac{Y_2}{L} \right)^3 \frac{y'}{h'^2} \frac{\partial \kappa'}{\partial x'} \frac{\partial v'}{\partial x'} + \frac{1}{\mathrm{Re}} \frac{Y_2}{L} \frac{\kappa'}{h'} \frac{\partial v'}{\partial y'} -
$$

$$
- \frac{1}{\mathrm{Re}} \left(\frac{Y_2}{L} \right)^3 \left(\frac{\kappa'}{h'} \right)^2 v' - \frac{1}{\mathrm{Re}} \frac{Y_2}{L} \frac{1}{h'^3} \frac{\partial \kappa'}{\partial x'} u' -
$$

$$
- \frac{1}{\mathrm{Re}} \frac{Y_2}{L} \frac{2\kappa'}{h'^2} \frac{\partial u'}{\partial x'}. \tag{VII.22}
$$

326

Let us reduce equations (VII.1) for a gas to dimensionless form y<f(x):

$$\frac{\varrho_1}{\rho_2}\left[\frac{1}{h'}u'\frac{\partial u'}{\partial x'}+v'\frac{\partial u'}{\partial y'}+\frac{Y_1}{L}\frac{\kappa u'v'}{h'}\right]=-\frac{gL}{U^2}g_x'\frac{\rho_1}{\rho_2}-\frac{1}{h'}\frac{\partial p'}{\partial x'}+$$
$$+\frac{\mu_1}{\mu_2}\frac{1}{Re}\left[\frac{1}{h'^2}\frac{\partial^2 u'}{\partial x'^2}+\left(\frac{L}{Y_1}\right)^2\frac{\partial^2 u'}{\partial y'^2}-\frac{Y_1}{L}\frac{1}{h'^3}y'\frac{\partial\kappa'}{\partial x'}\frac{\partial u'}{\partial x'}+$$ (VII.23)
$$+\frac{L}{Y_1}\frac{1}{h'}\frac{\partial u'}{\partial y'}-\frac{\kappa'^2 u'}{h'^2}+\frac{Y_1}{L}\frac{1}{h'^3}\frac{\partial\kappa'}{\partial x'}v'+-\frac{Y_1}{L^1}\cdot 2\frac{\kappa'}{h'}\frac{\partial v'}{\partial x'}\right];$$

$$\frac{\rho_1}{\rho_2}\left[\left(\frac{Y_1}{L}\right)^2\frac{1}{h'}u'\frac{\partial v'}{\partial x'}+\left(\frac{Y_1}{L}\right)^2 v'\frac{\partial u'}{\partial y'}-\frac{Y_1}{L}\frac{\kappa u'^2}{h'}\right]=$$
$$-\frac{gL}{U^2}\frac{Y_1}{L}g_y'\frac{\rho_1}{\rho_2}-\frac{\partial p'}{\partial y'}+\frac{\mu_1}{\mu_2}\frac{1}{Re}\left[\left(\frac{Y_1}{L}\right)^2\frac{1}{h'^2}\frac{\partial^2 v'}{\partial x'^2}+\frac{\partial^2 v'}{\partial y'^2}-\right.$$
$$-\left(\frac{Y_1}{L}\right)^3\frac{y'}{h'^2}\frac{\partial\kappa'}{\partial x'}\frac{\partial v'}{\partial x'}+\frac{Y_1}{L}\frac{\kappa'}{h'}\frac{\partial v'}{\partial y'}-\left(\frac{Y_1}{L}\right)^2\left(\frac{\kappa'}{h'}\right)^2 v'-$$
$$-\frac{Y_1}{L}\frac{1}{h'^3}\frac{\partial\kappa'}{\partial x'}u'-\frac{Y_1}{L}\frac{2\kappa'}{h'^2}\frac{\partial u'}{\partial x'}\right].$$ (VII.24)

The obtained expressions allow the influence of viscous forces on the investigated motion with an interface to be traced. If we consider that in the region which corresponds to motion of a gas [y≤f(x)], the forces of inertia are of the same order as the viscosity forces, then it is necessary according to equation (VII.23) to set

$$\frac{\rho_1}{\rho_2}\sim\frac{\mu_1}{\mu_2}\cdot\frac{1}{Re}\left(\frac{L}{Y_1}\right)^2,$$

that is, to select the scale Y_1 as follows:

$$\frac{Y_1}{L}=\frac{1}{\sqrt{\frac{UL}{\nu_1}}}.$$ (VII.25)

Here the order of thickness of the gas interlayer corresponds to the thickness of the boundary layer developed on a body moving in a gas. Substituting Y_1 by equation (VII.25) in equations (VII.21)-(VII.24) and neglecting the terms containing the small factor 1/Re, considering the equality (VII.20), we obtain:

$$\frac{1}{h'}u'\frac{\partial u'}{\partial x'}+v'\frac{\partial u'}{\partial y'}+\sqrt{\left(\frac{\mu_2\rho_2}{\mu_1\rho_1}\cdot\frac{1}{Re}\right)}\kappa'u'v'=$$
$$=-\frac{gL}{U^2}g_x'-\frac{1}{h'}\frac{\partial p'}{\partial x'}+\left(\frac{\mu_1\rho_1}{\mu_2\rho_2}\right)\frac{\partial^2 u'}{\partial y'^2};$$ (VII.26)

$$\left(\frac{\mu_2\rho_2}{\mu_1\rho_1}\frac{1}{Re}\right)\frac{u'\partial v'}{h'\partial x'}+\left(\frac{\mu_2\rho_2}{\mu_1\rho_1}\frac{1}{Re}\right)v'\frac{\partial v'}{\partial y'}-\frac{1}{h'}\sqrt{\left(\frac{\mu_2\rho_2}{\mu_1\rho_1}\frac{1}{Re}\right)}\kappa'u'^2=$$
$$=-\frac{gL}{U^2}\sqrt{\left(\frac{\mu_2\rho_2}{\mu_1\rho_1}\frac{1}{Re}\right)}g_y'-\frac{\partial p'}{\partial y'}.$$ (VII.27)

for $y \geq f(x)$ and

$$\frac{\mu_1}{\rho_2}\left(\frac{1}{h'}u'\frac{\partial u'}{\partial x'} + v'\frac{\partial u'}{\partial y'} + \right)\sqrt{\frac{v_1}{v_2}}\frac{\kappa'u'v'}{\sqrt{Re}}\right) = -\frac{gL}{U^2}\frac{\rho_1}{\rho_2}g_x' - \qquad (VII.28)$$
$$- \frac{1}{h'}\frac{\partial p'}{\partial x'} + \frac{\rho_1}{\rho_2}\frac{\partial^2 u'}{\partial y'^2} ;$$

$$\frac{\mu_1}{\mu_2}\frac{1}{Re}\frac{1}{h'}u'\frac{\partial v'}{\partial x'} + \frac{\mu_1}{\mu_2}\frac{1}{Re}v'\frac{\partial v'}{\partial y'} - \sqrt{\frac{\mu_1\rho_1}{\mu_2\rho_2}\frac{1}{Re}}\cdot\frac{1}{h'}\kappa'u'^2 =$$
$$\cdots - \frac{gL}{U^2}\sqrt{\frac{\mu_1\rho_1}{\mu_2\rho_2}\frac{1}{Re}}g_y' - \frac{\partial p'}{\partial y'} \qquad (VII.29)$$

for $y \leq f(x)$.

From the presented expressions it follows that the motion of a liquid and a gas depends on the relation between $\mu_1\rho_1/\mu_2\rho_2$ and $1/Re$. If the parameter $(\mu_2\rho_2/\mu_1\rho_1)$ $(1/Re) \sim 1$, so that $(\mu_1\rho_1/\mu_2\rho_2) \sim 1/Re$, expressions (VII.26) and (VII.27) become Euler equations, and for small values of the density relation, equations (VII.28) and (VII.29) lead to the condition $p = const = p_k$ for $y \leq f(x)$. Inasmuch as the value of $\mu_1\rho_1/\mu_2\rho_2$ under ordinary conditions is extremely small, the application of the methods of ideal fluid theory even in the investigated case of gas interlayers having a thickness on the order of a laminar boundary layer in a gas, can lead to satisfactory results.

If the parameter $(\mu_2\rho_2/\mu_1\rho_1)$ $(1/Re)$ is less than one so that $\mu_1\rho_1/\mu_2\rho_2 > 1/Re$, it is necessary to consider the influence of finiteness of the viscosity and density of the gas included in the film. A possible means of considering this is finding the correction to the solution obtained by the cavitation theory methods. This correction is caused by stagnation of the fluid near the interface caused by the effect of the gas viscosity forces. Up to now no one has undertaken such an effort.

Finally, if $(\mu_2\rho_2/\mu_1\rho_1)(1/Re) \ll 1$, equations (VII.26)-(VII.29) become laminar boundary layer Prandtl equations. This corresponds to very thin gas interlayers so that the forces of inertia and viscosity in the wall layer of the liquid are identical with respect to order of magnitude. The flow is characterized by constancy of pressures across the boundary layer, and the form of the boundary layer is determined not by the effective pressure forces, but, in essence, by the gas flow rate and method of injecting it.

As follows from equation (VII.21), in the investigated case it is necessary to take the following value as the scale Y_2

$$Y_2 = \frac{L}{\sqrt{Re}},$$

after which the initial system of equations (VII.21)-(VII.24) reduces to the form

$$u_2' \frac{\partial u_2'}{\partial x'} + v_2' \frac{\partial u_2'}{\partial y'} = -\frac{gL}{U^2} g_x' - \frac{\partial p_2'}{\partial x'} + \frac{\partial^2 u_2'}{\partial y'^2};$$

(VII.30)

$$0 = \frac{\partial p_2'}{\partial y'};$$

$$\frac{\rho_1 \mu_1}{\rho_2 \mu_2} \left(u_1' \frac{\partial u_1'}{\partial x'} + v_1' \frac{\partial u_1'}{\partial y'} \right) = -\frac{\rho_1 \mu_1}{\rho_2 \mu_2} \frac{gL}{U^2} g_x' -$$

$$- \frac{\mu_1}{\mu_2} \frac{\partial p_1'}{\partial x'} + \frac{\partial^2 u_1'}{\partial y'^2},$$

(VII.31)

$$0 = \frac{\partial p_1'}{\partial y'}$$

or in dimensional variables:

$$u_2 \frac{\partial u_2}{\partial x} + v_2 \frac{\partial u_2}{\partial y} = -g_x - \frac{\partial p_2}{\partial x} + v_2 \frac{\partial^2 u_2}{\partial y^2};$$

$$u_1 \frac{\partial u_1}{\partial x} + v_1 \frac{\partial u_1}{\partial y} = -g_x - \frac{\partial p_1}{\partial x} + v_1 \frac{\partial^2 u_1}{\partial y_2}.$$

(VII.32)

The boundary conditions of jointness of motion of a liquid and gas at the boundary y=f(x), as follows from equalities (VII.4), (VII.6), (VII.8), (VII.9), (VII.10), (VII.16), (VII.19) reduce to the expressions for y=f(x)

$$v_1 - u_1 \frac{df}{dx} = 0;$$

(VII.33)

$$v_2 - u_2 \frac{df}{dx} = 0;$$

(VII.34)

$$u_1 = u_2;$$

(VII.35)

$$\mu_1 \left(\frac{\partial u}{\partial y} \right)_1 = \mu_2 \left(\frac{\partial u}{\partial y} \right)_2,$$

(VII.36)

expressing impermeability of the boundary for the liquid and the gas, equality of the longitudinal velocities and continuity of the tangential stresses, respectively. According to (VII.7) and (VII.18) at the interface the normal stress -- pressure -- is continuous

$$p_1 = p_2 = p(x),$$

(VII.37)

which is constant across the boundary layer and is considered known.

At the surface of a permeable solid contour, the gas ventilation conditions are given: for example, on a porous surface the longitudinal component of the gas vanishes as a result of adhesion

$$y = 0, \quad u_1 = 0,$$

(VII.38)

329

and the normal component is defined by the gas injection velocity

$$y = 0; \quad v_1 = v_0(x).$$

(VII.39)

For y→∞, the velocity of the fluid approaches the velocity of a potential flow at infinity, so that

$$y \to \infty, \quad u_2 \to U(x).$$

(VII.40)

Laminar motions in the boundary layer of a plate with interface of two immiscible fluids were investigated by G. G. Chernyy for ratios between the viscosity and density of the moving media not very small [11]. The case of a gas film studied in reference [1] in which numerical integration of the system of differential equations of the boundary layer (VII.32) was used to calculate the tangential stress on the wall as a function of the Reynolds number, the physical properties of the gas and its flow rate during injection distributed along the length of the plate according to the law $v_0(x) \sim 1/\sqrt{x}$. As was demonstrated in [11], this assignment of the ventilation law, just as in a homogeneous fluid, leads to the self-similar problem. In reference [13] a study was made of the heat transfer characteristics in a laminar boundary layer with gas-liquid interface.

§VII.2. Two-Phase Laminar Boundary Layer[1]

Let us present the fundamentals of two-phase laminar boundary layer theory for the case where gas is injected at the body surface. When developing the theory the assumption is made that as a result of gas ventilation on the body surface a solid film is formed which is a liquid and gas boundary layer interface. For the case of flow over a plate, this two-phase laminar boundary layer problem was solved in the paper by Sparrow, Johnson and Eckert [1]. In the mentioned paper it was demonstrated that the presence of a two-phase boundary layer for a flat plate leads to sharp drag reduction. Practical realization of this drag reduction depends on the possibility of creation and maintenance of a continuous gas film. Realization of the continuous gas film is connected with difficulties arising from the necessity for insuring stability of the interface, for it will decay into separate bubbles and go over to turbulent flow conditions.

However, the solution to the problem of two-phase laminar boundary layers has practical significance, for it permits not only establishment of the upper admissible limit in drag improvement, but it permits an approach to the solution of the stability problem of gas and liquid interfaces and also the creation of the two-phase turbulent boundary layer theory.

Statement of the Problem and Basic Equations. When studying flow of a viscous fluid over the surface of a body, the case where the external flow is considered to depend on only one parameter is of great interest. The single-parametric solutions to the Faulkner and Skan problem of a steady-state laminar boundary layer with

---

[1]The basic results of §VII.2-VII.5 were obtained by A. M. Basin and V. B. Starobinskiy [3], [7], [22], [23].

single-term exponential distribution of the velocity U(x) [2] have found the greatest application in boundary layer theory:

$$U(x) = cx^m.$$

<div align="right">(VII.41)</div>

Here c and m are arbitrary positive constants, where m is dimensionless.

Let us use the exponential velocity distribution for solution of the problem of a laminar two-phase boundary layer [3].

Let us assume that gas is injected into the liquid boundary layer through surface pores of the body in such a way that a continuous gas film is created and maintained (Figure VII.2).

The basic equations of plane motion of a liquid and gas in a laminar boundary layer are written as follows (§VII.1):

<div align="right">(VII.42)</div>

$$u \frac{\partial u}{\partial x} + v \frac{\partial u}{\partial y} = U \frac{dU}{dx} + \nu_{1,2} \frac{\partial^2 u}{\partial y^2};$$

$$\frac{\partial u}{\partial x} + \frac{\partial v}{\partial u} = 0.$$

<div align="right">(VII.43)</div>

Here and hereafter the subscript "1" has been introduced to denote values pertaining to the gas, and the subscript "2" for values pertaining to the liquid; x and y are the coordinates along the wall and along the normal to it; u and v are the corresponding velocity components; U is the velocity at the outer boundary of the boundary layer.
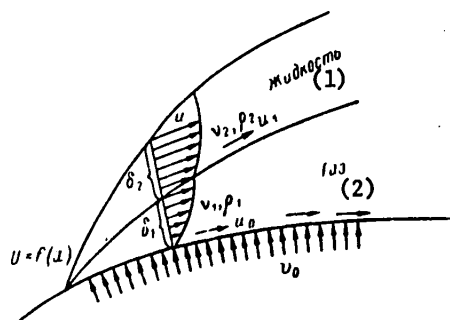

Figure VII.2. Diagram of a two-phase boundary layer

Key:
1. liquid
2. gas

When investigating a gas film let us neglect the influence of compressibility and evaporation of the liquid from the interface.

At the gas and liquid interface variation of the physical properties takes place in a very thin layer. Therefore in hydrodynamic respects this interface can be

<div align="center">331</div>

taken as a discontinuity surface on which the conditions of conservation of the flow of mass, momentum and energy must be satisfied (§VII.1).

Since in the investigated case we neglect the phase transformations at the liquid-gas interface and, consequently, the flow of mass across the discontinuity surface $y=\delta_1=f(x)$, these conditions reduce to the boundary conditions (VII.33)-(VII.40) obtained in §VII.1.

The normal stress -- pressure -- is constant across the boundary layer and is considered known

$$p_1 = p_2 = p(x).$$

(VII.44)

On a solid wall for y=0:

$$u = 0; \quad v = v_0.$$

(VII.45)

On the liquid and gas interface for $y=\delta_1$ the following conditions must be satisfied:

Equality of tangential velocities

$$u_1 = u_2.$$

(VII.46)

Equality of tangential stresses $\tau_1=\tau_2$, or

$$\mu_1 \left(\frac{\partial u}{\partial y}\right)_1 = \mu_2 \left(\frac{\partial u}{\partial y}\right)_2.$$

(VII.47)

Condition of impermeability of the boundary for liquid and gas

$$v_1 - u_1 \frac{d\delta_1}{dx} = 0; \quad v_2 - u_2 \frac{d\delta_1}{dx} = 0.$$

(VII.48)

Condition at infinity (for $y\to\infty$)

$$U(x) = cx^m.$$

(VII.49)

Expressions (VII.44)-(VII.49) jointly with equations (VII.42) and (VII.43) offer the possibility of theoretically solving the problem of determining the parameters of a two-phase laminar boundary layer.

The solution of the system of nonlinear differential equations (VII.42)-(VII.43) with boundary conditions (VII.45)-(VII.49) present great difficulties. Therefore, usually for the solution of this system the similarity method is used, assuming that the velocity profile in the boundary layer has similar form for all values of x. This assumption is equivalent to introduction of an additional condition on the injection velocity distribution.

For satisfaction of the continuity equation (VII.42), let us introduce the current function ψ into the investigation, setting

$$u = \frac{\partial \psi}{\partial y}; \quad v = -\frac{\partial \psi}{\partial x}.$$

Here equation (VII.41) is written in the form

$$\frac{\partial \psi}{\partial y} \cdot \frac{\partial^2 \psi}{\partial x \, \partial y} - \frac{\partial \psi}{\partial x} \cdot \frac{\partial^2 \psi}{\partial y^2} = U \frac{\partial U}{\partial x} + \nu_{1,2} \frac{\partial^3 \psi}{\partial y^3}. \tag{VII.50}$$

Let us apply the similarity transformation (see §IV.1) known from boundary layer theory to this equation. For the investigated case it is expedient to introduce the following formula for the current function:

$$\psi = \sqrt{\nu c x^{m+1}}\, \varphi(\eta), \tag{VII.51}$$

where

$$\eta = y \sqrt{\frac{c x^{m-1}}{\nu}}. \tag{VII.51a}$$

Using expression (VII.51), let us calculate the following values entering into equation (VII.50):

$$\left.
\begin{aligned}
u &= \frac{\partial \psi}{\partial y} = c x^m \varphi'(\eta); \\[6pt]
\frac{\partial^2 \psi}{\partial y^2} &= \frac{c\sqrt{c}}{\sqrt{\nu}} x^{\frac{3m-1}{2}} \varphi''(\eta); \\[6pt]
\frac{\partial^3 \psi}{\partial y^3} &= \frac{c^2}{\nu} x^{2m-1} \varphi'''(\eta); \\[6pt]
-v &= \frac{\partial \psi}{\partial x} = \\[6pt]
&= \sqrt{\nu c}\, x^{\frac{m-1}{2}} \left[\frac{m+1}{2}\varphi(\eta) + \frac{m-1}{2} \eta \varphi'(\eta) \right]; \\[6pt]
\frac{\partial^2 \psi}{\partial x \, \partial y} &= c x^{m-1} \left[m\varphi'(\eta) + \frac{m-1}{2} \eta \varphi''(\eta) \right].
\end{aligned}
\right\} \tag{VII.52}$$

Here the indices on the constants are omitted; the stroke denotes the derivative with respect to η.

Equation (VII.50) is reduced to the following third-order differential equation well known from laminar boundary theory after substitution of the values of the derivatives into the righthand side of U(x) according to formula [VII.41) [2]:

$$\varphi''' + \frac{m+1}{2} \varphi\varphi'' = m(\varphi'^2 - 1). \tag{VII.53}$$

This equation is valid both for the gas boundary layer and for the liquid.

When using equation (VII.53) for the gas layer it is necessary to set:

$$v - v_1; \quad 0 \leqslant y_1 \leqslant \delta_1; \quad \eta - \eta_1 = y_1 \sqrt{\frac{cx^{m-1}}{v_1}};$$

$$\varphi = \varphi(\eta_1) = \frac{\psi_1}{\sqrt{v_1 cx^{m+1}}}.$$

When calculating the parameters of the liquid layer, the transverse coordinate is reckoned from the liquid-gas interface.

For the case of a liquid it is necessary to set

$$v = v_2; \quad 0 < y_2 = y - \delta_1 \leqslant \infty;$$

$$\eta = \eta_2 = y_2 \sqrt{\frac{cx^{m-1}}{v_2}};$$

$$\varphi = \varphi_2(\eta_2) = \frac{\psi_2}{\sqrt{v_2 cx^{m+1}}}.$$

The boundary conditions (VII.45)-(VII.49) for equation (VII.53) have the form:

1. On a solid wall.

For y=0 or η_1=0; u=0, which corresponds to

$$\varphi_1'(\eta_1) = \varphi_1'(0) = 0;$$

$$v(0) = v_0 = - \left(\frac{\partial \psi}{\partial x} \right)_{\eta_1 = 0} = - \frac{m+1}{2} \sqrt{v_1 c} \, x^{\frac{m-1}{2}} \varphi_1(0). \qquad (VII.54)$$

Hence, we obtain

$$\varphi_1(0) = - \frac{2}{(m+1)} \cdot \frac{v_0}{cx^m} \left(\frac{cx^{m+1}}{v_1} \right)^{1/2} =$$

$$= - \frac{2}{(m+1)} \cdot \frac{v_0}{U(x)} \left[\frac{U(x)x}{v_1} \right]^{1/2} = -\varphi_0. \qquad (VII.55)$$

As is obvious from formula (VII.55), the value of ϕ_0 will not be a function of x except the case where the injection velocity v_0 is subject to the condition

$$v_0 \sim x^{\frac{m-1}{2}}. \qquad (VII.56)$$

2. At the interface $\eta_1 = \eta_\delta$ the boundary conditions (VII.46)-(VII.48) are written as follows.

The condition of absence of the gas flow rate dM=0 based on (VII.48) assumes the form

$$dM = \rho_1 (u \, dy - v \, dx)_{y=\delta_1} = 0.$$

Substituting the values of u and v into this expression according to the formulas (VII.52) and considering the notation of (VII.51a) and condition (VII.54), we obtain

$$dM = \rho_1 \left\{ cx^m \varphi_1'(\eta_\delta) \frac{1-m}{2} x^{-\frac{(m+1)}{2}} \sqrt{\frac{v_1}{c}} \eta_\delta + \right.$$

$$\left. + \sqrt{v_1 c} \, x^{\frac{m-1}{2}} \left[\frac{m+1}{2} \varphi_1(\eta_\delta) + \frac{m-1}{2} \eta_\delta \varphi_1'(\eta_\delta) \right] \right\} dx =$$

$$= \rho_1 \frac{m+1}{2} \sqrt{v_1 c x^{m-1}} \varphi_1(\eta_\delta) \, dx = 0.$$

Hence, it follows that the condition dM=0 is equivalent to the condition

$$\varphi_1(\eta_\delta) = 0, \tag{VII.57}$$

where δ_1 is the gas film thickness, and $\eta_\delta = \delta_1 \sqrt{\dfrac{cx^{m-1}}{v_1}}$.

An analogous expression can be written for the boundary layer of a liquid.

For calculation purposes it is more convenient to reckon the transverse of the coordinate for the boundary layer of a liquid beginning with the liquid-gas interface.

If we neglect evaporation of the liquid from the interface, the condition of absence of a flow rate assumes the form

$$\varphi_1(\eta_\delta) = \varphi_2(0) = 0, \tag{VII.58}$$

where $y_1 = \delta_1$; $\eta_1 = \eta_\delta$; $\eta_2 = 0$.

The other two boundary conditions on the interface assume the form

$$\varphi_1'(\eta_\delta) = \varphi_2'(0); \tag{VII.59}$$

$$\mu_1 \left(\frac{\partial u}{\partial y} \right)_{y_1 = \delta_1} = \mu_2 \left(\frac{\partial u}{\partial y} \right)_{y_2 = 0}. \tag{VII.60}$$

Let us transform condition (VII.60) considering expressions (VII.51) and (VII.52). Then we obtain

$$\frac{\mu_1 c \sqrt{c}}{\sqrt{v_1}} x^{\frac{3m-1}{2}} \varphi_1''(\eta_\delta) = \frac{\mu_2 c \sqrt{c}}{\sqrt{v_2}} x^{\frac{3m-1}{2}} \varphi_2''(0).$$

Hence it follows that

$$\varphi_1''(\eta_\delta) = R \varphi_2''(0). \tag{VII.61}$$

Here

$$R = \left[\frac{\rho_2 \mu_2}{\rho_1 \mu_1} \right]^{1/2}. \tag{VII.62}$$

335

The boundary condition at infinity assumes the form

$$\varphi_2' \rightarrow 1 \text{ for } \eta_2 \rightarrow \infty. \tag{VI.63}$$

Solution of the Equations. The solution of equation (VII.53) for the boundary layer of a gas will be found in the form of a Taylor series

$$\varphi_1(\eta_1) = \varphi_1(0) + \varphi_1'(0)\eta_1 + \frac{\varphi_1''(0)}{2!}\eta_1^2 + \frac{\varphi_1'''(0)}{3!}\eta_1^3 + \cdots \tag{VII.64}$$

The first two derivatives are found directly from the boundary conditions

$$\varphi_1(0) = -\varphi_0; \quad \varphi_1'(0) = 0.$$

For $\eta=0$ the remaining derivatives are easily expressed in terms of $\phi_1(0)$, $\phi'_1(0)$, $\phi''_1(0)$ using successive differentiation of the equation (VII.53)

$$
\begin{aligned}
\varphi_1''' &= -\frac{(m+1)}{2}\varphi_1\varphi_1'' - m; \\
\varphi_1^{IV} &= -\frac{(m+1)}{2}\varphi_1\varphi_1'''; \\
\varphi_1^{V} &= -\frac{(m+1)}{2}\left(\varphi_1''^2 - \varphi_1\varphi_1^{IV}\right) + 2m\varphi_1''; \\
\varphi_1^{VI} &= -\frac{(m+1)}{2}\left(4\varphi_1''\varphi_1''' + \varphi_1\varphi_1^{V}\right); \\
\varphi_1^{VII} &= -\frac{(m+1)}{2}\left(4\varphi_1'''^2 + 7\varphi_1''\varphi_1^{IV} + \varphi_1\varphi_1^{VI}\right) + \\
&\quad + 2m\left(3\varphi_1'''^2 + 4\varphi_1''\varphi_1^{IV}\right); \\
\varphi_1^{VIII} &= -\frac{(m+1)}{2}\left(15\varphi_1'''\varphi_1^{IV} + 11\varphi_1''\varphi_1^{V} + \varphi_1\varphi_1^{VII}\right) + \\
&\quad + 2m\left(10\varphi_1'''\varphi_1^{IV} + 5\varphi_1''\varphi_1^{V}\right).
\end{aligned}
\tag{VII.65}
$$

Expressions (VII.64) and (VII.65) are used to satisfy the boundary conditions at the liquid and gas interface for determination of $\phi'_1(0)$. Thus, using the boundary condition (VII.57) $\phi_1(\eta_\delta)=0$ and introducing it into expression (VII.64), we obtain

$$0 = -\varphi_0 + \frac{\varphi_1''(0)}{2!}\eta_\delta^2 + \frac{\varphi_1'''(0)}{3!}\eta_\delta^3 + \cdots$$

or

$$0 = -\varphi_0 + \varphi_1''(0)\left[\frac{\eta_\delta^2}{2} + \sum_{\kappa=3}\frac{\varphi_1^{\kappa}(0)\eta_\delta^{\kappa}}{\varphi_1''(0)\kappa!}\right].$$

Hence,

$$\varphi_1''(0) = \frac{\varphi_0}{\dfrac{\eta_\delta^2}{2} + \displaystyle\sum_{\kappa=3}\dfrac{\varphi_1^{\kappa}(0)\eta_\delta^{\kappa}}{\varphi_1''(0)\kappa!}}. \tag{VII.66}$$

In the righthand side of expression (VII.66) the value of $\phi''_1(0)$ in the first approximation is selected from the condition of insuring rapid convergence of the process of successive approximations. The values of $\phi''_1(0)$ presented below for a plate can be taken as the approximate value of $\phi''_1(0)$.

Let us differentiate the series of (VII.64) and use the boundary condition (VII.59) $\psi'_1(\eta_\delta)=\phi'_2(0)$. As a result, we obtain

$$\varphi'_2(0) = \varphi'_1(0)\left[\eta_\delta + \sum_{\kappa=3} \frac{\varphi_1^\kappa(0)\,\eta_\delta^{\kappa-1}}{\varphi'_1(0)\,(\kappa-1)!}\right]. \qquad \text{(VII.67)}$$

In order to use the boundary condition $\phi''_1(\eta_\delta)=R\phi''_2(0)$ it is necessary to differentiate the series (VII.64) twice. Then we find

$$R\varphi''_2(0) = \varphi''_1(0) + \varphi'''_1(0)\,\eta_\delta + \frac{\varphi_1^{IV}(0)}{2!}\,\eta_\delta^2 + \cdots$$

or

$$\varphi''_1(0) = \frac{R\varphi''_2(0)}{1 + \sum_{\kappa=3} \dfrac{\varphi_1^\kappa(0)\,\eta_\delta^{\kappa-2}}{\varphi''_1(0)\,(\kappa-1)!}}. \qquad \text{(VII.68)}$$

From equations (VII.64), (VII.66)-(VII.68), it is possible to find the gas boundary layer characteristics, that is, the frictional stress and total drag if the values of $\phi'_2(0)$ and $\phi''_2(0)$ are known for the external boundary layer of the liquid.

These values can be found as a result of solution of the differential equation (VII.53) for the following boundary conditions:

$$\left.\begin{array}{l} \varphi_2 = 0; \quad \varphi'_2 = A_0 \ \text{ for } \eta = 0; \\[4pt] \qquad \varphi'_2 = 1 \ \text{ for } \eta \to \infty. \end{array}\right\} \qquad \text{(VII.69)}$$

Here A_0 is a constant.

If the solution of this equation is obtained, it is possible completely to solve the stated problem by using the method of successive approximations [1]. First, the values of ϕ_0 and R of interest to us are calculated.

The dimensionless thickness of the gas film η_δ is designated in the first approximation, and $\phi''_1(0)$ is found by formula (VII.66) considering (VII.65). The value of $\phi'_2(0)$ is determined by the value found for $\phi''_1(0)$ using formula (VII.67), and $\phi''_2(0)$ is found by the known solution of the fluid layer boundary equation. Then $\phi''_1(0)$ is calculated again by formula (VII.68). If the calculated $\phi''_1(0)$ differs from $\phi''_1(0)$ taken in the preceding approximation, the calculation is repeated for the value of $\phi''_1(0)$ obtained by formula (VII.68). The calculations are performed to comparison of the preceding and subsequent approximation with required accuracy of $\phi''_1(0)$.

By the value found for $\phi''_1(0)$ it is easy to calculate all the boundary layer characteristics of interest to us.

The results of the numerical calculations are presented in the following sections.

Two-Phase Laminar Boundary Layer on a Plate. For the special case of a two-phase laminar boundary layer on a plate all the required formulas can be obtained from the preceding ones if the set $U(x)=U_0$ in them, that is, $c=U_0$, $m=0$.

Here the basic equation of the boundary layer (VII.53) assumes the following form:

$$\varphi'' + \frac{1}{2} \varphi\varphi'' = 0. \tag{VII.70}$$

Here $\phi=\phi_1$ for a gas, and $\phi=\phi_2$ for a liquid.

The boundary conditions (VII.54)-(VII.63) for a plate are written as follows:

$$\left.\begin{aligned}
\varphi_1(0) &= -\varphi_0; \quad \varphi'_1(0) = 0; \\
\varphi_1(\eta_\delta) &= \varphi_2(0) = 0; \quad \varphi'_1(\eta_\delta) = \varphi'_2(0); \\
\varphi''_1(\eta_\delta) &= R\varphi''_2(0); \\
\varphi'_2 &\to 1 \quad for\ \eta_2 \to \infty.
\end{aligned}\right\} \tag{VII.71}$$

The problem of a two-phase laminar boundary layer on a plate was investigated in detail by Sparrow, Johnson and Eckert [1].

In contrast to the presented solution in the above-mentioned paper instead of the parameters η_1, η_2 and η_δ the parameters η_{p1}, η_{p2} and $\eta_{p\delta}$ were introduced:

$$\left.\begin{aligned}
\eta_{p_1} &= \frac{\eta_1}{2} = \frac{y_1}{2} \sqrt{\frac{U_0}{x\nu_1}}; \\
\eta_{p_2} &= \frac{\eta_2}{2} = \frac{y_2}{2} \sqrt{\frac{U_0}{x\nu_2}}; \\
\eta_{p_\delta} &= \frac{\delta_1}{2} \sqrt{\frac{U_0}{x\nu_1}}.
\end{aligned}\right\} \tag{VII.72}$$

·In connection with the fact that the results of calculating the two-phase laminar boundary layer characteristics on a plate are presented in reference [1], it is expedient to present a comparison of the formulas obtained above with the formulas of the article.

In the above-presented formulas let us do the substitution of variables (VII.72), and let us denote

$$\varphi\left(\frac{\eta}{2}\right) = f(\eta_p). \tag{VII.73}$$

Then, we obtain

$$\left.\begin{aligned}
\varphi' &= \frac{\partial\varphi}{\partial\eta} = \frac{1}{2}\cdot\frac{\partial f}{\partial\eta_p} = \frac{1}{2}f'; \\
\varphi'' &= \frac{\partial^2\varphi}{\partial\eta^2} = \frac{1}{4}\cdot\frac{\partial^2 f}{\partial\eta_p^2} = \frac{1}{4}f''; \\
\varphi''' &= \frac{\partial^3\varphi}{\partial\eta^3} = \frac{1}{8}\cdot\frac{\partial^3 f}{\partial\eta_p^3} = \frac{1}{8}f'''.
\end{aligned}\right\} \tag{VII.74}$$

Substituting values of (VII.74) in equation (VII.70), we find

$$f''_{1,2} + f_{1,2}f''_{1,2} = 0.$$
<div align="right">(VII.75)</div>

Here $f = f_1$ for gas, and $f = f_2$ for a liquid.

When calculating the parameters of the liquid layer, the transverse coordinate is reckoned from the liquid-gas interface.

The boundary conditions (VII.71) assume the form

$$f_1(0) = -f_0 = -\frac{2v_0}{U_0}\left(\frac{U_0 x}{v_1}\right)^{1/2}; \quad f'_1(0) = 0;$$
$$f_1(\eta_b) - f_2(0) = 0; \quad f'_1(\eta_b) = f'_2(0);$$
$$f''_1(\eta_b) = Rf''_2(0); \quad f'_2 \to 2 \text{ for } \eta_2 \to \infty.$$
<div align="right">(VII.76)</div>

The velocity components in the gas film will be defined by the formulas

$$u = \frac{\partial \psi}{\partial y} = \frac{1}{2}U_0 f'(\eta_p),$$
$$v = -\frac{\partial \psi}{\partial x} = -\frac{1}{2}\sqrt{\frac{v_1 U_0}{x}}\left|f(\eta_{p_1}) - \eta_{p_1}f'(\eta_{p_1})\right|.$$
<div align="right">(VII.77)</div>

The solution of equation (VII.75) for a gas film also will be found in the form of the series

$$f_1(\eta_{p_1}) = f_1(0) + f'_1(0)\eta_{p_1} + \frac{f''_1(0)}{2!}\eta_{p_1}^2 + \frac{f'''_1(0)}{3!}\eta_{p_1}^3 + \cdots$$
<div align="right">(VII.78)</div>

The derivatives entering into this equation are defined by the same procedure as (VII.65), and they are equal to:

$$f_1(0) = -f_0; \quad f'_1(0) = 0; \quad f'''_1(0) = f_0 f''_1(0);$$
$$f_1^{IV}(0) = f_0^2 f''_1(0); \quad f_1^{V}(0) = -f''_1(0)[f''_1(0) - f_0^3];$$
$$f_1^{VI}(0) = f''_1(0)[16 f_0^2 f''_1(0) - f_0^5]$$
<div align="right">(VII.79)</div>

. . . .

$$f''_1(0) = \frac{f_0}{\frac{1}{2}\eta_{p\delta}^2 + \sum_{k=3}\frac{f_1^{\kappa}(0)\eta_{p\delta}^{\kappa}}{f''_1(0)\kappa!}};$$
<div align="right">(VII.80)</div>

$$f'_2(0) = f''_1(0)\left[\eta_{p\delta} + \sum_{k=3}\frac{f_1^{\kappa}(0)\eta_{p\delta}^{\kappa-1}}{f''_1(0)(\kappa-1)!}\right];$$
<div align="right">(VII.81)</div>

$$f''_1(0) = \frac{Rf''_2(0)}{1 + \sum_{\kappa=3}\frac{f_1^{\kappa}(0)\eta_{p\delta}^{\kappa-2}}{f''_1(0)(k-1)!}}.$$
<div align="right">(VII.82)</div>

As we have already pointed out, equations (VII.79)-(VII.82) permit all the two-phase laminar boundary characteristics to be found if the values of $f'_2(0)$ and $f''_2(0)$ found from solving the problem of a liquid boundary layer are known.

<div align="center">339</div>

This problem was solved by Sass and Sparrow [5], who obtained the solution to equation (VII.75) for $f=f_2$

$$f_2'' + f_2 f_2''' = 0 \qquad\qquad \text{(VII.83)}$$

under the following boundary conditions:

$$f_2(0) = 0; \quad f_2'(0) = A_0; \quad f_2' \to 2 \text{ for } \eta_{p_\delta} \to \infty,$$

where A_0 is a constant.

The table of values of $f_2'(0)$ and $f_2''(0)$ corresponding to the solution of equation (VII.83) is presented in reference [5]. Other parameters are determined by the method of successive approximations, the method indicated above.

The local friction is determined by the Newton formula

$$\tau_0 = \mu_1 \left(\frac{\partial u}{\partial y} \right)_{y=0} = \frac{1}{4} \mu_1 U_0 \left(\frac{U_0}{\nu_1 x} \right)^{1/2} f_1''(0). \qquad\qquad \text{(VII.84)}$$

From formula (VII.84) it follows that the local friction of a plate is proportional to $f_1''(0)$.

Let us compare expression (VII.84) for local friction with the analogous expression for the case where gas injection is not used. For this purpose let us represent expression (VII.84) in the form

$$\tau_0 = \frac{\mu_2 U_0}{4} \left(\frac{U_0}{\nu_2 x} \right)^{1/2} \left(\frac{\rho_1 \mu_1}{\rho_2 \mu_2} \right)^{1/2} f_1''(0). \qquad\qquad \text{(VII.85)}$$

The Blasius formula for plate friction with homogeneous liquid has the form

$$\tau_{00} = 1.328 \frac{\mu_2 U_0}{4} \left(\frac{U_0}{\nu_2 x} \right)^{1/2}. \qquad\qquad \text{(VII.86)}$$

The ratio of the local friction with blowing τ_0 to the value of τ_{00} in the absence of blowing is

$$\frac{\tau_0}{\tau_{00}} = \frac{\zeta_f}{\zeta_{f_0}} = \frac{f_1''(0) \cdot}{1.328} \left[\frac{\rho_1 \mu_1}{\rho_2 \mu_2} \right]^{1/2} = \frac{f_1''(0)}{1.328 R}. \qquad\qquad \text{(VII.87)}$$

Here ζ_f and ζ_{f_0} are the local friction coefficients.

The numerical values of $f_1''(0)$ as a function of the parameters f_0 and R and also the values of η_{p_δ} and $\tau_0/\tau_{00} = \zeta_f/\zeta_{f_0}$ are presented in Table VII.1.

The following curves are presented in Figure VII.3

$$\frac{\zeta_f}{\zeta_{f_0}} = \frac{\tau_0}{\tau_{00}} = F \left(\frac{2 v_{0L}}{U_0} \sqrt{\frac{U_0 L}{\nu_1}}; \quad \left[\frac{\rho_2 \mu_2}{\rho_1 \mu_1} \right]^{1/2} \right),$$

or

$$\frac{\zeta_f(x)}{\zeta_{f_0}(x)} = F\left(\frac{2v_{0_1}}{U_0}\sqrt{\frac{U_0 x}{v_1}};\ \left[\frac{\rho_1 \mu_1}{\rho_2 \mu_2}\right]^{1/2}\right),$$

characterizing the frictional drag reduction of a plate for a two-phase laminar boundary layer. It is obvious that the presence of a gas interlayer in a two-phase boundary layer leads to a sharp reduction in frictional drag of the plate.

It must be remembered that these results pertain to the case where the ventilation velocity is proportional to $x^{-1/2}$.
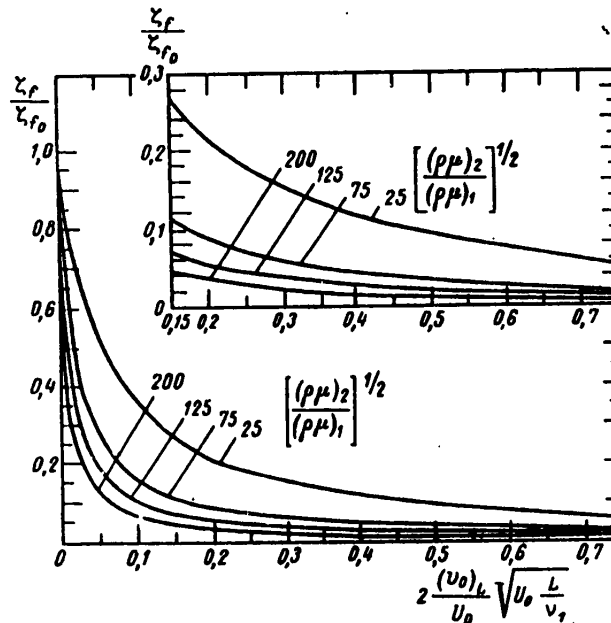
Figure VII.3. Frictional drag reduction of a plate for a two-phase laminar boundary layer

For approximate use of the results obtained in the case where the distribution of the ventilation parameters is given by a different law, it is possible to introduce the concept of reduced flow rate

$$J_0 = \left(\frac{U_0 l}{v_1}\right)^{1/2} \frac{1}{U_0 l} \int_0^l v_0(x)\, dx, \tag{VII.88}$$

where l is the length of the investigated section;

$v_0(x)$ is the ventilation velocity distribution law with respect to length l.

341

Table VII.1. Characteristics of a Two-Phase Laminar Boundary Layer

I_o	$f_1''(0)$	$\eta_{p\delta}$	$f_1'(\eta_{p\delta})$	$\dfrac{\tau_f}{\tau_{f_o}}$	$f_1''(0)$	$\eta_{p\delta}$	$f_1'(\eta_{p\delta})$	$\dfrac{\tau_f}{\tau_{f_o}}$
	$R=200$				$R=125$			
0,01	108,62	0,01357	1,474	0,4090	86,11	0,01515	1,312	0,5187
0,025	59,44	0,02900	1,724	0,2238	51,81	0,03114	1,600	0,3121
0,05	33,95	0,05425	1,844	0,1278	31,29	0,05653	1,769	0,1885
0,10	18,27	0,1044	1,918	0,06879	17,39	0,1070	1,872	0,1048
0,15	12,41	0,1550	1,944	0,04672	12,01	0,1574	1,913	0,07235
0,20	9,32	0,2058	1,957	0,03509	9,09	0,2084	1,932	0,05476
0,25	7,47	0,2562	1,966	0,02813	7,32	0,259	1,945	0,04407
0,35	5,21	0,360	1,973	0,01960	5,13	0,362	1,963	0,03090
0,50	3,41	0,520	1,983	0,01284	3,37	0,523	1,973	0,02030
0,75	1,88	0,813	1,984	0,00708	1,87	0,815	1,980	0,01127
	$R=75$				$R=25$			
0,01	62,90	0,01783	1,122	0,6315	27,38	0,02704	0,740	0,8247
0,025	42,20	0,03442	1,453	0,4237	22,24	0,04615	1,055	0,6633
0,05	27,46	0,06035	1,657	0,2757	17,22	0,07622	1,312	0,5187
0 10	16,09	0,1113	1,800	0,1615	11,81	0,1299	1,543	0,3557
0,15	11,33	0,1624	1,856	0,1138	8,94	0,1825	1,651	0,2693
0,20	8,69	0,2131	1,890	0,08727	7,23	0,2335	1,724	0,2178
0,25	7,07	0,2632	1,914	0,07098	6,02	0,285	1,769	0,1813
0,35	5,00	0,3667	1,938	0,0502	4,41	0,390	1,824	0,1328
0,50	3,31	0,527	1,957	0,03323	3,00	0,553	1,867	0,09036
0,75	1,84	0,820	1,967	0,01847	1,71	0,847	1,910	0,05151

The velocity distribution in a gas boundary layer can be obtained by formula (VII.77) considering expression (VII.78). We have

$$\frac{u}{U_0} = \frac{1}{2} f_1'(\eta_{p_1}) = \frac{1}{2}\left[f_1'(0) + f_1''(0)\,\eta_{p_1} + f_1'''(0)\,\frac{\eta_{p_1}^2}{2} + \dots \right]. \qquad \text{(VII.89)}$$

If we consider that f'₁(0)=0, then from (VII.89) we find

$$\frac{u}{U_0} = \frac{1}{2} f_1''(0)\left[\eta_{p_1} + \sum_{k=3}\frac{f_1^k(0)\,\eta_{p_1}^{\kappa-1}}{f_1''(0)\,(\kappa-1)!} \right]. \qquad \text{(VII.89a)}$$

The velocity at the boundary of two phases is calculated by the formula

$$\frac{u(\eta_{p\delta})}{U_0} = \frac{1}{2} f_1'(\eta_{p\delta}). \qquad \text{(VII.90)}$$

§VII.3. Calculation of a Two-Phase Laminar Boundary Layer for an Exponential Velocity Distribution Law at the Outer Boundary

The results of numerical solution obtained in §VII.2 of the basic two-phase laminar boundary layer equation using the BESM-2M computer [7] are presented. These results made it possible to investigate the effect of the presence of a gas layer on the velocity profiles in a two-phase laminar boundary layer and on the frictional drag of the body along which flow is taking place. In addition, numerical calculations offer the possibility of analyzing the nature of separation of the two-phase laminar boundary layer.

Basic Formulas. The equations of motion of a laminar boundary layer have the form (VII.42) and (VII.43). The boundary conditions of the problem are described by the expressions (VII.45)-(VII.49).

For numerical calculations on a digital computer it is more convenient to introduce the following values instead of $\phi(\eta)$ and the variable η by formulas (VII.51) and (VII.51a):

$$\psi = \sqrt{v_{1,2} c x^{m+1} \frac{2}{m+1}} \, \Phi(\xi);$$
(VII.91)

$$\xi = y \sqrt{\frac{m+1}{2} \cdot \frac{c x^{m-1}}{v_{1,2}}}.$$
(VII.92)

Under the given boundary conditions and with the adopted notation of (VII.91) and (VII.92), equations (VII.42) and (VII.43) can be transformed to the following known equation from [2] analogous to that presented in §VII.2

$$\Phi''' + \Phi\Phi'' = \beta(\Phi'^2 - 1),$$
(VII.93)

where the derivative sign denotes differentiation with respect to the variable ξ.

The parameter β is related to the parameter m by the following expression

$$\beta = \frac{2m}{m+1}.$$
(VII.94)

The velocities in the boundary layer are calculated by the formulas

$$\left. \begin{array}{l} u = c x^m \Phi'; \\[2ex] v = -\sqrt{\dfrac{2v_{1,2} c}{m+1}} \, x^{\frac{m-1}{2}} \left(\dfrac{m-1}{2} \xi \Phi' + \dfrac{m+1}{2} \Phi \right). \end{array} \right\}$$
(VII.95)

The boundary conditions for equation (VII.93) are written in following form.

On a solid wall (for $\xi=0$)

$$\left. \begin{array}{l} \Phi'_1(0) = 0; \\[2ex] v(0) = v_0 = -\sqrt{2v_1 c(m+1)} \, x^{\frac{m-1}{2}} \Phi_1(0) \end{array} \right\}$$
(VII.96)

343

or

$$\Phi_1(0) = -\frac{v_0 x^{\frac{1-m}{2}}}{\sqrt{2v_1 c(m+1)}}.$$ (VII.97)

In order to obtain similar solutions to equation (VII.93) it is necessary that $\Phi_1(0)$ not depend on x. For this purpose it is necessary to set

$$v_0 = kx^{\frac{m-1}{2}}.$$ (VII.98)

Self-similar solutions have physical meaning only for $m \leqslant 1$; k is a value which does not depend on x.

Substituting (VII.98) in (VII.97), we find

$$\Phi_1(0) = -\Phi_0,$$ (VII.99)

where

$$\Phi_0 = \frac{k}{\sqrt{2v_1 c(m+1)}}.$$ (VII.100)

At the liquid-gas region interface the condition is equivalent to the conditions (VII.57), (VII.58) (see §VII.2)

$$\Phi_1(\xi_\delta) = 0;$$ (VII.101)

$$\Phi_2(\xi_\delta) = 0,$$ (VII.102)

where ξ_δ is the dimensionless thickness of the gas film.

When calculating the liquid layer parameters, the transverse coordinate is reckoned from the liquid-gas interface. In this case condition (VII.102) assumes the form

$$\Phi_2(\xi_\delta) = \Phi_2(0) = 0.$$ (VII.102a)

The other two boundary conditions (VII.59) and (VII.61) are described as follows:

$$\Phi_1'(\xi_\delta) = \Phi_2'(0);$$ (VII.103)

$$\Phi_1''(\xi_\delta) = R\Phi_2''(0),$$ (VII.104)

where

$$R = \left[\frac{\rho_2 \mu_2}{\rho_1 \mu_1}\right]^{1/2}.$$ (VII.105)

The condition at infinity $\Phi' \to 1$ for $\xi \to \infty$.

Method of Solving the Equations. Equation (VII.93) was solved in advance for a fluid boundary layer. In this case we have the following boundary conditions:

$$\Phi_2(0) = 0; \quad \Phi_2'(0) = A_0;$$ (VII.106)

$$\Phi_2' \to 1 \text{ for } \xi_2 \to \infty.$$ (VII.107)

The calculation was performed for values of $A_0 = 0$ to 1.0 with a 0.1 interval and for values of the parameter $\beta = 1.0$ to 0.50.

The boundary conditions (VII.107) do not permit numerical calculations to be performed. Therefore the equation was solved for the following boundary condition:

$$\Phi_2' = 1 \text{ for } \xi_2 \to B.$$ (VII.107a)

The value of B must be selected quite large.

In the given case the basic calculations were performed for a value of B=12. The control calculations were performed for B=24, 36 and 6. A comparison of the calculation results for various B and also with the results of calculations performed for some special cases by other authors [2], [5] shows that the value of $\Phi'_2(\xi)$ for B=12 in practice coincides with the exact solution (with accuracy to four significant figures).

For $\beta < 0$ the solution of equations (VII.93) under the boundary conditions (VII.106) and (VII.107) can be ambiguous (see [2]). Therefore after solving the equation, the equation was solved again under the following boundary conditions:

$$\Phi_2(0) = 0; \quad \Phi_2'(0) = A_0; \quad \Phi_2''(0) = [\Phi_2''(0)] + 0.001,$$ (VII.108)

where $[\Phi''_2(0)]$ is the value of the second derivative.

In order to find the solution of equation (VII.93) under boundary conditions (VII.106) and (VII.107), we assume that the solution of this equation is a continuous function of $\Phi''_2(0)$. Here we also determine the value of $\Phi''_2(0)$ such that for $\xi_2 = B$ it was the root of the equation

$$\Phi_2' [B, \Phi_2''(0)] - 1 = 0.$$ (VII.109)

Equation (VII.109) is transcendental, and in order to find its root $\Phi''_2(0)$ let us use the Newton method, according to which $\Phi''_2(0)$ must be determined by the formula

$$_{n+1}\Phi_2''(0) = {}_n\Phi_2''(0) - \frac{\Phi_2'[B, {}_n\Phi_2''(0)] - 1}{{}_n f_2'(B)},$$ (VII.110)

where $\Phi'_2[B_n, \Phi''_2(0)]$ is the solution to equation (VII.93) for $\xi_2 = B$ with the initial conditions (VII.106) and (VII.107a) and $\Phi''_2(0) = {}_n\Phi''_2(0)$, and $f'_2(B)$ is the solution

$$f_2'' + \Phi f_2'' + \Phi'' f_2 - 2\beta \Phi' f_2'$$ (VII.111)

$$f_2 = \frac{\partial \Phi}{\partial \Phi_2''(0)}$$

345

with the boundary conditions

$$f_2 - f_2'(0) = 0; \quad f_2'' = 1 \text{ for } \xi_2 = 0. \tag{VII.112}$$

Equation (VII.111) and the boundary conditions (VII.112) are obtained by differentiation of the equation (VII.93) and the boundary conditions with respect to the parameter $\Phi''_2(0)$.

Let us note that the practical application of the given method when solving non-linear differential equations with similar boundary conditions gives good results and is easily realized on a computer.

The process of successive approximations quickly converges even in the case where the initial value of $\Phi''_2(0)$ is selected unsuccessfully. In all of the investigated cases it turned out to be sufficient to perform three to four iterations to satisfy the boundary conditions with high precision.

For the boundary layer of a gas, equation (VII.93) must satisfy the following boundary conditions:

for

$$\xi_1 = 0; \quad \Phi_1 = -\Phi_0; \quad \Phi_1' = 0; \tag{VII.113}$$

for

$$\xi_1 = \xi_\delta; \quad \Phi_1 = 0; \quad \Phi_1'' = F(\Phi_1'), \tag{VII.114}$$

where ξ_δ is the dimensionless thickness of the gas interlayer.

Under the boundary condition (VII.114) the function F will be determined from the relations given by equations (VII.103) and (VII.104) and the dependence of $\Phi''_2(0)$ on $\Phi'_2(0)$ for different β obtained from solutions of equation (VII.93) for the boundary conditions (VII.106) and (VII.107a). The function $\Phi''_1=F(\Phi'_1)$ for different values of the parameter β is given in table form.

For numerical solution of equation (VII.93) under boundary conditions (VII.113) and (VII.114) let us represent the relation in the form of a piecewise continuous function having breaks at the node points of the table, that is,

$$\Phi_1'' = a_i\Phi_1' + b_i, \tag{VII.115}$$

where a_i and b_i are determined by the formulas

$$a_i = \frac{_{i+1}\Phi_1'' - _i\Phi_1''}{_{i+1}\Phi_1' - _i\Phi_1'}; \tag{VII.116}$$

$$b_i = \frac{_i\Phi_1''_{i+1}\Phi_1' - _{i+1}\Phi_1''_i\Phi_1'}{_{i+1}\Phi_1' - _i\Phi_i'}, \tag{VII.117}$$

346

where $_i\Phi''_1$ and $_i\Phi'_1$ are the values of the i row of the table defining the functions $\Phi''_1 = F[\Phi'_1(\xi_\delta)]$.

Just as in the preceding case, let us assume that the solution of this equation is a continuous function of the value of $\Phi''_1(0)$, and let us take this value so that for $\xi_1 = \xi_\delta$ determined from the condition (VII.107a) $\Phi_1(\xi_\delta) = 0$, equation (VII.115) will be satisfied.

Applying Newton's method, we obtain

$$_{n+1}\Phi''_1(0) = {}_n\Phi''_1(0) - \frac{\Phi'_1(\xi_\delta) - a_i\Phi'_1(\xi_\delta) - b_i}{f'_1(\xi_\delta) - a_i f'_1(\xi_\delta)}, \qquad \text{(VII.118)}$$

where $_{i+1}\Phi''_1$, $_i\Phi''_1$, $_{i+1}\Phi'_1$ and $_i\Phi'_1$ are taken such that the following condition will be satisfied

$$_i\Phi'_1 < \Phi'_1(\xi_\delta) < {}_{i+1}\Phi'_1, \qquad \text{(VII.119)}$$

and $f''_1(\xi_\delta)$ and $f'_1(\xi_\delta)$ will be defined as a result of solving equation (VII.111) with the boundary conditions (VII.112).

When performing practical calculations by the given method it is necessary that the function F be given in a quite broad range of variation of the value of Φ'_1, and for a value of $\Phi''_1(0)$ selected in the first approximation, the condition (VII.119) will be satisfied.

In the case where the function $F(\Phi'_1)$ is monotonic, the given process of successive approximations is converging. In order to obtain a solution, 3-4 iterations are sufficient.

In the case where the function $F(\Phi'_1)$ is not monotonic, in the case of unsuccessful selection of the first approximation it can turn out that convergence will not occur.

In this case the solution of equation (VII.93) can be obtained as follows. Equation (VII.93) permits reduction by an order. Taking Φ as the independent variable and denoting $\Omega = \Phi'$, we obtain

$$\Phi'' = \frac{d\Omega}{d\Phi} \cdot \frac{d\Phi}{d\xi} = \Omega'\Omega;$$

$$\Phi''' = (\Omega'\Omega + \Omega'^2)\Omega.$$

The stroke in the righthand side of these equalities denote the derivative with respect to Φ.

Equation (VII.93) is rewritten as follows:

$$\Omega'' + \frac{\Omega'^2}{\Omega} + \Phi\frac{\Omega'}{\Omega} = \beta\left(1 - \frac{1}{\Omega^2}\right). \qquad \text{(VII.119a)}$$

Standard boundary conditions for the given equation for $\Phi = 0$; $\Omega = a$; $\Omega' = b$.

347

Under these boundary conditions the equation can be solved numerically by any approximate method (for example, the Runge-Kutta method).

The condition $\Phi=0$ is satisfied on the outer boundary of the boundary layer (condition VII.10). If we take values of a and b satisfying the relations $\Phi''=F(\Phi')$ which is easily expressed in terms of the introduced variables and functions, the solution to the equation found will correspond to a set of boundary conditions at the outer boundary of the boundary layer (VII.114).

The inner boundary will be determined from the condition (VII.113) $\Phi'=\Omega=0$, and the value of Φ_0 is not given in advance, but is found as the value of the independent variable in equation (VI.119a) for $\Omega=0$.

This solution technique is effective, but it required analysis of the solution obtained at points where $\Omega=0$, for velocity profiles are possible for which several points have $\Omega=\Phi'=0$.

Results of Numerical Solution of the Equations. For the boundary conditions (VII.106) and (VII.107a) equation (VII.93) was solved for values of $A_0=0$, 0.1, 0.2, 0.3, 0.4, 0.5, 0.6. 0.7, 0.8, 0.9, 0.95 and for values of the parameter $\beta=1$, 0.5, 0, -0.1, -0.2, -0.3, -0.45.

For the value of $\beta=0$ and also for certain selected values of β and A_0, the results of such calculations appear in [8]. The obtained results agree with these data.

The results of solving the equation are presented in Figure VII.4 in the form of the functions $u/U=\Phi'(\xi)$ for different β. These graphs characterize the velocity profiles for a body during flow of a viscous fluid over it under the condition that at the body wall $u=u_1$. Graphs were constructed for $u_1/U=0.1$ to 0.95

In Figure VII.5, curves are presented for the function $\Phi''_2(0)=F[\Phi'_2(0)]$, which were obtained as a result of solving equation (VII.93) with boundary conditions (VII.106) and (VII.107a). This function is used when compiling the boundary condition (VII.114).

Analysis of the data presented in Figure VII.4 indicates that with an increase in the value of $\Phi'(0)$ which is proportional to $u(0)=u_1$, the range of β expands where attached flow is possible. The maximum value of $\beta=-0.5$; then attached flow is possible only for $u(0)=U$; $u_1/U=1$.

The results of solving equation (VII.93) for a gas boundary layer are presented in Table VII.2 where values are given for $\Phi''_1(0)$, ξ_δ, $\Phi''(\xi_\delta)$ as a function of ϕ_0 for different values of β. In this case all the calculations are performed for a value of the parameter $R=[\rho_2\mu_2/\rho_1\mu_1]^{1/2}=200$. This value of the parameter corresponds to the case of injection of air into the boundary layer formed by the water, which is of practical importance.

In Figure VII.6, the relation is presented for the ratio of the frictional drag in the investigated case of a two-phase laminar boundary layer to the frictional drag in a homogeneous liquid as a function of the ventilation parameter ϕ_0 for values of $\beta=1$, 0.5, 0, -0.1. Investigation of this figure shows that injection of gas leads to significant frictional drag reduction. This reduction is greater the larger the ventilation parameter ϕ_0 and the value of β.

Table VII.2   Internal Boundary Layer Characteristics

Φ_0	$\beta = 1$			$\beta = 0.5$			$\beta = 0$			$\beta = -0.1$		
	$\Phi_1''(0)$	ξ_0	$\Phi''(\xi_0)$	$\Phi_1''(0)$	ξ_0	$\Phi''(\xi_0)$	$\Phi_1''(0)$	ξ_0	$\Phi''(\xi_0)$	$\Phi_1''(0)$	ξ_0	$\Phi''(\xi_0)$
0.005				41,386	0,0182	41,381	38,875	0,01885	38,879	33,038	0,0218	33,043
0.00707	13,042	0,0182	43,030	14,704	0,0481	14,688	21,020	0,0421	21,029	19,270	0,0436	19,283
0,0175	21,207	0,0421	27,186	10,114	0,0830	10,103	11,555	0,0786	11,576	10,895	0,0805	10,921
0,0350	12,651	0,0745	12,620	6,102	0,1590	6,091	6,449	0,1475	6,4945	6,0814	0,1525	6,1361
0,0707	6,649	0,1438	6,594	3,427	0,2875	3,4218	3,294	0,2915	3,3852	3,2248	0,2985	3,3357
0,141	3,540	0,2858	3,445	1,943	0,5162	1,9324	1,839	0,5085	1,9896	1,7880	0,5140	1,9838
0,247	2,106	0,4920	1,9401	0,9228	1,0750	0,9077	0,6612	1,151	1,0013	0,5852	1,188	1,0051
0,53	1,1605	1,016	0,8677									

	$\beta = -0.2$			$\beta = -0.3$			$\beta = -0.4$			$\beta = -0.45$		
$\Phi_1''(0)$	ξ_0	$\Phi''(\xi_0)$	$\Phi_1''(0)$	ξ_0	$\Phi''(\xi_0)$	$\Phi_1''(0)$	ξ_0	$\Phi''(\xi_0)$	$\Phi_1''(0)$	ξ_0	$\Phi''(\xi_0)$
			20,764	0,02195	20,7712						
28,642	0,02260	28,619	21,360	0,0259	21,369						
17,224	0,04530	17,241	15,174	0,0481	15,194						
10,564	0,0818	10,696	10,121	0,0839	10,159						
5,7257	0,1605	5,7911	5,855	0,1558	5,932	4,8441	0,1725	4,9359			
3,410	0,3012	3,451	2,983	0,3045	3,1353	2,8629	0,3085	3,0386			
1,315	0,575	1,348	1,696	0,5220	1,9631	1,6191	0,5295	1,9251			
0,4215	1,223	0,8621	0,4354	1,255	1,0415	0,3310	1,318	1,0520	0,1937	1,459	1,0188

349
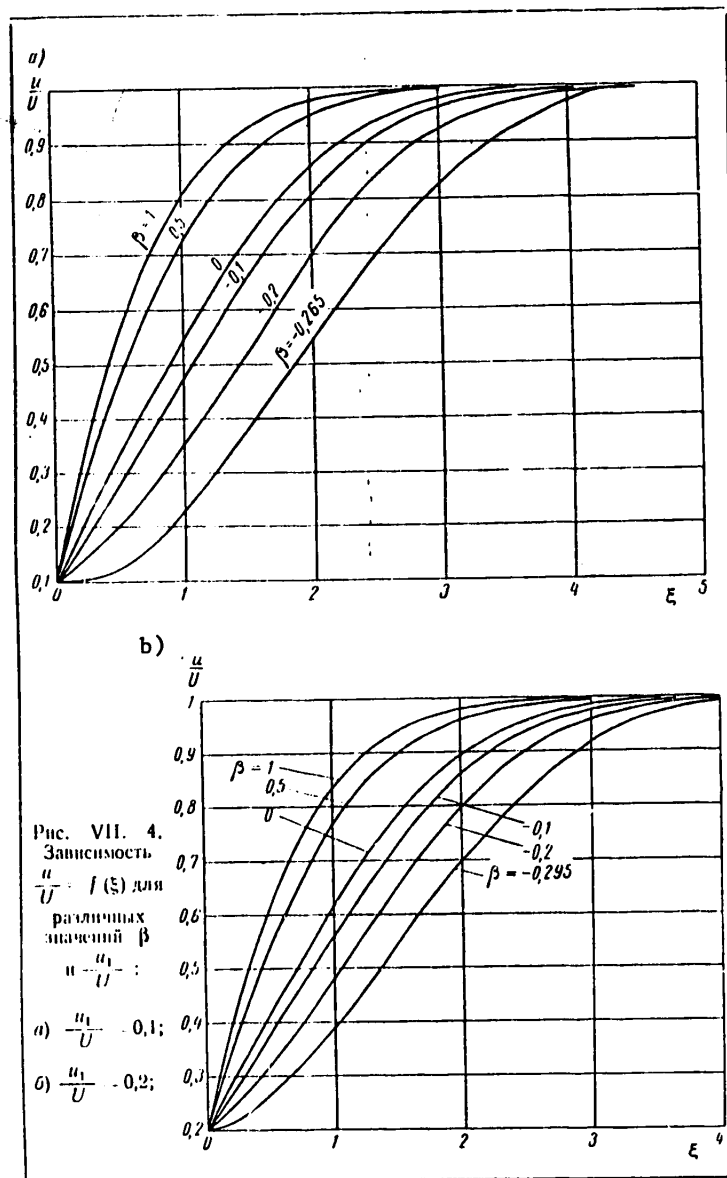
Figure VII.4. The function u/U=f(ξ) for different values of β
and u₁/U;
a) u₁/U=0.1; b) u₁/U=0.2
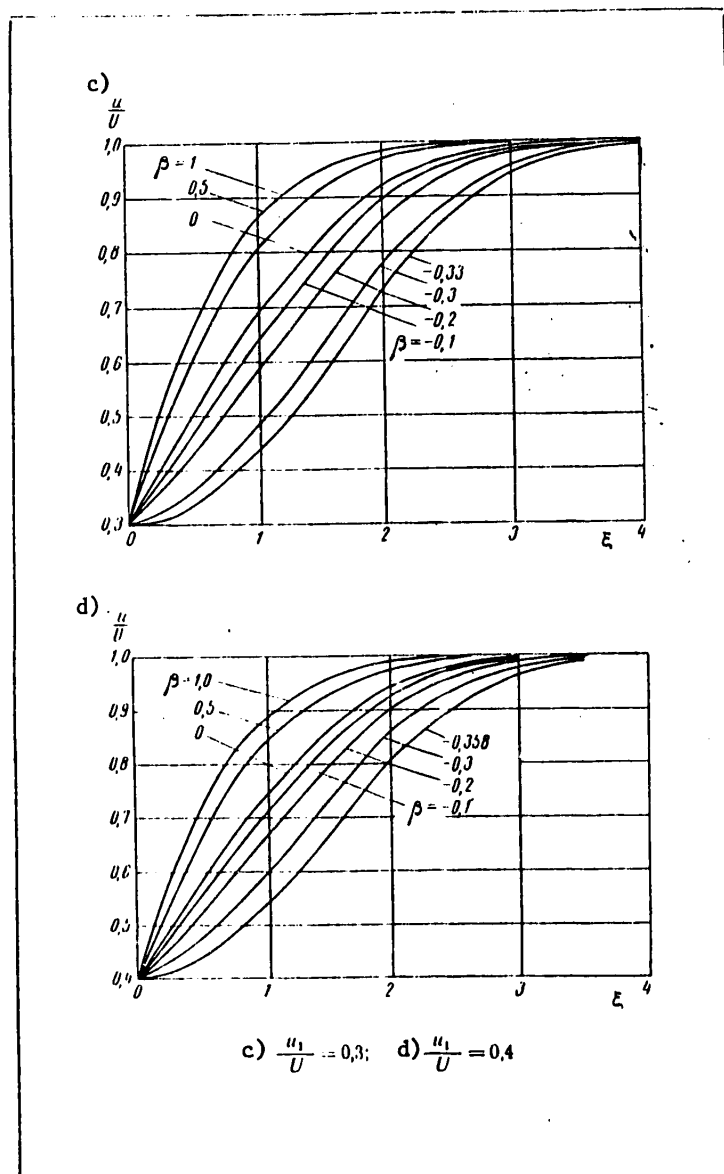
$$c) \; \frac{u_1}{U} = 0,3; \quad d) \frac{u_1}{U} = 0,4$$

Figure VII.4 (continued)

351
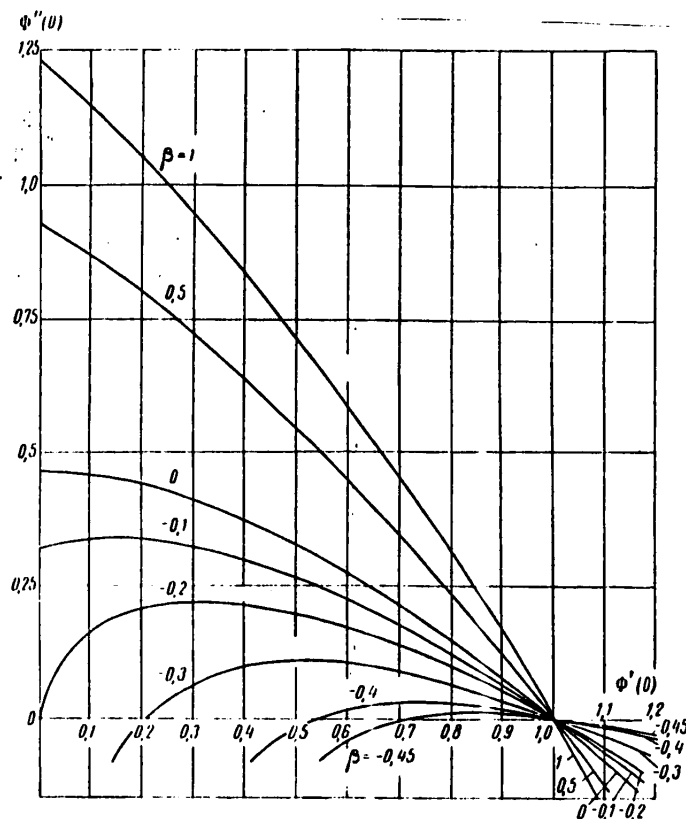
Figure VII.4 (continued)
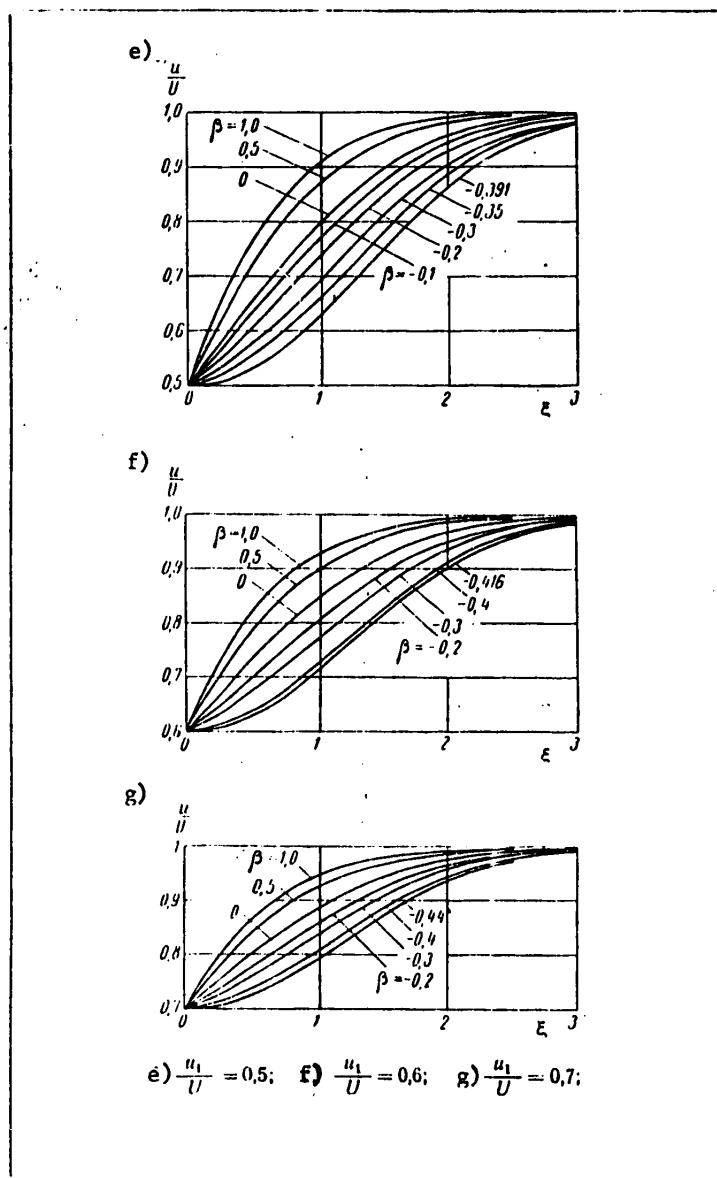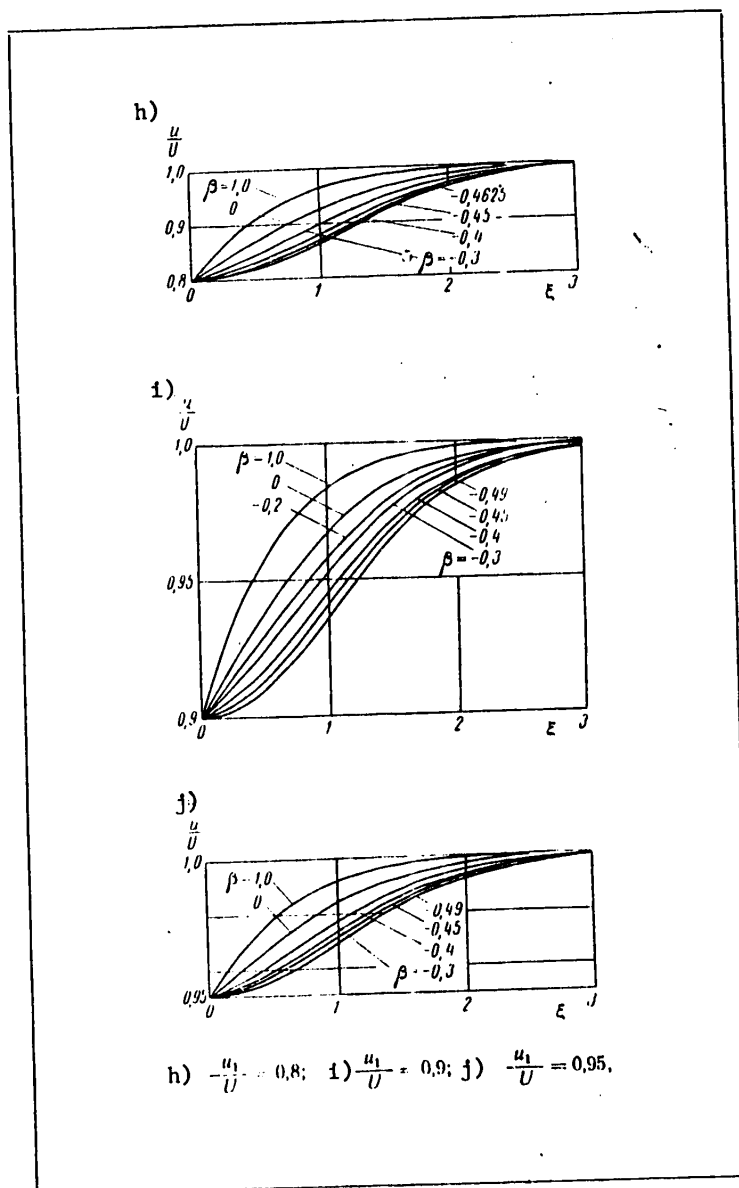
Figure VII.4 (continued)

353

Figure VII.5. $\Phi''(0)$ as a function of $\Phi'(0)$ for different values
of β

For values of $\beta < -0.1988$ in a single phase boundary layer separation takes place. On injecting gas in a formed two-phase boundary layer for each value of β from the range of $-0.1988 > \beta > -0.5$ the possible velocity profiles are presented in Figure VII.7 as a function of the value of the parameter Φ_0.

The velocity profile for relatively small values of the ventilation parameter is presented in Figure VII.7, b. This velocity profile, just as the initial one for $\Phi_0=0$, has a range of variation of the ξ-axis where the value of $\Phi''(\xi) \leqslant 0$. With a further increase in $\Phi(0)$ the velocity profile assumes the form presented in Figure VII.7, c. This velocity profile is attached and exists in some range of values of Φ_0. With further increase in the parameter Φ_0, a profile is formed as presented in Figure VII.7, d.

Let us note that the velocity profiles presented in Figure VII.7, a and b with return current were obtained on the basis of the boundary layer equations which are not applicable in the separation region.

At the same time, the profile presented in Figure VII.7, c is attached, and the boundary layer equations are applicable to it.

354
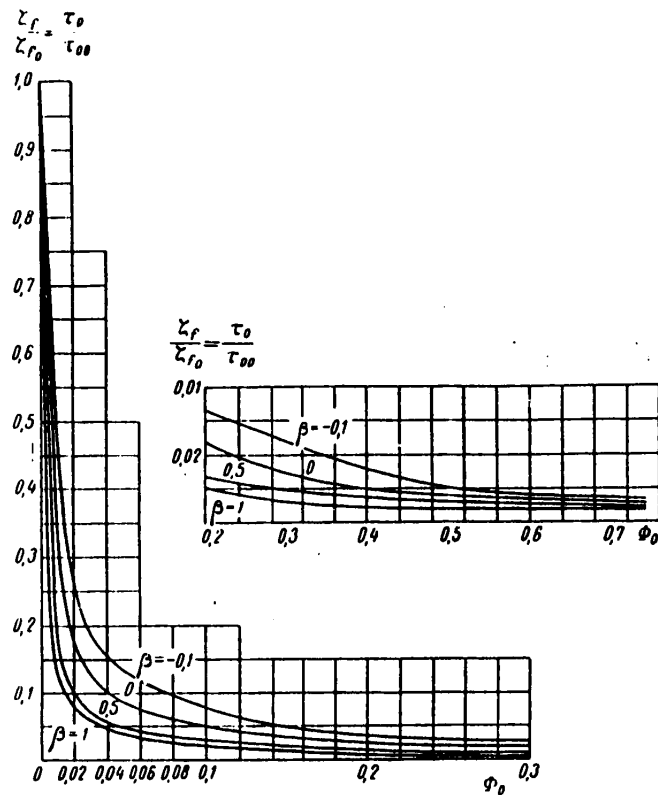
Figure VII.6. Effect of gas injection on frictional drag reduction
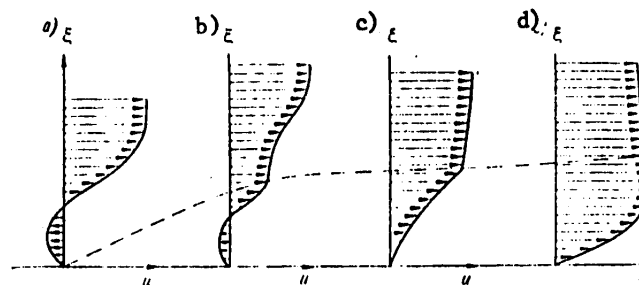
Figure VII.7. Velocity profiles for $\beta < 0.198$ for different values of Φ_0; a) $\Phi_0 = 0$; b) $\Phi_0 > 0$, but small; c) and d) attached profiles

355

§VII.4. Integral Expressions for a Two-Phase Boundary Layer

Let us consider a two-phase boundary layer consisting of a wall gas layer with density ρ_1 and an outer layer of liquid with density ρ_2 (see Figure VII.2). The Prandtl equation for a two-phase boundary layer can be written in the following form:

$$\frac{\partial (u^2)}{\partial x} + \frac{\partial (uv)}{\partial y} = U \frac{dU}{dx} + \frac{1}{\rho_{1,2}} \frac{\partial \tau}{\partial y}. \tag{VII.120}$$

Hereafter, just as earlier, the index "1" will denote values pertaining to a gas, and the index "2" the same values for a liquid.

From the continuity equation (VII.43) it is possible to write the following identity

$$\frac{\partial (Uu)}{\partial x} + \frac{\partial (Uv)}{\partial y} = u \frac{dU}{dx}. \tag{VII.121}$$

Subtracting equation (VII.120) from equation (VII.121), we obtain

$$\frac{\partial}{\partial x} [u(U-u)] + \frac{\partial}{\partial y} [v(U-u)] + \tag{VII.122}$$

$$+ \frac{dU}{dx}(U-u) = -\frac{1}{\rho_{1,2}} \frac{\partial \tau}{\partial y}.$$

Let us find the integral relation for the boundary layer as a whole. For this purpose let us integrate equation (VII.122) from 0 to the thickness of a two-phase boundary layer $\delta = \delta_1 + \delta_2$, assuming that for $y=0$, $u=u_0$ and $v=v_0$.

As a result, we obtain

$$\frac{d}{dx} \int_0^\delta [u(U-u)] dy - v_0(U-u_0) + \int_0^\delta (U-u) \frac{dU}{dx} dy$$

$$= -\frac{1}{\rho_1} \int_0^{\delta_1} \frac{\partial \tau}{\partial y} dy - \frac{1}{\rho_2} \int_{\delta_1}^\delta \frac{\partial \tau}{\partial y} dy. \tag{VII.123}$$

Equation (VII.123) can be transformed if we consider the known notation

$$\delta^* = \int_0^\delta \left(1 - \frac{u}{U}\right) dy; \quad \delta^{**} = \int_0^\delta \frac{u}{U}\left(1 - \frac{u}{U}\right) dy, \tag{VII.124}$$

and consider that

$$\int_0^{\delta_1} \frac{\partial \tau}{\partial y} dy = \tau_1 - \tau_0; \quad \int_{\delta_1}^\delta \frac{\partial \tau}{\partial y} dy = 0 - \tau_1 = -\tau_1. \tag{VII.125}$$

Substituting (VII.124) and (VII.125) in (VII.123), we obtain the integral relation of the pulses for a two-phase boundary layer as a whole

$$\frac{d}{dx}(U^2 \delta^{**}) + U \frac{dU}{dx} \delta^* - v_0(U-u_0) = \frac{\tau_0}{\rho_1} - \tau_1 \left(\frac{1}{\rho_1} - \frac{1}{\rho_2}\right) \tag{VII.126}$$

356

The integral relation of the pulses for the outer boundary layer will be obtained as follows.

Let us assume that the normal to the interface of the gas layer and liquid layer makes a small angle of $d\delta_1/dx$. Therefore when compiling the integral relation of the pulses it is possible to neglect the value on the order of $(d\delta_1/dx)^2$, for in this case the error is within the limits of accuracy of the assumptions made when compiling the boundary layer equations.

Hereafter, when calculating the liquid layer parameters, the transverse coordinate is reckoned from the liquid-gas interface.

Integrating equation (VII.122) from 0 to δ_2, we obtain

$$\int_0^{\delta_2} \frac{\partial}{\partial x} [u(U-u)]\,dy + \int_0^{\delta_2} \frac{\partial}{\partial y} [v(U-u)]\,dy +$$

$$+ \frac{dU}{dx} \int_0^{\delta_2} (U-u)\,dy - \frac{1}{\rho_2} \int_0^{\delta_2} \frac{\partial \tau}{\partial y}\,dy. \qquad (VII.127)$$

After transformations, equation (VII.127) assumes the form

$$\frac{d}{dx}(U^2\delta_2^{**}) + U \frac{dU}{dx} \delta_2^* = \frac{\tau_1}{\rho_2}. \qquad (VII.128)$$

Here

$$\delta_2^* = \int_0^{\delta_2}\left(1-\frac{u}{U}\right)dy; \quad \delta_2^{**} = \int_0^{\delta_2}\frac{u}{U}\left(1-\frac{u}{U}\right)dy. \qquad (VII.129)$$

For an internal boundary layer (gas layer) the integral relation can be obtained in two forms.

It is convenient to use the first form of the integral relation in the case where the velocity distribution is given in the form u/U_1 (U_1 is the velocity at the boundary of the gas and liquid layers); the second form, when the velocity profile is given in the form u/U.

In order to obtain the first type of integral relation let us write the continuity equation (VII.121) in the form

$$\frac{\partial (U_1 u)}{\partial x} + \frac{\partial (U_1 v)}{\partial y} = u \frac{\partial U_1}{\partial x}. \qquad (VII.130)$$

Subtracting equation (VII.120) from equation (VII.130), we obtain

$$\frac{\partial}{\partial x}[u(U_1-u)] + \frac{\partial}{\partial y}[v(U_1-u)] + \qquad (VII.131$$

$$+ \frac{dU_1}{dx}(U_1-u) + \left(U\frac{dU}{dx} - U_1\frac{dU_1}{dx}\right) = -\frac{1}{\rho_1}\frac{\partial \tau}{\partial y}.$$

On the basis of the theorem of differentiation of an integral with respect to a parameter it is possible to obtain

$$\int_{\delta_0}^{\delta_1} \frac{\partial}{\partial x} \left[u(U_1 - u) \right] dy = \frac{d}{dx} \int_{\delta_0}^{\delta_1} u(U_1 - u) \, dy -$$

$$- u(U_1 - u) \Big|_{y=\delta_1} \frac{d\delta_1}{dx} + u(U_1 - u) \Big|_{y=\delta_0} \frac{d\delta_0}{dx}.$$

In our case when $y=\delta_1$ and $u(U_1-u)=0$, for $u=U_1$, in addition, $d\delta_0/dx=0(\delta_0=0)$.

Thus, we have

$$\int_0^{\delta_1} \frac{\partial}{\partial x} \left[u(U_1 - u) \right] dy = \frac{d}{dx} \int_0^{\delta_1} u(U_1 - u) \, dy. \qquad (VII.132)$$

Integrating (VII.131) from 0 to δ_1, we obtain the integral relation for the gas layer

$$\frac{d}{dx}(U_1^2 \Delta^{**}) + U_1 \frac{dU_1}{dx} \Delta^* - v_0(U_1 - u_0) +$$

$$+ \left(U \frac{dU}{dx} - U_1 \frac{dU_1}{dx} \right) \delta_1 = \frac{1}{\rho_1}(\tau_0 - \tau_1). \qquad (VII.133)$$

The following notation has been introduced here:

$$\Delta^* = \int_0^{\delta_1} \left(1 - \frac{u}{U_1} \right) dy; \qquad \Delta^{**} = \int_0^{\delta_1} \frac{u}{U_1} \left(1 - \frac{u}{U_1} \right) dy. \qquad (VII.134)$$

The term $\left(U \frac{dU}{dx} - U_1 \frac{dU_1}{dx} \right) \delta_1 \approx 0$, for the pressure across the boundary layer is

constant, and at the point x=0 where this condition is violated, it is assumed that $\delta_1=0$.

Thus, the integral relation (VII.134) is rewritten as follows:

$$\frac{d}{dx}(U_1^2 \Delta^{**}) + U_1 \frac{dU_1}{dx} \Delta^* - v_0(U_1 - u_0) = \frac{1}{\rho_1}(\tau_0 - \tau_1). \qquad (VII.135)$$

The second form of the integral relation where the velocity profile is given in the form of the ratio u/U will be obtained by subtracting (VII.128) from (VII.126)

$$\frac{d}{dx}(U^2 \delta_1^{**}) + U \frac{dU}{dx} \delta_1^* - v_0(U - u_0) = \frac{1}{\rho_1}(\tau_0 - \tau_1). \qquad (VII.136)$$

Here

$$\delta_1^* = \int_0^{\delta_1} \left(1 - \frac{u}{U} \right) dy; \qquad \delta_1^{**} = \int_0^{\delta_1} \frac{u}{U} \left(1 - \frac{u}{U} \right) dy.$$

From the four obtained integral pulse relations (VII.126), (VII.128), (VII.135) and (VII.136) only any two relations are independent.

Pulse Equation for a Two-Phase Boundary Layer of a Flat Plate. Let us consider the special case of a two-phase boundary layer on a plate. Let us assume that the gas layer is created only as a result of vertical injection of gas with a velocity v_0. Here $u_0=0$; $U=$const.

Then from (VII.136), we obtain

$$U^2 \frac{d}{dx} \int_0^{\delta_1} \frac{u}{U} \left(1 - \frac{u}{U} \right) dy - v_0 U = \frac{1}{\rho}(\tau_0 - \tau_1),$$

or

$$\frac{d}{dx} \int_0^{\delta_1} u^2 \, dy - U \frac{d}{dx} \int_0^{\delta_1} u \, dy + v_0 U = \frac{1}{\rho}(\tau_1 - \tau_0).$$

Let us demonstrate that

$$\frac{d}{dx} \int_0^{\delta_1} u \, dy \qquad v_0. \qquad\qquad\qquad (VII.137)$$

Let us integrate the continuity equation from 0 to δ_1

$$\int_0^{\delta_1} \frac{\partial u}{\partial x} \, dy + \int_0^{\delta_1} \frac{\partial v}{\partial y} \, dy = 0,$$

or

$$\frac{d}{dx} \int_0^{\delta_1} u \, dy - U_1 \frac{d\delta_1}{dx} + v_1 - v_0 = 0.$$

Since $\delta_1(x)$ is the current line, then

$$\frac{d\delta_1(x)}{dx} = \frac{v_1}{U_1}.$$

Hence, we have the validity of formula (VII.137).

The pulse equation of a gas layer for a plate assumes the form

$$\frac{d}{dx} \int_0^{\delta_1} u^2 \, dy = \frac{1}{\rho_1}(\tau_1 - \tau_0). \qquad\qquad (VII.136a)$$

The pulse equation of the outer layer of a liquid (VII.128) for a plate assumes the form

$$\frac{d}{dx} \int_0^{\delta_2} u(U - u) \, dy = \frac{\tau}{\rho_2}. \qquad\qquad (VII.128a)$$

359

§VII.5. Use of Integral Relations for Approximate Solution of the Problem of a Two-Phase Laminar Boundary Layer

General Solution of the Problem by the K. K. Fedyayevskiy Method. Now let us solve the problem of a two-phase laminar boundary layer using integral relations from §VII.4.

The Prandtl and continuity equations for a gas and liquid boundary layer have the form

$$u \frac{\partial u}{\partial x} + v \frac{\partial u}{\partial y} = U \frac{dU}{dx} + \frac{1}{\rho_{1,2}} \frac{\partial \tau}{\partial y};$$ (VII.138)

$$\frac{\partial u}{\partial x} + \frac{\partial v}{\partial y} = 0.$$ (VII.139)

Here the index "1" pertains to a gas, and the index "2" to a liquid (see Fig VII.9).

In accordance with K. K. Fedyayevskiy (VI.42), let us take the tangential stress distribution law in the gas boundary layer in the following form:

$$\frac{\tau}{\tau_0} = a_0 + a_1 \eta_1 + a_2 \eta_1^2,$$ (VII.140)

where

$$\eta_1 = \frac{u}{\delta_1}.$$

The adopted tangential stress distribution law must satisfy the following boundary conditions:

For y=0:

$$\frac{\tau}{\tau_0} = 1; \quad u = u_0; \quad v = v_0;$$

$$\frac{\partial \tau}{\partial y}\Big|_{y=0} = \rho_1 \left(-U \frac{dU}{dx} + u_0 \frac{du_0}{dx} \right) + v_0 \frac{\tau_0}{\nu_1}.$$ (VII.141)

The last expression is obtained whe using equation (VI.138) if we set y=0 in it.
For y=δ₁:

$$\eta_1 = 1; \quad \frac{\tau}{\tau_0} = \frac{\tau_1}{\tau_0} = \bar{\tau}_1.$$ (VII.142)

When satisfying the above-indicated boundary conditions, we obtain the following values of the coefficients:

$$a_0 = 1; \quad a_2 = -a_0 - a_1 + \bar{\tau}_1 = -1 - A + \bar{\tau}_1;$$

$$a_1 = A = \frac{\rho_1 \delta_1}{\tau_0} \left(-U \frac{dU}{dx} + u_0 \frac{du_0}{dx} \right) + \frac{v_0 \delta_1}{\nu_1}.$$ (VII.143)

Here A is a generalized K. K. Fedyayevskiy form parameter.

Substituting (VII.143) in (VII.140), we obtain the following tangential stress distribution law in the gas layer

$$\frac{\tau}{\tau_0} = 1 + A\eta_1 - (1 + A - \bar{\tau}_1)\,\eta_1^2. \qquad (VII.144)$$

The velocity distribution will be determined from Newton's law, setting $\mu = \mu_1$,

$$\tau = \mu_1 \frac{\partial u}{\partial y}. \qquad (VII.145)$$

From expressions (VII.144) and (VII.145), after integration we obtain the following velocity distribution law in the gas layer

$$u_1 = u_0 + \frac{\tau_0}{\mu_1}\left[y + A\,\frac{y^2}{2\delta_1} + (-1 - A + \bar{\tau}_1)\frac{y^3}{3\delta_1^2} \right]. \qquad (VII.146)$$

The velocity at the interface of the gas and liquid layers will be determined from (VII.146), setting $y = \delta_1$,

$$U_1 = (u_1)_{y = \delta_1} = u_0 + \frac{\tau_0 \delta_1}{3\mu_1}\left(2 + \frac{A}{2} + \bar{\tau}_1\right). \qquad (VII.147)$$

The tangential stress distribution in the outer layer of liquid will be taken in the form

$$\frac{\tau}{\tau_1} = b_0 + b_1 \eta_2 + b_2 \eta_2^2. \qquad (VII.148)$$

Here

$$\eta_2 = \frac{y_2}{\delta_2} = \frac{y - \delta_1}{\delta_2}. \qquad (VII.149)$$

The values of b_i will be determined from the following boundary conditions for $y = \delta_1$:

$$
\left.
\begin{aligned}
& y_2 = 0;\quad \frac{\tau}{\tau_1} = 1; \\
& \frac{\partial \tau}{\partial y} = \rho_2\left(-U\,\frac{dU}{dx} + U_1\,\frac{dU_1}{dx}\right);
\end{aligned}
\right\} \qquad (VII.150)
$$

for $y = \delta_1 + \delta_2$:

$$y_2 = \delta_2;\quad \frac{\tau}{\tau_1} = 0. \qquad (VII.151)$$

On satisfaction of these boundary conditions we find

$$
\left.
\begin{aligned}
& b_0 = 1;\quad b_2 = -1 - A_1; \\
& b_1 = A_1 - \frac{\rho_2 \delta_2}{\tau_1}\left(-U\,\frac{dU}{dx} + U_1\,\frac{dU_1}{dx}\right).
\end{aligned}
\right\} \qquad (VII.152)
$$

Substituting (VII.152) in (VII.148), we obtain the following expression for the tangential stress distribution in a layer of liquid

$$\frac{\tau}{\tau_1} = 1 + A_1 \eta_2 + (-1 - A_1)\eta_2^2. \qquad (VII.153)$$

361

The velocity distribution in the liquid layer will be determined from Newton's law (VII.155), setting $\mu=\mu_2$,

$$u_2 = U_1 + \frac{\tau_1}{\mu_2}\left[y_2 + A_1 \frac{y_2^2}{2\delta_2} - (1 + A_1) \frac{y_2^3}{3\delta_2^2}\right].$$

(VII.154)

The value of U_1 can be excluded from the given equality by replacement of it by expression (VII.147).

It is obvious that for $y_2=\delta_2$, we should have $u_2=U$, where U is the given function characterizing the velocity distribution at the boundary of the boundary layer,

$$U = U_1 + \frac{\tau_1\delta_2}{6\mu_2} (4 + A_1).$$

(VII.155)

It is possible to consider equality (VII.155) as one of the equations characterizing the frictional drag law of a body in the presence of a two-phase laminar boundary layer. Three other equations for determining the four unknowns δ_1, δ_2, τ_0, τ_1 can be compiled using the two pulse equations [for the inner gas layer (VII.136) and for the outer liquid layer (VII.128)] and the mass conservation equation for the inner gas. The last equation can be written as follows in integral form:

$$\int_0^{\delta_1(x)} u_1\, dy = \int_0^x v_0\, dx = c(x).$$

(VII.156)

Let us call the value of $c(x)$ the integral ventilation law.

Substituting the velocity distribution u_1 in the inner gas layer according to (VII.146) in equality (VII.156), we find

$$c(x) = \int_0^{\delta_1}\left\{u_0 + \frac{\tau_0}{\mu_1}\left[y + A \frac{y^2}{2\delta_1^2} + (-1 - A + \bar{\tau}_1) \frac{y^2}{3\delta_1^2}\right]\right\} dy =$$

$$= u_0\delta_1 + \frac{\tau_0\delta_1^2}{12\mu_1} (5 + A + \bar{\tau}_1).$$

(VII.157)

From equations (VII.155) and (VII.157) the following relations can be obtained between the calculated values of τ_0 and τ_1 in the form

$$\mathrm{Re}_\ast^\ast = \mathrm{Re}_\delta \frac{6(\bar{c} - \bar{u}_0)\left\{(\bar{c} - \bar{u}_0)\left[4 + 2\frac{\mu_1\delta_2}{\mu_2\delta_1}(4 + A_1)\right] - (1 - \bar{u}_0)\right\}}{\left|\bar{c}(6 + A) + \bar{u}_0(A - 6) + 4A\right| + \frac{\mu_1}{\mu_2}(5 + A)(4 + A_1)(\bar{c} - \bar{u}_0)};$$

(VII.158)

$$\bar{\tau}_1 = \frac{-2\bar{c}(4 + A) + \bar{u}_0(3 + A) + (5 + A)}{2(\bar{c} - \bar{u}_0)\left(2 + \frac{\mu_1\delta_2}{\mu_2\delta_1}\right) - (1 - \bar{u}_0)}.$$

(VII.159)

Here the following notation is introduced

$$\mathrm{Re}_\ast = \frac{v \cdot l}{v_1};\quad v^\ast = \sqrt{\frac{\tau_0}{\rho_1}};\quad \mathrm{Re}_\delta = \frac{U\delta_1}{v_1};$$

$$\bar{u}_0 = \frac{u_0}{U};\quad \bar{c} = \frac{c(x)}{U\delta_1}.$$

(VII.160)

The values of $\delta*_1$, $\delta**_1$, $\delta*_2$, $\delta**_2$ entering into the integral relations are expressed by the following formulas:

$$\frac{\delta_1^{\cdot}}{\delta_1} = \int_0^1 \left(1 - \frac{u_1}{U}\right) d\eta_1 \quad 1 - \frac{u_0}{U} - \frac{1}{2} \frac{Re_{\cdot}^2}{Re_\delta}(5 - A - \bar{\tau}_1); \tag{VII.161}$$

$$\frac{\delta_1^{\cdot\cdot}}{\delta_1} \quad \int_0^1 \frac{u_1}{U}\left(1 - \frac{u_1}{U}\right) d\eta_1 \quad \frac{u_0}{U}\left(1 - \frac{u_0}{U}\right) -$$

$$- \frac{1}{6} \frac{u_0}{U} \frac{Re_{\cdot}^2}{Re_\delta}(5 + A + \tau_1) - \frac{1}{315}\left(\frac{Re_{\cdot}^2}{Re_\delta}\right)^2 \times \tag{VII.162}$$

$$\times \left(68 + \frac{113}{4} A + \frac{13}{4} A^2 + 32\tau_1 + \frac{105}{14}\bar{\tau}_1 A + 5\bar{\tau}_1^2\right);$$

$$\frac{\delta_2^{\cdot}}{\delta_2} \quad \int_0^1 \left(1 - \frac{u_2}{U}\right) d\eta_2 = \frac{1}{12} \frac{Re_{\cdot}^2}{Re_\delta}\bar{\tau}_1 \frac{\delta_2\mu_1}{\delta_1\mu_2}(3 + A_1); \tag{VII.163}$$

$$\frac{\delta_2^{\cdot\cdot}}{\delta_2} - \int_0^1 \frac{u_2}{U}\left(1 - \frac{u_2}{U}\right) d\eta_2 = \frac{u_0}{12U} \frac{Re_{\cdot}^2}{Re_\delta}(3 + A_1) +$$

$$+ \left(\frac{Re_{\cdot}^2}{Re_\delta}\right)^2 \frac{\delta_2\mu_1}{\delta_1\mu_2} \frac{\bar{\tau}_1}{36}\left(2 + \frac{A_1}{2} + \bar{\tau}_1\right)(3 + A_1) +$$

$$+ \left(\frac{Re_{\cdot}^2}{Re_\delta}\right)^2 \left(\frac{\delta_2\mu_1}{\delta_1\mu_2}\right)^2 \bar{\tau}_1^2 \left(\frac{13}{210} + \frac{9}{280} A_1 + \frac{1}{280} A_1^2\right). \tag{VII.164}$$

The integral relations assume the form:

$$\left.\begin{aligned}
\frac{d}{dx}(U^2\delta_1^{\cdot\cdot}) + U\frac{dU}{dx}\delta_1^{\cdot} - v_0(U - u_0) &= \frac{1}{\rho}(\tau_0 - \tau_1); \\
\frac{d}{dx}(U^2\delta_2^{\cdot\cdot}) + U\frac{dU}{dx}\delta_2^{\cdot} &= \frac{\tau_1}{\rho_2}.
\end{aligned}\right\} \tag{VII.165}$$

Together with the equalities (VII.157) and (VII.158) they form a closed system of equations for calculating the two-phase laminar boundary layer.

Thus, calculation of a two-phase laminar boundary layer reduces to solving a system of two differential equations which can be done by computer.

Calculating a Two-Phase Laminar Boundary Layer on a Flat Plate. Let us consider the special case of a two-phase laminar boundary layer on a plate. Let us assume that the gas layer is created only as a result of vertical injection of the gas with a velocity v_0 (u_0=0; U=const).

The velocity distribution in the gas boundary layer is defined by formula (VII.146)

$$u_1 \quad \frac{\tau_0}{\mu_1}\left|\; y_1 + A \frac{y_1^2}{2\delta_1} + (-1 - A + \bar{\tau}_1)\frac{y_1^3}{3\delta_1^2}\right|. \tag{VII.166}$$

For a plate, the parameter A defined by formula (VII.143) assumes the form

$$A \quad \frac{v_0\delta}{v_1}. \tag{VII.167}$$

The velocity distribution in the boundary layer of a liquid will be defined by the formula (VII.154), setting $A_1=0$,

$$u_2 = U_1 + \frac{\tau_1}{\mu_2}\left(y_2 - \frac{y_2^3}{3\delta_2^2}\right).$$

(VII.168)

The pulse equation (VII.136a) for a gas layer in the investigated case of a plate can be rewritten as

$$\frac{d}{dx}\int_0^{\delta_1} u_1^2\, dy = \frac{\tau_1 - \tau_0}{\rho_1};$$

(VII.169)

for a liquid layer the pulse equation assumes the form

$$\frac{d}{dx}\int_0^{\delta_2} u_2(U - u_2)\, dy = \frac{\tau_1}{\rho_2}.$$

(VII.170)

Substituting the expression for u_1 by formula (VII.166) in the integral in the lefthand side of the integral relation (VII.169) for a gas layer and integrating, we obtain

$$\int_0^{\delta_1} u_1^2\, dy = \frac{\tau_0^2 \delta_1^3}{\mu_1^2} F_1(A, \bar{\tau}_1),$$

where

$$F_1(A, \bar{\tau}_1) = \frac{68}{315} + \frac{113}{1260} A + \frac{13}{1260} A^2 + \frac{32}{315} \bar{\tau}_1 +$$

$$+ \frac{6}{252} A\bar{\tau}_1 + \frac{1}{63} \bar{\tau}_1^2.$$

(VII.171)

When obtaining equality (VII.171) it is considered that

$$A = \frac{v_0 \delta_1}{v_1} = f(x), \text{ since } v_0 = \frac{d}{dx}\int_0^{\delta_1} u_1\, dy.$$

As a result, the integral expression (VII.169) for the gas layer assumes the form

$$\frac{d}{dx}\left[\frac{\tau_0^2 \delta_1^3}{\mu_1^2} F_1(A, \bar{\tau}_1)\right] = \frac{\tau_1 - \tau_0}{\rho_1}.$$

(VII.172)

Let us consider the case where the boundary layer is such that τ_0 and τ_1 are constant along the layer.

In this case, from (VII.172), for $0<x<L$ we obtain

$$\frac{\tau_0^2 \delta_1^3}{\mu_1^2} F_1(A, \bar{\tau}_1) = \frac{\tau_1 - \tau_0}{\rho_1} x,$$

(VII.173)

or otherwise

$$\delta_1^3 = \frac{\bar{\tau}_1 - 1}{F_1(A, \bar{\tau}_1)} \cdot \frac{\mu_1^2}{\rho_1 \tau_0} x.$$

(VII.174)

Let us denote

$$F_2(A, \bar{\tau}_1) = \frac{\bar{\tau}_1 - 1}{F_1(A, \bar{\tau}_1)}.$$

(VII.175)

Then from (VII.174) we find

$$\delta_1 = \sqrt[3]{F_2(A, \bar{\tau}_1) \frac{v_1^2 x}{(v^*)^4}}.$$

(VII.176)

At the end of the plate for $x=L$; $\delta_1 = \delta_{1L}$, we obtain

$$\bar{\delta}_1 = \frac{\delta_{1L}}{L} = \sqrt[3]{\frac{F_2(A, \bar{\tau}_1)}{\text{Re}_x^2}}.$$

(VII.177)

Now let us use the pulse equation for a liquid boundary layer (VII.170).

From (VII.166) we find the following expression for the velocity U_1 at the gas and liquid interface

$$U_1 = \frac{\tau_0 \delta_1}{3\mu_1} \left(2 + \frac{A}{2} + \bar{\tau}_1\right).$$

(VII.178)

Substituting the expression for U_1 in (VII.168), we obtain the following velocity distribution law in a liquid layer

$$u_2 = \frac{\tau_0 \delta_1}{3\mu_1} \left(2 + \frac{A}{2} + \bar{\tau}_1\right) + \frac{\tau_1}{\mu_2} \left(y_2 - \frac{y_2^3}{3\delta_2^2}\right).$$

(VII.179)

The pulse thickness of the liquid layer will be defined by the formula

$$U^2 \delta_2^{**} = \int_0^{\delta_1} u_2(U - u_2) dy = \frac{\tau_0 \tau_1 \delta_1 \delta_2^2}{12\mu_1\mu_2} \left(2 + \frac{A}{2} + \bar{\tau}_1\right) +$$
$$+ \frac{13}{210} \frac{\tau_1^2 \delta_2^3}{\mu_2^2}.$$

(VII.180)

The integral relation for the boundary layer of a liquid (VII.170) assumes the form

$$\frac{d}{dx} \left[\frac{\tau_0 \tau_1 \delta_1 \delta_2^2}{\mu_1 \mu_2} F_3(A, \bar{\tau}_1) + \frac{13}{210} \frac{\tau_1 \delta_2^3}{\mu_2^2}\right] = \frac{\tau_1}{\rho_2}.$$

(VII.181)

The following notation was adopted

$$F_3(A, \bar{\tau}_1) = \frac{1}{12} \left(2 + \frac{A}{2} + \bar{\tau}_1\right).$$

(VII.182)

Assuming as before $\bar{\tau}_1 = $const for $0 \leq x \leq L$, after integration (VII.181) we obtain

$$\frac{\tau_0 \tau_1 \delta_1 \delta_2^2}{\mu_1 \mu_2} F_3(A, \bar{\tau}_1) + \frac{13}{210} \frac{\tau_1^2 \delta_2^3}{\mu_2^2} = \frac{\tau_1}{\rho_2} x.$$

(VII.183)

On introduction of the notation analogous to the preceding, the given equality is rewritten in the form

$$\frac{13}{210} \frac{\mu_1}{\mu_2} \bar{\tau}_1 \bar{\delta}_2^3 + \bar{\delta}_1 \bar{\delta}_2^2 F_3(A, \bar{\tau}_1) - \frac{\nu_2}{\nu_1} \frac{1}{\text{Re}_x^2} = 0.$$

(VII.184)

For determination of $\bar{\delta}_2 = \delta_{2L}/L_2$ it is necessary to solve a cubic equation. However, in the majority of cases the first term in equation (VII.184) is small by comparison with the rest, and it can be neglected. Then δ_2 will be defined by the following formula:

$$\delta_2 \cdot \frac{\delta_{2L}}{L} = \frac{1}{Re_*} \sqrt{\frac{1}{\delta_1} \cdot \frac{v_2}{v_1} \cdot \frac{1}{F_3(A, \bar{\tau}_1)}}. \tag{VII.185}$$

The other two relations for the unknowns in the investigated case can be obtained from the equalities (VII.155) and (VII.157).

Thus, from the equality (VII.155) and (VII.157) for $y = \delta_1 + \delta_2$; $u_2 = U$ $A_1 = 0$, we obtain

$$U \cdot \frac{\tau_0 \delta_1}{\mu_1} \left[4F_3(A, \bar{\tau}_1) + \frac{2}{3} \frac{\bar{\delta}_2}{\delta_1} \frac{\mu_1}{\mu_2} \bar{\tau}_1 \right]. \tag{VII.186}$$

This expression can be converted to the form

$$Re = Re_*^2 \delta_1 \frac{v_1}{v_2} \left[4F_3(A, \bar{\tau}_1) + \frac{2}{3} \frac{\bar{\delta}_2}{\delta_1} \frac{\mu_1}{\mu_2} \bar{\tau}_1 \right] \tag{VII.187}$$

or, otherwise,

$$Re_*^2 \cdot Re \frac{v_2}{v_1} \cdot \frac{1}{4F_3(A, \bar{\tau}_1) \bar{\delta}_1 + \frac{2}{3} \frac{\mu_1}{\mu_2} \bar{\delta}_2 \bar{\tau}_1}, \tag{VII.187a}$$

where $Re = UL/v_2$.

Expression (VII.187) characterizes the frictional drag of a plate in the presence of a two-phase laminar boundary layer.

In order to use expression (VII.157), it is necessary to be given the integral ventilation parameter $c(x)$. When defining $c(x)$ we consider that the ventilation parameter A remains constant along the boundary layer.

Then the ventilation velocity will be defined as

$$v_0 \cdot \frac{Av_1}{\delta_1}. \tag{VII.188}$$

In this case equality (VII.157) assumes the form

$$c(x) \int_0^x \frac{Av_1}{\delta_1} dx \quad \frac{\tau_0 \delta_1^2}{\mu_1}(5 + A + \bar{\tau}_1). \tag{VII.189}$$

After substitution of δ_1 from (VII.176) and performance of the integration, expression (VII.189) will be written as follows:

$$F_2(A, \bar{\tau}_1) F_4(A, \bar{\tau}_1) = \frac{3}{2} A. \tag{VII.190}$$

where it is denoted that

$$F_4(A, \bar{\tau}_1) = \frac{1}{12}(5 + A + \bar{\tau}_1). \tag{VII.191}$$

366

From equality (VI.190) it follows that under the given assumptions the value of $\bar{\tau}_1 = \tau_1/\tau_0$ is uniquely defined by the ventilation parameter A.

The equality (VII.190) in expanded form is written as follows:

$$\bar{\tau}_1^2 (70 - 20A) + \bar{\tau}_1 (280 - 58A + 30A^2) -$$
$$- (350 + 342A + 113A^2 - 13A^3) = 0. \tag{VII.192}$$

The relations obtained permit calculation of a two-phase boundary layer on a flat plate. Such calculations were performed for values of $[\rho_2\mu_2/\rho_1\mu_1]^{1/2} = 200$, 100, 75, 25 and for values of the ventilation parameter A=0.1, 0.05, 0.01, 0.005, 0.001.

The calculation results are presented in Figure VII.8 in the form of the functions $\tau_0/\tau_{00} = \varsigma_f/\varsigma_{f_0}$ -- the ratios of the frictional drag in a two-layer boundary layer to the mean frictional drag with respect to length on a plate in a single-phase layer and the ratio of U_1/U as a function of the ventilation parameter $A = v_0\delta_1/v_1$ for fixed values of $[\rho_2\mu_2/\rho_1\mu_1]^{1/2}$. The calculation points are plotted on the figure in the form of circles, and the data from exact solution of this problem taken from reference [1] are presented in the form of solid lines.

A comparison of the results of the given solution with exact solution indicates good qualitative correspondence.

Solution of the Problem of a Two-Phase Laminar Boundary Layer for a Plate by the Pohlhausen-Karman Method. In order to establish the upper obtained limit of drag reduction in the presence of a two-phase boundary layer it is possible to limit ourselves to the simple approximation solution of the problem for a plate presented below which was obtained by I. D. Zheltukhin by the Pohlhausen-Karman method.

Let us consider a two-phase laminar boundary layer for a flat plate on which vertical injection of the gas into the liquid layer is realized.

Let us assume that between the gas layer and the liquid layer there is an interface which is a distance δ_1 from the plate.

In the investigated case the boundary conditions are written in the following form.

For a flat wall when y=0

$$u = 0; \quad v = v_0. \tag{VII.193}$$

Here u and v are the velocity components along the x and y axes (see Figure VII.2).
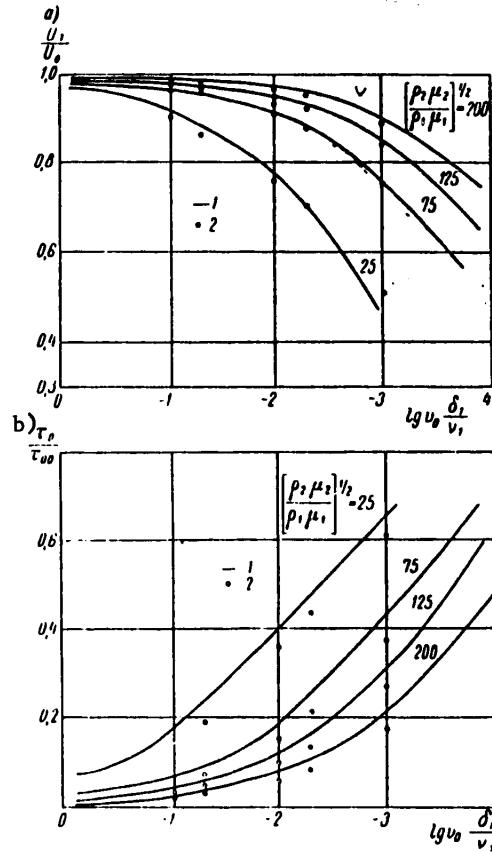
367

Figure VII.8. Results of calculating the characteristics of a two-phase laminar boundary layer: a -- sliding velocity at the interface as a function of the air injection parameter; b -- reduction of the plate friction as a function of the air injection parameter. 1 -- calculated data; 2 -- data from [1]

At the boundary of the boundary layer for $y=\delta_1+\delta_2=\delta$

$$u = U.$$ (VII.194)

At the gas and liquid interface, for $y=\delta_1$ the conditions (VII.46)-(VII.48) must be observed:

Equality of the tangential velocities

$$u_1 = u_2 = U_1;$$ (VII.195)

Equality of tangential stresses

$$\tau_1 = \tau_2,$$ (VII.196)

or

$$\mu_1 \left(\frac{\partial u_1}{\partial y} \right)_{y=\delta_1-0} = \mu_2 \left(\frac{\partial u_2}{\partial y} \right)_{y=\delta_1+0}.$$

(VII.197)

The condition of absence of a mass flow through the interface can be represented in the form

$$v_1 - u_1 \frac{d\delta_1}{dx} = 0; \quad v_2 - u_2 \frac{d\delta_1}{dx} = 0.$$

(VII.198)

Here the index "1" pertains to a gas layer, and the index "2," to a liquid layer.

The boundary layer equations for a gas and a liquid have the form of (VII.138) and (VII.139):

$$\left. \begin{array}{l} u \dfrac{\partial u}{\partial x} + v \dfrac{\partial u}{\partial y} = v_{1,2} \dfrac{\partial^2 u}{\partial y^2}; \\[2mm] \dfrac{\partial u}{\partial x} + \dfrac{\partial v}{\partial y} = 0. \end{array} \right\}$$

(VII.199)

The boundary conditions and equations (VII.199) offer the possibility of solving the stated problem of finding the characteristics of joint motion of gas and liquid layers.

The integral expressions (VII.136a) and (VII.128a) for gas and liquid layers have the form

$$\frac{d}{dx} \int_0^{\delta_1} u_1^2 dy = \frac{\tau_1 - \tau_0}{\rho_1};$$

(VII.200)

$$\frac{d}{dx} \int_{\delta_1}^{\delta_1+\delta_2} u_2 (U - u_2) dy = \frac{\tau_1}{\rho_2}.$$

(VII.201)

Here τ_1 is the frictional stress at the gas and liquid interface, τ_0 is the frictional stress at the wall.

The integral relation (VII.197) can be obtained directly by integrating the equation of motion for a gas within the limits from 0 to δ_1 considering condition (VII.195).

Let us take the form of the velocity profile in the boundary layer cross section in the form of a polynomial

$$\frac{u}{U_1} = m_0 + m_1 \frac{y}{\delta_1} + m_2 \frac{y^2}{\delta_1^2}.$$

(VII.202)

The coefficients m_1 are defined from the boundary conditions.

For gas layer, using condition (VII.193) on a plate for y=0, from equation (VII.199) we obtain

$$v_0 \left(\frac{\partial u}{\partial y} \right)_0 = v_1 \left(\frac{\partial^2 u}{\partial y^2} \right)_0.$$

(VII.203)

369

In addition, using condition (VII.196) and considering that on the interface ($y=\delta_1$, $u=U_1$, we find the velocity profile in the following form

$$\frac{u}{U_1} = \frac{2}{2+A}\frac{y}{\delta_1} + \frac{A}{2+A}\left(\frac{y}{\delta_1}\right)^2,$$ (VII.204)

where $A=v_0\delta_1/v_1$ is the dimensionless ventilation parameter.

For a layer of liquid, the coefficients of the polynomial m_1 will be defined from the conditions that at the interface $y=\delta_1$, $u=U_1$ and at the boundary of the boundary layer $y=\delta_1+\delta_2=\delta$; $u=U$; $\partial u/\partial y=0$. Then we obtain

$$\frac{u-U_1}{U-U_1} = 2\frac{y-\delta_1}{\delta-\delta_1} - \frac{(y-\delta_1)^2}{(\delta-\delta_1)^2}.$$ (VII.205)

Substituting the velocity profiles (VII.204) and (VII.205) in (VII.200) and (VII.201), we obtain the following expressions:

$$\frac{d}{dx}\left[U_1^2\delta_1\frac{20+15A+3A^2}{15(2+A)^2}\right] = v_1\frac{U_1}{\delta_1}\frac{2A}{2+A};$$ (VII.206)

$$\frac{d}{dx}\left[(\delta-\delta_1)(U-U_1)^2\left(\frac{1}{3}\frac{U}{U-U_1}-\frac{1}{5}\right)\right] = 2v_2\frac{U-U_1}{\delta-\delta_1}.$$ (VII.207)

The system of equations (VII.206), (VII.207) and condition (VII.197) expressing equality of the tangential stresses at the interface permits us to find the desired value of U_1, δ and δ_1.

Substituting (VII.204) and (VII.205) in (VII.197), we obtain

$$\mu_1\frac{U_1}{\delta_1}\frac{1+A}{2+A} = \mu_2\frac{U-U_1}{\delta-\delta_1}.$$ (VII.208)

Let us make the assumption that the ventilation parameter A remains constant, that is, let us propose that a larger quantity of gas is injected at the locations with greater friction, and a smaller quantity of gas, at the places with less friction.

Then from equations (VII.206) and (VII.207) we find

$$\delta_1^2 = \frac{v_1 x}{U_1}\frac{60A(2+A)}{20+15A+3A^2};$$ (VII.209)

$$(\delta-\delta_1)^2 = \delta_2^2 = \frac{4v_2 x}{\frac{1}{3}U-\frac{1}{5}(U-U_1)}.$$ (VII.210)

Let us define the remaining undefined value of U_1 from the condition (VII.208), which in the investigated case assumes the form

$$N\bar{U}_1^3 - \frac{\bar{U}_1}{3} - \frac{2}{15} = 0,$$ (VII.211)

where

$$\bar{U}_1 = \frac{U_1}{U - U_1};$$

(VII.212)

$$N = \frac{1}{15} \cdot \frac{\mu_1 \rho_1}{\mu_2 \rho_2} \frac{(1 + A)^2 (3A^2 + 15A + 20)}{A (2 + A)^3}.$$

(VII.213)

Calculation of the drag reduction as a function of gas flow rate is made in the following sequence.

Let us be given the value of the ventilation parameter A which is related to the gas flow rate across one end of the plate by the expression

$$\frac{Q}{UL} = \sqrt{\frac{2}{3} \frac{v_1 U_1}{v_2 U} \frac{A}{Re}},$$

(VII.214)

where

$$Re = \frac{UL}{v_2}.$$

Let us calculate the value of N by formula (VII.213).

Let us solve equation (VII.211) with respect to $\bar{U}_1$, and from formula (VII.212) let us find the value of the ratio U_1/U.

Let us determine the friction at the wall and thickness of the gas layer by the following formulas:

$$\left.\begin{array}{c}
\dfrac{\tau_0}{\tau_{00}} = \sqrt{\dfrac{\mu_1 \rho_1}{\mu_2 \rho_2}} \left(\dfrac{U}{U_1}\right)^{3/2} \sqrt{\dfrac{20 + 15A + 3A^2}{24 (2 + A)^2}}; \\[4mm]
\dfrac{\delta}{\delta - \delta_1} = \sqrt{\dfrac{v_1 U}{v_2 U_1}} \sqrt{\dfrac{2A (2 + A)}{20 + 15A + 3A^2}}.
\end{array}\right\}$$

(VII.215)

Here τ_{00} is the friction at the wall in a homogeneous liquid.

The numerical calculations (Table VII.3) were performed for the case where air under normal conditions is the gas [$(\mu_1 \rho_1 / \mu_2 \rho_2) = 1.15 \cdot 10^{-5}$].

The sliding velocity at the interface and friction reduction as a function of the air injection in a laminar film are presented in Figure VII.9.

It is obvious that small gas flows lead to sharp variation of the frictional drag. Thus, a tenfold reduction of friction by the comparison with the friction in water ($\tau_0/\tau_{00}=1/10$) is reached for a value of the parameter $(v_0/U)\sqrt{Re}=3.4 \cdot 10^{-2}$ (which corresponds to $A \sim 10^{-3}$). Here the speed of motion at the interface ($y=\delta_1$) is 0.93 of the speed of the oncoming flow ($U_1/U=0.93$).

For very small values of the ventilation parameter, the friction reduction is less significant. Thus, for a value of the ventilation parameter $(v_0/U)\sqrt{Re}=10^{-3}$, the friction is reduced by only 25%.

Table VII.3. Variation of the thickness δ_{1L} as a function of Re

$Re = \dfrac{UL}{v_2}$	10^4	10^6	10^8	10^{10}
$Q \cdot \ell/\text{sec}$	$3.4 \cdot 10^{-3}$	$3.4 \cdot 10^{-2}$	$3.4 \cdot 10^{-1}$	3.4
UL	10^{-2}	1	10^2	10^4
$\bar{\delta}_1 = \dfrac{\delta_{1L}}{l.}$	$2 \cdot 10^{-3}$	$2 \cdot 10^{-4}$	$0.63 \cdot 10^{-4}$	$2 \cdot 10^{-5}$

Low gas flow rates correspond to very small thicknesses of the gas interlayer. Thus, for a model of length L=1.0 m at a velocity U=1.0 m/sec, the thickness of the gas layer at the trailing edge is δ_{1L}=0.2 mm.

From §VII.2, an exact solution to the problem of a laminar gas film is presented, which for the special case of ventilation (A=const) was reduced to a system of two ordinary nonlinear differential equations of the Blasius type with analogous boundary conditions (VII.44-VII.48). It is interesting to compare the results of the numerical solution presented in §VII.2 with the results of the calculation obtained by the above-presented formulas. This comparison was made by I. D. Zheltukhin and presented in Figure VII.10 and VII.11. The sliding velocity at the boundary layer and friction reduction on the plate are shown in these figures as functions of the gas injection parameter $A = v_0 \delta_1 / v_1$.
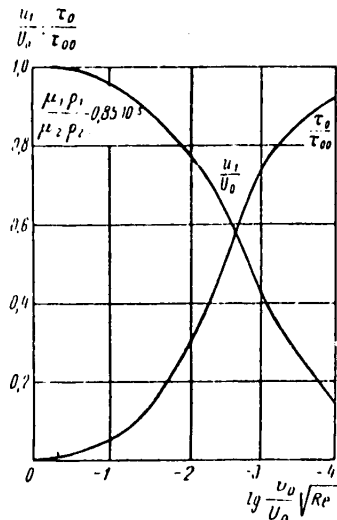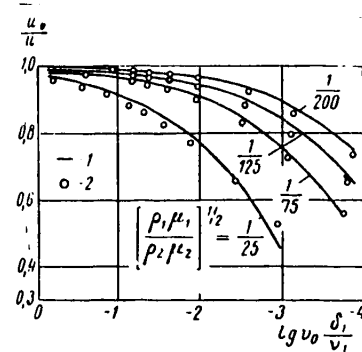

Figure VII.9. Sliding velocity at the interface and friction reduction of the plate as a function of the air injection parameter into a laminar interlayer

VII.10. Sliding velocity at the interface as a function of injection of various gases into a laminar interlayer.
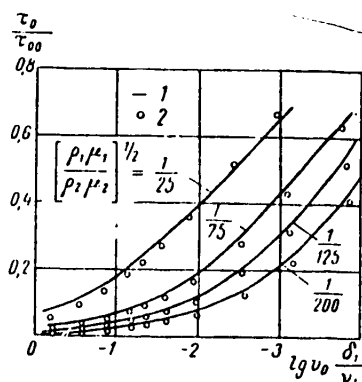1 — data of I. D. Zheltukhin;
2 — data of [1]

372

Figure VII.11. Reduction of plate friction as a function of the injection of various gases into a laminar boundary layer
1 -- data of I. D. Zheltukhin; 2 -- data of [1]

It is obvious that the approximate solution compares satisfactorily with the exact one. It must be noted that the exact solution is obtained for a different ventilation law also for the case where the condition of constancy of the tangential stresses on the plate is not satisfied.

§VII.6. Turbulent Motion in a Two-Phase Boundary Layer (Diffusion Gas Saturation Conditions)

The diffusion or bubble gas saturation conditions are characterized by motion of a gas-liquid mixture (a liquid carrying gas bubble) in the wall region. The parameters of this motion depend on the density and viscosity of the mixture, the method of injection of the gas into the flow, and the effect of the gravitational forces, and so on.

In order to trace the influence of the first of the indicated factors, let us consider the case where the dimensions of the bubbles suspended in the liquid are so small compared to the characteristic scale of motion, for example, thickness of the viscous sublayer, that they cannot be used in the calculation in general. Then it is possible to consider the gas bubbles as a continuously (and not discretely) distributed admixture in the liquid, and the two-phase mixture, as a homogeneous medium with values of the density and viscosity that vary from point to point.

If we neglect the effect of gravity and molecular diffusion of the component suspended in the liquid, the equations of motion of such a medium can be represented in the form [14]

$$\frac{\partial}{\partial x}(\rho u^2) + \frac{\partial}{\partial y}(\rho u v) = -\frac{dp}{dx} + \frac{\partial}{\partial y}\left[\mu \frac{\partial u}{\partial y} + \rho(-\overline{u'v'})\right]; \qquad (VII.216)$$

$$\frac{\partial u}{\partial x} + \frac{\partial v}{\partial y} = 0; \qquad (VII.217)$$

$$\frac{\partial cu}{\partial x} + \frac{\partial cv}{\partial y} = -\frac{\partial j}{\partial y}. \qquad (VII.218)$$

373

Here

$$c \text{ is the gas concentration by volume;}$$

$$\rho = \rho_1 c + \rho_2 (1 - c) \text{ is the density of the mixture;}$$

$$\mu (c) \text{ is the viscosity of the mixture;}$$

$$j = -\overline{c'v'} \text{ is the turbulent diffusion flow of the admixture}$$

$$(VII.219)$$

It is characteristic that the continuity equation (VII.217) has the same form that it does for a homogeneous liquid: a mixture of two incompressible components behaves just as an incompressible liquid in spite of the fact that the density in the flow field varies as a result of concentration variation.

The system of equations (VII.216)-(VII.218) of a boundary layer must be solved under known conditions at infinity, for y→∞;

$$u \to U(x), \quad c \to 0 \qquad (VII.220)$$

and the boundary conditions for y=0 expressing the method of injecting the gas into the flow, its injection velocity and the material conservation balance.

Hereafter, a flow is investigated in a two-phase boundary layer on a flat plate, across the permeable (porous) surface of which gas is injected into a liquid flow. In this case the boundary conditions are represented in the form

$$y = 0, \quad u = 0, \quad v = v_0 = q, \qquad (VII.221)$$

where q is the volumetric flow rate of the gas per second across a unit area of permeable surface. The gas supplied to the porous surface on the side y_{-0} is dissipated in the flow; the gas from the y_{+0} side, by convection $c_0 \cdot v_0$ and diffusion j_0, such that the boundary condition for the concentration equation (VII.218) will be the expression

$$y = 0, \quad q = j_0 + c_0 v_0$$

or considering (VII.221)

$$y = 0, \quad q = j_0 + c_0 q. \qquad (VII.222)$$

Equality (VII.222) expresses the material balance for y=0.

Following the usual procedure for analyzing turbulent boundary layers, we proceed from equations (VII.216)-(VII.218) to the integral expressions. Assuming that the boundaries of the diffusion and dynamic boundary layers coincide so that the condition (VII.222) is satisfied for the same finite value of y=δ hereafter called the boundary layer thickness, let us integrate equation (VII.216) at the limits from y=0 to y=δ; we obtain

$$\int_0^\delta \frac{\partial}{\partial x} (\rho u^2) \, dy + \rho u v \Big|_0^\delta = \tau \Big|_0^\delta ,$$

or after transformations

$$\frac{d}{dx}\int_0^\delta \rho u^2\, dy - \rho_2 U^2\, \frac{d\delta}{dx} + \rho_2 U v_\delta = -\tau_0.$$

Let us multiply equation (VII.217) by $\rho_2 U$, and let us integrate at the limits $(0, \delta)$

$$\frac{d}{dx}\int_0^\delta \rho_2 U u\, dy - \rho_2 U^2\, \frac{d\delta}{dx} + \rho_2 U v_\delta - \rho_2 U v_0 = 0.$$

Comparing the difference of the relations obtained, we arrive at the following form of the integral pulse equation:

$$\frac{d}{dx}\int_0^\delta \left[\frac{u}{U} - \frac{\rho}{\rho_2}\frac{u^2}{U^2}\right] dy = \frac{\tau_0}{\rho_2 U^2} + \frac{q}{U}, \qquad (VII.223)$$

used to analyze bubble gas saturation in reference [15]. Let us transform the lefthand side of (VII.223)

$$\frac{d}{dx}\int_0^\delta \left[\frac{u}{U} - \frac{\rho}{\rho_2}\frac{u^2}{U^2}\right] dy = \frac{d}{dx}\int_0^\delta \frac{\rho}{\rho_2}\left(\frac{u}{U} - \frac{u^2}{U^2}\right) dy +$$

$$+ \frac{d}{dx}\int_0^\delta \frac{u}{U}\left(1 - \frac{\rho}{\rho_2}\right) dy.$$

In accordance with determining the concentration, according to (VII.219)

$$1 - \frac{\rho}{\rho_2} = 1 - \left[\frac{\rho_1}{\rho_2}c + (1 - c)\right] = c - \frac{\rho_1}{\rho_2}c.$$

From the equation (VII.218) considering (VII.220-221) it follows that

$$\frac{d}{dx}\int_0^\delta c\frac{u}{U}\, dy = \frac{q}{U},$$

therefore

$$\frac{d}{dx}\int_0^\delta \left(\frac{u}{U} - \frac{\rho}{\rho_2}\frac{u^2}{U^2}\right) dy = \frac{d}{dx}\int_0^\delta \frac{\rho}{\rho_2}\left(\frac{u}{U} - \frac{u^2}{U^2}\right) dy + \frac{q}{U} - \frac{\rho_1 q}{\rho_2 U},$$

and equation (VII.223) reduces to the form

$$\frac{d}{dx}\int_0^\delta \frac{\rho}{\rho_2}\left(\frac{u}{U} - \frac{u^2}{U^2}\right) dy = \frac{\tau_0}{\rho_2 U^2} + \frac{\rho_1 q}{\rho_2 U}, \qquad (VII.224)$$

usually used when analyzing the movements of a compressible gas and applied to the problem of two-phase flow in a turbulent boundary layer in references [16], [17].

The pulse equation serves as the basis for calculating the boundary layer characteristics of practical importance -- thickness, velocity profiles and

concentration, frictional stresses at the wall. The calculation is constructed
on the possibility of reducing the series of unknowns entering into the equation
to one unknown which can be done using semi-empirical turbulence theories.

When constructing the velocity profile at the boundary layer cross section, let us
use the Karman formula, in accordance with which [18]

$$\tau = \rho \varkappa^2 \frac{u'^4}{u''^2}$$

(VII.225)

in the turbulent core of the boundary layer.

Assuming that in a boundary layer on a plate

$$\tau = \tau_0,$$

(VII.226)

after simple transformations [19] we find:

$$u' = \frac{du}{dy} = \sqrt{C}e^{-\varkappa \int \sqrt{\frac{\rho}{\rho_0}}\,d\varphi};$$

$$\frac{v_*^2}{v_0}\frac{d\varphi}{d\eta} = \sqrt{C}e^{-\varkappa \int \sqrt{\frac{\rho}{\rho_0}}\,d\varphi},$$

(VII.227)

where $\varphi = \frac{u}{v_*}$, $\eta = \frac{y v_*}{v_0}$ are universal variables used when analyzing turbulent

motion; v_0, ρ_0 are the kinematic viscosity and density of the gas-liquid mixture
at the wall; $v_* = \sqrt{\tau_0/\rho_0}$ is the dynamic velocity, C is the integration constant. In
the turbulent boundary layer of a homogeneous liquid, this constant is defined from
the condition at the viscous sublayer boundary:

$$\varphi = \alpha; \quad \eta = \alpha; \quad \left(\frac{d\varphi}{d\eta}\right)_{\eta = \alpha + 0} = \frac{1}{\varkappa \alpha}.$$

(VII.228)

Applying condition (VII.228) also to the investigated case of an inhomogeneous
liquid, from (VII.227) we find

$$\frac{d\eta}{d\varphi} = \eta = \frac{1}{d\varphi/d\eta} = \varkappa \alpha \exp\left[\varkappa h \int_{\bar{\alpha}}^{\bar{\varphi}} \sqrt{\frac{\rho}{\rho_0}}\,d\bar{\varphi}\right],$$

(VII.229)

where $\bar{\varphi} = \frac{u}{U}; \quad \bar{\alpha} = \frac{u}{h}; \quad h = \frac{U}{v_*}.$

Let us use the obtained expression for calculating the pulse loss thickness by the
method indicated in [19],

$$\delta^{**} = \int_0^\delta \frac{\rho}{\rho_2}\left(\frac{u}{U} - \frac{u^2}{U^2}\right)dy - \frac{\rho_0}{\rho_2}\frac{v_0}{v_*}h\int_0^1 \frac{\rho}{\rho_0}\bar{\varphi}(1-\bar{\varphi})\eta\,d\bar{\varphi}$$

$$= \varkappa \alpha \frac{\rho_0}{\rho_2}\frac{v_0}{v_*}h\int_0^1 \frac{\rho}{\rho_0}\bar{\varphi}(1-\bar{\varphi})e^{\varkappa h I(\bar{\varphi})}\,d\bar{\varphi},$$

(VII.230)

where when calculating $\delta**$ it is convenient to replace the lower integration limit in the formula

$$I(\bar{\varphi}) = \int_u^{\bar{\psi}} \sqrt{\frac{\rho}{\rho_u}}\, d\bar{\varphi} \simeq \int_0^{\bar{\varphi}} \sqrt{\frac{\rho}{\rho_u}}\, d\bar{\varphi} \qquad \text{(VII.231)}$$

by zero. By the evidence in [19], this does not lead to significant errors.

As a rule, the value of χh is significantly greater than one, as a result of which, when calculating the integral in formula (VII.230) it is convenient to apply the method of integration by parts several times, so that

$$J \quad \int_0^1 \psi(\bar{\varphi}) \exp\left[\chi h I(\bar{\varphi})\right] d\bar{\varphi} = \frac{e^{\chi h I(x)}}{\chi h \Phi(x)}\left[\psi(x) - \frac{1}{\chi h \Phi}\left(\psi' - \psi\frac{\Phi'}{\Phi}\right) + \frac{1}{(\chi h)^2 \Phi^4}(3\psi\Phi'^2 - \psi\Phi\Phi'' - 3\psi'\Phi\Phi' + \psi''\Phi^2) - \cdots\right]\Big|_{x=0}^{x=1}, \qquad \text{(VII.232)}$$

where

$$\Phi = \sqrt{\frac{\rho}{\rho_u}}; \quad \psi = \frac{\rho}{\rho_u}\,\bar{\varphi}\,(1-\bar{\varphi}); \quad I(\bar{\varphi}) = \int_0^{\bar{\varphi}} \sqrt{\frac{\rho}{\rho_u}}\, d\bar{\varphi}.$$

At the integration limits $\psi(0)=\psi(1)=0$, $\Phi(0)=1$, $\Phi(1)=\sqrt{\rho_2/\rho_0}$, therefore finally under the condition $\exp[\chi h I(x)]\gg 1$ and $1/\chi h I(1)\ll 1$, we obtain

$$J = -\frac{e^{\chi h I(1)}\psi'(1)}{(\chi h)^2 \Phi^2(1)},$$

or, since $\psi'(1)=-\rho_2/\rho_0$,

$$\delta** = \frac{u}{\chi}\frac{\mu_0}{\mu_2}\frac{v_2}{U}\,e^{\chi h I(1)}. \qquad \text{(VII.233)}$$

Substituting (VII.233) in the initial equation (VII.222) and neglecting its value $\rho_1 q/\rho_2 U$ in the righthand side, we obtain

$$h^2 \frac{\rho_2}{\rho_0} d\left[\frac{\mu_0}{\mu_2}e^{\chi h I(1)}\right] = \frac{x}{u} d\left(\frac{Ux}{v_2}\right). \qquad \text{(VII.234)}$$

For simplicity let us assume that the values of μ_0 and ρ_0 as a result of giving a defined injection law do not depend on the longitudinal coordinate x; then equation (VII.234) is easily integrated. Under the condition x=0, h=0, with accuracy to terms on the order of $1/\chi h I(1)$, its integral has the form

$$\frac{\rho_2}{\rho_0}\frac{\mu_0}{\mu_2} h^2 e^{\chi h I(1)} = \frac{x}{u}\frac{Ux}{v_2}. \qquad \text{(VII.235)}$$

In the absence of blowing $\rho_0=\rho_2$, $\mu_0=\mu_2$, $I(1)=1$, $h=h_2$

$$h_2^2 e^{\chi h_2} = \frac{x}{u}\frac{Ux}{v_2}. \qquad \text{(VII.236)}$$

Dividing one by the other, finally we find

$$\lg \frac{\zeta_{f_*}}{\zeta_f} + F\left[\sqrt{\frac{\zeta_{f_*}}{\zeta_f}} H - 1\right] = G,$$

(VII.237)

where

$$H = \sqrt{\frac{\rho_0}{\rho_2}} I(1) = \sqrt{\frac{\rho_0}{\rho_2}} \int_0^1 \sqrt{\frac{\rho}{\rho_0}} \, d\varphi;$$

$$F = (\lg e) \times \sqrt{\frac{2}{\zeta_{f_*}}} = 1.52 \, Re_x^{1/14};$$

$$G = \lg \frac{\mu_2}{\mu_0}.$$

(VII.238)

In order to apply the formula obtained to calculation of the motion of liquid bearing gas bubbles to us, first of all it is necessary to discover the nature of the gas concentration distribution in a cross section of the boundary layer, and secondly, to establish the form of the function $\mu(c)$.

For solution of the first problem let us consider the investigation of movement of an inhomogeneous liquid without pressure gradient along an infinite plane. In this case, from equations (VII.216), (VII.218) we have the expressions

$$\frac{\partial}{\partial y} \left[\rho \left(-\overline{u'v'}\right)\right] = 0;$$

(VII.239)

$$\frac{\partial}{\partial y} \left(-\overline{c'v'}\right) = 0,$$

(VII.240)

expressing constancy of the turbulent shearing stress and turbulent diffusion flows in the entire halfspace occupied by the inhomogeneous liquid. Without violating generality, it is possible to set

$$-\overline{u'v'} = K \frac{du}{dy};$$

(VII.241)

$$-\overline{c'v'} = \alpha K \frac{\partial c}{\partial y},$$

(VII.242)

where K is the turbulent momentum exchange factor, and the factor α takes into account the difference between the exchange of momentum and matter.

After integration, equations (VII.235) and (VII.236) lead to the relations

$$\rho K \frac{du}{dy} = \tau_0;$$

(VII.243)

$$\alpha K \frac{\partial c}{\partial y} = -j_0.$$

(VII.244)

Dividing one by the other, we obtain

$$\frac{u}{\rho_1 c + \rho_2 (1 - c)} \frac{\partial c}{\partial u} = -\frac{j_0}{\tau_0},$$

or since $\rho_1 = \rho_2$, after integration with the conditions $c=0$ for $u=U$, we obtain

$$\ln(1-c) = \frac{\rho_2 j_0}{\alpha \tau_0} U \left(\frac{u}{U} - 1 \right). \qquad \text{(VII.245)}$$

Considering that according to (VII.222) $j_0=(1-c_0)q$, from (VII.245), for $u=0$ we find the following expression for calculating c_0:

$$(1 - c_0) = e, {}^{-(1-c_0) \cdot b} \qquad \text{(VII.246)}$$

$$b = \frac{2q}{uU\zeta_f}. \qquad \text{(VII.247)}$$

Hence it follows that c_0 does not depend on x if the gas injection law corresponds to b=const. For calculation of H [equality (VII.238)] it is necessary to know the distribution ρ/ρ_0; using (VII.245) and (VII.246), we obtain

$$\frac{\rho}{\rho_0} = e^{(1-c_0) \cdot b\bar{\varphi}}, \qquad \text{(VII.248)}$$

$$H(c_0) = -\frac{\sqrt{1-c_0}}{\ln \sqrt{1-c_0}}\left[\frac{1}{\sqrt{1-c_0}} - 1 \right]. \qquad \text{(VII.249)}$$

Now let us turn to the establishment of the form of the functional relation $\mu(c)$. The viscosity of a gas and water emulsion is higher than the viscosity of a homogeneous liquid. This follows from the fact that the surface tension forces try to maintain a spherical shape of a small gas bubble which is manifested as an increase in shear resistance, that is, an increase in viscosity. In the case of low concentrations by volume, the variation of the viscosity can be considered by the A. Einstein formula

$$\mu = \mu_2 [1 + 2.5c], \qquad \text{(VII.250)}$$

and for large concentration by volume, the generalized formula obtained in [20], [21] and having the form

$$\mu = \mu_2 \cdot e^{2.5c}. \qquad \text{(VII.251)}$$

Let us use the relations obtained for calculations by formula (VII.237).

In Figure VII.12 the relative value of ζ_f/ζ_{f_2} is presented as a function of c_0. The dependence of c_0 on the parameter b [formula (VII.247)] and the parameter

$$\lambda = \frac{2q}{uU\zeta_{f_0}} = b \cdot \frac{\zeta_f}{\zeta_{f_0}}, \qquad \text{(VII.252)}$$

calculated by the values of ζ_f/ζ_{f_2} found from (VII.237) is illustrated in Figure VII.13 and VII.14. The function $\zeta_f/\zeta_{f_2}=f(\lambda)$ was constructed in Fig VII.15. The curves presented in Figures VII.12 to VII.16 were calculated for a value of Re=10^7. Inasmuch as formula (VII.237) includes the Reynolds number to a power of 1/14, the results obtained can be used to estimate the ratio of not the local, but the total surface friction coefficients in the Reynolds number range of 10^6 to 10^9.
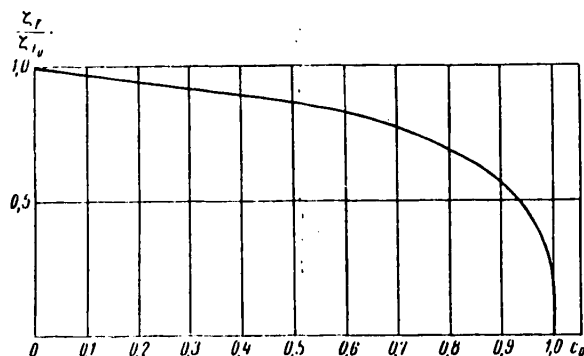
Figure VII.12. Relative local surface friction coefficient in a
turbulent two-phase boundary layer on a plate as a function of
gas content at the wall

The performed calculations pertain to an idealized system of a homogeneous medium
with density and viscosity differing from water; they are of interest primarily
for the fact that they indicate the significantly lower efficiency of the bubble
conditions of gas saturation by comparison with film. In the case of bubble gas
saturation, as follows from the presented data, the effect depends to a great extent
on how successfully the liquid density is reduced directly at the wall. The fact
that a drag reduction of 30-60%, which is of practical interest, is reached at
$c_0 > 0.8$, indicates the necessity for using the gravitational force in the calculation.
The influence of the characteristic features of the method of injecting the gas,
for example, in the case of porous surfaces, the porosity of the material, the
pore diameter and uniformity of pore distribution with respect to size, appears to
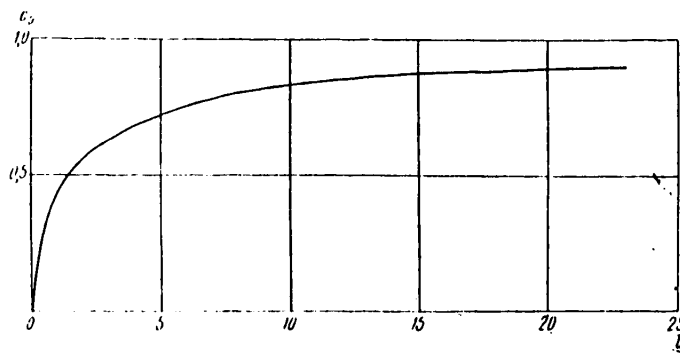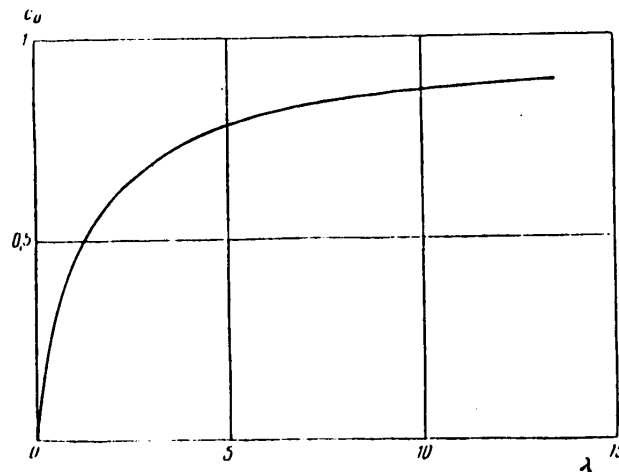be very important.

Figure VII.13. Gas content at the wall in a two-phase turbulent
boundary layer on a plate as a function of the dimensionless injection
parameter b defined by formula (VII.247)

380

Figure VII.14. Gas content at the wall in two-phase turbulent boundary layer on a plate as a function of the dimensionless injection parameter λ defined by formula (VII.252)
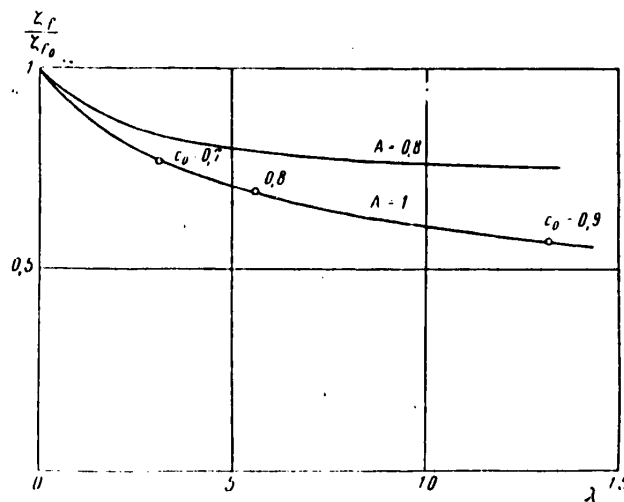

Figure VII.15. Relative local surface friction coefficient in a turbulent two-phase boundary layer on a plate as a function of the dimensionless injection parameter λ defined by formula (VII.252) for two values of the effective porosity A=0.8 and A=1

In order to demonstrate this fact, let us consider a porous permeable material having N holes -- capillary mouths, each with a diameter d -- on the surface. The process of escape of the gas bubbles into the flow can be represented as entry of previously manufactured spheres with diameter D into the flow. The source of such particles will be the portion of the surface equal to $(\pi/4)Nd^2(D/d)^2$ defining the effective porosity of the wall.

381

Previously we assumed a porosity of 100%, considering an ideal material on which it would be possible to obtain a value of $c_0 \rightarrow 1$. From the presented argument it follows that for real material values of c_0 close to one are reached if

$$\frac{\pi}{4} N d^2 \left(\frac{D}{d}\right)^2 \gamma = 1.$$

The coefficient γ considers the finite rate of formation of a gas bubble or, in other words, the difference in the square of the mean separation diameter of a bubble D^2 from the average instantaneous value of its diameter averaged over the bubble formation time squared $\overline{D'}^2$. Assuming that all the bubbles are spheres, it is possible to write

$$\frac{d}{dt}\left(\frac{\pi D'^3}{6}\right) - \frac{q}{N} \text{ и } dt = \frac{\pi}{2} \frac{N}{q} D'^2 dD',$$

$$\overline{D'^2} = \frac{\int_0^T D'^2 \, dt}{\int_0^T dt} = \frac{\int_0^D D'^4 \, dD'}{\int_0^D D'^2 \, dD'} = \frac{3}{5} D^2, \text{ т. e. } \gamma = 0,6.$$
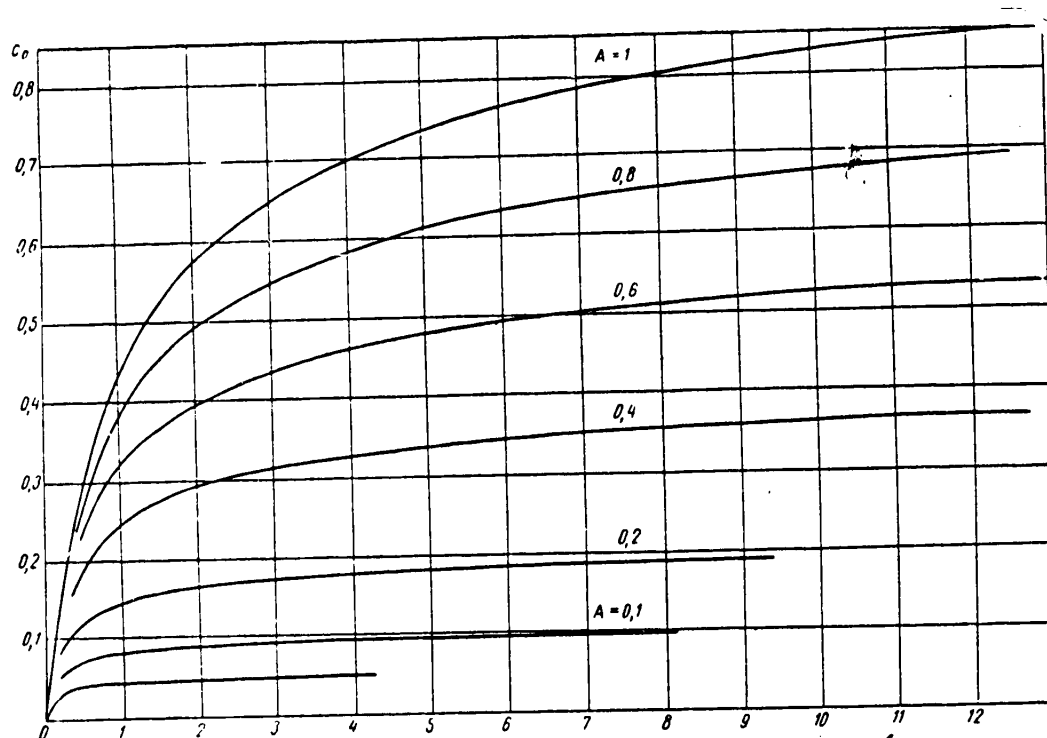

Figure VII.16. Gas content at the wall in a two-phase turbulent boundary layer on a plate as a function of the dimensionless ventilation parameter b determined by formula (VII.247) for different values of the effective porosity A.

Thus, it is possible to estimate the effect of a finite value of the porosity used for gas-saturation of a porous material. We shall consider that q -- the flow rate reduced to a unit area of permeable surface -- enters into the flow only from that portion of the area which corresponds to the effective porosity

$$A = \frac{\pi}{4} N d^2 \left(\frac{D}{d}\right)^2 \cdot \gamma,$$

then it is necessary to put the value of b/A in formula (VII.246) instead of b and multiply the calculated value of c_0 by A.

The results of this calculation are illustrated in Figure VII.16. Figure VII.15 shows the relation for ζ_f/ζ_{f_2} as a function of the ventilation parameter λ for a porous surface with effective porosity 0.8 and 1.

BIBLIOGRAPHY

1. Sparrrow, E. M.; Johnson, V. K.; Eckert, E. P. "Two-Phase Boundary Layer and Total Drag Reduction of a Plate," (translated from the English), TR. AMERIK. OBSHCH. INZH.-MEKH. "PRIKLADNAYA MEKHANIKA" [Works of the American Society of Engineering Mechanica,Applied Mechanics], Series E, Vol 29, No 2, 1962.

2. Loytsyanskiy, L. G. LAMINARNYY POGRANICHNYY SLOY [Laminar Boundary Layer], Fizmatgiz, 1960.

3. Basin, A. M.; Starobinskiy, V. B. "Two-Phase Laminar Boundary Layer with an Exponential Law of Velocity Distribution Along the Outer Boundary," TR. LIVT [Works of the Leningrad Institute of Water Transportation], No 92, 1967.

4. Sedov, L. I. PLOSKIYE ZADACHI GIDRO-I AERODINAMIKI [Two-Dimensional Problems of Hydro and Aerodynamics], GTTI, 1950.

5. Sass, ; Sparrow, E. M. "Film Boiling in a Boundary Layer with Induced Motion," (translated from the English), TR. AMERIK. OBSHCH. INZH.-MEKH., SERIYA C, TEPLOPEREDACHA [Works of the American Society of Engineering Mechanics, Series C, Heat Transfer], Vol 83, No 3, 1961.

6. Sass; Sparrow, E. M. "Film Boiling of a Superheated Fluid on a Flat Plate with Forced Convection," TR. AMERIK. OBSHCH. INZH.-MEKH., SERIYA C, TEPLOPEREDACHA, Vol 83, No 3, 1961.

7. Basin, A. M.; Gurbanov, G. G.; Starobinskiy, V. B. "Calculating a Two-Phase Laminar Boundary Layer for a Power Law of Velocity Distribution Along the Outer Boundary," TR. LIVT, No 98, 1967.

8. Klyauzer, F. "Turbulent Boundary Layer," PROBLEMY MEKHANIKI [Problems of Mechanics], No II, 1959.

9. Schubauer, H. B.; Chan, K. M. "Turbulent Flow," TURBULENTNYYE TECHENIYA I TEPLOPEREDACHA [Turbulent Flows and Heat Transfer], Moscow, IL, 1963.

10. Libby; Baronti; Napolitano. "Investigation of an Incompressible Turbulent Boundary Layer with Pressure Gradient," (translated from the English), RAKETNAYA TEKHNIKA I KOSMONAVTIKA [Rocket Engineering and Astronautics], No 3, 1964.

11. Chernyy, G. S. "Laminar Movements of Gas and Liquid in a Boundary Layer with an Interface," IZV. AN SSSR, OTN [News of the USSR Academy of Sciences, Department of Technical Sciences], No 12, 1954.

12. Levich, V. G. FIZIKO-KHIMICHESKAYA GIDRODINAMIKA [Physical-Chemical Hydrodynamics], FM, 1959.

13. Kazenin, D. A. "A Possible Exchange System in a Boundary Layer with Phase Conversion Surface," IFZH [Engineering Physics Journal], Vol VII, No 11, 1964.

14. Bay, Shi-I. TURBULENTNOYE TECHENIYE ZHIDKOSTEY I GAZOV [Turbulent Flow of Liquids and Gases], Moscow, IL, 1962.

15. Hirata, M.; Nishiwaki. "Skin Friction and Heat Transfer for Liquid Flow Over Porous Wall with Gas Injection," INTERNAT. JOURNAL OF HEAT AND MASS TRANSFER, Vol 6, p 9, 1963.

16. Loytsyanskiy, L. G. "Alteration of the Drag of Bodies by Filling the Boundary Layer with Liquids with Other Physical Constants," PMM [Applied Mathematics and Mechanics], Vol VI, 1942.

17. Fedyayevskiy, K. K. "Frictional Drag Reduction by Varying the Physical Constants of the Liquid at Walls," IZV. AN SSSR, OTN, No 9-10, 1943.

18. Loytsyanskiy, L. G. MEKHANIKA ZHIDKOSTI I GAZA [Liquid and Gas Mechanics], GTTI, 1957.

19. Lapin, Yu. V. "Friction and Heat Exchange in a Compressible Turbulent Boundary Layer in the Presence of Material Injection," ZHTF [Journal of Technical Physics], Vol XXX, No 8, 1960.

20. Deryagin, B. V.; Levi, S. M. FIZIKO-KHIMIYA NANESENIYA TONIKH SLOYEV NA DVIZHUSHCHUYUSYA PODLOZHKU [Physics and Chemistry of Applying Thin Layers to Moving Substrate], Izd. AN SSSR, 1959.

21. Richardson, E. DINAMIKA REAL'NYKH ZHIDKOSTEY [Dynamics of Real Fluids], Izd. Mir, 1965.

22. Basin, A. M.; Starobinskiy, V. B. "Integral Methods in the Theory of Calculation of a Two-Phase Boundary Layer," TR. LIVT, No 113, 1968.

23. Basin, A. M.; Starobinskiy, V. B. "Two-Phase Boundary Layer and Frictional Drag Reduction," DOKLADY K XVII KONFERENTSII PO TEORII KORABLYA (KRYLOVSKIYE CHTENIYA) [Reports at the 17th Conference on Ship Theory (Krylov Lectures)], NTOSP, 1967.

CHAPTER VIII. FRICTIONAL DRAG REDUCTION OF A SHIP BY CREATION OF ARTIFICIAL
CAVITIES (GAS FILMS) ON ITS BOTTOM

§VIII.1. Brief Survey of Experimental-Theoretical Research

The results of theoretical and experimental studies presented in the preceding
chapters permit the following possible methods of viscous drag reduction of ships
by boundary layer control to be noted:

1. Suction of the boundary layer in order to protract the transition point of the
laminar boundary layer to turbulent.

2. Suction of the boundary layer to prevent separation of it and at the same time
provide form drag reduction.

3. Projection of the region of transition of a laminar boundary layer to turbulent
by distributed damping of disturbances (Tollmien-Schlichting instability waves)
as a result of applying elastic coatings.

4. Variation of physical characteristics of a fluid in the boundary layer near
a wall by injection of material with different physical constants into the boundary
layer.

Let us consider the enumerated methods of viscous drag reduction by boundary layer
control from the point of view of the practical possibility of their application on
transport vessels.

The problem of the applicability of boundary layer suction to provide frictional
drag reduction as a result of maintaining laminar flow conditions in the boundary
layer was investigated in detail in Chapters IV and V. As was demonstrated there,
the efficiency of this method of boundary layer control (if we ignore the struc-
tural difficulties connected with its application) depends to a significant degree
on the surface state of the body and the degree of turbulence of the external flow.
Significant flow turbulence in seas and rivers complicates the effective use of
this method of drag reduction for transport vessels.

Boundary layer suction to prevent separation of the boundary layer and at the same
time provide form drag reduction is one of the first methods to be substantiated
scientifically. Its application on vessels with high form drag can turn out to be
expedient. However, practical implementation of suction is accompanied with sur-
mounting enormous structural difficulties. Therefore it has not found practical
application to this time.

385

The most effective method of drag reduction for transport vessels is alteration of the physical constants of the fluid near the wall by injection of a material with different physical constants into the boundary layer. In this case it is possible to use air as the injected material. In the published literature the given method of drag reduction has come to be called "air lubrication."

Air lubrication for frictional drag reduction has been proposed many times. Laval attempted the first experiment in air lubrication in 1882. Self-propellled river boats equipped with an air lubrication system proposed by L. M. Lapshin were tested in the USSR in 1938 and 1957 [1], [2].

For the tests, the bottom of the vessel was separated into compartments by longitudinal planks. Air was injected in the forward end of the bottom through tubes cut into the bottom flush with the surface. In the tests the author was only interested in the final effect -- reduction of the water resistance to the ship.

In the theoretical studies by K. K. Fedyayevskiy [3], [4] and L. G. Loytsyanskiy [5] on the problem of frictional drag reduction by altering the fluid density at the wall, it was assumed that as a result of gas injection the fluid density varies continuously according to a given law from the injected gas density to the density of the oncoming fluid. The fluid density variation law was selected from the condition of obtaining a flow with similar velocity profiles in the boundary layer and finding the solution in simplest form.

The possibility of practical implementation of air lubrication with such density distribution was not investigated in these experiments.

Using a power law for the velocity profile in a turbulent boundary layer, K. K. Fedyayevskiy obtained a simple formula for the friction coefficient in the presence of a fluid with different constants near the wall

$$\zeta_f = \zeta_{f_0} \frac{\nu}{\nu_0} \left(\frac{\rho_0}{\rho}\right)^{\frac{1}{1-m}}$$

Here ζ_f is the friction coefficient in the presence of a fluid with different physical constants at the wall;

ζ_{f_0} is the friction coefficient for the same Reynolds number, but with uniform flow;

ρ_0, ν_0 are the density and kinematic viscosity of the fluid at the wall;

ρ, ν are the density and kinematic viscosity of a fluid in the flow;

$$m = \frac{2n}{1+n};$$

n is the exponent in the velocity distribution law.

In reference [5], L. G. Loytsyanskiy also tried to find a theoretical solution to the problem of estimating the possible gain with respect to drag by injecting a liquid into the plate boundary layer.

For a turbulent boundary layer L. G. Loytsyanskiy obtained the following formula:

$$\zeta_f = \zeta_{f_*}\left(\frac{v_0}{v}\right)^{0.2}\left(\frac{\rho_0}{\rho}\right)^{0.8}\left(\frac{n}{n_1}\right)^{0.2};$$

$$n_1 = \frac{7}{72}; \quad n = \frac{7}{90} + \frac{7}{360}\frac{\rho_0}{\rho}.$$

As the formulas of K. K. Fedyayevskiy and L. G. Loytsyanskiy demonstrate, aeration of a turbulent boundary layer in the water leads to very large drag reduction.

The frictional drag factor calculated in references [3], [5] for a flat plate with turbulent flow conditions was 1/130 of the value of ζ_{f_0} for a homogeneous fluid.

The experiments did not confirm the results of these calculations. Usually when injecting a gas into a liquid boundary layer the drag reduction is no more than 30-40%.

As I. D. Zheltukhin demonstrated, the cause of divergence of the theoretical and experimental data is that when solving the stated problem certain characteristic features of the gas-liquid flows were not taken into account.

The weakest points in the research [3] and [5] are:

a) The assumption of monotonicity of the transition of the properties of the medium from the gas properties at the wall to liquid properties at the boundary layer boundary.

When injecting a gas through a porous surface into the boundary layer usually interfaces are formed at which the properties of the medium can be discontinuous and not vary monotonically;

b) In the above-indicated research it is ignored that the wall material and, especially, the wettability factor which is absent in homogeneous flows, have great influence on the characteristics of fluid motion in the boundary layer.

In the paper by I. D. Zheltukhin, the first effort was made to consider the influence of the above-indicated peculiarities of gas-liquid flows on the frictional drag of a liquid flowing over a flat plate with gas injected through a porous surface.

The solution of the problem of a gas-saturated boundary layer on a porous surface is given under the assumption that the conditions of movement of the fluid in the gas film are laminar. A study is made of the processes occurring when injecting gas into a turbulent boundary layer. The author demonstrated that in the investigated case the drag reduction is explained not by a decrease in fluid viscosity, but by the processes occurring near the solid wall.

Thus, in the published theoretical and experimental research, a study was made of the flow characteristics in the boundary layer for a defined injection law and density distribution across the layer.

387

In connection with the fact that realization of the scheme giving continuous variation of the density of the mixture across the boundary layer is in practice impossible, K. K. Fedyayevskiy stated the idea of expediency of blowing air through the slots or holes under the bottom of the vessel so that a gas interlayer will be formed.

In order to discover the possibility of obtaining such an air interlayer K. K. Fedyayevskiy set up some special experiments in 1943 [4]. In these experiments a study was made of the ratio of the friction coefficient with air lubrication to the friction coefficient without it as a function of the flow rate factor.

The problems connected with discovering the physical conditions of the existence of gas interlays, their form and dimensions were not investigated in the published papers. Nevertheless, during practical use of gas interlayers for drag reduction knowledge of the dimensions and physical conditions of formation of these interlayers has decisive significance. Therefore the above-mentioned papers did not offer specific recommendations with respect to the practical use of gas interlayers for frictional drag reduction of a ship, but they only demonstrated the theoretical possibility of their application theoretically and experimentally.

The shape and size of artificial cavities occurring on injection of gas at the lower side of a flat horizontal plate over which flow is taking place were first studied theoretically and experimentally by A. A. Butuzov [6], [7] under the direction of A. N. Ivanov. For the theoretical solution of the problem the assumption was made that the pressure at the interface of the gas interlayer and the liquid remains constant. This condition will be satisfied with great accuracy when the fluid density in the flow hitting the plate is many times greater than the density of the material in the gas interlayer. For the case of gas interlayers of practical importance for frictional drag reduction of a ship this condition is always met.

Under the given assumption, the boundary condition at the liquid and gas interface is equivalent to the boundarycondition assumed in developed cavitation theory [8]. Hence, it follows that the mathematical methods of developed cavitation theory are applicable to the solution of the problem of the shape and size of the gas interlayer (cavities).

Using the methods of linear cavitation theory [9], A. A. Butuzov solved the problem of the shape and size of the cavity occurring behind a wedge-shaped appendage on the lower side of a flat horizontal plate.

As a result of the theoretical solution, it was established that the length of the cavity cannot exceed an amount defined by the Froude number ($Fr_k = u_0/\sqrt{g\ell_k}$) calculated by the oncoming flow velocity U_0 and by the cavity length ℓ_k. The analogous problem was solved by V. B. Starobinskiy for the case of a bounded flow [10], [11].

For proper estimation of the drag reduction achieved by creating thin gas interlayers (films, cavities) and development of the method of recalculating the results of model tests to full-scale situations, it is necessary to study the flow of a viscous liquid over a body with gas interlayers (cavities).

The solution of this complex problem can be reduced approximately to calculation of two-phase boundary layers.

A theoretical investigation of two-phase boundary layers is presented in Chapter VII. The calculation techniques presented in Chapter VII are based on the assumption that the injected gas forms a continuous interlayer with expressed hydrodynamic gas-liquid interface. The gas injection law is taken from the condition of obtaining similar velocity profiles in the boundary layer.

The calculation results demonstrated that the presence of a two-phase boundary layer (air-water) leads to sharp frictional drag reduction of the streamlined body.

Practical realization of a two-phase boundary layer and the corresponding frictional drag reduction on a ship depend on the possibility of creating and maintaining a continuous gas interlayer.

In addition to the theoretical solution of the stated problem special experimental studies [7] were performed which confirmed the theoretical conclusions and demonstrated the possibility of significant frictional drag reduction of transport vessels by equipping the vessel with a special "air lubrication" system.

The theoretical and experimental results obtained in the USSR at this time permit an efficient approach to calculation of the "air lubrication" system for a transport vessel. The most prospective is to use "air lubrication" on inland transport ships.

Among the foreign papers it is necessary to note the Danish patent of Gram [12] in which it was proposed that air interlayers supported by means of automated valves be formed on the bottom divided by longitudinal and transverse partitions into a large number of sections.

In this chapter some of the results of the theoretical and experimental studies of the problems of frictional drag reduction of ships by creating cavities on the bottom are discussed.

On the basis of the linear theory of developed cavitation, a study is made of the problem of determining the shape and the dimensions of artificial cavities under conditions of unlimited and limited depth of flow. With significant flow restrictions with respect to depth, it becomes impossible to use the methods of linear cavitation theory. Therefore the solution of the indicated problem has been investigated here without linearizing the boundary condition.

§VIII.2. Investigation of the Shape and Sizes of an Artificial Cavity Formed on the Lower Side of a Horizontal Plate

Statement of the Problem, Basic Assumptions. Let us propose that an artificial cavity (gas interlayer) is formed on the bottom of a ship as a result of gas (air) injection behind a thin wedge-shaped appendage which is in the form of a flat plate placed at a small angle with respect to the bottom.

389

Let us present the solution of the problem of the shape and dimensions of an artificial cavity formed behind an appendage under the conditions of an unlimited fluid obtained by A. A. Butuzov [7].

Let us make the following assumptions in order to simplify the problem:

a) Let us consider the fluid ideal, incompressible and having weight. The motion of the fluid is assumed to be laminar and irrotational;

b) The bottom of the vessel is replaced by a horizontal plate which extends infinitely in the longitudinal direction;

c) The cavity is formed on the lower side of the plate as a result of gas (air) injection behind an appendage, the dimensions of which are small by comparison with the length of the cavity;

d) Let us consider the pressure on the bottom of the cavity constant. The gas flow in the aft end of the cavity is not considered, and it is replaced by an imaginary flow around an appendage of the same form as the forming cavity, but symmetrically arranged.

Thus, in order to close the cavity, the Ryabushinskiy cavitation system is used;

e) Let us assume that the cavity (gas interlayer) is thin. This allows the methods of linear cavitation theory to be used when solving the problem.

The fluid motion will be considered in the coordinate system bound directly to the plate. The adopted coordinate system and basic notation are presented in Figure VIII.1.

When solving the problem it is necessary to satisfy the following boundary conditions:

1. The condition of constancy of pressure on the surface of a gas film.

Let us write the Bernoulli equation for the current line ABC (Figure VIII.1).

$$p_0 + \frac{\rho}{2} U_0^2 = p_\kappa + \frac{\rho}{2} [(U_0 + u)^2 + v^2] - \rho g \eta(x). \qquad \text{(VIII.1)}$$

The following notation is adopted here:

U_0 is the flow velocity at infinity;

p_0 is the pressure at the bottom level at infinity;

p_k is the pressure in the cavity;

u and v are the induced velocities along the x and y axes, respectively;

ρ is the fluid density;

$\eta(x)$ is the y-axis of the cavity profile;

390

a is the length of the appendage:

ℓ is the cavity length;

g is the gravitational acceleration (the direction of the gravitational acceleration is indicated in Figure VIII.1).
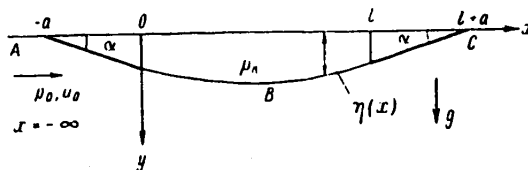

Figure VIII.1. Coordinate system and basic notation

Assuming the squares of the induced velocities to be small, condition (VIII.1) can be rewritten in the form

$$\frac{u}{U_0} = \frac{\sigma}{2} + \frac{g\eta(x)}{U_0^2},$$ (VIII.2)

where

$$\sigma = \frac{p_0 - p_K}{\frac{\rho}{2} U_0^2}$$ (VIII.3)

is the cavitation number.

2. The condition of not spreading at solid boundaries

$$\frac{v}{U_0 + u} = \frac{d\eta^*(x)}{dx}.$$

Neglecting the squares of the induced velocities,

$$\frac{v}{U_0} = \frac{d\eta^*(x)}{dx}.$$ (VIII.4)

Here $\eta^*(x)$ is the equation of the appendage profile.

3. The condition of closure of the cavity

$$\eta(\ell + a) - \eta(-a) = \int_{-a}^{\ell+a} \frac{d\eta}{dx}\, dx = \frac{1}{U_0} \int_{-a}^{\ell+a} v\, dx = 0.$$ (VIII.5)

4. The condition at infinity

$$\left. \begin{array}{l} u \to 0 \\ v \to 0 \end{array} \right\} \text{ for } \left. \begin{array}{l} x \to \infty \\ y \to \infty. \end{array} \right\}$$ (VIII.6)

391

The assumption of thinness of a cavity permits conditions (VIII.2)-(VIII.5) to be used for y=0, that is, the boundary conditions can be carried over to the x-axis.

The set of presented boundary conditions permits the given problem to be formulated as a standard boundary problem or reduced to an integral equation. The former is used when solving the problem of finding the shape and dimensions of cavities formed during flow of a weightless liquid, and the latter, when solving the problem considering gravity.

Let us present the formulation of these problems.

Boundary Problem. The given problem is formulated as follows as a boundary problem: it is required that the function of the complex induced velocity dw(z)/dz=u-iv, z=x+iy, which is analytical in the halfplane be determined. The limiting values of this function are continuous for $y\to0^+$ with the exception of the points x=-a; x=ℓ+a; y=0. This function must be subject to the following conditions

$$\frac{v}{U_0} = 0 \text{ for } -\infty < x < -a; \quad y = 0; \tag{VIII.7}$$

$$\frac{v}{U_0} = \frac{d\eta^*}{dx} \text{ for } -a < x < 0; \quad y = 0. \tag{VIII.8}$$

The condition of constancy of the pressure at the cavity profile (VIII.2)

$$\frac{u}{U_0} = \frac{\sigma}{2} + \frac{g\eta(x)}{U_0^2} \text{ for } 0 < x < l, \tag{VIII.9}$$

where

$$\eta(x) = \eta^*|_{x=0} + \frac{1}{U_0} \int_0^x v\,dx. \tag{VIII.10}$$

The value of σ is subject to definition.

The condition corresponding to closure of the cavity with respect to the Ryabushinskiy diagram

$$\frac{v}{U_0} = -\frac{d\eta^*}{dx} \text{ for } l < x < l+a, \tag{VIII.8a}$$

$$\frac{v}{U_0} = 0 \text{ for } l+a < x < \infty. \tag{VIII.7a}$$

The cavity closure condition

$$\int_{-a}^{l+a} v\,dx = 0, \tag{VIII.11}$$

$$\frac{dw}{dz} \to 0 \text{ for } z \to \infty. \tag{VIII.12}$$

Integral Equation of the Problem. In order to formulate the given problem as an integral equation, we shall consider the complex velocity dw/dz as induced by sources distributed on the x axis (y=0),

392

$$\frac{dw}{dz} = u - iv = \frac{1}{2\pi} \int_{-a}^{l+a} \frac{q(\xi)\, d\xi}{z - \xi},$$ (VIII.13)

where

$$q = \pm 2U_0 \frac{d\eta^*}{dx} = \pm 2U_0 \eta^{*\prime} \quad \text{for} \quad \begin{cases} -a < x < 0 \\ l < x < l + a \end{cases}$$

$$q = 2U_0 \frac{d\eta}{dx} = 2U_0 \eta' \qquad \qquad 0 < x < l.$$ (VIII.14)

In this representation, the boundary condition of not spreading is satisifed automatically.

Accordingly, it is possible to write

$$\frac{u}{U_0} = \frac{1}{\pi} \int_0^l \frac{\eta'(\xi)\, d\xi}{x - \xi} + \frac{1}{\pi} \int_{-a}^0 \frac{\eta^{*\prime}(\xi)\, d\xi}{x - \xi} - \frac{1}{\pi} \int_l^{l+a} \frac{\eta^{*\prime}(\xi)\, d\xi}{x - \xi}.$$ (VIII.15)

The last two terms in formula (VIII.15) depend on the appendage profile.

Let us introduce the notation

$$\varphi(a, x) = \frac{1}{\pi} \int_{-a}^0 \frac{\eta^{*\prime}(\xi)\, d\xi}{x - \xi} - \frac{1}{\pi} \int_l^{l+a} \frac{\eta^{*\prime}(\xi)\, d\xi}{x - \xi}.$$ (VIII.16)

Considering (VIII.16), formula (VIII.15) is rewritten as follows:

$$\frac{u}{U_0} = \frac{1}{\pi} \int_0^l \frac{\eta'(\xi)\, d\xi}{x - \xi} + \varphi(a, x).$$ (VIII.17)

Substituting (VIII.17) in (VIII.2), we obtain the integro-differential equation for determining the cavity profile

$$\frac{g}{U_0^2} \eta(x) + \frac{1}{\pi} \int_0^l \frac{\eta'(\xi)\, d\xi}{\xi - x} + \frac{\sigma}{2} = \varphi(a, x).$$ (VIII.18)

In equation (VIII.18), the parameter σ is subject to definition.

Equation (VIII.18) must be solved under the following conditions at the ends:

$$\eta|_{x=0} = \eta|_{x=l} = \eta^*|_{x=l};$$
$$\eta'|_{x=0} = -\eta'|_{x=l} = \eta^{*\prime}|_{x=l}.$$ (VIII.19)

Artificial Cavity Behind a Wedge Without Considering Gravity. The solution to this problem is obtained in closed form and can be used for the case of motion of a body with high velocities. The length of the appendage will be taken equal to a=1; the velocity U_0=1. Setting g=0 in the boundary condition (VIII.2), we obtain the system of boundary conditions (VIII.7)-(VIII.12) corresponding to the mixed boundary problem for determining the analytical function dw/dz.

393

For the investigated case (of a halfplane) the solution is given by the Keldysh-Sedov formula [14], and it has the form

$$\frac{dw}{dz} = \frac{1}{\pi} \sqrt{z(z-l)} \left\{ \alpha \int_{-1}^{0} \frac{dx}{\sqrt{-x(l-x)}\,(x-z)} \right. $$

$$\left. - \frac{\sigma}{2} \int_{0}^{l} \frac{dx}{\sqrt{x(l-x)}\,(x-z)} + \alpha \int_{l}^{l+1} \frac{dx}{\sqrt{x(x-l)}\,(x-z)} \right\}. \qquad (VIII.20)$$

For realization of the requirement that $\frac{dw}{dz}\Big|_{z\to\infty} \to 0,$ it is necessary to observe the condition

$$\alpha \int_{-1}^{0} \frac{dx}{\sqrt{-x(l-x)}} + \alpha \int_{l}^{l+1} \frac{dx}{\sqrt{x(l-x)}} $$

$$- \frac{\sigma}{2} \int_{0}^{l} \frac{dx}{\sqrt{x(l-x)}} = 0. \qquad (VIII.21)$$

Formula (VIII.21) makes it possible to find the relation between the cavitation number σ and the cavity length l

$$\frac{\sigma}{\alpha} = \frac{2}{\pi} \ln \frac{2\sqrt{1+l}+l+2}{2\sqrt{1+l}-(l+2)}. \qquad (VIII.22)$$

From formula (VIII.20) it is obvious to determine the equation of the cavity section

$$\eta(x) = \alpha - \frac{\alpha}{\pi} \left[\arcsin \frac{(2+l)x-l}{lx+l} + x - \right. \qquad (VIII.23)$$

$$\left. - (1+l)\arcsin \frac{(2+l)x-(1+l)i}{-lx+(1+l)l} - \frac{\pi l}{2} \right].$$

The asymptotic formula for the drag factor of a thin body (appendage) of arbitrary shape, forming the cavity has the form

$$C_x = \frac{R}{\frac{\rho}{2} U_0^2 \eta_{max}} = \frac{\pi}{4} \sigma, \qquad (VIII.24)$$

where C_x is the drag factor with respect to the characteristic dimension equal to the product of the cavity length l times the angle of inclination of the body at the point of takeoff of the cavity α.

Artificial Cavity Behind a Wedge Considering Gravity. Let us transform the integro-differential equation (VIII.18), introducing the following variables:

$$\bar{a} = \frac{a}{l}; \quad \bar{\eta} = \frac{\eta}{l}; \quad \bar{x} = \frac{x}{l}; \quad \bar{\xi} = \frac{\xi}{l}; \quad f = \frac{1}{Fr_l^2} = \frac{gl}{U_0^2}. \qquad (VIII.25)$$

Here $Fr_l = U_0/\sqrt{gl}$ is the Froude number with respect to the cavity length.

For the case of a straight-necked wedge the integrals entering into expression (VIII.16) are calculated in finite form for $\phi(a, x)$.

As a result, the equation (VIII.18) assumes the form

$$\bar{\eta}(\bar{x}) + \frac{1}{\pi} \int_{0}^{1} \frac{\bar{\eta}'(\bar{\xi})\,d\bar{\xi}}{\bar{\xi} - \bar{x}} + \frac{\sigma}{2} = \frac{a}{\pi} \ln \frac{(\bar{x} + \bar{a})[(1 + \bar{a}) - \bar{x}]}{\bar{x}(1 - \bar{x})}. \tag{VIII.26}$$

The conditions at the ends (VIII.19) are rewritten as follows:

$$\left.\bar{\eta}\right|_{\bar{x}=0} = \left.\bar{\eta}\right|_{\bar{x}=1} = \bar{a}\alpha; \\ \left.\bar{\eta}'\right|_{\bar{x}=0} = -\left.\bar{\eta}'\right|_{\bar{x}=1} = \alpha. \tag{VIII.27}$$

It is easy to see that the integro-differential equation (VIII.26) is analogous with respect to form to the Prandtl equation from finite-span foil theory. Instead of the circulation $\Gamma(\bar{x})$, this equation includes $\bar{\eta}(\bar{x})$ is the y-axis of the cavity section. In this equation there is also a constant σ subject to determination and the additional condition at the ends (VIII.27) corresponding to it.

For the calculations, equation (VIII.26) was rewritten in the form

$$\int_{0}^{1} \frac{q(\bar{\xi})\,d\bar{\xi}}{\bar{x} - \bar{\xi}} + \frac{\pi f_1}{a} \int_{0}^{\bar{x}} q(\bar{\xi})\,d\bar{\xi} + \frac{\pi\sigma}{2a} = $$
$$= -\pi f_1 + \ln \frac{(\bar{x} + \bar{a})[(1 + \bar{a}) - \bar{x}]}{(1 - \bar{x})\bar{x}}, \tag{VIII.28}$$

where

$$q(\bar{x}) = \frac{\bar{\eta}'(\bar{x})}{a} —$$

is the relative source density, and

$$f_1 = f\bar{a} = \frac{ga}{U_0^2}.$$

For approximate solution of equation (VIII.28) the function $q(\bar{x})$ was approximated by a continuous broken line. Satisfying equation (VIII.28) at n points located in the middles of the intervals $(\bar{\xi}_i, \bar{\xi}_{i+1})$, $0 = \bar{\xi}_0 < \bar{\xi}_1 < \cdots < \bar{\xi}_n = 0.5$ and, on the basis of symmetry following from the Ryabushinskiy system, setting $q(0.5)=0$, $q(x)=-q(1-x)$, we obtain a system of n linear algebraic equations for determination of (n-1) values of q_i and the constant σ. The system obtained in this way was solved on a computer.

As a result of analyzing the numerical calculations, A. A. Butuzov drew the following theoretical conclusions.

1. The length of an artificial cavity formed on a flat bottom behind a thin wedge-shaped appendage cannot exceed some value ℓ_k defined by the Froude number $\mathrm{Fr}_k = U_0/\sqrt{g\ell_k} = 0.416$ to 0.438.

2. For the value of the Froude number $Fr_\ell = Fr_k$ on a smooth bottom, cavities having a length of $\ell = \ell_k$ and different maximum thickness are theoretically possible.

The results presented here are valid for the case where the length of the appendage is small by comparison with the cavity length.

In order to obtain results that are valid for any relations between the appendage and cavity lengths, A. A. Butuzov [6], [26] generalized the Ryabushinskiy scheme to the case where the cavity closes on a fictitious appendage significantly shorter than the primary appendage or the cavity.

The problem of determining the cavity parameters by a modified Ryabushinskiy system (Figure VIII.2) in the case of a thin cavity reduced to solving an integro-differential equation with respect to the function $\eta = \eta(x)$, which is the cavity equation. This equation has the form

$$f\bar{\eta}(\bar{x}) + \frac{1}{\pi} \int_0^1 \frac{\bar{\eta}'(\bar{\xi})\,d\bar{\xi}}{\bar{\xi} - \bar{x}} + \frac{\sigma}{2} + \frac{\beta}{\pi} \ln \frac{1 - \bar{x}^2}{(1 + \bar{a}_2) - \bar{x}} =$$

$$= \frac{\alpha}{\pi} \ln \frac{\bar{x} + \bar{a}_1}{\bar{x}} . \tag{VIII.29}$$

The following notation is also introduced here:

$$\bar{a}_1 = \frac{a_1}{l} ; \quad \bar{a}_2 = \frac{a_2}{l} .$$

The additional conditions of smooth conjugation of the cavity outline with the appendage outlines imposed on the function $\bar{\eta}(x)$ at the ends of the interval $0 \leqslant x \leqslant 1$ will have the form

$$\bar{\eta}'(0) = \alpha; \quad \bar{\eta}(0) = \bar{a}_1\alpha; \quad \bar{\eta}'(1) = -\beta; \quad \bar{\eta}(1) = \beta\bar{a}_2. \tag{VIII.30}$$

The parameters α, $\bar{a}_1$, $\bar{a}_2$, f are considered given, and the parameters σ and β are considered unknown.
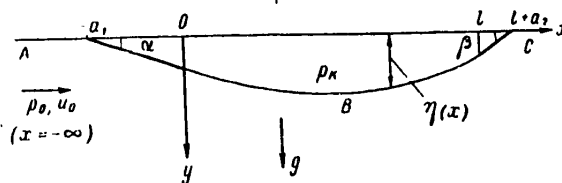

Figure VIII.2. Modified Ryabushinskiy system

Equations (VIII.29) and (VIII.30) are transformed to equations (VIII.26), (VIII.27) if we set $a_1 = a_2$ and $\beta = \alpha$.

For approximate numerical solution of the integrodifferential equation (VIII.29), the function $q(x)=(1/\alpha)\bar{n}'(x)$, just as for (VIII.28), was approximated by a continuous broken line satisfying the first and third conditions of (VIII.30). Here, in accordance with the expression

$$\frac{1}{\alpha}\,\bar{\eta}(x) = \bar{a}_1 + \int_0^x \bar{q}\,d\bar{\xi}$$

the function $(1/\alpha)\bar{n}'(\bar{x})$ was approximated by segments of a parabola smoothly conjugate to each other. The integrodifferential equation (VIII.29) was satisfied at n points selected in the middles of the intervals $\bar{\xi}_i; \bar{\xi}_{i+1}; \bar{x}_{i,i+1} = \frac{1}{2}(\bar{\xi}_i + \bar{\xi}_{i+1});$

in addition, the fourth condition of (VIII.30) was satisfied

$$\frac{1}{\alpha}\,\bar{\eta}(x) = \bar{a}_1 + \int_0^1 \bar{q}\,d\bar{\xi} = \frac{\beta}{\alpha}\,\bar{a}_1.$$

Thus, a system of n+1 linear algebraic equations was compiled.

The solution of the system of linear equations (VIII.29) and calculation of the function $\bar{n}(x)$ and the appendage drag factor C_x were performed on the EVMM-20 computer.

The appendage drag factor C_x was determined by the formula

$$C_x = \frac{R}{\frac{\rho}{2}U_0^2 a_1 \alpha},\tag{VIII.31}$$

where

$$\tag{VIII.32}$$

$$R = \alpha \int_{a_1}^0 (p - p_\kappa)\,dx;$$

$$p - p_\kappa = -\rho U_0 u(x) + \rho g y + p_0 - p_\kappa;\tag{VIII.33}$$

$$y = \alpha(a_1 + x).\tag{VIII.34}$$

The results of calculating the parameters β/α and C_x/α as functions of for for $\bar{a}_1=0.2(a_2/a_1=0.1)$ are presented in Figure VIII.3.

For other values of $\bar{a}_1$ and $a_2/a_1=0.1$, 0.2, 0.4, these functions have the same nature. It is obvious that with an increase in the parameter f (that is, with intensification of the effect of weightlessness of the fluid) the values of β/α and C_x/α decrease monotonically, vanishing for some value of $f=f\big|_{\beta=0}$. For $f>f\big|_{\beta=0}$ the cavity intersects the bottom line ($\beta<0$), which indicates impossibility of the existence of thin cavities on a flat bottom in some range of values of the parameter $f>f\big|_{\beta=0}$. The value of the parameter $f=f\big|_{\beta=0}$ has the meaning of a limit.

The limiting value of f_k or, in other words, the limiting value of the Froude number $Fr_k=1/\sqrt{f_k}$, for given speed of the ship U_0 corresponds to the limiting cavity

length $l_\kappa = \frac{U_0^2}{g}f_\kappa = \frac{U_0^2}{g}\frac{1}{Fr_\kappa^2}\cdots$ Hence, it follows that even in the investigated

case with given speed of the ship, a thin cavity of length exceeding the limiting length cannot be obtained.

Cavities of limiting length are of the greatest interest from the point of view of using them for drag reduction of a ship inasmuch as these cavities are closed ($\beta=0$) and, consequently, can be obtained for very small, theoretically zero air flow rates. The drag of thin appendages behind which these cavities are formed must also be very small $\left(\frac{C_\lambda}{\alpha}\Big|_{\beta=0} = 0\right)$.
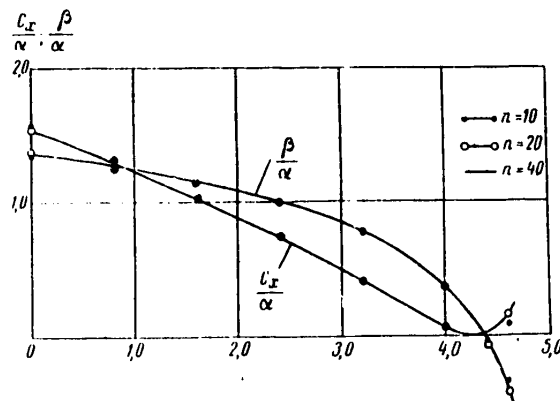

Figure VIII.3. Curves for the variation of C_x/α and β/α as functions of the parameter f(n is the number of selected calculated points)

A cavity of limiting length corresponds to the limiting cavitation number $\sigma_k=\sigma\big|_{\beta=0}$ and the limiting relative thickness of the cavity $(\eta_{max})_k=(\eta_{max})_{\beta=0}$. These parameters make it possible to find the gas pressure in a cavity of limiting length and the maximum thickness of the cavity.

The calculations demonstrated that variation of the parameter f_1 $(f_1=\bar{f}a_1)$ from zero $(a_1=0)$ to infinity $(a_1=\infty)$, that is, variation of the Froude number with respect to the appendage length $Fr_a=U_0/\sqrt{ga_1}$ from infinity to zero leads to a monotonic increase in the limiting Froude number along the length of the cavity Fr_k from a value of 0.425 to 0.657. The limiting Froude number Fr_k as a function of the parameter $F_1=ga_1/U^2_0$ and also the parameters of limiting cavities $(\eta_{max}/\alpha\ell)_k$ and $(\sigma/a)_k$ as a function of the same parameter are presented in Figure VIII.4.

The application of a modified Ryabushinskiy system permits not only determination of the values of the limiting Froude number Fr_k for the entire range of the ratio of the appendage length to cavity length $a_1=a_1/\ell$, but also establishment of the detailed characteristics of thin cavities of limiting length.
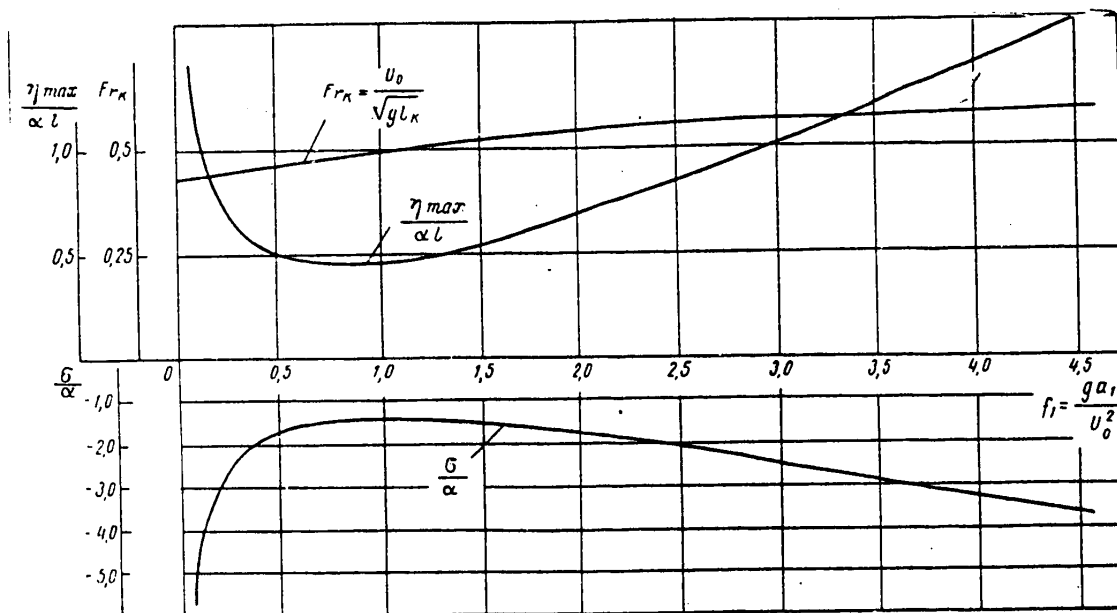
Figure VIII.4. Limiting Froude number Fr_k and parameters of the limiting cavities $\eta_{max}/\alpha l$ and σ/α as a function of the parameter $f_1 = g a_1/U_0^2$

Comparison of Theoretical and Experimental Results. The above-presented theoretical data on artificial cavities formed on a flat horizontal bottom were checked out experimentally in a flume with plate equipped with washers [6]. The plate was 945 mm long, 200 mm wide and 20 mm thick. The rear tip of the appendage was 315 mm from the forward edge of the plate. The cavities were formed by injecting air on the bottom surface of the plate behind wedge-shaped appendages.

During the air injection tests, the following values were measured: the flow velocity in front of the plate (by a Prandtl tube), the pressure in the cavity (a micromanometer), the air flow rate (Venturi tube). The geometric parameters of the cavities were determined visually, and also by photography. The tests were run in oncoming flow velocity range of 0.5 to 0.7 m/sec.

Appendages with the following dimensions were tested: 1) $a_1 = 100$ mm; $\alpha = 0.1$; 2) $a_1 = 50$ mm, $\alpha = 0.12$; 3) $a_1 = 25$ mm, $\alpha = 0.12$; 4) $a_1 = 12$ mm, $\alpha = 0.167$.

Observations of the cavity development with an increase in air flow rate confirmed the main theoretical conclusion regarding the existence of a cavity of limiting length.

The experiments demonstrated that for very small air flow rates the cavities had a profile resembling the theoretical profile of limiting cavities. Increasing the

air flow rate by 20 times led to an increase in the air taken from the end of the cavity region by two loops leading to the side plates, but in practice had no influence on the geometric dimensions of the cavities. Further significant increase in the air flow rate led to an increase in cavity thickness and loop thickness.

Figure VIII.5 shows a comparison of the relations for the values of

$$Fr_{\kappa} = \frac{U_0}{\sqrt{g l_{\kappa}}}; \quad \frac{\eta_{max}}{a a_1} \text{ and } \frac{\eta_{max}}{\sigma(a_1 + l)} \text{ as a function of the parameter } f_1 = g a_1/U_0^2 \text{ obtained}$$

theoretically and by the experimental data for limiting cavities. In Figure VIII.5 the solid lines are used for the theoretical curves, and dotted lines for the experimental curves. Experimentally obtained cavities, the maximum thickness of which almost do not change at all with an increase in the air flow beginning with almost zero values of the air flow, were considered limiting. Data are presented in the same figure for an appendage a_1=12 mm (αa_1=2 mm).

From Figure VIII.5 it is obvious that with the exception of thickness, according to the theoretical and experimental data, all of the remaining basic geometric parameters of limiting cavities (length and width) correspond to each other. The difference in the theoretically and experimentally obtained thickness of the cavity becomes significant only for cavities which are long by comparison with the appendage dimensions, and the appendage dimensions themselves are small. For a small appendage the influence of the surface tension forces is significant. Thus, the theoretical proposition that the cavity surface is tangent to the appendage surface is not properly realized.
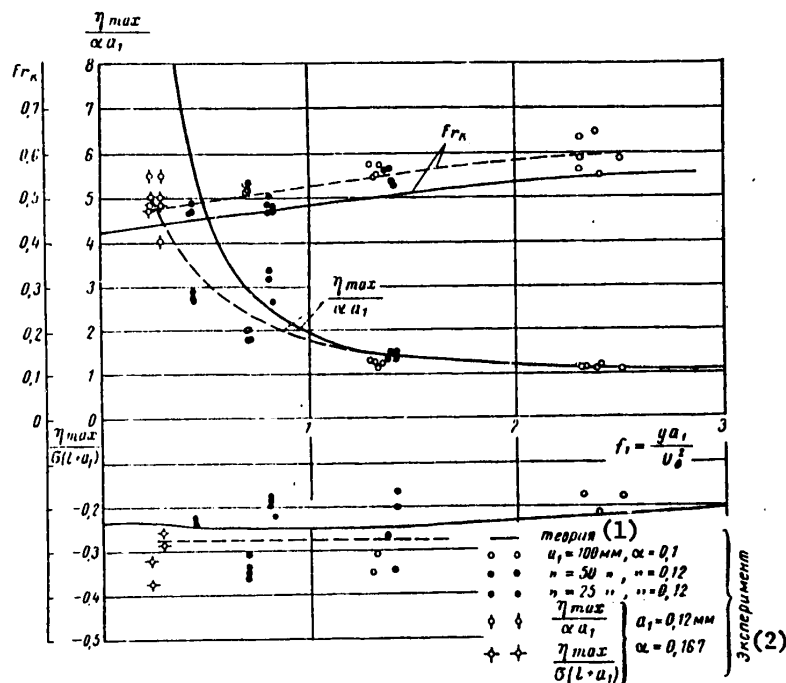

Figure VIII.5. Theoretical and experimental relations for Fr_k, $\eta_{max}/\alpha a_1$, $\eta_{max}/\sigma(a_1+l)$ as functions of the parameter f_1=ga_1/U_0^2

Key: 1 -- theory; 2 -- experiment

a)

$f_1 = 2.39; \ \frac{1}{\alpha} G = -2.52; \ Q = 0.04$. liter/sec

b)

$f_1 = 2.51; \ \frac{1}{\alpha} G = -2.77; \ Q = 0.24$ liter/sec

c)

$f_1 = 2.44; \ \frac{1}{\alpha} G = -5.46; \ Q = 3.20$ liter/sec

d)

$f_1 = 2.59; \ \frac{1}{\alpha} G = -2.16$
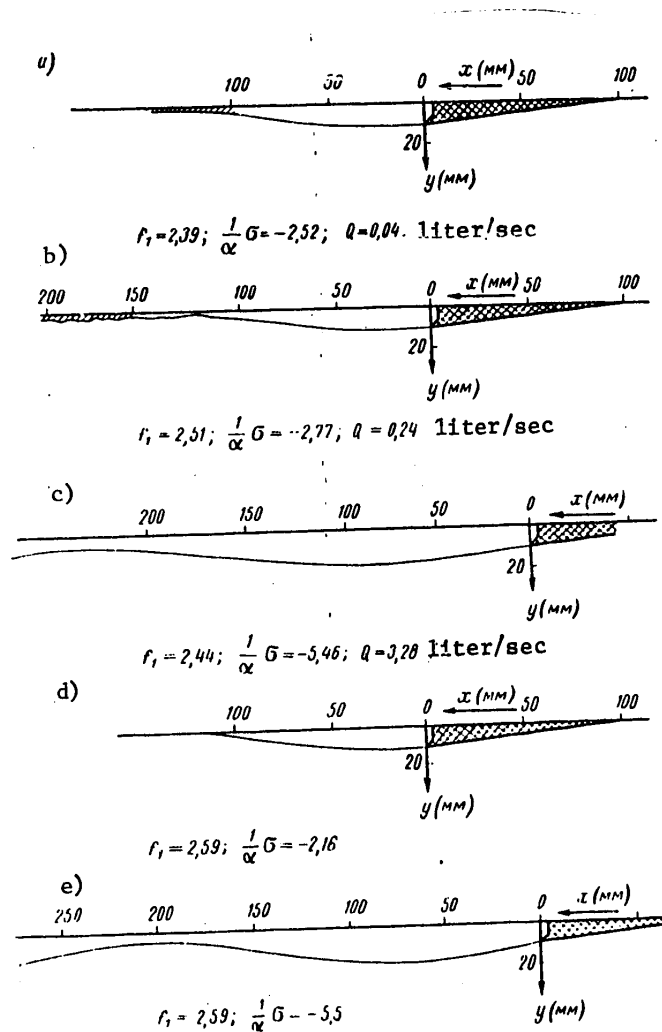
e)

$f_1 = 2.59; \ \frac{1}{\alpha} G = -5.5$

Figure VIII.6. Theoretical and experimental picture of the development
of a cavity with an increase in air flow rate Q: a, b, c -- experimental
profiles; d, e -- theoretical profiles

Accordingly, it is of interest to compare the outlines of the cavities obtained
experimentally and theoretically for large-sized appendages. A comparison of this
type is presented in Figure VIII.6. Here a, b and c are experimental outlines,
d and e are theoretical outlines. Cases a and b correspond to d, and case c
corresponds to e. It is obvious that there is a satisfactory correspondence
between the theoretically and experimentally obtained values. Thus, all of the
basic theoretical conclusions are qualitatively confirmed by the experimental
results.

§VIII.3. Effect of Limitation of the Flow on the Shape and Dimensions of an Artificial Cavity Formed on the Lower Side of a Horizontal Plate

Solution of the Linear Two-Dimensional Problem. In order to consider the effect of limitation of the flow on the form and dimensions of an artificial cavity, according to V. B. Starobinskiy [10], [11], let us consider plane flow of an ideal, incompressible fluid, but one with weight, in a strip of width H extending infinitely in both directions (Figure VIII.7).
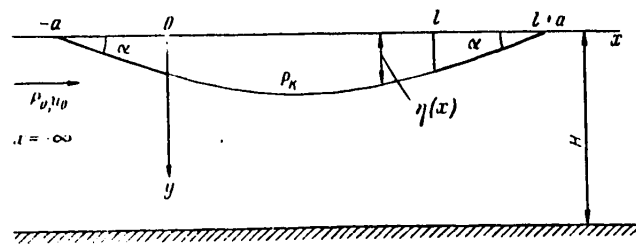

Figure VIII.7. Diagram of a cavity in a limited flow

In the investigated case the problem of cavitating flow around an appendage is solved under the same assumptions and boundary conditions as for the case of an unlimited fluid. In addition to the boundary conditions (VIII.7)-(VIII.12), it is necessary to consider an additional boundary condition at the bottom of the body of water

$$\frac{v}{U_0} = 0 \quad \text{for} \quad y = H; \ -\infty < x < |\infty.$$
(VIII.35)

The set of boundary conditions (VIII.7)-(VIII.12) and (VIII.35) permits the given problem to be formulated as a standard boundary problem or reduced to an integral equation.

For a weightless fluid, the solution of the investigated mixed boundary problem can be obtained in closed form directly by the Keldysh-Sedov formula for a strip [15], [16].

Let us take $U_0=1$; $g=0$. Then for the complex velocity $dw(z)/dz$ we obtain the following expression

$$\frac{dw(z)}{dz} = u - iv = \frac{1}{2Hi} \sqrt{\mathrm{sh}\,\frac{\pi z}{2H} \cdot \mathrm{sh}\,\frac{\pi(\xi - l)}{2H}} \times$$

$$\times \left\{ \frac{a}{2} \int_0^l f(z,\,\xi,\,l)\,d\xi - i \left[\int_{-a}^0 \frac{d\eta^*}{d\xi} f(z,\,\xi,\,l)\,d\xi + \right. \right.$$

$$\left. \left. + \int_l^{l+a} \frac{d\eta^+}{d\xi} f(z,\,\xi,\,l)\,d\xi \right] \right\}.$$
(VIII.36)

The following notation is introduced here

$$f(z, \xi, l) = \frac{\operatorname{cth} \frac{\pi(\xi - z)}{2H}}{\sqrt{\operatorname{sh} \frac{\pi\xi}{2H} \cdot \operatorname{sh} \frac{\pi(\xi - l)}{2H}}} . \qquad (VIII.37)$$

Using expression (VIII.36), it is possible to define the parameters characterizing the cavity: the profile shape, the appendage drag, and so on. In particular, from the condition of closure of the cavity (VIII.5), it is possible to obtain an expression defining the relation between the cavity length ℓ and the cavitation number σ. For a straight-necked wedge with angle of taper α, the condition (VIII.5) is written as follows

$$\alpha \int_{-a}^{0} \frac{d\xi}{\psi(\xi, l)} + \alpha \int_{l}^{l+a} \frac{d\xi}{\psi(\xi, l)} - \frac{\sigma}{2} \int_{0}^{l} \frac{d\xi}{\psi(\xi, l)} = 0, \qquad (VIII.38)$$

where

$$\psi(\xi, l) = \sqrt{\operatorname{sh} \frac{\pi\xi}{2H} \cdot \operatorname{sh} \frac{\pi(\xi - l)}{2H}} .$$

After transformations, the desired expression can be reduced to the form

$$\frac{\sigma}{\alpha} = \frac{2F \left[\operatorname{arcsin} \sqrt{\dfrac{\operatorname{ch} \frac{\pi}{2H}(l + 2a) - \operatorname{ch} \frac{\pi l}{2H}}{\operatorname{ch} \frac{\pi}{2H}(l + 2a) - 1}} ; \sqrt{\dfrac{2}{\operatorname{ch} \frac{\pi l}{2H} + 1}} \right]}{F \left[\frac{\pi}{2} ; \sqrt{\dfrac{\operatorname{ch} \frac{\pi l}{2H} - 1}{\operatorname{ch} \frac{\pi l}{2H} + 1}} \right]}, \qquad (VIII.39)$$

or

$$\frac{\sigma}{\alpha} = \frac{2F \left[\operatorname{arcsin} \sqrt{\dfrac{\operatorname{sh} \frac{\pi a}{2H} \cdot \operatorname{sh} \frac{\pi}{2H}(l + a)}{\left[\operatorname{sh} \frac{\pi}{4H}(l + 2a) \right]^{2}}} ; \dfrac{\sqrt{2}}{\operatorname{ch} \frac{\pi l}{4H}} \right]}{F \left[\frac{\pi}{2} ; \operatorname{th} \frac{\pi l}{4H} \right]} .$$

Here F is a first type elliptic integral.

From expression (VIII.36) it is possible to obtain the form of the cavity profile by the formula

$$\eta(x) = a\alpha + \int_{0}^{x} v \, dx. \qquad (VIII.40)$$

For the case of a fluid that has weight, the set of boundary conditions (VIII.7)-(VIII.12) and (VIII.35) permits the given problem to be reduced to an integral equation.

For this purpose let us use the Schwartz integral for the strip [16]

$$f(z) = v + iu = \frac{i}{2H} \int\limits_{-\infty}^{\infty} v_0(\xi) \, \mathrm{cth} \, \frac{\pi}{2H}(\xi - z) \, d\xi +$$

$$+ \frac{i}{2H} \int\limits_{-\infty}^{\infty} v_1(\xi) \, \mathrm{th} \, \frac{\pi}{2H}(\xi - z) \, d\xi. \qquad \text{(VIII.41)}$$

Here $v_0(\xi)$ and $v_1(\xi)$ are values of the real part $f(z)=v+iu$ for $y=0$ and $y=H$, respectively.

From the boundary condition of stagnation at the cavity profile $v/U_0 = \partial\eta(x)/\partial x$ when $y=0$ and from expression (VIII.41), we obtain the following expre sion for u/U_0:

$$-\frac{u}{U_0} = \frac{1}{2H} \int\limits_{-a}^{l+a} \eta'(\xi) \, \mathrm{cth} \, \frac{\pi}{2H}(\xi - x) \, d\xi. \qquad \text{(VIII.42)}$$

In this expression let us isolate the terms which depend on the appendage profile

$$\frac{u}{U_0} = -\frac{1}{2H} \int\limits_{-a}^{0} \eta^{*'}(\xi) \, \mathrm{cth} \, \frac{\pi}{2H}(\xi - x) \, d\xi -$$

$$- \frac{1}{2H} \int\limits_{0}^{l} \eta'(\xi) \, \mathrm{cth} \, \frac{\pi}{2H}(\xi - x) \, d\xi + \frac{1}{2H} \int\limits_{l}^{l+a} \eta^{*'}(\xi) \, \mathrm{cth} \, \frac{\pi}{2H}(\xi - x) \, d\xi. \qquad \text{(VIII.43)}$$

Substituting (VIII.43) in the boundary condition of constancy of pressure at the cavity profile (VIII.9), we obtained the desired integrodifferential equation for determining the cavity profile

$$\frac{g\eta(x)}{U_0^2} + \frac{1}{2H} \int\limits_{0}^{l} \eta'(\xi) \, \mathrm{cth} \, \frac{\pi}{2H}(\xi - x) \, d\xi = -\frac{\sigma}{2} + \varphi. \qquad \text{(VIII.44)}$$

Here

$$\varphi = -\frac{1}{2H} \int\limits_{-a}^{0} \eta^{*'}(\xi) \, \mathrm{cth} \, \frac{\pi}{2H}(\xi - x) \, d\xi +$$

$$+ \frac{1}{2H} \int\limits_{l}^{l+a} \eta^{*'}(\xi) \, \mathrm{cth} \, \frac{\pi}{2H}(\xi - x) \, d\xi. \qquad \text{(VIII.45)}$$

In expression (VIII.44), the term φ isolates the integrals which depend on the appendage profile $\eta^*(x)$.

The function obtained as a result of solving equation (VIII.44) must satisfy the boundary conditions which assume the following form for a straight-necked wedge

$$\eta(0) = \eta(l) = a\alpha; \quad \eta'(0) = -\eta'(l) = \alpha, \qquad \text{(VIII.46)}$$

where α is the angle of inclination of the wedge; a is the length of the wedge.

The cavitation number is unknown, defined in the process of solving the problem.

From formula (VIII.44), it is easy to obtain the limiting transition to the case of deep water. If we assume that H→∞, then

$$\operatorname{cth} \frac{\pi}{2H}(\xi - x) \rightarrow \frac{2H}{\pi(\xi - x)}$$

and equation (VIII.44) assumes the form

$$-\frac{\mu_0(x)}{U_0^2} + \frac{1}{\pi} \int_0^l \frac{\eta'(\xi)\,d\xi}{\xi - x} = -\frac{\sigma}{2} + \varphi. \qquad (VIII.47)$$

Equation (VIII.47) coincides with formula (VIII.18).

For the case of a straight-necked wedge (α=const) the value of φ will be defined by the formula

$$\varphi = \frac{\alpha}{2H}\left[\int_{-a}^{0} \operatorname{cth} \frac{\pi}{2H}(x - \xi)\,d\xi - \int_{l}^{l-a} \operatorname{cth}\frac{\pi}{2H}(x - \xi)\,d\xi \right]. \qquad (VIII.48)$$

As a result of calculating the integrals in the righthand side of equation (VIII.48) and transformations, we obtain

$$\varphi = -\frac{\alpha}{\pi}\ln\frac{\operatorname{ch}\frac{\pi l}{2H}\left(\frac{x}{l} - \frac{1}{2}\right) - \operatorname{ch}\frac{\pi l}{4H}}{\operatorname{ch}\frac{\pi l}{2H}\left(\frac{x}{l} - \frac{1}{2}\right) - \operatorname{ch}\frac{\pi l}{2H}\left(\frac{a}{l} + \frac{1}{2}\right)}. \qquad (VIII.49)$$

When investigating the influence of gravity and the limited nature of flow on the cavity characteristics, equation (VIII.44) is used. Let us reduce equation (VIII.44) to dimensionless form, assuming the following notation:

$$\bar{x} = \frac{x}{l}; \quad \bar{\eta} = \frac{\eta}{l}; \quad \bar{a} = \frac{a}{l}; \quad \bar{\xi} = \frac{\xi}{l}; \\ f = \frac{1}{F_l^2} = \frac{gl}{U_0^2}; \quad l_H = \frac{l}{2H}. \qquad (VIII.50)$$

In this notation equation (VIII.47) is rewritten as

$$f\bar{\eta}(\bar{x}) + l_H \int_0^1 \bar{\eta}'(\xi)\operatorname{cth} l_H(\bar{\xi} - \bar{x})\,d\bar{\xi} = -\frac{\sigma}{2} + \varphi. \qquad (VIII.51)$$

This equation must satisfy two boundary conditions at the ends of the cavity

$$\bar{\eta}(0) = \bar{\eta}(1) = \bar{a}\alpha; \\ \bar{\eta}'(0) = -\bar{\eta}'(1) = \alpha. \qquad (VIII.52)$$

Let us write equation (VIII.51) in a form which is more convenient for calculation

405

$$l_H \int_0^1 q(\bar{\xi})\, c\,\text{th}\, l_H(\bar{\xi} - \bar{x})\, d\bar{\xi} + \frac{f_1}{a} \int_0^{\bar{\lambda}} q(\bar{\xi})\, d\bar{\xi} + \frac{\sigma}{2a} = -f_1 + \frac{\varphi}{a},$$ (VIII.53)

Here $\qquad\qquad q(\bar{\xi}) = \dfrac{\bar{\eta}'(\bar{\xi})}{a}; \quad f_1 - \overline{fa} = \dfrac{ga}{U_0^2}.$

The approximate solution of equation (VIII.53) can be obtained by reducing it to a system of algebraic linear equations.

In the investigated case it is expedient to obtain the system by replacing the integrals entering into (VIII.53) by finite sums and satisfaction of this equation at points located in the middles of the breakdown intervals. In the interval where $\bar{x} = \bar{\xi}$ and also where the variable $\bar{x} = -\bar{\xi}$ is adjacent to the ends of the integration interval (0.1), the value of $\bar{\eta}'(\bar{\xi})$ was approximated analogously to the case of an unlimited fluid.

The solution to the system of algebraic equations was found on the M-20 computer. Calculations were performed for the following values of the parameters: a=0.1, 0.05, 0.025, 0.0125, ℓ_H=0.2, 1.0, 1.6, 2, 2.6, 3.6, 5.0, 7.0. The value of the parameter f was selected in the calculation process.

Analysis of the performed calculations indicates that, just as in the case of deep water (see §VIII.2), for each fixed value of the shallow water parameter ℓ_H there is a value of the parameter f for which the cavity characteristics undergo discontinuous variation.

Here the cavity profile somehow "intersects" the bottom, that is, for $f > f_k$ the solution to the problem becomes physically unrealistic. This is equivalent to the fact that the value of the parameter $f = g\ell/U_0^2$ cannot exceed f_k.

Consequently, even under limited flow conditions for given velocity U_0, the cavity length ℓ also cannot be greater than that which is determined by the value of the parameter f_k, that is, even in this case there is a cavity of limited length.

It is easy to demonstrate that a cavity of limited length can have different shapes.

The calculation results permit consideration of the influence of the depth of the fluid on the cavity shape and dimensions.

The influence of the shallow water parameter can be analyzed by the curves $(\sigma/\alpha)(f)$ and $(\delta/\alpha\ell)(f)$ for different values of ℓ_H which are presented in Figures VIII.8 and VIII.9. Here, δ denotes the maximum thickness of the cavity. By these relations it is easy to determine a narrow range of variation of the parameter f for different values of ℓ_H for which discontinuous variation of the cavity parameters takes place.

From an investigation of these figures it follows that with a decrease in fluid depth, that is, from an increase in the value of the parameter ℓ_H, the values of f_k increase. Consequently, with a decrease in fluid depth the length of the limiting cavity increases.

406

Let us consider the nature of variation of the cavity parameters for flow velocities close to critical ($Fr_H = U_0/\sqrt{gH} \to 1.0$).

Figure VIII.10 gives the results of calculating the relation $Fr_H = U_0/\sqrt{gH}$ as a function of Fr_K $\dfrac{U_0}{\sqrt{g(l_K + 2a)}} \cdot \dfrac{U_0}{\sqrt{gL}}$. As follows from this figure, the values of Fr_H do not exceed one anywhere, that is, $Fr_H < 1$ when $Fr_L \to 0$.

Analysis of expression (VIII.53) shows that for a value of $Fr_H \to 1$ discontinuous variation of the cavity parameters takes place for any values of $l_H = l/2H$. Therefore the straight line $Fr_H = 1$ is an asymptote to the curve $Fr_H = f(Fr_K)$ presented in Figure VIII.10.

Thus, for the linear statement of the problem, the conclusion is obtained that for $Fr_H \geq 1$, existence of a cavity of finite length is impossible.

This conclusion is not confirmed by the experimental data. Lack of correspondence between the theoretical and experimental data is explained by inadmissibility of linearization of the boundary condition for $Fr_H \geq 1$. The analogous conclusion is obtained in the linear theory of plane surface waves under shallow water conditions.

For $Fr_H \geq 1$ it is possible to obtain an approximate solution only as a result of solving the nonlinear problem while keeping terms of higher order of smallness.

Thus, the theoretical studies of the forms and dimensions of artificial cavities under limited flow conditions permit the following conclusions to be drawn:

1. For each fixed value of the velocity U_0 and water depth H, there is a Froude number Fr_l calculated by the cavity length, which is limiting for the given values of U_0 and H. The cavity length cannot exceed the value defined by the limiting Froude number Fr_K.

2. With an increase in the Froude number with respect to fluid depth $Fr_H = U_0/\sqrt{gH}$, the value of the limiting Froude number calculated by the cavity length $Fr_K = U_0/\sqrt{g l_K}$ decreases, and the cavity length increases.

3. The linear theory is unsuitable for investigating the shapes and sizes of artificial cavities when $Fr_H \geq 1.0$. In this case the solution of the problem can be obtained only when maintaining nonlinear boundary conditions.

Solution of the Nonlinear Two-Dimensional Problem. Let us present the results of solving a nonlinear two-dimensional problem of finding the form and the dimensions of artificial cavities for Froude numbers with respect to depth $Fr_H \geq 1$ obtained by V. B. Starobinskiy [11].

When stating the problem let us also make the same assumptions as were made when solvint the linear problem, but under the boundary condition at the cavity surface we shall not neglect the squares of the induced velocities as was done before.
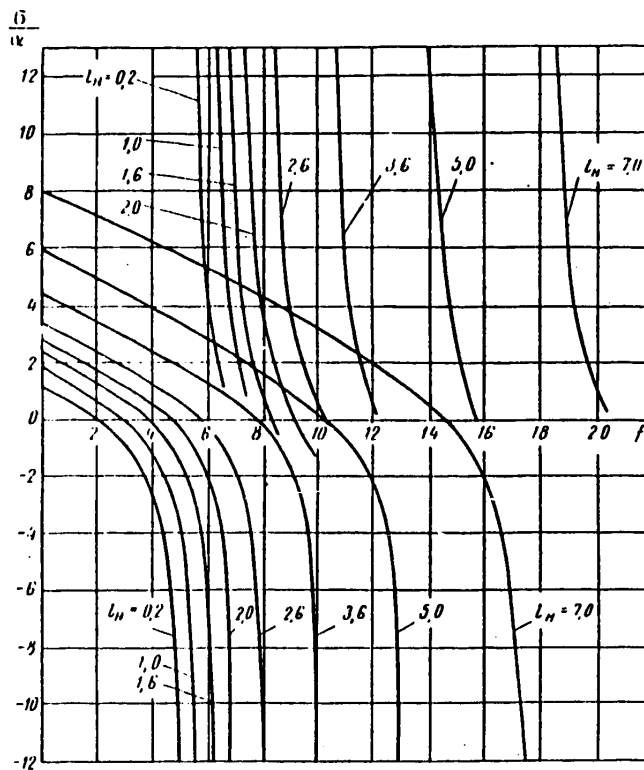
Figure VIII.8. Curves $\sigma/\alpha = \phi(f)$ for $\ell_H = $const

Let us write the Bernoulli equation for the current line ABC (Figure VIII.11)

$$\frac{\rho U_0^2}{2} + p_0 + \rho g H = \frac{\rho v_K^2}{2} + p_K + \rho g y(x). \qquad (VIII.54)$$

Here v_k is the velocity at the cavity of the boundary.

Let us define the velocity v_k in terms of the modulus of the derivative of the function conformally mapping the investigated flow region onto a rectilinear strip of unit width

$$v_K = U_0 \left| \frac{dw_0}{dz_1} \right|. \qquad (VIII.55)$$

Here $z_1 = \overline{x}_H + i\overline{y}$.

408
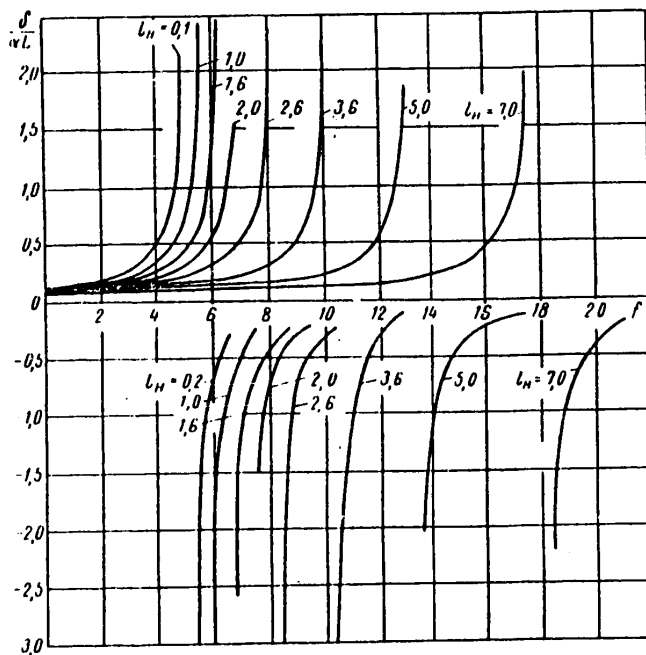
Figure VIII.9. Curves $\sigma/\alpha L = \phi(f)$ for $\ell_H = const$
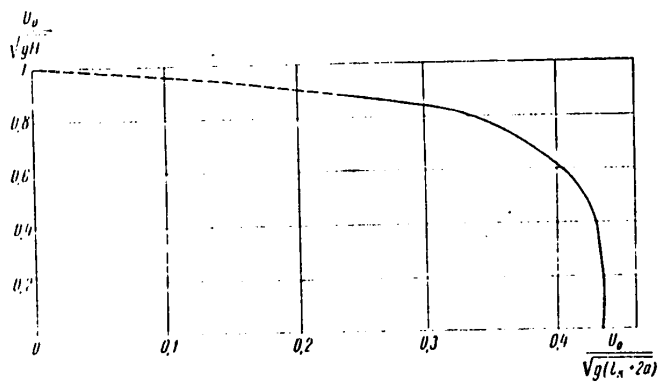
Figure VIII.10. $Fr_H = U_0/\sqrt{gH}$ as a function of $Fr_\kappa' \cdot \dfrac{U_0}{\sqrt{g(\ell_\kappa + 2a)}}$.

409
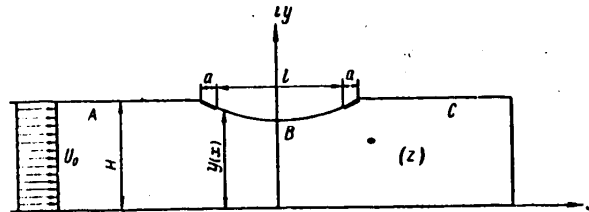
Figure VIII.11. Diagram of the solution of the nonlinear problem

Let us introduce the following notation:

$$\bar{x}_H \quad \frac{x}{H}; \quad \bar{y}(\bar{x}) = \frac{y(x)}{H}; \quad \mathrm{Fr}_H = \frac{U_0}{\sqrt{gH}}; \quad \nu_H = \frac{1}{\mathrm{Fr}_H^2}; \quad \left. \begin{array}{c} \\ \\ \end{array} \right\} \qquad \text{(VIII.56)}$$

$$\sigma \quad \frac{2(p_0 - p_k)}{\rho U_0^2} .$$

Substituting (VIII.55) and (VIII.56) in (VIII.54), we obtain

$$\left| \frac{dw_0}{dz_1} \right|^2 + 2\nu_H \bar{y}(\bar{x}_H) = 1 + \sigma + 2\nu_H = c. \qquad \text{(VIII.57)}$$

The investigated problem of determining detached flow over a wedge was reduced to the problem of finding the function realizing conformal mapping of the flow region onto a rectilinear strip with satisafaction of the condition (VIII.57) at the boundary of the region.

For investigation of the forms and dimensions of artificial cavities with Froude numbers with respect to depth Fr_H close to and greater than one, V. B. Starobinskiy used the asymptotic method of narrow strips [15], [18]. The concept of Academician M. A. Lavrent'yev regarding approximate calculation of the derivative of the conformal mapping in the case of narrow regions was used as the basis for this method. It turned out that in the case where the mapping region i. narrow and the boundary of the region is sufficiently smooth, the derivative of the conformal rapping at the boundary can be calculated by the following formula:

$$\left| \frac{dw_0}{dz_1} \right| \approx I\left(\bar{y}, \frac{d\bar{y}}{dx_H}, \frac{d^2\bar{y}}{dx_H^2} \cdots \right), \qquad \text{(VIII.58)}$$

that is, the value of $|dw_0/dz_1|$ is defined only by the local boundary characteristics.

Then the boundary condition (VIII.57), which is a nonlinear partial differential equation will in this case become an ordinary differential equation, the solution of which is appreciably simpler.

Let us write the formula in the form (VIII.58) for determination of $|dw_0/dz_1|$ of the mapping of the curvilinear strip close to rectilinear on a rectilinear strip [18]

410

$$\left| \frac{dw_0}{dz_1} \right|^2 \quad \frac{1}{\bar{y}^2} \left[1 + \frac{2}{3} \bar{y}\bar{y}'' - \frac{1}{3} (\bar{y}')^2 \right] + \cdots \tag{VIII.59}$$

The following restriction is imposed on the boundary $\bar{y}(\bar{x}_H)$,

$$\bar{y}^k(\bar{x}_H) \sim O(\varepsilon^{nk}), \tag{VIII.60}$$

where k=1, 2, ..., m; ε is a small value; n is an arbitrary positive number.

Direct use of equation (VIII.59) for the given problem is impossible as a result of the fact that the flow region does not satisfy the conditions (VIII.60) at the points A and B (see Figure VIII.12a). Consideration of this singularity of the boundary is theoretically necessary, for only in this case will it be possible to consider the influence of the wedge on the formation of the cavity.

V. B. Starobinskiy proposed the following method of reducing the given boundary conditions to the conditions offering the possibility of using formula (VIII.59).
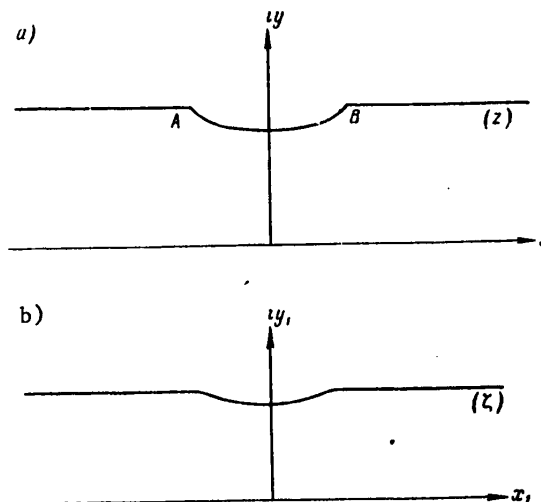

Figure VIII.12. Conformal mapping diagram:
a -- basic diagram; b -- conformal mapping region

Let us perform an additional conformal mapping of the region z_1 (Figure VIII.12a), occupied by the cavity onto the region ζ (Figure VIII.12b) realized by the function [11]

$$w_1 \quad \frac{1}{\pi} \ln \frac{e^{\frac{\pi(l+2a)}{H}}}{\frac{\pi}{\pi} - a} \left\{ 1 - \left[1 - e^{\pi\left(\frac{l+2a}{H} - \zeta \right)} \right]^{\frac{\pi}{n-a}} \right\}^{-1}. \tag{VIII.61}$$

411

Here α is the reduced slope of the wedge, ℓ is the cavity length, a is the length of one wedge, H is the depth of the water.

The function (VIII.61) becomes a rectilinear strip of width H with projected circular lune width $\ell+2a$ and reduced joining angle α to a rectilinear strip of unit width. Here the profile boundary is mapped onto the plane (Figure VIII.12b) in such a way that condition (VIII.60) will be satisfied. The problem reduces to finding the approximate solution of the differential equation of the type

$$\left|\frac{dw_1}{d\zeta}\right|^2 \left|\frac{dw_0}{dz_1}\right|^2 + 2\nu_H \bar{y} = c. \qquad \text{(VIII.62)}$$

where $|dw_1/d\zeta|$ is the modulus of the derivative of the function of conformal mapping of the flow region onto the plane ζ calculated by formula (VIII.61);

dw_0/dz_1 is the modulus of the derivative of the function of conformal mapping of the region ζ obtained when mapping the flow region by the function w_1 onto a rectilinear strip of unit width. Formula (VIII.59) can be used to calculate $|dw_0/dz_1|^2$.

The discussed method of solving the problem is convenient when using computers.

A simpler solution can be obtained if we use the N. Ya. Yakimov theorem [19], according to which the formula of the type of (VIII.59) can also be used in the case where the boundary satisfies the required conditions not on the entire region, but only in a defined vicinity of the investigated point. In this case it is possible to define the velocity caused by the appendages with respect to a linear theory. If we assume that the velocity caused by the appendages is constant along the length of the cavity, the solution to the problem can be obtained in closed form. This is also done below.

The formula for determining the velocity caused only by a wedge, in this case is analogous to formula (VIII.49) and has the form

$$\bar{u}_к = \frac{u_к}{U_0} = \varphi_1 = \frac{u}{\pi} \ln \frac{\operatorname{ch} \pi l_H \bar{x} - \operatorname{ch} \pi l_H \left(\bar{a} + \frac{1}{2}\right)}{\operatorname{ch} \pi l_H \bar{x} - \operatorname{ch} \pi \left(\frac{1}{2} - l_H\right)}. \qquad \text{(VIII.63)}$$

The adopted coordinate system is shown in Figure VIII.11, $u_к$ is the velocity induced by the wedge.

The equation which must be satisfied at the cavity boundary from (VIII.62) assumes the form

$$u_к^2 \left|\frac{dw_0}{dz}\right|^2 + 2\nu_H \bar{y} = c, \qquad \text{(VIII.64)}$$

where $|dw_0/dz|^2$ is the square of the modulus of the derivative of the conformal mapping function for the calculation of which formula (VIII.59) can be used.

The curves for the variation of $\bar{u}_к$ along the cavity length are presented in Figure VIII.13 for different values of ℓ/H. It is obvious that the value of $\bar{u}_к$ varies little with variation of x with the exception of the ends of the interval. Therefore in the first approximation it is possible to make $\bar{u}_к$ constant.

412

If we assume that the velocity caused by the appendages is constant along the cavity length, the solution to the problem can be obtained in closed form.
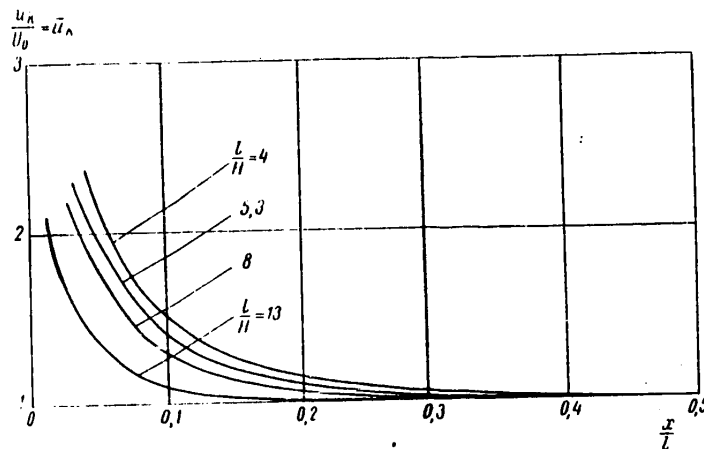

Figure VIII.13. Curves for the variation of $\overline{u}_k = u_k / U_0$ with respect to cavity length for different values of ℓ / H

Let us denote

$$\nu_1 = \frac{\nu_H}{\overline{u}_k^2}; \qquad c_1 = \frac{c}{\overline{u}_k^2}.$$ (VIII.65)

Then it is possible to write equation (VIII.61)

$$\left| \frac{dw_0}{dz} \right|^2 + 2\nu_1 \overline{y} = c_1.$$ (VIII.66)

Now if we substitute the value of $|dw_0/dz|^2$ calculated by formula (VIII.59) in (VIII.66), equation (VIII.66) assumes the form

$$\frac{1}{\overline{y}^2} + \frac{2}{3} \frac{\overline{y}''}{\overline{y}} - \frac{1}{3} \frac{\overline{y}'}{\overline{y}^2} + 2\nu_1 \overline{y} = c_1.$$ (VIII.67)

Let us introduce the notation $\psi = \overline{y}' = d\overline{y}/d\overline{x}$. In this case (VIII.67) is written as follows [17]:

$$\overline{y} \frac{d\psi^2}{d\overline{y}} - \psi^2 = -3 + 3c_1\overline{y}^2 - 6\nu_1\overline{y}^3.$$ (VIII.68)

The common integral of this equation is

$$\psi^2 = 3 + c_0\overline{y} + 3c_1\overline{y}^2 - 3\nu_1\overline{y}^3,$$ (VIII.69)

where c_0 is the integration constant defined in the given case from the condition of takeoff of the cavity from the appendage.

413

By definition $\bar{y}=1+\eta(\bar{x}_\eta)$. Let us substitute this value in (VIII.69), we obtain

$$\psi^2 = 3 + c_0 + 3c_1 - 3v_1 + (c_0 + 3c_1 - 9v_1)\eta + \\ + (3c_1 - 9v_1)\eta^2 - 3v_1\eta^3. \qquad \text{(VIII.70)}$$

The solution to equation (VIII.70) can be expressed in terms of elliptic functions. For this purpose let us represent the righthand side of equation (VIII.70) in the following form:

$$\psi^2 = (\eta - p)(\eta - q)(\eta - r), \qquad \text{(VIII.70a)}$$

where p, q, r are the roots of the polynomial in the righthand side of (VIII.70).

From investigation of equation (VIII.70) it follows that for the existence of the required solution it is necessary that the roots p, q, r be real. One of them is positive, and two are negative. For determinacy $p > q > r$. Then the y-axis of the cavity profile $|\eta| < |q|$.

Since $\psi = \dfrac{d\bar{y}}{dx_H} = \dfrac{d\eta}{dx_H}$, then equation (VIII.70) can be rewritten in the following form:

$$\frac{d\eta}{dx_H} = \sqrt{(\eta - p)(\eta - q)(\eta - r)}. \qquad \text{(VIII.71)}$$

Let us assume that for $\bar{x}_H = 0$; $\eta = q$. This is equivalent to the fact that the y-axis coincides with the axis of symmetry of the cavity.

Performing integration of (VIII.71), we obtain

$$\int_0^{\bar{x}} dx_H = \int_0^{\eta} \frac{dt}{\sqrt{(t-p)(t-q)(t-r)}} = \frac{2}{\sqrt{p-r}} F(\varphi, S), \qquad \text{(VIII.72)}$$

where

$$\sin\varphi = \sqrt{\frac{(p-r)(\eta-q)}{(p-q)(\eta-r)}}; \quad S = \sqrt{\frac{p-q}{p-r}}. \qquad \text{(VIII.73)}$$

Inversion of (VIII.72) gives [13]

$$\varphi = \text{am}\left(\frac{\sqrt{p-r}}{2}\bar{x}_H, S\right), \qquad \text{(VIII.74)}$$

where am is the elliptic amplitude.

From (VIII.73) and (VIII.74) it follows that

$$\sin\left|\text{am}\left(\frac{\sqrt{p-r}}{2}\bar{x}_H, S\right)\right| = \sqrt{\frac{(p-r)(\eta-q)}{(p-q)(\eta-r)}}. \qquad \text{(VIII.75)}$$

414

By definition [13]

$$\sin\left[\operatorname{am}\left(\frac{\sqrt{p-r}}{2}\bar{x}_H\right)\right] = \operatorname{sn}\frac{\sqrt{p-r}}{2}\,\bar{x}_H. \qquad\text{(VIII.75a)}$$

After transformations from (VIII.72), we obtain the following formula for determing the cavity profile:

$$\eta = \frac{q - r\,\dfrac{p-q}{p-r}\operatorname{sn}^2\left(\dfrac{\sqrt{p-r}}{2}\bar{x}_H,\,S\right)}{1 - \dfrac{p-q}{p-r}\operatorname{sn}^2\left(\dfrac{\sqrt{p-r}}{2}\bar{x}_H,\,S\right)}. \qquad\text{(VIII.76)}$$

Calculations of the cavity profiles were made by this formula for Froude numbers with respect to depth Fr_H=0.7, 1.0, 1.1, 1.25 for cavitation numbers σ=-0.2, -0.1, -0.01 for a=0.05. The cavity profiles obtained as a result of the calculation for Fr_H=0.7 are presented in Figure VIII.14. Comparison of the cavity profiles indicates that for variation of the cavity number from -0.1 to -0.01, the cavity length varies little. In addition, the length of the obtained cavity is in this case close to the length obtained from calculations by linear theory. This permits consideration that in the first approximation the cavity length for σ=-0.2 is close to the limiting length. Beginning with this assumption, the dotted curve is used in Figure VIII.15 to plot $Fr_H=U_0/\sqrt{gH}$ as a function of $Fr'_k=U_0/\sqrt{g(\ell_k+2a)}$ by the results of the performed calculations. Comparison of these results with the results calculated by linear theory indicates significant divergence for Fr_H>0.8.

Thus, consideration of nonlinearity of the boundary conditions permits determination of the characteristics of artificial cavities for Fr_H close to and greater than one.
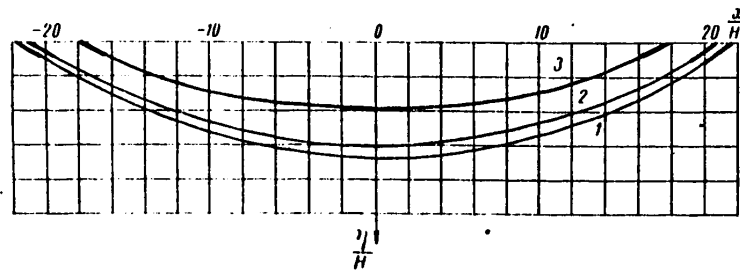

Figure VIII.14. Cavity profiles for $Fr_H=u_0/\sqrt{gh}$=0.7.
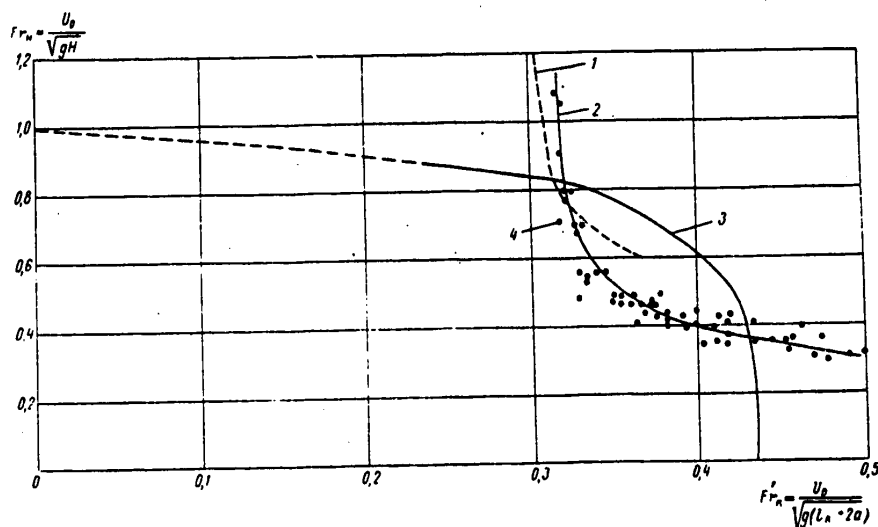1 -- σ=-0.2; L/H=4.35; 2 -- σ=-0.1; L/H=4.19; 3 -- σ=-0.01; L/H=3.58

Figure VIII.15. $Fr_H = u_0/\sqrt{gH}$ as a function of $Fr'_k = U_0/\sqrt{g(\ell_k + 2a)}$.
Comparison of theoretical and experimental results.
1 -- nonlinear theory; 2 -- experiment; 3 -- linear theory;
4 -- experimental points

Comparison of Theoretical and Experimental Results. An experimental study was made of the shapes and dimensions of artificial cavities in a bounded flow in a flume in order to check out the theoretical conclusions. The experimental conditions corresponded to a high degree to the prerequisites set down as the basis for the theoretical study (horizontal plate, plane flow).

The cavity was created on the lower side of a rectangular channel, the height of which could be varied. The channel height variation offered the possibility of investigating the formation of cavities with different channel restrictions.

A wedge 2 mm high and 12 mm long was used to form the cavity.

During the experiment the following values were measured: the flow velocity, pressure in the cavity, air flow rate to form the cavities, shape and dimensions of the cavities.

The tests were performed for the following channel depths: H=23.5, 15.5, 11.5, 7.5, 3.5 cm.

The experiments demonstrated that with variation of the cavitation number (an increase in the air flow rate) for fixed channel depth, the cavity thickness increases, and when reaching the limiting thickness, the cavity exists without an appendage, moving ahead against the flow, or it is arranged so that the appendage is in its midsection.

416

Comparison of the tests obtained for different channel depths indicates that the general nature of the influence of the cavitation number is retained for all constrictions of the flow. With a decrease in channel depth, the relative thickness of the cavity which takes off the appendage decreases significantly.

Analysis of the experimental data demonstrated that the Froude number calculated by the cavity length $Fr_\ell = U_0/\sqrt{g\ell}$ for given ℓ/H remains constant.

A comparison of the theoretical and experimental results is presented in Figure VIII.15 on which the theoretically and experimentally obtained curves for the variation of the Froude number with respect to channel depth $Fr_H = U_0/\sqrt{gH}$ are plotted as a function of the Froude number with respect to limiting cavity length $Fr_k = U_0/\sqrt{g(\ell_k + 2a)}$.

From Figure VIII.15 it is obvious that the theoretical results correctly reflect the nature of the influence of the limited nature of the flow and the artificial cavity parameters.

The conclusions obtained as a result of the theoretical study offer the possibility of analyzing the experimental data. Thus, theory demonstrated that for a cavity of limiting length variation of the cavitation number only leads to variation of its thickness. When performing tests in a flume, the form of the cavity was close to limiting. This made it possible to obtain the universal function $Fr_k = f(Fr_H)$ for the cavities presented in Figure VIII.15.

The results of measuring the air flow rated used for cavity formation demonstrated that with a decrease in channel depth the air flow rate increases somewhat with an identical value of σ/α.

§VIII.4. Results of Experimental Studies of the Creation of Artificial Cavities (Gas Films) on Flat-Bottomed Model Ships

Results of Experiments with a Schematized Model. The primary goal and content of the experimental studies performed by A. A. Butuzov, the results of which are discussed below, was to study the physical laws determining the shape and dimensions of gas films -- artificial cavities -- on the bottom of a model ship by injecting air and comparison of the theoretical and experimental data.

The test object was a schematized model on which the main part of the bottom was made of plexiglass.

The model had straight-wall symmetry with respect to the midstation form. A third of the model was occupied by a cylindrical insert, and the forward and aft branches of the water line were given by a second-degree parabola.

The primary dimensions of the model were as follows: maximum displacement $V_m = 0.499$ m^3, length between perpendiculars $L_m = 6.0$ meters, extreme beam $B_m = 0.60$ m, extreme draft $T_m = 0.18$ m.

A single cavity was investigated on the schematized model. A coordinate grid was plotted on plexiglass on the bottom of a model on the outside for determination of the cavity (gas film) dimensions in plan view during observations from the .

towing cradle. For uniform air distribution at its emission point along the width of the model, metal boxes were installed on the model (Figure VIII.16). The lower part of the box was in the form of two horizontal sheets separated in the transverse direction by a slot which was covered by a wedge-shaped appendage and could be covered by a plank flush with the bottom. In order to prevent surfacing of the air along the sides, vertical keels were installed on the bottom of the model which were arranged parallel to the fore-and-aft plane of the model at a distance equal to the slot length from each ·other. The keels installed on the model were 2.55 m long, 50 and 25 mm high. The distance between the forward edge of the keel and the forward perpendicular of the model was 1.7 meters. The distance between keels was 0.5 meters, the distance from the slot to the forward perpendicular was 1.85 meters.

During the tests the following measurements were taken: the towing speed, the towrope drag of the model, the trim of the model, gas film dimensions in plan and amount of injected air, pressure in the gas film by gauges and also observation and photographing of the gas film through the plexiglass keel using a hydroperiscope.
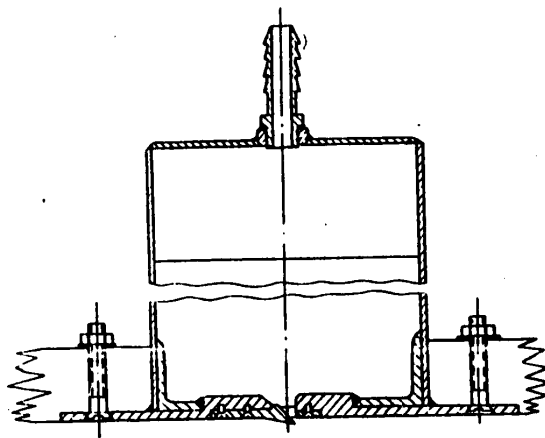

Figure VIII.16. Schematized model for investigating a single cavity

The model was also tested with a blind slot, with and without keels.

The experimental observations demonstrated the following:

a) An artificial cavity (gas film) has a clearly outlined rear boundary and retains its shape and dimension stably. Inside the gas film the pressure is almost constant. This indicates similarity between gas films and artificial cavities.

Additional proof of the correctness of this conclusion is the fact that at model towing speeds of $U_0=3$ m/sec and higher, it was possible to distinguish the "reentrant jet" known from observations of cavitating flows, the spray from which fanned out in the direction of the lateral keels.

418

The air from the gas film was removed in two sheets adjacent to the lateral keels;

b) The formation of a stable gas film depends to a significant degree on the presence of an appendage. The slot turned out to be ineffective without the appendage, for the gas film did not form behind it with small air flow rates;

c) The experiments confirmed the theoretical conclusion of the existence of a limiting Froude number for a gas film which does not depend on the dimensions of the appendage or the amount of injected air. At slow speeds of the model, the limiting Froude number of the gas film $Fr_k = U_0 / \sqrt{g \ell_k}$ according to the experimental data was close to the theoretical value of $Fr_k = 0.423$, and $Fr_k = 0.475$ obtained experimentally in a flume;

d) The air flow rate in the presence of an appendage ahead of the slot had in practice little influence on the gas film thickness. In the absence of an appendage, the air flow rate has a significant influence on the thickness of the gas film. According to the theoretical conclusions, the thickness of the gas film is proportional to the appendage height;

e) The presence of a gas film leads to planing-up of the model and increased trim by the stern;

f) The greatest drag reduction for the model with respect to the bare hull drag was from 10 to 20%, depending on the draft of the model.

Results of Experiments with River Boat Models. The test subjects were models of the "Bol'shaya Volga" class vessel and the design 461b barge. The primary purpose of the tests was to investigate the drag of a vessel in the presence of gas films on the bottom.

Analysis of the test results led to the following conclusions.

1. At high flow rates, the gas is removed from the gas films in the form of two sheets adjacent to the parts of the model bottom close to the sides. The sheet width essentially depends on the towing speed. Near the calculated speed the sheets are comparatively narrow. With a decrease in speed, the air sheets gradually expand, they approach the center line of the bottom, and the air escapes from the gas film in the form of formless "chunks" primarily just as in the case of the schematized model.

2. The air flow rate in practice has little influence on the gas film dimensions.

3. Experiments confirmed the previous conclusion of the existence of a limiting Froude number with respect to the length of the gas film Fr_ℓ. This is obvious from Figure VIII.17 in which the relation is presented for the Froude number Fr_ℓ as a function of velocity for different values of the air flow rate, for two models of different scales (1:10 and 1:20).

4. In all cases air injection leads to a decrease in the towrope drag. The relative drag reduction of a model of the "Bol'shaya Volga" ship (by comparison with bare hull drag) for model speeds corresponding to actual speeds, is 9 and 8.5%

419

for a flow rate of Q=8.5 ℓ/sec. Drag reduction of the model reduced to the drag of a model with side keels and blind slots is 13%.

It must be noted that the version of formation of gas films on the bottom of a model of the "Bol'shaya Volga" was not optimal. As further experimental studies have demonstrated, by developing hydrodynamically optimal dimensions of the appendages forming the gas films and finding the most efficient method of air injection under the bottom of the ship, the gain in drag of the model can be increased significantly at the calculated speed.
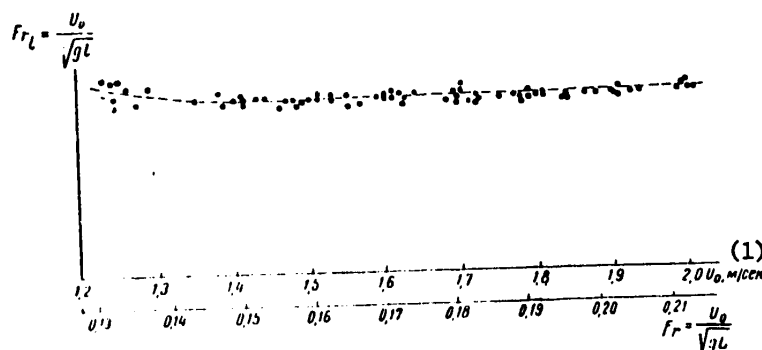

Figure VIII.17. Froude number $Fr_\ell = U_0/\sqrt{g\ell}$ as a function of the speed of a model U_0 for different air flow rates Q

Key:
   1. m/sec

Figure VIII.18 shows the towrope drag curves for a model of the design 461-B barge on which the devices creating the gas film system were selected optimal by the model test results. The upper curve pertains to a model with appendages shaping the gas films in the absence of air injection at the bottom of the model; the curve located below pertains to a model with a bare hull. The lower curves were obtained for different air flow rates. In the figure it is obvious that at the calculated speed, the gain in model drag in practice does not depend on the flow rate and reaches 18-22% of the bare hull drag. For speeds less than the calculated speed, increasing the air flow rate leads to an increased gain with respect to drag, which is explained by the presence of air sheets behind the gas films, the width of which depends essentially on the air flow rate and towing speed of the model.

Influence of Shallow Water on the Drag of a Ship Equipped with a Device to Create a Gas Film System. In order to check the possibility of air lubrication for a ship moving under restricted waterway conditions and to check the theoretical results, tow tests were run on a model of the design 461 B barge under shoal conditions (H/T=2.0; H is the basin depth; T is the draft of the ship).
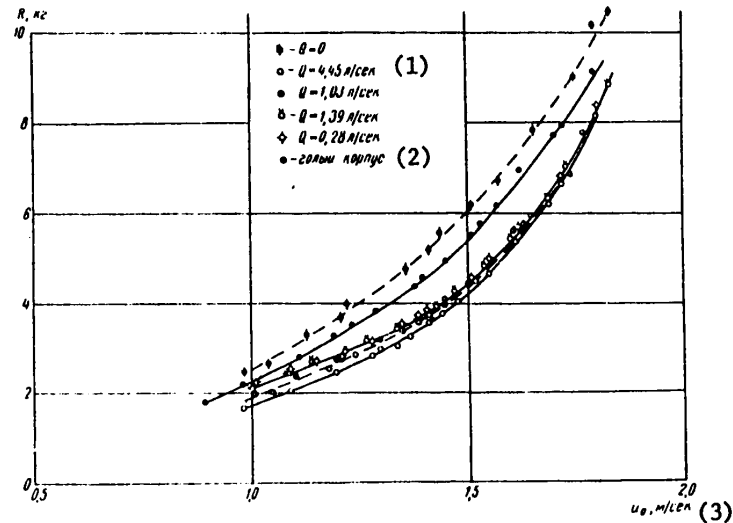
Figure VIII.18. Curves for the towrope drag of a design 461B
model for different air flow rates Q

Key:

1. ℓ/sec
2. bare hull
3. m/sec

The model test results demonstrated that the air flow rate has little influence on
the cavity length, and they confirmed the theoretical conclusion of the presence
of a limiting cavity length.

The results of the tests to measure cavity lengths were processed by constructing
a relation for the Froude number calculated by the cavity length $Fr_k = U_0/\sqrt{g(\ell_k+2a)}$
as a function of the Froude number $Fr'_H = U_0/\sqrt{g(H-T)}$. The indicated function is
presented in Figure VIII.19. Comparison of Figures VIII.19 and VIII.15 obtained
by the theoretical data indicates satisfactory qualitative agreement between the
theoretical and experimental results.

Model tests to measure the towrope drat and air flow rate for H/G=2-0 are presented
in Figure VIII.20, and they demonstrated that the greatest gain with respect to
drag under shoal conditions is less than under deep water conditions, and it is
reached at the lower speed. This is explained by the fact that the cavity length
under shoal conditions increases more rapidly, and the bottom of the model is
completely covered with air lubrication at lower speed (U_0=1.15 m/sec) than under
deep water conditions (U_0=1.40 m/sec).

If we compare the values of the dimensionless drag reduction factor (Figure VIII.21)

$$\Delta C_x \quad \frac{2\Delta R}{\rho U_0^2 LB} - \frac{2(R - R_{Q=0})}{\rho U_0^2 LB},$$

it is possible to note that the value of ΔC_x in deep

water at a speed of U_0=1.40 m/sec differs insignificantly from the value of ΔC_x
under shoal conditions at a speed of U_0=1.15 m/sec. Here $\Delta R = R - R_{Q=0}$ the difference
between the model drag with air lubrication and drag for Q=0.

427

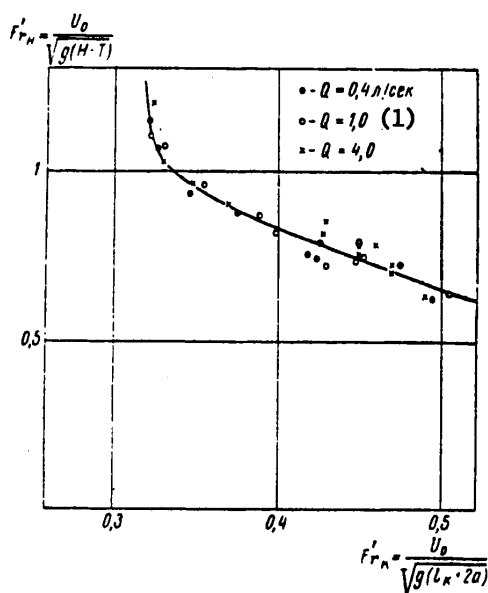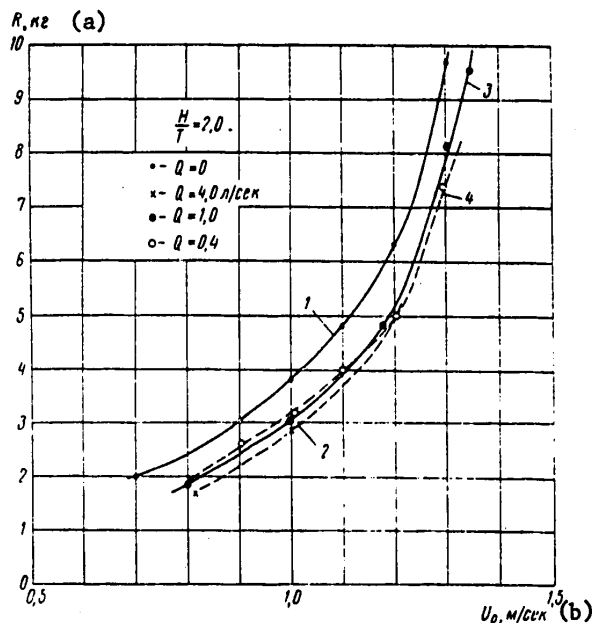Figure VIII.19. Experimental dependence of

$$\mathrm{Fr}'_{\text{н}} = \frac{U_0}{\sqrt{g\,(H-T)}} \qquad \text{on} \qquad \mathrm{Fr}'_{\text{к}} = \frac{U_0}{\sqrt{g\,(l_{\text{к}} - 2a)}} .$$

Key:
1. ℓ/sec

Figure VIII.20. Towrope drag curves for H/T=2.0.
1 -- without lubrication; 2, 3, 4 -- with lubrication
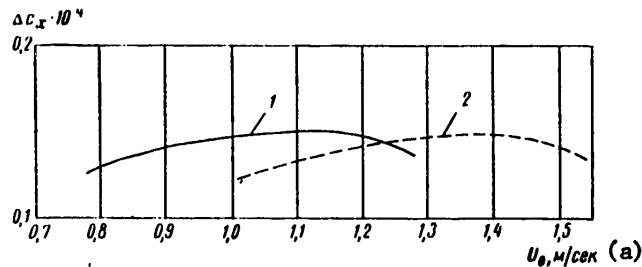
Key:
a. R, kg; b -- m/sec

Figure VIII.21. Effect of shoal water on drag reduction
1 -- for H/T=2; 2 -- in deep water

Key:
    a. m/sec

§VIII.5. Estimation of Drag Reduction of a Ship Equipped with a Device for Creating Artificial Cavities (Gas Films) on its Bottom by Model Test Data

Let us discuss an approximate method of calculating the drag reduction of a ship with a system of gas films arranged on its bottom. This method is based on the assumption that the effectiveness of the device providing for frictional drag reduction of a ship will be unchanged for a model and a full-scale ship with identical Froude numbers [27].

By the efficiency of the device creating the gas film system on the bottom of a model, we mean the ratio

$$k = \frac{\Delta R_m}{\Delta R_0}.$$ (VIII.77)

Here ΔR_m is the experimentally obtained gain with respect to drag;

ΔR_0 is the ideal gain with respect to frictional drag which can be obtained by calculating if we assume that the appendage drag is equal to zero and that the air cov rs the entire flat part of the bottom.

The value of ΔR_0 is constant for given velocity, and it is found as the difference between the frictional drag of a plate with a length equal to the distance between the forward and aft perpendiculars of the model and beam equal to the distance between the side keels and total drag of two plates separated by a solid gas film.

The results of calculating the efficiency $k=\Delta R_m/\Delta R_0$ for the 461 B barge model are presented in Figure VIII.22. It is obvious that the highest efficiency of the device corresponds to speeds close to the calculated speed for which the gas films cover the greatest part of the bottom. It is obvious that the efficiency k, which contains the experimental value of ΔR_m in the numerator takes into account the influence of the appendage drag on the efficiency of the device and also the influence of escape of air from the gas films.
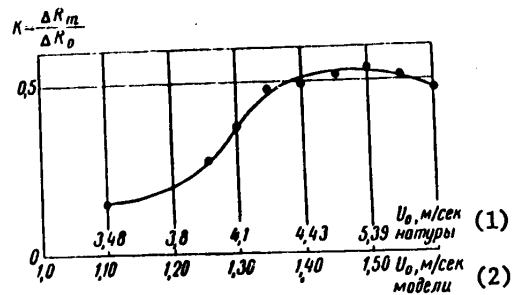
423

Figure VIII.22. Efficiency of air lubrication for the 461 B barge model

Key:
1. U_0, m/sec, full-scale
2. U_0, m/sec, model

An approximate estimate of the gain with respect to drag of a full-scale vessel can be made by the formula

$$\Delta R = k\Delta R_f + \zeta_{\text{rough}} \frac{\rho}{2} \cdot U_0^2 S_0. \tag{VIII.78}$$

Key: 1. rough

Here ΔR_f is the "ideal" gain with respect to frictional drag calculated for a full-scale vessel;

S_0 is the bottom area in the vicinity of the parallel middle body of a ship covered with air;

ζ_{rough} is the roughness factor of the skin of a ship's hull.

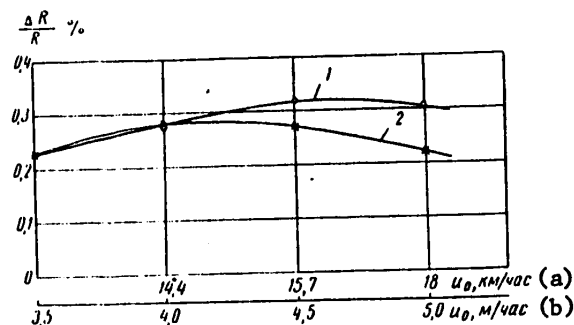The value of ΔR_f is calculated under the same assumptions as for the case of an "ideal" gain ΔR_0 on a model.

Figure VIII.23. Gain with respect to drag.
1 -- calculation; 2 -- full-scale

Key:
a. km/hr; b. m/hr

424

The results of calculating the expected absolute gain with respect to drag
ΔR with respect to the bare hull towrope drag of the 461 B barge are presented in
Figure VIII.23. It is obvious that the expected drag reduction with respect to
the towrope drag of the barge (curve 1) is 22-32% -- in the barge speed range of
3.5-5.0 m/sec (12.5-18 km/hr).

A full-scale test of the effectiveness of the drag reduction of a barge equipped
with a device creating a system of air cavities on its bottom was performed in
the Kuybyshev Reservoir on the Volga in May-June 1965 [27].

Figure VIII.24 shows the results of full-scale testing of the 461 B barge in the
form of the towrope drag curves for the barge. The middle curve corresponds to
the bare hull towrope drag in the presence of a pusher boat, the lower curve was
obtained when pushing the barge with simultaneous injection of air on its bottom.
The upper curve corresponds to the towrope drag with appendages with which the
barge is equpped to create an air lubrication system.

From a comparison of the curves presented in Figure VIII.24 it is obvious that the
application of air lubrication on the bottom of the 461 B barge led to total drag
reduction of the barge on the order of 23-25% of the bare hull drag in the speed
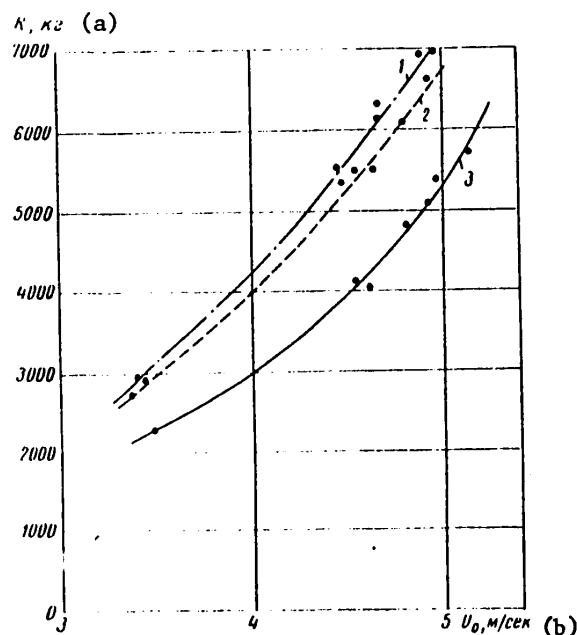range of 11-18 km/hr.

Figure VIII.24. Results of full-scale testing of the 461 B barge
1 -- hull with appendages; 2 -- bare hull; 3 -- hull equipped with
an air lubrication system
Key:
   a -- R, kg; b -- m/sec

425

Hence, it is possible to draw the conclusion that the full-scale tests demonstrated the efficiency of using air lubrication for drag reduction of flat-bottomed heavy-cargo river vessels.

Figure VlII.23 shows a graph of the drag reduction reduced to the bare hull drag (curve 2) constructed using curves presented in Figure VIII.24, obtained as a result of analyzing the full-scale tests. Comparison of curves 1 and 2 demonstrates satisfactory correspondence between the calculated value of the gain with respect to drag and its value obtained from the full-scale testing in the speed range of 11-18 km/hr.

§VIII.6. Results of Investigating Artificial Cavities Created on the Bottom of Planing Vessels

In the preceding sections a study was made of the problems pertaining to the case of creating artificial air cavities on the flat bottom of slow superships having large parallel middlebody. The application of air lubrication for these vessels, in which the frictional drag is a significant part of the total drag, turns out to be most efficient. Another class of ship in which it is possible to expect drag reduction of the water as a result of artificial cavities is planing vessels. Planing vessels have frictional drag of about 60% of the total drag. The experiments performed by a collective of authors directed by I. T. Yegorov [23], [24] demonstrated that it is possible to achieve effective frictional drag reduction on shallow-draft planing vessels by injecting air behind the step, that is, by creating an artificial cavity on the bottom.

For planing vessels the conditions of creating air cavities differ significantly from the conditions for slow superships.

In the investigated case of a high-speed vessel the cavity parameters are significantly influenced by the conditions of motion, closeness of the free surface of the water, variable trim of the vessel, bottom shape as a whole and center of gravity position.

Results of a Theoretical Study of Artificial Cavities Created on a Planing Surface. In order to discover the laws of formation of an artificial air cavity on a planing surface A. A. Butuzov solved the two-dimensional linearized problem of cavitating flow in the case of cavity formation on a body planing over the free surface of a fluid with weight [20]. This problen is solved under assumptions with respect to the fluid and the nature of its motion made for the solution of analogous problems presented in §VIII.2.

The planing surface (Figure VIII.25) CDEE'HJ' consists of three rectilinear segments CD, DE, HJ and the section EE'H of arbitrary shape located inside the cavity. The free surfaces ahead of and behind the planing body can be considered as surfaces of cavities of great extent, the pressure on which is given ($\sigma=0$). Accordingly, they can be taken as bounded, semi-infinite, horizontal plates A'A and KK'. These surfaces have been introduced in order not to investigate free surfaces of infinite length, the introduction of which leads to great difficulties for numerical calculations.

426

Figure VIII.25. Diagram of a planing surface with cavity:
a -- general diagram; b -- simplified diagram; c -- system without
a cavity.

The vertical position of a planing body and the position of the fictitious horizontal surface KK' must be determined from solution of the problem inasmuch as they depend on the given pressure on the free surfaces.

In Figure VIII.25, BC, GH and IK denote fictitious planes, the inclination of which is selected so as to insure smooth closure of the free surfaces AB, JI and the cavity surface EG. The distances between the points A and B, J and I are assumed to be selected quite large, and the dimensions of the plates BC and GH so small that the adopted schematization of the flow insures absence of influence on the cavity parameters and pressure distribution with respect to the planing surface,

427

]

excluding small vicinities of the points C and H. The fictitious plates GH, JI are equivalent with respect to their purpose to the fictitious bodies used for closure of cavities in the Ryabushinskiy type systems. The sum of the horizontal components of the pressure forces acting on the plates BC and GH corresponds with respect to magnitude to the spray drag of a planing surface with cavity. Let us present a solution of the stated problem according to the paper by A. A. Butuzov.

Derivation of the equations of the problem does not differ from the derivation given in §VIII.2. The equations are a system of integrodifferential equations with respect to the contours of the free current lines $y=\eta^{(i)}(x)$ (i=1, 2, 3, — see Figure VIII.25a):

$$f\eta^{(k)}(x) + \frac{1}{\pi} \sum_{i=1}^{3} \left\{ \int_{R_{0,i}}^{R_{1,i}} \frac{\frac{d\eta^i}{d\xi} d\xi}{\xi - x} + \ln\left|\frac{R_{1,i} - x}{R_{2,i} - x}\right| \beta_i \right\} +$$

$$+ \frac{1 \pm (-1)^k}{4} \sigma = \frac{1}{\pi} \left\{ \sum_{i=1}^{2} \ln\left|\frac{R_{2,i} - x}{R_{0,i+1} - x}\right| \alpha_i + \right.$$

$$\left. + \ln\left|\frac{R_{2,1} - x}{R_{0,2} - x}\right| (\alpha_1^* - \alpha_1) \right\}.$$

(VIII.79)

Here

$$R_{0,k} < x < R_{1,k}; \quad k = 1, 2, 3.$$

$$f = \frac{1}{F_L^2} = \frac{gL}{U_0^2}; \quad \sigma = \frac{2(p_0 - p_K)}{\rho U_0^2};$$

L is the characteristic line dimension taken as the unit length; hereafter $L = R_{0,3} - R_{2,1}$.

The functions $\eta^{(i)}(x)$ must also satisfy the following ten conditions:

$$\frac{d}{dx} \eta^{(1)}(R_{0,1}) = 0; \quad \frac{d}{dx} \eta^{(1)}(R_{1,1}) = -\beta_1;$$

$$\frac{d}{dx} \eta^{(2)}(R_{0,2}) = \alpha_1^*; \quad \frac{d}{dx} \eta^{(2)}(R_{1,2}) = -\beta_2;$$

$$\frac{d}{dx} \eta^{(3)}(R_{0,3}) = \alpha_2; \quad \frac{d}{dx} \eta^{(3)}(R_{1,3}) = -\beta_3;$$

$$\eta^{(1)}(R_{0,1}) = 0;$$

$$\eta^{(1)}(R_{1,1}) - \beta_1 b_1 + \alpha_1 a_1 + \alpha_1^* a_1^* = \eta^{(2)}(R_{0,2});$$

$$\eta^{(2)}(R_{0,3}) + \Delta = \eta^{(2)}(R_{1,2}) - \beta_2 b_2;$$

$$\eta^{(2)}(R_{1,2}) - \beta_2 b_2 + \alpha_2 a_2 = \eta^{(3)}(R_{0,3}).$$

(VIII.80)

The parameters β_1, β_2, β_3 and are unknowns in the relations (VIII.79) to (VIII.80).

Equations (VIII.79) were solved approximately. For this purpose in the intervals $\xi_i^{(k)} < x^{(k)} < \xi_{i+1}^{(k)}$, $i=0,1,\ldots,r-1$ ($r=m$ for $k=1$, $r=n$ for $k=2$, $m=p$ for $k=3$

$R_{0,k} = \xi_0^{(k)} \xi_1^{(k)} < \ldots < \xi_r^{(k)} = R_{1,k}$, the functions $q^{(k)} = (d/dx)\eta^{(k)}$ were approximated by segments of straight lines continuously conjugate to each other and satisfying the first six conditions of (VIII.80).

For the corresponding approximation of the functions $\eta^{(k)}(x)$, the 7th, 8th and 10th conditions of (VIII.80) were satisfied. As a result of satisfaction of expression (VIII.79) at the points $x_i^{(k)} = (1/2)(\xi_i^{(k)} + \xi_{i+1}^{(k)})$, a system of linear algebraic equations was compiled. The system consisted of m+n+p equations and contained m+n+p+1 unknowns:

$$q_1^{(1)}, \ldots q_{m-1}^{(1)}, \ q_1^{(2)}, \ldots q_{n-1}^{(2)}, \ q_1^{(3)}, \ldots q_{p-1}^{(3)}, \ \beta_1, \ \beta_2, \ \beta_3, \ \sigma.$$

Another, missing equation, followed from the 9th condition of (VIII.80).

The system of linear algebraic equations was solved on the M-20 digital computer.

For efficient use of computer engineering and in order to obtain good approximation in the segments of the free surface outside the planing plate, the breakdown points of the intervals were selected so that near solid walls the intervals form portions of the length of the nearest elements of these walls, and they increase more and more on going away from the solid surfaces, remaining, however, less than some segment in which the segment of sinusoidal profile of the wave can be sufficiently satisfactorily approximated by a segment of a second-degree parabola.

After solution of the system of linear equations, all the necessary values are defined.

The component of the lift factor for the given flat bottom segment

$$\Delta C_y = \frac{2\,\Delta Y}{\rho U_0^2 L} = \int \Delta p(x)\,dx. \tag{VIII.81}$$

Here Δp is the pressure acting on each flat segment of the bottom which water flows over,

$$\Delta p = \frac{2(p - p_0)}{\rho U_0^2} = \Delta p_1 + 2f\eta(x).$$

The pressure Δp consists of two components: the hydrodynamic pressure Δp_1 and hydrostatic pressure $2f\eta(x)$. The hydrostatic pressure can be found in terms of the planing-up of the rear edge of the body (α=const). The hydrodynamic pressure is defined in terms of the density of all sources

$$\Delta p_1 = \frac{1}{\pi} \int_{R_{0,1}}^{R_{1,1}} \frac{\eta'(\xi)\,d\xi}{x - \xi}. \tag{VIII.82}$$

In this equation $\eta=\eta(\xi)$ is the boundary current line equation, that is, the equation of solid and liquid boundaries investigated in the set.

When calculating the hydrodynamic pressures acting on the given two-dimensional segment, the integral (VIII.82) is split in two, one of which corresponds to all solid boundaries, and the other, to free current lines. The use of the selected approximation $\eta'(\xi)$ by a broken lines makes the integral (VIII.82) a table integral.

A component of the residual drag coefficient is expressed in terms of

$$\Delta C_x \approx \Delta C_y \alpha_i. \tag{VIII.83}$$

where α_i is the angle of attack of the investigated segment of the bottom.

The coefficients C_x, C_y are determined as a result of summing the individual components ΔC_x and ΔC_y for the flat segments of the bottom and the section covered by the cavity.

The segments R_{11}, R_{21} and $R_{12}R_{22}$ are investigated only when calculating the wave drag.

In order to check the efficiency of the applied system, calculations were made for a planing plate without cavity (Figure VIII.25c), and they were compared with the available results for a plate presented in the paper by L. I. Sedov [14]. The comparison demonstrated good coincidence.

By the results of solving the obtained system of algebraic equations, the y-axes of the free boundaries of the cavity and also C_x, C_y and the distance of the pressure center from the trailing edge of the planing surface, and the dimensionless values ℓ_g/L were calculated.

Let us present some results of numerical calculations obtained by A. A. Butuzov using the M-20 digital computer.

Calculations of flow over a planing surface with cavity were performed for the simplest shape of planing surface $\gamma/\alpha=0$; $\psi/\alpha=0$ (the values of γ, ψ and α are presented in Figure VIII.25b). The results of these calculations for the case of $L_1=0.2L$; $\ell_k=0.6L$; $b_2=0.005L$; $F_L=U_0/\sqrt{gL}=3.0$ are presented in Figure VIII.26 in the form of curves for the values of ω/α, σ/α, c_y/α, ℓ_g/L, C_x/C_y^2 as a function of the parameter $h/\alpha L$ characterizing the step height. In Figure VIII.26 these curves are denoted by 1,2,3,4,5, respectively. The angle between the actual plate closing the cavity and bottom line $\omega=\alpha+\beta_2+\psi$ is denoted by ω, and the curve C_x/C_y^2 was obtained for L=const.

430
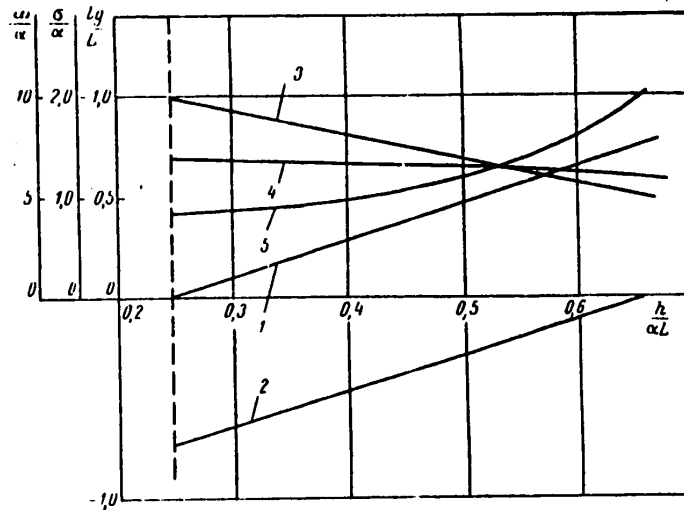
Figure VIII.26. Values of ω/α, σ/α, ℓ_g/L, C_y/α, C_x/C_y^2 as a function of the parameter $h/\alpha L$. The scale of C_x/C_y^2 coincides with the scale of ℓ_g/L, and C_y/α, with σ/α

The vertical dotted line shown in Figure VIII.26 corresponds to the limiting value of $h/\alpha L = 0.2473$ ($\omega = 0$), for when $h/\alpha L < 0.2473$ the cavity outline intersects the bottom line ($\omega < 0$). The value of $h/\alpha L = 0.6548$ ($\sigma/\alpha = 0$) corresponds to the case of an ordinary stepped craft.

From the curve $C_x/C_y^2 = f(h/\alpha L)$ characterizing the variation of the drag R for constant vertical load (p=const) as a function of $h/\alpha L$, it follows that in the limiting case of smooth closure of the cavity ($h/\alpha L = 0.2473$; $\omega = 0$), the planing surface has minimum pressure drag. This drag is 2.36 times less than the drag experienced by an ordinary stepped craft. The condition $\omega = 0$ is the most favorable, for under this condition, expenditures of power on injecting gas into the cavity are theoretically not required, and these conditions can be insured (as follows from the graph of $C_y/\alpha = \Phi$ ($h/\alpha L$)) for p=const as a result of a decrease in the ordinary step height ($\sigma = 0$) and a shift of the load toward the bow.

According to Figure VIII.26, for transition from the case of $\sigma = 0$ to the case of $\omega = 0$ with p=const, the step height must be decreased by 80%, and the load center of gravity shifted 15% toward the bow.

As the calculations demonstrated, these conclusions are qualitatively valid for Froude numbers no less than one. With an increase in the velocity ($F_L > 1$), a cavity that closes smoothly to the bottom formed on a planing surface of given shape and dimensions with fixed load (p=const, ℓ_g/h:ℓ/L=const), becomes elongated. The angle of attack of a planing surface decreases in this case, and the wetted length ahead of the cavity increases somewhat.

The influence of the shape of the bottom of a planing surface on its lift-drag ratio in the case of a cavity smoothly closed on the bottom ($\omega = 0$) was investigated by performing numerical calculations for different values of γ/α, h/α, ψ/α and $F_L = 3$.

431

The calculations demonstrated that an ordinary appendage ($h=\psi=0$) installed on a flat bottom ($h=\psi=0$) favorable for slow vessels is not favorable for high-speed draft for which the favorable bottom shape from the point of view of drag reduction R is the shape with a bottom fold after the step ($\psi>0$).

Shape and Size Control of an Artificial Cavity. The application of artificial air cavities on the bottom of planing vessels for frictional drag reduction is connected with certain difficulties related to the fact that for simple bottom shapes, the cavity length at high speeds becomes appreciably greater than the possible dimensions of the vessel. Accordingly, it becomes necessary to alter the shape of the cavity so that it will close on the bottom of the vessel.

It is known that in the case of detached cavitating flow over bodies in real fluids the main part of the energy expended on the motion is expended in the tail section of the cavity. Here, nonsteady closure of the cavity is observed as a result of pulsation of its tail section accompanied by escape of gas from the cavity in the case of artificial cavitation. For usual nonsteady closure of a cavity, the gas flow rate can be large, and it is possible for gas to get into the propulsion unit.

Accordingly, recently efforts have been made to find methods of controlling the shape and size of an artificial cavity which will insure smooth closure of the jets in the tail section of the cavity and minimum (theoretically zero) gas consumption.

Smooth closure of the jets can be accomplished with negative cavitation number in the tail of the cavity [21] or considering the fact that the fluid has weight (limiting cavities investigated in §VIII.2).

As was demonstrated above, for planing vessels it is possible to control the cavity by appropriate selection of the form of the planing surface. A deficiency of this method of artificial cavity control is that it operates efficiently only at calculated speed. For speeds less than calculated speed, the closure of the cavity will not be smooth.

Therefore the problem arises of finding methods of shape and size control for an artificial cavity which will permit cavitating drag reduction and reduction of gas consumption to a minimum in the largest possible range of speeds.

Noncavitating foils in the tail section of the cavity can be used as one such means [25].

In order to discover the basic qualitative laws, V. I. Migachev solved the two-dimensional problem of unbounded jet flow of an ideal weightless fluid over a wedge in the presence of vortices simulating noncavitating foils, and he investigated the condition under which smooth closure of the cavity takes place. As a result of solving this problem, the theoretical possibility of controlling the cavity characteristics by noncavitating foils was demonstrated (Figure VIII.27).

The solution to the problem of symmetric flow over a wedge in the presence of vortices obtained by V. I. Migachev [22] is also presented below.

Let us consider an unbounded flow of ideal weightless fluid over a wedge in which vortices with an intensity of $+\Gamma$ and $-\Gamma$, respectively, are located at the points z_f and $\bar{z}_f$ (Figure VIII.28). The wedge has an angle of taper of $2\pi\alpha$ and web length of 1. The velocity at infinity is 1 and is directed along the x-axis. The cavitation number is σ.
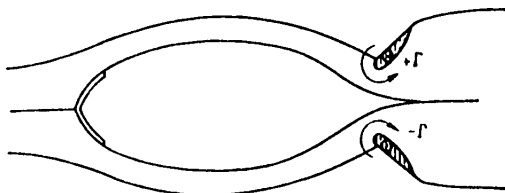

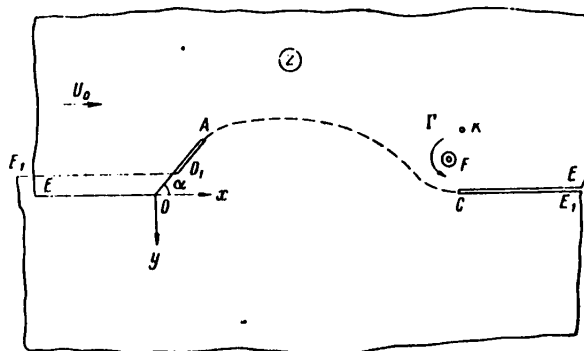Figure VIII.27. Diagram of cavity control using noncavitating foils

Figure VIII.28. Symmetric flow over a wedge in the presence of vortices

In the investigated case of flow with symmetry, the real axis is the current line and can be considered a solid wall. Therefore it is possible to consider only the upper half of the flow. The problem is solved by the method of continuation through the free current line (the Schiffman method) [21].

On the auxiliary plane u (Figure VIII.29) the real axis is an image of the solid boundary and physical plane, and the imaginary axis is an image of the free current line.

For solution of the problem it is sufficient to define

$$\frac{dz}{du} = F_1(u); \quad \frac{dw}{du} = F_2(u),$$

where $w_{(z)} = \phi + i\psi$ is the complex potential of the total induced velocity.

.433

Let us find the function dz/du. At the points K_1 and $\overline{K}_1$ ($u=k_1=-m+in$; $u=\overline{k}_1=-m-in$) the function z(u) has third-order nulls, and at the points F_1 and $\overline{F}_1$ ($u=f_1=-c+id$ and $u=\overline{f}_1=-c-id$), simple poles.

Applying the Schwartz-Christoffel formula to the polyhedron $EOAO_1E_1CE$, we have

$$\frac{dz}{du} = \frac{c_1}{v_K}\left(\frac{u+u}{u-a}\right)^u \frac{(u-\bar{k}_1)^2(u-k_1)^2 u}{(u-f_1)^2(u-\bar{f}_1)^2(u^2-1)^2};$$

$$z(u) = \int_a^u \frac{dz}{du}\,du,$$

(VIII.84)

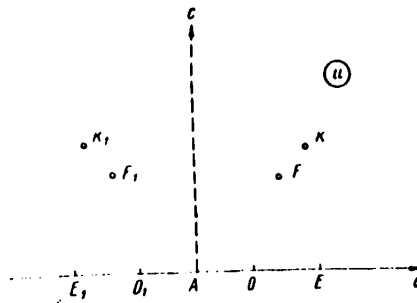where $v_k=\sqrt{1+\sigma}$ is the velocity at the cavity boundary.

Figure VIII.29. Auxiliary cavity

The function dw/du has zeros at the points K, $\overline{K}$, K_1 and $\overline{K}_1$, and simple poles at the points F, $\overline{F}$, F_1, $\overline{F}_1$. Taking this into account, analogously to the preceding, we have

$$\frac{dw}{du} = c_1 \frac{(u-k)(u-\bar{k})(u-k_1)(u-\bar{k}_1)u}{(u-f)(u-\bar{f})(u-f_1)(u-\bar{f}_1)(u^2-1)^2}.$$

(VIII.85)

From formulas (VIII.84) and (VIII.85) we determine the complex velocity

$$\frac{dw}{dz} = v_K\left(\frac{u-a}{u+a}\right)^u\left(\frac{u-k}{u-k_1}\right)\left(\frac{u-\bar{k}}{u-\bar{k}_1}\right)\left(\frac{u-f_1}{u-f}\right)\left(\frac{u-\bar{f}_1}{u-\bar{f}}\right).$$

(VIII.86)

Formulas (VIII.84)-(VIII.86) give the general solution of the problem.

The following coefficients are unknown: c_1, a, m, n, c, d defined by the conditions of the problem.

In order to determine these coefficients we have the following system of equations:

$$z(0) = e^{-iu\pi};$$

(VIII.87)

$$\frac{dw}{dz}(1) = 1;$$

(VIII.88)

434

$$\frac{dw}{du} = \frac{i\Gamma}{2\pi}\left(\frac{1}{u-f} - \frac{1}{u-f_1} + \frac{1}{u-\bar{f}} - \frac{1}{u-\bar{f}_1}\right) - \tag{VIII.89}$$

$$- \frac{N}{(u-1)^2} + \frac{N}{(u+1)^2};$$

$$z(c+id) = x_f + iy_f. \tag{VIII.90}$$

Equations (VIII.94)-(VIII.97) completely define all of the unknown coefficients of the problem. However, equations (VIII.84)-(VIII.86) with these coefficients define the more general problem than the stated problem (see Figure VIII.30).
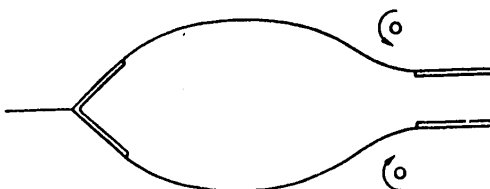

Figure VIII.30. Generalized diagram of flow over a wedge in the presence of vortices

In order to obtain the solution to the stated problem it is necessary to add the condition of closure of the cavity to the system (VIII.87)-(VIII.90)

$$\text{Res}\left(\frac{dz}{du}\right)_{u=1} = 0. \tag{VIII.91}$$

It is possible to transform the system (VIII.87)-(VIII.90) to the following form:

$$m^2 = \frac{c^2 - d^2 + r}{2(1+r)} + \frac{1}{2}\sqrt{\frac{r+(c^2+d^2)^2}{1+r}}; \tag{VIII.92}$$

$$n^2 = \frac{d^2 - c^2 - r}{2(1+r)} + \frac{1}{2}\sqrt{\frac{r+(c^2+d^2)^2}{1+r}}; \tag{VIII.93}$$

$$c_1 = 4N(1+r); \tag{VIII.94}$$

$$a = \frac{B-1}{B+1}; \tag{VIII.95}$$

$$N = \frac{\sqrt{1+\sigma}\,e^{-i\pi a}}{4(1+r)J_0^a}; \tag{VIII.96}$$

$$\begin{aligned}\text{Jm} \\ \text{Re}\end{aligned}\left\{\frac{e^{-i\pi a}}{J_0^a}J_a^{c+id}\right\} = \begin{cases}y_f \\ x_f\end{cases}; \tag{VIII.97}$$

$$B = (1+\sigma)^{1/2a}\left[\frac{(1-m)^2+n^2}{(1+m)^2+n^2}\right]^{1/a}\left[\frac{(1+c)^2+d^2}{(1-c)^2+d^2}\right]^{1/a}; \tag{VIII.98}$$

$$r = \frac{2\gamma\,cdJ_0^a}{\pi e^{-i\pi a} - 2\gamma c\,dJ_0^a}; \quad \gamma = \frac{\Gamma}{v_\kappa} = \frac{\pi r}{2c\,dJ_0^a(1+r)}; \tag{VIII.99}$$

$$J_a^u = \int_a^u\left(\frac{u+a}{u-a}\right)^a\frac{[(u+m)^2+n^2]\,u\,du}{[(u+c)^2+d^2][(u^2-1)^2]}.$$

435

The cavity closure condition assumes the form:

$$\frac{aa}{1-a^2} + \frac{2(1+c)}{(1+c)^2+d^2} - \frac{2(1+m)}{(1+m)^2+n^2} = 0. \qquad \text{(VIII.100)}$$

Giving the angle of taper of the wedge $2\pi\alpha$, the vortex coordinates x_f and y_f, the cavitation number σ and circulation Γ from (VIII.92)–(VIII.99), we find all the necessary coefficients. The closure condition (VIII.100) gives the set of initial values for which smooth closure of the cavity is observed.

It is possible to express the cavitation number σ explicitly beginning with equation (VIII.100) in terms of c, d, r, α

$$\sigma = \left[-\frac{2}{\alpha}\frac{\varphi_0}{\varphi_1} + \frac{1}{\varphi_1}\sqrt{1+4\frac{\varphi_0^2}{\alpha^2}} \right]^{2\alpha} - 1, \qquad \text{(VIII.101)}$$

where

$$\varphi_0 = 2\left[\frac{1+c}{(1+c)^2+d^2} - \frac{1+m}{(1+m)^2+n^2} \right];$$

$$\varphi_1 = \frac{|(1-m)^2+n^2|^{1/\alpha}\,|(1+c)^2+d^2|^{1/\alpha}}{|(1+m)^2+n^2|^{1/\alpha}\,|(1-c)^2+d^2|^{1/\alpha}}.$$

For a zero cavitation number the cavity cannot be closed in a finite part of the plane.

From formula (VIII.100) it is possible to find that the cavity can be closed only for $\Gamma>0$. This corresponds to the foil position in Figure VIII.30. This is explained physically by the fact that smooth closure in the tail section of the cavity is possible only for negative curvature of the cavity in the region which is observed only with negative pressure gradient (where the pressure drops on transition from the cavity to the fluid) [21]. The negative pressure gradient, in turn, is observed when the vortex (or the nose of the foil section) is located near the cavity boundary and there is no critical point between them, that is, the condition $\Gamma>0$ is observed.

It must be noted that the given flow system is also realized when the vortices are replaced by discharges.

The flow parameters for $\alpha=0.0278$ were calculated by formulas (VIII.92)–(VIII.100). The results of calculating ℓ_k and γ as a function of σ for $x_f=5.0$ and $y_f=0.2$ are presented in Figure VIII.31. As is obvious from the graph, for any cavitation number, except $\sigma=0$, circulation γ is realized for which the vortex at the point (5, 0.2) closes the cavity smoothly.
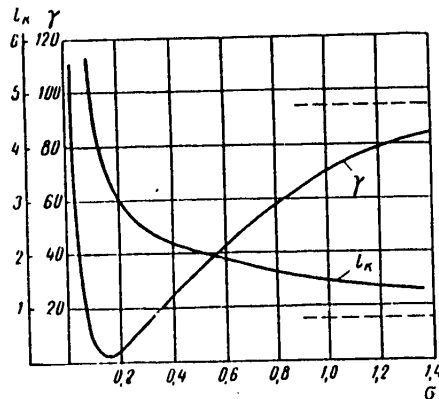
Figure VIII.31. Results of calculating flow parameters

However, when replacing the vortex by a noncavitating profile the range of cavitation numbers for which the cavity is smoothly closed is significantly more narrow and is defined by the relation

$$\gamma < \frac{C_{ym}\bar{b}}{2\sqrt{1+\sigma}},$$

where $\bar{b}$ is the chord of the foil reduced to the web length of the wedge; C_{ym} is the maximum value of C_y of the foil for which cavitation is absent.

The cavity length varies sharply only near $\sigma=0$.

BIBLIOGRAPHY

1. Ryzhov, L. M. "Problem of Drag Reduction of a Ship by Injecting Water under the Bottom," GIIVT [Works of the Gor'kiy Institute of Water Transportation Engineers], Vol 8, 1940.

2. Shanchurova, V. K. "Influence of Water Injection under the Bottom of a Ship on Water Drag and Speed of the Vessel," RECHNOY TRANSPORT [River Transportation], No 10, 1958.

3. Fedyayevskiy, K. K. "Frictional Drag Reduction by Varying the Physical Constants of the Fluid at the Wall," IZV. AN, OTN [News of the USSR Academy of Sciences, Technical Sciences Division], No 9-10, 1943.

4. Fedyayevskiy, K. K. "Frictional Drag Reduction by Varying the Fluid Density at the Wall. Industrial Aerodynamics," No 24, LOPASTNYYE MASHINY I TECHENIYA V KANALAKH [Blade Motors and Flows in Channels], Oborongiz, 1962.

5. Loytsyanskiy, L. G. "Variation of the Drag of Bodies by Filling the Boundary Layer with a Fluid with Different Physical Constants," PMM [Applied Mathematics and Mechanics], No 1, 1942.

6. Butuzov, A. A. "Results of Theoretical Analysis of the Parameters of Cavities Created on the Bottom of a Ship," DOKLADY K XVI KONFERENTSII PO TEORII KORABLYA, MAY 1966 (KRYLOVSKIYE CHTENIYA) [Reports at the 16th Conference on Ship Theory, May 1966 (Krylovskiy Lectures)], Leningrad, NTOSP, No 73, 1966.

7. Butuzov, A. A. "Limiting Parameters of an Artificial Cavity Formed on the Bottom Surface of a Horizontal Wall," IZV. AN SSSR "MEKHANIKA ZHIDKOSTI I GAZA" [News of the USSR Academy of Sciences, Liquid and Gas Mechanics], No 2, 1966.

8. Pernik, A. D. PROBLEMY KAVITATSII [Cavitation Problems], Leningrad, Sudpromgiz, 1963.

9. Tulin, M. P. "Supercavitating Flow Past Foils and Struts. Cavitation in Hydrodynamics," PROC. OF A SYMPOSIUM HELD AT NPL, 1956.

10. Starobinskiy, V. B. "Detached Flow of a Fluid of Finite Depth Over a Thin Wedge," TR. LIVT [Works of the Leningrad Institute of Water Transportation], izd. Transport, 1964.

11. Starobinskiy, V. B. "Problem of Frictional Drag Reduction of Vessels Under Shoal Conditions by Creating a System of Artificial Cavities on the Bottom of Such Vessels," DOKLADY K XV KONFERENTSII PO TEORII KORABLYA. (KRYLOVSKIYE CHTENIYA) [Reports at the 15th Conference on Ship Theory. (Krylovskiy Lectures)], NTOSP, No 64, 1965.

12. "Vorrichtung zur Verringerung des Reibungs - widerstandes von Schiffen mit einem unter dem Boden angeordneten Luftkissen," KNAT FINE GRAM (DANEMARK).

13. Gradshteyn, I. S.; Ryzhik, I. M. TABLITSY INTEGRALOV, SUMM, RYADOV I PROIZVEDENIY [Tables of Integrals, Sums, Series and Products], Moscow, Fizmatgiz, 1962.

14. Sedov, L. I. PLOSKIYE ZADACHI GIDROMEKHANIKI I AERODINAMIKI [Two-Dimensional Problems of Hydromechanics and Aerodynamics], Moscow, Fizmatgiz, 1952.

15. Lavrent'yev, M. A.; Shabat, B. V. METODY TEORII FUNKTSIY KOMPLEKSNOGO PEREMENNOGO [Methods of the Theory of Functions of a Complex Variable], Moscow, Fizmatgiz, 1958.

16. Muskhelishvili, N. I. SINGULYARNYYE INTEGRAL'NYYE URAVNENIYA [Singular Integral Equations], Gostekhizdat, 1946.

17. Ivanilov, Yu. P.; Monseyev, N. N.; Ter-Krikorov, A. M. "Asymptotic Nature of the M. A. Lavrent'yev Formulas," DAN SSSR [Reports of the USSR Academy of Sciences], Vol 123, No 2, 1958.

18. Monseyev, N. N. "Asymptotic Methods of the Narrow Strip Type," NEKOTORYYE PROBLEMY MATEMATIKI I MEKHANIKI [Some Problems of Mathematics and Mechanics], Novosibirsk, USSR Academy of Sciences, Siberian Division, 1961.

19. Yakimov, M. L. "Approximate Formula for Tension During Conformal Mapping of Regions Having a Narrow Segment," SIBIRSKIY MATEMATICHESKIY ZHURNAL [Siberian Mathematics Journal], Vol 3, No 6, 1962.

20. Butuzov, A. A. "Theoretical Analysis of Detached Cavitation Created on a Planing Surface," DOKLADY K XVII NAUCHNO-TEKHNICHESKOY KONFERENTSII PO TEORII KORABLYA [Reports at the 17th Scientific-Technical Conference on Ship Theory], Leningrad, TR. NTOSP [Works of the Scientific and Technical Society of the Shipbuilding Industry], No 88, 1967.

21. Birchhoff, G.; Sarantonello, E. STRUI, SLEDY, I KAVERNY [Jets, Wakes and Cavities], Moscow, izd. Mir, 1964.

22. Migachev, V. I. "Symmetric Jet Flow Over a Wedge in the Presence of Vortices," TR. LIVT, No 113, 1967.

23. Basin, M. A.; Yegorov, I. T.; Isayev, I. I.; Kramarev, Ye. A.; Sadovnikov, Yu. M. "Peculiarities of Using Gaseous Media to Alter the Hydrodynamic Characteristics of Solid Bodies Moving in a Fluid," ANNOTATSII DOKLADOV II VSESOYUZNOGO S"YEZDA PO TEORETICHESKOY I PRIKLADNOY MEKHANIKE [Annotations of Reports of the Second All-Union Conference on Theoretical and Applied Mechanics], USSR Academy of Sciences, 1964.

24. Isayev, I. I.; Sadovnikov, Yu. M. "Study of the Possibility of Creating Artificial Cavities on Planing Surfaces," Leningrad, TR. NTOSP, No 88, 1967.

25. Yegorov, I. T. "Methods of Increasing Lift and Increasing the Lift/Drag Ratio of Lifting Foils Under Detached Flow Conditions and in the Deep Stage of Cavitation," TR. NTOSP, Leningrad, izd. Sudostroyeniye, No 88, 1967.

26. Butuzov, A. A. "Artificial Cavitating Flow Behind a Thin Wedge Placed on the Lower Surface of a Horizontal Wall," IZV. AN SSSR, MEKHANIKA ZHIDKOSTI I GAZA [News of the USSR Academy of Sciences, Fluid and Gas Mechanics], No 2, 1967.

27. "Towrope Drag Reduction of Ships," RECHNOY TRANSPORT [River Transporation], No 8, 1967.

10845
CSO: 8344/1852

- END -